e-ISSN : 2320-0847
p-ISSN : 2320-0936

American Journal of Engineering Research (AJER)

Volume 3 Issue 11– November 2014

www.ajer.org ajer.research@gmail.com

Editorial Board

American Journal of Engineering Research (AJER)

American Journal of Engineering Research

Volume-3 Issue-11

American Journal of Engineering Research

American Journal of Engineering Research (AJER)
e-ISSN : 2320-0847 p-ISSN : 2320-0936
Volume-03, Issue-11, pp-01-09
www.ajer.org

Research Paper Open Access

Study of Space-Time Coding Schemes for Transmit Antenna Selection

[1]Munia Patwary, [2]Adnan Quaium, [3]Afroza Akter Munni, [4]Christin Nabonita Halder Jui, [5]Sonia

[1,2,3,4,5] *(Department of Electrical and Electronic Engineering / American International University-Bangladesh, Bangladesh)*

ABSTRACT : *Multiple-Input Multiple-Output (MIMO) is a spatial diversity technique and diversity techniques have been applied to overcome multipath fading in wireless communication. MIMO system can improve the quality (BER) or the data rate of the communication by means of adequate signal processing techniques at both ends of the system. The capacity can increase linearly with the number of antennas and thus increase the reliability of wireless communication. However, due to several limitations and hardware complexities, antenna selection has been chosen as alternative to restrain numerous advantages of MIMO. This article reviews results on familiar antenna selection diversity, followed by a discussion of performance of different space-time coding gains and error probability at the transmit side.*

Keywords *– Diversity, MIMO, MRC, STBC, STTC, TAS*

I. INTRODUCTION

In the last few years, there have been many revolutionary changes in the telecommunication industry. The wireless industry has already embraced Multiple Input Multiple Output (MIMO) systems for the resulting impressive improvements in capacity and bit error rates (BERs). Wireless communication system is striving further for higher ever data rates and to improve performance by increasing transmission rates and spectral efficiency. Using multiple transmit antenna as well as receive antennas, a MIMO system exploits spatial diversity, higher data rate, greater coverage and improved link robustness without increasing total transmission power or bandwidth [1]. The MIMO channels can be exploited to increase the bandwidth efficiency through the layered structure or to achieve a full diversity order through space-time coding techniques, such as space-time block codes (STBCs) and space-time trellis codes (STTCs) [2]. In this paper, Transmit Antenna Selection is discussed with appropriate equations, table and figures for different schemes- TAS/MRC, TAS/STBC and TAS/STTC mainly. The performance analyses of these schemes in different papers are also discussed here. The paper is organized as follows. The section II gives antenna overview, section III discusses antenna selection algorithms, section IV elaborates the space-time codes, section V presents comparison and performance analysis of the space-time codes- STBC and STTC, and section VI draws the conclusion. These comparisons are useful for design and implementation of multiple antenna wireless system.

II. ANTENNA OVERVIEW

In a typical multiple input multiple output (MIMO) transmitter/receiver system, there are M independent sources of signals and noise dispersed or assembled in some manner in space and there is an array of N sensors usually placed in some best designed configuration. Each sensor receives, or the transmitter transmits, a different mixture or combination of the source signals. Assume a MIMO system with N_T transmit and N_R receive antennas is selected. At the transmitter, we only choose a subset with N ($N \leq N_t$) transmit antennas for transmission. It is denoted by (N_t, N; N_r). Let C_k denote the channel power gain associated with transmit antenna k.

$$C_k = \sum_{i=1}^{n_R} h_{k,i} \vee^2, \qquad 1 \leq k \leq N_t \tag{1}$$

The random variables C_k are rearranged in an ascending order of magnitude and denoted by: $C_{(1)} \leq C_{(2)} \leq \ldots \leq C_{(N_t)}$. Out of $\binom{N_t}{N}$ choices, the subset which maximizes the total received power will be selected. In an N_t X N_r MIMO system, totally (N_t X N_r) channels are required to be estimated between transmitters and receivers. The received training symbols can be expressed as:

$$y = Hx + n \tag{2}$$

where x is the transmitted training signal, y is the received signal and n is the noise response. The channel response H is assumed to be random and quasi-static within two transmission blocks [1].

Most of the current hand-held devices can support one or at most two antennas for their limited size and power. In a number of applications, the only practical means of attaining diversity is deployment of antenna arrays at the transmitter and/or the receiver. However, considering the fact that receivers are typically required to be small; it may not be practical to arrange multiple receive antennas at the remote station, and this encourages us to consider transmit diversity. So, for high data rate downlink transmission, a high diversity order is possible only if space-time codes with a large number of transmit antennas are engaged at the base station, though design and implementation of such space-time codes is challenging.

III. ANTENNA SELECTION ALGORITHMS

TRANSMIT ANTENNA SELECTION WITH MRC

Transmit antenna selection requires a feedback path from the receiver to the transmitter. The main purpose of the feedback is to inform the transmitter which antennas to select. When the transmitter is fully aware of the channel coefficients, the maximum capacity available in the channel will be attained [3]. The surplus capacity supplied by transmit antenna selection is quantified and analyzed. Figure 1 shows the transmit antenna selection system.

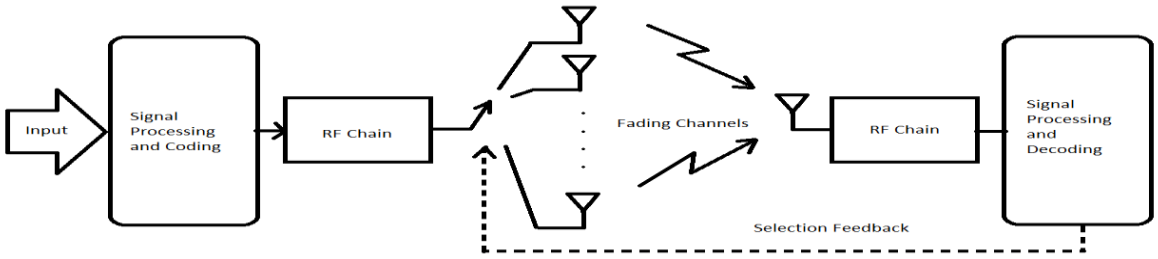

Figure 1: Transmit Antenna Selection

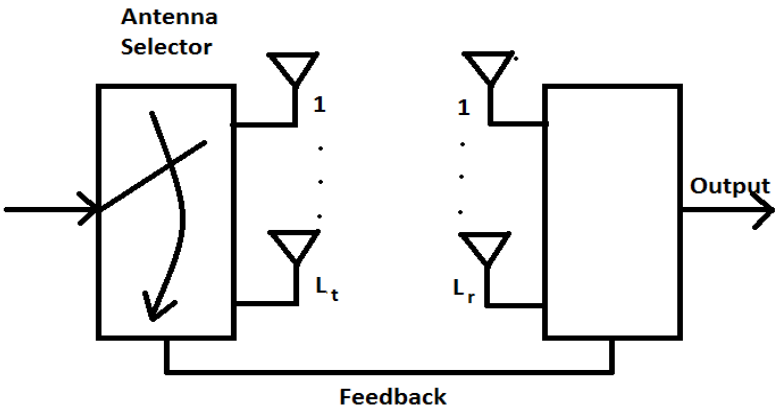

Figure 2: (a) Transmit Antenna Selection (TAS)

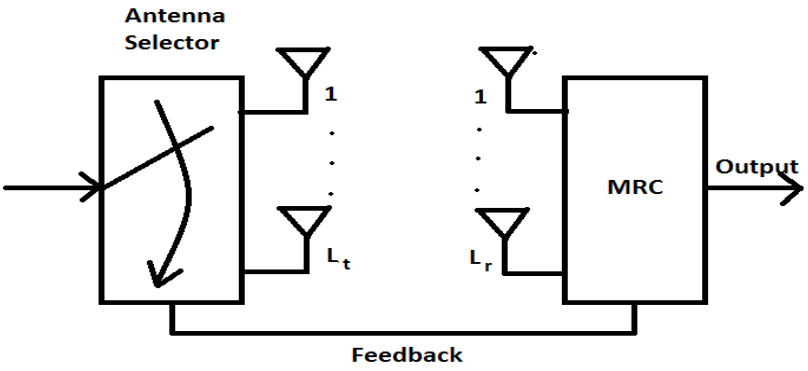

Figure 2: (b) TAS/MRC

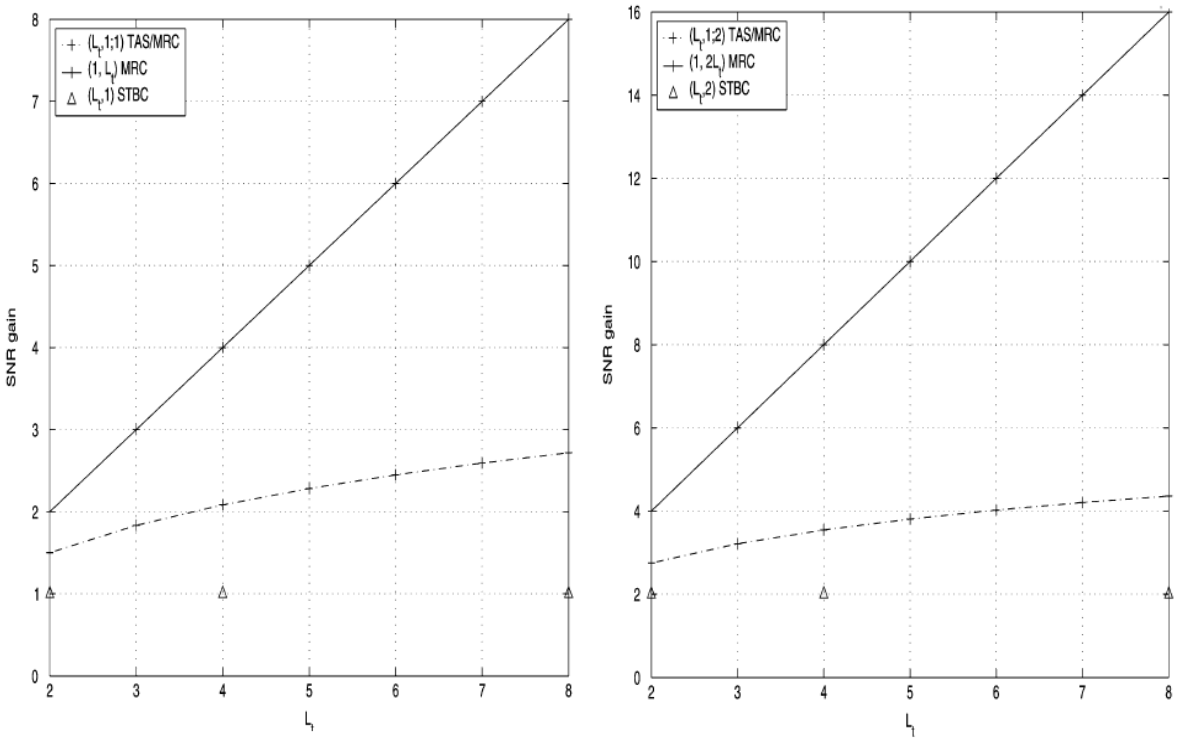

(a) (b)

Figure 3: Average SNR gain comparison for (a) diversity orderL_t, and (b) diversity order $2L_t$

The maximal-ratio combining (MRC) is the optimal linear combining process. In [4], the average SNR gain comparison for diversity order L_t and diversity order $2L_t$ is shown. Each graph shows the TAS/MRC, MRC and STBC curves and it is apparent that the TAS/MRC is giving the best SNR gain. For diversity order $2L_t$, the SNR gain is exactly double for TAS/MRC and STBC, and almost double for MRC when compared to the curves for diversity orderL_t.

In [11], the error performance of the TAS/MRC scheme for an asymptotic scenario of high SNRs is investigated, which shows the diversity gain of the TAS/MRC scheme over Nakagami-m fading channels. There an (L_t, 1;L_r) TAS/MRC system equipped with L_t transmit and L_r receive antennas in a flat Nakagami-m fading environment is considered. The analytical and simulation results of the TAS/MRC scheme for some modulation schemes over Nakagami-m fading channels are presented there.

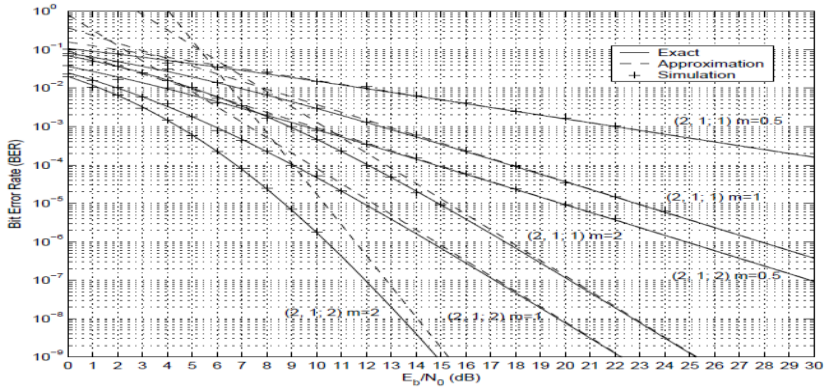

Figure 4: The exact, approximation and simulation BER for the (2, 1; 1) and (2, 1; 2) TAS/MRC schemes, BPSK

Fig.4. in [11] shows the comparison between the exact expressions, the asymptotic expressions and the simulation results for the (2, 1; 1) and (2, 1; 2) TAS/MRC schemes when Nakagami-m fading parameters m are equal to 0.5, 1 and 2.

IV. SPACE-TIME CODED SYSTEMS

Space-Time Codes (STC) were first introduced by Tarokh et al. from AT&T research labs [8] in 1998 as a novel means of providing transmit diversity in wireless fading channels using multiple transmit antennas. Space-time block coding is a method used in wireless communication to transmit multiple copies of a data stream across a number of antennas and to exploit the various received versions of the data to improve the dependability of data transfer. It involves the transmission of multiple surplus copies of data to recompense for fading and thermal noise in the hope that some of them may arrive at the receiver in a better state than others.

1. TRANSMIT ANTENNA SELECTION WITH STBC

The Space-time Block Codes (STBC) is a promising signaling technique. It uses the MIMO structure to improve the sturdiness of communication link. Space-time block codes are designed to achieve the maximum diversity order for a given number of transmit and receive antennas subject to the constraint of having a simple decoding algorithm [5]. In 1998, Alamouti designed a simple transmission diversity technique for systems having two transmit antennas [6], which provides full diversity and requires simple linear operations at both transmission and reception side.

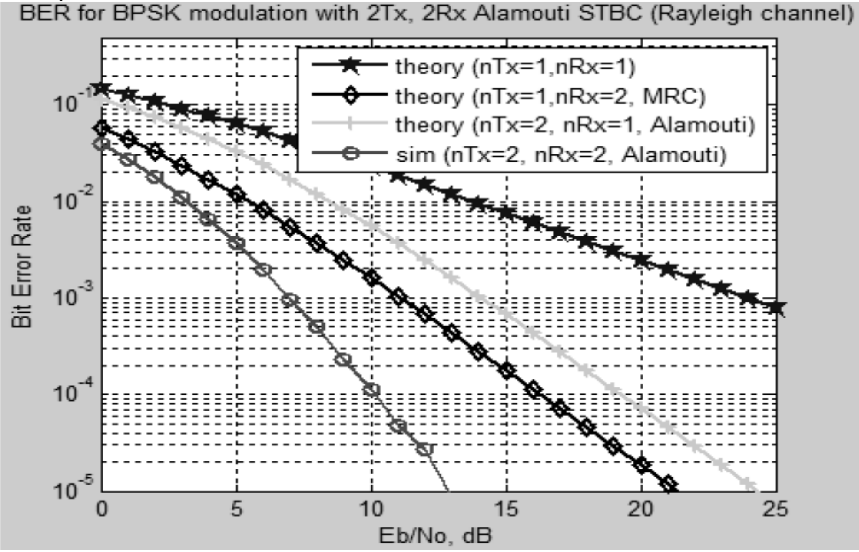

Figure 5: BER for BPSK modulation with 2X2 Alamouti STBC (Rayleigh channel)

The performance limit of MIMO system for different antenna configuration is measured through Bit Error Rate (BER) which is particularly a smart dimension for wireless communications. Figure 5 [5] shows four different curves for different combinations of Tx and Rx. The Alamouti scheme [Alamouti, 98] is the simplest STBC with N_t = 2 [7]. The table below, as in [5], shows the comparison of different diversity schemes where the Alamouti curve for 2Tx and 2Rx is showing the best curve with less BER.

Type of scheme	Type of modulation	No. of Tx antenna	No. of Rx antenna	BER	SNR
Conventional System (SISO)	BPSK	1	1	0.01208	13dB
MRC	BPSK	1	2	0.001606	13dB
Alamouti (2x1)	BPSK	2	1	0.0004341	13dB
Alamouti (2x2)	BPSK	2	2	$1.1e^{-005}$	13dB

Table 1: Comparison of different diversity schemes

2. TRANSMIT ANTENNA SELECTION WITH STTC

Space-time trellis codes (STTC), originally proposed by Tarokh et al., incorporate jointly designed channel coding, modulation, transmit diversity and optional receive diversity [8]. Space-time trellis code (STTC) is a MIMO technique which provides full diversity and coding gain, but only transmits one data symbol per time slot. The encoding processing can be represented by a trellis for Space-time Trellis Codes. For example, the trellis of a 4-state 4-PSK STTC with N_t = 2 is as below [8].

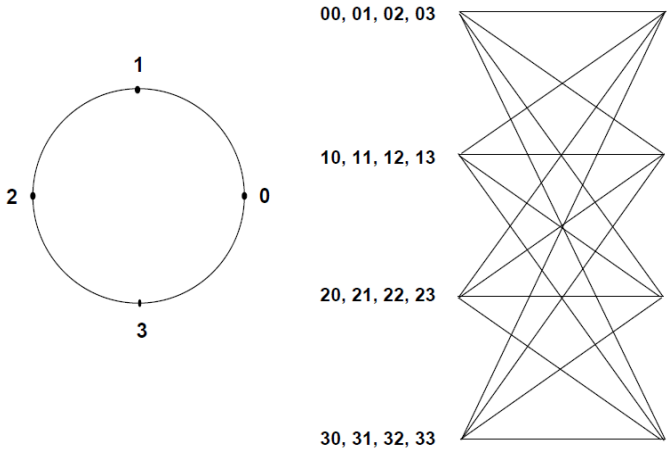

Figure 6: Tarokh's 4-state QPSK space-time trellis code

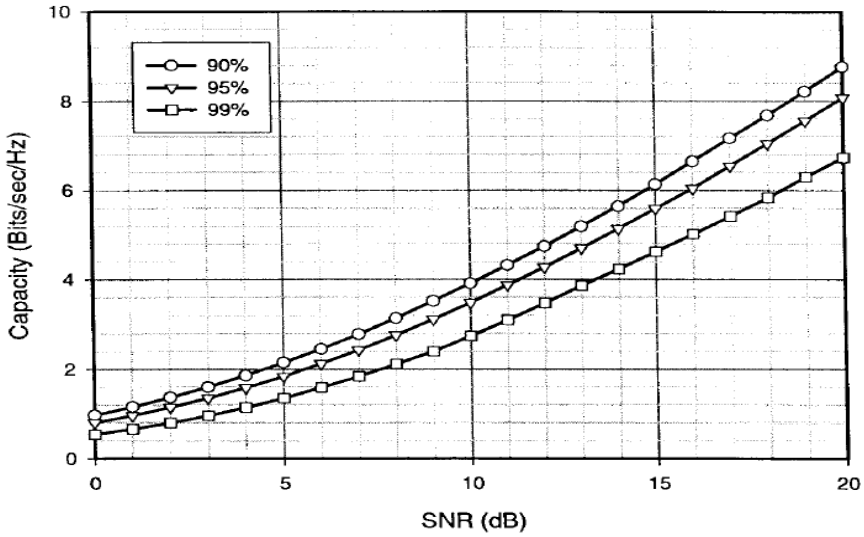

Figure 7: Outage capacity for two receive and two transmit antennas

STTCs have to employ Viterbi algorithm, which is usually complex. A carefully designed STTC can attain a full diversity order with certain constriction from memory order.

V. COMPARISON AND PERFORMANCE ANALYSIS OF STBC AND STTC

Any space-time code can be analyzed in terms of the measures presented for space-time trellis codes, namely diversity advantage and coding advantage. The performance curve is affected by the diversity advantage and coding advantage in different ways. Diversity advantage affects the slope of the FER versus SNR graph in a way – greater the diversity, the more negative the slope. Coding advantage affects the horizontal shift of the graph – greater the coding advantage, the greater the shift to the left [10].

In [13], the performance of STBC and STTC are compared in terms of frame error rate keeping the transmit power, spectral efficiency and number of trellis states fixed. There, it has been discovered that a simple concatenation of space-time block codes with traditional AWGN (additive white Gaussian noise) trellis codes outperforms some of the best known space-time trellis codes at SNRs (signal to noise ratios) of interest.
The MRCs, STBCs and STTCs – the all three technique can achieve a full diversity order. However, when they are implemented in practical systems, certain problems emerge and MRC is incompatible since its diversity order is solely determined byN_T. We are trying to focus on transmit antenna selection in this paper and hence, STBC and STTC are more significant here.

In [7], it has been stated that for STBCs, n_T > 2 means a full code rate cannot be achieved with complex constellations, and SNR loss relative to receive diversity is large; for STTCs, n_T > 2 means a large memory order is needed to guarantee a full diversity order besides having a very complex decoding algorithm, and design difficulty is also tremendous.

Space-time block codes and space-time trellis codes are two exceptionally different diversity schemes. In [14], the simulation and comparative analysis of STBC and STTC in MIMO technique are presented, where fig.6 is also shown. There it is seen that, as the number of transmitting and receiving antenna increases, the error probability is improved for both STBC and STTC with the increase of signal to noise ratio. The comparison between STBC and STTC (fig.8a), shows that the error probability of STTC is lower than that of STBC for higher SNR and so the coding gain of STTC is higher than that of STBC when applied for two transmit and two receive antennas, but both the codes achieve same diversity. Fig.8 (b) shows that coding gain of STTC is higher than STBC, when applied for three transmitting and three receiving antennas, both the codes achieving same diversity.

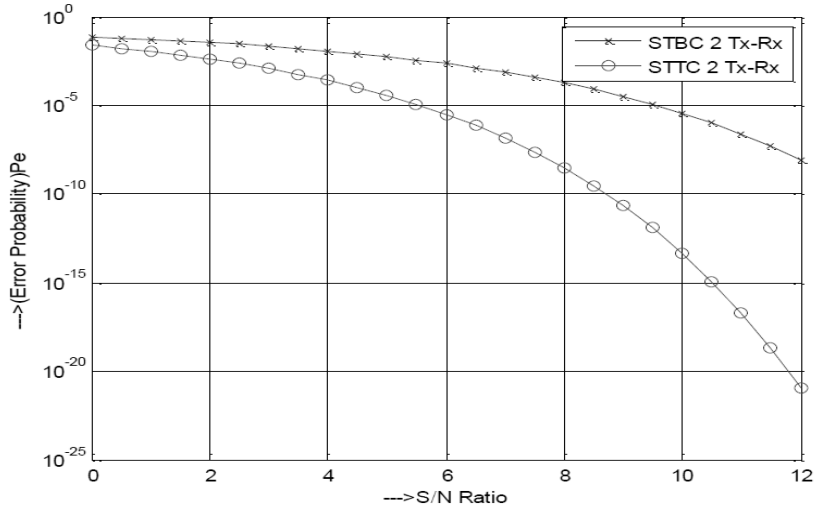

(a)

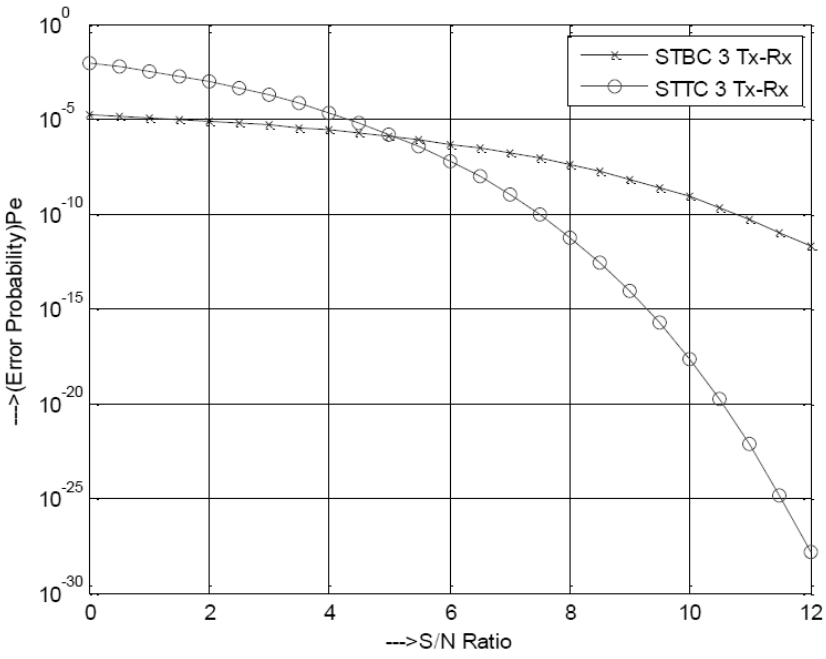

(b)

Figure 8: Comparison of STBC and STTC for coded MIMO system for (a) 2 Tx-Rx antennas and (b) 3 Tx-Rx antennas

Coding gain of STTC is higher than STBC, when applied for four transmitting and four receiving antennas [15], both the codes achieving same diversity. The error probability is improved as compared to three transmit and three receive antennas [14]. Also, for five transmitting and five receiving antennas, the error probability of STTC is lower than that of STBC for high SNR so the coding gain of STTC is higher than STBC, both the codes achieving same diversity and the error probability being further improved as compared to four transmit and four receive antennas [14].

STTC Scheme	Error Probability (dB)	STBC Scheme	Error Probability (dB)
2Tx-2Rx antennas	-209.5078	2Tx-2Rx antennas	-80.4527
3Tx-3Rx antennas	-278.3268	2Tx-2Rx antennas	-117.4714
4Tx-4Rx antennas	-347.1669	2Tx-2Rx antennas	-189.8716
5Tx-5Rx antennas	-416.0032	2Tx-2Rx antennas	-304.5842

Table 2: Comparison of STTC and STBC in terms of Error Probability (SNR=12dB)

VI. CONCLUSION

In this paper, we deduce that the coding gain of STTC is higher than that of STBC for higher SNR as the error probability of STTC is lower than STBC, the same diversity being achieved by both the codes. The diversity can be increased by increasing the number of transmit and receive antennas. The same phenomena are applicable for two transmit and two receive antennas, three transmit and three receive antennas, four transmit and four receive antennas, and five transmit and five receive antennas. The error probability for four transmit and four receive antennas is improved when compared to three transmit and three receive antennas, and the error probability for five transmit and five receive antennas is further improved when compared to four transmit and four receive antennas.

REFERENCES

[1] M. W. Numan, M. T. Islam and N. Misran, "Performance and complexity improvement of training based channel estimation in MIMO systems", Progress In Electromagnetics Research C, Vol. 10, pp. 1-13, 2009

[2] Zhuo Chen, Jinhong Yuan and Branka Vucetic, "Analysis of Transmit Antenna Selection/Maximal-Ratio Combining in Rayleigh Fading Channels", IEEE Transactions on Vehicular Technology, Vol. 54, pp. 1312-1321, No. 4, July 2005

[3] S. P. Premnath, J. R. Jenifer and Arunachalaperumal, "Performance enhancement of MIMO systems using Antenna Selection Algorithm", International Journal of Emerging Technology and Advanced Engineering, Volume 3, Special Issue 1, pp. 229-233, January 2013

[4] Dr. JT Wang, "Analysis of Transmit Antenna Selection/Maximal-Ratio Combining in Rayleigh Fading Channels, IEEE Transactions on Vehicular Technology, Vol. 54, No. 4, July 2005

[5] Nazia Parveen and D. S. Venkateswarlu, "Implementation of Space-Time Block Coding (STBC) Using 2 Transmit and 2 Receive Antennas", International Journal of Emerging Technology and Advanced Engineering, Volume 2, Issue 10, pp. 175-178, October 2012

[6] J. Akhter and D. Gesbert, "Extending orthogonal block codes with partial feedback", IEEE Transactions on Wireless Communication, Vol. 3, pp.1959-1962, Nov. 2004

[7] Zhuo Chen, Jinhong Yuan and Branka Vucetic, "Performance Analysis of Transmit Antenna Selection in MIMO systems", Telecommunications Laboratory

[8] Harsh P. Shah, B. E., "Performance Analysis of Space-Time Codes", Thesis, Master of Science in Electrical Engineering, the University of Texas at Dallas, December 2003

[9] Lei Poo, "Space-Time Coding for Wireless Communication: A Survey", Stanford University

[10] S. Sandhu and A. J. Paulraj, "Space-time block codes versus space-time trellis codes", in Proceedings of the ICC, 2001

[11] Zhanjiang Chi, "Performance Analysis of Maximal-Ratio Combining and Space-Time Block Codes with Transmit Antenna Selection over Nakagami-m Fading Channels", 20 March 2007

[12] Shahab Sanayei and Aria Nosratinia, "Antenna Selection in MIMO Systems", IEEE Communications Magazine, pp. 68-73, October 2004
[13] S. Sandhu, R. Heath and A. Paulraj, "SPACE-TIME BLOCK CODES VERSUS SPACE-TIME TRELLIS CODES", IEEE, pp.1132-1136, 2001
[14] T. P. Zinzuwadia, K. R. Borisagar, B. S. Sedani, "Simulation and Comparative analysis of STBC and STTC in MIMO Technique", International Journal of Darshan Institute on Engineering Research & Emerging Technologies, Vol. 2, No. 1, 2013
[15] Space-Time Codes and MIMO Systems by Mohinder Jankiraman, Artech House Boston, London www.artechhouse.com

American Journal of Engineering Research (AJER)
E-ISSN: 2320-0847 p-ISSN: 2320-0936
Volume-03, Issue-11, pp-12-17
www.ajer.org

Research Paper

Assessment of Regional Development Using Taxonomy Model (A Case of Razavi Khorasan, Iran)

Hadi Ivani[1*], Maryam Sofi[2*]

[1] *Faculty of Art and Architecture, Payame Noor University, Iran (Corresponding author)*
[2*] *MSc student of Geography & Urban Planning, Payam Noor University, Iran*

ABSTRACT : *Today, for balanced growth in all regions of the country, economists believe that the idea of dynamic growth pole was unsuccessful because not only did it fail in decreasing regional inequalities in the country, but it also caused existing inequality-ties to intensify. In order to, the aim of current research is assessment of regional development using taxonomy model in the Razavi Khorasan province of Iran. Applied methodology is based on descriptive- analytical methods. we have used of numerical taxonomy as an most common approaches to categorize of development level in the Khorasan Razavi cities. Results show that Torbat-E- Jam (0.5) city has the highest level of development in case study region, while Fariman (0.15) has the lowest level. Finally, in the end of this presented some solve ways.*

KEY WORDS: *Urban Development, Regional Development, Razavi Khorasan, Taxonomy*

I. INTRODUCTION

Regional development is a broad term but can be seen as a general effort to reduce regional disparities by supporting (employment and wealth-generating) economic activities in regions. In the past, regional development policy tended to try to achieve these objectives by means of large-scale infrastructure development and by attracting inward investment. Awareness of the need for a new approach is driven by observation that past policies have failed to reduce regional disparities significantly and have not been able to help individual lagging regions to catch up, despite the allocation of significant public funding. The result is under-used economic potential and weakened social cohesion. Substantial disparity in regional incomes is a reality in every geographically large country, and the causes of the disparity are numerous and complex. The enduring character of many cases of regional backwardness is also a reality, for example, the Appalachians in the United States, Northern Shaanxi in China, Chiapas in Mexico, and Madura in Indonesia. The persistence of regional poverty has led many prominent social scientists to see the primary causes of entrenched regional poverty to be interrelated in a self-reinforcing manner (Démurger & et al, 2001). Based on the expert's views in development, there are various definitions for the term of "development". Among them can be mentioned the following cases: the increase in economic production and productivity, improving both the qualitative and quantitative indicators of living standards, improving the level of hygienic and security services, the reduction of unemployment and inflation and meeting social and economic needs (Tudaro, 2008; Fanni & et al, 2014).

II. BACKGROUND

Iran with its unique climactic conditions has experienced different climactic landscapes over its long history. Therefore, in different regions of Iran, the development has not done equally well and there are some inequalities in obtaining the benefits of development. Development that nowadays is the first and foremost purpose of all governments has different forms. One of the important forms of development is economic development but this is not the way development be conceived, so development is not limited to a purely economic phenomenon. Therefore, the main purpose of development must be an optimal growth paradigm for public income that covers any stratum of society. Development besides the amount of production and income includes changes in the political, institutional, social, and bureaucratic structures and revising them and the public opinion of people as well as production and income (Azkia, 1999).

One of the topics that recently have been proposed in the culture of regional and parochial planning is inequality in regional development, but its status is not clearly defined. These inequalities, which are used by various reasons that can be historical, social, economic, geographical, demographic, and/or political, have different and imbalanced growth rates across areas and regions (Mansoori, 1996).In the recent years, Iran's development policy followed the growth pole theory. In this strategy, the development of cities becomes a priority, with the goal of their economic and social development spreading to rural villages. As well, this theory posits that the economic growth of cities stimulate the agricultural production of their neighboring regions. The evidence shows that with the implementation of "the growth pole" policy, cities could not provide the necessary services that the theory had suggested they would, and this caused rural–urban migration (Hamsi, 1981).For understanding the spatial structure of regions and predicting the changes and evolutions of development, Freidman proposes the central- peripheral paradigm. Freedman says "every system of geography includes two spatial subsystems: one of them is the center that is the pioneering heart and dynamism of the system and another one is the peripheral that can be considered as the rest of the system and is in the state of dependency or accepting sovereignty toward the center" (Hilhorst, 1967).

The relationship of the center-periphery maybe considered as akin to a colonial relationship. Generally, the polarization of structure is toward the center from the periphery by replacing internal factors. According to the proposed theoretical framework, the common aspect or factor of all is to paying attention to regional inequalities and also to the growth and development of less developed areas. Based on the proposed theories, namely the growth pole and center periphery theories, the main cause of the existing inequalities among the regions is the internal factors. This is to say, while the basic economic theory emphasizes on seeking the root cause of the lack of development factors over the foreign factors, and the foreign factors play the primary and determining role in making inequalities among the regions. The inexorable process of globalization has accelerated in recent decades. Driven, inter alia, by the processes of technological change, migration, innovation and connectivity, the world has been more tightly woven together (Lee & et al, 2003). While the positive impacts of globalization have been reaped in the form of rapid economic growth, globalization has also given rise to a range of issues including rapid transmission of financial shocks, international crime and drug trafficking, increasingly volatile and turbulent international financial and product markets, issues of food and energy security and widening income and social inequalities (Kalantari, 2001).

These issues cannot be effectively dealt with except through coordinated global and regional action, and require effective regional and global governance mechanisms. Partly as a response to these challenges, there has been a broadening of regional integration processes and many forms of intra-regional cooperation. Many of the key policy actions and policy dialogues to address the impact of the multiple crises were initiated at the regional and sub-regional levels. Much of this has been done by regional organizations and groupings which have evolved as important players in determining the development agenda at all levels. The regional dimension of development is now being recognized as being critical for an effective and coordinated response for addressing an ever-growing number of Tran's boundary issues. With the regional development architecture evolving rapidly, this is an opportune time for the UN system, in particular the Regional Commissions, to reposition itself to engage more effectively with regional processes. Therefore, the Regional Commissions have come together to undertake a study, which would identify ways in which the UN system, and the Regional Commissions in particular, could engage more deeply and more effectively with the policy frameworks and initiatives developed by regional and sub-regional organizations. The study will document the rise of the most salient and effective regional integration and cooperation mechanisms in different regions, and draw upon selected examples, particularly in the areas of trade and investment; macroeconomic, financial and monetary policy coordination; and regional connectivity including transport. It will provide recommendations for the UN system, in particular the Regional Commissions, for enhanced and coherent support of regional and sub-regional initiatives and priorities (Xang, 2005; Tik, 1987).

III. METHODOLOGY

Various methods and model are used to assess the level and rate of development in regions. Some of these methods are consisting of Oskologram, taxonomy, factor analysis, cluster analysis and Morris noted that each have advantages and disadvantages. In this research, we have used of numerical taxonomy as an most common approaches to categorize of development level in the Khorasan Razavi cities. Finally, it is presented some suggestions to solve the problem.

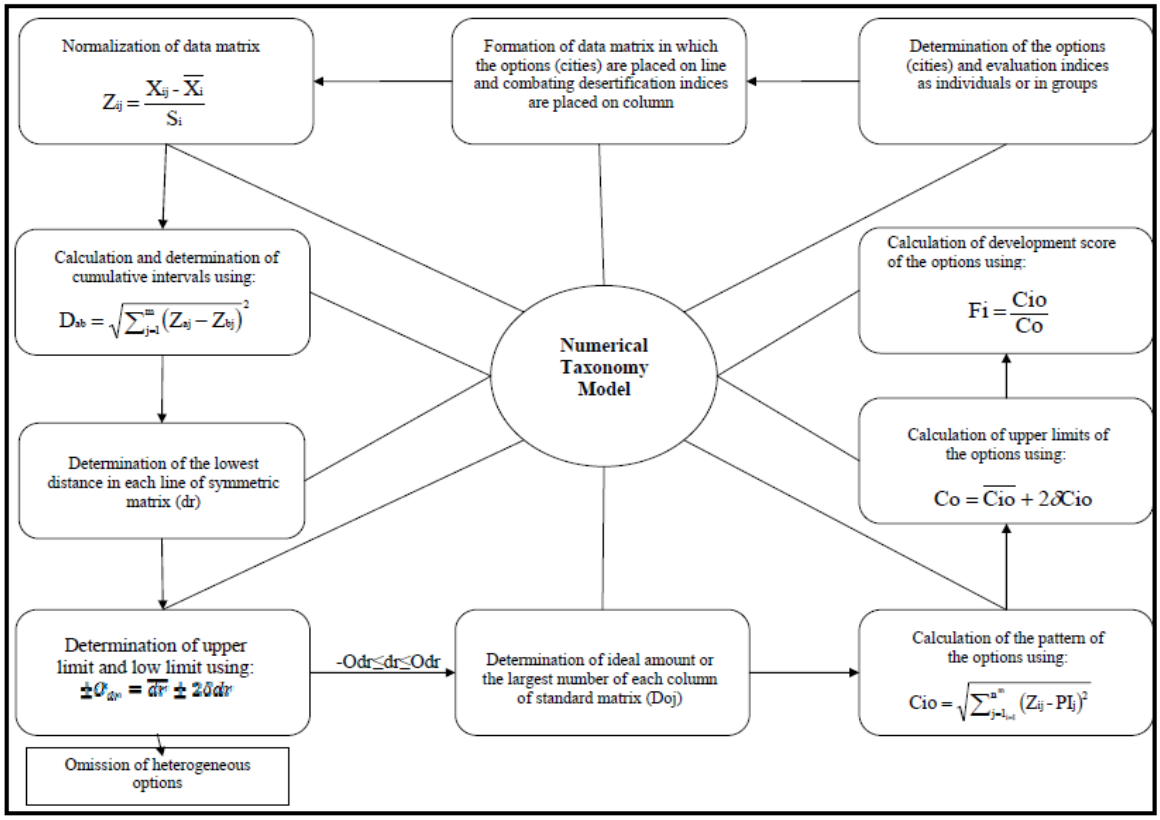

Fig. 1. Steps of numerical taxonomy analysis.
Source: Sadeghi Ravesh & et al. 2013.

IV. CASE STUDY REGION

Razavi Khorasan is a province that is located in the northeastern of Iran and Mashhad city is the center and the capital city of this province. Other cities and townships are Quchan, Dargaz, Chenaran, Sarakhs, Fariman, Torbat-e Heydarieh, Torbat-e Jam, Taybad, Khaf, Roshtkhar, Kashmar, Bardaskan, Nishapur, Sabzevar, Gonabad, Kalat, Khalilabad and Mahvelat. Razavi Khorasan is one of the three provinces that were created after the division of Khorasan Province in 2004. In 2014 it was placed in Region 5with Mashhad as the location of the region's secretariat (Wikipedia, 2014). In Persian, "Khor" means "sun" and "san" means "the place", "the dwelling". Khorasan being situated in the East of Iran is the "place where the sun rises". Historical Khorasan, also known as "Great Khorasan" included present day Khorasan as well as Transoxiana and Afghanistan. It was in the 19th century, during the reign of the Qajars, that the frontiers as we know them today were established. The older Persian province of Khorasan included parts which are today in Iran, Afghanistan, Tajikistan, Turkmenistan and Uzbekistan. Some of the main historical cities of Persia are located in the older Khorasan: Nishapur and Tus (now in Iran), Merv and Sanjan (now in Turkmenistan), Samarkand and Bukhara (both now in Uzbekistan), Herat and Balkh (now in Afghanistan), Khujand and Panjakent (now in Tajikistan). In its long history, Khorasan knew many conquerors and empires: Greeks, Mauryans, Arabs, Seljuk Turks, Safavids, Pashtuns (ethnic Afghans) and others. The major ethnic groups in this region are Persians with Kurdish, Turks and Turkmen minorities. Most of the people in the region speak closely related modern day dialects of Persian. The largest cluster of settlements and cultivation stretches around the city of Meshed northwestward, containing the important towns of Quchan, Shirvan, and Bojnurd. The language spoken in Khorasan is Persian.

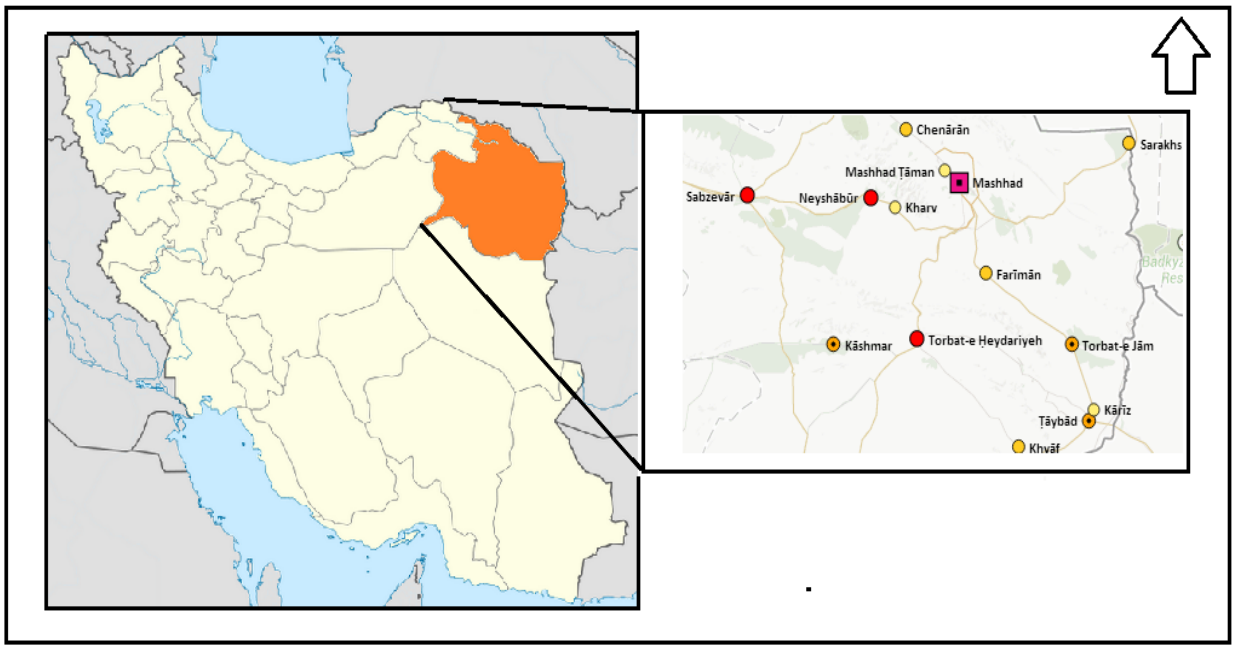

Fig. 2. A view of case study region.

Results

In this study, the options are the urban areas of Khorasan province (units studied), and evaluation indexes are main regional development factors in urban areas which imply amount of investments, activities and operations about regional development in urban and province level.

Step 1: Formation of data's matrix:

$$X = \begin{vmatrix} 75/45 & 9/09 & 37/5 & 12/18 & 12/92 \\ 0 & 1/82 & 0/20 & 0 & 1/34 \\ 0/20 & 3/64 & 5/33 & 1/85 & 1/44 \\ 0/04 & 7/27 & 1/43 & 3/25 & 2/52 \\ 0/20 & 9/09 & 5/12 & 7/37 & 2/40 \\ 0 & 9/09 & 1/64 & 2/71 & 2/40 \\ 0 & 7/27 & 5/94 & 4/50 & 4/18 \end{vmatrix}$$

In contionuous, we have Infrastructure index table as below:

Table (1)

Infrastructure indexes in Razavi Khorasan cities

	Network length	Urban Gas delivery	Rural gas delivery	Rural power	Rural telephone
Mashhad	75.45	9.09	37.5	12.18	12.92
Bakharz	0	1.82	0.20	0	1.34
Binalod	0.20	3.64	5.33	1.85	1.44
Taibad	0.04	7.27	1.43	3.25	2.52
Torbat Jam	0.20	9.09	5.12	7.37	2.40
Khavaf	0	1.64	2.71	1.64	2.40
Fariman	0	7.27	5.94	4.50	4.18
Avg	10.84	6.75	8.17	4.55	3.89
X	26.38	2.70	12.15	10.83	3.79

Step 2: Converting data matrix to Standard data matrix:

$$Z = \begin{vmatrix} 2/45 & 0/87 & 2/41 & 0/70 & 2/38 \\ -0/41 & -1/83 & -0/66 & -0/42 & -0/67 \\ -0/40 & -1/15 & -0/23 & -0/24 & -0/64 \\ -0/41 & 0/19 & -0/55 & -0/12 & -0/36 \\ -0/40 & 0/87 & -0/25 & -0/26 & -0/39 \\ -0/41 & 0/87 & -0/53 & -0/16 & 0/39 \\ -0/41 & 0/19 & -0/18 & -0/004 & 0/076 \end{vmatrix}$$

Step 3: Calculating composite intervals between areas:

$$D = \begin{vmatrix} 0/000 & 5/9541 & 5/40152 & 5/07578 & 4/87776 & 4/63927 & 4/59936 \\ 5/9541 & 0/000 & 0/82504 & 2/168432 & 2/74994 & 2/91515 & 2/24518 \\ 5/40152 & 0/82504 & 0/000 & 1/41099 & 2/0356 & 2/28862 & 1/53836 \\ 5/07578 & 2/168432 & 1/41099 & 0/000 & 0/75696 & 1/01336 & 0/58348 \\ 4/87776 & 2/74994 & 2/0356 & 0/75696 & 0/000 & 0/8348 & 0/85612 \\ 4/63927 & 2/91515 & 2/28862 & 1/01336 & 0/8348 & 0/000 & 0/84132 \\ 4/59936 & 2/24518 & 1/53836 & 0/58348 & 0/85612 & 0/84132 & 0/000 \end{vmatrix}$$

Table (2)

Matrix Composites distances between regions of Razavi Khorasan

Region	**Mashhad**	**Bakharz**	**Binalod**	**Taibad**	**Torbat- E-Jam**	**Khaf**	**Fariman**	**Shortest distance**
Mashhad	0	5.9541	5.40152	5.07578	4.877	4.6	4.5	4.59
Bakharz	5.95	0	0.82	2.168	2.74	2.915	2.24	0.82
Binalod	5.40	0.82	0	1.41	2.035	2.2	1.5	0.82
Taibad	5.07	2.16	1.41	2.03	2.2	1.53	0.583	0.583
Torbat- E-Jam	4.8	2.7	2.03	0.75	0	0.83	0.85	0.75
Khaf	4.63	2.91	2.2	1.01	0.834	0	0.84	0.834
Fariman	4.5	2.2	1.5	0.58	0.856	0.84	0	0.583
	$\bar{X}(D) = 1/28688$				$S(D) = 1/63281$			
	$D_{(+)} = 4/5525$				$D_{(+)} = 1/97874$			

Step 4: Calculating the developmental paradigm:

Table (3)

Development patern in Razavi Khorasan province

city	**Development patern**
Fariman	0.73995
Binalod	1.021518
Taibad	1.14289
Bakharz	1.463
Khaf	2.2126
Mashhad	2.35
Torbat- E- Jam	2.39

According to the fourth development plan, investment and production developments should be done through:
- Priority making and acceleration of performance, and exploiting uncompleted governmental plans;
- Limiting governmental investment in ruling fields and common public and private investment in order to encouraging the activities of private section;
- Establishing support organizations for encouraging the activities of research, progress and development of innovation, technology development, human resource development, exploiting improvement and competency accepting;

- Establishing new organization and supporting current ones and providing proper facilities for developing occupations and entrepreneurs and encouraging entrepreneurships (Organization of management and planning, 2005). Today, for balanced growth in all regions of the country, economists believe that the idea of dynamic growth pole was unsuccessful because not only did it fail in decreasing regional inequalities in the country, but it also caused existing inequality-ties to intensify. In this way, accurate regional programming to achieve balanced development is necessary. Based on the view-point of these economists, the purpose of balanced development should be create the best conditions and to develop the society in all areas. As well, interregional life differences should be minimized and finally eradicated. The first step in regional programming is the identification of the existing situation of that region; and this identification itself requires the analysis of different economic, social and cultural sectors. To devote budgets and sources among regions, the identification of the rank of the region in related sectors.

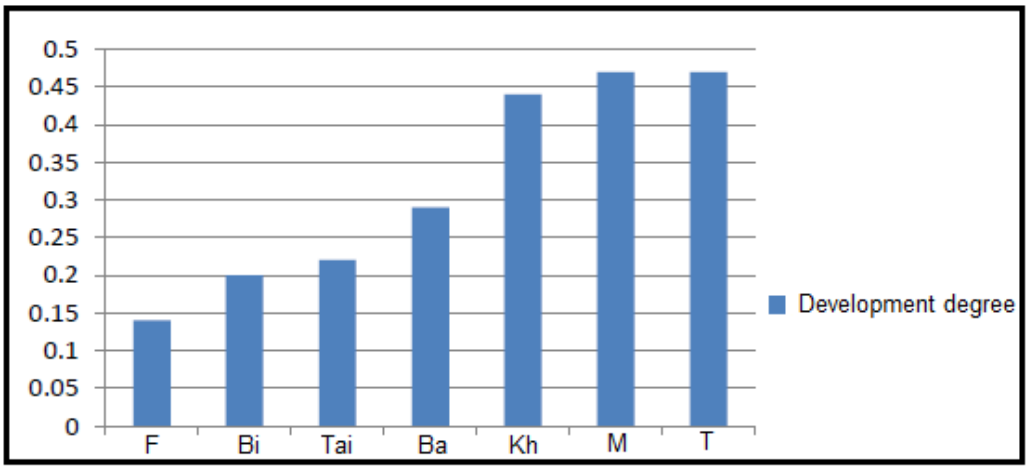

Fig. 2. Development degree of Razavi Khorasan.

Suggestions

[1] Attention to the urban population of cities in Raazavi Khorasan Province in providing of services with spatial movements of human elements in the framework of complete spatial ideas;
[2] repeated reviewing in distribution of health programs, basic structure and curing services;
[3] Improve the sense of social trust between government and citizens.

REFERENCES

[1] Azkia, M. (1999). An introduction in sociology and developing countries. Tehran: EtelaatPublications.
[2] Demurger, H. Jhag, K. Erta, N. (2001). New towns and future urbanization in Iran. TWPR, 22(1), 67–86.
[3] Fanni, Z. Khakpoor, BA. Heydari, A. (2014). Evaluating the regional development of border cities by TOPSIS model (case study: Sistan and Baluchistan Province, Iran). Sustainable Cities and Society 10 (2014) 80–86.
[4] Hamsi, M. (1981). A discussion based on the factors affecting migration of people inIran. Iran Geographical Institution Publications., first period, No. 3.
[5] Hansen, E. (1997). Threshold effects in non-dynamic panels: estimation, testing, andinference. Journal of Econometrics, 93(2), 266.
[6] Hilhorst, J. (1967). Regional Development Theory. Canada: Mouton & Co.
[7] Kalantari, Kh. (1998). Programming and regional development (methods and hypothe-ses). Tehran: Khoshbin Publications.
[8] Lee, U. (1987). A criticism on taxonomy method in determining rural regions development, Chahar Mahal va Bakhtiari province, the department of planning and coordination, the organization of planning and budget of Chahar Mahal va Bakhtiari province, p.66.
[9] Mansoori Sales, M. (1996). Measuring the degree of being development of cities in theprovince of Tehran. Tehran: Shahid Beheshti university (master thesis).
[10] Sadeghi Ravesh, A. Ahmadi, H..Zehtabian, Gh.R. Tahmouresd, M. (2013). Application of Numerical Taxonomy Analysis in Sustainable Development Planning of Combating Desertification. DESERT 17 (2013) 147-159.
[11] Tudaro, P. (2008). Income expectations, urban migration and employment in Africa.International Labor Review, 104(5), 23.
[12] Wikipedia. (2014).
[13] Xang, T. (2005). Government and growth, translation, Tehran, the organization of management and planning.

American Journal of Engineering Research (AJER)
e-ISSN : 2320-0847 p-ISSN : 2320-0936
Volume-03, Issue-11, pp-20-29
www.ajer.org

Research Paper Open Access

1000 YEARS RULE?...
(A New theory on " Kanni Theevu")

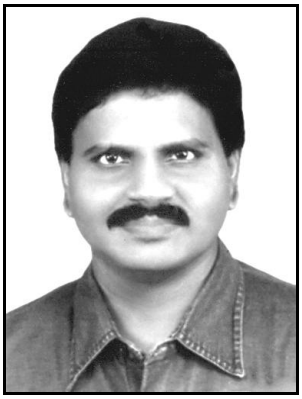

M.Arulmani, B.E.
(Engineer)
m.arulmani58@gmail.com

V.R.Hema Latha, M.A., M.Sc., M.Phil.
(Biologist)
vrhemalatha58@gmail.com

ABSTRACT: The Present "**EARTH PLANET**" is going to be **destroyed**?... The Present Earth populations do not have any hope for sustainability of life due to **threat of global warming**?... **No… No… No…**

This scientific research speculates that the Earth planet we will have **life period** for another **1000 years.** The new genetically evolved human populations are going to live in the newly formed Island called "**KANNI THEEVU**" under the new environment of Fourth generation radiation called "**j-Radiation**". The Kanni Theevu shall also be called as "**SOUTHERN HOLY LAND**".

KANNI LOGO
(Southern Holy Land)

It is speculated that after the period of 1000 years live, the present '**Atmospheric energy level**' may reach '**Zero level**' which may lead to the **earth atmosphere** under absolute darkness and the earth life may come to an end. The environment state of earth planet after 1000 years shall be called as '**ZERO POINT OF EARTH**'.

KEY WORDS:
a) Philosophy of "**ENERGY LEVEL CHANGE**"?...
b) Philosophy of "**KANNI THEEVU**"?...
c) Philosophy of "**4th GENERATION HUMAN**"?...
d) Philosophy of "**PARADISE**"?...

I. INTRODUCTION:

Scientists focus that the **universe** was formed **13.7** billion years ago and the **Earth planet** we live today was formed just **4.54** billion years ago. Scientists also confirm that the **Universe expands** consistently but could not clarify that when the **universe comes to an end.**

This research focus that '**ENERGY**' is required for sustainability of life. It is further emphasized that the present '**ENERGY LEVEL**' of earth atmosphere is about **30%** and the energy level is expected to reach **zero level** after **1000 years**.

"Be Happy… Nature shall pull on Life existence for another 1000 years"

…Author

Hypothesis and Narrations

a) Philosophy of varied Energy level?...

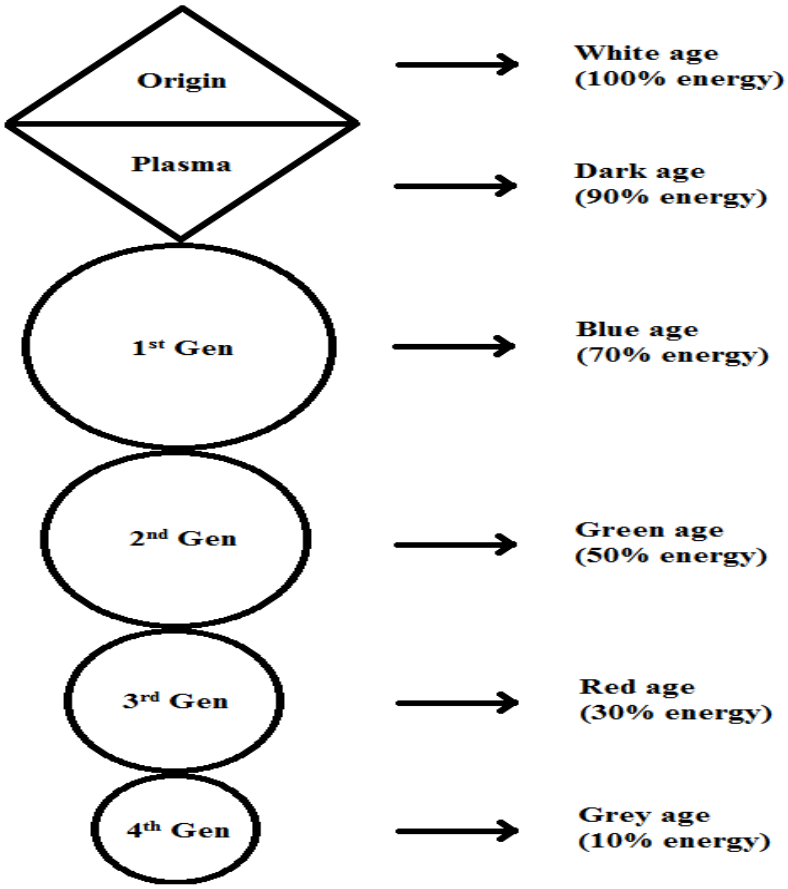

(MODEL ENERGY LEVEL OF UNIVERSE)

It is hypothesized that the first human population shall be considered originated on Earth Planet during '**Dark age**' around 5,00,000 years. The '**Dark age human**' (Indos) shall be considered having distinguished

genetic value and having high Immunity and lived for long span of say thousands of years due to presence higher atmospheric energy level in the **early universe**.

Further during the course of expanding universe the human populations considered lived under varied environmental conditions say **Blue age, Green age, Red age** with consistent reduced Energy level in **different atmospheric age**. The philosophy of various atmospheric energy level above earth planet in different age shall be described as above.

b) Philosophy of "white age"?...

It is hypothesized that the '**white age**' shall be considered as the stage of early universe when **virgin populations** (Angels) considered lived in '**white planet**' (white mars) under '**J-RADIATION**' (Zero hour radiation) having absolutely pure and **very high energy level**. During white age the Earth planet shall be considered totally submerged under "**Ocean Water**" and there was no existence of Life on Earth Planet. The **white planet** having absolute pure environment shall be called as '**PARADISE**' or '**J-NADU**'. The model human of White age shall be described as below.

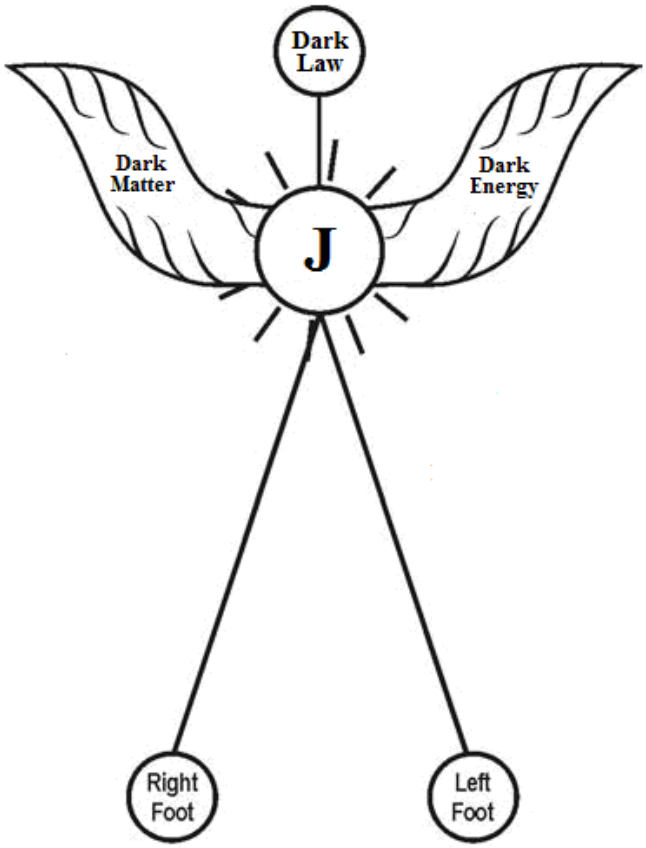

ENERGETIC FLYING HUMAN
(White Age)

c) Philosophy of KANNI THEEVU?...

It is hypothesized that '**Kanni theevu**' shall be considered as the genetically varied Island and dwelling place of '**4th generation human population**' evolved due to impact of '**j-Radiation**' (Fourth generation radiation) and considered belong to distinguished family of **γ**-radiation, **β**-radiation, **α**-radiation in the last three nuclear age say **Blue age, Green Age, Red Age**.

KANNI THEEVU LOGO
(Law of 4th Generation)

d) Philosophy of 4th generation human?...

It is hypothesized that the white age human considered having only '**Three chromosome**' (called as Trisomy) having only '**single chamber heart**' with single type blood say "**White blood**" (Universal acceptor). During the course of different age of expanding universe **different human species** considered evolved with different chromosome level and with consistently **increased heart chambers** say with 46 chromosome and four chamber heart in **red age** (so called 3rd Generation of modern time).

It is hypothesized that **fourth generation human** (**also called as j-66 Human**) shall be considered having **66 chromosome**, with **five chamber heart** having evolution of new blood type '**j-type blood**' in addition to conventional type of **AB, A, B, O**. The '**j-66 human**' shall be considered adopted to current new radiation level and could sustain for the span of another **1000 years**. The fourth generation population consider having no discrimination of **Caste, race, colour** etc. and having sense of "**Unity and Peace**"

(i)

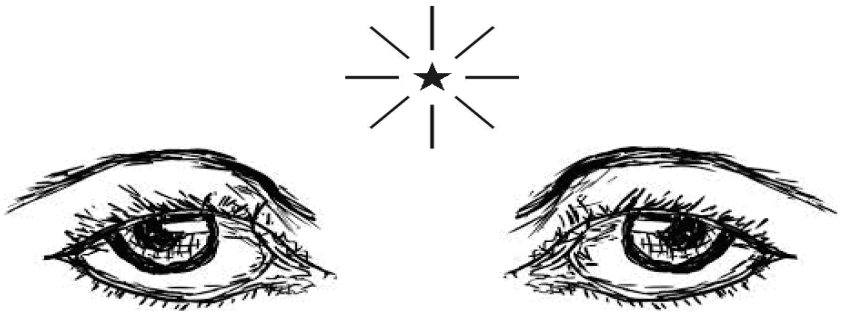

QUEEN OF PEACE
(Model j-66 Human)

(ii)

MODEL KANNI THEEVU
(j-66 Human Populations)

***"QUEEN OF PEACE** shall be considered as **MOTHER** of 4th Generation having **5 chambered heart**"*

…Author

e) Case study on five chamber heart?...

Case study shows that only '**bees**' have five chamber heart. But recently there has been one reported case in **Russia** in which a boy was born with **five chamber heart** (3 ventricle, 2 article).

Further a second case that a baby boy in **Louisvillie**, **ky**, born with 5 chamber heart now at the **age of 20** who is still fine and leading normal life **without undergoing any surgery**.

f) Philosophy of "Perfect Dark body"?...

Scientists focus that the **Absolute black body** can't exist as **100% efficiency** of Absorption is not possible.

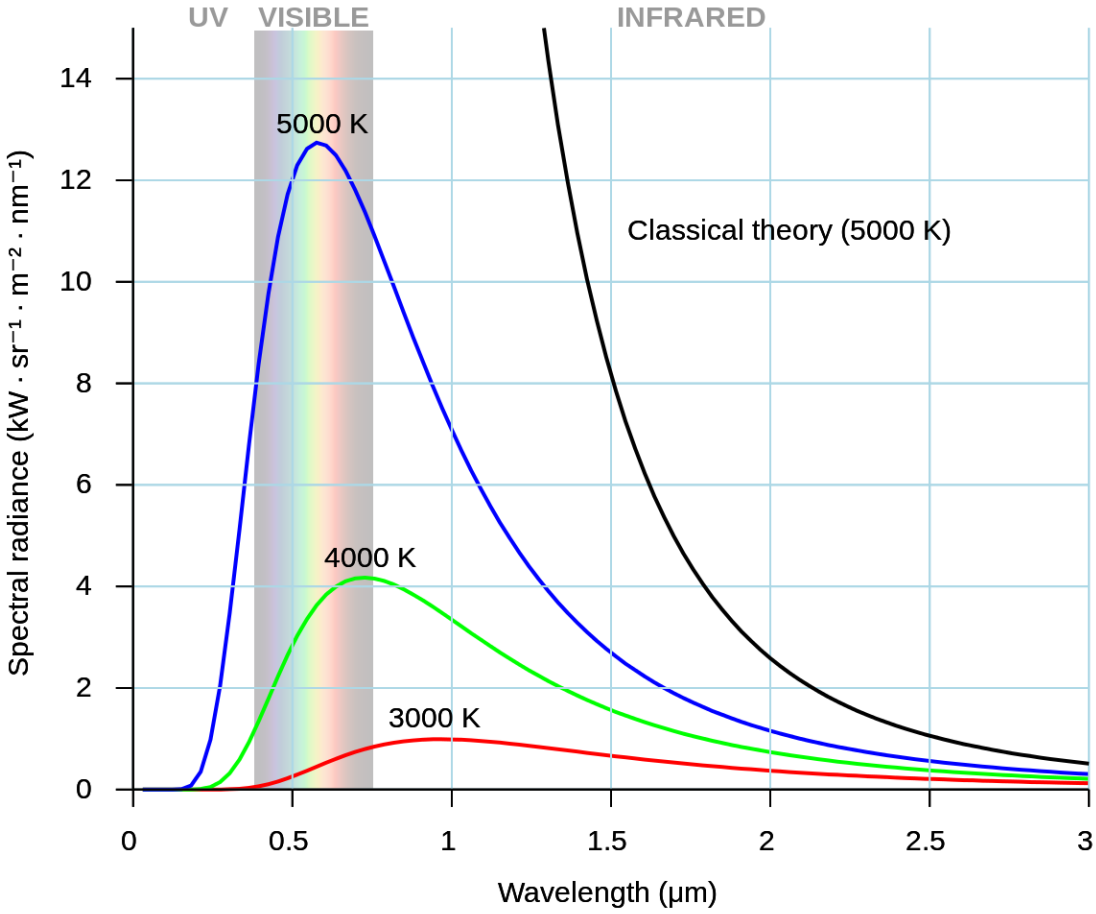

As the temperature of a black body decreases, its intensity also decreases and its peak moves to longer wavelengths. Shown for comparison is the classical Rayleigh–Jeans law and its ultraviolet catastrophe.

Dark body differs from **black body?... YES… YES… YES…** It is hypothesized that the white age human population shall be considered as "**Perfect white body**" having 100% efficiency of emission. Similarly the Dark age populations lived on Earth planet shall be considered as '**perfect dark body**' having 100% efficiency of absorption. Black body shall be considered as species to dark body. The various human species lived under different age of environment having different energy grading of dark body as described below:

i. White age - perfect white body (100% emission)
ii. Dark age - perfect dark body (100% absorption)
iii. Blue age - 70% dark body (**γ**-family)
iv. Green age - 50% dark body (**β**-family)
v. Red age - 30% dark body (**α**-family)
vi. Fourth generation - 10% dark body (**j**-family)

g) Case study on solar efficiency?...

Case study shows that though the **SUN** is the source of Infinity level of energy in a white light spectrum, but it is possible to capture only small portion of that spectrum and convert them into electricity using **photovoltaic cells**. The solar power efficiency normally around **20%** at standard testing centre but in some cases higher efficiency is achieved by multiple junction cells say **44.7%**.

Similarly the **thermal efficiency** of IC Engines is around **25%** and the fossil fuel generation has a maximum efficiency of about **28%**.

It is hypothesized that the present environment of atmosphere above earth planet shall be considered under "**Red Age**" (modern time) having maximum energy efficiency around **30%**. The energy level may consistently get reduced during post modern time and became "**Zero Level**" in another 1000 years.

h) Searching for other planet?...

Case study shows that global level intensive research is going on for possibility of shifting future generations to other planets for sustainability of life. **It is the clarification of author that:**

"When the "ENERGY LEVEL" of universe becomes "ZERO" where is the question of shifting the life to other planets?"

…M. Arulmani, Tamil based Indian.

2. Conclusion:

It is speculated by the author that the 1000 years life on '**KANNI THEEVU**' shall be considered as begining of '**NEW LIFE**' with '**perfect peace**'.

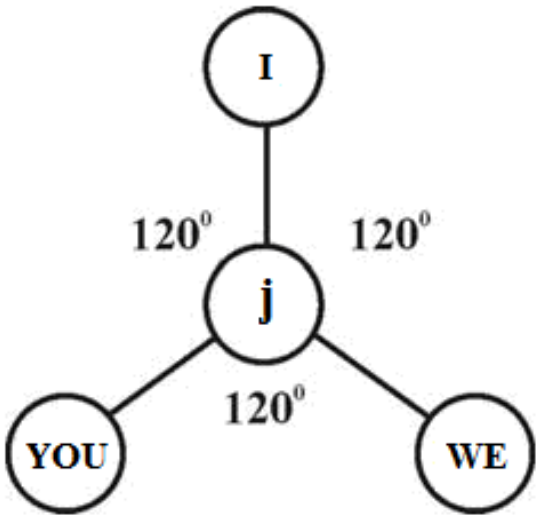

LAW OF NEW LIFE
(KANNI THEEVU)

i. **YOU** is like **LOVE**
ii. **WE** is like **MERCY**
iii. **I** is like **HOPE**

Further the philosophy of "**Kanni Theevu**" shall be described within the following scope.

i) The Island of **perfect happiness**
ii) The Island where **No casteism**
iii) The Island where **No Racism**
iv) The Island where **No need of UPS**
v) The Island where **No need of Judges**.
vi) The Island where **No need of Court expenses**

vii) The Island where **No need of Jail**
viii) The Island where **No Border Dispute**
ix) The Island where **No River Water Dispute**
x) The Island where **No Missile Test launch**
xi) The Island where **No need of UNO membership**

3. Previous Publication:

The philosophy of origin of first life and human, the philosophy of model Cosmo Universe, the philosophy of fundamental neutrino particles have already been published in various international journals mentioned below. Hence this article shall be considered as **extended version** of the previous articles already published by the same author.

[1] Cosmo Super Star – IJSRP, April issue, 2013

[2] Super Scientist of Climate control – IJSER, May issue, 2013

[3] AKKIE MARS CODE – IJSER, June issue, 2013

[4] KARITHIRI (Dark flame) The Centromere of Cosmo Universe – IJIRD, May issue, 2013

[5] MA-AYYAN of MARS – IJIRD, June issue, 2013

[6] MARS TRIBE – IJSER, June issue, 2013

[7] MARS MATHEMATICS – IJERD, June issue, 2013

[8] MARS (EZHEM) The mother of All Planets – IJSER, June issue, 2013

[9] The Mystery of Crop Circle – IJOART, May issue, 2013

[10] Origin of First Language – IJIRD, June issue, 2013

[11] MARS TRISOMY HUMAN – IJOART, June issue, 2013

[12] MARS ANGEL – IJSTR, June issue, 2013

[13] Three principles of Akkie Management (AJIBM, August issue, 2013)

[14] Prehistoric Triphthong Alphabet (IJIRD, July issue, 2013)

[15] Prehistoric Akkie Music (IJST, July issue, 2013)

[16] Barack Obama is Tamil Based Indian? (IJSER, August issue, 2013)

[17] Philosophy of MARS Radiation (IJSER, August 2013)

[18] Etymology of word **"J"** (IJSER, September 2013)

[19] NOAH is Dravidian? (IJOART, August 2013)

[20] Philosophy of Dark Cell (Soul)? (IJSER, September 2013)

[21] Darwin Sir is Wrong?! (IJSER, October issue, 2013)

[22] Prehistoric Pyramids are RF Antenna?!... (IJSER, October issue, 2013)

[23] HUMAN IS A ROAM FREE CELL PHONE?!... (IJIRD, September issue, 2013)

[24] NEUTRINOS EXIST IN EARTH ATMOSPHERE?!... (IJERD, October issue, 2013)

[25] EARLY UNIVERSE WAS HIGHLY FROZEN?!... (IJOART, October issue, 2013)

[26] UNIVERSE IS LIKE SPACE SHIP?!... (AJER, October issue, 2013)

[27] ANCIENT EGYPT IS DRAVIDA NAD?!... (IJSER, November issue, 2013)

[28] ROSETTA STONE IS PREHISTORIC "THAMEE STONE" ?!... (IJSER, November issue, 2013)

[29] The Supernatural "CNO" HUMAN?... (IJOART, December issue, 2013)

[30] 3G HUMAN ANCESTOR?... (AJER, December issue, 2013)

[31] 3G Evolution?... (IJIRD, December issue, 2013)

[32] God Created Human?... (IJERD, December issue, 2013)

[33] Prehistoric "J" – Element?... (IJSER, January issue, 2014)
[34] 3G Mobile phone Induces Cancer?... (IJERD, December issue, 2013)
[35] "J" Shall Mean "JOULE"?... (IRJES, December issue, 2013)
[36] "J"- HOUSE IS A HEAVEN?... (IJIRD, January issue, 2014)
[37] The Supersonic JET FLIGHT-2014?... (IJSER, January issue, 2014)
[38] "J"-RADIATION IS MOTHER OF HYDROGEN?... (AJER, January issue, 2014)
[39] PEACE BEGINS WITH "J"?... (IJERD, January issue, 2014)
[40] THE VIRGIN LIGHT?... (IJCRAR, January issue 2014)
[41] THE VEILED MOTHER?... (IJERD, January issue 2014)
[42] GOD HAS NO LUNGS?... (IJERD, February issue 2014)
[43] Matters are made of Light or Atom?!... (IJERD, February issue 2014)
[44] THE NUCLEAR "MUKKULAM"?... (IJSER, February issue 2014)
[45] WHITE REVOLUTION 2014-15?... (IJERD, February issue 2014)
[46] STAR TWINKLES!?... (IJERD, March issue 2014)
[47] "E-LANKA" THE TAMIL CONTINENT?... (IJERD, March issue 2014)
[48] HELLO NAMESTE?... (IJSER, March issue 2014)
[49] MOTHERHOOD MEANS DELIVERING CHILD?... (AJER, March issue 2014)
[50] E–ACHI, IAS?... (AJER, March issue 2014)
[51] THE ALTERNATIVE MEDICINE?... (AJER, April issue 2014)
[52] GANJA IS ILLEGAL PLANT?... (IJERD, April issue 2014)
[53] THE ENDOS?... (IJERD, April issue 2014)
[54] THE "TRI-TRONIC" UNIVERSE?... (AJER, May issue 2014)
[55] Varied Plasma Level have impact on "GENETIC VALUE"?... (AJER, May issue 2014)
[56] JALLIKATTU IS DRAVIDIAN VETERAN SPORT?... (AJER, May issue 2014)
[57] Human Equivalent of Cosmo?... (IJSER, May issue 2014)
[58] THAI-e ETHIA!... (AJER, May issue 2014)
[59] THE PHILOSOPHY OF "DALIT"?... (AJER, June issue 2014)
[60] THE IMPACT OF HIGHER QUALIFICATION?... (AJER, June issue 2014)
[61] THE CRYSTAL UNIVERSE?... (AJER July 2014 issue)
[62] THE GLOBAL POLITICS?... (AJER July 2014 issue)
[63] THE KACHCHA THEEVU?... (AJER July 2014 issue)
[64] THE RADIANT MANAGER?... (AJER July 2014 issue)
[65] THE UNIVERSAL LAMP?... (IJOART July 2014 issue)
[66] THE MUSIC RAIN?... (IJERD July 2014 issue)
[67] THIRI KURAL?... (AJER August 2014 issue)
[68] THE SIXTH SENSE OF HUMAN?... (AJER August 2014 issue)
[69] THEE… DARK BOMB?... (IJSER August 2014 issue)
[70] RAKSHA BANDHAN CULTURE?... (IJERD August 2014 issue)
[71] THE WHITE BLOOD ANCESTOR?... (AJER August 2014 issue)

[72] THE PHILOSOPHY OF "ZERO HOUR"?... (IJERD August 2014 issue)

[73] RAMAR PALAM?... (AJER September 2014 issue)

[74] THE UNIVERSAL TERRORIST?... (AJER September 2014 issue)

[75] THE "J-CLOCK"!... (AJER September 2014 issue)

[76] "STUDENTS" AND "POLITICS"?... (IJERD October 2014 issue)

[77] THE PREGNANT MAN?... (AJER September 2014 issue)

[78] PERIAR IS ATHEIST?... (IJSER September 2014 issue)

[79] A JOURNEY TO "WHITE PLANET"?... (AJER October 2014 issue)

[80] Coming Soon!... (AJER October 2014 issue)

[81] THE PREJUDICED JUSTICE?... (IJERD October 2014 issue)

[82] BRITISH INDIA?... (IJSER October 2014 issue)

[83] THE PHILOSOPHY OF "HUMAN RIGHTS"?... (IJERD October 2014 issue)

[84] THE FOSTER CHILD?... (AJER October 2014 issue)

[85] WHAT DOES MEAN "CRIMINAL"?... (IJERD October 2014 issue)

4. REFERENCE

a) Intensive Internet "e-book" study through, Google search and wikipedia
b) M.Arulmani, "3G Akkanna Man", Annai Publications, Cholapuram, 2011
c) M. Arulmani; V.R. Hemalatha, "Tamil the Law of Universe", Annai Publications, Cholapuram, 2012
d) Harold Koontz, Heinz Weihriah, "Essentials of management", Tata McGraw-Hill publications, 2005
e) M. Arulmani; V.R. Hemalatha, "First Music and First Music Alphabet", Annai Publications, Cholapuram, 2012
f) King James Version, "Holy Bible"
g) S.A. Perumal, "Human Evolution History"
h) "English Dictionary", Oxford Publications
i) Sho. Devaneyapavanar, "Tamil first mother language", Chennai, 2009
j) Tamilannal, "Tholkoppiar", Chennai, 2007
k) "Tamil to English Dictionary", Suravin Publication, 2009
l) "Text Material for E5 to E6 upgradaton", BSNL Publication, 2012
m) A. Nakkiran, "Dravidian mother", Chennai, 2007
n) Dr. M. Karunanidhi, "Thirukkural Translation", 2010
o) "Manorama Tell me why periodicals", M.M. Publication Ltd., Kottayam, 2009
p) V.R. Hemalatha, "A Global level peace tourism to Veilankanni", Annai Publications, Cholapuram, 2007
q) Prof. Ganapathi Pillai, "Sri Lankan Tamil History", 2004
r) Dr. K.K. Pillai, "South Indian History", 2006
s) M. Varadharajan, "Language History", Chennai, 2009
t) Fr. Y.S. Yagoo, "Western Sun", 2008
u) Gopal Chettiar, "Adi Dravidian Origin History", 2004
v) M. Arulmani; V.R. Hemalatha, "Ezhem Nadu My Dream" - (2 Parts), Annai Publications, Cholapuram, 2010
w) M. Arulmani; V.R. Hemalatha, "The Super Scientist of Climate Control", Annai Publications, Cholapuram, 2013, pp 1-3

American Journal of Engineering Research (AJER)
e-ISSN : 2320-0847 p-ISSN : 2320-0936
Volume-03, Issue-11, pp-30-37
www.ajer.org

Research Paper Open Access

Earthquake Response Mitigation of RC Building Using Friction Pendulum System

Sudarshan B. Sanap[1], Pradip D. Jadhao[1], S. M. Dumne[2]
[1]*Department of Civil Engineering, K K Wagh Institute of Engineering Education & Research Nashik, Maharashtra, India*
[2]*Department of Applied Mechanics, Government Polytechnic Aurangabad, Maharashtra, India*

ABSTRACT : *Earthquake hazard mitigation is very sensitive issue now a day's therefore researchers are struggling for optimum solution since last few decades. Base isolation technique is one of the effective techniques which give better results seismic hazard mitigation under earthquake excitation particularly in building structures, bridges and water tanks etc. Base isolation reduces not only the effects of earthquake acceleration to be transmitted to the structures, but also protects the content of building while simultaneous supporting the mass of structure. This study proposed a realistic ten storey RC building which is model as shear type lumped mass having single degrees-of-freedom at each floor level. This building is isolated by Friction Pendulum System of sliding base isolated type and excited under unidirectional ground motion due to four realistic earthquakes namely, Imperial Valley, 1940, Loma Prieta, 1989, Kobe, 1995 and Northridge, 1994. The governing equation of motion for the building solved using Newmarks method whereas isolation system is modelled by Wen's model. The effectiveness of proposed isolation system and building response has been evaluated by coding in MATLAB 8.2 computing software. Further, effectiveness of isolation system is also studied in terms of peak responses of building. The results obtained from the study underscored that Friction Pendulum System works effectively in limiting the building responses during excitation due to earthquakes.*

KEYWORDS : *Earthquake Response, Base isolation, Friction Pendulum System, Mitigation*

I. INTRODUCTION

Earthquake is natural and unpredictable phenomena, which has tremendous destructive energy in the form of ground shaking during an earthquake leads to enormous amounts of energy released. This release of energy can cause by sudden dislocation of segments of crust, volcanic eruptions. In the process of dislocations of crust segments, however, leads to the most destructive earthquakes may cause significant life hazard therefore, past disastrous earthquakes underlined the need of seismic hazard mitigation. Structural vibrations produced due to earthquake can be controlled by various means that is, increasing strength, stiffness and ductility. The researchers are considerably involved in developing seismic resistance through various techniques as conventional and Non-conventional technique. The non-conventional technique in which controlling devices are added based on which control system is employed that is, active, passive or combined. Further, passive control system in which base isolation system is one of the most popular technique and works with the concept of reducing fundamental frequency of structural vibration to a value lower than the seismic energy containing frequency. During earthquake, flexible device get momentum as a result building gets decoupled from the ground motion leads to avoid certain devastating hazard.

In relevant to above study, many past researchers have established their research findings but few of them are outlined and reviewed as Jangid and Datta [1] (1995) presented an updated review on behaviour of various base isolated systems applied to the buildings subjected to seismic excitation. The study includes literatures on theoretical aspects, parametric behaviour of base isolation building and experimental studies to verify some theoretical findings. P. Bhaskar Rao and R. S. Jangid [2] (2001) studied the performance of sliding systems under near-fault motions and found that friction coefficient of various sliding isolation systems is

typically dependent on relative velocity at the sliding interface. The response of building system is analysed to investigate the performance of sliding system and concluded that sliding base isolation found very effective in controlling seismic response. Matsagar and Jangid [4] (2004) performed the computational study on structural responses and bearing displacement for the various isolation systems during impact upon adjacent structures. From the study, it is observed that increase in the building flexibility causes to increase in superstructure acceleration and decreases in bearing displacement marginally. S. M. Dumne *et al* [5] (2012) studied the effectiveness of semiactive hybrid control involving base isolation for seismic performance of connected dissimilar buildings. The effective analysis in terms of peak responses have been evaluated by taking numerical example of realistic coupled RC buildings subjected to unidirectional earthquake excitation. From the numerical study, it is observed that semiactive hybrid control involving sliding base isolation not only effective in controlling the seismic responses but also avoids the damages due to pounding. The specific objectives of study are (i) determination of seismic response of building with and without base isolation system (ii) study the seismic performance of Friction Pendulum base isolation system in terms of peak response reduction and (iii) comparative study of peak responses of base isolated and non-isolated building.

II. PROBLEM IDENTIFICATION

A realistic ten storey RC building isolated with Friction pendulum system (FPS) and assuming strata at the foundation level is hard which is excited by unidirectional ground motion due to earthquake. The details of design parameters are, plan dimension 20m X 30 m, grade of concrete M20, size of column 300 X 300 mm, beam size 300 X 450 mm, slab thickness 135 mm, structural damping equal to 5% and thickness of infill wall is 230 mm. The plan and elevation of proposed building model are shown in figure 1.

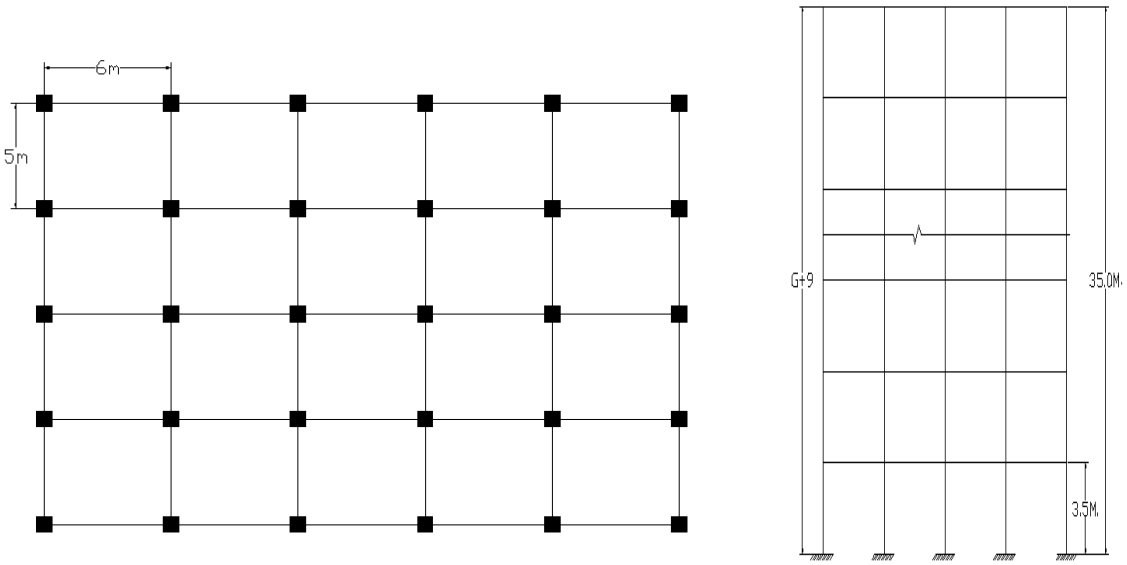

Fig. 1 Plan and Elevation of the proposed building model

III. STRUCTURAL MODEL OF BUILDING

The building model is idealized as a linear shear type lumped mass with single lateral degrees of freedom at each floor levels including isolation floor. The structural building model is assumed to remain in linear elastic state, therefore, does not yield during excitation. The numerical study has been performed corresponding to unidirectional excitation due to four real earthquakes. During this study, it is assumed that spatial variation of ground motion and also effect due to soil structure interaction is neglected. The governing equations of motion for multi degrees-of-freedom building with isolated base are expressed in matrix form as

$$[M]\{\ddot{u}\} + [C]\{\dot{u}\} + [K]\{u\} = -[M]\{r\}\ddot{u}_g + \left[B_p\right]\{f_b\} \qquad (1)$$

where, [*M*], [*C*], and [*K*] are the mass, damping and stiffness matrices of building respectively, $\{u\}=\{u_b,u_1,u_2,u_3.....u_n\}$, $\{\dot{u}\}$ and $\{\ddot{u}\}$ are the vectors of relative floor displacement, velocity and acceleration response respectively, $\ddot{u}_g$ is the ground acceleration due to earthquake, $\{r\}$ is the vector of influence coefficient

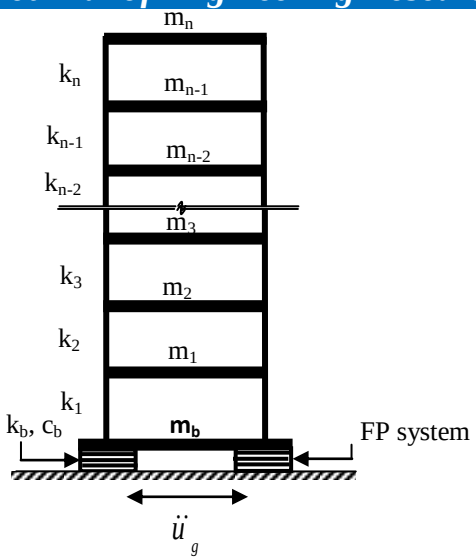

having all elements equal to one, $[B_p]$ is the bearing location vector, $\{f_b\}$ is the vector of bearing force and (u_b) is the bearing displacement.

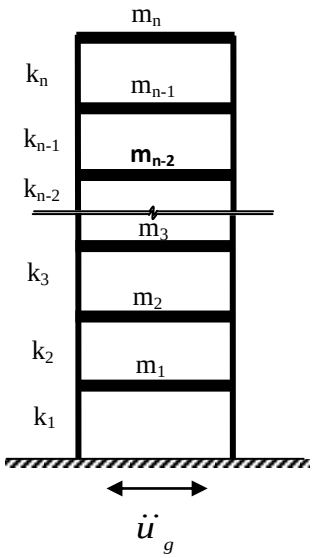

Fig. 2 Structural model of building with and without FP System

The classical stiffness and damping matrix may not be suitable since superstructure and substructure have significant difference in stiffness and damping so non-classical type of matrices are to be constructed. Under which, it is constructed by first evaluating the classical stiffness and damping matrix for building without isolation then stiffness and damping matrix for building with base isolation is superimposed by assembling matrix due to superstructure and substructure.

Computation of bearing force : The Friction- Pendulum system is based on well-known engineering principle of pendulum motion having combine action of sliding and restoring force by geometry. The cross section and schematic diagram is shown in figure 3. This system is equipped with re-centring force provided by gravitational action, which is achieved by means of an articulated slider moves on spherical concave chrome surface. When the slider is in contact with polished chrome surface then there will be maximum coefficient of friction in the order of 0.1 or less and may be minimum of 0.05 or less corresponding to low velocity of slider.

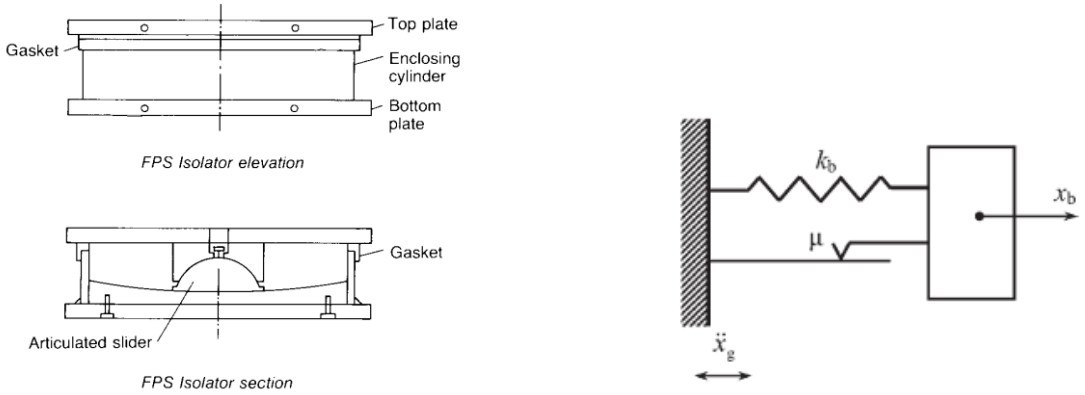

Fig. 3 Cross-section and schematic diagram of FPS system

In this system, the structure is supported on spherical shaped bearings and load is applied through a small area covered by high strength composite materials. The residual displacement after an earthquake is reduced due to self centring action. The friction pendulum system (FPS) provides isolation effects through the parallel action of friction and restoring spring. The bearing force yielded by FPS is given by,

$$f_b = k_b u_b + f_r \quad (2)$$

Where, k_b is the stiffness of bearing provided through inward gravity action, u_b is the bearing displacement, f_r is the friction force generated at the interface of isolation system and its modelling is described as friction force is modelled by two approaches referred as, conventional model and hysteretic model. In the study, hysteretic model is considered to compute the frictional force in which hysteretic displacement (Z) is evaluated using Wen's equation. The frictional force mobilized at the interface of system is

$$f_r = f_s \, x \, z \quad (3)$$

Where, f_s is the limiting frictional force and expressed by

$$f_s = \mu \, M_t \, g. \quad (4)$$

where, M_t is the total mass of building including mass of isolation floor, g is the gravitational acceleration, μ is the friction coefficient of sliding system that depends on the instantaneous velocity of base floor and expressed by the equation. The friction coefficient (μ) of sliding system with Teflon-steel bearing can be modelled by using an equation is described below

$$\mu = \mu_{max} - (\Delta\mu) exp(-a|\, v_b \,|) \quad (5)$$

where, μ_{max} is the maximum friction coefficient at large velocity of sliding (after levelling off), μ_{min} is the minimum friction coefficient at small velocity of sliding, Δμ is the difference of maximum and minimum friction coefficient respectively at large and small velocity at the interface of system, and its value is assumed to be independent of relative velocity (Δμ=0) at the sliding interface which leads to coulomb-friction idealization, a is the calibration constant for a given bearing pressure and interface condition is taken as 20 sec/m and z is the hysteretic displacement evaluated by Wen's model, satisfying the nonlinear first order differential equation as

$$q\dot{z}_b = -\beta \, |v_b||z_b| \, z_b|^{n-1} - \tau \, v_b|z_b|^n + A v_b \quad (6)$$

where, q is the yield displacement of bearing, β and τ are the strengthening coefficients of lead plug that control the shape and size of hysteresis loop, n and A are the integer constant that controls the smoothness of transition from elastic to plastic state. The parameters of wen's model are so selected so as to provide a rigid- plastic shape that is, β= 0.5, τ= 0.5, n= 2, Q= 25mm and A= 1. The parameter of isolation system, namely stiffness (k_b) and damping (c_b) are so selected to provide desired value of isolation period (T_b) and damping ratio (ξ_b) respectively as $T_b = 2\pi\sqrt{\frac{M_t}{\alpha_b k_b}}$ and $\xi_b = \frac{c_b}{2 M_t \omega_b}$ where, M_t is the total mass of building including isolation floor, respectively, k_b and c_b are the stiffness and damping of isolation system respectively, and ω_b is the natural frequency of bearing

IV. SOLUTION PROCEDURE

The governing equation of motion for multi-storeyed building involving sliding base isolation is solved numerically by Newmark's step by step method assuming linear variation in acceleration over a small time interval (Δt). The time interval is kept very small to achieve stability of Newmark's integration method. The algorithm developed for governing equation of motion of building and bearing used is simulated through

Earthquake	Recording station	Component	PGA(g)
Imperial Valley, 1940	El-Centro	N00E	0.348
Loma Prieta, 1989	Los Gatos Presentation Centre	N00E	0.570
Northridge, 1994	Japan Meteorological Agency	N00E	0.834
Kobe, 1995	Sylmer Converter Station	N00E	0.843

Table 1 Details of earthquake ground motions

MATLAB® version 8.2 computing software. Further, graphs from results are drawn using Origin 8.0 software.

V. NUMERICAL STUDY

A structural model of lumped mass system having 5% of critical damping with ten storey's of RC framed building in which each floor mass as 674.05 tonne and stiffness is of 5.17E+06 kN/m, respectively, which gives fundamental period of fixed base building is equal to 0.48 seconds. The mass of isolation floor is taken as 10% in excess of floor mass of superstructure floor. The parameters of friction pendulum system considered are as T_b=3 sec and μ_{max}=0.05. The response parameters of interest are, top floor displacement (u_f), acceleration (a_f), story drift (u_r), normalized bearing force (F_b/W), bearing displacement (u_b), normalized base shear (B_{sy}), Here bearing force (F_b), storey shear (S_{sy}) and Base shear (B_{sy}) are normalized by total weight of building (W). The building is subjected to unidirectional excitation for which four real earthquake ground motions are considered and details are given in table 1.

The comparison of peak responses of isolated building and fixed base building under all considered ground motions are shown in table 2 along with percentage reduction of peak responses are written in parenthesis with respect to the peak responses of fixed base building. It is noted that reduction in floor displacement, acceleration and base shear are in the range of 80-90% for the building under four different earthquakes which implies that base isolation mechanism underscored the most effective technique in mitigating the building responses.

Table 2 Comparison of peak responses of building under various earthquakes (T_b=3s, μ_b = 0.05)

Earthquake	Peak responses	Uncontrol	FPS control
Imperial Valley, 1940	u_f	5.7589	0.6637 (88.47)
	a_r	1.0817	0.1978 (81.71)
	B_{sy}/W	0.7086	0.0949 (86.60)
	u_b	---	6.147
Loma Prieta, 1989	u_f	14.6720	1.5673 (89.89)
	a_f	2.3784	0.3084 (87.03)
	B_{sy}/W	1.8605	0.2394 (87.13)
	u_b	---	31.576
Northridge, 1994	u_f	15.6566	1.4365 (90.82)
	a_f	2.7142	0.2913 (89.26)
	B_{sy}/W	1.8246	0.2072 (88.64)
	u_b	---	20.108
Kobe, 1995	u_f	16.3702	1.1392 (93.04)
	a_r	2.8304	0.2889 (89.79)
	B_{sy}/W	1.9778	0.1408 (92.88)
	u_b	---	12.307

Note: Value in parenthesis represents the percentage reduction in response.

The fig. 4 shows time varying response of proposed building and is observed that value of displacement response is lesser in all three earthquakes except Loma Prieta Earthquake. Further, fig. 5 and 6 reflects that top floor acceleration response and base respectively of building are reduced effectively due to presence of base isolation which clarify the effectiveness of friction pendulum system. Fig. 7 shows peak displacement response at each floor of building and is observed that initial peak displacement of upper floor of building reduced considerably except in case of Loma Prieta earthquake. From the fig. 8 one can comment that peak acceleration found to have large variation in lower floor acceleration and upper floor acceleration. Fig. 9 shows storey drift of building floor and it is noted that FPS is more effective in reducing storey drift except under Loma Prieta earthquake. Fig. 10 indicate that peak story shear response of building floors and observed that FPS is effective in reducing storey shear at each floor. From the fig. 11, one can conclude that various energy loops of bearing force-displacement reflects that smooth functioning of FPS bearing under all four considered earthquakes.

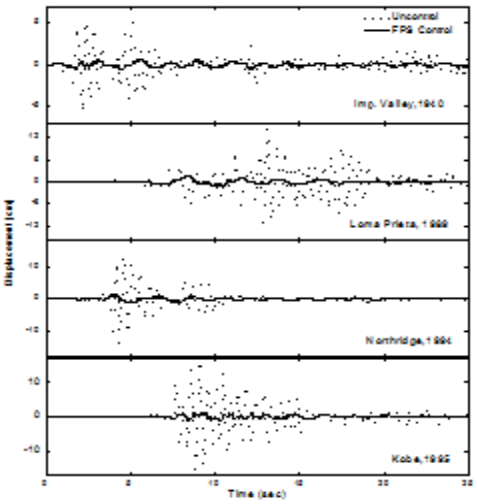

Fig. 4 Time varying displacement response of top floor
(T_b= 3s, μ_b=0.05)

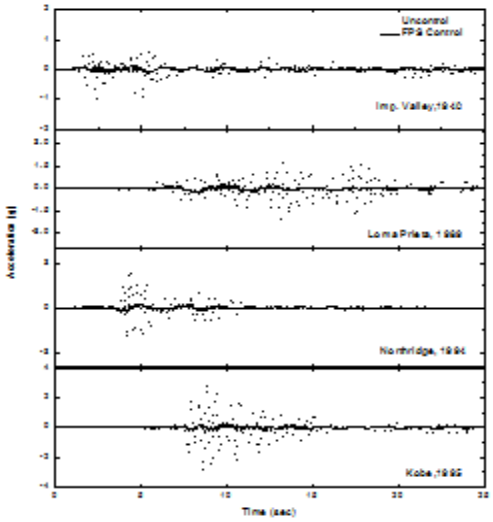

Fig. 5 Time varying acceleration response of top floor
(T_b= 3s, μ_b=0.05)

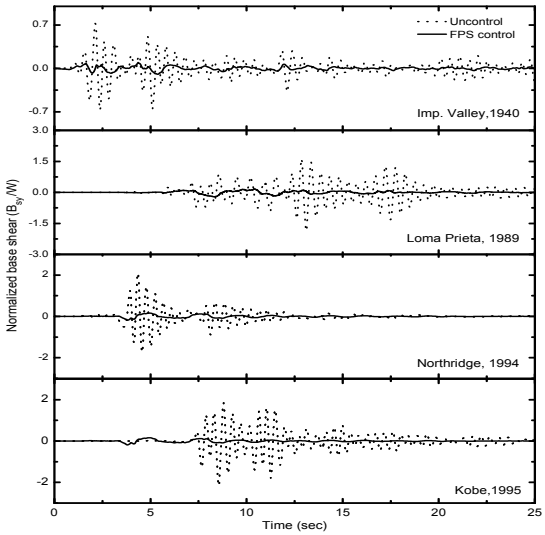

Fig.6 Time varying base shear response of building
(T_b= 3s, μ_b=0.05)

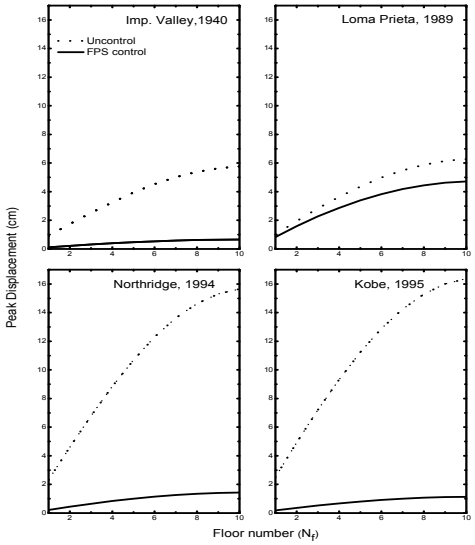

Fig. 7 Peak displacement response of building floors
(T_b= 3s, μ_b=0.05)

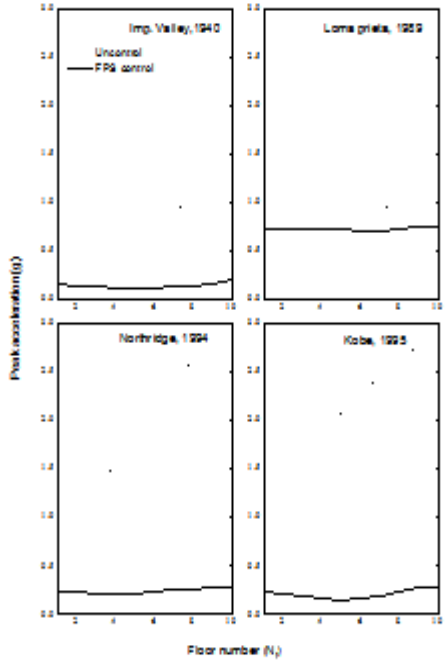

Fig. 8 Peak acceleration responses of building floors (T_b= 3s, μ_b=0.05)

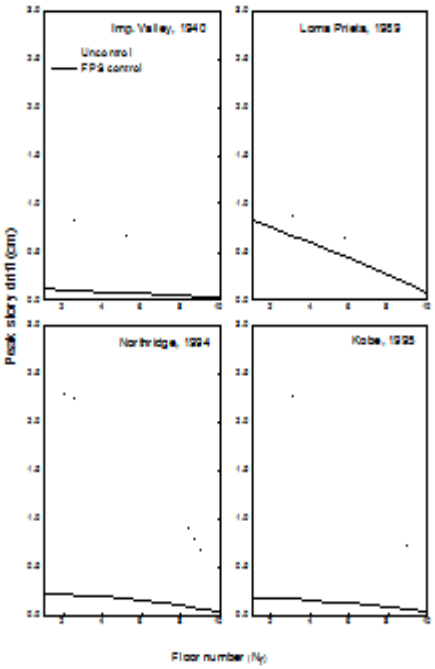

Fig. 9 Peak story drift response of building floors (T_b = 3s, μ_b=0.05)

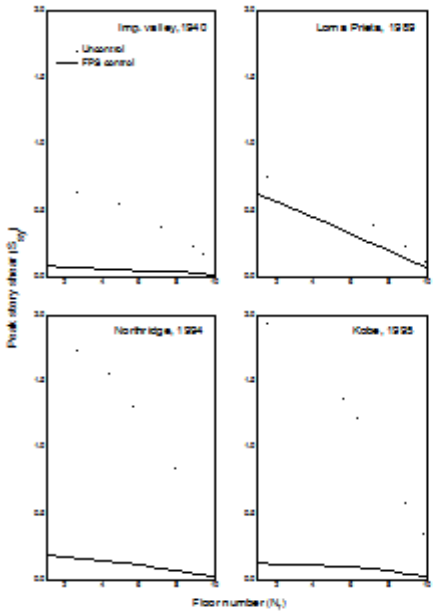

Fig. 10 Peak story shear response of building floors (T_b= 3s, μ_b=0.05)

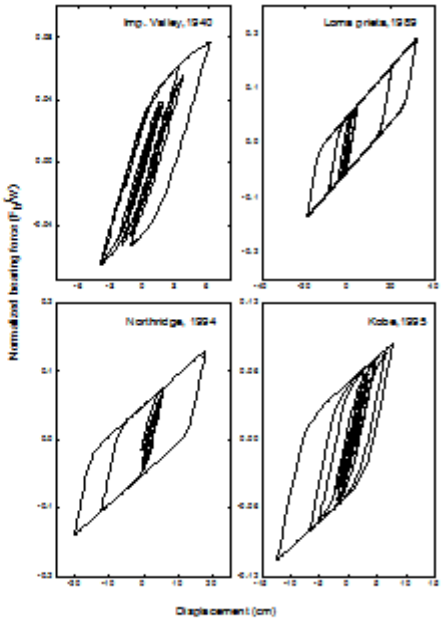

Fig. 11 Force-displacement behaviour of FP System for various earthquakes (T_b = 3s, μ_b =0.05)

VI. CONCLUSIONS

In this study, effectiveness of the proposed FPS control in terms of peak responses of building has been examined through MATLAB® version 8.2 using ten storied RC framed building. The proposed building model is excited to unidirectional excitation for which four real earthquake ground motions are taken. The numerical results are outlined and following precise conclusions are drawn

[1] The seismic responses of building isolated with Friction Pendulum system perform effectively in reducing the responses during earthquake.
[2] The mitigation of peak responses of building under FPS is about 85% in respect of fixed base building responses which reflects the well functioning of bearing used.
[3] The performance of FPS bearing in controlling peak responses that is, displacement, acceleration, and base shear is lesser under Loma Prieta earthquake as compared to other earthquakes considered.
[4] The energy loop from the bearing force-displacement shows that FPS bearing reflects enough seismic energy input during earthquakes.

REFERENCES

[1] Jangid, R.S. and Datta, T. K. (2003). Seismic behaviour of base-isolated buildings: a state-of –the art review. Proceedings of Institute of Civil Engineers, Structures & building; vol. 110 pp. 186-203.
[2] Bhasker, P. and Jangid R.S. (2000).Performance of sliding systems under near-fault motions. Nuclear Engineering and Design; 203 (2001) pp. 259-272.
[3] Housner, G.W., Bergman, L.A., Caughey, T.K., Chassiakos, A.G., Claus, R.O., Masri, S.F., Skelton, R.E., Soong, T.T., Spencer, B.F. and Yao, J.T.P. (1997). "Structural control: past, present and future", Journal of Engineering Mechanics, ASCE; Vol. 123(9), pp. 897-971.
[4] Maria Qing Feng, Masanobu and Shunji Fujii(1994). Friction- Controllable sliding isolation system. Journal of Engineering Mechanics, vol.119 pp.4368.
[5] Matsagar, V.A. and Jangid, R.S. (2004). Influence of isolator characteristics on the response of base-isolated structure. Engineering Structures; 26 (2004) pp. 1735-1749.
[6] S. M. Dumne, S. D. Bharti and M. K. Shrimali (2012). Semiactive hybrid control for response analysis of seismically excited coupled building. Proceeding of 4th International Conference on Structural Stability and Dynamics (ICSSD 12), Malaviya National Institute of Technology, Jaipur, Rajasthan, India, 4-6th January-2012, (2012) pp 143-150.
[7] R.S. Jangid (2000) Optimum frictional elements in sliding isolation systems, Computers and Structures, vol. 76. pp. 651-661.
[8] C.P. Providakis(2009) Effect of supplemental damping on LRB and FPS seismic isolators under near-fault ground motions,Soil dynamics and earthquake engineering, Procedia Engineering, vol. 29; pp. 80–90.

American Journal of Engineering Research (AJER)
e-ISSN : 2320-0847 p-ISSN : 2320-0936
Volume-03, Issue-11, pp-38-45
www.ajer.org

Research Paper Open Access

Development of Mathematical Models To Forecasting The Monthly Precipitation

Mustapha BEN EL HOUARI[1, 2], Omar ZEGAOUI[1], Abdelaziz ABDALLAOUI[2*]

[1)] *University Moulay Ismail, Faculty of Science, Department of Chemistry, Research Team "Applied Materials and Catalysis", BP 11201, Zitoune, Meknes, Morocco.*

[2)] *University Moulay Ismail, Faculty of Science, Department of Chemistry, Research Team "Analytical Chemistry and Environment", BP 11201, Zitoune, Meknes, Morocco.*

** Corresponding author: a.abdallaoui@gmail.com*

ABSTRACT: *The prediction of the precipitation is very important and challenging task in the modern world. In this study, the Multi Layer Perceptron (MLP) artificial neural network model was used for predicting the monthly precipitation in the region of Meknes in Morocco. Eight meteorological parameters (average temperature, maximum temperature, minimum temperature, pressure, moisture, visibility, wind speed and maximum wind speed) were used as predictors. The database used cover 209 months, from 1996 to 2013. The neural network architecture developed is [8-3-1]. The efficiency of the model measured by the calculation of the Root Mean Square Error and the linear correlation coefficient suggest that the studied meteorological parameters were related to the precipitation by nonlinear relationships. They also show that the ability of MLP neural network model was better than MLR, PLS and NLMR models.*

KEYWORDS**:** *MLP artificial neural network, MLR, NLMR, PLS, Precipitation, Prediction.*

I. INTRODUCTION

In the present-day context of climate change, precipitation has become one of the most important meteorological parameter. In semi-arid countries like Morocco, the prediction of this variable is primordial for different sectors such as agriculture and water resources management. In the last years, many studies have been conducted to rainfall forecasts in many countries such as Brazil [1], Mexico [2], or Turkey [3]. In general, theses authors have used Artificial Neural Networks (ANN) technique to predict the precipitation parameter. Indeed, artificial neural networks have been successfully used in various domains of science and engineering because of its ability to model both linear and non-linear systems without the need to make assumptions as are implicit in conventional statistical approaches. The ANN predictive technique has been used in weather events [4, 5], stock market [6]**,** particle interactions in high-energy physics [7], cloud classification and identification [8, 9], etc. Many models of ANNs have been developed for precipitation prediction such as Multi Layer Feed forward Neural Network (MLFN) [10]**,** Multi Layer Feed-forward Perceptron (MLFP) neural network [1]. However, for precipitation prediction, the Multi Layer Perceptron (MLP) neural network is the most widely used. In this paper, MLP neural network have been used to obtain a prediction model for the monthly precipitation in the region of Meknes in Morocco. The ANN analyses and their results are discussed and compared with the results obtained by using different traditional statistical models such as Multiple Linear Regression (MLR), Partial Least Squares regression (PLS) and Non-linear Multiple regression (NLMR). The meteorological parameters used as predictors for forecasting purposes are: average temperature (T), maximum temperature (T_{max}), minimum temperature (T_{min}), Pressure (Pr), moisture (H), Visibility (VV), wind speed (V) and maximum wind speed (V_{max}). The choice of these data is based on two criteria, namely the availability of data and the increased correlation between these parameters as demonstrated by others studies [11]**.** The objective of this study was to estimated daily precipitation from limited meteorological data using ANN model. The analyses and their results are discussed in this paper and compared with the results obtained by using the MLR, PLS, NLMR models. Finally we present the results obtained and the concluding remarks.

II. MATERIALS AND METHOD

Study Region and Data:

The study area comprises the region of Meknes (Figure 1). It is located in the central part of Morocco on plain of the Saïs with 33° 57' Northern latitude, 05° 33' Western longitude and 500 meter elevation. This region, with an area of approximately 4,560 km^2 is considered to be one of the best agricultural regions in Morocco.

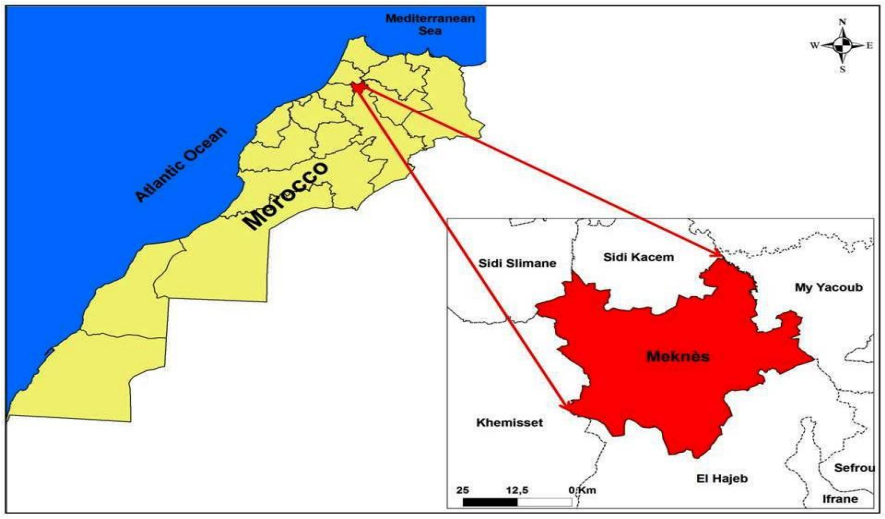

Figure 1: Geographic location of the region of Meknes

The average annual rainfall is close to 501.29 mm. The database used in this work cover 209 months, from 1996 to 2013. It contains the monthly precipitation (dependant variable: to explain) in addition to eight other meteorological variables (**T**: Average temperature**,** $\mathbf{T_{max}}$: Maximum temperature, $\mathbf{T_{min}}$: Minimum temperature**, Pr**: Pressure**, H**: moisture**, VV**: Visibility**, V**: Average wind speed and $\mathbf{V_{max}}$: Maximum wind speed**)**, chosen as independent variables (explanatory variables). Figure 2 show the evolution of the precipitation during the studied period. Summer is generally dry; the period of the largest rain lasts from October to May, with the number of days with monthly rain of 7 to 10 days. The average number of days with rain annually is estimated at 70 days and the annual total rainfall is around 501.29 mm.

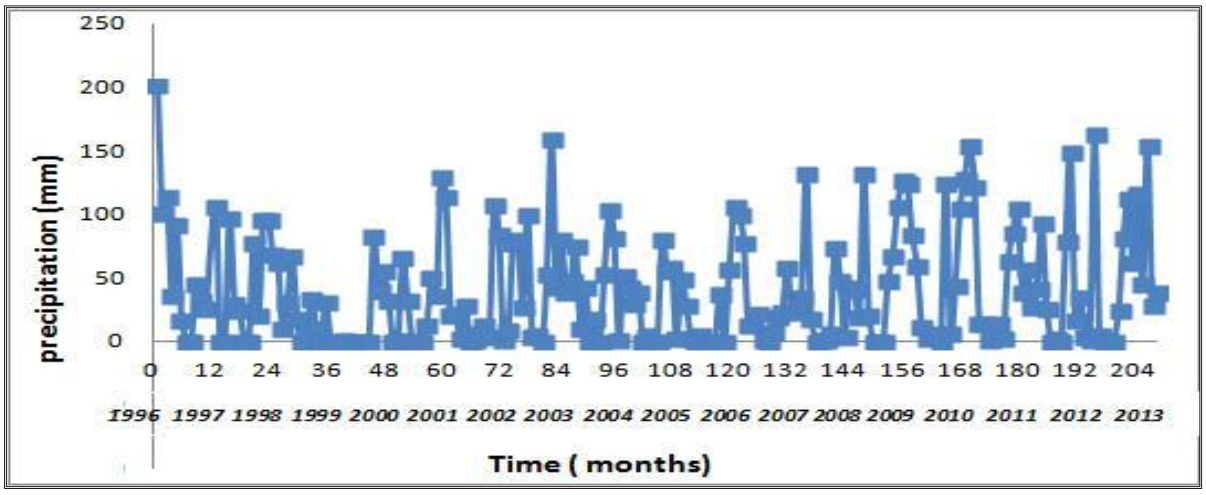

Figure 2: Evolution of the observed monthly precipitation in the region of Meknes between 1996 and 2013.

Performance evaluation of predictive model:

Two criteria are used to measure the model efficiency:

The Root Mean Square Error (RMSE) that represents the discrepancy between the computed and observed values is defined as: $$RMSE = [\frac{1}{n}\sum_1^n(\acute{Y}_i - Y_i)^2]^{1/2} \quad \textbf{(1)}$$

where **n** is the data number, $\acute{Y}_I$ are the predicted rainfall values, Y_i are the observed rainfall values

The linear correlation coefficient (R) is determined by: $$R = \frac{\mathbf{COV}(\acute{Y},\ Y)}{\boldsymbol{\sigma}_{\acute{Y}}.\boldsymbol{\sigma}_Y} \quad \textbf{(2)}$$

Where *COV* is the Covariance and σ the average deviation,

In analyzing the different predictive models, the best answers for the model, RMSE go to zero and R go to one.

III. METHODOLOGY

Multiple linear regression (MLR):

The MLR model is used to predict values of a dependent variable from explanatory or independent variables. It is used to find the best linear model to predict the dependent value that produces the minimum error.

$$Y = a_0 + a_1 X_1 + a_2 X_2 + \ldots + a_n X_n + e \quad \textbf{(3)}$$

Y is the dependant variable, a_0 is the regression constant and a_i (i = 1, 2, …n) are the regression coefficients and e is the error term.

Partial least squares regression (PLS):

Partial least squares (PLS) is a method for constructing predictive models when the factors are many and highly collinear. Note that the emphasis is on predicting the responses and not necessarily on trying to understand the underlying relationship between the variables.

Such as linear regression, PLS regressions equation is:

$$Y = b_0 + b_1 X_1 + b_2 X_2 + \ldots + b_n X_n + e \quad \textbf{(4)}$$

Y is the dependant variable, b_0 is the regression constant and b_i (i = 1, 2, … n) are the regression coefficients and e is the error term.

Non-linear multiple regression (NLMR):

The purpose of the non-linear regression is to adjust the values of variables in the model to find the best curve which predicts Y in function of X. It can be expressed simply as:

$$Y_i = f(X_i, \theta) + \varepsilon_i \qquad i = 1,2,\ldots n \quad \textbf{(5)}$$

Where Yi are the answers, f a nonlinear function depending on the vector $X_i = (X_{i1}, \ldots X_{ik})$ and the parameter $\theta = (\theta_1, \ldots \theta_p)$. ε_i is the residue.

Artificial Neural Network (ANN):

An artificial neural network is an interconnected group of artificial neurons that has a natural property for storing experiential knowledge and making it available for use. ANN consists of a large number of processing elements called neurons, which are arranged in different layers in the network: an input layer, an output layer and one or more hidden layers [12].

The basic ANN architecture is shown in Figure 3

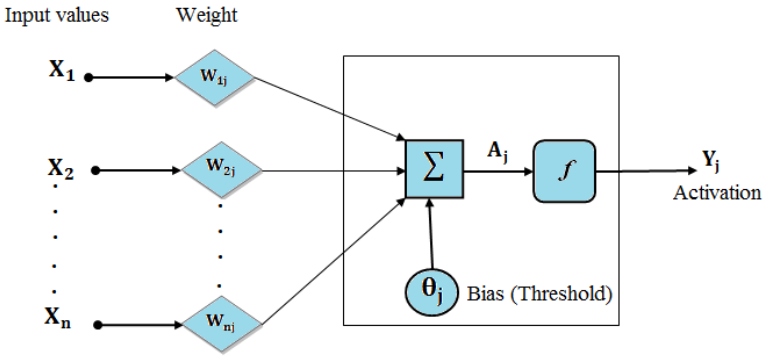

Figure 3: Schematic presentation of neural network [13**].**

The neuron receives input signals, processes them and sends an output signal [14]**.** Each neuron is connected with at least one other neuron and each connection is represented by a real number called a weight. The weights are adjusted iteratively so that the network attempts to produce the desired output [15]. Mathematically, the process can be expressed following the equation (6) [14]**.**

$$Y_k = f[\sum_{k=1}^{n} W_k X_k + b_k] \quad \textbf{(6)}$$

Where W_k represents the synaptic weight, X_k is the input value (k = 1, 2..., n), b_k is the bias of neuron, f is the transfer function, and Y_k is the output. In this work, the sigmoid activation function has used in hidden layer [1]. It defined for any variable X as:

$$f(X) = \frac{1}{1+\exp(-X)} \quad \textbf{(7)}$$

For the output layer, a linear transfer function has used [8].

$$a = f(n) = n \quad \textbf{(8)}$$

Among the 209 data set, 169 was chosen randomly for the training phase and the rest (40 data) for the test phase. Precisely 20%, this is the best distribution of the test phase. The first option is connected to the distribution of the database in two bases: training phase and test phase based on the calculation of the root mean square error. RMSE in Table 1.

Table 1: Root mean square error of training and testing phase for different distributions of the data.

	RMSE Training phase	RMSE Testing phase
Training phase : 90% Testing phase : 10%	0.22	0.20
Training phase : 80% Testing phase : 20%	**0.19**	**0.18**
Training phase : 70% Testing phase : 30%	0.21	0.20

A study has been conducted to choice the number of hidden neurons. The RMSE results of the integrated ANN obtained for different hidden layer are presented in table 2.

Table 2: Root mean square error of training and testing phase for different Number of neuron of the hidden layer.

Number of the neuron of hidden layer	2	**3**	4	5	6	7
RMSE Training phase	0.23	**0.19**	0.24	0.29	0.20	0.29
RMSE Testing phase	0.20	**0.18**	0.20	0.21	0.20	0.19

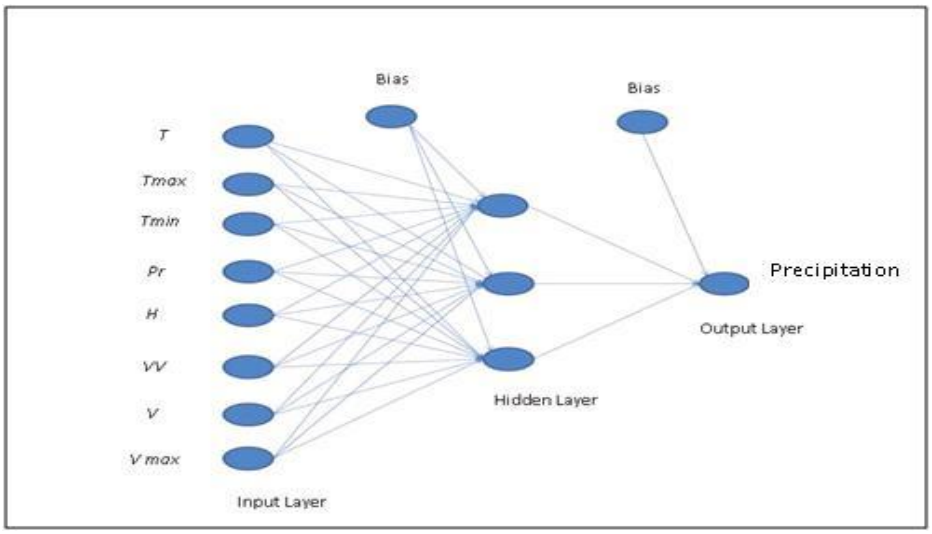

Figure 4: The developed neural network architecture [8-3-1].

An optimal ANN architecture may be considered as the one yielding the best performance in terms of error minimization. According to the results by increasing the number of neuron of the hidden layer, the training and testing RMSE values show that the best structure obtained is with 3 neurons of the hidden neurons corresponding to the lowest RMSE values. So the developed neural network architecture is [8-3-1], as presented in figure 4.

The model used in this study is the type of multilayer perceptron (MLP) artificial neural network with a back propagation of the square error. The rule of the back-propagation is to propagate the errors through the network and allow the adaptation of the hidden units. The Levenberg-Marquardt is used to optimize the weights of the network with transfer functions: sigmoid and linear.

IV. RESULTS AND DISCUSSION

Statistical models (MLR, PLS, NLMR)

We obtained the equations (9), (10) and (11) respectively after analyze by the MLR, PLS and NLMR:

[MLR] : $$\mathbf{Y_{MLR}} = 2766.61 - [4.11 \times T] - [13.50 \times T_{max}] + [16.37 \times T_{min}] - [2.39 \times Pr] - [0.91 \times H] - [9.34 \times VV] - [0.09 \times V] + [2.89 \times V_{max}] \quad \mathbf{(9)}$$

[PLS] : $$\mathbf{Y_{PLS}} = 2149.23 - [4.10 \times T] - [12.91 \times T_{max}] + [16.29 \times T_{min}] - [1.96 \times Pr] + [2.19\ 10^{-2} \times H] + [3.54 \times VV] - [3.31 \times V] + [4.36 \times V_{max}] \quad \mathbf{(10)}$$

[NLMR]: $$\mathbf{Y_{NLMR}} = 37423 + [16.6 \times T] - [44.6 \times T_{max}] + [27.2 \times T_{min}] - [732.94 \times Pr] - [1.37 \times H] - [48.14 \times VV] - [1.16 \times V] + [14.97 \times V_{max}] - [0.40 \times T^2] + [0.54 \times T^2_{max}] - [0.55 \times T^2_{min}] + [0.35 \times Pr^2] + [5.69\ 10^{-3} \times H^2] + [3.05 \times VV^2] + [3.73\ 10^{-2} \times V^2] - [0.30 \times V^2_{max}] \quad \mathbf{(11)}$$

The signs of the coefficients for the variables in the model (MLR) are similar to the PLS model with the exception of the moisture H and Visibility VV. This compatibility signs shows the probable existence of a strong correlation between the two models.

The correlation coefficients obtained by statistical models (MLR, PLS, NLMR) for training series are respectively 0.68, 0.80 and 0.82. In fact, the NLMR method is most effective, the correlation coefficient between the observed and predicted monthly precipitation is significantly important (R = 0.82) compared to the MLR and PLS methods.

Artificial Neural Network (ANN):

In this study, ANN model has been developed with 8 neurons in the input layer (**T**, $\mathbf{T_{max}}$, $\mathbf{T_{min}}$, **Pr**, **H**, **VV**, **V** and $\mathbf{V_{max}}$), three neurons in the hidden layer and one neuron in the output layer for the prediction of precipitation. Table 3 shows the regression coefficient and the root mean square error of training and testing phases obtained by using the four prediction models. It is clear that the developed ANN model shows the best correlation coefficient (R=0.97 and 0.98 for training and testing phases respectively) corresponding to a RMSE = 0.19 and 0.18 respectively while the MLR calculation lead to a wrong correlation value (R=0.68 and 0.81 for training and testing phases respectively) corresponding to a RMSE = 3.7 and 3.5 respectively.

Table 3: Error criteria during training and testing process of different model.

Model	Training phase		Testing phase	
	R	RMSE	R	RMSE
MLR	0.68	3.7	0.81	3.5
PLS	0.80	2.6	0.84	2.4
NLMR	0.82	2.5	0.85	2.3
ANN	**0.97**	**0.19**	**0.98**	**0.18**

The Figure 5 shows the relationships and coefficients of regression between the observed and the predicted precipitation values using the MLR, PLS, NLMR and ANN models. The figures 5A, 5B and 5C indicate clearly

that the points obtained by using MLR, PLS and NMLR prediction models are not uniformly scattered around the regression lines. However, figure 5D relative to ANN prediction model shows a good correlation between observed and predicted rainfall values. These results and those presented in table 3 suggest that the studied meteorological parameters are related to the precipitation by nonlinear relationships. Also, these results show that the ability of ANN model to predict the precipitation values are better than MLR, PLS and NLMR models, the ability of ANN model to predict the mid-range values was better than the ability of MLR model as shown in ANN diagram, the points are scattered closer to the straight line than the clusters in MLR, PLS and NLMR diagrams (Figure 5).

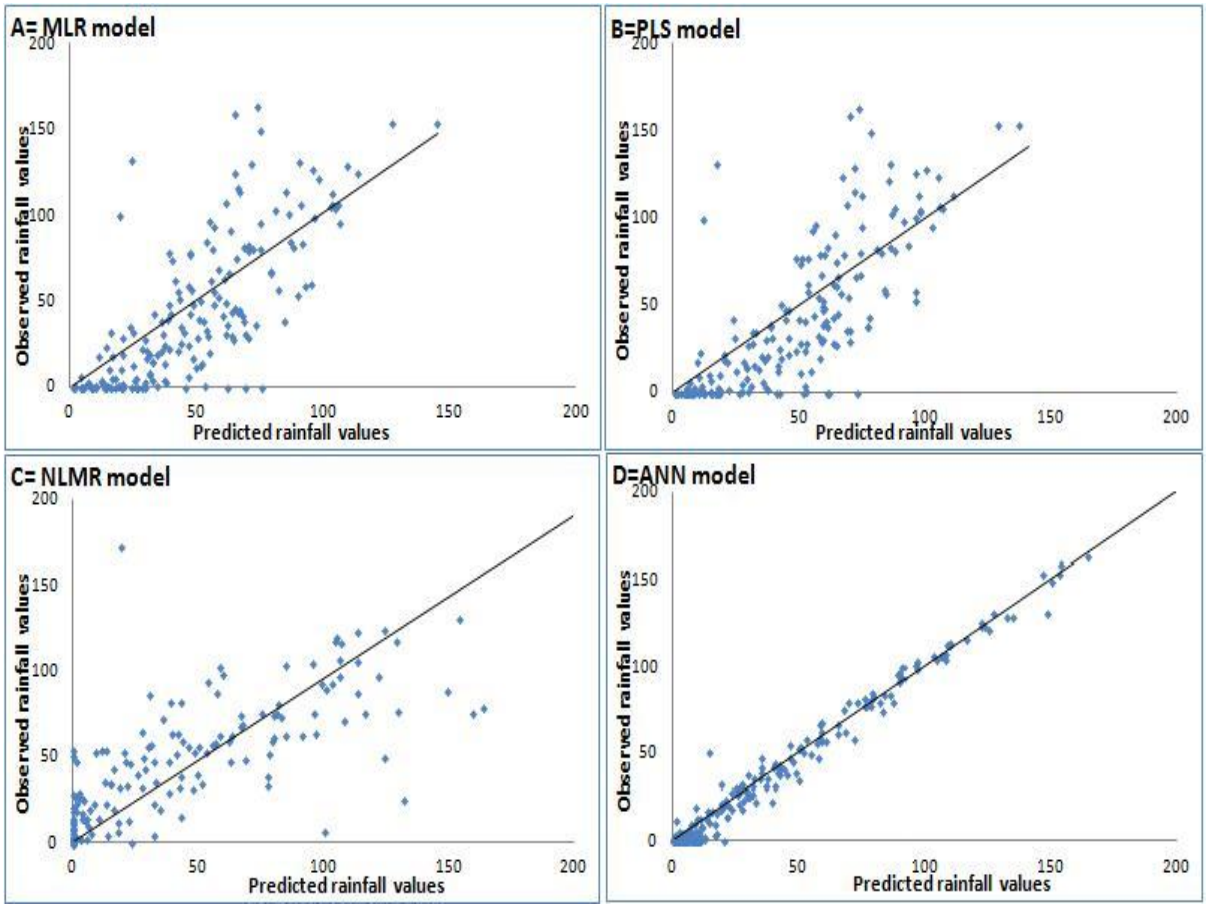

Figure 5: Comparison between the observed total precipitation data and the results obtained from (A): MLR, (B): PLS, (C): NLMR and (D): ANN models

The residue is the error committed by the models established by each individual method on a sample of model construction; Figure 6 shows the plots of the distribution of the residuals based on the simulated values obtained during the training and testing phases using the four predictive models. The figures 6A, 6B and 6C show that the points representing the residues are not uniformly scattered around the abscissa axis zero. However, the figure 6D shows that the points representing the residues fall on the abscissa axis zero, indicating that the more perfectly prediction model is the ANN in comparison with the MLR, PLS and NLMR prediction models.

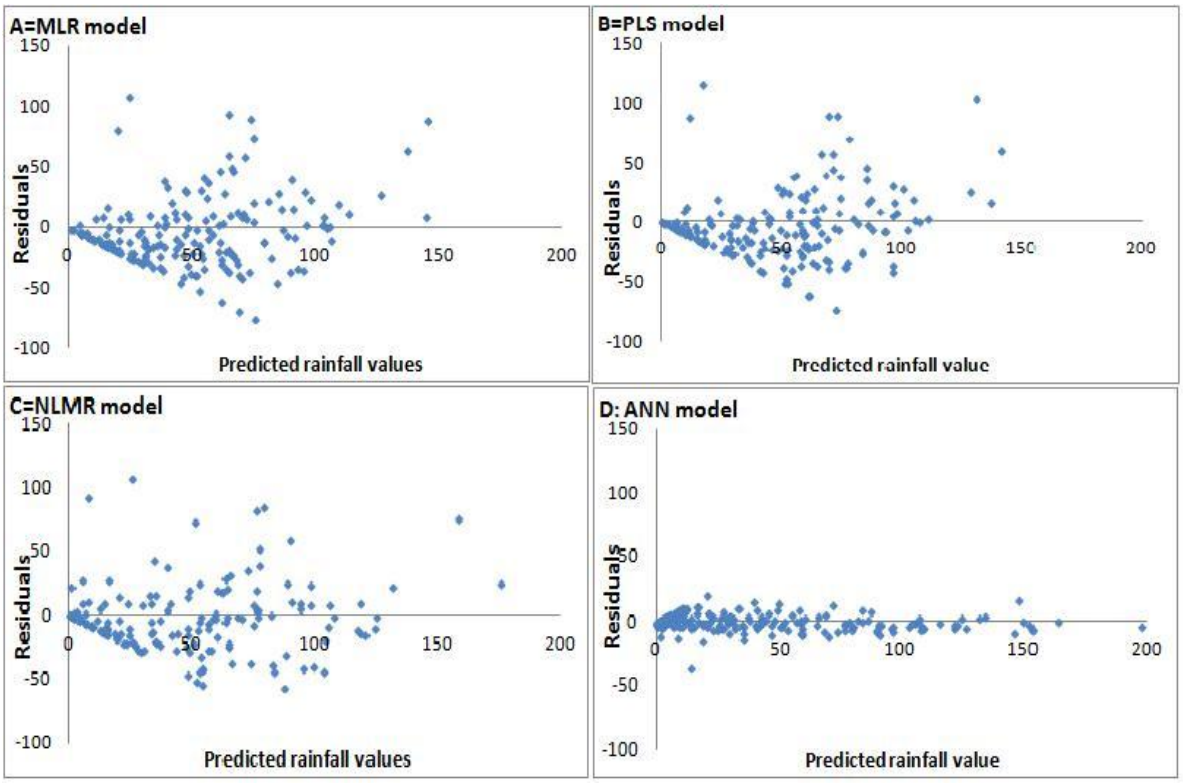

Figure 6: Distribution of residuals obtained by the four prediction models.

V. CONCLUSION

ANN model has been developed to predict the monthly precipitation parameter for the region of Meknes, Morocco. Based on the RMSE and R values, the appropriate architecture of the neural network was [8-3-1] and the ANN model appears capable of providing accurate predictions of the monthly precipitation by comparison with the conventional statistical models (MLR, PLS, NLMR). The results show a significant capacity for prediction for monthly precipitation contents with a linear correlation coefficient (R) of 97% and a low Root Mean Square Error (RMSE) of 0.19 for the database used. For multiple linear regression (MLR), Partial least squares regression (PLS) and Non-linear multiple regression (NLMR) the results are less significant with a linear correlation coefficient (respectively 0.68, 0.80 and 0.82). This shows that the parameters are associated with the monthly precipitation by a non-linear relationship. For the prediction of monthly precipitation, the use of a neural model configuration [8-3-1] gave better results.

REFERENCES

[1] M.C.V. Ramirez, N.J. Ferreira, and H.F. Velho, Artificial neural network technique for rainfall forecasting applied to the Sao Paulo region, *Journal of Hydrology*, *301*, 2005, 146-162.

[2] C. Tereza, Downscaling large-scale circulation to local winter rainfall in north–eastern Mexico, *International Journal of Climatology*, *17*, 1997, 1069-1082.

[3] K. Saplioglu, M. Cimeny, and B. Akman, Daily precipitation prediction by artificial neural networks. Proceedings of the 4th International Scientific Conference on Water Observation and Information System for Decision Support Water Observation and Information System for Balkan Countries. Ohrid, Republic of Macedonia, 2010.

[4] C. Marzbam, and G. Stumpf, Multiresolution wavelet transform and neural networks methods for rainfall estimation from meteorological satellite and radar data. *J. App. Meteor.*, *35*, 1996, 617-626.

[5] K. Hsu, H.V. Gupta, X. Gao, and S. Sorooshian, Rainfall Estimation from Satellite Imagery, Chapter 11 of Artificial Neural Networks in Hydrology, *Edited by R.S. Govindaraju and A.R. Rao, Published by Kluwer Academic Publishers*, 2000, 209-234.

[6] E. Collins, S. Ghosh, and C. Scofield, An application of a multiple neural network learning system to emulation of mortgage underwriting judgements. *Proceedings of the IEEE International Conference on Neural Networks*, 1988, 429.

[7] R. Kantowski, and C. Marzban, A neural network for locating the primary vertex in a pixel detector, *Nucl. Instrum. Methods phys. Res*, *355*, 1995, 582-588.

[8] R.L. Bankert, Cloud classification of a advanced very high resolution radiometer imagery in maritime regions using a probabilistic neural network. *J. Appl. Meteor*, *33*, 1994, 909-918.

[9] J.E. Peak, and P.M. Tag, Sesmentation of satellite imagery using hierarchical thresholding and neural networks. *J. Appl. Meteor*., *33*, 1994, 605-616.

[10] K.C. Luk, J. Ball, and A. Sharma, An application of artificial neural networks for rainfall forecasting. *Mathematical and Computer modelling*, *33(6)*, 2001, 683-693.

[11] H. AL-Naimi.Rasheed, M. AL-Salihi. Ali, I. Bakr. Dher, Neural network based global solar radiation estimation using limited meteorological data for Baghdad, Iraq. *International Journal Of Energy And Environment*, 2014, 79-84.

[12] A.J.P. Kumar, and D.J.K. Singh, 2008. Artificial neural network-based wear loss prediction for a 390 aluminium alloy, *J. of Theoretical and Applied Information Technology, 4(10)*, 2008, 961-964.

[13] H. El Badaoui, A. Abdallaoui, I. Manssouri, and H. Ousmana, The prediction of moisture through the use of neural networks MLP type. *Journal of Computer Engineering*, 2013, 66-74.

[14] S. Haykin, Neural Neural Network and Its Application in IR, *a comprehensive foundation, 2nd edition Upper Saddle Rever, New Jersey: Prentice Hall*, 1999, 842p.

[15] M. Safa, S. Samarasinghe, and M. Mohsen, Modelling fuel consumption in wheat production using neural networks. *18th World International Congress on Modelling and Simulation, Cairns, Australia, 13-17 July 2009*, 2009, 775-781.

American Journal of Engineering Research (AJER)
e-ISSN: 2320-0847 p-ISSN : 2320-0936
Volume-03, Issue-11, pp-46-54
www.ajer.org

Research Paper Open Access

Karnophuli River Front Development, Chittagong, Bangladesh

Md.Kamrul Islam[1], Sudipta Chowdhury[2]
[1]*Student, Department of urban and Regional Planning.Chittagong University of Engineering and Technology, Bangladesh*
[2]*Student, Department of urban and Regional Planning.Chittagong University of Engineering and Technology, Bangladesh*

***ABSTRACT**: In Bangladesh there are so many rivers. Every river has some specialty and historical background. That is why the river can be an attractive place for recreation and social interaction. The Karnophuli riverfront development project has taken to develop the condition along the river bank and to increase the natural beauties of the river as well as the surrounding areas. Though Chittagong has various natural resources and it is naturally a beautiful city but it has lack of planning orders which gradually make this beautiful city so much hazy, inconvenient and intolerable. The unplanned situation of the Patenga-Sadarghat-kalurghat has been reducing the beauty of the river as well as the city. This study is prepared to provide some recommendation and some design to enrich and beautify the bank of the Karnophuli River (west side) so that the people of the Chittagong city can go there and can enjoy the beautiful scenario of the river.*

***KEYWORD**: River front, Development, Karnophuli, Recreation, Social interaction*

I. INTRODUCTION

B**ackground of the study :** Bangladesh is a riverine country. The total area of this country is 147,998 sq km. among which 13,830 sq km water land. About 800 rivers including tributaries flow through the country constituting 24,140 km of water way. Most of the country's land is formed through silt brought by the rivers. Some important rivers in Bangladesh are Padma, Meghna, Jamuna, Brahmaputra, etc. Karnophuli is one of the most important rivers in this country. Chittagong whichis the main port and second largest city of Bangladeshis located on the banks karnophuli. With the increased urbanization in city, the river is also experiencing various developments and needs emergency attention for controlled development to project the haphazard construction and river pollution.[1]

II. OBJECTIVE AND SCOPE OF THE STUDY

The goal of the study is to propose development activities in the front side the west of the Karnophuli river of Chittagong. Study focus on some development activities in the west side of the Karnophuli river of Chittagong such as potential and pedestrian site beautification. This approach may convince the west side to tourist spots in Chittagong.

III. METHODOLOGY

Topic Selection: The selected project name is "Redevelopment plan for karnophuli river front" under the course "Urban Planning Techniques Studio".

Selection of the Study Area: After selecting the topic a study area is needed for the study. The project area is the western bank of the Karnophuli River starting from Kalurghat Bridge to potenga.

Analyzing existing situation: By analyzing the existing situation, the condition of the study area is learned along with the position of building and their uses (commercial, industrial, residential), area of port, open space and aesthetic beauty of the river.

Problem identification and scope of the studies: After analyzing the study area we select the problem and scope of study area are identified. What problem it is facing today and what are the scopes that are destroying day by day. Then thegoal and objective of the work is decided.

Settling of goal
After analyzing the project the goal are settled the goal of this work is toprepare a suitable redevelopment plan for karnophuli river front in Chittagong

Literature review:A literature review is a body of text that determines the aims to review the critical points of current knowledge including substantive findings as well as theoretical and methodological contributions to a particular topic. Literature reviews are secondary sources, and as such, do not report any new or original experimental work.

Data Collection
There are two types of data collection process. They are
[1] Primary Data Collection
[2] Secondary Data Collection

Primary Data Collection: Primary Data is collected through visual survey. Data are also collected by photographic survey. Primary data also collected from discussion with local people. Then data has been analyzed.

Secondary Data Collection: Secondary data have been collected from CDA (Chittagong development authority), CCC (Chittagong City Corporation), and AUTOCAD map and port authority.

Data analysis: After collecting the primary and secondary data one should have perform the data analysis process...

Recommendation: After analyzing data some plan will be prepared including ample car parking facilities, boat club, landing Facilities, toilet, dressing & Sitting Arrangements, and others.

Conclusion: Finally prepared a report is prepared on this topic which helps to understand this base map and the overall work.

IV. LITERATURE REVIEW

Riverfront (Re) development: In general, a riverfront is the zone of interaction between urban development's and the River and a riverfront area is considered as a unique and irreplaceable resource where it is the interface between land, water, air, sun and productive plants. Moreover, the riverfront is a place integrating land with water and having a natural attraction to people. Waterfront development refers to any development in front of water and a water body; a river, lake, ocean, bay, creek or canal. In the development area, considered that a waterfront development may not necessarily need to be directly fronting water but May only need to look attached to the water. They believe that commanding a view of water can still be considered as a waterfront property. [2]

Riverfront Development practice in Bangladesh

Photo1-Hatirjheel-Begunbari project

In Bangladesh the Government has introduced some important projects. For Example Hatirjheel-Begunbari project, Padma river front development in Rajshahi city, Bongobondhu Eco-park project in the bank of Jamuna River etc. Hatirjheel-Begunbari project area included 46 acres of Rajuk's land, 34 acres of other government agencies, and 81 acres of Court of Wards and 141 acres of private land. Hatirjheel-Begunbari project to be opened on Dec 15Rajuk's, assisted by the Local Government and Engineering Department (LGED), Dhaka Wasa, Special Work Organization of Bangladesh Army, is implementing the project costing over Taka 1971 crore. [3]

Photo 2: River front besides the Bongobondhu Bridge

3.4. Guideline for the development related to rivers and river reserves

Specifically, the guideline for riverfront development concept aims four objectives, as follows:

[1] To explain and encourage the implementation of guideline in the development planning of riverfront areas.
[2] To be a reference and a guideline for any development near to the river areas.
[3] To provide uniform guidelines for all parties involved in the riverfront development process.
[4] To control all types of riverfront developments.

IV. EXISTING CONDITION

Introduction: Karnophuli River the largest and most important river in Chittagong and the Chittagong hill tracts. In Chittagong the Karnophuli made a most significant change in its course from Kalurghat downwards... This fact is of much historical importance in so far as it helps locate the eastern bounds of the town during the Mughal and early British period.

Location: Karnophuli is the largest and most important river in Chittagong and the Chittagong Hill Tracts. It is 667 meters (2,188 ft)-wider river in the south-eastern part of Bangladesh which is originate from the Lushai hills in Mizoram, India.. It flows 270 km (170 mi) southwest through Chittagong Hill Tracts and Chittagong into the Bay of Bengal. The mouth of the river hosts Chittagong's sea port, the main port of Bangladesh. [4]

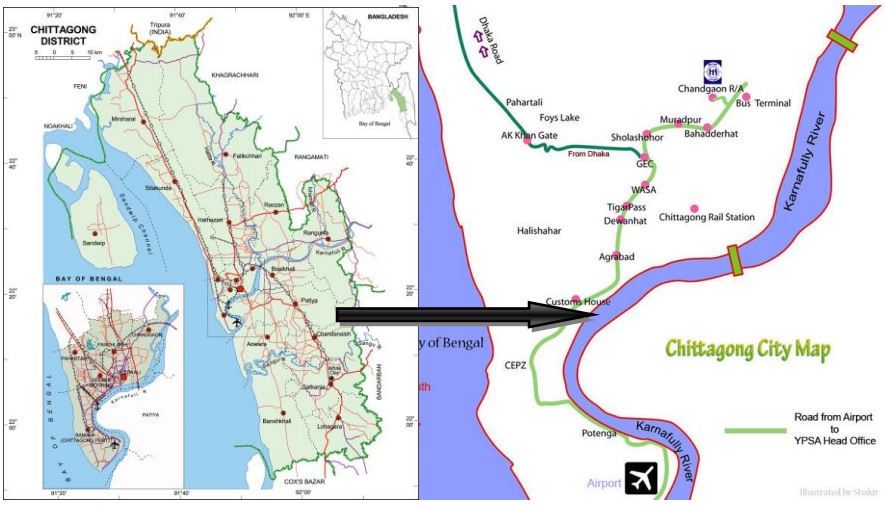

Map3: Location map of Karnophuli River

Project Area: The project area is the western bank of the Karnophuli River stretching from Kalurghat Bridge to potenga.

Karnophuli River pollution : The polluting industries of Chittagong, the second largest city of Bangladesh, such as 19 tanneries, 26 textile mills, 1 oil refinery, 1 TSP plant, 1 DDT plant, 2 chemical complexes, 5 fish processing units, 1 urea fertilizer factory, 1 asphalt bitumen plant, 1 steel mill, 1 paper mill (solid waste disposal hourly 1450 m^3), 1 rayon mill complex, 2 cement factories, 2 pesticide manufacturing plants, 4 paint and dye manufacturing plants, several soap and detergent factories and a number of light industrial units directly discharge untreated toxic effluent into Karnophuli river. From the survey of effluents from different industries, it has been found that the discharge is generally composed of organic and inorganic wastes.

Marine pollution: All kinds of waste either in solid or liquid form are dumped into the water, resulting in the deterioration of the aquatic environment. Most of the pollutants are in sediment form, municipal and industrial wastes, agrochemical residues and pollutant discharges from ships and boats although this pollution has existed over the years, information regarding the nature of pollutants and the damage. They cause to marine fisheries and other resources are very scant.

Photo 4: Pollution of water from ship discharge

Bangladesh is not an industrialized country. The considerable discharge of untreated industrial effluents has led to the degrading of the aquatic and marine ecosystems of Bangladesh and has had an impact on fisheries. The second largest urea plant in the country has recently been established on the south bank of the Karnophuli River. It has provision for treatment facilities, but the plant is reported to still contribute to river pollution

Pollution by waste disposal: There is no proper waste disposal system in the bank of the Karnophuli River. Different types of waste like human waste, Residential waste, unused products, fertilizer, Bags, oil etc is thrown into river. There is also many hanging latrine in the bank of the river. While using the toilet, the filth goes to the river and pollutes water. Again the people of the area bath in the river though the latrine is situated beside the bath and swimming places. This is very harmful for their health.

Photo 5: Pollution by waste disposal

Photo 6: Illegal encroachments

Illegal activities: In Sadarghat area, different illegal activities increase day by day in river side .Many people playing card with money. Sometimes they playing card in different illegal way. Local people have no safety way in this area by these illegal activities. Tin-shed and concrete structure builds after filling up a vast stretch of Karnophuli River at Bakolia in Chittagong, Bangladesh. Encroachment still continues on the bank of

Karnophuli River posting a threat to the River upstream towards the fourth bridge on it. After encroachment of a vast stretch of river bank in Char Bakolia illegal occupants' in a latest move are now constructing concrete structures and filling up the water bodies of karnophuli river..

Erosion: Another problem in this area is erosion in river bank of the Sadarghat is increasing day by day. Crease causes of erosion, there is no embankment of the river side. There is no enough deck for good loading and unloading. Though existing deck is made of wood this deck is destroyed any time which create a great lose in economics field. For this reason the existing situation of the deck can have vulnerable in any time.

V. ANALYSIS

Karnophuli River Front Development Project and Detailed Area Plan: The River Karnophuli is the pride of Chittagong. Virtually the whole Chittagong is laced and crisscrossed by the river Karnophuli. Communities large and small along the Karnophuli River have started discovering their river heritage, turning back to their riverfront and recognizing them as tremendous community and economic assets. People with more close to their home recreation facilities, including riverfront trails, boating and nature viewing are included here. In view of mass demand Chittagong Development Authority (CDA) has decided to develop a project on uplifting of the bank of the Karnophuli by involving the communities and all other stakeholders involved in the process

Karnophuli River Front Development Project and other countries

We read some project in water front development and which principle they emphasized most. In Malaysia they select ten principles for sustainable water development. They emphasized on

- ✓ Secure the quality of water and the environment.
- ✓ Waterfronts are part of the existing urban fabric.
- ✓ The historic identity gives character.
- ✓ Mixed-use is a priority.
- ✓ Public access is a prerequisite.
- ✓ Planning in public-private partnerships speeds the process.
- ✓ Public participation is an element of sustainability.
- ✓ Waterfronts are long term projects.
- ✓ Revitalization is an ongoing process.
- ✓ Waterfronts profit from international networking. [12]

Expected End of Project Situation

Economic Benefit

- Improved Link within City
- Creation of jobs
- Increase the quality of life style
- Enhance property values
- Expand local business
- Increase local tax revenues
- Attract or relocating businesses
- Promote local community

Environmental Quality Impact
- Ecological functions of the Karnophuli River will be maintained / improved.

Social Impact
- The Development will increase social interaction amongst people.
- It will encourage people to visit the riverbank.
- Participatory planning process will encourage community ownership of the project.

Target Beneficiaries
- People of Chittagong; and
- Tourists

Preliminary Planning Concept
- The bank will be developed with a sense of belonging of Chittagong people;
- River-side drive will be a pleasant experience to all visitors which will be connected to City Road Network as well as trails and different activities;
- Basic concept of beautification is to bring the river back to the front of the city's landscape;
- Cyclone/ Tidal flow will be considered in the planning process;
- Beautification will be with manicured gardens and tasteful illuminations;
- There will be something for each age group and community;
- Ample car parking facilities;
- The entire stretch will be dotted with several floating restaurants;
- Open-air theatre will be developed in natural environment;
- Water based recreational facilities will be developed in the project.
-

VI. PROPOSAL

River Network:A large number of economic activities take place along the Karnophuli River using the numerous Ghats situated along the river. These Ghats play an important role in fish supply to the local and national market, provide riverine communication through trawlers and small ships between Chittagong city and its surrounding districts. There should be a wide pedestrian footpath (at least 30' to 40') along the river side so that people can walk easily and they can sit and gossip freely with the other people.

Embankment and Road along KarnophuliRiver : In order to provide protection to the riverbank and to enhance traffic circulation in the southern part of this zone, an embankment has been proposed by CDA in DAP between Strand Road and intersection of the Karnophuli Approach Road at Shah Amanat Bridge. A road should be within shah Amanat Bridge to Kalurghat Bridge. The road should be located 300ft opposite from the river bank. Beside this road 5 fat road curve should be given and then landscaping should be started.

Improvement of River Ghats: Considering that inland water transport along Karnophuli River will continue to play an important role in the future, it is proposed that all the river Ghats and areas surrounding these should be improved and modernized to better serve the traffic which uses them.

Leisure, Recreation: About 1705 acres of the land of the Parkir Char area are proposed for the Beach related some of the water bodies need to be improved by plantation on bank sides. Such pond can be used for community used. There is no sufficient facility for recreation activities in this area. For better mental and health improvement of the local people it is mandatory to provide land for different types of recreation activities like parks, play ground, green and sports complex. Taking into consider this demand for recreational purpose the present study of DAP recommends a certain amount land in the study area.An area eastern side of CDA Kalpalok Residential area up to Karnophuli River bank, may be developed as a river side amusement such as sport, leisure centre etc. The triangular area south of the industrial area and near to Karnophuli River may be reserved for an urban park. A butterfly park may be incorporated which may operate as a commercial venture.

Photo 7: Sitting arrangement

Photo 8: Road along the river side

Parks and Open Spaces: To enhance the city environment and make it habitable, it is necessary to build some parks and new Urban Green blocks in this zone. Some such locations are at Chandgaon crossing, near Kalpalok residential area, and south of Noa khal mouth. This green park should be kept open for public visit and leisure. There will be a park beside the Karnophuli Bridge which will be the recreational place for people. The areas of this park will be2.5 Acres. Another park will be in the side of Kalpolok residential area. This will be 7.5 Acres.

Shops: There should be some small shops. For example-clamps necklace, shops of *fuchka*, *Chotpoti*, various types of flowers shops should be available along the river side. But there should not be any large shops or departmental shops in the river side.

Vehicles: Motors vehicles are not allowed in the footpath regions. If anyone wants to go with motor vehicles then he/she must park it in the parking lot.

Picnic spot: The river side can be a turned into an attractive place if any picnic spot are available in this side. The potenga sea beach and the parker char is the most attractive and beautiful place for picnic spots. Some specials project should be taken to develop this place.

Boat cruise: There are no felicities to travel with boat along the river side. So there should be some option to travel with boat. This will create an employment of the people in this region.

Bus and Truck Terminal: There are two sites that have been recommended for transport related use. The site located atomizer Tack and another site located on the north of Silver Crossing has been designated for inter district bus terminal and truck terminal respectively. The terminals are to be developed taking into account environmental enhancement and proper traffic circulation. It is mandatory to design a green buffer of trees surrounding the terminals.

Illegal encroachment: Any illegal development, infrastructures are allowed to the river side. Some special rules should be made to protect illegal encroachment along the river side.

Green belt along River and Khal sides: The south bank of the Karnophuli River needs to be protected from saline water intrusion and storm surges by polders. A green belt is recommendation along the embankment. All major khals, such as Shikolbaha khal should be rehabilitated; backlines should be marked and fixed. Along the backline there should be a buffer zone of green belt, up to 100 ft. wide on both sides.

The east bank of the Karnophuli River needs to be protected by embankment from saline water intrusion. A green belt is recommendation along the embankment. All major khals should be rehabilitated; back lines should be marked and fixed. Along the back line there should be a buffer zone of green belt, up to 100 ft wide on both sides.

Photo 9: Proposed Green belt along River

Photo 10: Proposed Landscaping

Treatment Plants: Major part of the area, particularly adjacent to the Karnophuli River, has been proposed to develop for industrial use. There is always a risk of pollution of the Karnophuli from the industrial units. All polluting industries must have treatment plant, and must not discharge into the river without treatment. In the karnophuli river front development project we provide a treatment plant. This treatment plant project is situated in Chaktai Channel which total area 3 acres. In this project we provide these plants to purify the water of industrials waste.

Bus and Truck Terminal: Karnophuli bridge south side has been designated for inter district bus terminal and truck terminal respectively. The terminals are to be developed taking into account environmental enhancement and proper traffic circulation. It is mandatory to design a green buffer of trees surrounding the terminals. The area of the bus and Track terminal is 5 acre.

Pedestrian walkway: In the whole area (Kalurghat to Sadarghat).There will be a pedestrian walkway. This walk way should be used for pedestrian purposes. No vehicles are allowed in this walkway. The wide of the pedestrian would be 16 ft. various types of landscaping and monument should be in side of this walkway. The walkway should not be straight. It should be curved so that it removes monotones view.

Resort: In the Char area there will be two or more resort which will be connected with Cable Car or boat facilities. This area will create beauty as well as economic benefit.

Art gallery : An art gallery will be beside the kalpolok residential area. Area for art gallery will be 20000 sq. ft.

Open Theatre: An open theatre will be in the side of the river bank. And beside this theatre many public facilities will be given.

Parking: Parking is the safety place for the keeping cars. In the karnophuli river front development project we provide parking facilities in the road side. In this project we provide place for the parking the cars in safety who will come here to visit. Parking is the act of stopping and leaving it unoccupied. Parking on one or both sides of a road is often permitted, though sometimes with restrictions. Parking facilities are constructed in combination with some buildings, to facilitate the coming and going of the buildings' users. Two parking lots are provided. One is situated only little distance from the proposed bus terminal and another is beside the Kalpolok residential area which will serve the vehicles of the commercial area and the people who will visit this area. Both parking will serve minimum 80-100 vehicles.

Archeology museum: Public institution dedicated to preserving and interpreting the primary tangible evidence of humans and their environment. Types of museums include general (multidisciplinary) museums, natural-history museums, science and technology museums, history museums, and art museums. In Roman times the word referred to a place devoted to scholarly occupation (Museum of Alexandria). The public museum as it is known today did not develop until the 17th18th century Museum is the place where people can know about the real historic background and monument of ancient Chittagong. In the karnophuli river front development project we provide the Archeology museum where people can gather knowledge about the historic books and historic monument. On this project in Kalurghat area there is an Archeology museum which total area is 1 acre. In the

Archeology museum the ancient history and ancient monument should be presented of Chittagong region as well as whole Bangladesh.

Stadium and gymnasium:A stadium and gymnasium will be located beside the commercial place. The area for the Stadium 2 acres and the area for the gymnasium will be 1500sq. ft. the stadium will be used for indoor games purposes.

VII. CONCLUSION

This paper aimed to explore the effectiveness of Karnophuli riverfront development in Chittagong, Bangladesh. The analysis and the proposal part confirmed that the developer's level of awareness of the regulations, which directly or indirectly relate to the control of riverfront developments. The majority indicated that they were somewhat familiar with the regulations. Nevertheless, bear in mind, some regulations were designed specifically for certain areas, and some may be not necessary to others. Moreover, the results showed that Chittagong does not currently have sufficient regulations and guidelines to control riverfront development. Now there are some plans for the Chittagong to control the haphazard growth of buildings. For example there is a master plan for Chittagong city, there is structure plan, detail area plan etc. But in terms of riverfront development, there is no specific plan to control or to beautify the Karnophuli river front development. More than that, the failure of the Bangladesh government and the responsible institutions, specifically to enforce the regulations and guidelines, has resulted in unsuccessful riverfront developments in this country. Therefore, in order to strengthen regulations and guidelines for riverfront developments in Chittagong, the government and the policy makers are required to do more with the regulations in the future. In this paper, we also identified several components that should be included in riverfront development guidelines in an effort to practice riverfront developments in a good manner. Improvement is required in order to enhance and maintain sustainable riverfront developments in the future, in this country.

VIII. ACKNOWLEDGEMENT

At first, all praises belong to the Almighty Allah, the most clement, most generous and most bounteous to all living creatures and their actions. We express our profound gratitude and indebtedness to our respective visiting teacher **Engr. Planner. M.Ali Ashraf**, Chairman, Bangladesh Institute of Planners (Chittagong Chapter). We owe much to **Ms, Israt Jahan**, Associate professor, Department of Urban & Regional Planning and**A.T.M Shahjahan,** Lecturer, Department of Urban & Regional Planning, Chittagong University of Engineering and Technology, for their cordial encouragement, constant guidance, inspiration and valuable suggestion to prepare this report. We would like to pay homage the planning office, CUET. Our special thanks owe towards the students of CUET. Without their help the data used in this report could never be collected. We would also like to thank our friends and classmates, for their effective discussion and suggestion to conduct the study.

REFERENCES

[1] http://en.wikipedia.org/wiki/Karnaphuli_River (Accessed: 06/06 /2014)

[2] http://www.banglapedia.org/HT/K_0101.HTM (Accessed: 06/06 /2014)

[3] http://travelingluck.com/Asia/Bangladesh/Bangladesh+ (general)/_1198381_Karnaphuli+River.html (Accessed: 06/06 /2014)

[4] Breen, A., & Rigby, D. (1996). The new waterfront: A worldwide urban success story. New York: McGraw-Hill.

[5] Ryckbost, P. (2005). Redeveloping urban waterfront property. USA: University of Michigan.

[6] http://news.priyo.com/business/2012/07/31/hatirjheel-begunbari-57065.html(Accessed: 08/06 /2014)

American Journal of Engineering Research (AJER)
e-ISSN : 2320-0847 p-ISSN : 2320-0936
Volume-03, Issue-11, pp-55-60
www.ajer.org
Research Paper Open Access

Review and Locating of Health-Care Centers Using Fuzzy-AHP Techniques (A case of Zabol City)

Dr. Gholam Ali Khammar[1*], Hossein Majidi Meskin[2]
[1] *Assistant Professor of Geography & Urban Planning, University of Zabol, Zabol, Iran*
[2] *MSc student of Geography & Urban Planning, University of Zabol, Zabol, Iran*

ABSTRACT : *The location of facilities is critical in both industry and health care centers. In most cities of Iran, the lack of appropriate space allocation and optimal positioning of physical elements and services, particularly health care centers led to increasing of urban and civilian's problems. In order to, the aim of current research is review and locating of health-care centers using Fuzzy-AHP Techniques in Zabol city. Applied methodology is based on qualitative and quantitative methods with point on socio-economic indicators to adjusting the level of settlements in the spatial system of the Zabol region. Results show that almost all medical centers are located in areas 2 of Zabol city and citizens have many difficulties in terms of access to these centers.*

KEY WORDS: *Health facilities, Zabol city, Fuzzy-AHP Techniques, Spatial System*

I. INTRODUCTION

During the 19th and early 20th centuries, the synergies between urban planning and public health were evident in at least three areas: creation of green space to promote physical activity, social integration, and better mental health; prevention of infectious diseases through community infrastructure, such as drinking water and sewage systems; and protection of persons from hazardous industrial exposures and injury risks through land-use and zoning ordinances. During the middle of the 20th century, the disciplines drifted apart, to a certain extent because of their success in limiting health and safety risks caused by inappropriate mixing of land uses (Majidi, 2006). The disciplines recently have begun to reintegrate. During the last 20 years, shared concerns have included transportation planning to improve air quality, encourage physical activity, prevent injuries, and promote wellness. In addition, some original crossover ideas, such as the potential for parks and recreational facilities to contribute to physical activity and mental health, have reemerged. Relatively recently, urban planning has focused on the effects of community design on energy use and greenhouse gas emissions to affect the growing public health concern of climate change. Finally, emergency preparedness (evacuation planning) and access to health care (e.g., assurance of accessibility and adequacy of facilities) are topics important to both disciplines (Refahi & et al, 2003; Qajari, 2008).

In health care, the implications of poor location decisions extend well beyond cost and customer service considerations. If too few facilities are utilized and/or if they are not located well, increases in mortality (death) and morbidity (disease) can result. Thus, facility location modeling takes on an even greater importance when applied to the siting of health care facilities. Everything usually begins with the architects and designers meeting with the clinical staff and other professionals who will be working in the new or enhanced space. A design specification is generated based on considerations such as workflow, patient Volumes, types of activities, proximity to key partners, and the basic necessary infrastructure such as heating, ventilation, and cooling (Xang, 2013; Utnm, 2014). It's critical that IT be involved in the design specification stage before the specification is generated. Key decisions at this point in the process include defining what applications and technology will be used in the new or remodeled space. From an IT perspective, everything that's planned should be within the guidelines of the IT strategic plan for the organization. It is fine to test new technology, but it should be part of a vision for the larger organization (Yama, 2008). To make a balance between different aspects, urban planning is a conventional tool used which also can be a significant tool for promoting the interaction among planners and officials and the local community (Diamantini & Zanon 2000). In making sustainable urban development, urban planning can play an eminent role. In order to make balance between four aspects economic, environmental,

social, and governance is the aim of sustainable urban development .This paper examines the spatial distribution of healthy land use in Zabol city according to urban fabric divisions. Also partly are considered the consistent or not consistent position in relation to the centers of adjacent land uses and because almost all the clinics are located in the city of Zabol in Area 2 and it hasn't an balanced in distribution, our goal is the provide of best locations for the construction of health centers in the Zabol city as balanced. This problem has faced citizens of Zabol with big challenges and led to limit their access to other areas.

Case study Region : Zabol is the second city of Sistan and Baluchistan province and it is the first city of Sistan region. This province is located between $25^{//}$ $3^{/}$ to $31^{//}$ $29^{/}$ northern widths and $58^{//}$ $49^{/}$ to $36^{//}$ $20^{/}$ eastern lengths. It is limited to Sothern Khorasan with the Oman Sea to the north, Afghanistan to the south, Pakistan to the east, and Hormozgan province to the west. According to the census of 2006, the population of this province estimated at 2,405,742 people. Based on the latest division of the country Sis-tan and Baluchistan has 14 counties, 36 cities, 40 boroughs, 102vials, 8908 coded villages (Fanni, khakpour & Heydari, 2014).

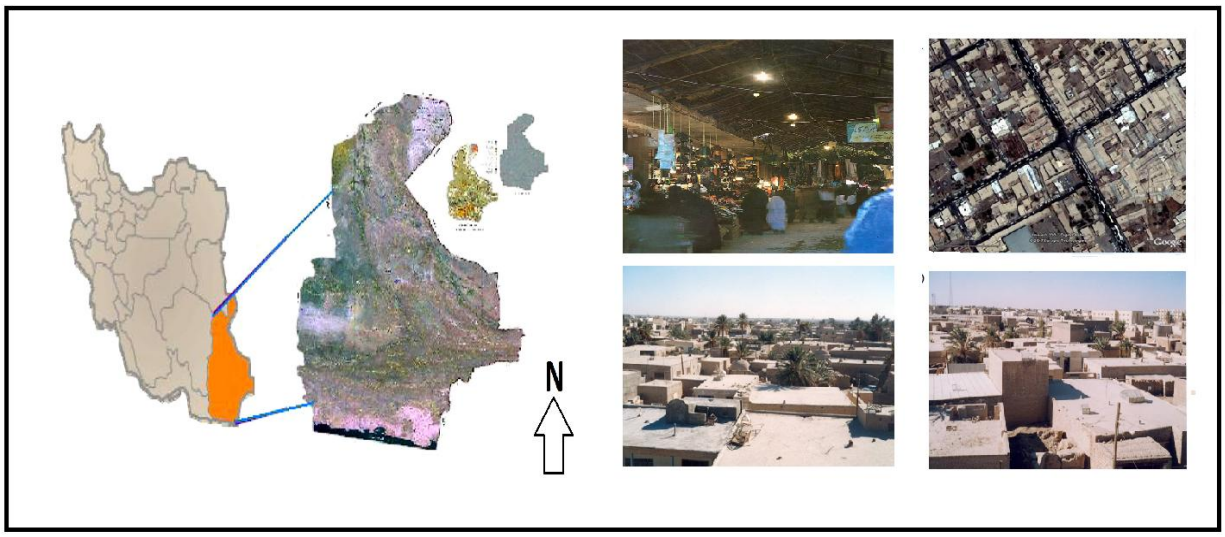

Fig. 1. Case study region.

Also Zabol city is located in the near of Hamon Lake and the region agriculture lands are irrigated by Hirmand River water. Lake Hamun is a seasonal lake that is often dry. The people of Zabol speak a Persian language variant known as Sistani or Seistani which is very similar to Dari, also known as Afghan Persian. The tribes of the area include the Shahraki, Arbabi, Narui, Barahui, Gorgij, Herati, Ghanbari, Afshar, Barani, Sarani, Fakhireh, Mir, Dahmardeh, Rashki, Sanchooli, Pahlevan, Faghiri, Divaneh, Gorg, Nohtani, and Sayyadi. In recent years these tribal names appear in the surnames of the inhabitants of the area. There are also hundreds of Baluchis, Brahuis families and some Pashtuns in this city. Zabol area is well known for its "120 day wind", a highly persistent dust storm in the summer which blows from north to south. Zabol is connected by road to Zaranj across the border in Afghanistan. The Delaram- Zaranj Highway provides road connectivity to the rest of Afghanistan. Zabol thus provides Afghanistan access to the Arabian Sea and Persian Gulf via the Port of Chabahar.

II. METHODOLOGY

In present study the data were collected from libraries, documents and field study. In the case of library, data were collected by studying books, articles and internet. Then, field study was done and including observation, discussion and filling questionnaire and data were analyzed by using a qualitative range. For further clarification of the issue data were analyzed in AHP and Fuzzy techniques. In current research according to surveys and current information's and for combined criteria were used of GIS and the main methods of data fusion, fuzzy logic and Analytic Hierarchy Process (AHP) and the map of the best locations for the construction of health centers was obtained. Then, using inference functions and fuzzy operators were ranking these criteria to Fuzzy measures.

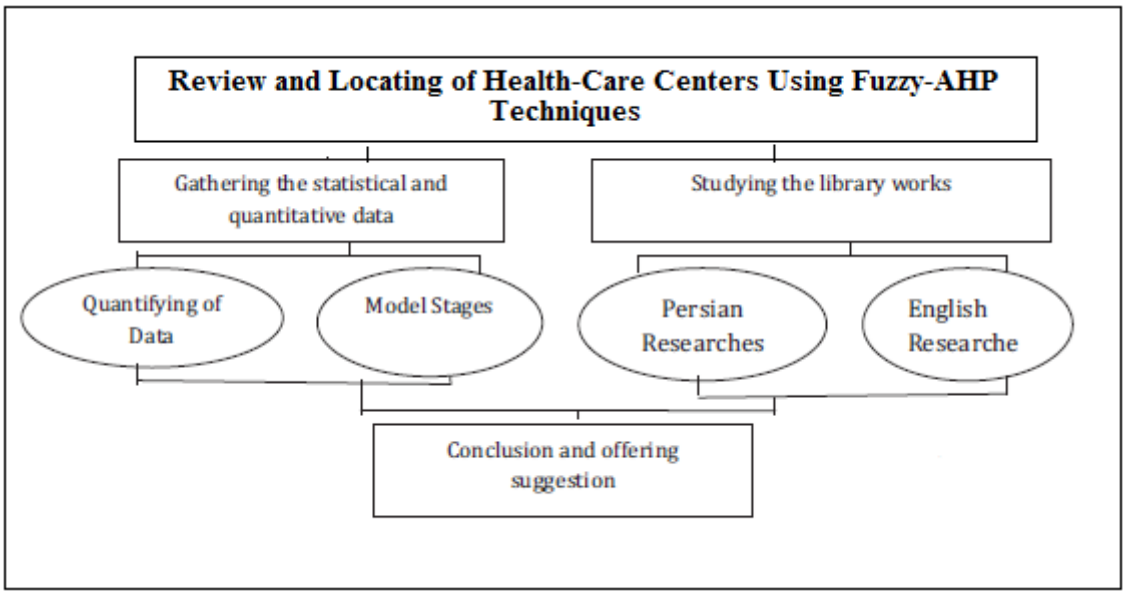

Fig. 2. Conceptual research diagram.

III. RESULTS

World-wide cities are growing at a rate of 2% annually (UN, 1999). While in 2000 about half of the world's population lived in cities, almost 2/3 (60, 3%) will reside in urban areas in 2030. Especially African, Asian and Latin American cities are characterized by high urban growth rates (3,5% for Africa, 2,4% for Asia and 1,7% for Latin America) caused by natural population growth and rural-urban migration as well as by the underlying pull- and push factors such as the lacking infrastructure in rural areas and the hope for employment in the cities. As a result of the uncontrolled and uncoordinated growth of urban agglomeration characterized by informal land acquisition, fragmentation of peri urban land, inefficient use of land, poorly functioning land markets etc. urban development is far from being sustainable.

Consistent with compatible land uses : In term of urban planning, land use which placed in the sphere of influence should be consistent with each other in terms of authenticity and coordinates and Causing a nuisance and do not work together properly. For land use rate layers, current land uses in Zabol city have divided to six classes. Then the degree of compatibility between land uses were determined and classified based on land-use map of the city and in some cases field observations. Then specific point was awarded to each class.

Table (1) Land use valuation based on their fitness degree

Land use	Value
Bayer, Farming, garden	6
Parks, educational, administrative	5
Sports, industrial, cultural	4
Military Facilities	3
Commercial and Residential	2
Sanitary	1

Proximity to residential centers : Human life place is the most important part of the city and it is allocated a major portion of the land use. So that more than 60 percent in small towns and about 40 percent of large cities are covered by residential land use (PourMohammadi, 2003).

Accessibility to main transportation networks : Fast and timely access to medical care is considered as the basic needs of families because timely delivery of patients to these centers is of crucial importance (Azizi, 2004).

Distance from industrial sites : Industrial land uses are incompatible with health centers and cause problems such as buildup noise pollution. However, these land uses can cause environmental pollution, Therefore comply with the basic principles of location is an important factor.

Proximity to Urban Green Space : In current research, whatever the distance between green spaces and health care centers be closer, it can get good grades and the opposite of this situation is probably too.

Table (2) Rate of data layers based on the Distance

Score	Distance from data layers				
	Industrial workshops	Residential centers	Medical Centers	Green Spaces	Main ways
1	0-300	More than 500	0-300	More than 1000	More than 500
2	300-600	500-400	300-600	1000-800	500-400
3	600-900	400-300	600-900	800-600	400-300
4	900-1200	300-200	900-1200	600-400	300-200
5	1200-1500	200-100	1200-1500	400-200	200-100
6	More than 1500	100-0	More than 1500	200-0	100-0

After the value of existing data layers, the data's will be weighted. Weight of the layers was done using analytic hierarchy process.

Healthy land use : Zabol city has one municipality region and five districts with attention to its size in Iranian urban system (20845200 Km^2). One district with an area equivalent to 48/331 acres, in generally is include of south and southeast part of Zabol city. The district has only one hospital in medical facilities (Amir Al Moemenin Hospital). The two districts have an area equal to 8/457 hectares. This area has many hospitals consist of Imam Khomeini and all its clinics in the Zabol city (Al Zahra, Salamat, Shafa, Beheshti & Shohada). Three Zabol city district has cover an area with 308 hectares based on Tash Consulting Engineers. This area doesn't have suitable area in status of medical facilities. Four district of Zabol city has an area with equal to 31/711 hectares. In general, in the current situation Zabol city has two hospitals and five clinics. The total area of these centers is about 54,955. Calculated per capita, according to the centers of population in 2006 is equal to 0.42. As shown in the figure 2, the healthiest facilities are located in the central part of Zabol city. However, in other areas of the city are deprived of health facilities and account for a small percentage of it. Amir Al Momenin's hospital has located in the entrance road of Zabol to Zahedan city. This hospital has multifunctional services to whole of Zabol city due to its role and due to its 2 Km^2 distance of residential area. If at least one clinic covered population (10,000 people) and the minimum radius of its access to the residential neighborhoods (750- 650 m) to require clinics to consider the criterion, one area with 36,971 inhabitants, has minimum required three clinics. District 2 with 41,619 populations and taking the five clinics in this area and it has very suitable status quantities scale. Three district with 35,546 inhabitants is requires three clinic. Four areas with 7391 inhabitants needed to one clinic. Finally, district five, with 22,732 inhabitants needs two other clinics.

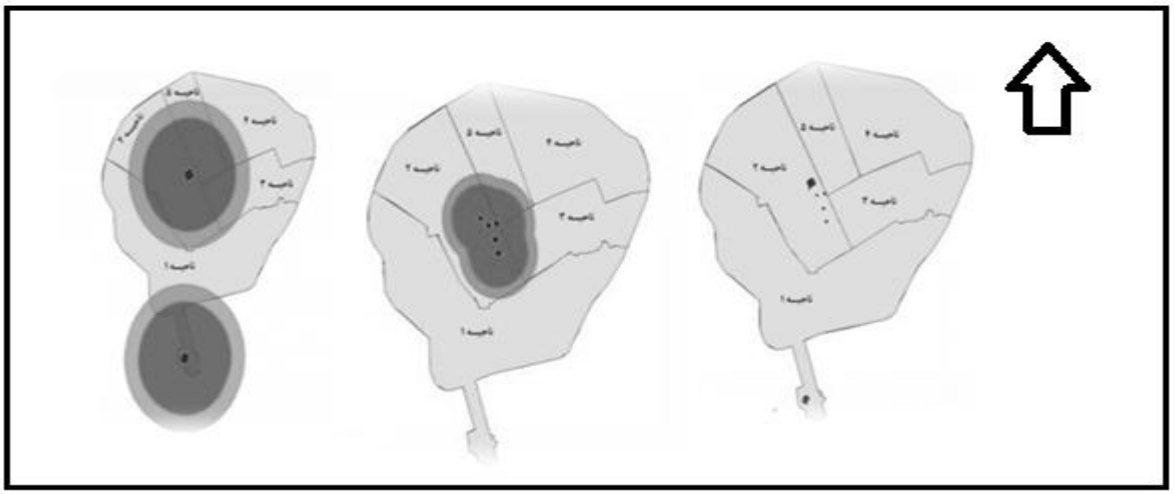

Fig. 3. location of health centers in the districts of Zabol city.

In this research, proximity to the main road is the most important factor in the location of health centers and then the standards of living in residential care, suitable use, away from industrial centers; health centers and close to the green were next factors.

Table (3) Weights to the criteria's

Criteria	Weight	Priorities
Close to main road	0.366	1
Close to residential area	0.310	2
Suitable land use	0.132	3
Distance from industry centers	0.122	4
Close to green space	0.047	5
Distance from healthy centers	0.023	6

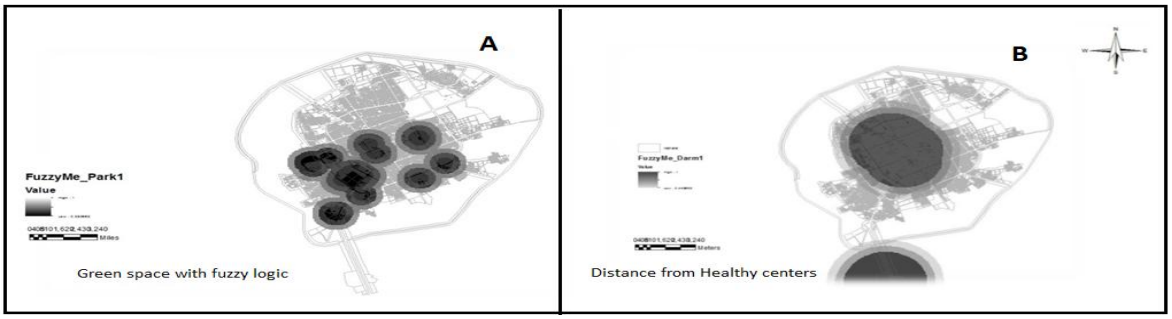

Fig. 3. Fuzzification of layers (Green space & Health center).

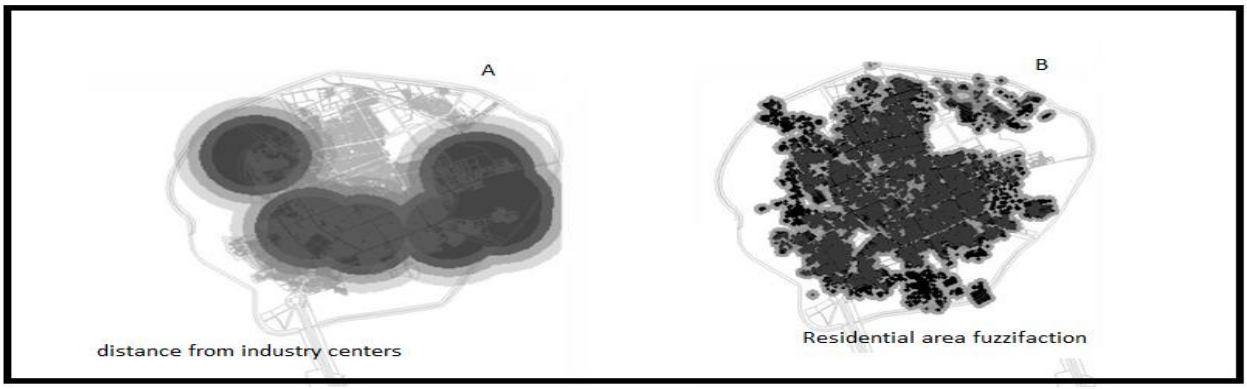

Fig. 4. Fuzzification of layers (industry centers & Residential area).

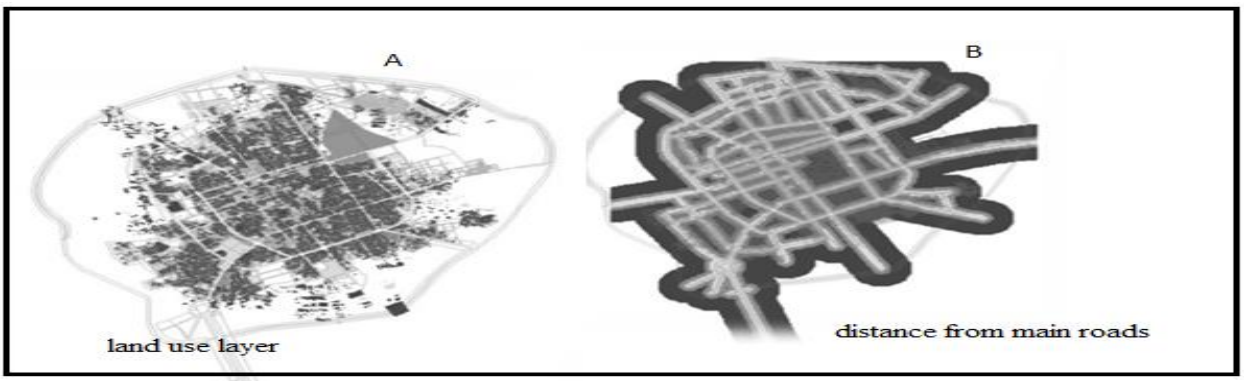

Fig. 5. Fuzzification of layers (Land use layer & distance from main roads).

IV. CONCLUSION

In this paper the problems of health centers in Zabol were realized and it was found that medical centers in Zabol not balanced distribution. (Hypotheses), and almost all health centers are located in district 2 in the Zabol city and this problem led to created trouble for people from other areas in terms of access to these facilities. In order to, the best place to build a new health center in the city is first group of locations (4.0 to 5/0).

Suggestions

[1] municipality as the responsible organization about master plans, must provide more suitable laws about urban land use and urban land use allocation.
[2] Making the proper medical facilities in the city, to reduce the volume of referrals from other parts to the Zabol city.
[3] Use the experience of other countries in locating of health facilities.

REFERENCES

[1] **Azizi, H.** land use in Iran. Standard press.
[2] **Diamantini, H. Zanon, J.** 2000. History of political relations of Iran and England. Tehran: National Works
[3] **Fanni, Z. Khakpoor, BA. Heydari, A.** 2014. Regional development in Zahedan, SCS.
[4] **Majidi, U.** 2006. Dictionary of Urbanism, Streetwise Press.
[5] **Pourmohammadi, M.** 2002. Urban land use planning, Samt press.
[6] **Qajari, L.** 2008. Iran and healthly facilities after Islamic event. Gatreh press.
[7] **Refahi, Y. et al,** 2003. Housing renewal policies, house prices and urban competitiveness. Applied Geography, 30. Society., p. 952.
[8] **UN,** 1999. Health report.
[9] **Utnm, O.** 2014. Urban and settlement. Report for 2000.
[10] **Xang, J.** 2013. Dividing Up the Investment Pie: Have We Overinvested in Housing? Business Review (Federal Reserve Bank of Philadelphia), 13-23.
[11] **Yama, Y.** 2008. Encouraging Mixed Use in Practice. Incentives, Regulations, and Plans: The Role of States and Nation-states in Smart Growth Planning.

American Journal of Engineering Research (AJER)
e-ISSN : 2320-0847 p-ISSN : 2320-0936
Volume-03, Issue-11, pp-61-69
www.ajer.org
Research Paper Open Access

Parametric Study of Jatropha Blended Gasoline Fuel In Compression Ignition Engine Of A Small Capacity Diesel Engine

[1]Benjamin Ternenge Abur, [2]Abubakar Adamu Wara, [3]Gideon Ayuba Duvuna and [4]Emmanuel Enenoma Oguche

[1] *Department of Mechanical Engineering, Abubakar Tafawa Balewa University, Bauchi-Nigeria.*
[2] *Technology Incubation Center, Gusau, Zamfara-Nigeria.*
[3] *Department of Mechanical Engineering, Federal Polytechnic Mubi, Adamawa-Nigeria.*
[4] *Industrial Skills Training Center, Kano*

ABSTRACT : *In this study, Jatropha Biodiesel was tested in a single cylinder direct-injection diesel engine to investigate the operational parameters of a small capacity diesel engine under six engine loads. Here the jatropha oil is used as a non edible oil to produce the biodiesel. The investigated blends were 40/60%, 30/70%, 20/80% and 100% jatropha biodiesel at various loads. The jatropha biodiesel was obtained from National Research Institute for Chemical Technology Zaria-Nigeria and was within EN, BIS and Brazil specifications for biodiesel. Each blend was tested on a short term basis of three hours. The result shows that the brake thermal efficiency increased for all tested blends at lower engine loads and decreases at higher engine loads. The specific fuel consumption (S.F.C) increased for lower blends compared to neat jatropha oil while higher engine powers were obtained for lower blends compared to neat jatropha oil. In all the investigated operational parameters, the diesel reference fuel had better performance to jatropha biodiesel blends except in the percentage heat loss to the exhaust where jatropha biodiesel blends had better performance.*

KEYWORDS: *Jatropha, Biodiesel, Brake Power, Brake Thermal Efficiency, Specific Fuel Consumption.*

I. INTRODUCTION

The enormous amount of energy being consumed across the world is having adverse effect on the ecosystem of the planet. The technologies for fossil fuels extraction, processing, transportation and their combustion have environmental concerns (Munear, 2005). With dramatic growth in the use of compression ignition engines in recent years for transportation, power generation, agriculture, earth moving machines and several industries due to its inherent fuel economy, ease in operation, maintenance and long life.The demand for conventional petroleum fuels and environmental degradation resulting from diesel combustion can no longer be ignored (Naveen Kumer, 2005).To provide long lasting solution to these twin problem, the use of alternative fuels have been effectively utilized for partial or complete substitution of conventional petroleum fuels in compression ignition engines.Non edible vegetable oils have demonstrated potentials as alternative fuels which could be use in existing diesel engines without any major engine hardware modifications at a relatively low price (). Some positive attributes exhibited by the oils include; biodegradable, higher heat content, liquid nature-portability, lower aromatic content and lower sulphur content.

Jatropha curcas (Linaeus), a non edible oil bearing and drought hardy shrub with ecological advantages is found to be the most appreciated renewable alternative source of bio-diesel (Tint et al, 2009). Vegetable oil in neat form is not suitable for diesel engine due to its high viscosity. The commonly employed methods of reducing the viscosity of vegetable oils are blending with diesel, emulsification, pyrolysis, cracking and transesterification. The transesterification method of vegetable oils to mono alkyl esters (biodiesel) appears to be the best route amongst all these methods (Xie, 2006).Several researchers have prepared blends of varying proportions of jatropha curcas oil and diesel and compared the performance with diesel fuel in compression ignition engines. Relatively high viscosity, lower volatility and reactivity of unsaturated hydrocarbon chains of these oils cause problems of high emissions and low break thermal efficiency (Vellgulh, 1983). Straight vegetable oils are too vicious and create difficulties over prolonged use in the diesel injection diesel engines (Ziejewski, 1984).

Many researchers observed that bio-diesel containing 10-12% oxygen on weight basis causes reductions in engine torque and power due to its lower energy content. However, some studies have also reported that bio-diesel can cause a slightly higher engine power than conventional diesel fuel. This is because of complete combustion with the fuel oxygen in the fuel rich flame zone. The complete combustion also reduces exhaust emission such as hydrocarbons, smoke and carbon monoxide (Usta et al., 2005).The aim of the study is to determine the operational parameters of a biodiesel fuel compression ignition engine test for blends of 60/40%, 70/30%, 80/20% and 100/00% for jatropha bio-diesel fuel.

II. MATERIALS AND METHODS

The Engine Test bed : A Petter AA1, TD114 diesel engine was used for the test. It is a single cylinder, two stroke, horizontal type unit with a cylinder bore of 70mm, piston stroke of 57mm and a compression ratio of 17:1. It has maximum torque of 8.2Nm at 3600rpm, maximum brake power of 2.6kW at 3600rpm, fuel injection timing of 24° to 33° BTDC. The engine unit was connected with other appropriate accessories (instrumental unit).

Experimentation : The experiment aims at determining the operational parameters of a compression ignition engine run on jatropha biodiesel. Thus, the Petter AA1, TD114 diesel engine was operated as an Automobile engine. Each of the blends consisted of six test runs that lasted for three hours since the engine is a small capacity- laboratory base. The engine speed and torque were operated manually and the following parameters measured; engine temperature, fuel consumption, exhaust temperature and developed power. The engine was first run on the reference diesel fuel and consequently on the blends of jatropha biodiesel after which the engine was serviced and replaced with new lubrication oil and fuel system flushed with the next test fuel blends. The jatropha oil was obtained from National Research Institute for Chemical Technology, Zaria Kaduna State Nigeria (NARICT).

Methods : The operational parameters of the engine were evaluated from Equations 1 to 9 (Eastop, 1993)

(a) Power Developed.

The power developed in an engine is given by:

$$P=\frac{2\Pi NT}{60} \quad \text{.....} \quad 1$$

Where N is the number of revolutions per minute and T is torque.

(b) Measurement of Air consumption

The expression for air consumption in kg/hr is given by:

$$M_a = 2.98\sqrt{\frac{P}{T}}hmm \quad \text{Kg/hr} \quad \text{.....2}$$

Where P is measure in millibar and T in °K

(c) Measurement of fuel consumption

The fuel consumption is determined by measuring the time (t) taken for an engine to consume a given a volume of fuel:

$$M_f = \frac{28.8 \times S_{gf}}{t} \quad \text{kg/hr} \quad \text{.....3}$$

Where: S_{gf} is the specific gravity of the fuel.

t, time taken to consume a given quantity of fuel.

(d) Specific fuel consumption

This is defined as the fuel consumption rate divided by brake power:

$$\text{S.f.c} = \frac{M_f}{P_B} \times 10^3 \quad \text{(g/kwh)} \quad \text{.....4}$$

(e) Brake Thermal Efficiency.

The maximum overall efficiency of energy conversion is expressed as the brake thermal efficiency given as:

$$\eta_b = \frac{P_B}{M_f \times H} \times 3600 \quad \text{..... 5}$$

Where P_B is measured in kW and M_f is measured in kg/hr.

(f) Percentage heat Loss in Exhaust
The heat carried away by the exhaust gases expressed as a percentage of the heat input is:

$$\text{Percentage heat loss in exhaust} = \frac{(M_a \times M_f) \times C_p \times \Delta t \times 100}{M_f \times H} \quad \text{..... ... 6}$$

Where: H is the calorific value of the fuel measured in kJ/kg

Δt Is the difference between exhaust and ambient temperatures

C_p Is the specific heat of exhaust gases.

(g) Volumetric Efficiency
For this study, the volumetric efficiency is given as:

$$\eta_v = \frac{M_a}{60\ N} \times \frac{1}{V_s \rho_a} \quad \text{for a two stroke engine} \quad \text{.....7}$$

Where M_a is in kg/hr,

V_s = Swept volume

ρ_a = Density of air

(h) Correction of Brake Power to Standard Atmospheric Pressure and Temperature.
The most significant correction is made to brake power:

$$P_B(corrected) = P_B(measured) \times \frac{749\ mmHg}{P_O} \times \frac{273 + t_o}{273 + t_s} \quad \text{..... ... 8}$$

Where t_s is the standard condition and t_o is the observed condition.

(i) Measurement of Air/Fuel ratio
It is given by:

$$A/F = \frac{m_a}{m_f} \quad \text{..... .... 9}$$

(j) Measurement of Exhaust Temperature
Exhaust temperature was measured by a chrome/Alumel thermocouple conforming to BS1827.

(k) Measurement of Torque
The hydraulic dynamometer measures the engine torque and displays it on the torque meter located on the instrumentation unit.

(l) Measurement of speed
Engine speed was measured electrically by a pulse counting system.

III. ENGINE PARAMETERS

Tables 1, 2 and 3 shows diesel engine test parameters, properties of biodiesel jatropha obtained from NARICT and properties of diesel and Jatropha biodiesel blends.

Table 1: Specification of Diesel Engine Test Bed

S/No	Parameters	Value
1	Ambient Temp	32° C
2	Engine Bore	70mm
3	Engine Stroke	57mm
4	H_2	35.8mm of water
5	Density of Air	1.1548kg/m^3
6	Quantity of fuel consumed	8ml
7	Swept volume	$2.19\times 10^{-4} m^3$

Table 2: Properties of Biodiesel Jatropha obtained from NARICT

S/No	Fuel properties	ASTM P_s 975 diesel	ASTM 121 Biodiesel	Biodiesel Jatropha obtained from NARICT	Unit
1	Aniline point	_	_	27	^{0}C
2	Specific gravity at 60^{0}F	0.85	0.88	0.88	
3	API gravity	_	_	29.1	
4	Carbon Residue	<0.35	0.05	1.21	Wt%
5	Kinematic viscosity at 40^{0}C	1.3-4.1	1.90-6.0	5.82	Cst
6	Colour			>1.0	
7	Diesel index			23.5	
8	Calorific value	45	41	44	KJ/Kg
9	Flash point	60-80^{0}C	-100 to 170^{0}C	133	^{0}C
10	Cloud point	-5 to 5^{0}C	-3 to 12^{0}C	-3	^{0}C

(Source: NARICT)

Table 3: Properties of Diesel, Biodiesel Jatropha

Fuel blend	Specific gravity	Calorific value (KJ/kg)
Diesel	0.8400	39000
B60	0.8530	41139
B70	0.8553	41090
B80	0.8576	40174
B100	0.8621	39174

IV. RESULTS

Tables 4 – 10 show the summaries for analyzed results in comparison with the reference diesel fuel. The parameters analyzed are the thermal efficiency, specific fuel consumption, power, percentage heat loss, exhaust gas temperature, volumetric efficiency and the air-fuel ratio for the diesel and the biodiesel blends.

Table 4: Brake Thermal Efficiency for the Tested Blends (%)

S/No	Torque (Nm)	Diesel	B60	B70	B80	B100
1	0.5	5.37	1.28	3.54	3.35	3.69
2	2.2	17.99	5.48	9.13	11.05	11.50
3	3.3	18.86	9.63	9.28	9.40	10.75
4	4.6	22.28	10.77	9.93	10.43	11.40
5	5.4	20.00	11.40	9.17	10.76	11.33
6	5.8	18.29	10.62	9.38	12.06	12.23

Table 5: Specific fuel consumption (s.f.c) for the Tested Blends (g/kwh)

S/No	Torque (Nm)	Diesel	B60	B70	B80	B100
1	0.5	1718.84	2660.30	2469.30	2673.94	2489.76
2	2.2	513.10	861.79	959.14	810.28	799.03
3	3.3	489.30	908.01	943.39	952.79	780.05
4	4.6	404.42	812.39	881.50	859.06	805.18
5	5.4	461.11	766.94	954.97	832.12	810.91
6	5.8	404.57	823.56	933.47	742.99	750.93

Table 6: Percentage heat loss to exhaust for the tested blends (%)

S/No	Torque (Nm)	Diesel	B60	B70	B80	B100
1	0.5	29.16	9.74	10.67	10.12	16.54
2	2.2	29.21	8.30	8.41	9.18	15.55
3	3.3	23.20	6.57	6.57	6.23	11.98
4	4.6	21.90	6.77	6.19	6.46	11.86
5	5.4	17.58	6.72	5.18	6.49	10.92
6	5.8	17.89	5.40	4.47	6.65	10.86

Table 7: Table 6 Power Developed for the Tested Blends (W)

S/No	Torque (Nm)	Diesel	B60	B70	B80	B100
1	0.5	116.83	116.69	116.82	116.82	116.82
2	2.2	514.06	499.32	499.32	495.65	495.65
3	3.3	757.29	743.32	743.32	737.66	723.56
4	4.6	1036.43	830.82	824.44	818.15	792.73
5	5.4	1194.15	911.22	893.60	876.24	841.18
6	5.8	1272.93	1033.39	1001.35	981.35	941.27

Table 8: Exhaust gas temperature for the tested blends (°C)

S/No	Torque (Nm)	Diesel	B60	B70	B80	B100
1	0.5	134	97	97	96	125
2	2.2	168	110	118	108	153
3	3.3	197	128	130	122	181
4	4.6	201	132	134	127	186
5	5.4	212	134	136	131	187
6	5.8	247	137	138	134	195

Table 9: Air/Fuel ratio for the tested blends

S/No	Torque (Nm)	Diesel	B60	B70	B80	B100
1	0.5	110.51	60.69	66.49	62.57	68.71
2	2.2	82.77	42.80	39.18	47.53	49.35
3	3.3	57.39	27.17	26.55	26.83	30.50
4	4.6	49.54	26.88	23.95	26.49	29.17
5	5.4	37.09	26.11	19.49	25.34	26.60
6	5.8	31.46	20.15	16.33	25.22	25.11

Table 10: Volumetric Efficiency for the tested blends (%)

S/No	Torque (Nm)	Diesel	B60	B70	B80	B100
1	0.5	61.79	52.51	53.40	54.42	55.64
2	2.2	60.79	53.37	53.78	55.13	56.44
3	3.3	60.29	54.58	55.41	56.55	57.66
4	4.6	59.96	53.99	51.56	56.27	58.07
5	5.4	60.00	54.47	50.86	57.62	58.94
6	5.8	59.99	51.84	47.61	58.52	58.90

V. DISCUSSION OF RESULTS

Brake Thermal Efficiency : Diesel, the reference fuel shows a decreasing trend of brake thermal efficiency as exhibited in figure 1 with increase in engine speed. Generally, there is consistent decrease in the brake thermal efficiency with the addition of jatropha oil in biodiesel jatropha blends. The decreasing trend shows no significant difference between higher and lower jatropha oil/diesel fuel blends. This work is contrast with the earlier work of (Nwafor, 2004) who reported higher brake thermal efficiency as compared to diesel. The maximum brake thermal efficiency has been observed with B100 with a value of 12.23%.

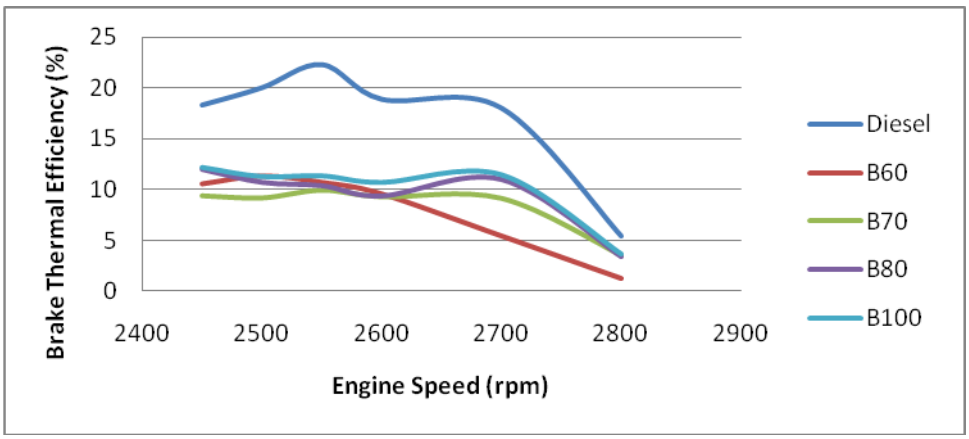

Figure 1: Variation of Brake Thermal Efficiency with Engine Speed for Diesel and all Tested Blends

Spcific Fuel Consumption : Generally, the engine clearly exhibit more fuel consumption pattern as the engine speed increases with higher blends having more rate of fuel consumption. For the biodiesel jatropha, B100 exhibited the lowest specific fuel consumption at all speeds and load conditions. This signifies that lower engine speeds are required for fuel economy. This is in confirmative to the work of (Nwafor, 2004).

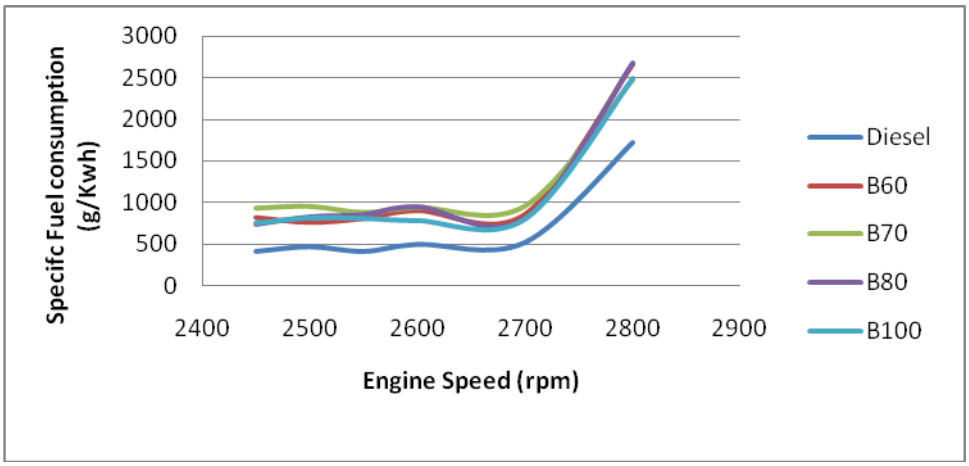

Figure 2: Variation of Specific Fuel Consumption with Engine Speed for Diesel and all Tested Blends

Brake Power : Higher powers were obtained at lower engine speeds for diesel and jatropha biodiesel blends. There were decreases in the brake power as engine speed increases for increased percentage substitution of jatropha oil. The optimum brake power for the jatropha biodiesel blends were for B60 while B100 exhibited the minimum brake power. The diesel referenced fuel clearly demonstrated superior characteristics of power output available for work. This conforms to the work of (Neto da Silva, 2003) in which they observed that 5% of biodiesel and diesel resulted in increase in torque and power output while 30% blends gave a reduction in torque and power output. The works of Gideon and Wara (2012) also ascertain to that.

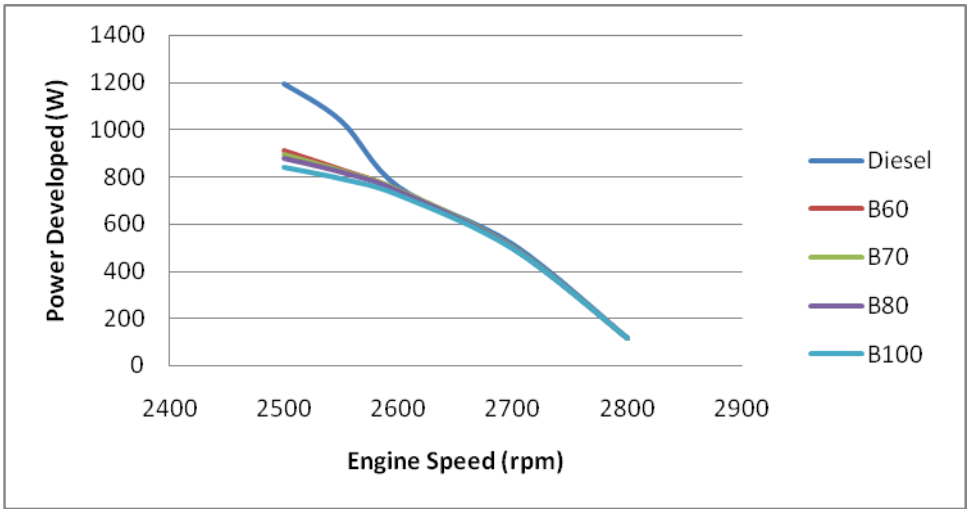

Figure 3: Variation of Brake Power with Engine Speed for Diesel and all Tested Blends

Exhaust Gas Temperature : The biodiesel jatropha blends exhibited good characteristics in exhaust gas temperature as it reduces for increased in the engine speed. This characteristic is healthy as less useful heat energy is lost through the gases. In comparison to diesel reference fuel, the experimental result showed that exhaust gas temperature were lower for biodiesel jatropha blends in comparison to diesel with B80 having the optimum result. This is in confirmative to the earlier work of Gideon and Wara (2012). However, this is contrast to the work of (Usta et al., 2005) which they reported that blends of biodiesel demonstrated higher exhaust temperatures than that of diesel reference fuel.

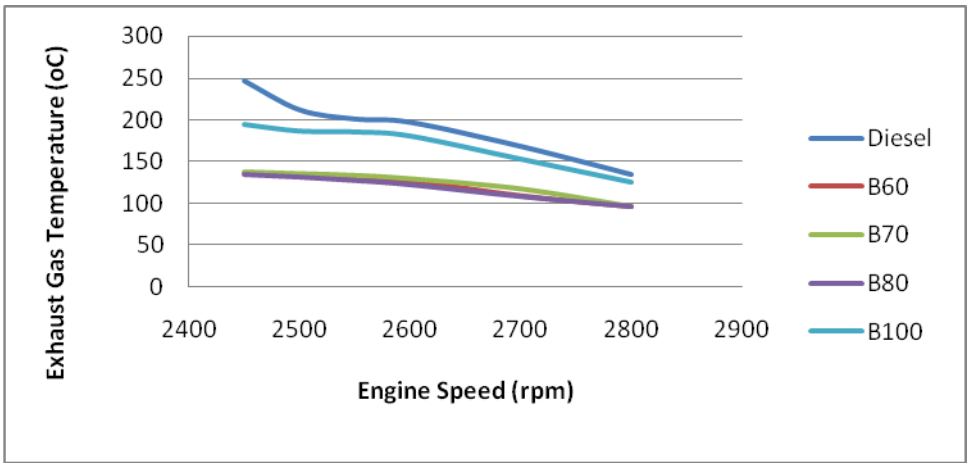

Figure 4: Variation of Exhaust Temperature against Engine Speed for Diesel and all Tested Blends

Percentages heat loss to Exhaust : The percentage heat loss shows a reduction with increasing engine speed as noted in the exhaust gas temperature for both diesel and jatropha oil/diesel blends. For higher biodiesel jatropha blends, there were significant reductions in the percentage heat losses with B80 having the minimum. It is noted that the biodiesel jatropha fuel blends lost less useful heat energy when compared to diesel reference fuel. This useful heat is lost through the flue gases leaving.

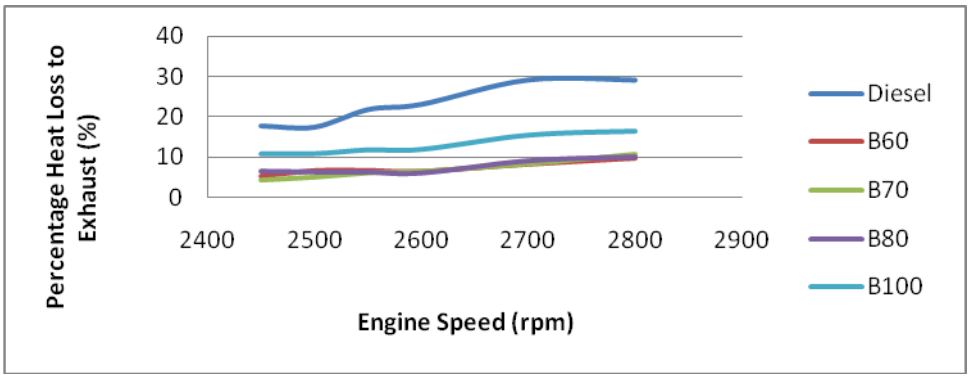

Figure 5: Variation of Percentage Heat Loss against Engine Speed for Diesel and all Tested Blends

Air / Fuel Ratio : The air /fuel ratio values increases at higher engine speeds for diesel reference fuel and other biodiesel jatropha blends with diesel having higher values. The maximum air / fuel ratio value observed for biodiesel jatropha blends was for B100. There were increased in engine noise for higher biodiesel jatropha blends and this could be attributed to the deficient air/fuel ratio.

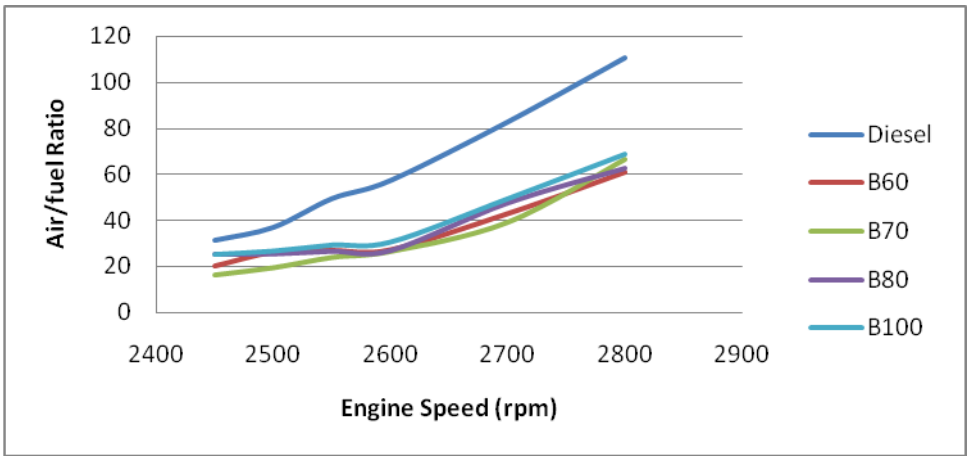

Figure 6: Variation of Air/Fuel ratio against Engine Speed for Diesel and all Tested Blends

Volumetric Efficiency : There were no significant difference in the volumetric efficiencies at lower and higher speeds for diesel reference fuel and biodiesel jatropha blends. However, the diesel reference demonstrated better volumetric efficiency at all speeds with B100 having the best among the biodiesel jatropha blends.

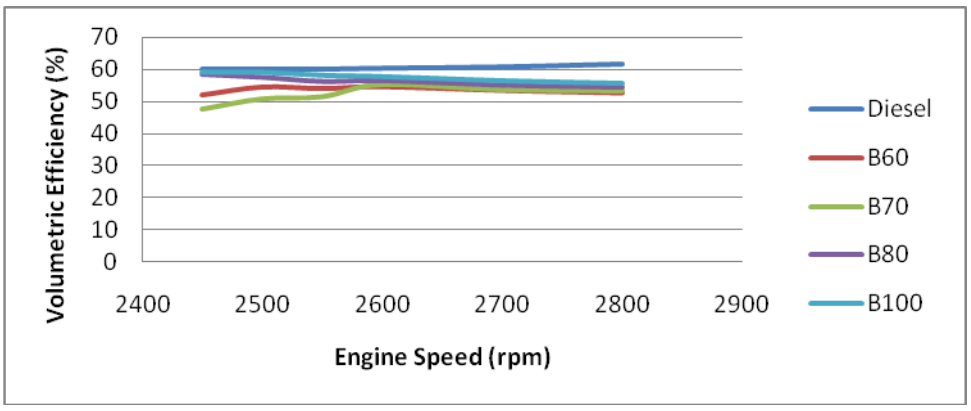

Figure 7: Variation of Volumetric Efficiency against Engine Speed for Diesel and all Tested Blends

VI. CONCLUSION

The operational parameters of a single cylinder two stroke engine run on biodiesel jatropha as an automobile engine were determined. The study shows that diesel reference fuel exhibited superior performance characteristics when compared to biodiesel jatropha blends in terms of brake power, specific fuel consumption, brake thermal efficiency, air/fuel ratio and volumetric efficiency while biodiesel jatropha blends demonstrated better performance for exhaust gas temperatures and percentage heat loss to exhaust. Furthermore, for the biodiesel jatropha blends, B100 gave best optimum result due to its relatively high brake thermal efficiency and low specific fuel consumption despite its high percentage of heat loss to flue gases.There was no reaction of the biodiesel jatropha blends with engine parts as there was no engine starting problems, wear out of components or breakdown. No long term assessment, emission characteristics or endurance tests including breakdown of biodiesel jatropha were carried out.

REFERENCES

[1] Barnwal B K and Sharma M P (2005). Prospects of biodiesel production from vegetable oils in India. Renewable and Sustainable Energy Reviews, Vol. 9, pp 363-378.

[2] Duraisamy M K, Balusamy T and Senthilkumar T (2011). Reduction of NO_X Emissions in Jatropha Seed oil-fueled CI Engine. ARPN Journal of Engineering and Applied Sciences, Vol. 6, No. 5, pp 34-39.

[3] Duvuna G.A and Wara A. A (2012). Determination of Operational Parameters of a Single Cylinder Two Stroke Engine Run on Jatropha Biodiesel. Advanced Materials Research, Vol. 367 pp 525-536.

[4] Kritana Prueksakorn and Shabbir H. Gheewala (2006). Energy and Greenhouse Gas Implications of Biodiesel Production from Jatropha curcas. The 2nd Joint International Conference on "Sustainable Energy and Environment (SEE 2006)". 21-23 November, Bangkok, Thailand.

[5] Loganathan M, Anbarasu A and Velmurugan A (2012). Emission Characteristics of Jatropha-Dimethyl Ether Fuel Blends on A DI Diesel Engine. International Journal of Scientific and Technology Research, Vol. 1, No. 8, pp 28-32.

[6] Munear T, Asift M. (2005). Energy Supply, its demand and security issues for developed and emerging economies. Renewable and Sustainable Energy Review

[7] Nagaraja AM, Prabhukumar G.P (2004). Characterization and optimization of rice bran oil methyl ester for CI engines at different injections pressures. Society of Automotive Engineers. 28: 0039.

[8] Naik S N, Meher L C and Vidya Sagar D (2006). Technical aspects of biodiesel production by transesterification - A review. Renewable and Sustainable Energy Reviews, Vol. 10, pp 248-268.

[9] Naveen Kumar and Abhay Dhuwe (2004). Fuelling an agricultural diesel engine with derivative of palm oil. Society of Automotive Engineers, Vol. 28, pp 39.

[10] Naveen Kumar and Sharma P.B (2005). Jatropha Curcus A. sustainable source for production of Bio-diesel: Journal of scientific and Industrial Research (JSIR), Vol. 64, pp 883- 889.

[11] Neto da Silva F., Salgado Prata A and Rocha Teixeira J (2003). Technical Feasibility Assessment of Oleic Sunflower Ethyl Ester Utilization in Diesel Bus Engine, Energy Conservation and Management, Vol. 44, No. pp 2857-2878

[12] Nwafor O.M.I (2004) Emission Characteristics of Diesel Engine Operating on Rapeseed Methyl Ester, Renewable Energy, Vol. 29, pp 119-129

[13] Pramanik K (2003). Properties and use of jatropha curcas oil and diesel fuel blends in c.i engines: Renewable Energy Vol. 28

[14] Ramadhas A S, Jayaraj S and Muralidharan C. 2004. Use of vegetable oils as IC engine fuels- A review. Renewable Energy, Vol. 29, pp 727-742.

[15] Roberte E Bailis and Jennifer E Baka (2010). Greenhouse Gas Emissions and Land Use Change from Jatropha Curcas-Based Jet Fuel in Brazil. Environmental Science Technology, Vol. 44, pp 8684–8691.

[16] Shailendra Sinha and Avinash Kumar Agarwal (2005). Combustion characteristics of ricebran oil derived biodiesel in a transportation diesel engine. Society of Automotive Engineers, Vol. 26, pp 354.

[17] Suryawanshi J G and Despande N V (2004). Experimental investigations on a pungamia oil methyl ester fuelled diesel engine. Society of Automotive Engineers, Vol. 28, pp 18.

[18] Tint Tint Kywe and Mya Oo (2009): Production of bio-diesel from Jatropha oil in pilot plant, proceedings of world academy of science, engineering and technology Vol. 28, No. , pp.

[18] Usta N, Ozturkb E, Canb O, Conkura E S, Nasc S, Con A H, Cana A C and Topeua M (2005). Combustion of Bio-diesel Fuel Produced from Hazelnut Soapstock/Waste Sunflower Oil Mixture in a Diesel Engine, Energy Conservation and Management, Vol. 46, No. pp 741-755

[19] Xie W and Haito Li (2006). Alumina-supported potassium iodine as a heterogenous catalyst for bio-diesel production from soya bean oil: Journal of Molecular Catalysis A: Chemical Vol. 255 No. 1-2, pp 1-9.

American Journal of Engineering Research (AJER)
e-ISSN : 2320-0847 p-ISSN : 2320-0936
Volume-03, Issue-11, pp-70-76
www.ajer.org

Research Paper Open Access

Static Linear and Nonlinear Analysis of R.C Building on Sloping Ground with Varying Hill Slopes

K.S.L.Nikhila[1], Dr.B.Pandurangarao[2]
[1](Professor&Dean, Department of Civil Engineering V.R.Siddhartha Engineering College, Vijayawada)
2(M.Tech Student, Department of Civil Engineering V.R.Siddhartha Engineering College, Vijayawada)

ABSTRACT: *Earthquake field investigations repeatedly confirm that irregular structures suffer more damage than their regular counterparts. This is recognized in seismic design codes, and restrictions on abrupt changes in mass and stiffness are imposed. Irregularities in dimensions affect the distribution of stiffness, and in turn affect capacity, while mass irregularities tend to influence the imposed demand. Elevation irregularities have been observed to cause story failures due to non-uniform distribution of demand-to-supply ratios along the height. Plan irregularities, on the other hand, cause non-uniform demand-to-capacity ratios amongst the columns. In this paper the structure chosen for study is a 4, 5 storied commercial complex building. The building is located in seismic zone IV on a rock soil site. Three dimensional mathematical models for the same are generated in ETABS software. The structural elements, M40 grade of concrete, floor diaphragms are assumed to be rigid. Seismic loads were considered acting in the horizontal direction along either of the two principal directions and the ground slope choosen in between 0° and 25° and building that which produce less torsion effect for setback - stepback with irregular configuration in horizontal and vertical direction is modeled and analyzed.*

KEYWORDS: *Setback-Stepback, Static linear analysis, Static Nonlinear Analysis ,Base shear, Target displacement, Hinge Status*

I. INTRODUCTION

In many parts of India it is a common practice to construct buildings on hill slopes, if there is a natural hill sloping terrain. The building on a sloping terrain undergo severe torsion under earthquake excitation due to considerable variation in the height of ground floor columns .Buildings constructed on hill slopes are highly unsymmetrical in nature. The scarcity of plain ground in hilly areas compels construction activity on sloping ground resulting in various important buildings such as reinforced concrete framed hospitals,colleges,hotels and offices resting on hilly slopes. Since the behavior of building during earthquake depends upon the distribution of mass and stiffness in both horizontal and vertical planes of the buildings, both of which vary in case of hilly building with irregularity and asymmetry due to stepback –setback configuration .Such constructions in seismically prone areas makes them exposed to great shears and torsion as compared to conventional buildings.
Hence, while adopting practice of multistorey buildings in these hilly and seismically active areas, utmost care should be taken for making these buildings earthquake resistant.

Every structure is subjected to elastic and inelastic behavior .Since inelastic behavior is intended in most of structures subjected to infrequent earthquake loading , the use of nonlinear analysis is essential to capture behavior of structures under seismic effects .Due to simplicity, the structural engineering profession has been using the nonlinear static procedure (or)Pushover analysis, described in FEMA-356 and ATC-40 .It is widely accepted that ,when pushover analysis is used carefully, it provides useful information that cannot be obtained by linear static or dynamic analysis procedures. In the implementation of pushover analysis, modeling is one of the important steps. The model must consider nonlinear behavior of structure/ elements .Such a model requires the determination of the nonlinear properties of each component in the structure that are quantified by strength and deformation capacities.

II. OBJECTIVES

The objective of this work is to study the linear, nonlinear behavior and performance of building frame on sloping ground depends on various hill slopes and number of stories. The objective of study is as follows:

1. To study the variation of base shear, displacement, drifts with respect to variation in various hill slopes
2. To study the target displacement, performance i.e. plastic hinges formation in various hilly slopes. And finding the angle that subjected to less torsion and which is safe in increasing the height of building.

III. LITEARTURE REVIEW

Mr.Satish Kumar and Mr.D.K.Paul have presented the methodology of analysis for irregular buildings with rigid floor system where center of mass and center of stiffness of each floor lie on different vertical axes .A.K.Jain evaluated the eccentricity distribution for floor eccentricity and storey eccentricity for different types of lateral load distribution along the height of the building. Mr.B.G.Birajdar and Mr. S.S.Nalawade presented the results obtained from seismic analysis performed on three different configuration.viz. Stepback building, Setback building, Stepback-Setback building. 3-D analysis including torsional effect has been carried out by using response spectrum method. It has been found that combination of stepback –setback building was less affected by torsion as compared to stepback building. Hence they observed that Stepback-Setback buildings are found to be more suitable on sloping ground.

IV. ANALYSIS METHODS

Static analysis methods are broadly classified as linear static and nonlinear static analysis .In linear static analysis will produce the effect of the higher modes of vibration and the actual distribution of forces in the elastic range i.e, which the response of building is assumed as linear elastic manner .This analysis is carried out as per IS1893-2002(Part-1) Nonlinear static analysis is an improvement over linear static and linear dynamic analysis in the sense that it allows the inelastic behavior of the structure .The nonlinear analysis of a structure is an iterative procedure .It depends on the final displacement ,as the effective damping depends on the hysteric energy loss due to inelastic deformations h in turn depends on the final displacement .This makes the analysis procedure iterative. Difficulty in the solution is faced near the ultimate load, as the stiffness matrix at this point becomes negative definite due to instability of the structure becoming a mechanism. Software available to perform nonlinear static analysis as ETABS,(Extended Three Dimensional Building System) and Structural Analysis Program finite element program that works with complex geometry and monitor deformations at all hinges to determine ultimate deformation. It has built-in defaults for ACI 318 material properties and ATC-40and FEMA 273 hinge properties. Also it has capability for inputting any material or hinge property. ETABS 9.7 deals with the buildings only. The analysis in ETABS 9.7 involves the following four step.1) Modeling,,2) Static analysis, 3)Designing, 4)Pushover analysis Steps used in performing.

Fig A. Graph shows the curve Force Vs. Deformation

1. Point A corresponds to unloaded condition.
2. Point B represents yielding of the element.
3. The ordinate at C corresponds to nominal strength and abscissa at C corresponds to the deformation at which significant strength degradation begins.
4. The drop from C to D represents the initial failure of the element and resistance to lateral loads beyond point C is usually unreliable.
5. The residual resistance from D to E allows the frame elements to sustain gravity loads. Beyond point E, the maximum deformation capacity, gravity load can no longer be sustained.

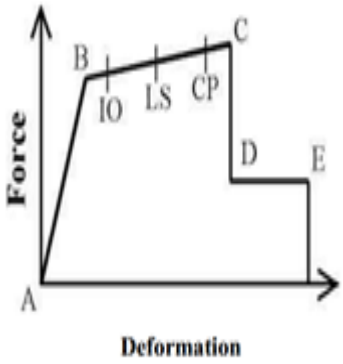

PLASTIC HINGE MECHANISM : In deciding the manner in which a beam may fail it is desirable to understand the concept of how plastic hinges form where the beam is fully plastic. At the plastic hinge an infinitely large rotation can occur under a constant moment equal to the plastic moment of the section. Plastic hinge is defined as a yielded zone due to bending in a structural member at which an infinite rotation can take

place at a constant plastic moment Mpof the section. The number of hinges necessary for failure does not vary for a particular structure subject to a given loading condition, although a part of a structure may fail independently by the formation of a smaller number of hinges. The member or structure behaves in the manner of a hinged mechanism and in doing so adjacent hinges rotate in opposite directions. Theoretically, the plastic hinges are assumed to form at points at which plastic rotations occur. Thus the length of a plastic hinge is considered as zero. The values of moment, at the adjacent section of the yield zone are more than the yield moment up to a certain length ΔL, of the structural member. This length ΔL is known as the hinged length. The hinged length depends upon the type of loading and the geometry of the cross-section of the structural member. The region of hinged length is known as region of yieldorplasticity.

Mechanism : When a system of loads is applied to an elastic body, it will deform and will show a resistance against deformation. Such a body is known as a structure. On the other hand if no resistance is set up against deformation in the body, then it is known as a mechanism.

Plastic moment condition: The bending moment at any section of the structure should not be more than the fully plastic moment of the section.

V. DESCRIPTION OF STRUCTURES.

The structure choosen is of type setback –stepback which is 4 storied, 5-storied with different hill slopes varying from 0 to 25 degress.. The presence of abrupt reduction of the lateral dimension of the building at specific levels of the elevation. This building category is known as 'setback and stepback building'. The structure chosen material in which is subjected to less torsion effect.

Detailed data of buildings

General details of building				
No of Storey				4 Storey,5Storey
Storey Height				Floor to Floor Height=3.5mts
				Plinth Height=1.75mts
Building frame system				OMRF
The concrete floors are modeled as				Rigid
Building use				Commercial Building
Foundation type				Stepped
Seismic Zone				IV
Soil Type				ROCK
Material Properties				
Grade of concrete				M40
Grade of steel				415N/mm^2
Youngs Modulus of M40 concrete,E				5000√fck
Density of concrete				25KN/m^3
Poison's ratio (of concrete)				0.2
Density of Brick masonary				19KN/m^3
Structural members				
Thick ness of Slab				0.12mts
All beam Size				For 4 storied=0.23*0.45mts
				For 5 storied=0.30*0.45mts
All Column Size				For 4 storied=0.23*0.50mts
				For 5 storied=0.30*0.50mts
Thickness of wall				Full brick wall=0.230mts
				Half brick wall=0.115mts
Assumed Dead load intensities				
Floorfinishes				1.5KN/m^3
Live load				3KN/m^3
Earthquake LL on slab as per Clause 7.3.1 and 7.3.2 of IS 1893(part-1)-2002				
Roof				0 KN/m^2
Floor				0.25 x 3.0 = 0.75kN/m^2
EARTHQUAKE PARAMETERS				
Time period T				0.09h/√d
Importance factor				1
Sa/g				1/T,2.50
Response Reduction Factor				3
LOAD CASES FOR PUSHOVER ANALYSIS				
Pushover cases	Names	Loads	Controlled by	
1	Gravity	DL+0.25LL	Forces	

2	PUSH X	EQX	Displacements	
3	PUSHY	EQ	Displacements	

SKETCHES

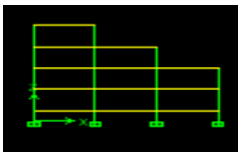

4-BAY 0^0

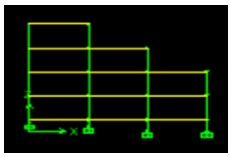

4-BAY 5^0

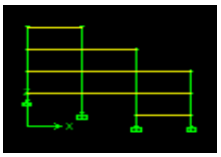

4-BAY 10^0

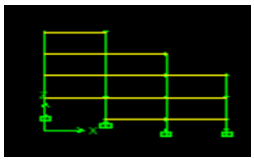

4-BAY 16.32^0

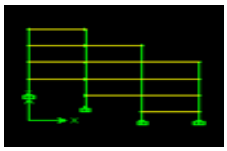

4-BAY21.58^0

FIGURES AND TABLES FROM STATIC LINEAR ANALYSIS

DISPLACEMENTS

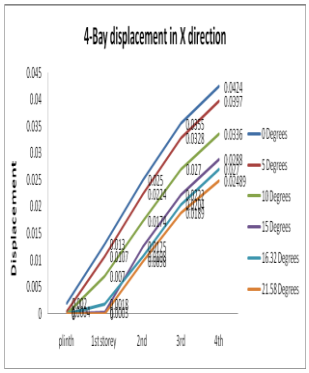

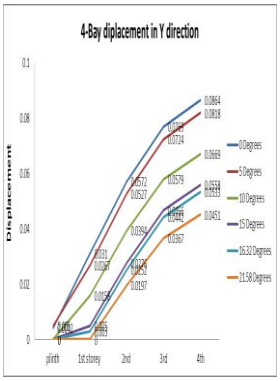

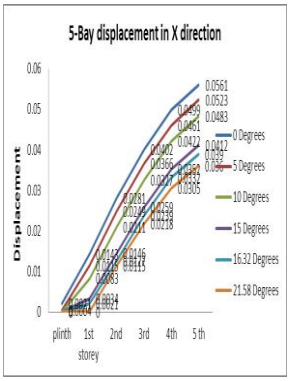

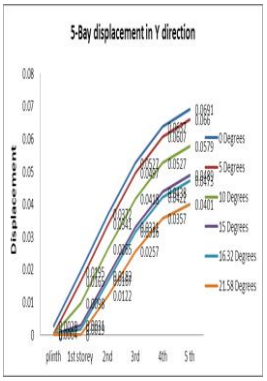

DRIFTS

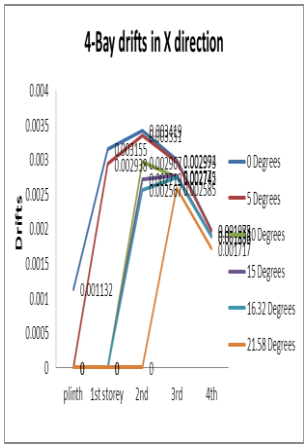

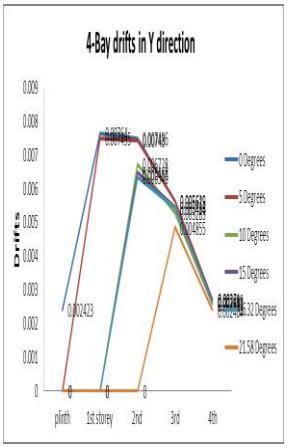

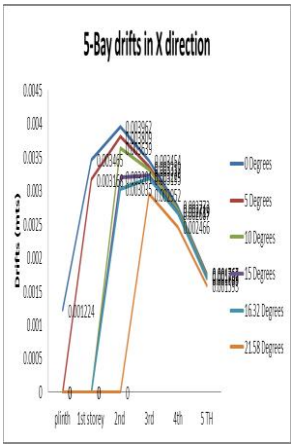

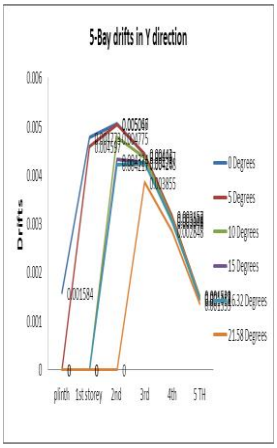

STOREY SHEARS

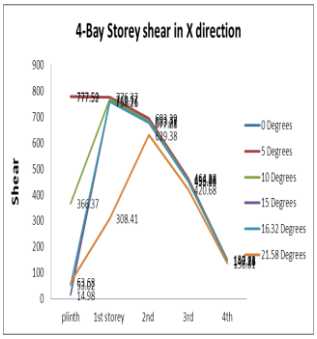

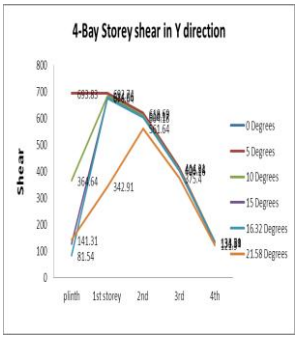

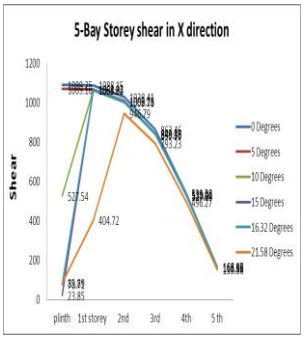

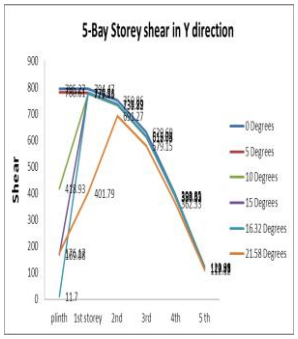

BASE SHEAR

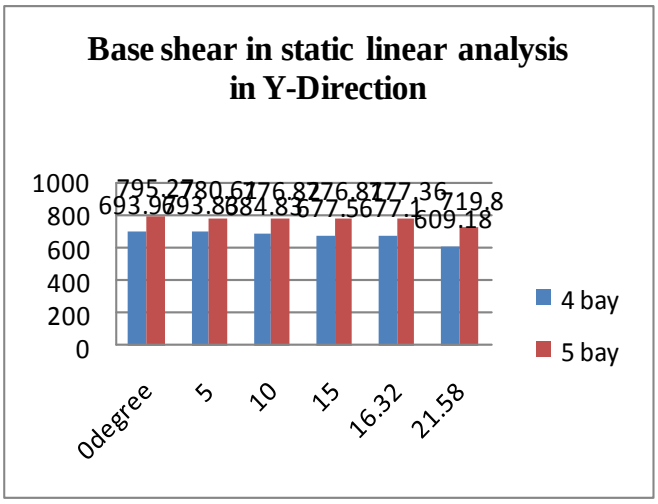
Base shear in static linear analysis in Y-Direction
1000
800
600
400
200
0
693.96
693.88
684.83
677.56
677.1
609.18
719.8
4 bay
5 bay
0degree
5
10
15
16.32
21.58

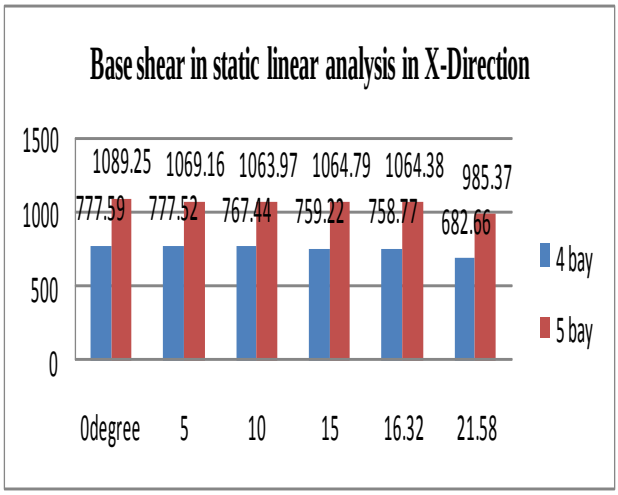
Base shear in static linear analysis in X-Direction
1500
1000
500
0
1089.25
1069.16
1063.97
1064.79
1064.38
985.37
777.59
777.52
767.44
759.22
758.77
682.66
4 bay
5 bay
0degree
5
10
15
16.32
21.58

TABLES FROM NONLINEAR STATIC ANALYSIS

X-DIRECTION **Y-DIRECTION**

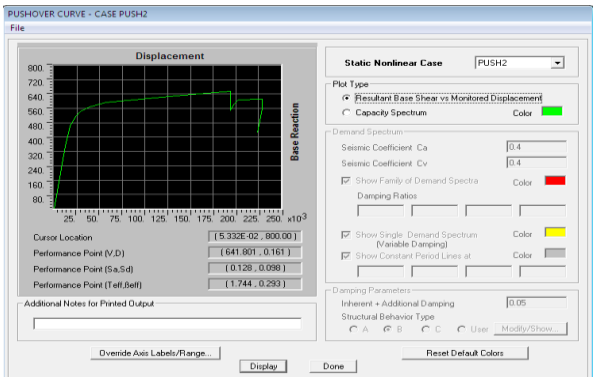

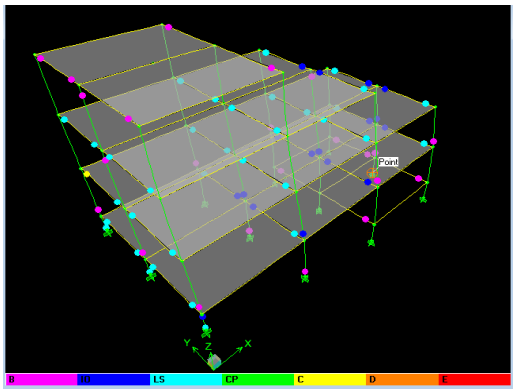

HINGE PERFORMANCE OF STRUCTURE **m PUSHOVER CURVE IN X- DIRECTION**

V. CONCLUSION

[1] The performance of reinforced concrete frames was investigated using the pushover analysis

[2] From this analysis the observations are as the angle of slope increases base shear increases and displacement decreases.

[3] The base shear acts more in longitudinal direction than in transverse direction.

[4] It is observed that left columns, which are on the higher side of the sloping ground and are short, are most affected. Special attention is required while designing short columns.

[5] As the slope increases no of hinges will decreases.

[6] From this we observed that for 15, 16.32 degrees are safe upto 5- bay .But as the bay increases more no of hinges are to be formed and subjected to collapse region.

[7] In static linear analysis we observed that as the angle of slope increases storey shear decreases and base shear decreases

MODELS	TARGET DISPLACEMENT(mm)	BASESHEAR (KN)	PERFORMANCE LEVEL	NO OF HINGES
4-Bay 0^0	128	546.409	LS-CP	382
5^0	126	546.5862	LS-CP	382
10^0	119	569.034	C-D	356
15^0	105	603.184	LS-CP	330
16.32^0	96	612.650	LS-CP	330
21.58^0	101	596.305	C-D	304
MODELS	**TARGET DISPLACEMENT(mm)**	**BASESHEAR(KN)**	**PERFORMANCE LEVEL**	**NO OF HINGES**
5-Bay 0^0	141	646.88	LS-CP	474
5^0	137	646.8	LS-CP	474
10^0	133	657.660	A-B	448
15^0	123	698.460	LS-CP	422
16.32^0	114	703.851	LS-CP	422
21.58^0	121	702.473	D-E	396

[8] As the angle of slope increases displacement and drifts decreases.

[9] For the buildings studied, it is found that the plastic hinges are less in case of buildings resting on sloping ground as the slope increases. Most of these elements are in the range of LS-CP and some of the elements lie in the range of C-D which indicates failure of elements lies in the range of collapse point increases the seismic vulnerability of the structure and such elements which are in LS-CP state requires retrofitting

REFERENCES

[1] ATC-40: Seismic Evaluation and Retrofit of Concrete Buildings.
[2] FEMA-356: Prestandard and Commentary For The Seismic Rehabilitation of The Buildings.
[3] Nonlinear static pushover analysis of irregular space frame structure , Govind M1, Kiran K. Shetty2, K. Anil Hegde3 1M. Tech Final Year (Structures), Department of civil engineering, M.I.T Manipal, Karnataka, India 2Associate Professor (senior scale), Department of civil engineering, M.I.T Manipal Karnataka, India 3Senior Structural Consultant, Vimal Anil Structural Consultants, Mangalore, Karnataka, India
[4] A Performance study and seismic evaluation of RC frame buildings on sloping ground Mohammed Umar Farooque Patel1, A.V.Kulkarni2, Nayeemulla Inamdar3 1(Asst Professor, Civil Engineering Department, BLDE Engg College,Bijapur, India) 2(Professor Civil Engineering Department, BLDE Engg College, Bijapur, India) 3(Asst Professor, Civil Engineering Department, BLDE Engg College,Bijapur, India)
[5] Seismic Analysis of Buildings Resting on Sloping Ground with Varying Number of Bays and Hill Slopes
[6] Dr. S. A. Halkude1, Mr. M. G. Kalyanshetti2, Mr. V. D. Ingle3 (Civil Engg. Dept. W. I. T. Solapur, University, India)
[7] Pushover analysis of unsymmetrical framed structures on sloping Ground 1n. Jitendra babu, 2k.V.G.D balaji & 3s.S.S.V gopalaraju 1Assistant professor, k l university, guntur, india 2professor, gitam university, visakhapatnam - 530 045, andhra pradesh, india 3professor & head gitam university, hyderabad, india
[8] Effect of Irregular Configurations on Seismic Vulnerability of RC Buildings Ravikumar C M1,*, Babu Narayan K S1, Sujith B V2, Venkat Reddy D1 1Department of Civil Engineering, National Institute of Technology, Surathkal, 575025, India 2Department of Studies in Civil Engineering, U.B.D.T College of Engineering, Davangere, 577004, India cmravibdt@gmail.com, sujithbv@gmail.com
[9] Seismic analysis of buildings resting on sloping Ground by B.GBirajdar1,S.S.Nalawade2.
[10] Effects of plastic hinge properties in nonlinear analysis of reinforced concrete buildings by Mehmet Intel,Hayri Baytan Ozmen .Dept of Civil Engineering Pamukkale University.
[11] Pankaj Agarwal –Earthquake Resistant Design Of Structures.
[12] A.K.Chopra-Dynamics of Structures.

American Journal of Engineering Research (AJER)
e-ISSN : 2320-0847 p-ISSN : 2320-0936
Volume-03, Issue-11, pp-77-84
www.ajer.org
Research Paper Open Access

Genetic Algorithm Based Transmission Expansion Planning System

Dike, Damian Obioma
Electrical & Electronic Engineering Department, Federal University of Technology, Owerri Nigeria.

ABSTRACT: *This paper presents an application of genetic algorithm (GA) to the solution of Static Transmission Expansion Planning (STEP) to determine the optimal number of transmission circuits required in each network corridor and their respective network adequacy while satisfying various economic and technical constraints. The uncertainties in generation and distribution networks as a result of power system deregulation cannot be modeled effectively using the conventional mathematical methods. GA, been a probabilistic based approach has the ability to resolve the transmission expansion planning problem in the face of such uncertainties. The model presented in this work will help in the identification of overloaded lines using Gauss Seidel (GS) load flow technique. Result from GS is then used as input in the GA simulation to show the extra lines needed to accommodate present load flow in the system. The model was tested on IEEE 14 – bus test network.The model developed and simulation results obtained may be useful in an electric power systems undergoing deregulation. Such is the case in Nigeria presently where the generation and distribution components are increasing significantly without any commensurate boost in the transmission sector. This leads to line overloads necessitating commensurate and immediate expansion of the grid.*

KEYWORDS: ***Deregulation, Gauss Seidel, Genetic algorithm,*** *Transmission expansion planning and System overload.*

I. INTRODUCTION

The basic principle of TEP is to minimize the network construction and operational costs while satisfying the requirement of delivering electric power safely and reliably to load centers along the planning horizon [1]. The expansion of a transmission network may include the construction of new overhead lines or underground cable in new corridors, and the upgrading of existing lines or cables in corridors already in use by increasing the number or the capacity of lines or cables, increasing the rated voltage, the improvement on the capacity and control equipment (FACTS, Capacitor banks etc.). In a more broad sense, one may also consider the introduction of generators in appropriate places to allow a better balance between generation and loads, and better use of the network, increasing the transmission capacity of the network.
From the stake-holders point of view, transmission expansion should attend the following targets [2].

- Encourage and facilitate competition among market participants;
- Provide non-discriminatory access to cheap generation for all consumers;
- Alleviate transmission congestion;
- Minimize the investment, the risk of investments and operation costs;
- Increase the reliability of the network;
- Increase the flexibility of system operation while reducing the network charges;
- Minimize the environmental impacts;
- Allow better voltage level regulation.

Even though the principles are quite simple, the complexity of the problem and the impact on society due to the heavy investments that have to be made, together with the costs incurred due to failures, make TEP on as a challenging issue. The following are some of the factors that distinguish TEP as a challenging field in power system analysis [2].

- Complexity of the problem; TEP is a complex problem because it has a mixed integer nonlinear programming nature. It is also a complex mathematical problem as it involves, typically, a large number of variables.

- Usually, heavy investments must be made. This kind of investments goes a long way to strain the economy of the country or region undergoing such expansion plans.

Transmission expansion planning addresses the problem of strengthening an existing transmission network to optimally serve a growing electricity market while satisfying a set of economic and technical constraints. Various techniques, including simulated annealing, tabu search, evolution strategies, greedy randomized adaptive search procedure (GRASP), probabilistic reliability criteria (PRC), and probabilistic load flow (PLF), have been used to study the problem [3] – [7]. It is difficult to obtain the optimal solution of a composite power considering the generators and transmission lines simultaneously in an actual system, and therefore, transmission expansion planning is usually performed after generation expansion planning.

This paper presents a method for determining the optimal number of transmission circuits required in each network corridor using genetic algorithm (GA). Gauss – siedel power flow algorithm was used to determine the line flows and voltage magnitudes in each network corridor and network bus respectively. The static transmission expansion planning (STEP) problem was formulated using a DC power flow model [8], [9].

This paper is organized as follows; Section II describes in details the Genetic Algorithm theory. Section III describes the mathematical modeling of the chosen solution method. Section IV describes the application of GA theory to solve transmission expansion planning, i.e. implementation. Section V shows the results obtained from the application of GA in transmission expansion planning. Section VI summarizes the conclusion of the work.

II. GENETIC ALGORITHM (GA)

The use of Genetic Algorithm for problem solving is not new. The pioneering work of J.H. Holland in the 1970's proved to be a significant contribution for scientific and engineering applications.

GA is inspired by the mechanism of natural selection, a biological process in which the stronger individuals are likely to be the winners in the competing environment. Here, GA uses the direct analogy of such natural evolution. It presumes that the potential solution of a problem is an individual and can be represented by a set of parameters.

Standard genetic algorithm is a random search method that can be used to solve non-linear system of equations and optimize complex problems. The base of this algorithm is the selection of individuals. It doesn't need a good initial estimation for sake of problem solution, In other words, the solution of a complex problem can be started with weak initial estimations and then be corrected in evolutionary process of fitness [10].

GA also combines various operators namely; selection, crossover, and mutation operators with the goal of finding the best solution to a problem. GA searches for this optimal solution until a specified termination criterion is met. A proto-typical GA consists of the following steps

- Generate initial generation
- Measure fitness
- Select a mating pool
- Mutate randomly selected member of the mating pool
- Pair the members of the mating pool.
- Perform crossover to obtain the new generation
- Iteration continues until some stopping condition is satisfied.

The Mutation operator selects one of existed integer numbers from the mating pool and then changes its value randomly. Reproduction operator, similar to standard form, reproduces each individual proportional to the value of its objective function. Therefore, the individuals which have better objective functions will be selected more probable than other chromosomes for the next population [15].

The selection operator selects the individual in the population for reproduction. The more fit the individual, the higher its probability of being selected for reproduction. The crossover operator involves theswapping of genetic material (bit-values) between the two parent strings. Based on predefined probability, known as crossover probability, an even number of individuals are chosen randomly. Each individuals (children) resulting from each crossover operation will now be subjected to the mutation operator in the final step to forming the new generation. The mutation operator enhances the ability of the GA to find a near optimal solution to a given problem by maintaining a sufficient level of genetic variety in the population, which is needed to make sure that the entire solution space is used in the search for the best solution.

In the context of TEP, the alternative expansion plans are referred to as the individuals. These individuals are what make up the mating pool as stated above. The power flows in the network together with other line flow constraints are all modeled mathematically and constitute part of the Algorithm [10], [11].

III. MATHEMATICAL MODELLING

In this section, the mathematical models as proposed in [8], [12] and [13] are outlined. It consists of a Power flow model and a static transmission expansion planning (STEP) model.

A. Power flow model

This provides a model of the nonlinear relationships among bus power injections, power demands, bus voltages and angles with the network constants providing the circuit parameters.

The power flow model provides information on the electrical performance of the lines with actual power flows in such lines. They also provide information about the line and transformer loads as well as losses throughout the system and voltages at different points in the system [12].

In developing power flow equations, a 3 – phase balanced system operation is assumed; hence per – phase analysis is utlized to obtain the necessary equations.

$$S_i \triangleq S_{Gi} - S_{Di} \quad (1)$$

$$I_i = I_{Gi} - I_{Di} \quad (2)$$

$$I_i = \sum_{k=1}^{n} Y_{ik} V_k \quad (3)$$

$$S_i = V_i I_i^* = V_i \sum_{k=1}^{n} Y_{ik}^* V_k^* \quad (4)$$

$$V_i \triangleq |V_i| e^{\angle V_i} = |V_i| e^{j\theta_{ik}} \quad (5)$$

$$\theta_{ik} = \theta_i - \theta_k \quad (6)$$

$$Y_{ik} \triangleq G_{ik} + jB_{ik} \quad (7)$$

$$S_i = \sum_{k=1}^{n} |V_i||V_k|(G_{ik}\cos\theta_{ik} + B_{ik}\sin\theta_{ik}) \quad (8)$$

Resolving into real and imaginary parts we obtain

$$P_i = \sum_{k=1}^{n} |V_i||V_k|(G_{ik}\cos\theta_{ik} + B_{ik}\sin\theta_{ik}) \quad (9)$$

$$Q_i = \sum_{k=1}^{n} |V_i||V_k|(G_{ik}\sin\theta_{ik} - B_{ik}\sin\theta_{ik}) \quad (10)$$

Gauss – Siedel power flow modification was also adopted as highlighted in this section.

Recall from equation 4 that:

$$S_i = V_i I_i^* = V_i \sum_{k=1}^{n} Y_{ik}^* V_k^* \quad i = 1,2,\ldots\ldots n$$

$$S_i^* = V_i^* \sum_{k=1}^{n} Y_{ik} V_k \quad i = 2,3,\ldots\ldots,n \quad (11)$$

$$\frac{S_i^*}{V_i^*} = Y_{ii}V_i + \sum_{\substack{k=1 \\ k\neq i}}^{n} Y_{ik}V_k, \quad i = 2,3,\ldots\ldots\ldots,n \quad (12)$$

$$V_i = {}^{1}/_{Y_{ii}}\left[\frac{S_i^*}{V_i^*} - \sum_{\substack{k=1 \\ k\neq i}}^{n} Y_{ik}V_k\right], i = 2,3,\ldots\ldots\ldots,n \quad (13)$$

$$V_i = {}^{1}/_{Y_{ii}}\left[\frac{(P_i^{sch} - jQ_i^{sch})}{V_i^*} - \sum_{\substack{k=1 \\ k\neq i}}^{n} Y_{ik}V_k\right], i = 2,3,\ldots\ldots n \quad (14)$$

Where P_i^{sch} and Q_i^{sch} are the net real and reactive powers expressed in per-unit. Thus, for buses where real and reactive power are injected into the bus, such as generator buses, P_i^{sch} and Q_i^{sch} have positive values.For Load buses where real and reactive powers are flowing away from the bus, P_i^{sch} and Q_i^{sch} have negative values.

$$P_i = \Re\left\{V_i^*\left[V_i Y_{ii} + \sum_{\substack{j=1 \\ j\neq i}}^{n} Y_{ij}V_j\right]\right\} \quad j \neq i \quad (15)$$

$$Q_i = \Im\left\{V_i^*\left[V_i Y_{ii} + \sum_{\substack{j=1 \\ j\neq i}}^{n} Y_{ij}V_j\right]\right\} \quad j \neq i \quad (16)$$

For the voltage controlled buses, the bus voltage must be equal to the specified voltage. Also, the maximum and minimum reactive powers at these buses are also specified and the value of $Q_i (for\ i = 1,2,3,\ldots.n)$ must lie between these limits. [23], [24].

Thus, the conditions to be met are as follows:

1. $|V_i| = |V_i|_{spec}\ for\ i = 2,3,\ldots\ldots.n$
2. $Q_{i\,min} < Q_i < Q_{i\,max}\ for\ i = 2,3,\ldots\ldots.n$

If during any of the iterations, we find out that Q_i is outside the limits specified, Q_i is fixed at the minimum or the maximum value as the case may be and then the bus is treated as a PQ bus (load bus).

B. Static transmission expansion planning model

Generally, transmission expansion planning could be classified as static or dynamic. Static expansion determines where and how many new transmission lines should be added to the network up to the planning horizon [8]. Implicitly, we could infer the major goal of Static TEP is finding an appropriate number of new circuits that should be added to the transmission network.

The Static transmission expansion planning problem was formulated as follows using a DC power flow model [8], [9].

$$TC = \sum_{i,j\in\Omega} C_{ij} \times n_{ij} \quad (17)$$

Where

TC: Construction cost of lines along the planning horizon

C_{ij}: Construction cost of each line in corridor $i-j$.

Equation 19 represents the construction cost of new lines which should be added to the network for delivering safe and reliable electric power to load centers over the planning horizon. Several constraints are also modeled in a mathematical representation to ensure that the mathematical solutions are in line with planning requirements. These constraints are stated in the following sections [8].

$$P_i = \sum_{j=1}^{NB} P_{ij} + d_i \, (i = 1,2,\dots\dots,NB), (\forall i,j \in \Omega) \quad (18)$$

Where, NB = total number of buses in the network

P_i &d_i: Generation and demand on bus i

P_{ij}: Power flow of each branch $i-j$

Equation is known as the Dc power flow node balance constraint.

Also,

$$P_{ij} = \gamma_{ij} \times \left(n_{ij}^0 + n_{ij}\right) \times \left(\theta_i - \theta_j\right) \quad (19)$$

Where

γ_{ij}: Total Susceptance of circuits in corridor $i-j$

θ_i&θ_j : Voltage phase angles of buses i & j respectively

The power flow limit on the transmission line is modeled thus:

$$|P_{ij}| \leq Nl_{ij} \times P_{ij}^{max} \quad (20)$$

$$Nl_{ij} = n_{ij}^0 + n_{ij} \quad (21)$$

Where,

Nl_{ij}: Total number of circuits (new & existing) in corridor $i-j$

P_{ij}^{max}: Maximum power flow in corridor $i-j$.

By replacing P_{ij} and Nl_{ij} in equation 3.25 above with their respective expressions in equation 3.24 and 3.26 the following expression can be obtained

$$|(\theta_i - \theta_j)| \times |\gamma_{ij}| \leq P_{ij}^{max}$$

$$0 \leq n_{ij} \leq n_{ij}^{max}$$

Equation models the maximum number of lines that can be installed in each corridor of the network. Where, n_{ij}^{max} is the maximum number of constructible circuits in corridor $i-j$

IV. IMPLEMENTATION

The Gauss – Siedel power flow model was implemented using MATLAB. The flowchart used in implementing the Gauss – Siedel Power flow model is shown in Figure 1 and that of the Genetic algorithm is shown in Figure *2*.The output of the Gauss –Siedel load flow algorithm constitutes the input of the Genetic algorithm flowchart. The various blocks in the Genetic Algorithm flowchart are described in section**II**.

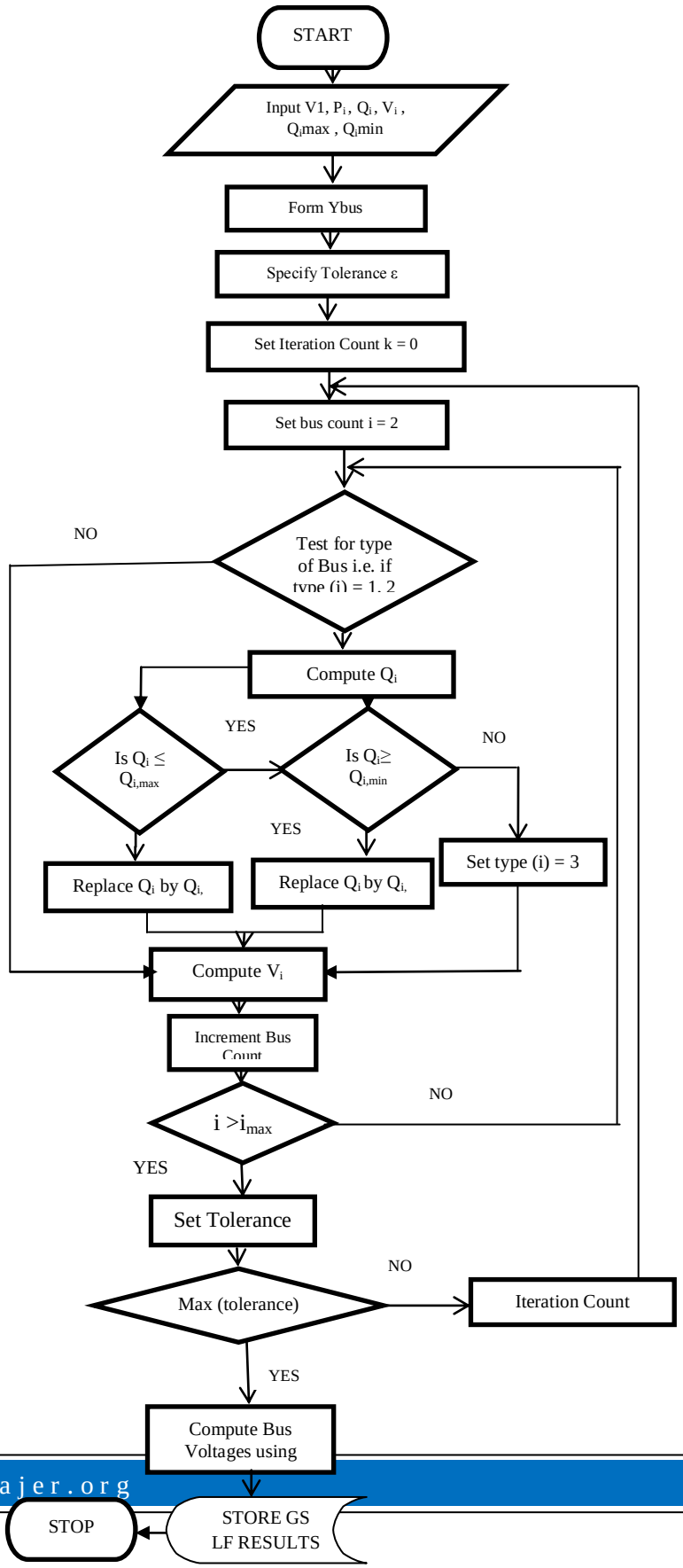
START
Input V1, Pi, Qi, Vi ,
Qimax , Qimin
Form Ybus
Specify Tolerance ε
Set Iteration Count k = 0
Set bus count i = 2
NO
Test for type
of Bus i.e. if
type (i) = 1, 2
Compute Qi
YES
Is Qi ≤
Qi,max
Is Qi≥
Qi,min
NO
YES
Replace Qi by Qi,
Replace Qi by Qi,
Set type (i) = 3
Compute Vi
Increment Bus
Count
NO
i >imax
YES
Set Tolerance
NO
Max (tolerance)
Iteration Count
YES
Compute Bus
Voltages using
STOP
STORE GS
LF RESULTS

Fig 1 Gauss – Siedel (GS) Power Flowchart

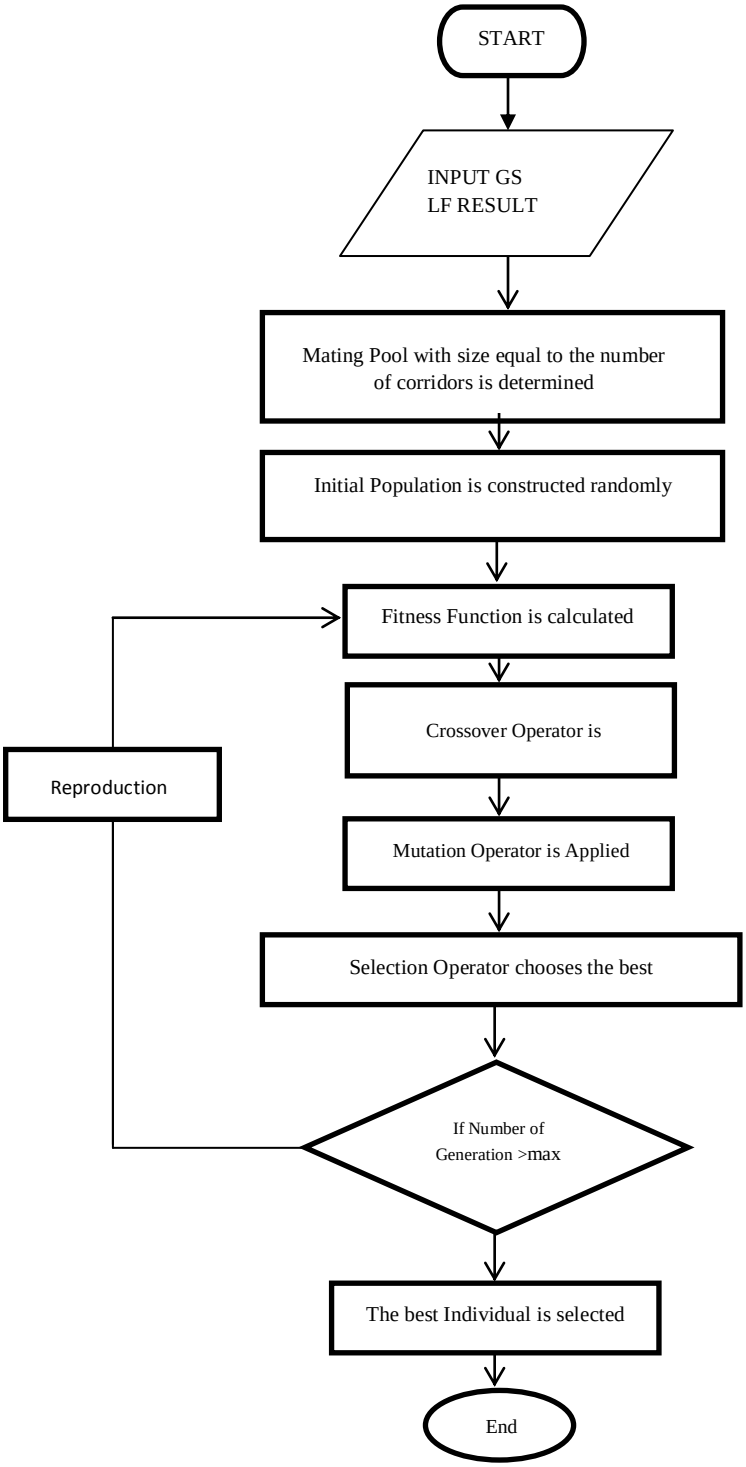

Fig. 2 Genetic Algorithm Flowchart

V. RESULTS AND DISCUSSION

IEEE 14 – bus network was used as a test system to demonstrate the effectiveness of the chosen method.The network data for the IEEE 14 – bus test network was gotten from [14].The voltage magnitude, voltage angle and line flow of the IEEE 14 – bus network as calculated are shown in tables I and II. Also, the optimal number of extra lines required in each network corridor as calculated is tabulated in Table III.

Table I: Voltage Magnitude And Voltage Angle

Bus Number	Voltage Magnitude(p.u.)	Voltage Angle
1.	1.0600	0
2.	1.0186	-4.6495
3.	1.0047	-13.0577
4.	0.9940	-10.2633
5.	0.9998	-8.7037
6.	0.9721	-15.0821
7.	0.9828	-13.8216
8.	1.0131	-13.8216
9.	0.9596	-15.7607
10.	0.9537	-15.9883
11.	0.9590	-15.6947
12.	0.9559	-16.1048
13.	0.9509	-16.1923
14.	0.9359	-17.1686

Table II: Line Flows

From Bus	To Bus	Line Flow (p.u.)
1	2	2.0220
1	5	2.8506
2	3	0
2	4	0
2	5	0.3277
3	4	0
4	5	0
4	7	0
4	9	0
5	6	0
6	11	0
6	12	0
6	13	0
7	8	0
7	9	0.6353
9	10	0.2140
9	14	0.1568
10	11	0.0373
12	13	0.0274
13	14	0

Table III: Number of New Circuits and Network Adequacy

S/NO	BRANCH	NEW CIRCUITS	NETWORK ADEQUACY (YEARS)
1.	1 – 2	4	6
2.	1 – 5	5	1
3.	2 – 5	0	5
4.	9 – 10	0	5

Table I and Table II show us the status of the network during the expansion year. A load growth coefficient of 1.07 was used to ascertain how the network would fare with yearly increase in demand. The transmission network adequacy is a measure of the length of time within which the transmission expansion plan would still be viable. The following can be inferred from the results so obtained:

- Line flow in branch 1 – 2 already exceeds the transmission capacity of the Line, thus the TEP proposes that 4 extra lines of the same capacity be constructed to relieve the already existing line in the branch. It also stipulates that the extra lines would become inadequate 6 years after expansion.
- Line flow of the line in corridor 1 – 5 also exceeds the transmission capacity of the line, much more than that of the line in corridor 1 – 2. Thus the TEP proposes that extra 5 lines of same capacity be constructed to relieve the already the congested line. However, the network adequacy of this plan is just 1 year. Improving the network adequacy would require an increase in the generation capacity, possibly in bus 2.
- Lines in corridors 2 – 5 and 9 – 10 both do not require extra lines; however the network adequacy of both lines is set at 5 years.

VI. CONCLUSION

This work addresses transmission system expansion planning using genetic algorithm. The number of transmission lines to decongest the branches and the corresponding network adequacy were both determined using this method. This work also provides a practical approach that could serve as a useful guide for the decision maker in selecting a reasonable expansion plan in the face of the prevalent circumstances.The model was also tested on IEEE 30 – bus network in order to ascertain the viability of the chosen methodology on diverse network models. They also suggest that transmission congestion occurs when actual or scheduled flows of electricity on a transmission lines are restricted below the level that grid users desire or when actual or scheduled flows exceeds the transmission capacity of the line.

REFERENCES

[1] Jalilizadeh, Saieed, et al, "Technical and Economic Evaluation of Voltage level in Transmission network expansion planning using GA," *Energy Conversion and Management*, 2007.

[2] Buygi, M. Oloomi; Shanechi, H.M; Balzer, G; Shahidehpour, M.; " Network Planning in unbundled power systems," *IEEE Trans. Power Syst.*,vol. 21, no. 3, pp. 1379 – 1387, Aug. 2006.

[3] A.S Braga, J.T Saraiva, "Transmission Expansion Planning and Long term marginal prices calculation using simulated annealing," *in proc. IEEE Power Tech. Conf.*, Bologna: Italy, June. 2003.

[4] Hiroyuki Mori and Yoshinori Iimura, "Transmission network expansion planning with hybrid meta-heuristic method of parallel tabu-search and ordinal optimization," *in proc. International Conf. on ISAP*, Kaohsiung, Taiwan, Nov. 2007

[5] Armando M. Leite da Silva, Warlley S. Sales, Leonidas C. Resende et al, "Evolution strategies to transmission expansion planning considering unreliability costs," *in proc. 9th International Conf. on Probabilistic methods applied to power systems*, Stockholm: Sweden; June, 2006.

[6] Silvio Binato, GersonCouto de Oliveira, and Joao Lizardo de Araijo, "A greedy randomized adaptive search procedure for transmission expansion planning," *IEEE Trans. Power Systs.*,vol. 16, no. 2, pp. 247 – 253, May, 2007.

[7] J. Choi, Trungtinh Tran, A. El-Keib, Robert Thomas, et al, "A method for transmission system expansion planning considering probabilistic reliability criteria," *IEEE Trans. Power Syst.*, vol. 20, no. 3, pp. 885 – 895, Aug. 2005.

[8] MeisamMahdavi, Hassan Monsef, "Review of static transmission expansion planning," *Journal of Electrical and Control Engineering*, vol. 1, No. 1, pp. 11 – 18, 2011.

[9] D.J. Silva, M.J. Rider, R. Romero and C.A. Murari, "Transmission expansion network planning considering uncertainties in demand," *in Proc. IEEE Power Eng. Society General Meeting*, vol. 2, pp. 1424 – 1429 , 2005.

[10] M. OloomiBuygi, H.M Shanechi, G. Balzer, M. Shahidepour, " Transmission planning approaches in restructured power systems," *in proc. IEEE Power Tech. Conf.*, Bologna, Italy, June 2003.

[11] Barros, Joao Ricardo P.; Melo, Albert C.G. and Silva, Armando M. Leite, "An approach to the explicit consideration of unreliability costs in transmission expansion planning," *Euro. Trans. Elect.Power*, vol. 17, pp. 401- 412, 2007.

[12] B.R. Gupta, "Power system analysis and design," S. Chand and Company, Ram Nagar, New Delhi, India, 2005.

[13] Arthur R. Bergen, Vijay Vittal, "Power System Analysis," Prentice Hall, Upper Saddle River, New Jersey, 2000.

[14] Power Systems Test Case Archive, [Online]. www.ee.washington.edu/research/pstca/pf14/pg_tca14bus.htm (Accessed 8th October 2013).

[15] H. Shayeghi, M. Mahdavi, H. Haddadian, "DCGA based transmission network expansion planning considering network adequacy," *World Academy of Science, Engineering and Technology*, vol. 24, pp. 807 – 812, 2008.

American Journal of Engineering Research (AJER)
e-ISSN : 2320-0847 p-ISSN : 2320-0936
Volume-03, Issue-11, pp-85-92
www.ajer.org

Research Paper Open Access

Simulation of the Effect of Bucket Tip Angle on Bucket Splitter of a Pelton Turbine

A. J. Ujam[1]*, S. O. Egbuna[2] and N. E.Nwocha[3].
1. Department of Mechanical Engineering, Enugu State university of Science and Technology,(ESUT), Enugu.
2. Department of Chemical Engineering, Enugu State University of Science and Technology,(ESUT), Enugu.
3. Department of Mechanical Engineering, Nnamdi Azikiwe University, Awka.

ABSTRACT: *The flow interaction in the rotating bucket of a pelton turbine influences the system power output. This work therefore sets out to investigate the effect of bucket tip angle on the power delivered to the bucket splitter. Simulation program was developed using Matlab to simulate the relationship between bucket tip angle, energy coefficient, bucket exit angle, and hydraulic efficiency to obtain an expression of power delivered to the bucket splitter. Research shows that at 3° bucket tip angle, the power delivered to the bucket splitter was maximum and decreases as the tip angle increases.*

Keyword: *Pelton turbine, bucket splitter angle, bucket tip angle, energy coefficient, power.*

I. INTRODUCTION

The high demand for a clean source of energy continues to increase as indicated by the increase in distributed generation technologies and adoption of renewable energy resources. Climate change and global warming have made renewable energy the most appropriate and fitting means of answering all these changes in our environment. Micro-hydro power plant (MHPP) is considered as one of the most reliable renewable energy in the world **[1]**. It is also one of the earliest small scales renewable energy and is still an important source of energy today. MHPP is appropriate in most cases for individual users or groups who are independent of the electricity supply grid. A MHPP is generally a hydroelectric power installation that can produce up to 100 KW of power. It does not encounter the problem of population displacement and is not expensive as solar or wind energy **[2]**.

There are many of MHPP around the world, usually in developing countries as they can provide an economical source with continuous supply of electrical energy compared to other small scale renewable energy. MHPP usually built on mountainous areas where hydropower resources are available to provide electricity for remote or rural areas. Furthermore, MHPP is often isolated from electricity supply grid. Therefore, it requires control to maintain constant frequency and voltage output in order to directly sustain load demands. This work focuses on the influence of tip angle and pressure distribution on the bucket surface which account for the power output of a MHPP (pelton turbine). Pelton bucket tip angle determines the power delivered to the bucket splitter

II. WORKING EQUATIONS:

Considering the flow inside the Bucket (figure1), a theoretical approach was carried out to estimate the pressure amplitudes during the initial impact and the power delivered to the splitter angle, since no pressure sensor is mounted directly on the tip of the bucket.

A kinematic study is performed to determine the angle of attack which is the tip angle at the instant of impact and consequently to determine the relationship between the tip angle, exit angle, energy coefficient and hydraulic efficiency, to develop an expression of power delivered to the splitter angle.

The jet is assumed to be 2D, and a longitudinal cut along bucket J symmetry plane was considered. The jet is animated by the absolute velocity u, while the bucket tip J moves with the peripheral velocity u_b. The first contact between bucket J tip and jet upper generator occurs with relative velocity V_r. The angle of impact of the tip γ is determined.

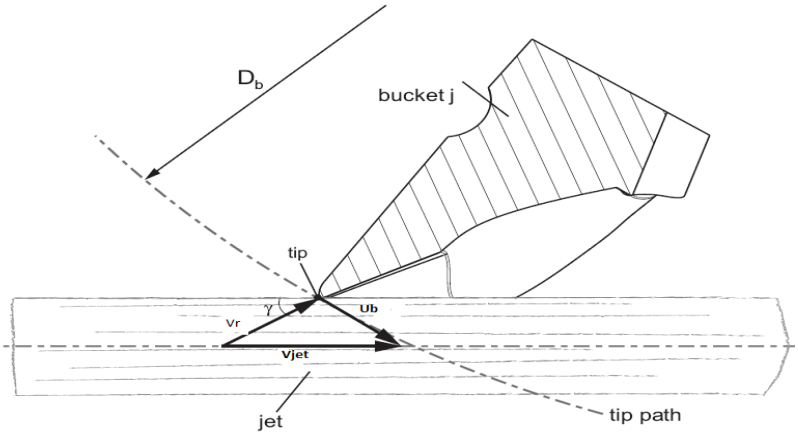

Fig. 1 2-D Velocity triangle at instant of impact

The position of bucket tip in a fixed frame of reference which origin coincides with the center of rotation of the runner is determined as follows:

$$\begin{cases} Xb\ (t) = \frac{D_b}{2}\ \mathrm{Cos}\ (wt + wto) \\ Zb(t) = \frac{D_b}{2}\ Cos(wt + wto) \end{cases} \qquad [1]$$

wto is the arc between the datum and the first contact point.

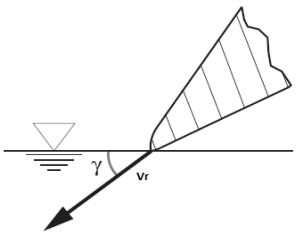

Fig. 2 Edge impact on the water surface

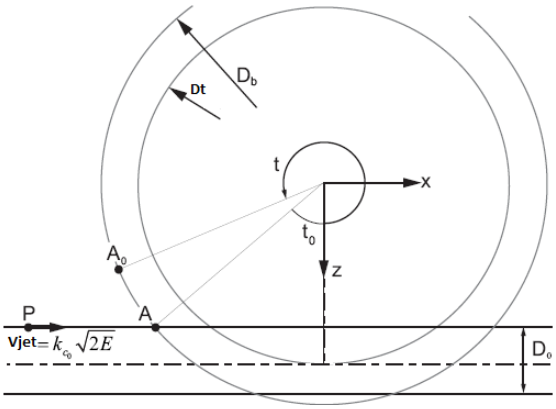

Fig.3 Kinetic path of the tip

wto = arcos $(\frac{Dt-Dn}{Db})$ [2]

The velocity of the bucket j tip is obtained by developing equation 1

$$\begin{cases} Uxb\ (t) = \frac{Dx_{b\ (t)}}{dt} = \frac{Db}{2}\sin(wt + wto)\,.\,\omega \\ Uzb(t) = \frac{Dz_{b\ (t)}}{dt} = -\frac{Db}{2}sin(wt + wto).\,\omega \end{cases}$$ **[3]** [3]

Consider the jet of diameter D_n oriented parallel to the x- axis. Let p be the water particle travelling on the jet upper generator at constant velocity $V_{jet} = k_{co}\,x\sqrt{2E}$ that is to encounter bucket j tip at position A. Particle p position is given by

$$\begin{cases} Xp\ (t) = k_{co}\,x\sqrt{2E\ x\ t} \\ Zp\ (t) = \frac{D_t - D_n}{2} \end{cases}$$ [4]

And its velocity is

$$\begin{cases} Vxp\ (t) = \frac{d_{xp\ (t)}}{dt} = k_{co}\,x\sqrt{2E} \\ Vzp\ (t) = \frac{d_{zp}}{dt} = 0 \end{cases}$$ [5]

The relative velocity component of particle p with respect to the bucket j tip is $V_r = V_{jet} - U$, at the instant of impact **[3].** Thus

$$\begin{cases} V_r xp\ (t) = k_{co}\,x\sqrt{2E}\ x\ \frac{Db}{2}\sin(wt + wto)\,.\,\omega \\ V_r zp = \frac{D_b}{2}\,Cos(wt + wto).\,\omega \end{cases}$$ [6]

The relative angle of impact of the tip is expressed as

γ = arc tan $(\frac{V_r zp}{V_r xp})$ + ρ [7]

Where γ *is* the tip angle and ρ is the angle of setting of bucket j.

ρ = arc sin $(\frac{2r}{D_b})$ [8]

Introducing the energy coefficient $\varphi_1$the expression for the angle of attack γ is given by:

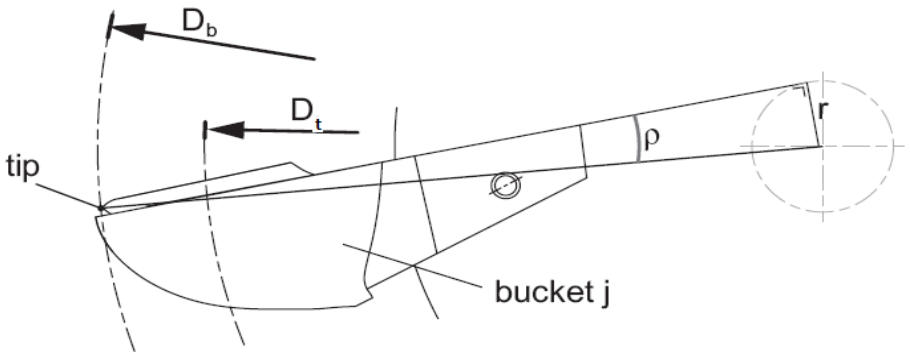

Fig. 4 Bucket angle of setting

$$arc\ coty = \left(\frac{D_t - D_n}{\varphi_1^{1/2} k_{co} - \frac{D_b}{D_t}\sqrt{1-\left(\frac{D_t-D_n}{D_b}\right)^2}}\right)$$ **[4]** [9]

The angle γ is a function of three parameters, $\gamma = \gamma(\varphi_1, D_n, k_{co})$.

From equation 9,

$$\varphi_1^{1/2} = \left(\frac{D_t - D_n}{coty\ k_{co} - \frac{D_b}{D_t}\sqrt{1-\left(\frac{D_t-D_n}{D_b}\right)^2}}\right)$$

$$ie\ \varphi_1 = \left(\frac{D_t - D_n}{coty\ k_{co} - \frac{D_b}{D_t}\sqrt{1-\left(\frac{D_t-D_n}{D_b}\right)^2}}\right)^2$$ [10]

The hydraulic efficiency η is by definition expressed as:

$$\eta = \frac{p_t}{p_h} = \frac{p_t}{\rho QE}$$ **[5]** [11]

With substitutions equations 10 & 11 finally reduce to

$$\eta = 2\left(\frac{V_{jet}}{\sqrt{\varphi}} - \frac{1}{\sqrt{\varphi}}\right) \text{ x } (1 + (1 - \Delta) \text{ x } \cos\beta_2$$ **[5]**

$$\eta = \frac{p_{wheel}}{p_h} = \frac{p_{wheel}}{\rho gH} = 2\left(\frac{V_{jet}}{\sqrt{\varphi}} - \frac{1}{\sqrt{\varphi}}\right) \text{ x } (1 + (1 - \Delta) \text{ x } Cos\beta_2$$

$$P_{wheel} = 2\rho gH\left(\frac{V_{jet}}{\sqrt{\varphi}} - \frac{1}{\sqrt{\varphi}}\right) \text{x } (1 + (1 - \Delta) \text{x } Cos\beta_2$$ **[6]** [12]

Equation 12 shows the relationship between tip angle, exit angle, hydraulic efficiency and energy coefficient to develop the power delivered to the splitter and the wheel by the fluid through the nozzle **[4-6]**.

2.1 Determination of Nozzle Velocity V_2jet

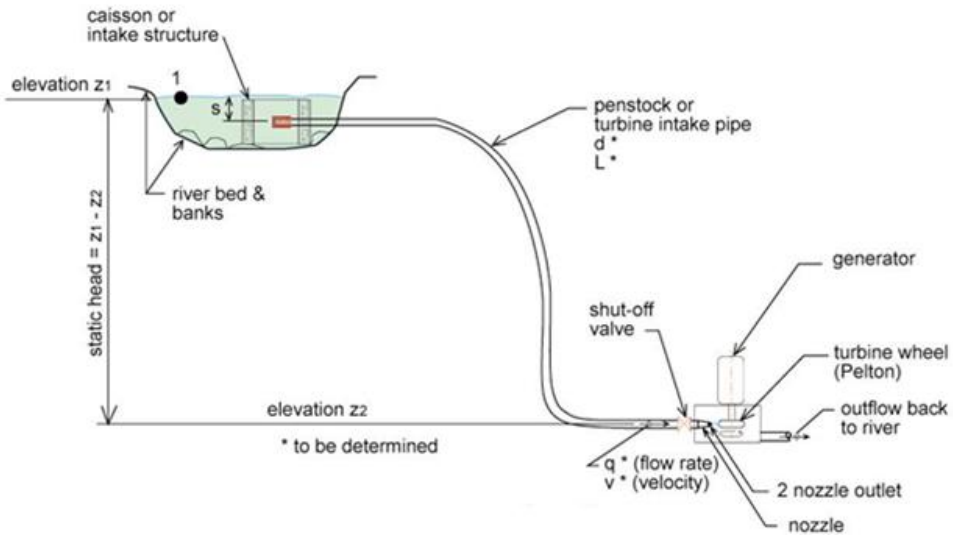

Fig. 5 Flow from the reservoir to the nozzle outlet

Water to drive a pelton wheel is supplied through a pipe from a river bed or lake as shown above, The maximum power output will be determined using the static head to check the influence of head on the power output of a pelton wheel and also the bucket shape runner or wheel. The head loss due to friction in the pipeline will be considered while minor losses neglected.

Calculations for hydro turbine jet impact velocity are based on the same sort of calculations done for pump systems, except there is no pump. The energy is provided by the difference in elevation between the inlet and outlet of the system, shown above .The inlet (point1) is defined as the surface elevation of the water source and the outlet is at the nozzle outlet (point2), the velocity v_1 is the velocity of fluid particle at the water source surface; velocity v_2 is the velocity of the water jet at the nozzle. The pressure head at point 1 and 2 is equal to zero. Applying the Bernoulli's equation to link the flow from the reservoir to the nozzle outlet, we have

$$Z_1 - Z_2 - H_f = \frac{V_2^2}{2g}$$

$$V_{jet}\ (\text{m/s}) = \sqrt{2\,x\,g\,(Z_1(m) - Z_2(m) - H_f\,(m)} \quad \textbf{[7, 8]} \qquad [13]$$

2.2 Shaft Power Output $\dot{W}_{shaft}$:

The shaft output is not only influenced by the force generated on the bucket as the jet impinges on the bucket splitter angle causing the rotary motion of wheel thereby affecting the shaft power output and the torque on shaft but also the head which delivered energy through the nozzle to the bucket.

The torque to the shaft is

$T = F_{bucket}\, r_m$

$\dot{w}\dot{W}_{shaft} = \rho\, Q\, U\, (U - V_{jet})\, (1 - \cos\beta_2) = 2\rho Q\, (U^2 - UV_{jet})$ **[9, 10]** [14]

Since $V_{jet} >$ U, shaft work being done is negative since work is done on the system and torque is maximum when U = 0.

III. SIMULATION

Simulation was performed to investigate the effect of power delivered by the bucket Tip Angle to the bucket splitter which then generates a force on the bucket surface to drive or retards bucket motion.

3.1 Basic Equations

The simulation model equations used in estimating the power delivered by the bucket tip angle to the bucket splitter and also the pressure distributed on the bucket surface in the study were derived from section 2.0

3.2 Simulation Flow Chart

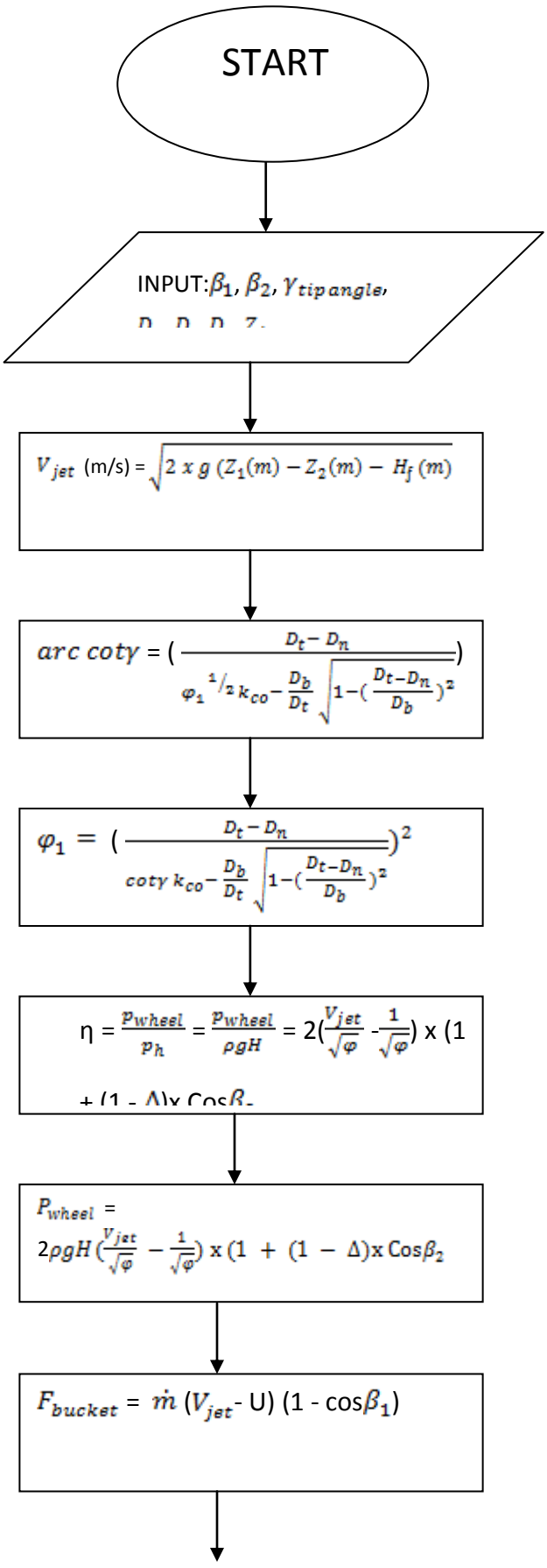

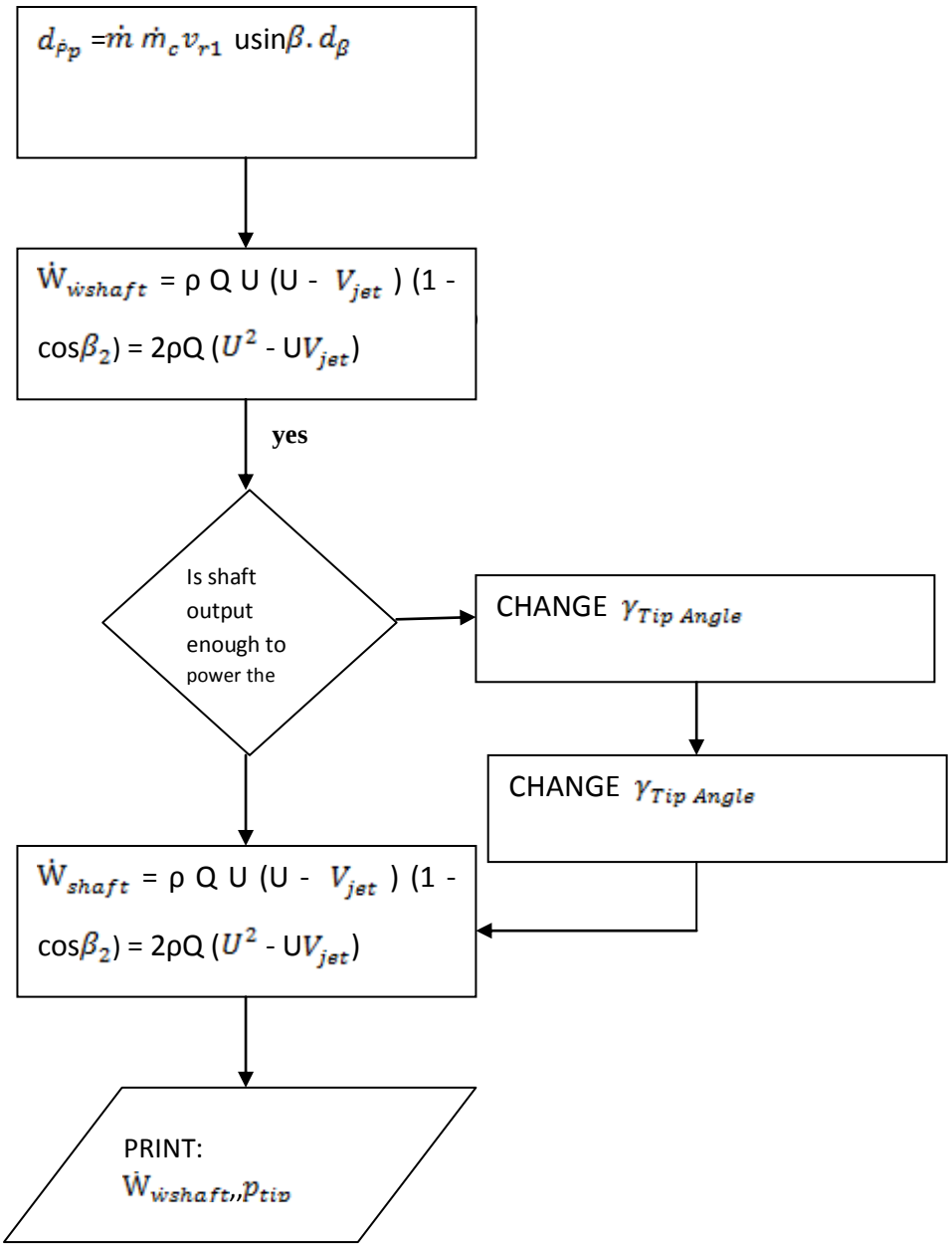

Fig 6: Simulation program flow chart

3.3 Results and Discussions

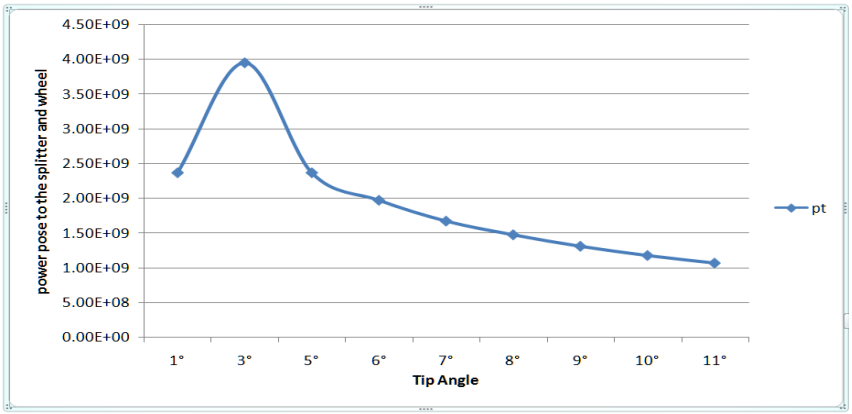

Fig.7: Relationship between the power delivered to the splitter angle and bucket tip angle

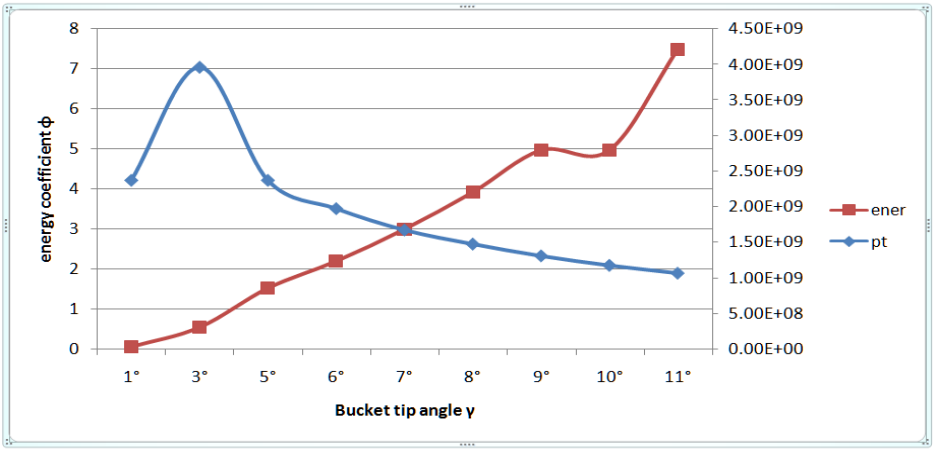

Fig. 8: Relationship between the bucket tip angle, energy coefficient and power directed to the splitter and the wheel using simulation to predict our results.

The results of our study show that power delivered to the bucket splitter and the wheel due to the bucket tip angle increases from 1° and got the peak at 3° where power output values were (2.3677 x 10^{09} kW and 3.9526 x 10^{09} kW respectively) and that there was a continuous decrease in the power delivered to the splitter as the tip angle increases from 5° to 11°, that is 2.3677 x 10^{09} kW to 1.0657 x 10^{09} kW. The energy coefficient was minimum at 1° with a slightly increase at 3°tip angle after which it increases continuously to maximum at 11° tip angle.

IV. CONCLUSION

The results of our study show that power delivered to the bucket splitter and the wheel due to the bucket tip angle was greater at 3° where power output was 3.9526 x 10^{09} kW showing that the pelton bucket with hemispherical cup shape should be designed with a tip angle of 3° to deliver a better power output on the system

REFERENCES

[1]. Nwocha E. N (2013) "***Effect of head and Bucket Splitter Angle on the Power Output of a Pelton Turbine".*** MENG Thesis, Department of Mechanical Engineering, Nnamdi Azikiwe University, Awka, Nigeria.

[2]. W. F. Durand (1939). ***"Articles on the history of pelton turbine"***. International Journal on pelton

[3]. Adriana Catanase, Mircea BĂRGLĂZAN, Cristina HORA, (2004) ***"Numerical Simulation of A Free Jet In Pelton Turbine"***, The 6th International Conference on Hydraulic Machinery and Hydrodynamics Timisoara, Romania.

[4]. J. Turbo mach (July 2006) ***"flow analysis inside a pelton turbine bucket"***. Journal of turbo machinery–128, issue 3,500 (page 12).

[5]. Brekke, H. B. Velensek and M. Bajd, B. Velensek and M. Bajd, Eds(1984), ***"A general study of the design of vertical pelton turbines"***. In *turboinstitut*., vol. 1, pp.383–397. Proceedings of the conference on hydraulic machinery and flow measurements.

[6]. Brackbill, J. U., Kothe, D. B., and Zemach, C. (1992), ***"A continuum method for modeling surface tension"***. *Journal of Computational Physics 100* 335–354

[7]. Kelley, J. B (1950). ***"The Extension Bernoulli's Equation"***. American J. Phys. pp. 202 – 204. India.

[8]. Church chill, S.W. (1977***). "Friction Factor Equation Span of Fluid Flow Regimes, Chemical Eng"***. Vol.7, pp.91 – 92.

[9]. Richard L. Roberts on (2008).***"Ocean Energy".*** Wentworth Institute of Technology Senior Design Project, Mechanical Engineering.

[10]. I. U. Attaneyake (2000). ***"Analytical study on flow through pelton turbine using boundary layer theory".*** International journal of Engineering & technology by IJET VOL: 9 NO: 19. Mechanical engineering dept, Open University of sri Lanka Nawala.

American Journal of Engineering Research (AJER)
e-ISSN : 2320-0847 p-ISSN : 2320-0936
Volume-03, Issue-11, pp-93-108
www.ajer.org

Research Paper Open Access

Chemical Recycle of Plastics

Sara Fatima
(Department of Chemical Engineering, Aligarh Muslim University, India)

ABSTRACT: *Various chemical processes currently prevalent in the chemical industry for plastics recycling have been discussed. Possible future scenarios in chemical recycling have also been discussed. Also analyzed are the effects on the environment, the risks, costs and benefits of PVC recycling. Also listed are the various types of plastics and which plastics are safe to use and which not after rcycle.*

Keywords - *Plastic Recycle, Mixed Plastic Waste (MPW), Polyvinyl chloride (PVC)*

I. INTRODUCTION

About 50% of the plastic waste collected as general waste is recycled today. The remaining half is disposed of at landfill sites or simply burned in incinerators. In countries like Japan, the capacity of landfill sites is continually decreasing. However, this plastic waste can be recycled and used as raw material, solid fuel and waste power generation and as heat source.

Furthermore, flame-retardant materials such as polyvinyl chloride (PVC) are known to cause corrosion in incinerators during combustion due to their constituent halogen substances; these materials also produce halogen compounds such as dioxins. Moreover, CO_2 discharged from the combustion of polymers causes environmental problems such as global warming and acid rain. In addition, suspected endocrine disrupting chemicals, typically Bisphenol A, can dissolve out of polycarbonate (PC).

Common recycled plastics include:

1. Polyethylene Terephthalate (PETE): Excellent clarity, strength, toughness, and barrier to gas and moisture. These are commonly used in soft drinks, water, salad dressing bottles, and peanut butter jars.
2. High Density Polyethylene (HDPE): Excellent stiffness, strength, toughness, resistance to moisture and permeability to gas. These are commonly used in milk, juice, and water bottles; trash and retail bags.
3. Polyvinyl Chloride (PVC): Excellent versatility, clarity, ease of bending, strength, and toughness. These are commonly used in juice bottles, cling films, and PVC piping.
4. Low Density Polyethylene (LDPE): Excellent ease of processing, strength, toughness, flexibility, ease of sealing, and barrier to moisture. These are commonly used in frozen food II

II. CHEMICAL PROCESSES FOR PLASTIC WASTE RECYCLE

Processes in recycling of plastics can be divided into three categories:

1. Chemical recycling of mixed plastic waste (MPW).
2. Chemical recycling of PVC-rich waste.
3. Alternatives for chemical recycling (incineration, mechanical recycling).

Processes used under each of these categories are discussed below:

1. Chemical recycling of mixed plastic waste

Listed are the processes that were operational in practice, temporarily shut down since the necessary waste supply was not ensured, or which had a fair chance of becoming operational in the short term as of year 2000:

- Texaco gasification process
- Polymer cracking process
- BASF conversion process
- Use as reduction agent in blast furnaces
- VEBA Combo Cracking process
- Pressurized fixed bed gasification of SVZ

These processes are discussed below one by one:

1.1 Texaco gasification process

Texaco has had commercial experience with its gasification process for over 50 years. During this period, it has proven its high reliability and feedstock flexibility in 100 installations worldwide. Experiments with mixed plastics waste were carried out at the pilot plant site (10 t/day) in Montebello, California, USA. The Texaco process (Figure 1) consists of a **liquefaction step** and an **entrained bed gasification step**. In liquefaction, the plastic waste is mildly thermally cracked (de-polymerization) into synthetic heavy oil and some condensable and non-condensable gas fractions. The non-condensable gases are reused in the liquefaction as fuel (together with natural gas). The heavy oil is filtered to remove large inorganic particles. The oil and condensed gas are then injected to the entrained gasifier. Also, Cl-containing gases from the plastic waste are fed to the gasifier. The gasification is carried out with O and steam at a temperature of 1200 – 1500 ºC. The gasification pressure is normally adjusted to the pressure of the process which will consume the resulting synthesis gas. After a number of cleaning processes (amongst others, HCl and HF removal), a clean and dry synthesis gas is produced, consisting predominantly of CO and H_2, with smaller amounts of CH_4, CO_2, H_2O and some inert gases. Virtually all Cl present in MPW is captured by washing the raw syn-gas under addition of NH_3 and converted into saleable NH_4Cl. S from MPW is won back in a pure, saleable form. Ash from the process is converted into slag and fines. Filtrated waste water from the scrubber and quench is distilled, yielding reusable water, crystallized NH_4Cl and a brine purge that is re-circulated to the gasifier.

De-polymerization step involves following chemical reactions in general. PET waste is dissolved in the dimethyl ester of benzene-1, 4-dicarboxylic acid (dimethyl terephthalic acid) and then heated with methanol under pressure at 600 K. This produces the two monomers of PET, ethane-1, 2-diol and the dimethyl ester which are subsequently purified by distillation.

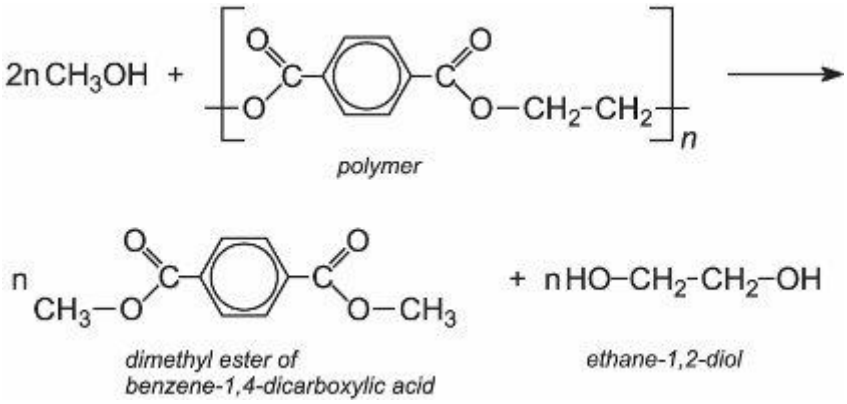

Input specifications are:

- Material texture Dry to the touch, not sticky, free flowing
- Physical description Shredded or chipped
- Size Less than 10 cm
- Physical fines content Less than 1% under 250 μm
- Bulk density > 100 g/liter
- Form at delivery baled or agglomerated
- Plastics content > 90 wt%
- Free metals < 1 wt%
- PVC content < 10 wt%
- Ash content < 6 wt%
- Residual moisture< 5 wt%
- Paper content < 10 wt%

Products are:

- Synthesis gas: 150 tons of mixed plastics per day produce roughly 350,000 Nm^3 per day of clean synthesis gas. This gas (predominantly H_2/CO) can be used as feedstock in petrochemical processes.
- Pure S.
- Saleable NH_4Cl.
- Vitrified slag.
- Fines.

1.2 The Polymer Cracking Process

BP Chemicals has led promotion of Polymer Cracking technology for feedstock recycling since its beginnings in the early 1990's. Support has been provided by a Consortium of European companies to develop the technology for recycling of plastics. The consortium members at the time of the successful pilot plant trials in 1997 were BP Chemicals, Elf Atochem, EniChem, DSM, and CREED. The "Polymer Cracking Process", a fluid bed cracking process, was first tested on small lab-scale equipment in the early 1990's. The pure research phase has now ended with successful demonstration of the process at continuous pilot plant scale at BP's Grangemouth site using mixed waste packaging plastics. This pilot plant, which started up in 1994, has a nominal 400 ton per year feed capacity, but runs continuously on a campaign basis at 50 kg/hr scale as it has limited product storage. The technology is now in the development phase with modifications in progress to the BP pilot plant to allow optimization and scale-up. Some elementary preparation of the waste plastics feed is required, including size reduction and removal of most non-plastics. This prepared feed is fed directly into the heated fluidized bed reactor (Figure 2). The reactor operates at approximately 500°C in the absence of air. The plastics crack thermally under these conditions to hydrocarbons which vaporize and leave the bed with the fluidizing gas. Solid impurities, including metals from e.g. PVC stabilizers and some coke, are either accumulated in the bed or carried out in the hot gas as fine particles for capture by cyclone. The decomposition of PVC leads to the formation of HCl, which is neutralized by bringing the hot gas into contact with a solid lime absorbent. This results in a $CaCl_2$- fraction that has to be land filled. The purified gas is cooled, to condense most of the hydrocarbon as valuable distillate feedstock. This is then stored and tested against agreed specifications before transfer to the downstream user plant. The remaining light hydrocarbon gas is compressed, reheated and returned to the reactor as fluidizing gas. Part of the stream could be used as fuel gas for heating the cracking reactor, but as it is olefin-rich, recovery options are being considered. Hydrocarbon is recovered in two stages since the heavy fraction becomes a wax at about 60°C. Once recovered, the light and heavy fractions could be combined together in a commercial plant ready for shipment to downstream refinery processing. The process shows very good results concerning the removal of elements like Cl. With an input of 10,000 pap (or 1%) Cl, the products will contain around 10 ppm Cl. This is somewhat higher than the specifications of 5 ppm

typical for refinery use. However, in view of the high dilution likely in any refinery or petrochemical application, BP assumes that this is acceptable. Also, metals like Pb, Cd and Sb can be removed to very low levels in the products. Further, all the hydrocarbon products can be used for further treatment in refineries.

Utilities include:

- electric power 60 kW/ton feed plastic (approx)
- cooling water 40 m^3/ton feed plastic
- steam 1.2 ton/ton feed

1.3 BASF Conversion Process

Before the waste plastics can be fed to the process (Figure 3), a pretreatment is necessary. In this pretreatment the plastics are ground, separated from other materials like metals and agglomerated. The conversion of the pretreated mixed plastic into petrochemical raw materials takes place in a multi-stage melting and reduction process. In the first stage the plastic is melted and de-halogenated to preserve the subsequent plant segments from corrosion. The hydrogen chloride separated out in this process is absorbed and processed in the hydrochloric acid production plant. Hence, the major part of the Cl present in the input (e.g. from PVC) is converted into saleable HCl. Minor amounts come available as NaCl or $CaCl_2$ effluent. Gaseous organic products are compressed and can be used as feedstock in a cracker. In the subsequent stages the liquefied plastic waste is heated to over 400 ºC and cracked into components of different chain lengths. About 20-30% of gases and 60-70% of oils are produced and subsequently separated in a distillation column. Naphtha produced by the feedstock process is treated in a steam cracker, and the monomers (e.g. ethylene, propylene) are recovered. These raw materials are used for the production of virgin plastic materials. High boiling oils can be processed into synthesis gas or conversion coke and then be transferred for further use. The residues consist of 5% minerals at most, e.g. pigments or Al lids. It seems likely that metals present in PVC-formulations mainly end up in this outlet. The process is carried out under atmospheric pressure in a closed system and, therefore, no other residues or emissions are formed.

Products are:

- HCl, which is neutralized or processed in a hydrochloric acid production plant
- naphtha to be treated in a steam cracker
- monomers, e.g. ethylene, propylene, which can be used for the production of virgin plastic materials
- high boiling oils, which can be processed into synthesis gas or conversion coke and then transferred for further use

1.4 Use of Mixed Plastic Waste in Blast Furnaces

For the production of pig iron for steel production, iron ore (Fe_2O_3) has to be reduced to Fe. This process takes place in a blast furnace. Coke, coal and heavy oil are normally used as reducing agents in this process. Iron and steel companies try to lower the consumption of coke, by partly replacing it with coal, gas or fuel oil (30% in weight seems to be the maximum), via coal injection technology. Recently, new developments have started to replace the conventional reducing agents by plastics waste. Though others like British Steel (UK) have done trials as well, the best-known pioneer in this field is Stahlwerke Bremen(SB), Germany. It is a large German steel manufacturer which operates two blast furnaces to produce over 7000 t/day, or some 3 Million ton per annum pig iron. Currently, German blast furnaces are the only plants in Europe using plastics waste in this way. However, other blast furnace companies have also used waste as a reducing agent, like waste oil. SB uses plastic waste as a substitute for fuel oil. In the blast furnace plastics are injected to the tuyeres in a similar way as coal or fuel oil. From a silo or big bags the plastics are filled on a screen where the fraction > 18 mm is separated. Also, no fibers or metal particles like wires or nails are allowed in the plastic waste. The smaller plastic waste particles (< 18 mm) go to the injection vessel where the injection pressure of about 5 bars is built up. The discharge and dosing work pneumatically without mechanical support. For continuous operation, it was found that a minimum value for the bulk density of 0.3 t/m3 should be set. One advantage of plastic waste is its low S content compared with coal. However, plastic waste has a relatively high Cl content due to the presence of PVC. The main part of the Cl forms HCl going into solution in the washer. Various groups have expressed concern about the possible formation of dioxins and furans. However, measurements during experiments have

indicated that the emissions of dioxins and furans were not significantly elevated, in relation to the strongly reducing atmosphere at 2100 ºC.

1.5 VEBA COMBI Cracking (VCC) Process

The plant configuration includes a de-polymerization section and the VCC section (Figure 4). De-polymerization is required to allow further processing in the VCC section. In the de-polymerization section the agglomerated plastic waste is kept between 350-400ºC to effect de-polymerization and de-chlorination. The overhead product of the de-polymerization is partially condensed. The main part (80 %) of the Cl introduced with PVC is present as HCl in the light gases. It is washed out in the following gas purification process, yielding technical HCl. The condensate, containing 18 % of the Cl input, is fed into a hydro-treater. The HCl is eliminated with the formation water. The resulting Cl-free condensate and gas are mixed with the de-polymerisate for treatment in the VCC section. The de-polymerizate is hydrogenated in the VCC section at 400-450ºC under high pressure (about 100 bars) in a liquid phase reactor with no internals. Separation yields a product which after treatment in a fixed-bed hydro-treater is a synthetic crude oil, a valuable product which may be processed in any refinery. From the separation a hydrogenated residue stream also results, which comprises heavy hydrocarbons contaminated with ashes, metals and inert salts. This hydrogenation bitumen is a byproduct which is blended with the coal for coke production (2 wt %). It is most likely that the major part of any metals present in a PVC formulation end up in this residue flow. Light cracking products end up in off-gas, which is sent to a treatment section for H_2S and ammonia removal. As indicated above, the main part of the Cl present in the input (i.e. from PVC) is converted into usable HCl.

Products are:

- HCl
- Syn-crude from the VCC section (This liquid product is free of Cl and low in O and N)
- hydrogenated solid residue (blended with the coal for coke production)
- off-gas

The input specifications for the plastic waste input in the de-polymerization section are:

- particle size < 1.0 cm
- bulk density ≥ 300 kg/m^3
- water content < 1.0 wt%
- PVC < 4% (≤ 2 wt% Cl)[7]
- inerts < 4.5 wt% at 650 ºC
- metal content < 1.0 wt%
- content of plastic ≥ 90.0 wt%

1.6 SVZ gasification process

The Sekundärrohstoff Verwertungs Zentrum (SVZ) operates a plant that converts several waste materials, included plastics, into synthesis gas, methanol and electricity. It originated from a coal gasification plant, but after several major investments it is currently mainly operating on waste material. It is currently fully operational. Waste and material that are accepted include contaminated wood, waste water purification sludge (including industrial sludges), waste derived fuel from MSW, paper fractions, plastic fractions, the light fraction of shredder waste, and liquid organic waste that arises from SVZ-related plants. The total capacity is about 410,000 tons per annum for solid material and 50,000 tons per annum for liquid material. The capacity for plastic waste is estimated at some 140,000 tons per annum in the near future. The MPW is fed into a reactor, together with lignite (in the form of briquettes) and waste oil. This reactor is a solid bed gasification kiln. O and steam are used as gasification media, and are supplied in counter flow with the input materials. This processes synthesis gas (a mixture of hydrogen and CO), liquid hydrocarbons, and effluent. The liquid hydrocarbons are further processed by oil pressure gasification. The raw gases from this process, as well as from the solid bed reactor, are purified by the rectisol process. There components like H_2S and organic S compounds are removed. The clean synthesis gas is used for various purposes. The main part, around 70 %, is used for the production of methanol. About 20 % is used for electricity production. The remainder is used in other processes. Waste gas

products are incinerated; in the flue gas cleaning an amount of gypsum is produced which is proportional to the amount of S in the input. The gasification process has a high tolerance for various input parameters. The plant has proven to be capable of dealing with mixed plastics waste, waste derived fuel (a mixture of plastics, wood and paper), the shredder light fraction of car wrecks, and the plastic fraction from shredded white goods and electronics. Acceptance criteria for input is indicated below:

- Particle size: > 20 to 80 mm
- Cl content: 2% as default, though higher concentrations are tolerable
- Ash content: up to 10% or more
- Caloric value: not critical

2. Chemical recycling of PVC-rich waste
The processes in this category are:

- BSL incineration process
- AKZO Nobel steam gasification process
- Linde gasification process
- NKT pyrolysis process

2.1 BSL Incineration process

The plant (Figure 5) consists of a pretreatment of the waste, the thermal treatment and energy recovery, the flue gas purification, the purification of the HCl and a waste water treatment installation. The waste is incinerated in the rotary kiln and a post-combustion chamber, directly after the rotary kiln, at temperatures of 900 to 1200ºC. During this treatment HCl is released and recovered. Based on the heat capacity of the waste, halogen content, and potential slag formation, an optimal mixture of wastes is determined. In this way a continuous production of high-quality HCl can be assured. Also, the formation of dioxins and furans can be diminished in this way. In the next step, the flue gas purification, the HCl is absorbed from the flue gas by water. Also, other impurities are removed from the gas. The raw HCl is then purified to a useful feedstock. The inert products from the incineration are dependent on the chemical composition of the waste. It is likely that the main part of any metals present in a PVC-formulation will end up in this slag.

Products are:

- HCl of high quality, which can be used in several production processes;
- Steam;
- Inert slag.

The process has been designed for a mix of high-chlorinated wastes (solvents, chlorinated tars, plastics). Hence, such kilns are usually fed with a mix of different wastes (e.g. PVC waste and other waste streams with a lower caloric value) in order to obtain a waste stream with an optimum composition. If the kiln were fed 100% PVC waste, this would on average produce an input with too high caloric values, leading to problems with temperature control. The Cl content, on the other hand, is not critical. As long as the caloric value is within the acceptable range, the accepted Cl content can be higher than 50%. The accepted particle size for the incineration process is 10x10x10 cm.

2.2 Steam Gasification Process

Akzo Nobel, as a producer of Cl and vinyl-chloride, started to study a process for feedstock recycling of mixed plastic waste containing PVC in 1992. Based on an investigation, Akzo Nobel chose in 1994 to use fast pyrolysis technology in a circulating fluid bed reactor system. This technique has been developed by Battelle, Columbia, USA, for biomass gasification. The process (Figure 6) consists of two separate circulating fluid bed (CFB) reactors at atmospheric pressure:

- A gasification (or fast pyrolysis) reactor in which PVC-rich waste is converted at 700-900 ºC with steam into product gas (fuel gas and HCl) and residual tar.
- A combustion reactor that burns the residual tar to provide the heat for gasification.

Circulating sand between the gasifier and combustor transfers heat between the two reactors. Both reactors are of the riser type with a very short residence time. This type of reactor allows a high PVC waste throughput. The atmosphere in the gasifier is reducing, avoiding the formation of dioxins. Depending on the formation of tars (as happened in the trial with mixed PVC waste), a partial oxidation (a gasifier) may be required to convert these tars into gaseous products. The product stream consisting of fuel gas and HCl is quenched to recover HCl. HCl is purified up to specification for oxy-chlorination. Additives in the waste stream, mainly consisting of chalk and metal stabilizers present in a PVC-formulation, are separated from the flue gas or as a bleed from the circulating sand. The output of the reactor is a synthesis gas with variable composition, which is dependent on the input. If the input contains a lot of PP and PE, relatively a lot of ethylene and propylene will be formed. With proportionally more PVC, HCl and CH_4 will be more evident in the product gas. In any case CO and H_2 will be the main components. Also the feed/steam ratio will influence the composition of the gas. A broad spectrum of materials like wood, biomass, mixed plastic and pure PVC waste is acceptable as input.

2.3 Linde Gasification Process

Linde KCA in Germany is offering a process to gasify waste materials in a slag bath. The basic technology was developed in the 1950s for gasification of lignite and coal. The process was made suitable to treat PVC waste with the following objectives:

- Maximum possible conversion of the Cl contained in the PVC into an HCl gas suitable for use in oxichlorination
- Maximum possible conversion of the chemically bound energy of the waste PVC into other forms of energy;
- Disposal of the unavoidable waste products of the process in a way complying with environmental regulations.

The European Council of Vinyl Manufacturers (ECVM) has pronounced a preference for this process for the treatment of PVC-rich waste. They regard the process as robust and economical. A pilot plant based on the Linde process was planned, supported by a financial commitment of 3 Million Euro from ECVM and constructed in year 2000. The plastic waste as delivered passes a conditioning process (Figure 7) in which it is pre-crushed and separated from steel and non- ferrous metals before entering the reactor. A pressurized reactor filled with slag is heated up to 1400-1600 ºC. The slag mainly consists of silicates. PVC, sand, O and steam are fed into the reactor according to the process conditions. The process is exothermic. Resulting products in the reducing atmosphere are a synthesis gas (CO / H_2) containing HCl and a slag. It is likely that this slag contains most of any metal stabilizers present in the PVC-formulation. HCl is absorbed with water from the synthesis gas. The resulting hydrochloric acid has to be purified from heavy metals chlorides and other halogens. Pure HCl gas is produced by distillation of the hydrochloric acid. The HCl-free synthesis gas can be used as feed for chemical processes or as a fuel gas to produce power. With these process waste streams containing up to 100% PVC waste can be recycled. This can be all kinds of PVC, hard and softened types. Conditioning of waste to meet the requirements for handling by the slag bath gasifier includes crushing and screening of the waste to the required particle size and then separation of iron and heavy non-ferrous metals from the waste by magnet or gravity sifter, respectively. Washing steps are not necessary. Also, drying of the waste is not necessary, because moisture is not a problem for the process.

2.4 NKT Pyrolysis process

The investigation into the treatment of PVC cable waste started in 1993 on a laboratory scale and was continued in 1995 on a semi-technical scale. This project was financed by the Danish Environmental Protection Agency (EPA) and NKT Research Centre. During the period February 1998 - June 1999, a PVC building waste project was carried out. In this project, the process was optimized for the treatment of mixed PVC building waste on a semi-technical scale. This project is financially sponsored by the Danish EPA, the NKT holding, ECVM and the Norwegian company Norsk Hydro. The process transforms PVC waste into chemical products/raw materials (Figure 8). In the pretreatment section light plastics such as PE, PP, wood and the like are sorted out. Also, sand, iron, steel, brass, copper and other metallic pollutants are separated from the PVC. The chemical and thermal degradation of the PVC waste takes place in a reactor at low pressures (2-3 bar) and moderate temperatures (maximum 375ºC). In the process Cl from the PVC reacts with fillers, forming calcium chloride. Simultaneously, the metal stabilizers that may be present in PVC-waste (lead, cadmium, zinc and/or barium) are converted to metal chloride. This consists of over 60 % lead and may be purified and re-used. After completion of the reactions, three main intermediate products are formed: a solid phase product, a liquid product and a gas phase product. From the gas phase produced in the reactor (see figure 2.8), HCl is collected by absorption in water, and the light gases (mainly carbon dioxide, propane and ethane) are released after incineration. The liquid phase is separated into an organic condensate and an aqueous condensate. Hydrogen chloride solutions are reused in the downstream separation process. The solid phase is treated in a multistage extraction-filtration process. By controlling pH, temperature and the amount of water added, heavy metals are separated from the coke in the filtration and/or evaporation step. Part of the chloride that is not internally re-used finally comes available as calcium chloride from the evaporation step.

Products are:

- Calcium chloride product (< 1 ppm lead), which may be used as thaw salt or for other purposes
- Coke product (< 0.1 wt% lead and Cl, respectively), which may be used as fuel in a cement kiln
- Metal concentrate (up to 60 wt% lead), which may be further purified and re- used
- Organic condensate, which may be used as fuel for the process

3. Alternatives to chemical recycle

These processes for chemical recycle of plastics include:

- Vinyloop® process
- Cement Kilns
- Municipal solid waste incinerators
- Landfill and mechanical recycling

Each of these processes is discussed below.

3.1 The Vinyloop® PVC-recovery process

Solvay has developed Vinyloop® as a response to a challenge from one of its customers, Ferrari Textiles Techniques (France). This company is specialized in the production of architectural tarpaulin and canvas in PVC/polyester compound. They consider it important that their products be recyclable. The process is quite simple in principle. First, the products to be recycled are cut and reduced in size. After that, PVC and its additives are selectively dissolved in a specific solvent such that they become separated from other elements. Finally, PVC is recovered by means of precipitation and dried and is ready for a new life. As indicated, this has to be labeled as mechanical recycling, since the PVC polymer is not broken down into its feedstock. Yet, unlike classical mechanical recycling processes, where the full PVC formulation is kept intact, here the components that make up the full formulation are separated. The Vinyloop® process is therefore capable of dealing with rather complicated formulations. Solvay claims that the regenerated PVC is comparable in quality to the primary product. The process deals with selectively collected PVC products. The quality has to be about the same as for mechanical recycling. Pilot plant results show that the Vinyloop® process is suitable for recycling all PVC-

compound materials tested so far: cables, pharmaceutical blister packs, floor coating, car dashboards, etc. The process is a closed loop system; i.e. there are no emissions to water.

3.2 Cement kilns

Cement kilns produce a clinker by sintering alkali raw materials such as lime ($CaCO_3$), clay (SiO_2 and Al_2O_3) and gypsum ($CaSO_4$) in a kiln at a very high temperature (1450°C in the solid fraction). The kiln can, in fact, be seen as a rotary kiln with a much longer length (200 meters). Furthermore, the solid materials flow in the opposite direction to the incineration gases. The length of the kiln results in a long residence time of incineration gases at high temperatures: 4 to 6 seconds at 1,800°C and 15 to 20 seconds at 1,200°C. Compared to regular waste incineration the O content, however, is much lower. Two processes are used to produce a clinker: a so-called wet process and a dry process. In the dry process the alkali raw materials are introduced in dry form into the kiln. In the wet process, these materials are introduced in the form of slurry. A clear disadvantage of the wet process is that it needs much more energy than the dry process (5,000 MJ/ton and 3,600 MJ/ton clinker), as in the dry process no water has to be evaporated. Because of the high temperatures, organic substances like MPW are effectively destroyed. Acidic substances such as HCl and SO_x are neutralized by the alkali raw materials, which act in fact as a caustic scrubber. Metals are bound in the clinker or in the fly ash. Fly ash is captured with an electro filter and subsequently added to the clinker. In general, no other flue gas cleaning is applied. Cement kilns have proved to be relatively robust with regard to their input material. In most cases the input material should be chipped or shredded. The PVC content is generally limited by license obligations, 1-2% Cl often being the maximum for individual waste streams.

3.3 Municipal solid waste incinerators

Municipal Solid Waste Incinerators (MSWIs) are in principle built for the treatment of municipal or similar industrial wastes. In such a kiln the waste, after it is tipped into storage and has been made more homogeneous, is transferred to a grid-type kiln. This rolling grid is placed under a certain slope, so that the waste is slowly transported with such a speed, that full incineration takes place. At the end of the grid slag remain. The slag is treated in order to recover the ferrous and non-ferrous fraction. In some countries these slag are re-used, mainly in road construction. Just like in the case of a rotary kiln, the flue gases pass through cleaning equipment such as an electro filter, an acid scrubber, a caustic scrubber, an active carbon scrubber and a DeNOx installation in order to comply with the demands of the EU incineration directive. In modern MSWIs, the energy is also recovered as much as possible. The flue gas cleaning process leads to fly ash and flue gas cleaning residue, which has to be land filled. The main part of any metals present in a PVC formulation ends up in these residues. A large fraction of the Cl input into the MSWI ends up in the flue gas cleaning residue. Normal municipal solid waste and similar material, including the regular plastics and PVC content, can easily be accepted by MSWIs. For dedicated waste streams, some elements have to be taken into account. First, if one wants to produce re- usable slag, the heavy metal input into the incinerator should be limited.

3.4 Landfill and Mechanical Recycling

Finally, other relevant treatment options for PVC or plastics waste include landfill and mechanical recycling. Mechanical recycling of plastics (be it PVC or other plastics), needs dedicated collection of the plastic waste in question. This seems only feasible for selected PVC flows. Landfill can accept PVC in any waste context (pure PVC, MPW, mixed materials).

III. ENVIRONMENTAL COMPARISON

Human and ecotoxicity

In this qualitative analysis, since it concerns MPW with a Cl-containing material like PVC, dioxin formation is a point of attention. As a general rule, reducing environments and high temperatures promote the breakdown and prevent the formation of dioxins. This would suggest that blast furnaces and gasification processes like VEBA and Texaco have advantages in this respect. However, drawing conclusions is rather difficult. In principle, one should take into account aspects such as the Cl content in the feedstock produced, their future fate, etc. This is well beyond the scope of this study.

Ozone depletion

The most important ozone-depleting substances have been phased out. There is no reason to assume why one of the technologies at stake would score worse or better than others concerning this aspect.

Photochemical Ozone Creation (POCP), eutrophication (NP) and acidification (AP)

The themes of photochemical ozone creation, eutrophication and acidification often tend to be correlated with energy use. Additionally, however, the processes avoided related to the useful by-products are relevant, as well as the quality of the flue gas cleaning. Here, one often sees the following difference between coal and oil as replaced products. Usually, oil refining results in relatively important emissions of NOx, SOx and VOC. If the recycling process produces a product that avoids this process step, it will score relatively well on POCP, NP and AP. Here this effect may be relatively less important since many processes produce feedstock that still have to be processed further in refineries. Mechanical recycling, however, can score somewhat better under favorable conditions (minor effort for collection, etc.).

Waste and other resource use

One aspect that needs to be addressed here is the fate of Cl in the process. In some processes (VEBA, BASF and Texaco) the Cl becomes generally available as a product (HCl or NH_4Cl). The advantage is that this prevents the production of primary materials and that a waste salt is produced in the process that has to be land filled. In its current form, the Polymer cracking and probably also the SVZ process has the disadvantage that the Cl comes available as a residue that has to be land filled. In blast furnaces Cl has no added value and will leave the furnace in the slag or as HCl emission. Classical MSWIs may let the Cl end up in part in the flue gas cleaning residues. In virtually all cases, any metals present in a PVC-formulation probably end up slag, fly-ash, or another residual flow.

IV. FIGURES AND TABLES

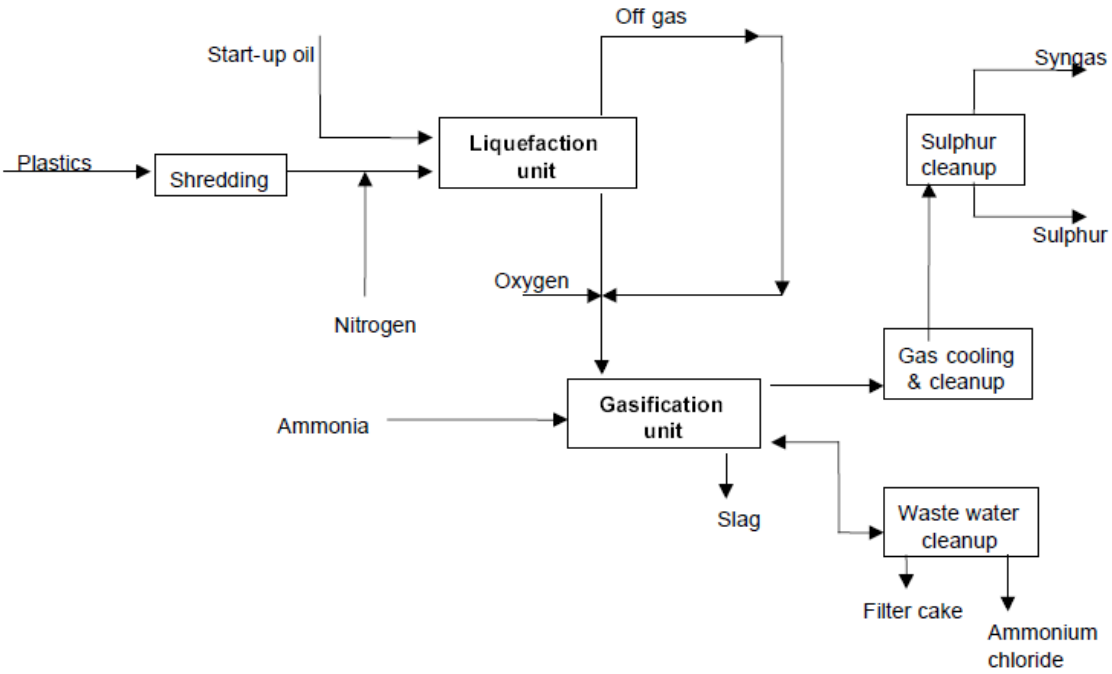

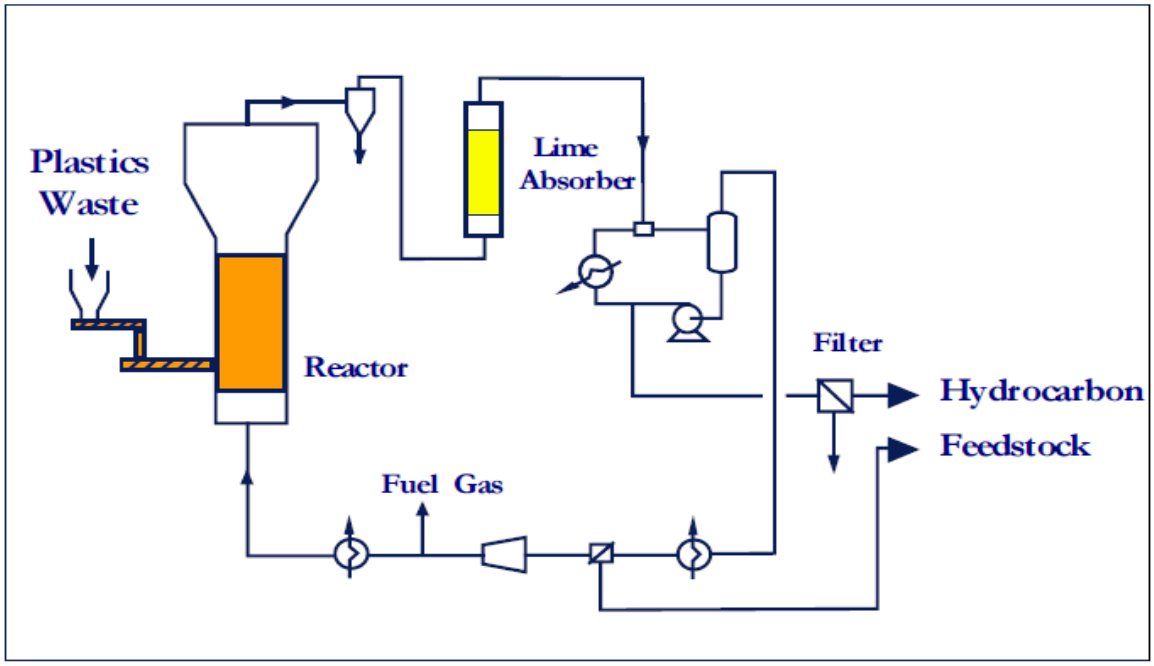

Figure 2: BP Process for Plastic recycles

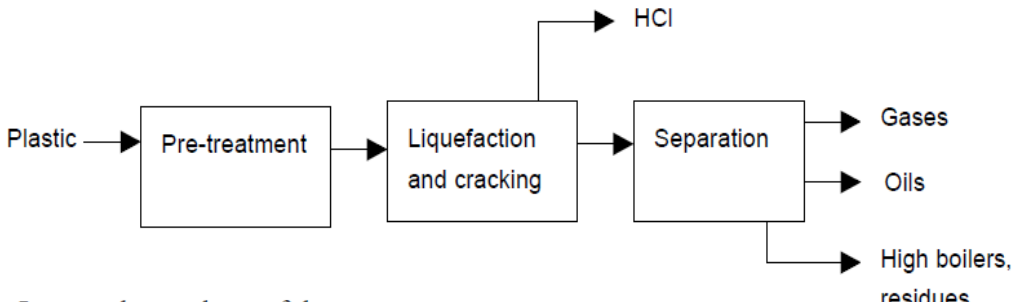

Figure 3: The BASF Pyrolysis process for plastic recycles

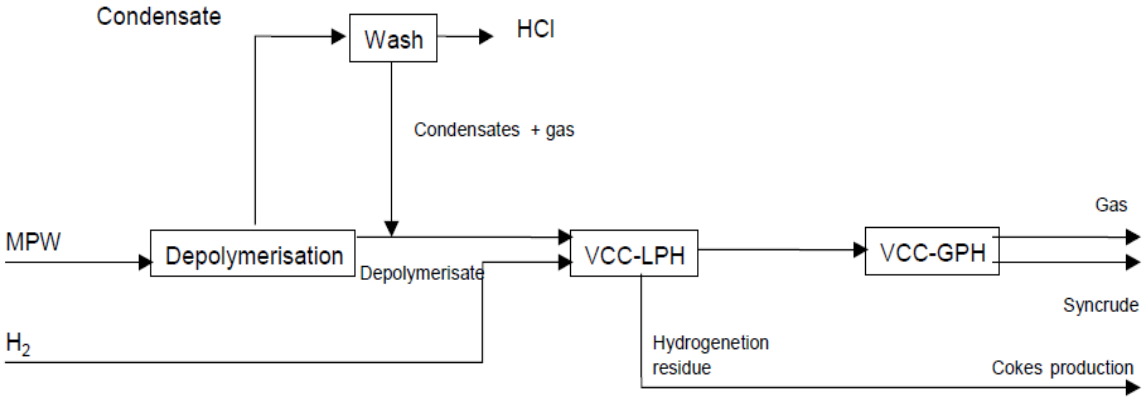

Figure 4: Veba Combi process for Plastic Recycle

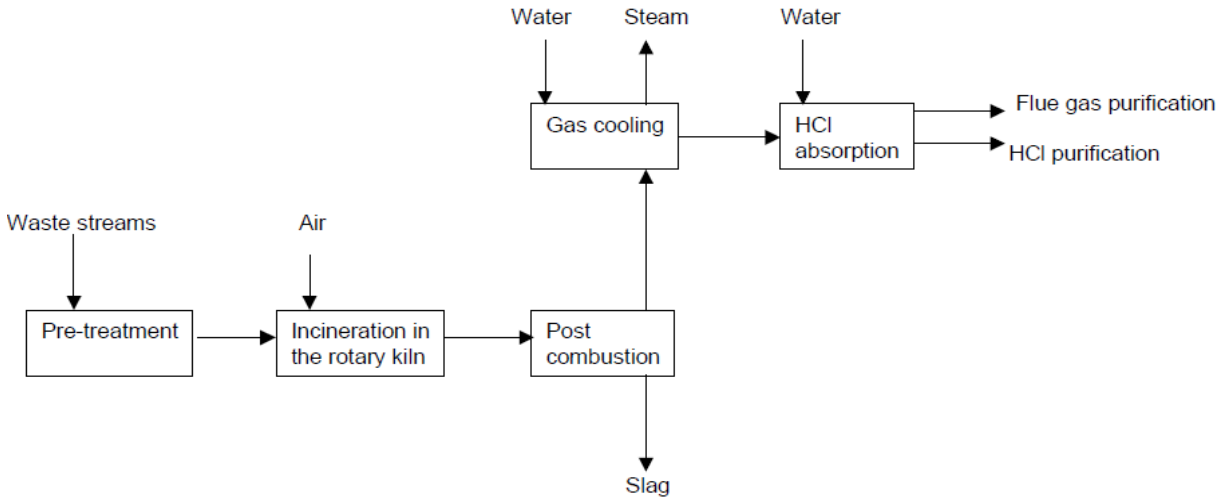

Figure 5: BSL incineration process for Plastic recycles

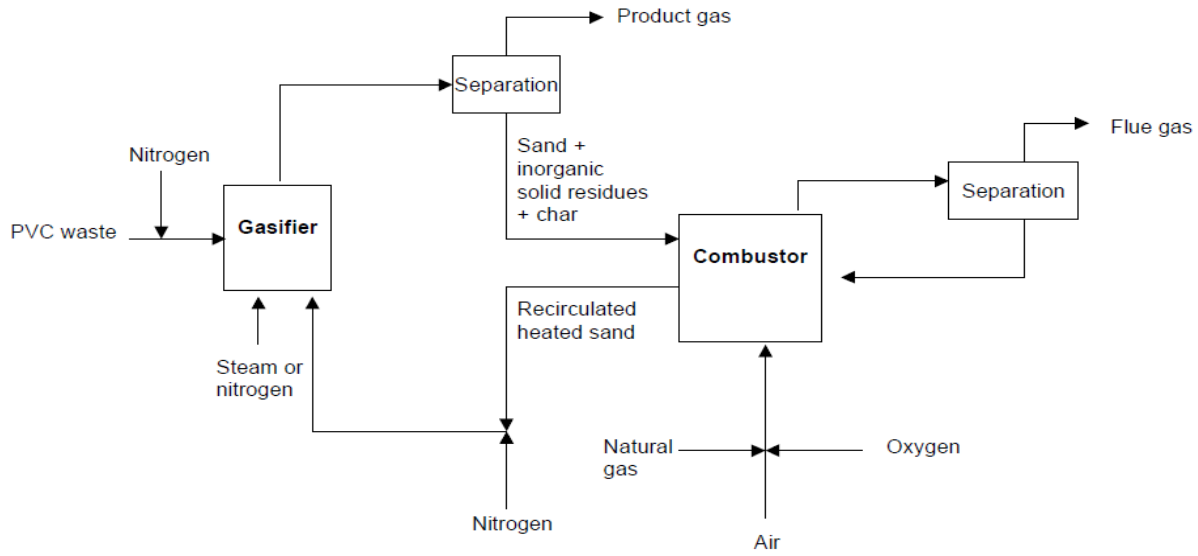

Figure 6: AKZO Steam gasification process for plastic recycles

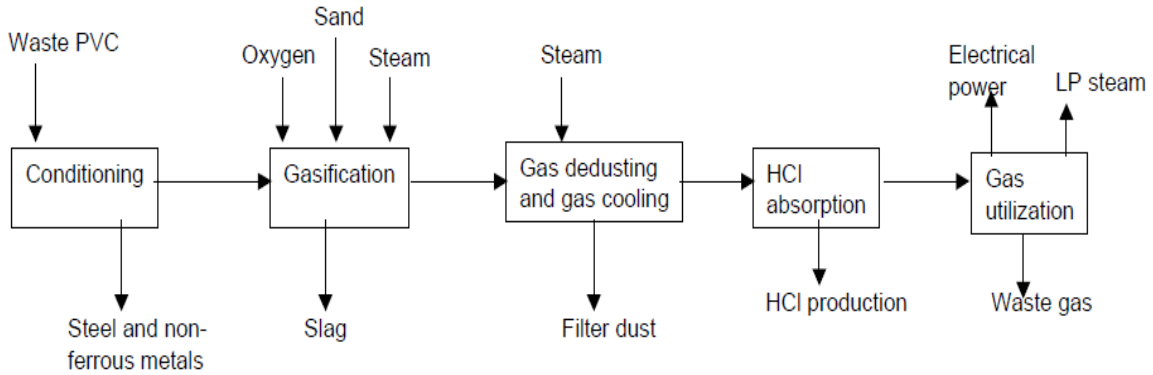

Figure 7: Linde Gasification process for Plastic recycles

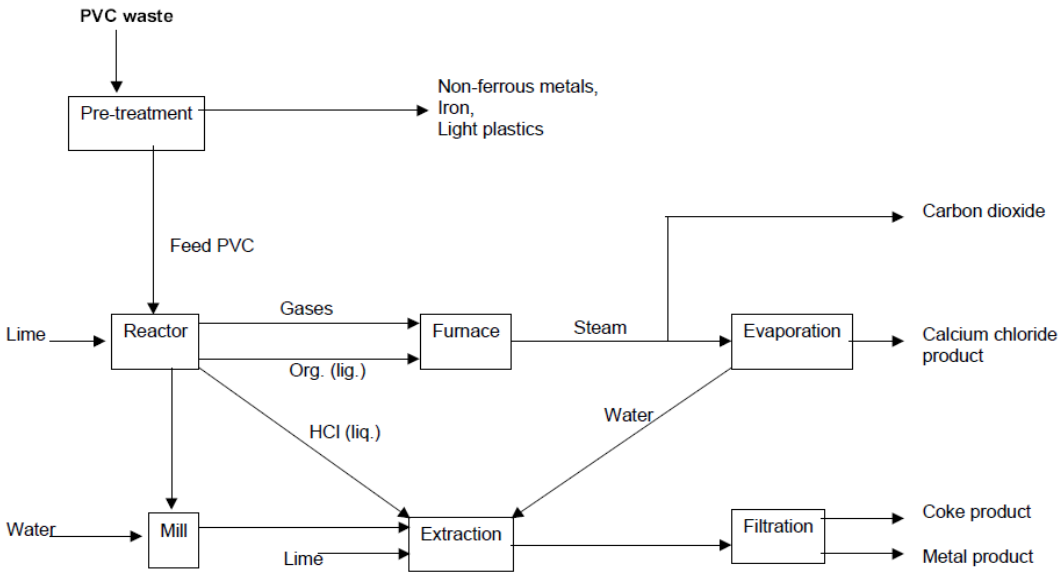

Figure 8: NKT Pyrolysis process for Plastic recycles

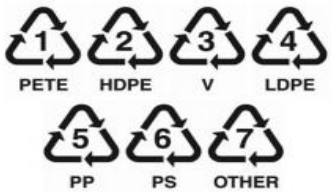

Figure 9: Numbers denotation of plastics, internationally

Table 1: Input specifications for the Polymer Cracking Process

Material	Unit	Normal	Limits
Polyolefin	wt. %	80	min. 70
Polystyrene	wt. %	15	Max. 30
PET	wt. %	3	Max. 5
PVC	wt. %	2	Max. 4
Total Plastic Content	wt. %	95	min. 90
Ash	wt. %	2	Max. 5
Moisture	wt. %	0.5	Max. 1
Metal pieces	wt. %		Max. 1
Size	mm	1-20	
Fines sub-250 micron	wt. %		Max. 1
Bulk Density	Kg/m^3	400	300

Table 2: Cost specification of the Polymer Cracking process (in £ per ton in 1999)

Costs		Income	
Capital charges	152	Products	100
Fixed costs	90	Gate fee	172
Variable costs	30		
Total	**272**	**Total**	**272**

Table 3: Inputs and outputs of the SVZ process

Inputs		Outputs	
MPW-agglomerate	763 g	Methanol	712 g
Waste oil	256 g	Synthesis gas	204 g
Lignite	1.25 kg	Electricity	2,28 MJ
Water	7.9 l	CO_2	6,32 kg
O	1,47 kg	Water vapor	9,9 kg
Fuel oil	40 g	Effluent	9,9 kg
Natural gas	0,1 m^2	Gypsum	0,1 kg
		Slag	0,9 g

Table 4: A review of technical aspects and gate fees (as of December, 1999)

Process	Input	Max. input Cl	Gate fee (Euro). Excl. collection /pretreatment	Status	Products/fate - Organic fraction - Cl - Metals	Capacity	Future potential
Texaco	MPW	5 %	100 (50)	Pilot	Syngas NH_4Cl-product In vitrified slag	-	Uncertain*
Polymer Cracking	MPW	2 %	200 (100-175)	Pilot	Liquid/gas $CaCl_2$ (landfill) In various residues	-	Uncertain*
BASF	MPW	2.5 %	250 (160)	Demo (closed)	Liquid/gas HCl (product) In residues	15 ktpa before 1996	-
Blast Furnace	MPW	1.5 %	Few-100?	Operational	Coal replacement Cl (to water) In iron or slag	162,5 ktpa in 1998	5 Mio tpa in the EU**
Veba	MPW	2 %	250	Operational (to be closed)	Gas/syncrude HCl (product) Hydrogenated resid.	87 ktpa before 2000	-
SVZ	MPW	2-5%	150	Operational	Singes/Methanol Cl to waste In landfill class 1 slag	110 ktpa in 1998	
BSL	PVC-rich, Various mixes	> 50 %	250	Operational	Energy HCl (product) Various solid residues	15 ktpa in 2000	
Kazoo Nobel	PVC-rich, Various mixes	High	Not known yet	Lab/pilot	Syngas HCl (>90 %) Various solid residues	-	
Linde	PCV-rich, Various mixes	> 50 %	200	Pilot operational from 2001	Syngas HCl (product) Various solid residues	2 ktpa in 2000	25 ktpa . 2005
NKT	PVC-rich, Various mixes	High	125-250	Pilot	Coke $CaCl_2$-product Metalchloride	< 1 ktpa in 1999	25 ktpa in future
Vinyloop ®	PVC-rich waste	High	350	Pilot, operational from 2001	PVC resin Other by-products	< 1 ktpa	17 ktpa in 2002
MSWI	MSW ca	n.r.	100-150	Operational	Energy (20-40 %); Cl and metals to waste	N/A	N/A
Cement kilns	MPW	1-2 %	Few-100?	Operational	Energy (100 %), metals and Cl in cement	Some 100+ ktpa	3 Mio tpa in the

Mechanical recycling	PVC mono waste flow	High	Some 200+, much lower for cables	Operational	Recovered PVC	N/A	N/A
Landfill	MSW ca	n.r.	1-280	Operational	-	N/A	N/A

Table 5: A review of options for chemical recycling of MPW and PVC-rich waste, including cement kilns

Technology	**Status**	**Capacity**	**Future potential**
MPW			
Texaco (NL)	Pilot/on hold	-	Uncertain*
Polymer cracking (UK)	Pilot/on hold	-	Uncertain*
BASF (D)	Closed in 1996	15 ktpa before 1996	-
VEBA (D)	Closed by 1-1-2000	87 ktpa before 2000	-
Blast furnaces	Operational (D)	162,5 ktpa in 1998	5 Mio tpa in the
SVZ (D)	Operational	110 ktpa in 1998	
Cement kilns	Operational		3 Mio tpa in the
PVC-rich waste			
BSL (D)	Operational	15 ktpa in 1999	
Linde (D/F)	Pilot under constr.	2 ktpa in 2001	15 ktpa > 2005
NKT (Dk)	Pilot under constr.	< 1 ktpa in 1999	15 ktpa in future

* Typical capacities considered are 50 ktpa up to 200 ktpa

** Theoretical potential *** No decision on realization yet

Table 6: Tentative cost comparison of treatment of MPW or PVC-rich waste, including collection and pre-treatment

Technology	**Typical waste input**	**Max. PVC content**	**Tentative costs over the full chain (Euro per ton)**
Mixed plastic waste			
Landfill	MSW	n.r.	250
MSWIs	MSW	n.r	325
Cement kilns	MPW	2-3%	275-335
Blast furnaces	MPW	2-3%	400
Chemical recycling of MPW	MPW	10% or less	500
PVC-rich waste			
Chemical recycling of PVC	PVC-rich mixture	n.r.	390
Mech. recycling cables	Cable sheeting	n.r.	50
Mech. recycling flooring	Flooring waste	n.r.	350
Mech. recycling other	Profiles etc.	n.r.	250

V. CONCLUSION

Figure 9 shows the different numbers given by plastic industry to different plastic products. Following plastics are a big no-no to be used after recycle from health point-of-view:

1) Plastic No. 3

Found in condiment bottles, teething rings, toys, shower curtains, window cleaner and detergent bottles, shampoo bottles, cooking oil bottles, clear food packaging, wire jacketing, medical equipment, siding, windows and piping, No. 3 plastics are at risk of releasing toxic breakdown products like phthalates into food and drinks. Also, the manufacturing of PVC is known to release highly toxic dioxins into the environment.

2) Plastic No. 6

Better known as polystyrene or Styrofoam, No. 6 plastics are found in disposable plates and cups, meat trays, egg cartons, carry-out containers, aspirin bottles and compact disc cases. You should particularly watch out for insulated Styrofoam cups which, when heated, can release potentially toxic breakdown products like styrene into your coffee or tea. Number 6 plastics have also become notorious for being one of the most difficult plastics to recycle.

3) Plastic No. 7

The so-called "miscellaneous" plastic, No. 7 is a catch-all for various types of plastics, including those found in baby bottles, three- and five-gallon water bottles, 'bullet-proof' materials, sunglasses, DVDs, iPod and computer cases, signs and displays, certain food containers and nylon. Number 7 plastics are made up of various resins, which fit into no other categories; while some are safe, some are suspect. Some contain Bisphenol A (BPA), a synthetic estrogen that could disrupt the human hormone system, causing various health effects.

Concerning the environmental performance of the different chemical recycling processes, we made a comparative analysis based on existing practices for treatment of MPW. MSWIs have a number of disadvantages, like a relatively low energy recovery compared with chemical recycling. Chemical recycling plants for MPW do not differ substantially in a mutual comparison. As for cement kiln incineration, it is unlikely that it will score substantially different to blast furnaces since in both cases coal (or oil) is replaced as a primary resource. It may be that chemical recycling plants which also recycle the Cl (e.g. as HCl) have some advantages. As for PVC-rich waste, it is likely that mechanical recycling scores better than chemical recycling provided it concerns high-quality recycling and the need for pretreatment is limited. Hence, clear environment winners between the four technologies discussed could not be identified.

REFERENCES

[1]. Tukker, A, Simons, L and Wiegersma, S. (**1999**), "Chemical Recycling of Plastics Waste (PVC and Other resins)", A report, Netherlands.

American Journal of Engineering Research (AJER)
e-ISSN : 2320-0847 p-ISSN : 2320-0936
Volume-03, Issue-11, pp-109-117
www.ajer.org

Research Paper Open Access

Survey on various design of microchip patch antenna

A.Anusuya[1], J.Janetstephy[2], prof.G.Jegan[3]
[1, 2,3]*Faculty of Electronics and Communication, Sathyabama University.*

ABSTRACT-*Due to fast advancement in wireless communication technology, use of small size antenna has rapidly increased. Not only the size of the antenna its cost, performance, ease of installation everything have been taken care while designing the antenna. To meet this entire requirement micro-strip antenna is proposed. Nowadays microstrip antennas are used in many places such as aircrafts, spacecraft's, satellite and missile applications. In this paper, we discuss the microstrip antenna, types of microstrip antenna, various substrates used for designing the antenna and the literature survey which we have done.*

Key words: *Microstrip patch antenna (MPA), Microstrip slot antenna (MSA), printed dipole antenna (PDA)*

I. INTRODUCTION:

Antenna is a transducer designed to transmit or receive electromagnetic waves. Microstrip antenna has several advantages over conventional antenna. It consists of a radiating patch on one side of dielectric substrate and has a ground plane on other side. Microstrip antennas are used for many commercial purposes due to their light weight and low cost. The recent demands of compact wireless devices propel the demand of pattern reconfigurable antennas. Reconfigurable microstrip antenna provides numerous application and offer more versatility as compared to conventional antennas which offer one function in a single antenna. They can provide diversity function in operating frequency, radiation pattern and polarization to mobile communications. The main disadvantages of microstrip patch antenna radiation performance including narrow bandwidth. Various techniques have been included to overcome these disadvantages.

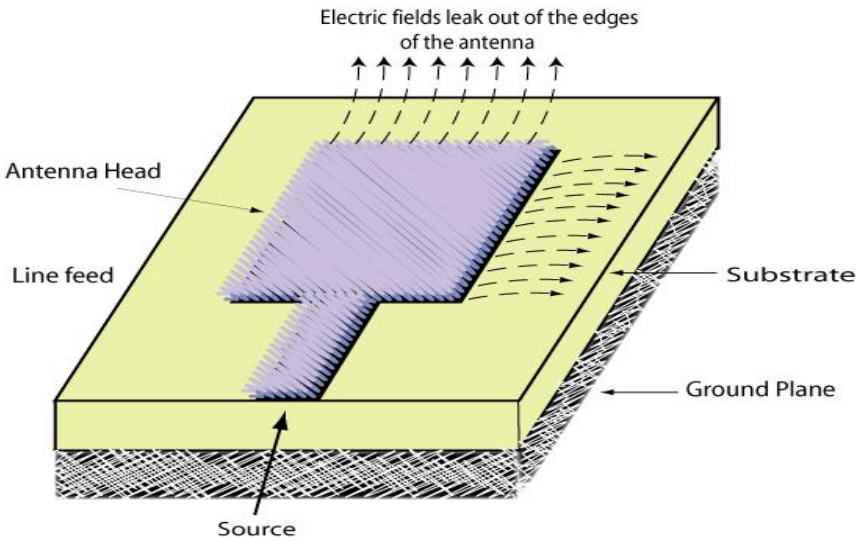

Comparisons of microstrip patch antenna, microstrip slot antenna and printed dipole antenna:

S.NO	CHARACTERISTICS	MPA	MSA	PDA
1	Profile	Thin	Thin	Thin
2	Fabrication	Very easy	Easy	Easy
3	Polarization	Both linear and circular	Both linear and circular	Linear
4	Dual frequency operation	Possible	Possible	Possible
5	Shape flexibility	Any shape	Mostly rectangular and circular	Rectangle and triangle
6	Spurious Radiation	Exists	Exists	Exists
7	Bandwidth	2-50%	5-30%	-30%

MPA-Microstrip patch antenna

MSA-Microstrip slot antenna

PDA-Printed dipole antenna

FEEDING TECHIQUE:

Microstrip patch antenna can be fed by a variety of methods. These methods can be classified into two categories-contacting and non-contacting. In the contacting method, the RF power is fed directly to the radiating patch using a connecting element such as a microstrip line. In the non-contacting method, electromagnetic field coupling is done to transfer power between the microstrip line and the radiating patch. There are four most popular technique used here they are i) Microstrip line ii) Coaxial line iii) aperture coupling iv) proximity coupling. Microstrip patch antennas have radiating element on one side of a dielectric substrate and thus may be fed by any of this four technique. Matching is usually required between the fed line and the antenna input impedances.

MICROSTRIP LINE FEED:

Microstrip line fed is conducting strip, usually of much smaller width compared to patch. It is easy to fabricate, simple to match by controlling the inset position. If we increases the thickness of the substrate surface waves and spurious fed radiation increases. And its bandwidth is very limited. The purpose of the inset cut in the patch is to match the impedance of the fed line to the patch, without the need for any additional matching element. This is achieved by properly controlling the inset position.

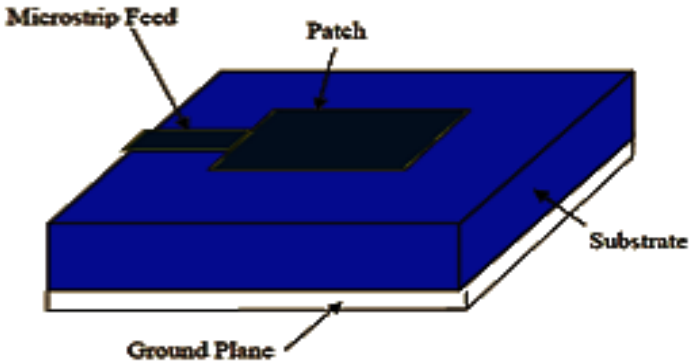

Figure Microstrip Line Feed

COAXIAL FEED:

It is a common technique used for feeding microstrip patch antenna. Inner conductor of the coaxial connector extends through the dielectric and is soldered to the radiating patch, while the outer conductor is connected to the ground plane. The advantage of this type of feeding scheme is that the fed can be placed at any desired location inside the patch in order to match its input impedance. Its major disadvantage is that it provide narrow bandwidth and is difficult to model since a hole has to be drilled in the substrate and the connector protrudes outside the ground plane, thus not making it completely planar for thick substrates.

APERTURE COUPLE FEED:

Coupling between the patch and the feed line is made through a slot or an aperture in the ground plane. In this technique transmission line is shielded from the antenna by a conducting plane with a hole to transmit energy to antenna as shown in fig.

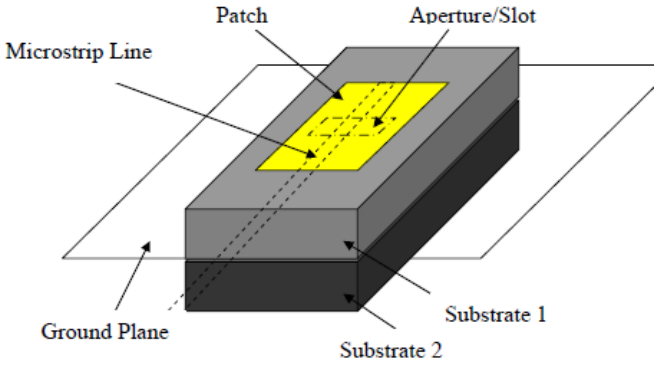

The upper substrate can be made with a lower permittivity to produce loosely bound fringing fields, yielding better radiation. The lower substrate can be independently made with a high value of permittivity for tightly coupled fields that don't produce spurious radiation. The disadvantage of this method is increased difficulty in fabrication.

PROXIMITYCOUPLE FEED:

This type of feed technique is also called as the electromagnetic coupling scheme. It has the largest bandwidth, has low spurious radiation. Fabrication of proximity coupling is very difficult. Length of feeding substrate and width to length ratio of patch is used to control the match. Its coupling mechanism is capacitive in nature.

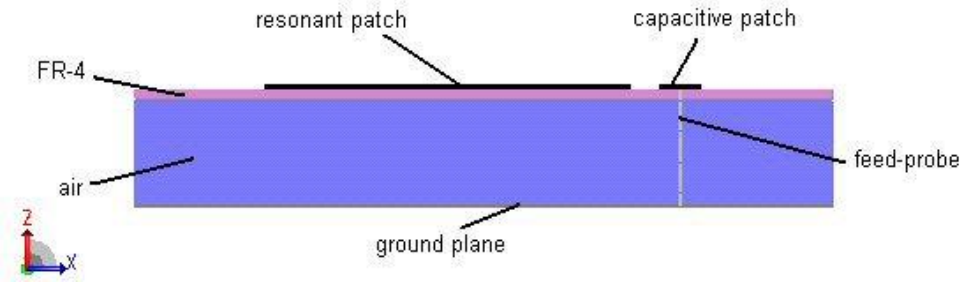

ANALYSIS OF SUBSTRATES USED FOR ANTENNA DESIGN:

Material	Symbol	RDC ε_R	TDC +/-	DF **tan** δ	TC **of** ε_R**(ppm/C)**	MD **(gr/cc)**	SH **(J/g/°C)**	TC **W/m°C**	CTE **PPM/°C x/y/z**
Bakelite		4.8							22/28/173
Rogers Duroid 5870	PTFE/ Random glass	2.33	0.02	0,0012	-129	2.2	0.96	0.26	31/48/237
Rogers Duroid 5880	PTFE/ Random glass	2.2	0.02	0.0012	-129	2.2	0.96	0.26	31/48/237
Rogers Duroid 6002	PTFE/ Random glass	2.94	0.04	0.0012	0	2.1	0.93	0.44	16/16/24
Rogers Duroid 6006	PTFE/ Random glass	6	0.15	0.0027	-350	2.7	0.97	0.48	38/42/24

Rogers Duroid 6010	PTFE/ Random glass	10.2-10.8	0.25	0.0023	-390	2.9	1	0.41	24/24/24
FR-4	glass/ epoxy	4.8		0.022				0.16	FR-4
Polyethylene		2.25							
Polyflon CuFlon	PTFE	2.1		.00045					12.9
Polyflon PolyGuide	Polyolefin	2.32		0.0005					108
Polyflon Norclad	thermoplastic	2.55		0.0011					53
Polyflon Clad Ultem	thermoplastic	3.05		0.003		1.27			56
PTFE	PTFE	2.1		0.0002		2.1	0.96	0.2	
Rexolite No. 1422		2.55							
Rogers R/flex 3700	Thermally stable thermoplastic	2.0		0.002					8
Rogers RO3003	PTFE ceramic	3	0.04	0.0013	13	2.1	0.93	0.5	17/17/24
Rogers RO3006	PTFE ceramic	6.15	0.15	0.0025	-169	2.6	0.93	0.61	17/17/24
Rogers RO3010	PTFE ceramic	10.2	0.3	0.0035	-295	3	0.93	0.66	17/17/24
Rogers RO3203	PTFE ceramic	3.02							
Rogers RO3210	PTFE ceramic	10.2							
Rogers RO4003	Thermoset plastic ceramic glass	3.38	0.05	0.0027	40	1.79		0.64	11/14/46
Rogers RO4350B	Thermoset plastic ceramic glass	3.48	0.05	0.004	50	1.86		0.62	14/16/50
Rogers RO4403	Thermoset plastic ceramic glass	3.17							
Teflon		2.1		0.0001		2.13-2.22			
Rogers TMM 3	ceramic/ thermos	3.27	0.032	0.002	37	1.78	0.87	0.7	15/15/23
Rogers TMM 4	ceramic/ thermoset plastic	4.5	0.045	0.002	0	2.07	0.83	0.7	16/16/21
Rogers TMM 6	ceramic/ thermoset	6	0.08	0.0023	-11	2.37	0.78	0.72	18/18/26
Rogers TMM 10	ceramic/ thermoset	9.2	0.23	0.0022	-38	2.77	0.74	0.76	21/21/20
Rogers TMM 10i	ceramic/ thermoset	9.8	0.245	0.002	-43	2.77	0.72	0.76	19/19/20
Ultralam 2000	glass reinforced	2.24-2.6	-.04	0.0019	-100				9.5/9.5/120

LITERATURE SURVEY

1. FREQUENCY RECONFIGURABLE MICRO PATCH-SLOT ANTENNA WITH DIRECTIONAL RADIATION PATTERN

In this author designed antenna with reflector at the back of an antenna. In this paper microstrip patch antenna and microstrip slot antenna were presented, where the slot antenna is positioned at the ground plane underneath the patch. This antenna is capable of reconfigure up to six different frequencies band from 1.75GHz to 3.5GHz. In this frequencies three different frequency produced by microstrip slot antenna and other three different frequencies is produced by microstrip patch antenna with bidirectional radiation pattern. Here the substrate used is Taconic RF35 with a permittivity of thickness 3.04. The patch of the antenna is designed to operate at4.13GHz. Here, inset feed is used to match the impedance between the patch and for analysis technique transmission line method is used.

2. CIRCULAR POLARIZATION WIDEBAND E-SHAPED PATCH ANTENNA FOR WIRELESS APPLICATIONS

In this paper, polarization switching is presented for reconfigurable wideband E-shaped patch antenna. This design consists of two slots which are switched on and off using pin diode. And, two antennas allowing switching either between linear and circular polarization or between two circular polarizations are demonstrated. This microstrip antenna operates at 2.45GHz frequencies. Antenna is constructed on grounded two layers of dielectric sheet (air and FR4), and a vertical probe connected from ground to the upper patch. The substrate FR4 with relative dielectric constant of 4.2, thickness of h=10mm, and loss tangent=0.02.

3. PATCH ANTENNA FREQUENCY RECONFIGURABLE LOW-PROFILE CIRCULAR MONOPOLAR

Here, antenna comprises of a centre-fed circular patch surrounded by four sector-shaped patches. Eight varactor diode are introduced to bridge the gap between the circular patch and the sector shaped patches. By changing the reverse bias voltage of the varactor diodes, the antenna can be switched in the operating frequency. Here the measured efficiency rises from about 45% to about 85% as the operating frequency increases from 1.64GHz to 2.12GHz. The antenna is printed on a 6.34mm thickness Rogers dielectric (ε_R =2.33) which is realized by stacking two 3.17mm thickness substrates and removing the middle two copper layer. To understand how the dimension of the antenna affects the performance, a parametric study was performed. The operating frequency tuning range from 1.64GHz to 2.12GHz by changing the reverse bias voltage of the varactor diode from 0V to 20V. Stable monopole like radiation patterns are achieved at all operating frequencies.

4. FREQUENCY RECONFIGURABLE MICROSTRIP PATCH ANTENNA WITH CIRCULAR POLARIZATION

A simple design of circularly-polarize microstrip antennas with frequency agilityis described. With a coaxial probe, two orthogonal resonant modes of the square patch antenna are simultaneously excited. Here only one DC voltage is required to vary the circular polarization operating frequency, and experimental results indicate that the circular polarization frequency can be switched between 1.97GHz and 2.53GHz. Antenna structure is based on a probe-fed microstrip patch antenna with capacitive loadings. A square radiating patch with a side length of 32mm is fabricated an FR4 substrate of thickness of 0.4mm and relative permittivity 4.4. The copper foil of other substrates with thickness 1.6mm serves as the ground plane. Measured results demonstrate that by controlling one dc voltage, the prototype can perform frequency switching from 1.97GHz to 2.53GHz. Moreover, within the bandwidth, the prototype has a return loss of less than 10db, an axial ratio of lower than 3d, gain variations of about 3db, and stable broad side radiation pattern.

5. RECONFIGURABLE TX/RX ANTENNA SYSTEMS LOADED BY ANISOTROPIC CONDUCTIVE CARBON FIBER COMPOSITE MATERIALS

Here, potential use of reinforced continuous carbon fiber composite (RCCFC) material to build reconfigurable TX/RX communication systems. The frequency agile characteristic is obtained by the rotation of the antennas on the ground plane which is made of anisotropic RCCFC material. Probe-fed rectangular microstrip patch antennas are fabricated and the reconfigurable characteristics are investigated both numerically and experimentally. RT/Duroid 5880 substrate with thickness of h=1.5mm is used to fabricate the antenna. In many wireless and sensor applications, the antennas are used and deployed over a horizontal plane so that the normal vectors of ground planes of antenna are parallel. In this case, the TX/RX performance over a horizontal plane becomes important. In modern, aircraft and automobiles, fuselage is mainly made of composite material,

especially RCCFC. The frequency of operation of a probe-fed patch antenna can be reconfigurable by rotating the patch around the probe, operating over an anisotropic ground plane made of RCCFC composite. The RCCFC ground acts as a mode filter, allowing radiating modes with a current distribution component parallel to the fiber direction to the excited by suppressing modes with current flows perpendicular to the fiber direction. In this only three frequency of operation is changed and the polarization of the radiated field does not change.

6. POLARIZATION RECONFIGURABLE OMNIDIRECTIONAL ANTENNA COMBINING DIPOLE AND LOOP RADIATORS

The omnidirectional circular polarization waves can be generated in the azimuthal plane by adopting two metal probe act as the dipole and printed spoke-like metal strips fabricated on two substrates act as the loop. 48-pin diodes placed on the two substrates to atter the current direction of the loop which makes the antenna polarization reconfigurable. The polarization states of this antenna can be switched between left-hand circular polarization (LHCP) and right-hand circular polarization (RHCP). The feeding type used is microstrip line fed. This antenna is designed for the frequency of 1.575GHz for GPS system. The polarization state of this antenna depends on the direction of the RF current in the loop at initial time. Antenna is designed with the use of Rogers/duroid 5870 substrate (h=1.57mm, permittivity=2.3) pin-diode of type BAR50-02V.

7. EFFECTS OF DIELECTRIC PERMITTIVITY ON RADIATION CHARACTERISTICS OF CO-AXIALLY FEED RECTANGULAR PATCH ANTENNA

In this paper author discuss about various dielectric materials and its effects on radiation characteristics of rectangular patch antenna such as resonance frequency, bandwidth, gain, return loss, input impedance, radiation pattern and current distributions are investigated. And the dielectric material selected here having zero loss tangent. Here there is only small space between radiating element and ground plane main power is radiated towards broad size co-axial probe feed is used,here outer conductor is connected to ground plane and the inner conductor of co-axial connector is extends through dielectric and soldered to patch. Inner conductor of co-axial cable transfers the power from strip line to microstrip antenna from slot in the ground plane. Here different substrates used to compare the return loss.

8. EFFECTS OF ANTENNA DESIGN PARAMETERS ON THE CHARACTERISTICS OF A TERAHERTZ COPLANAR STRIPLINE DIPOLE ANTENNA

This paper presents the antenna design parameters dependency on the impedance and radiation characteristics of a terahertz coplanar stripline dipole antenna. This antenna response is numerically investigated by applying a semi-infinite substrate and by generating a constant voltage source to drive signal on the antenna. In this way one can analyse the antenna characteristics without the photoconductive material response and the substrate lens geometrically effects antenna consists of centre-dipole connected to long bias has a travelling wave characteristics supporting a standing wave of current. The travelling wave behaviour produces stable antenna input impedances and minimal changes in the antenna radiation patterns. Gas substrate is used where this substrate was approximated with a semi-infinite greens function layer. The centre dipole is designed to resonate at around 1.0THz. The length of the centre dipole is increased so that the antenna becomes more distinct at low frequencies. By further increasing the centre dipole length could lower the cut off frequency and thus produce better impedance bandwidth.

9. ENHANCING THE BANDWIDTH OF A MICROSTRIP PATCH ANTENNA USING SLOTS SHAPED PATCH

In this three different geometry shapes U,E and H are developed from a rectangular patch of the width (w) =32mm and length (L) =24mm. the E-shaped patch antenna has the highest bandwidth followed by U-shape patch antenna and H-shape patch antenna. The substrate used here is alumina 96% with the dielectric constant of 9.4 and loss tangent of 4.0e-4. Parameter's used in this antenna design is i)frequency of operation-2GHz ii) height of substrate=2mm iii) dielectric constant=9.4 iv) width of patch=32mm v) length of the patch(L)=24mm vi) loss tangent=4.0e-4. This antenna is used for the WLAN. This antenna is to operate in the frequency range from 1GHz to 3GHz. The dielectric constant is kept high in order to get a reduced antenna size.

10. DESIGN OF COMPACT MICROSTRIP ANTENNA USING CERAMIC SUBSTRATE

Here, the proposed idea is to model the microstrip antenna with new material for substrate having very high dielectric constant. The basic idea of this paper is to get the desired functioning of microstrip patch antenna with less size with respect to height and width of the substrate as well as the patch with the use of ceramic substrate. The substrate used in this design is belongs to ceramic family which is named by forsterite. By using this ceramic family substrate efficient and concise antenna is designed. It gave the effect on the radiations and bandwidth of the antenna. This substrate (forsterite) has the dielectric constant 6.2. this substrate has low

microwave loss, good insulation at high temperatures, and as smooth surface. This ceramic substrate has high coefficient of thermal expansion, it bonds easily with metals and glass. Its resonant frequency is equals to 1.80GHz with the help of this substrate the dimensions of the antenna are greatly reduced. The bandwidth efficiency and directivity of this suggested model is also enhanced at low cost. Moreover, due to such a high dielectric constant material reduces the robustness and mechanical stability of the antenna.

11. A FREQUENCY RECONFIGURABLE STACKED PATCH MICROSTRIP ANTENNA WITH APERTURE COUPLER TECHNIQUE

This antenna is capable to accommodate at S/X band separately by using the same antenna. Two patches at different substrates are activated sequentially by changing modes at the feed line to achieve frequency reconfigurability. Operating frequency of this antenna is 2GHz to 8GHz. Antenna was based on a design of stacked patch microstrip patch antenna with aperture coupler technique. This antenna was composed of three layer of substrates, which are substrate1 and substrate2 by using Rogers/duroid 5880 materials with a dielectric constant, r=2.2, thickness h=0.78mm and tangent loss=0.0009 is used and FR4 material is used as substrate3 with a dielectric constant r=4.7, thickness h=1.6mm and tangent loss=0.0009 is used. According to the simulation results the FRSPMA can operate at the two states either ON state or OFF state. During the ON state, this antenna basically operates at s-band frequency which is at 2.16GHz with return loss is 34.01db. The gain obtained is 5.773db which is higher during the OFF state compared to ON state. The bandwidth during ON state is narrow width 92.9MHz. However, the bandwidth during OFF state can be considered large bandwidth width 247.7MHz. This antenna can cover large area during both states with the angular width (3db) 147.1 and 142.2 respectively.

12. PATCHANTENNA DESIGN ANALYSIS FOR WIRELESS COMMUNICATION

A simulation of sixteen (hexadecimal) faced microstrip patch antenna design using slot on the edge is discussed here. Here probe fed model is used. The simulated results of the antenna achieve the radiation parameters such as s-parameter radiation pattern and VSWR. In s-parameter. The parameter value reaches less than -10dB for the resonant frequencies 0.9GHz, 0.87GHz to 0.90GHz and VSWR value is obtained as less than 2 for that same frequency. This antenna will be useful for 900MHz band in wireless communication application.

13. RECTANGULAR MICROSTRIP PATCH ANTENNA USING CO-AXIAL PROBE FEEDING TECNIQUE TO OPERATE IN S-BAND

Here, the design of antenna is based on rectangular microstrip antenna. Its operating frequency is from 2GHz to 2.5GHz. Substrate used here is Flame Retardant 4 with the thickness of 1.6mm and its dielectric constant is approximately 4.4 and fed type used here is probe-fed. The return loss of the antenna obtained is -23dB at the centre frequency of 2.25GHz. From this, it indicates that the 9.61% of power is reflected and 90.84% of power is transmitted. The bandwidth obtained from the return loss result is 2% which signifies 46MHz. A perfectly matched antenna would have a VSWR of 1:1. This indicates how much power is reflected back or transferred into a cable. VSWR obtained from this antenna design is 1.13dB which is approximately equals to 1.1:1. This indicates that the level of mismatch is not very high.

14. FREQUENCYRECONFIGURABLE MICROSTRIP CIRCULAR PATCH ANTENNA FOR WIRELESS DEVICES

Here, frequency reconfigurable circular antenna design is proposed. In this, antenna a circular patch antenna with circular slot using two pin diode at the centre frequency 10 GHz was designed and simulated frequency reconfiguration is achieved in the frequency range of 9.69-10.2GHz. Thesubstrate used is FR-4 with its permittivity of 4.54 and thickness of 1.6mm. The dimensions of the microstrip circular patch element were calculated at the centre frequency of 10GHz by conventional design procedure. Here, electromagnetic simulation software was used to simulate the proposed structure. Frequency reconfigurations were achieved for three different cases.Case i) when both diodes was in off-states Case ii) when one-diode is in on-state Case iii) when both diode is on on-state. In first case, the return loss is -14.84dB at the resonant frequency of 9.69GHz. In second case, the return loss is -11.87dB at the resonant frequency of 9.83GHz.Whereas in third case, the return loss is -13.84dB at the resonant frequency of 10.18GHz.

15. DESIGN OF FREQUENCY RECONFIGURABLE MICROSTRIP PATCH ANTENNA

In this design, rectangular patch antenna with slots at the centre frequency 10GHz that can be reconfigured in the frequency range 10-10.5GHz. Reconfiguration is done by switching the diodes into on/off condition. Substrate used here is FR-4 with their permittivity of 4.54and its thickness is 1.50mm. slots and switches are also used here in order to achieve both the frequency and polarization reconfigurability. Specially here three different polarization states have been achieved: righthand, lefthand, linear and circular polarization. This reconfigurable antenna can further be modified by using RF-MEMS switches for fast switching process. As mentioned in previous paper here also those three modes have been specified. In first case, the return loss is -13dB at the resonant frequency of 10.5GHz. In second case, the return loss is -19dB at the resonant frequency of 10.3GHz.Whereas in third case, the return loss is -42dB at the resonant frequency of 10.2GHz.

16. RECONFIGURABLE MICROCHIP PATCH ANTENNA USING MEMS TECHNOLOGY

Here, the design of reconfigurable microchip patch antenna is based on MEMS technology. Operating frequency is in the range of 5-8GHz for the application of wireless communication has been designed. MEMS based switch is inserted in the patch to control its configuration patch antenna using switchable slots shows different resonant features with different states of the switch. Here, capacitive type MEMS switch is used. Fed line width is 1.5564mm and fed-line length is 2.456mm.in this design return loss of -10dB is obtained and VSWR lie in the range of 1-2 which is achieved for all frequencies. Resonant frequency of 6GHz was designed. Different operating frequency of 5.38, 5.68, 5.75GHz were obtained using RF MEMS switch.

17. DESIGN AND SIMULATION OF MICROSTRIP PATCH ARRAY ANTENNA FOR WIRELESS COMMUNICATION AT 2.4GHZ

Here, rectangular microstrip patch array antenna at 2.4GHz for wireless communications that provides a radiation pattern along a wide angle of bean and achieves a gain of 11.6db. In this, author designed an array of rectangular patch antenna of the centre frequency 2.4GHz sweeping between 1.2-3.6GHz. And the substrate used here is Rogers/duroid 5880 for analysing the antenna transmission line model is used. The fed type used here is edge type feeding. The performance parameters were achieved with gain 12db and beam width 40degree in E-plane and 26 degrees in H-plane for patch array antenna.

18. DESIGN OF COMPACT MULTIBAND MICROSTRIP PATCH ANTENNAS

In this design, antenna for important wireless applications which lie in the band starting from 900MHz to 5.5GHz which includes the GSM (880-960) GPS (1568-1592 MHz) ,DCS (1710-1880MHz), and PCS(1850-1990MHz), UMTS(1920-2170MHz), IEEE 802.11 b/g(2400-2484) and WLAN IEEE802.11a bands (5.15-5.35GHz,5.725-5.825GHz). In this design different type of antenna such as i) rectangular fractal antenna ii) multi-standard patch antenna iii) circularly polarized microstrip patch antenna iv) E-shape and U-shape v) multi-standard patch antenna. Gain and directivity is calculated for each antenna. This antenna will cover the wide band operation and can be applied to multiband wireless communication system due to its small size and low fabrication cost. Antenna gain and radiation pattern are acceptable at almost all bands of operation.

19. 2.45GHz MICROSTRIPPATCH ANTENNA WITH DEFECTED GROUND STRUCTURE FOR BLUETOOTH

In this paper, author analysed rectangular patch antenna with DGS (Defected Ground Structure) for wireless application. Their antenna design simulated at 2.45GHz frequency. And their feeding technique is done by quarter transformer feeding. This feeding is mostly used for impedance matching. Here, they used rectangular patch antenna. This patch antenna dimension is 15mmx18mm using the dielectric substrate having permittivity 3.2 and thickness is 0.762mm. The dimension of quarter transformer feed which is used for a rectangular patch antenna of the resonant frequency 5GHz are length 9.5mm and width 0.56mm and feed line width is 1.83mm which results in a good match with 50ohm.

20. AN ELECTRONICALLY RECONFIGURABLE MICROSTRIP ANTENNA WITH SWITCHABLE SLOTS FOR POLARIZATION DIVERSITY

In this paper, electronically reconfigurable microstrip antenna for both circular and linear polarization switching was presented. The prototype fabricated on a substrate of dielectric constant with permittivity of 4.4 and height(h) of 1.6 is fed by a proximity feed fabricated using the same substrate. By controlling the bias voltage of two pin-diodes, the polarization of the antenna can be switched between three states. Two states for linear polarization and one state for circular polarization. The fundamental resonant modes of the unslotted cross shaped patch are at 1.8GHz and 2.4GHz with orthogonal polarization. The properselection of slot size modifies the horizontal and vertical length of the patch equally so that two resonant frequencies are lowered to 1.12GHz and 1.44GHz. This antenna achieves a cross-polar level better than -10dB in linear polarization and 1.18%in circular polarization. This antenna is compact and simple because it uses only few active and passive components and it requires less area to occupy the patch. Frequency and polarization diversity in this design provides some potential application for wireless communication.

CONCLUSION:

Theoretical survey on microstrip patch antenna has done in this paper. While designing the antenna the things which we have to consider is substrate which we are going to use, feeding type, dielectric constant of the substrate and its height and width. When we use the substrate from the ceramic family it gives the low microwave loss and also good

insulation at high temperature. Particular microstrip patch antenna can be designed for specific applications. And it is believed that, this small size antenna will continue to benefit the human race for future years.

REFERENCES:

[1]. 1.Lei Ge and Kwai man Luk, "Frequency-Reconfigurable low-profile Circular Monopolar Patch Antenna",IEEE Transactions And Propagation,Vol.AA,No.B,2014.

[2]. 2.Aidin Mehdipour,Tayeb A. Denidni,"Reconfigurable TX/RX Antenna Systems Loaded by Anisotropic Conductive Carbon- Fibre Composite Material", IEEE Transaction On Antenna And Propagation,Vol.62,No.2,2014.

[3]. 3.Jeen-sheen Row and Jia-fu Tsai," Frequency-reconfigurable Microstrip Patch Antennas with Circular Polarization",IEEE Transactions And Wireless Propagation Letters,Vol.13,2014.

[4]. 4.Ali Ramadan, Mohammed Al- Husseini ,"A Directional Polarization Reconfigurable Microstrip Antenna ",IEEE Transaction Paper-2011.

[5]. 5.J.Salai Thillai Thillagam, Dr.P.K.Jawahar,"Patch Antenna Design Analysis for Wireless Communication", International Journal Of Advanced Research Electrical Electronics and Instrumentation Engineering-2013

[6]. 6.K.S.Tamilselvan,S.Mahendrakumar,"Design Of Compact Multiband Microstrip Patch Antennas", Journal Of Global Research In Computer Science,Vol-3,No.11,NOV-2012.

[7]. 7.Huda A.Majid,Mohammad K.A.Rahim,"Frequency Reconfigurable Microstrip Patch-Slot Antenna With Directional Radiation Pattern", progress in Electromagnetic Research,Vol.144,319-328,2014.

[8]. 8.Rajeshwar Lal Dua,Himanushu Singh,Neha Gambhir,"2.45Ghz Microstrip Patch Antenna with Defected Ground Structure for Bluetooth", International Journal of Soft Computing and Engineering ,Vol-1,Issue-6,January-2012.

[9]. 9.Dr.Thirmurugan.T,Sundar .k,eta.,"Circular Polarization wideband E-shaped Patch Antenna for Wireless Applications",International Journal of Engineering and Technical Research,Vol-2,Issue-3,March-2014.

[10]. 10.B.Sai sandeep, S.Sreenath kashyap,"Design and Simulation of Microstrip Patch Array Antenna for Wireless Communications At 2.45Ghz",International Joural of Scientific and Engineering Research,Vol-3,Issue-11,November-2012.

[11]. 11.Boli and Quan Xue."Polarization Reconfigurable Omnidirectional Antenna Combining Dipole and Radiators",IEEE Antenna And Wireless Propagation Letters,Vol-12,2013.

[12]. 12.K.Praveen Kumar,K.Sanjeev Rao eta.,"The Effect of Dielectric Permittivity on Radiation Characteristics of Co-axially feed Rectangular Patch Antenna",Intenational Journal of Advanced Research in Computer and Communication Engineering,Vol-2,Issue 2,Feb-2013.

[13]. 13.Truong Khang Nguyen and Ikmo park,"Effects of Antenna Design Parameter on The Characteristics Of a Terahertz Coplanar Stripline Dipole Antenna",Progress in Electromagnetics and research,Vol-28,129-143,2013.

[14]. 14.M.S.Nishamol,V.P>Sarin eta.,"An electronically Reconfigurable Microstrip Antenna With Switchable Slot For Polarization Diversity",IEEE Transcations Of Antenna And Propagation,Vol-59,No-9,Sep-2011.

[15]. 15.Atser A.Roy,Joseph M,Eta.,"Enhancing the Bandwidth of a Microstrip Patch Antenna Using Slot Shaped Patch",American Journal of Engineering Research,Vol-02,Issue-09,pp-23-30.

[16]. 16.Arun Sharma,Jagatijit singh Chahal."Design of Compact Microstrip Antenna Using ceramic Substrate", Journal of Engineering Computers And Applied Sciences,Vol-2.No 6 ,June 2013.

[17]. 17.N.Ramli,M.T.Ali,eta.,"Frequency Reconfigurable Stacked patch Microstrip Antenna with Aperture Coupler Technique,2012 IEEE Symposium On wireless Technology& Application,Sep 23-26,2012.

[18]. 18.Alak Majumder,"Rectangular Microstrip patch antenna Using Coaxial Probe feed ing Technique to operate in S-Band".International Joural Of Engineering Trends and technology,Vol-4,Issue 4,April 2013.

[19]. 19.Ghanshyam Singh and Mithilesh Kumar,"Design Of Frequency Reconfigurable Microstrip Patch Antenna",2011 6th International Conference on Industrial and Information System,ICIIS 2011,Aug-16-19,2011.

[20]. E. Ramola , Dr.T.Pearson,"Reconfigurable Microstrip Patch Antenna using MEMS:,IOSR Journal of Electronics And Communication Engineering,Vol-4,Issue 4(Jan-Feb 2013),PP 44-5.

American Journal of Engineering Research (AJER)
e-ISSN : 2320-0847 p-ISSN : 2320-0936
Volume-03, Issue-11, pp-118-124
www.ajer.org

Research Paper Open Access

The Trends and Tides of Poultry Farm Building in Makurdi, Benue State, Nigeria

V.D Chia[1] , B.O Ugwuishiwu[2]
Eco-Hydrological Systems Research Unit (EHSRU), Department Agricultural & Bioresources Engineering, University Nsukka, Nigeria[1]
Department Agricultural & Bioresources Engineering, University of Nsukka, Nigeria[2]

ABSTRACT: *Adequate poultry housing is needed to protect birds from rain, direct sunlight, heat, cold, turbulent winds, dust etc. Birds are unlikely to perform satisfactorily if the housing is poor, therefore correct housing must be provided to meet the optimum environmental requirements for birds' performance either through growth or egg production. Moreso, poultry houses cannot function satisfactorily unless they are properly equipped and supplied with the needed appliances. In the light of this, nine farms where chosen from different parts of Makurdi (Wurukum, Welfare Quarters, Judges Quarters, Achusa and Lobi Quarters) and visited. Their housing structures and equipment were evaluated. Different aspects of their designs were compared with those found in the relevant literature. All the building accessed were naturally ventilated, open-sided houses. However, some aspects such as the stock density, orientation of buildings, space between buildings, roof designs needed improvement, while other aspects were almost non-existent such as bio-security and environment control. Typical house dimensions ranged from lengths (11m - 22m), widths (6m - 12m) and heights (3.0m - 4.7m). In Makurdi, there is need for an ideal poultry house which should be well ventilated, dry, clean and spacious.*

KEYWORDS: *Makurdi, Poultry, Farm buildings, Trends, Environment*

I. INTRODUCTION

Agriculture continues to be the most important sector of the Nigerian economy in terms of provision of employment in spite of its declining contribution to the nation's foreign exchange earnings. About 65% of Nigerians are estimated to depend on agriculture for their livelihood while 34.8% of the GDP and over 38% of non-oil foreign exchange earnings are contributed by the agricultural sector. The poultry sub-sector is the most commercialized of all the subsectors of Nigeria's agriculture (FAO, 2006).The term "poultry" covers a wide variety of birds of several species. The term is relevant whether the birds are alive or dressed. It includes chickens, turkeys, ducks, geese, swans, guineas, pigeons, peafowl, ostriches, pheasants and other game birds (Ekwue et al, 2003). The types of poultry that are commonly reared in Nigeria are chickens, ducks, guinea fowls, turkeys, pigeons and more recently ostriches. Those that are of commercial or economic importance given the trade in poultry, however, are chickens, guinea fowls and turkeys, amongst which chickens predominate (FAO, 2006).

According to FAO (2006), there are two distinct poultry production systems in Nigeria, as in most developing countries of Africa and Asia. The two systems are conventionally referred to as commercial poultry production and rural poultry production. The commercial system is industrial in nature and is therefore based on large, dense and uniform stocks of modern poultry hybrids. It is capital and labour intensive and demands a high level of inputs and technology. On the other hand, rural poultry production is by convention a subsistence system which comprises of stocks of non-standard breeds or mixed strains, types and ages. It is generally small-scale, associated with household or grass-root tenure and little or no veterinary inputs. Poultry houses are either naturally ventilated or mechanically-ventilated. Naturally ventilated houses are very common in developing regions of the world and in small to medium-size poultry operations. In such houses, it is important during hot weather to facilitate the flow of air into and out of the poultry house. Mechanically-ventilated systems are common in areas where climates are harsh and temperature extremes exist.

The majority of hot-weather mechanically -ventilated systems are negative-pressure systems, and these are of two types; inlet ventilation and tunnel ventilation. The latest technology available for housing of poultry to ensure that the optimum house temperature is maintained is by the use of tunnel-ventilated houses (Ernst, 1995). In tunnel-ventilated houses, the right air velocity and air humidity (which are important for hygienic condition) are carefully monitored and modified to maintain optimum conditions. In effect, the litter stays dry and the birds stay healthy and management required for these houses, the benefits are decreased mortality, increased bird weight and reduced feed conversion rates compared to the conventional naturally-ventilated, open-sided buildings. Mabbett (2011) has it that tunnel ventilation in combination with evaporative cooling will provide the necessary control of poultry house environments prevailing in tropical Africa. Indeed, proper use and control of such systems is the key to profitable poultry production in such areas. Hence, income generation is greater on tunnel ventilation farms than naturally ventilated farms.

Poultry as an important sector of agriculture which gives returns to the breeder on shorter generation interval. According to the Central Bank of Nigeria's report in 1999, Poultry eggs and meat contribution of the livestock share recorded improvement in Gross Domestic product (GDP) increasing from 26% in 1995 to 27% in 1999 which significantly sustained by availability and use of improved vaccines, curtailed mortality rates in birds, reduction in the tariff on imported day old chicks and parent stock. Furthermore, the relative ease of compounding efficient feed from available local feedstuffs, use of modern housing facilities that reduce mortality rate and enhance optimal performance of the birds are other factors that enhance the record (Ojo and Afolabi, 2000). Nigerians own many varieties of farm animals including poultry. Poultry ranks highest in number among the farm animals on the farm; mostly 80 – 90 % owned by small scale farmers (Idi, 2000). Poultry production is increasing very rapidly and the consumption is increasing faster than that of other kinds of meat beside beef (Bukar, 2003). The population of poultry in the country was estimated to be 104.3 million; chickens (72.4 million), pigeons (15.2 million), ducks (11.8 million), guinea fowl (4.7 million) and turkeys (0.2 million) (FDLPCS, 1992).

In Makurdi, Benue State which is the study area, many poultry farms have sprung up due to the need for animal protein. This demand for poultry meat has increased remarkably over the past years due to increased population which gives rise to increased growth in the number of fast food restaurants featuring chicken in the state. Hence it is pertinent to access the housing conditions of the birds so as to ascertain whether they conform to the recommended standards.The objectives of this study include; to access the structures of the poultry farm building in the study area; to investigate the type and number of birds that are and can be accommodated in each building; to appraise the building materials for the construction of the building; and to describe the type and size of the facilities as well as the method of waste disposal and environmental control.

II. METHODOLOGY

Study Area : Makurdi is the capital of Benue State-Nigeria. Makurdi is located at the North Eastern part of Benue State and lies on latitude 7º30'N and longitude 8º35'E. It is located within the flood plain of lower River Benue valley. The physiographic characteristics span between 73-167 m above sea level. Due to the general low relief sizeable portions of Makurdi is water logged and flooded during heavy rainstorms. This is reflected in the general rise in the level of groundwater in wells during wet season. The drainage system is dominated by River Benue which traverses the town into Makurdi North and South banks. It shares boundaries with Gwer West and Guma Local Government Areas including Nassarawa State.The town is divided by the River Benue into the North and South banks, connected by two bridges: the railway bridge and the dual carriage bridge. Makurdi lies in the tropical guinea savanna zone of Central Nigeria, experiences a typical climate with two distinct seasons. The dry season lasts from late October to March and the rainy season which begins in April to October is the period of intensive agricultural activities by the inhabitants mostly Tivs, Idomas, Jukuns and Igedes.

Temperatures are generally high throughout the year due to constancy of isolation with the maximum of 32^{o}C and mean minimum of 26^{o}C. The hottest months are March and April. The rainfall here is convective, and occurs mostly between the months of April and October and is derived from the moist and unstable southwest trade wind from St. Helena Subtropical Anticyclones (STA). Mean annual rainfall total is 1190 mm and ranges from 775-1792 mm. Rainfall distribution is controlled by the annual movement and prevalence of Inter-Tropical Discontinuity (ITD).The mean monthly relative humidity varies from 43% in January to 81% in July-August period (Tyubee, 2009).The geology is of cretaceous sediments of fluvial-deltaic origin with well-bedded sandstones of hydrogeological significance in terms of groundwater yield and exploitation (Kogbe *et al.*, 1978). Makurdi town which started as a small river port in 1920 has grown to a population of 297,393 people (NPC, 2006).

Data Collection :A total of nine farms where chosen from different parts of Makurdi (Wurukum, Welfare Quarters, Judges Quarters, Achusa Old GRA, Lobi Quarters) were selected at random and visited as a part of the survey of the trends and tides of poultry farm buildings in the area of study. The survey assessed the layout (arrangement) of the poultry structures and their facilities, investigated the type and number of birds that are and can be accommodated in each building, and appraised the building materials for construction. The size and materials for the construction of the structural elements (columns, beams, roofs, walls and floors) were also noted. The type and sizes of the facilities such as waterer and feeders as well as methods of waste disposal and environmental control are described. The summary of the farms visited is shown in table 1 and 2 below.

Table 1 Details of some poultry farms in Makurdi.

S/No	Name of Farm/Farmer	Location	Number of Poultry Birds	Type of Poultry Birds
1	Sam Poultry Farms	Wurukum	400	Broiler
2	Martytex Animal Care Services	Wurukum	2000	1800 Broilers 200 Layers
3	Rose Farms	Welfare Quarters	300	Broilers
4	Sophie Farms	Old GRA	500	Broilers
5	Adura Baba Integrated Farms	Achusa	1000	Broilers
6	Valliepride Farms	Achusa	1500	Broilers
7	Averd Farms	Judges Quarters	1800	1000 Broilers 500 layers 200 Geese 100 Turkeys
8	Ashaver Farms	Judges Quarters	1500	1000 Broilers 500 Layers
9	Shihel Farms	Lobi Quarters	2000	Broilers

III. RESULTS AND DISCUSSION

All the poultry farms utilize naturally ventilated buildings with similar and in some cases different design specifications. Some of which are detailed in table 1 and 2 below. However, the following are

S/ No	Name of Farm/Farmer	No. of buildings	Typical building Dimensions in meters (Length, Width, Height)	Stock density (birds/m^2)	Building orientation	Space between buildings (metres)	Roof Design
1	Sam Poultry	1	11, 6, 4.0	5–7	North- South	-	Flat
2	Martytex Animal Care services	4 1	9, 8, 3.5 6, 11, 3.0	5–7 3-4	North- South	2 -	Gable Flat
3	Rose Farms	1	9, 6, 3.0	5–7	East - West	-	Gable
4	Sophie Farms	1	22, 8, 3.5	3-4	North- South	-	Flat
5	Adura Baba Integrated Farms	4	7, 6, 3.7	3-4	North- South	2	Flat
6	Valliepride Farms	5	11, 6, 3.9	5–7	East - West	2.5	Flat
7	Averd Farms	4	22, 10, 4.0	3-4	East - West	4	Gable
8	Ashaver Farms	3	15, 9, 4.7	5–7	North- South	3	Semi - monitor
9	Shihel Farms	2	22, 12, 4.5	3-4	East - West	5	Gable

Table 2. Features of the farms in Makurdi.

summarized during the field visits which were conducted between November 2013 and February 2014. Some pictures from the field visits are also presented.

Access and Services : All farms were easy to access as they were either near the main road or had good roads leading to them. Most the farms do not have processing plants and feed mill exception of Adura Baba Integrated Farms which have a processing plant and a feed mill. Averd farms has its own feed mill. Hence, the other farmers purchase feeds from feed dealers (Hybrid feeds, Vital feeds, Top feeds, etc). None of the farm were with hatcheries or breeding farms. All farms had water and electricity supply.

Stocking Density : The average stocking density (floor space) was 5 – 7 birds/m^2 and most farms were not producing at their maximum capacity (e.g. Rose farms and Sophie farms). Hence, the farmers productive potentials were not actually realized since birds grow better with enough space. The recommended stocking density by FAO (2011) is 3 - 4 bird/m^2.

Farm Houses : The number of houses on the farm varied significantly (Table 2). The houses were basically north-south or east-west-oriented. East-west orientation is preferred in the tropics (Makurdi inclusive) as it helps to minimize exposure to direct sunlight. Typical house dimensions ranged from lengths (11m - 22m), widths

(6m - 12m) and heights (3.0m - 4.7m). Today, a height of 3.9m - 5.3m is preferred for greater ventilation in order to reduce heat stress on birds (Ernst, 1995). Similar sizes and types of materials were used for elements of building construction. These elements are discussed below.

1. **Foundation :** The foundation of all the farms are made of poured concrete. It is the best foundation materials because it is hard, durable and strong in compression. Concrete blocks were used for the foundation wall.

2. **Floors :** All farms visited had the deep litter arrangement in place The floors of the building consisted dirt with sawdust, wood shavings or rice hulls 5 – 10cm deep. For a deep litter arrangement, FAO (2011) recommends that concrete floors of 80 –100mm thickness obtained from a stiff 1:2:4 or 1: 3:5 (cement: sand: gravel) mix laid on a firm base of at least 150mm ground level. This was however difficult to ascertain whether this was followed in constructing the floors. The floors were disinfected between grow-outs using commercial disinfectants.

3. **Walls :** Most of the walls of the farms visited were open-sided walls were by masonry blocks were raised to about 1m or their walls were mainly one to three rows of concrete blocks with a hexagonal wire mesh (1.25cm) completing the upper part of the walls. Lengths of timber were used alongside the wire mesh as a means of securing the wire mesh to the block.

4. **Doors :** The doors were usually made of similar materials as the walls (wire mesh and timber or wood/ wood and zinc sheets). Most of the main entrance doors were made of zinc metal sheets.

5. **Roof Shapes and Covering (Roofing system) :** Most of the farms made use of the flat roofing design except Averd farms and Ashaver, farms; and Shihel farms used the double-pitched(gable) roof design. Gabled roofs reduce solar heat loading. All the farms used zinc roofing sheets as roof cover. Zinc is a good covering material since it is impervious to rain and keeps out radiation (Ekwue et al, 2003). It is however, a good absorber and emitter of radiant heat. For better environmental control using zinc, roofs should be insulated and/or have heights of 4m to 5m (Lindley and Whitaker, 1996).

6. **Windows :** Shutters or curtains made from feed sacks or jute materials were used to cover the buildings that had window openings. All window frames were covered by wire mesh.

Feeders and Drinkers : None of the farms visited used automatic feeders or drinkers. The common feeders were of galvanized steel and wooden trough types (0.6m – 1.6m length, base width of 5 – 8cm for 8 weeks old birds and 20 – 25 cm for adult birds) and common drinkers of plastics with the capacity range of 2 – 8 litres.

Ventilation : The buildings of the farm visited were open-sided. They relied on natural airflow through the buildings (natural ventilation) commonly found in the topics. Chickens tolerate cold weather better than wet sticky foul-smelling litter resulting from inadequate ventilation.

Brooding : Chicks were normally brooded in the entire house by placing waste feed bags and polyethene bags around the entire floor structure and providing heat using electric bulbs. FAO (2011) recommends that the brooding building should be isolated from other buildings by 30m or more and should be self-contained in terms of field supplies and storage equipments. Most of the farms visited were using the same building for brooding (Rose farms, Sam poultry farms, Sophie farms) and the ones using different building for brooding did not use the specified distance for isolation. Full-sided wall poultry house is recommended for brooding day-old chicks; this was not observed in any of the farms.

Water Supply : All farms got their water either from the private wells or drilled boreholes as it is difficult to gain access to portable water from public supply in Makurdi metropolis.

Bio-Security : The only means of bio-security seemed to be chlorination of the water for birds. No farms had any footbaths at the doors to the buildings, though the floor was regularly disinfected. In all the farms visited, protective clothing or footwear were not provided for service personnel or visitors who entered these facilities. Moreso, quarantined periods were not established for new animals to be introduced into a group or facilities.

Waste Disposal/Management : Waste litter generated from these farms was given to other farmers to be used as fertilizers, packaged in bags and sold or disposed using the public disposal system. Averd farms packaged litter from layers and sells to interested persons, but dispose litter from broilers using public disposal. Dead birds were either burned or given to the dogs.

IV. CONCLUSION

Generally speaking, the intensification of poultry farming in Makurdi and Benue State at large has been towards large commercial flock production. With this trend has come an increase in confinement housing for poultry, hence the investment needs in terms of buildings and equipment. Poultry buildings or constructions entail providing sheds or environment for accommodating birds and store rooms (feeds and equipment). The extent to which these birds are exposed to the environment (sunshine, rain, wind) is determined partly by the system of management and this includes the design of the housing used for birds.This work presents the trends and tides of poultry house building in Makurdi, Benue State. The essentials of poultry buildings as they relate to housing of birds and equipment have been delve into and the different types of houses and equipment for operational activities in a poultry production management system were compared with current standards. However, it is pertinent to state that there is great need for improvement in the areas of stock density, orientation of buildings, space between buildings, roof designs and bio-security.

The recommended stocking density by FAO (2011) is 3 - 4 bird/m^2. The stocking density used by farmer in Makurdi is 5-7 bird/m^2 which gives less space for the birds. Less space creates stressed social behaviour, allowing disease vulnerability and cannibalism and leaving weaker birds deprived of feed. Getting the stocking density right is important to the farmer to ensure proper return on his investment.The orientation of some of the buildings in Makurdi are in North - south. According to Czarick and Fairchild (2008) in Daghir (2008), naturally ventilated houses should always be orientated in an east–west direction. The reason for this is to minimize the possibility of direct sunlight entering the house. Direct sunlight striking upon a bird can dramatically increase the effective temperature a bird is experiencing. Direct sunlight can increase the surface temperature of a bird to well above 38°C, creating a heat stress situation at air temperatures that would not normally be thought of as problematic.

In terms of the space between buildings as a group or for brooding buildings, more attention is needed since none of the buildings accessed attained such recommendations. FAO (2011) recommends that If there are several poultry buildings in a group, it is desirable to have them separated by 10–15 metres in order to minimize the possibility of spreading disease. Brooding buildings should be isolated from other poultry buildings by 30 metres or more, and be self contained in terms of feed supplies and storage of equipment. The most used roof design in Makurdi is the flat roof design and Zinc metal sheets were used as their roof cover. The roof should be double-monitor type and be made with alu-zinc, Compared to the gable roof, this design, although more expensive to construct, allows considerable light in the centre of the building which improves ventilation considerably.

The only bio-security measure practiced in the Makurdi is the chlorination of water for the birds. More attention should be given to other bio-security measures such as providing footbath at the doors to the buildings, protective clothing or footwear should be provided for service personnel or visitors who enter these facilities and specific quarantined periods should be established for new animals to be introduced into a group or facilities.

REFERNCES

[1] **Bukar, M. T. (2003).** Effect of frequency of ejaculation on semen characteristics in two breeds of turkey (Meleagris gallovapo) in a tropical environment. An unpublished B. Agric. Tech. project, Animal Production Programme, Abubakar Tafawa Balewa University, Bauchi, Nigeria, pp68.

[2] **C. B. N. (1999).** Central Bank of Nigeria Annual Report and statement of Account. CBN component in broiler starter mash with Gliricidia sepium. Animal production in the New Millennium; challenges and options. Book of proceeding. Edited by S. Ukachuckwu et al.

[3] **Daghir, N.J. (2008).** Poultry production in hot climates. Wallingford, UK, CAB International.

[4] **Ekwue, E.I. Gray, M. and Brown, A. (2003).** Poultry Farm Buildings in Trinidad: Present and Future Prospects West Indian Journal of Engineering Vol. 25. No.2, I – 17.

[5] **Ernst, R.A . (1995).** Housing for Improved Performance in Hot Climates. In. Daghir, N.J.(ed.): Poultry Production in Hot climates: 67-100, CAB INTERNATIONAL, UK.

[6] **FAO (1998).** Food and Agriculture Organization. Production Year Book, Rome, Italy, pp52.

[7] **FAO (2004).** Animal Production and Health manual. Small-scale Poultry Production Technical guide. FAO Technology Review. Rome, Italy. ISSN 1810- 1119.

[8] **FAO (2006).** Animal Health and Production. Poultry Sector and country review. Accessed at
a. http//www. Fao.org/avianflu/en/farmingsystems.html.

[9] **FAO (2011).** Rural structures in the tropics. Design and development. Rome, Italy, Pp 149-
a. 204; 225 – 295. ISBN 978-92-5-107047-5

[10] **FDLPCS (1992).** Nigerian Livestock Resources, Vol. 1, Executive Summary and Atlas. A publication of the Federal Department of Livestock and Pest Control Services, Abuja, Nigeria, 30pp.

[11] **Idi, R.D. (2000).** Semen characteristics and fertility of some breeds of cock in Bauchi. Unpublished M. Sc. Thesis, Abubakar Tafawa Balewa University, Bauchi, Nigeria, pp95.

[12] **Kogbe, C. A., Torkaski, A., Osijuk, D., and Wozney, D. E., (1978).** Geology of Makurdi in the Middle Benue Valley, Nigeria. Occasional Publication of Department of Geology, Ahmadu Bello University, Zaria.
[13] **Lindley, J.A. and Whitaker, J.H. (1996).** Agricultural buildings and structures. Revised edition. American Society of Agricultural & Biological Engineers (ASABE).
[14] **Mabbett, T. (2011).** African Farming and Food Processing. Retrieved from http://www.africanfarming.net/livestock/poultry/hot-tips-on-housing-and-enviroment-for- poultry
[15] **NPC (2006).** National Population Census Figures, National Population Commission, Abuja, Nigeria.
[16] **Ojo, S. O. and Afolabi, J. A. (2000).** Economic analysis of replacing the fish meal publications, Abuja, Nigeria.
[17] **Tyubee, B. T., (2009).** The influence of ENSO and North Atlantic sea surface temperature anomaly (SSTA) on extreme rainfall events in Makurdi, Nigeria. Meteorol. Climate Sci., 7: 28-33.

APPENDIX

Some pictures taken from field visit.

Picture 1: Pictures from Averd farms

Picture 2: Pictures from Rose farms

Picture 3: Pictures from Martytex animal services farms

Picture 4: Pictures from Ashaver farms.

American Journal of Engineering Research (AJER)
e-ISSN: 2320-0847 p-ISSN : 2320-0936
Volume-03, Issue-11, pp-125-130
www.ajer.org

Research Paper Open Access

Improving Microstrip Patch Antenna Directivity using EBG Superstrate

Hayat Errifi [1], Abdennaceur Baghdad [2], Abdelmajid Badri [3], Aicha Sahel [4]
[1, 2, 3, 4] *(EEA & TI Laboratory, Faculty of sciences and techniques/ Hassan II University Mohammedia-Casablanca, Morocco)*

ABSTRACT: *Electromagnetic Band-Gap (EBG) structures are popular and efficient techniques for microwave applications. EBG structures have two main configurations, first EBG substrate and second EBG superstrate. In first case, the patch of antenna is surrounded with EBG structure that suppress the propagation of surface wave and in second case, layer of EBG structure that call EBG superstrate set above the patch of antenna to increase the directivity and to reduce the side lobes of the radiation pattern. In this paper, we study the influence of the EBG superstrate on the performances of an aperture coupled rectangular microstrip patch antenna. The return loss, radiation pattern and directivity are studied using HFSS software. The simulation results show that the gain, directivity and S11 parameter of the antenna with EBG cover are increased at X band (8-12GHz). Compared with the patch feed with the same aperture size but without superstrate, the performance of the proposed antenna is significantly improved.*

KEYWORDS : *Patch antenna; HFSS; EBG Structure; Return Loss; Gain; and Directivity.*

I. INTRODUCTION

Microstrip antennas are widely used in various applications because of low profile, low cost, lightweight and conveniently to be integrated with RF devices. However, microstrip antennas have also disadvantages such as the radiation of electromagnetic energy in different directions from radiation source (i.e. patch) witch cause the electromagnetic energy duo to the patch and feed of microstrip antenna, divide in all direction in the space that it results to reduce directivity, gain and wide radiation beam [1].BG structures are periodic structures that are composed of dielectric, metal or metallo-dielectric materials. These structures can prevent or assist wave propagation in special directions and frequencies therefore they can be used as spatial and frequency filters [2].There are several configurations of EBG structures according to their application in antenna. Two main configurations are:

a. EBG structures place on antenna substrate that by creation band gap in certain frequency range Suppress from propagation of surface wave. This configuration is defined as EBG substrate. In this configuration both of mushroom-like EBG and uniplanar EBG is used [3].
b. EBG structure place at certain distance above radiation source of antenna i.e. patch and by creation ultra-refraction phenomenon, concentrate radiation in various direction normal to EBG structure. This configuration is defined as EBG superstrate or Metamaterial superstrate and only the uniplanar EBG is used in this one [4].

In this paper, we consider the problem of enhancing the directivity of an aperture coupled microstrip patch antenna. the paper is organized as follows: Section II explains the design procedure of an aperture coupled microstrip patch antenna (ACMPA) covered by EBG structure and section III is about the simulation results achieved by using single layer and two layers EBG superstrate in addition to the analysis of a comparative performance for better understanding. Section IV gives conclusion and anticipated future work.

DESIGN OF PATCH ANTENNA WITH EBG SUPERSTRATE : An aperture coupled patch antenna eliminates the direct electrical connection between the feed and radiating conductors by employing two dielectric substrates separated by a ground plane. This allows independent optimization of both the microstrip transmission line feed and radiating patch; patch and feed line are electromagnetically coupled through an aperture made on the ground. Such a design can be well explained with the help of following diagram:

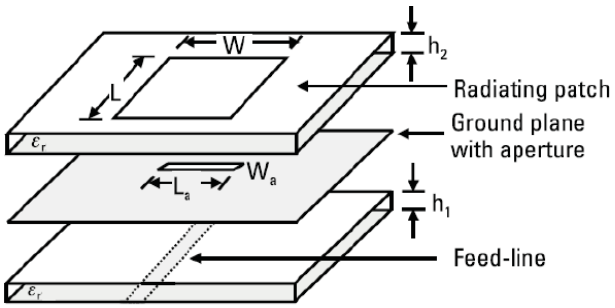

Fig. 1: Geometry of the basic aperture coupled microstrip antenna

Fig. 1 represents conventional aperture coupled microstrip patch antenna. The basic microstrip patch antenna consists of three layers. The dielectric substrate is placed between a ground plane (lower layer) and radiating metallic patch (top layer). The proposed microstrip patch antenna is realized on the Roger RT/duroid substrate with permittivity εr=2.2 and thickness (h) of substrate is 0.79 mm, the ground plane and radiating patch is made of copper. The operating frequency of antenna (fr), at which we wish to achieve the maximum directivity, is 7 GHz. The dimension of radiating patch is calculated by equations (1), (2), (3) and (4) where L, W is length and width of radiating patch [5].
Effective dielectric constant is calculated from:

$$\varepsilon eff = \frac{\varepsilon r+1}{2} + \frac{\varepsilon r-1}{2}\left(1+\frac{12h}{W}\right)^{-1/2} \quad (1)$$

Width of metallic patch:

$$W = \frac{c}{2fr\sqrt{\frac{2}{\varepsilon r+1}}} \quad (2)$$

Length of metallic patch:

$$L = L_{eff} - 2\Delta L \quad (3)$$

Calculation of length extension

$$\frac{\Delta L}{h} = 0.412\,\frac{(\varepsilon eff+0.3)\left(\frac{W}{h}+0.264\right)^{1}}{(\varepsilon eff-0.258)\left(\frac{W}{h}+0.8\right)^{1}} \quad (4)$$

The patch dimension (W × L) has been calculated as(11.86mm×9.15mm)and for ground plane dimension has been calculated as (Wg = 60 mm, Lg = 45 mm)[6].

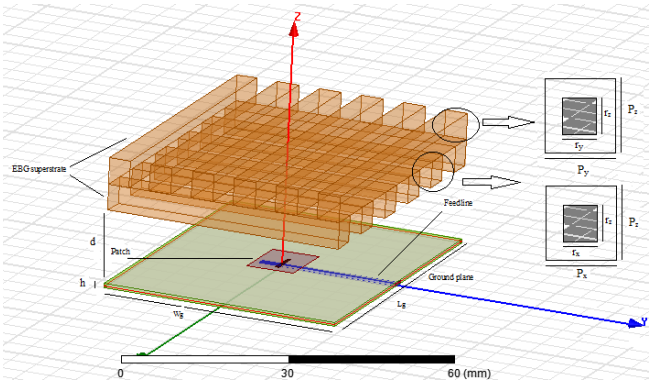

Fig. 2: Geometry of the EBG patch antenna

EBG structure places above the patch of antenna for concentrating of radiation energy normal to itself.Fig. 2 shows configuration of microstrip antenna with EBG superstrate. The EBG material iscomposed of two layers, the first layer has a rectangular lattice (Px=12.7 mm, Pz= rZ), and the dielectric rods have a rectangular cross section (rx= 4mm, rz= 5mm), for the second layer it has a rectangular lattice (Py=15.72 mm, Pz= rZ), and the dielectric rods have a rectangular cross section (ry= 5mm, rz= 5mm). The cover has sex layers of rods in the x-direction, and sex layers in the y-direction (see Fig 2). The length of the rods (in the x and y direction)is chosen to be the same as the dimension of the ground plane. The distance between the substrate and the cover is chosen to be d = 14 mm.

The dielectric material is taken to have a dielectric constant ε_r= 9.2 which corresponds to the dielectric constant of the "Rogers TMM 10 (tm)" in the microwave frequency range. Adjustment of first superstrate layer is the most important stage in antenna design and it is about one third of operation wavelength (λ/3) above ground plane which cause to gain increase. The second layer, improve beam shaping and directivity. The distance of second layer from first layer is taken almost zero.

Below, we will present the simulation results in terms ofthe computed radiation patterns, return loss and directivity of the proposed antenna. We use HFSS, which is 3D High Frequency Structure Simulator software [7].

II. SIMULATION RESULTS AND DISCUSSION

Now-a-days, it is a common practice to evaluate the systemperformances through computer simulation before the realtime implementation. A simulator *"Ansoft HFSS"* based onfinite element method (FEM) has been used to calculate return loss, radiation pattern and directivity. Thissimulator also helps to reduce the fabrication cost because only the antenna with the best performance would be fabricated [8].

Reflection characteristics : The reflection characteristic of the antenna design for high directivity operation is shown in Fig. 3. For comparison the results are also presented for the aperture coupled feeding patch antenna without the EBG superstrate.

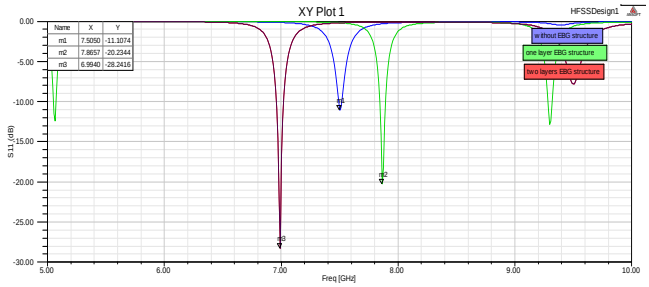

Fig. 3. Reflection coefficients of the source antenna with and without EBG structure

The return loss should be minimal at the resonance frequency for better performance; it can be seen that the reflection behavior of the unloaded antenna (without EBG superstrate) shows high resonance over the X band. After the feed antenna is loaded with one layer superstrate, it can be seen that the reflection losses were minimized (-20.23 dB at 7.86 GHz), however the operation frequency is still far from the desired. Adding a second layer helps to further minimize the reflection losses, the results of the frequency response of the S_{11} parameter show that the double-layer EBG superstrate provides a good impedance matching (S_{11} = -28.24 dB) with the source antenna that was initially designed with an air medium above it at a frequency of 7 GHz exactly.

Directivity : Fig. 4 shows the results of directivity as a function of frequency for the double layer EBG superstratebased antenna, a single layer EBG superstrate based antenna and the feed antenna. It can be seen that the antenna design using double layer EBG superstrate provides much better performance than that of the other two antenna configurations in term of directivity. The firstlayer has important role in this enhancement [9].

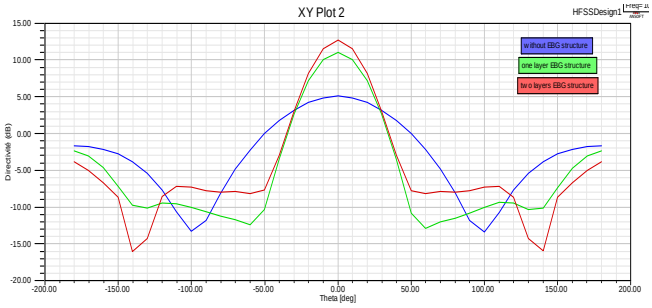

Fig. 4. Results of directivity of an antenna with single layer and double-layer EBG superstrate as well as that of the source antenna

To obtain an optimum response for directivity the air gap between the superstrate and the ground plane was varied to produce the final characteristic of directivity as shown in Figure4. The corresponding value is 14 mm. A maximum directivity of 11.78 dB is obtained at the frequency of 7GHz. Therefore it is important to control the air gap thickness in order to obtain a better performance from the antenna.

The maximum directivity of an aperture antenna is [10]:

$$D_{\max} = \frac{4\pi A}{\lambda^2} \qquad (5)$$

Where A is the area of the aperture. Since $A \approx 60 \times 45$ mm^2 and λ = 37.5 mm in the present configuration, one has D_{max}= 13.8 dB. The directivity of our designed EBG antenna (11.78 dB) is close to the maximum directivity (13.8dB). That is physically possible for this size of antenna.

Radiation pattern and 3dB beamwidth : In figures (5 and 6)3-D radiation pattern of the antenna without EBG superstrate and antenna with two layers EBG superstrate is shown. It is clear from these figures that directivity has been improved by 6.71dB and total efficiency of Antenna increased from 36% to 85%.

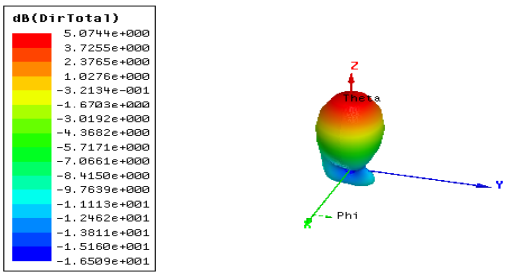

Fig. 5. 3D-Radiation pattern of microstrip antenna without EBG superstrate showing directivity of 5.07 dB

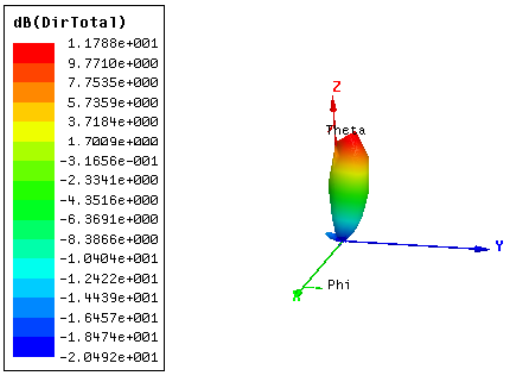

Fig. 6.3D-Radiation pattern of microstrip antenna with two layers EBG superstrate showing directivity of 11.78 dB

Fig. 7 displays Radiation pattern for the double layer EBG superstratebased antenna, a single layer EBG superstrate based antenna and the feed antenna.

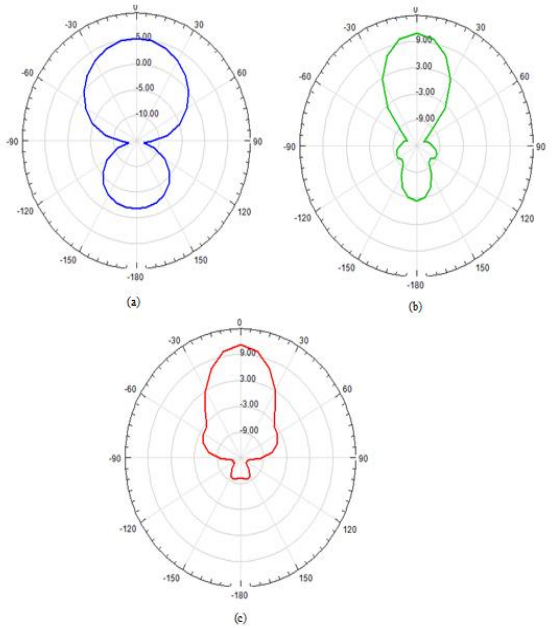

Fig. 7. Radiation pattern of (a) simple microstrip antenna (b) antenna with one layer EBG structure (c) antenna with two layersEBG structure

The results for the beamwidth are 75°, 34° and 30° at the frequency of 7.5 GHz, 7.86 GHz and 7 GHz for the simple antenna (a), antenna with one layer EBG superstrate (b) and antenna with two layers EBG superstrate respectively.It is obvious the use of two layers EBG superstrate, cause the increase of directivity of the antenna, the new antenna provides a narrower beamwidth (30° at E-plane) along the forward direction.A summary of the designed antennas is given in Table I. The table reveals that the designed antenna with two layers EBG superstrate had the best results in terms of frequency, return loss, directivity and beamwidth as those of antenna with one layer superstrate and antenna without the superstrate.

Table I. Comparison Forreturn Loss, Directivity And Beamwidth

Antenna	Freq	Return loss	Directivity	Beamwidth
Without EBG superstrate	7.5 GHz	-11.1 dB	5.07 dB	75°
with one layer EBG superstrate	7.86 GHz	-20.23 dB	10.97 dB	34°
with two layers EBG superstrate	7 GHz	-28.24 dB	11.78 dB	30°

III. CONCLUSION

In this paper, aperture coupled microstrip patch antenna with EBG superstrate has been studied. The main impetus for studying this antenna structure with EBG superstrate was the desire to realize increased directivity without using complex structures such as SRR (Split Ring Resonator) superstrate. The directivity characteristics of the composite structure have been investigated by using HFSS software, which has been found to be a useful tool for designing antennas of this type. Finally, it was found that both the directivity level, beamwith as well as reflection coefficient could be further enhanced by using EBG superstrate with two layers, rather than one. A very important need is to verify more of the simulation results with experimental measurements which will be reported in future work.

REFERENCES

Books:

[1] R. Garg, "Microstrip Antenna Design Handbook", Artech House, London, 2001

[2] F. Yang, "Electromagnetic Band Gap Structures in Antenna Engineering", Cambridge Universuty press, 2009

Journal Paper:

[3] sh. zhu, and R. Langley, "Dual band Wearable Textile Antenna on an EBG Substrate ", *IEEE transaction on antenna and propagation, Vol. 57, pages 926-935 (2009)*

Proceedings Paper:

[4] Dalin Jin, Bing Li , And Jingsong Hong, "gain improvement of a microstrip patch antenna using metamaterial superstrate with the zero refractive index", *Microwave and Millimeter Wave Technology conferece (ICMMT), page 1-3 (2012)*

Book:

[5] Balanis CA. Antenna theory, analysis and design. New York: John Wiley & Sons, Inc.; 1997.

Journal Paper:

[6] H. Errifi, A. Baghdad, A. Badri, "Design and optimization of aperture coupled microstrip patch antenna using genetic algorithm", *International Journal of Innovative Research in Science, Engineering and Technology,ISSN: 2319-8753, Vol. 3, Issue 5, May 2014.*

Book:

[7] HFSS software user guide.

Journal Paper:

[8] Mst. Nargis Aktar, Muhammad Shahin Uddin, Monir Morshed, Md. Ruhul Amin, and Md. Mortuza Ali, Enhanced gain and bandwidth of patch antenna using EBG substrates". *International Journal of Wireless & Mobile Networks (IJWMN) Vol. 3, No. 1, February 2011.*

Proceedings Paper:

[9] Basit Ali Zeb and Karu P. Esselle "A Simple EBG structure for dual-band circularly polarized antennas with high directivity", *in Proc. IEEE AP-S Int. Symp., 978-1-4673-0462-7/12/$31.00 ©2012 IEEE.*

Journal Paper:

[10] Min Qiu and Sailing He "High directivity patch antenna with both photonic bandgap substrate and photonic band gap cover, *Microwave and Optical Technology Letters / Vol. 30, No. 1, July 5 2001.*

American Journal of Engineering Research (AJER)

e-ISSN : 2320-0847 p-ISSN : 2320-0936
Volume-03, Issue-11, pp-131-138
www.ajer.org

Research Paper Open Access

A Neural Network Approach to GSM Traffic Congestion Prediction

M. A. Raheem[1, a] and O. U. Okereke[2, b]
[1, 2]*Department of Computer and Communication Engineering*
Abubakar Tafawa Balewa University Bauchi
Nigeria
[a]*marufakin@yahoo.com*, [b]*ouokereke@yahoo.com*

ABSTRACT : *In this paper, we propose a GSM congestion prediction model based on multilayer perceptron neural networks (MLP-NNs) with sigmoid activation function and Levenberg-Marquardt Algorithms (LMA) using twelve month real traffic data. The trained network model was used to predict traffic congestion along a chosen route. Regression analysis between predicted traffic congestion volumes and corresponding actual traffic congestion volumes shows a correlation coefficient of 0.986. This result clearly shows the effectiveness of Artificial Neural Networks (ANN) in traffic congestion prediction and control.*

KEYWORDS: *GSM congestion, prediction, neural networks, activation function, LMA*

I. INTRODUCTION

As wireless networks mature and the rate of subscriber growth levels off, the focus on customer retention and satisfaction becomes increasingly important. This occurs at a time when the widespread use of mobile communications has heightened consumer demand for quality service anytime, anywhere. Today, network operators face the challenges of improving the quality of service while increasing capacity and rolling out new services. Operators are fast realizing that they are in a highly competitive environment where subscribers can make or break them. Dissatisfaction by subscribers gives rise to a high rate of subscriber churn and low revenue for the operator.Congestion is a problem all GSM service providers are facing and trying to solve. It is a situation that arises when the number of calls emanating or terminating from a particular network is more than the capacity that the network is able to cater for at a particular time. It causes call signals to queue on the transmission channel. Consequently, the rate of transfer of voice signals is reduced or quality of signals received become distorted or both. At worst, the calls will not connect at all. There are technical mechanisms along the transmission link that tend to create or worsen congestion. When a Mobile Station (MS) dials a number, the call is routed to the nearest Base Transceiver Station (BTS) through the Air (Um) Interface. This receives, amplifies, and reroutes the call to the Base Station Controller (BSC) through the 'Abis' Interface. The BSC controls and manages multiple BTSs and communicates directlywith the Mobile service Switching Center (MSC) with an interface called the "A" Interface . Communication between two MSCs occurs on the 'E' Interface. The destination MSC finally routes the calls to its destination after the identity, authentication and credit status of the subscriber have been verified. The call set-up scenario is as shown in figure 1.

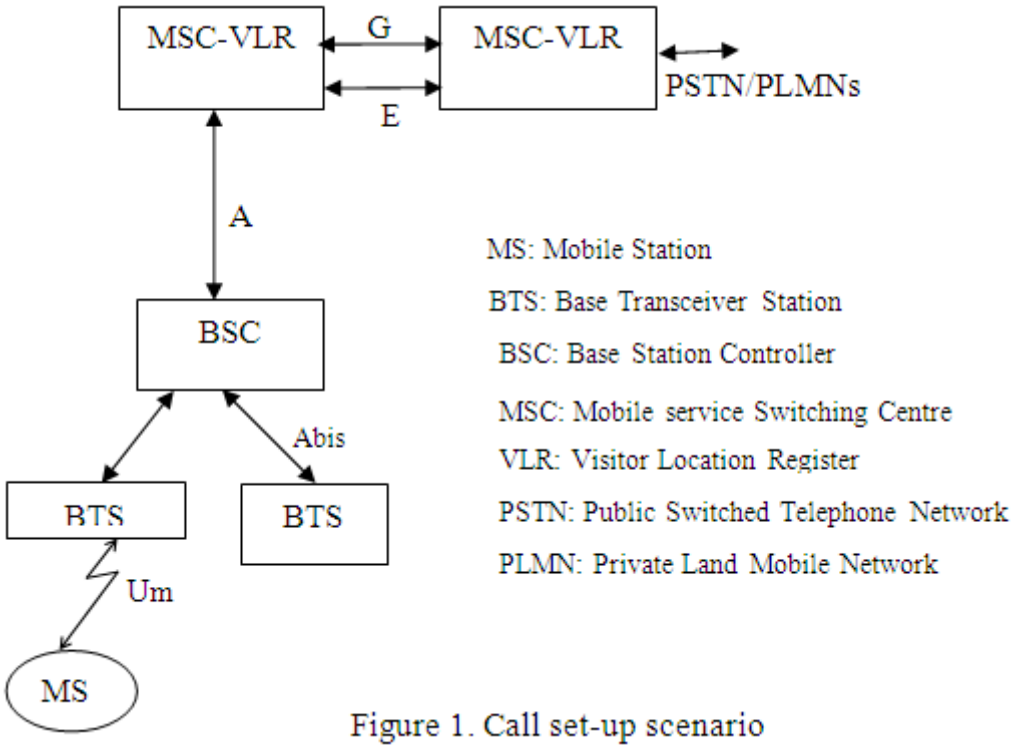

Figure 1. Call set-up scenario

Network Congestion : Congestion is defined as a state of network elements (e.g. switches, concentrators, cross-connects and transmission links) in which the network is not able to meet the negotiated network performance objectives for the already established connections and/or for the new connection requests (ITU-T, 1993). It is a network state in which performance degrades due to the saturation of network resources, such as communication links, processor cycles, and memory buffers (Andreas and Ahmet, 1999).From the view point of the network, four basic elements are related to congestion or indicate that a call could not be completed (Kuboye, 2006).

Traffic Channels Congestion (TCHC): Traffic channels (TCH) are voice channels. Out of the eight channels defined for each radio frequency carrier, most are used as traffic channels while some are used as control channels (Mehrotra, 1997). With absence of free voice channels during call initiation, traffic channels congestion (TCHC) results.

Dedicated Control Channel Congestion (DCCHC): Standalone dedicated control channels (SDCCH) provide authentication to mobile station, location updating and traffic channel assignments during idle periods (Mehrotra, 1997). Absence of free SDCCH for authentication results in an unsuccessful call attempt. This is called dedicated control channel congestion.

Common Control Channels Congestion (CCCHC): Common control channels support the establishment and maintenance of communication links between mobile stations and base stations (Harte et al., 1999). Random access channels (RACH), paging channels (PCH) and access grant channels (AGCH) are all common control channels. RACH is used for network assignment request, PCH for incoming call alert while AGCH assigns mobile stations to specific DCCH or SDCCH for onward communication. Calls cannot be established without the availability of any of these common control channels.

Pulse Code Modulation Congestion (PCMC Pulse code modulation (PCM) or E1 is the link required to connect the base station controller (BSC) and mobile service switching centre (MSC) or two MSCs together. Each PCM consists of thirty two timeslots. When there is no free timeslot to carry the call signals between the BSC and MSC or between the two MSCs (in case of inter-MSC call), then we have pulse code modulation congestion.

Congestion Control Strategies: Congestion control refers to the set of actions taken by the network to minimise the intensity, spread, and duration of congestion. It can be said that it is that aspect of a networking protocol that defines how the network deals with congestion. Despite the many years of research efforts, the

problem of network congestion control remains a critical issue and a high priority, especially given the growing size and demand of the networks.Several attempts had been made to forestall and manage congestion in GSM/GPRS network. A dynamic channel allocation model with one-level buffering was formulated by Ojesami *et al.* (2011) to control congestion in GSM network with a view to prevent call loss or degradation in quality of service of calls using Markov chain technique. They used object oriented program to evaluate the performance of the scheme based on three performance metrics: resource utilization, average queue length and blocking probabilities. The results obtained from the model show that the proposed scheme provides better performance benefits over fixed threshold techniques.

Kuboye (2010) proposed some optimization techniques that could be applied to minimize the problem of congestion on the GSM network in Nigeria. It was argued that implementation of dynamic half rate decoding, national roaming agreement between operators, regionalization and merging of GSM networks could ameliorate the problem of congestion.Dynamic load balancing technique was combined with Call Admission Control (CAC) to re-route calls that would have been dropped to another less busy cell within the BSC area (Alarape *et al.*, 2011). The combined algorithms were implemented on JAVA platform using real life call data record (CDR) collected from Globacom Nigeria Limited. New Call Blocking and Handoff Call Dropping Probabilities (NCBP and HCDP) were employed as performance index. NCBP and HCDP were computed for both CAC only and the combined scheme. The obtained results show significant reduction in the values of both NCBP and HCDP by 71.43% and 100% respectively, of cells considered for the new combined scheme when compared with that of the CAC only. Thus, the new combined scheme enabled the cells to accommodate more calls thereby increasing the call carrying capacity of the network. Markus *et al.* (2011) used multilayered feed-forward neural network with gradient descent backpropagation algorithm to model the telephone traffic situation on a PSTN. Regression analysis between predicted traffic congestion volumes and corresponding actual volumes clearly shows the utility and effectiveness of neural networks in traffic prediction and congestion control.

Realistic traffic models in the mobile network should cater for both the user communication rate and user movement in the network (Lam *et al.*, 1997). Little work has been done to develop adequate teletraffic models for mobile networks, such as those that support cellular or Personal Communications Services (PCS). The movement of the user implies that existing teletraffic models for the Public Switched Telephone Network (PSTN) cannot be used for mobile networks. Most mobile communications researchers simplify analysis by assuming a temporal and spatial uniform distribution of mobile calls. This could lead to wrong conclusions about real mobile networks (Lam *et al.*, 1997). From the foregoing, it is clear that previous studies on the subject matter were either carried out at the radio interface (cell level) on a mobile network or at the A or E-interface on a fixed network. However, with pulse code modulation congestion (PCMC) on a BS - MSC link or MSC - MSC link, the call would be blocked. This is true even if the radio interface is congestion-free. For a zero blocking probability, all the links between the MS and the MSC should be devoid of congestion. This present study seeks to address this missing link. Our attempt is to utilize the training capability of LMA to develop a model to predict, and thus control, telephone traffic congestion, more particularly PCMC, in a mobile network using artificial neural networks.

Artificial Neural Networks : Artificial neural networks (ANN) are mathematical tools originally inspired by the way human brain processes information (Hippert *et al.*, 2001). They are intelligent systems that are related in some way to a simplified biological model of the human brain. ANN are essentially function approximators that transform inputs into outputs to the best of their ability. They are composed of many simple elements, called neurons, operating in parallel and connected to each other in the forward path by some multipliers called the connection weights.The Levenberg-Marquardt Algorithm (LMA) is one of the variants of the basic backpropagation algorithm. This algorithm has been shown to be the fastest method for training moderate-sized feed-forward neural networks (up to several hundred weights). It also has an efficient implementation in MATLAB® software, since the solution of the matrix equation is a built-in function, so its attributes become even more pronounced in a MATLAB® environment (Demuth and Beale, 2008). The LMA uses this approximation to the Hessian matrix (**H**) in the following Newton-like update:

$$\mathbf{X_{k+1}} = \mathbf{X_k} - [\mathbf{J^T J} + \mu \mathbf{I}]^{-1} \mathbf{J^T e} \quad \ldots (1)$$

$\mathbf{X_k}$ is a vector of current weights and biases, **J** is the Jacobian matrix that contains first derivatives of the network errors with respect to the weights and biases, **e** is a vector of network errors, **μ** is a scalar, **I** is the identity matrix and $\mathbf{J^T}$ is the transpose of **J**. The expressions for **J** and **H** are given as:

$$\mathbf{H}(f) = \begin{bmatrix} \frac{\partial^2 f}{\partial x_1^2} & \frac{\partial^2 f}{\partial x_1 \partial x_2} & \cdots & \frac{\partial^2 f}{\partial x_1 \partial x_n} \\ \frac{\partial^2 f}{\partial x_2 \partial x_1} & \frac{\partial^2 f}{\partial x_2^2} & \cdots & \frac{\partial^2 f}{\partial x_2 \partial x_n} \\ \vdots & \vdots & \cdots & \vdots \\ \frac{\partial^2 f}{\partial x_n \partial x_1} & \frac{\partial^2 f}{\partial x_n \partial x_2} & \cdots & \frac{\partial^2 f}{\partial x_n^2} \end{bmatrix} \quad \ldots (2)$$

$$\mathbf{J} \begin{bmatrix} \frac{\partial f_1}{\partial x_1} & \cdots & \frac{\partial f_1}{\partial x_n} \\ \vdots & \ddots & \vdots \\ \frac{\partial f_n}{\partial x_1} & \cdots & \frac{\partial f_n}{\partial x_n} \end{bmatrix} \quad \ldots (3)$$

II. MATERIAL AND METHOD

The experimental procedure involves data collection and pre-processing, network modeling and training and simulation.

Data Collection and Pre-processing : Twelve month hourly traffic data retrieved from the automated traffic recordings of a MSC located in Bauchi metropolis was used. The various counters of the traffic data were careful selected by intuition so as to take those that actually affect congestion. Some of the variables selected include: Time of the day, Total call duration (in seconds), Peer office congestion, Seizure traffic (in Erlangs), Seizure attempts, Answer times, No answer after ringing times and Called subscriber busy times. Twenty four observations were made every day. Over the twelve month period, a total of 8,760 observations were made and extracted as data samples.The data were then preprocessed each time before being introduced to the Neural Network for training. Pre-processing involves scaling all the data in the range (-1, 1). This improves the accuracy of the neural network training.

Proposed Network Model and Training :A Multi-Layer Perceptron Feed-forward neural network with Levenberg-Marquardt Algorithm was used to train the network model. Training involves varying the network weights and biases and allowing the network to learn the different knowledge about the inputs and outputs. The number of neurons in the hidden layer (n) was varied to achieve optimum performance of the network. After a few experimental run, the number of neurons in the hidden layer was set at fifteen. The input parameters into the network include: Time of the day, Seizure attempts, Answer times, No answer after ringing times, Called party busy times, Seizure traffic (in Erlangs) and Total call duration (in seconds) as shown in figure 2. The output parameter is the peer office congestion times which measure the level of congestion of the trunk group. Equations (4) and (5) represent the input and output functions with their variables respectively.

$$I = f(T, S_a, A, N, C_b, S_t, T_c) \quad \ldots (4)$$

$$Y = f(C) \quad \ldots (5)$$

I = Input; Y = Output; T = Time of the day; S_a = Seizure attempts; A = Answer times
N = No answer after ringing times; C_b = Called subscriber busy times; S_t = Seizure traffic
T_c = Total call duration

Once the network weights and biases have been initialized, the network is ready for training. It is trained for function approximation and pattern association. A Mean Squared Error (MSE) of 10^{-4} was set as the error goal and the initial value of μ was set at 10^{-3}.

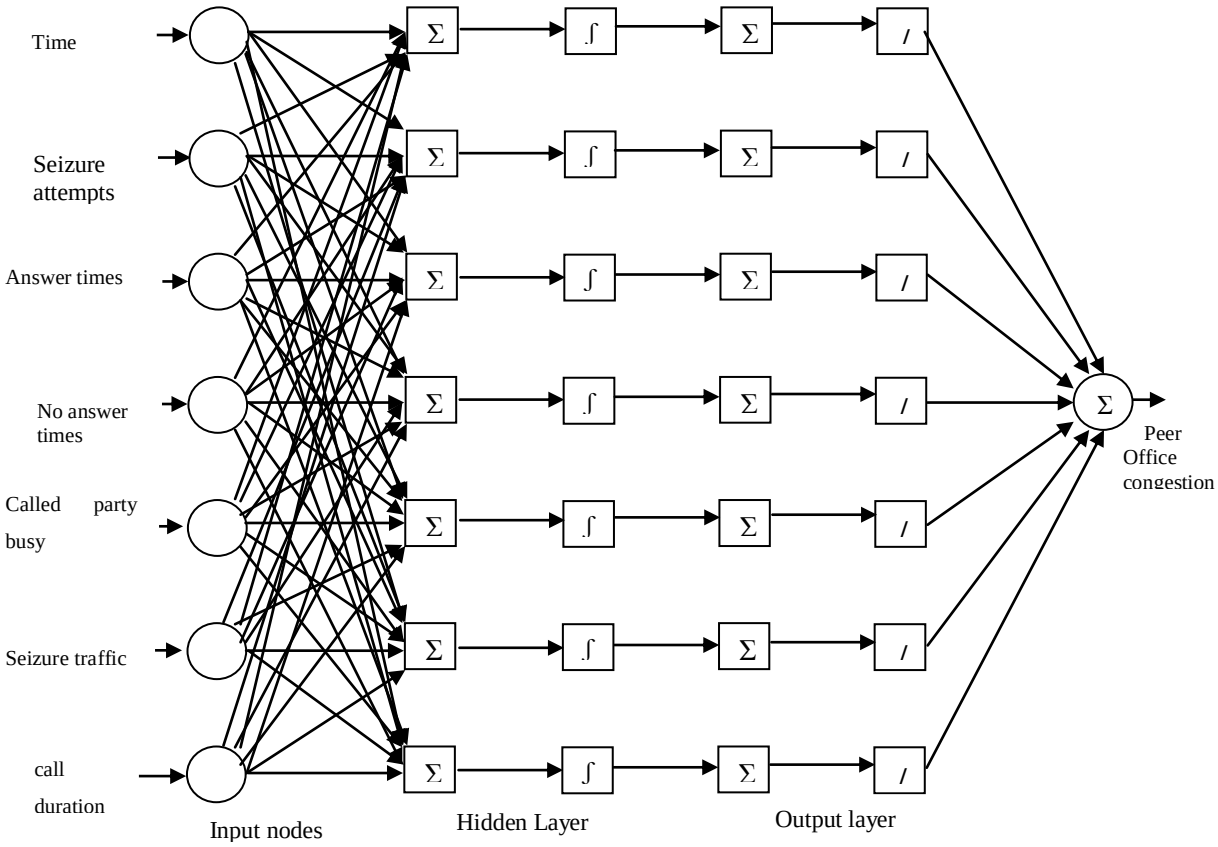

Figure 2: The two-layer feed-forward neural network

Simulation : After proper training of the network, simulation follows. Simulation involves presenting new set of inputs to the network and allowing the network to produce an output. After simulation, regression analysis was performed to determine the correlation between simulated outputs and targets.

III. RESULTS

A typical training session is shown in figure 3. It can be seen that this training instance took 0.04 seconds to complete 18 iterations. The error was minimized at 4.56 x 10^{-3}, very close to the set goal. The best validation performance of 1.4345 x 10^{-3} was achieved after twelve iterations.Figure 4 is the performance training window, which shows a plot of the training errors, validation errors, and test errors. It gives small mean-square error, no significant over-fitting and similar validation set errors and test set errors characteristics.

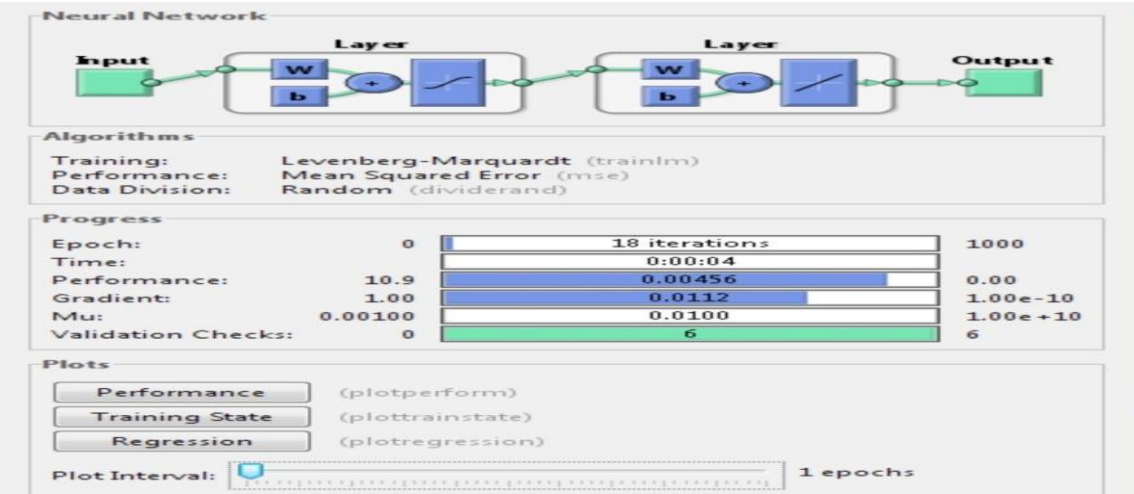

Figure 3. A typical training session using neural network tool

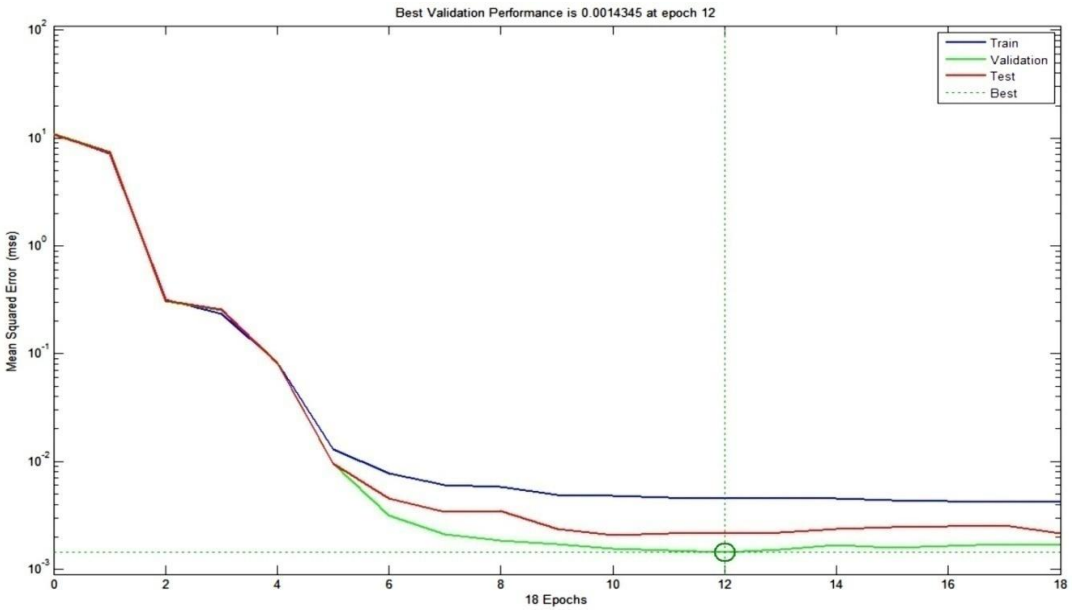

Figure 4. A plot of training, validation and test errors

Shown in figures 5(a)-(c) are prediction comparisons for three different days. It is clear that the simulated congestion volumes tracts the actual congestion volumes well.

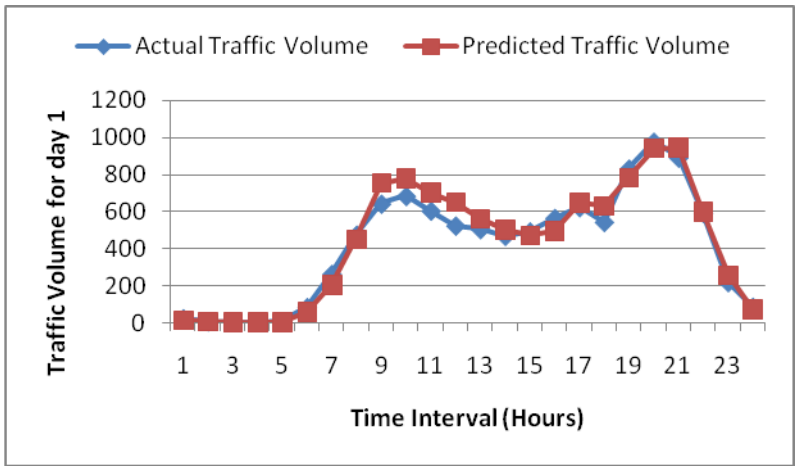

Figure 5(a). Actual congestion vs. predicted congestion (day 1)

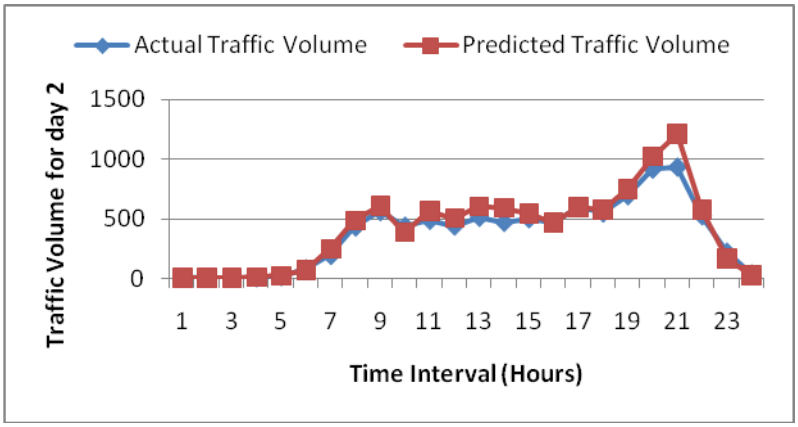

Figure 5(b). Actual congestion vs. predicted congestion (day 2)

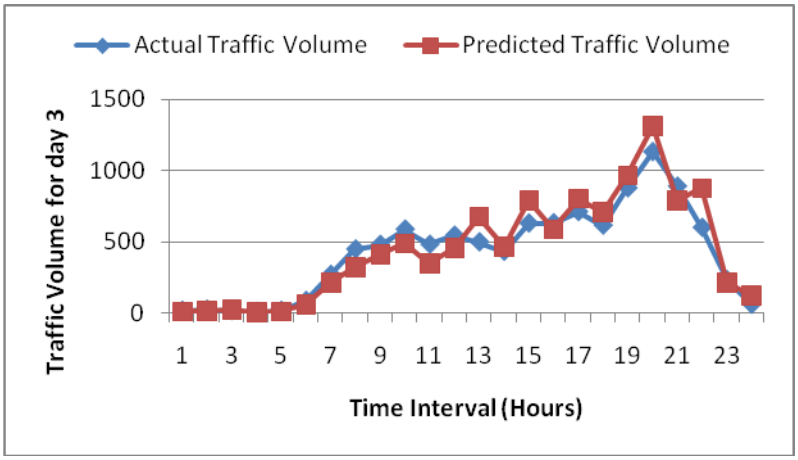

Figure 5(c). Actual congestion vs. predicted congestion (day 3)

Regression Analysis : To further evaluate the performance of the developed neural network model, a linear regression between the network outputs and the corresponding targets was carried out. Three parameters were returned. The first two, m and b, correspond to the slope and y-intercept of the best linear regression relating targets to network outputs respectively. A perfect fit gives a slope of 1 and zero intercept on the y-axis. The third variable returned (R-value) is the correlation coefficient between the outputs and targets. An R-value of 1 indicates perfect correlation between the targets and outputs. Figure 6 shows the regression plot carried out on the first day prediction. The network outputs were plotted against the targets as open circles. The best linear fit is indicated by a solid line while the perfect fit is indicated by the dash line. A slope of 0.93, an intercept of 10 and an R-value of 0.986 were obtained. This indicates a close relationship and high correlation between the actual outputs and the predicted outputs.

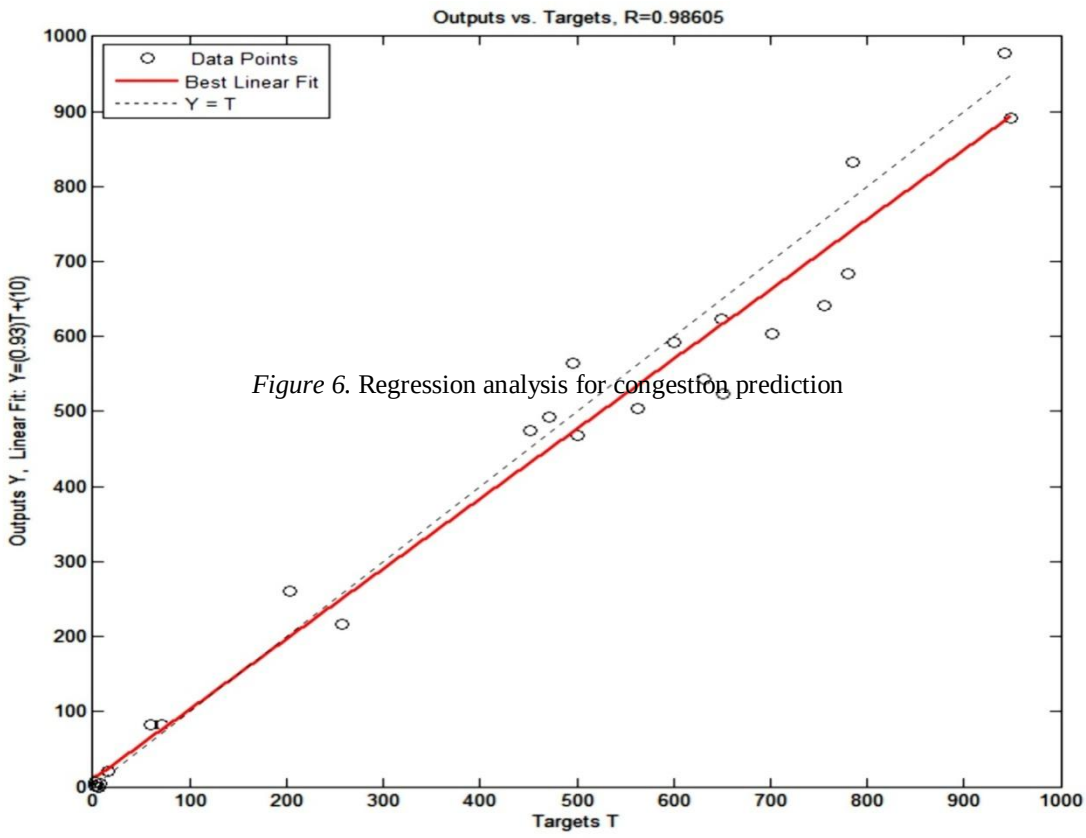

Figure 6. Regression analysis for congestion prediction

Figure 6. Regression analysis for congestion prediction

IV. CONCLUSION

Telephone traffic congestion pattern of a mobile network was studied. The multilayer perceptron feed-forward neural network was used to model the network. The network was trained using actual traffic data. The trained network was simulated with new input data and our results show that the behavior of the developed model is very close to a real network situation. With availability of relevant historical traffic data, artificial neural networks can model the behavior of mobile network to predict the occurrence of network irregularities.

REFERENCES

[1] Alarape, M.A.; Akinwale, A.T. and Folorunso, O. (2011). A Combined Scheme for Controlling GSM Network Calls Congestion. *International Journal of Computer Application*, **14**(3), *pp*: 47-53.

[2] Andreas, P. and Ahmet, S. (1999). *Congestion Control: Book CI Congestion-Control-Final.* (Tech. Doc.), University of Cyrus, Nicosia Cyrus.

[3] Demuth, H. and Beale, M. (2008). **Matlab Neural Network Toolbox Help.** Version R2008a, The MathWorks, Inc.

[4] Harte, L.; Levine, R. and Livingston, G. (1999). **GSM Superphones.** McGraw Hill **71**: 45-47.

[5] Hippert, H.; Pedreira, C. and Souza, R. (2001). Neural Networks for short-term load forecasting: A review and evaluation. *IEEE Transactions on Neural Networks*, **16***(1)*: 44–55.

[6] ITU-T Recommendation 1.371, (1993). **Traffic Control and Congestion Control in B-ISDN.**

[7] Kuboye, B.M. (2010). Optimization models for minimizing congestion in Global System for Mobile Communications (GSM) in Nigeria. *Journal of Media and Communication Studies* **2**(5), *pp*: 122-126.

[8] Kuboye, B.M. (2006). *Development of a framework for managing of congestion in GSM in Nigeria*. Unpublished master's thesis, department of electrical and electronics engineering, University of Portharcourt, Nigeria.

[9] Lam, D.; Cox, D.C. and Widom, J. (1997). Teletraffic Modeling for Personal Communications Services. *IEEE Communications Magazine*, February 1997, Pp. 79-87.

[10] Markus, E.D.; Okereke, O.U. and Agee, J.T. (2011). Predicting Telephone Traffic Congestion using Multilayer Feed-forward Neural Networks. *Journal of Advanced Materials Research*, **367**:191-198.

[11] Mehrotra, A. (1997). **GSM System Engineering.** Artech house, Inc., Pp: 70-73

[12] Ojesanmi, O.A.; Oyebisi, T.O.; Oyebode, E.O. and Makinde, O.E., (2011). Performance Analysis of Congestion Control Scheme for Mobile Communication Network, *International Journal of Computer Science and Telecommunications*, **2**(8).

American Journal of Engineering Research (AJER)
e-ISSN : 2320-0847 p-ISSN : 2320-0936
Volume-03, Issue-11, pp-139-149
www.ajer.org

Research Paper Open Access

BLACK MONEY?...

(A New theory on **"MONEY"**)

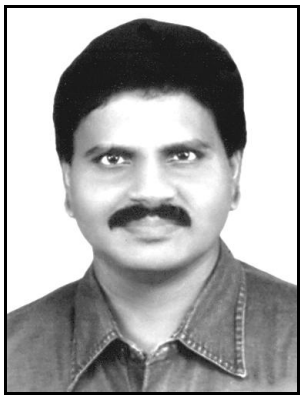

M.Arulmani,
B.E. (Engineer)

V.R.Hema Latha, M.A.,
M.Sc., M.Phil.
(Biologist)

ABSTRACT: *"**BLACK MONEY**" means "**ILLEGAL MONEY**"?... "BLACK" means "**SINFUL**"?... If so... "**CARBON MONEY**" earned by global national for "**CARBON CREDIT**" is **ILLEGAL**?... **SINFUL**?... The clergy men, Judges, magistrates, who wear long black robes are illegal?... **No… No… No…***
*This scientific research focus that the term "**MONEY**" shall be considered closely associated with "**MATTER**" of Universe composed of fundamental particles rather than denoting different currency of nations. (e.g) **BLACK MONEY** shall mean **BLACK MATTER**; **WHITE MONEY** shall mean **WHITE MATTER**.*

J

(WHITE MONEY LOGO)

This article further focus that in the **early universe** White Matter, Natural Metter (or) Holy Matter considered exist in **WHITE PLANET** (White Mars) even much before origin of matter in the **EARTH PLANET**. At one stage during expanding Universe the White Matter considered **transformed** to Earth Planet

and there after **Earthly Matter** considered evolved into distinguished **SPECIES MATTERS** with different combination of particles under different environmental conditions in **three nuclear Age**. The THREE-IN-ONE universal law of money shall be indicated as below.

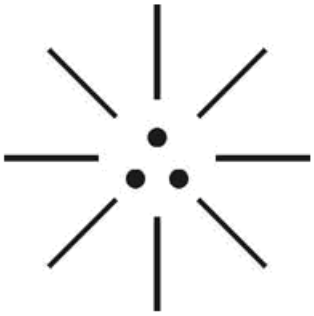

(Law of Money)

i) Right dot is **conduct** (Like "**Coin**")
ii) Left dot is **character** (Like "**Currency**")
iii) Centre dot is **moral** (Like "**Bond**")

*White Money means White Matter, Black Money means Black Matter. The International Philosophy of currency value such as India rupee, American dollar, European penny, KSA Riyal etc might be derived from the fundamental, of "**MONEY**"*

- Author

KEY WORDS:
a) Philosophy of **white money**?...
b) Philosophy of Black Money?...
c) Etymology of word **Money**?...
d) Etymology of word **Holy, Black, White**?...

I. INTRODUCTION:

Case study shows that the word "**BLACK**" is something concerned with illegal, violence, cruelty, sense of hating etc.,. Global level ethnicity also exist like **black race, white race**. The **international courts of law** also treat Black, Black Money is something like illegal, criminal and passing thousands of global level judgements day to day day. If so…

(i) BLACK BOX is Criminal?...
(ii) BLACK BODY is Criminal?...
(iii) BLACK BOARD is Criminal?...
(iv) BLACK HOLE is Criminal?...
(v) BLACK BELT is Criminal?...
(vi) BLACK DIAMOND is Criminal?...
(vii) BLACK FOREST is Criminal?...
(viii) BLACK MUSLIM is Criminal?...
(ix) BLACK AFRICAN is Criminal?...
(x) BLACK INDIAN is Criminal?...
(xi) BLACK BRITISH is Criminal?...
(xii) BLACK SHEEP is Criminal?...
(xiii) BLACK CAT is Criminal?...
(xiv) BLACK SMTTH is Criminal?...
(xv) BLACK SHIRT is Criminal?...
(xvi) BLACK ICE is Criminal?...
(xvii) BLACK SPOT is Criminal?...
(xviii) BLACK POWER is Criminal?...
(xix) BLACK ARMY is Criminal?...
(xx) BLACK FLAG is Criminal?...

(xxi) BLACK FLY is Criminal?...
(xxii) BLACK BIRD is Criminal?...

It is the humble submission of author to **INTERNATIONAL COURTS OF LAW** for transparent definition of what does means "**WHITE MONEY**", "**BLACK MONEY**"?... to pass error free judgment against **BLACK** and **WHITE.**

Hypothesis and Narrations

a) Dark money differs from Black Money?...

It is hypothesized that **Black money** shall be considered as **Earthly money** and integral pan of **Dark money** and white **money white** money shall be considered as the **accretion** of Dark money (**Natural assets**) . The Philosophy of dark money shall be indicated as below.

DARK MONEY
(Supernature)

b) Philosophy of source of "Black Money"?...

It is hypothesized that "**White Money**" shall be considered as the source of "**Black money**" as described below. In proto Indo Europe language root the White Money, Block Money, shall be called as "**KANDI**", "**KUNDI**" respectively. **Kandi, kundi**, shall mean genetically **varied money value matter.**

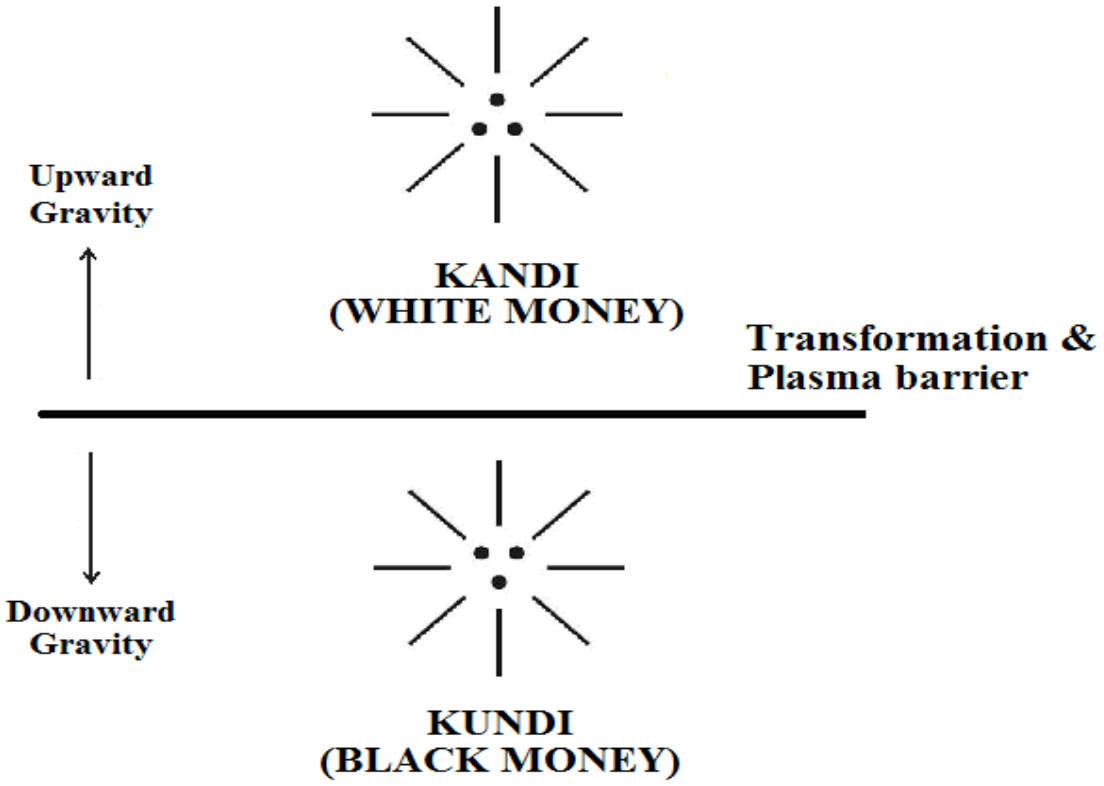

i) **KANDI** shall mean "**HOLY MATTERS**"(Natural)
ii) **KUNDI** shall mean "**EARTHLY MATTERS**"(Transformed)

- Author.

c) Human has money value?...

It is hypothesized that not only human, every matter of universe including planets has its **own money value** exists under different zone and environmental conditions. Similarly every human has also have their **own money value** in different zone as described below.

(i)

கண்டி
(WHITE MONEY)

(ii)

மண்டி
(Corrupt money under transfer)

(iii)

குண்டி
(BLACK MONEY)

d) Etymology of word "Money"?...

It is hypothesized that the etymology of word "**MONEY**" might be derived from proto Indo Europe language root word "**MANI**". **MANI** shall mean "**MATTER**" Consists of **three-in-one** fundamental particles **Photon, Electron, Proton**. Different **species matters** shall be considered having particles of distinguished **mass level**.

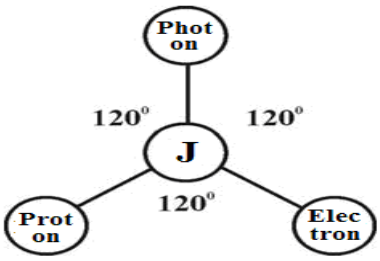

PHILOSOPHY OF MONEY
(Virgin Particles)

i) "கருமணி" means Dark hole
ii) கருகமணி means Anti neutrino particles
iii) வெள்ளி மணி means Neutrino particles
iv) தெய மணி means Virgin matter
v) ஆலய மணி means Temple matter
vi) நவ மணி means planet matter
vii) கண் மணி means Eye matter
viii) அருள் மணி means Gracious matter

- Author

Iris

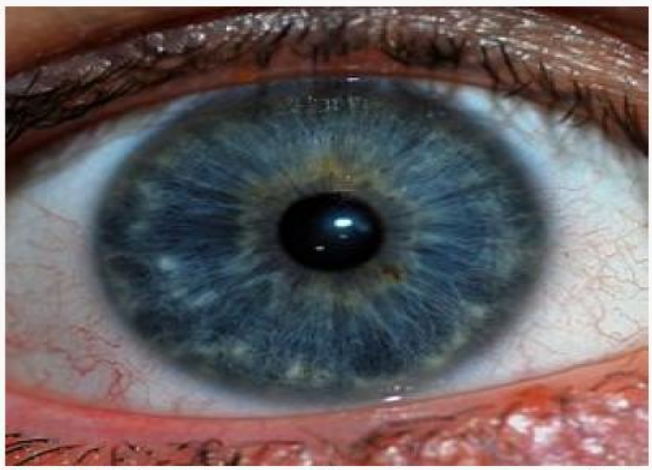

The **iris** is the blue area. The other structures visible are the pupil center and the white sclera surrounding the iris. The overlying cornea is pictured, but not visible, as it is transparent. Also pictured are the red-colored blood vessels within the sclera. These are easily visible on any person's eyes.

Human with different **eye iris** such as **Dark Blue Iris, Dark Green Iris, Dark Red Iris**, shall be considered as the most fundamental **species** of human exist under different **UV, RF, IR** environmental radiation considered having different "**Money Value**" (Genetically varied)**.**

e) Etymology of word Holy, Black, white?...

It is hypothesized that **BLACK, WHITE** shall be considered as the genetically distinguished and directly opposite in characteristics as described below. The etymology of word Black, white might be derived from proto Indo Europe root word **PIRAI, OUIR** respectively.

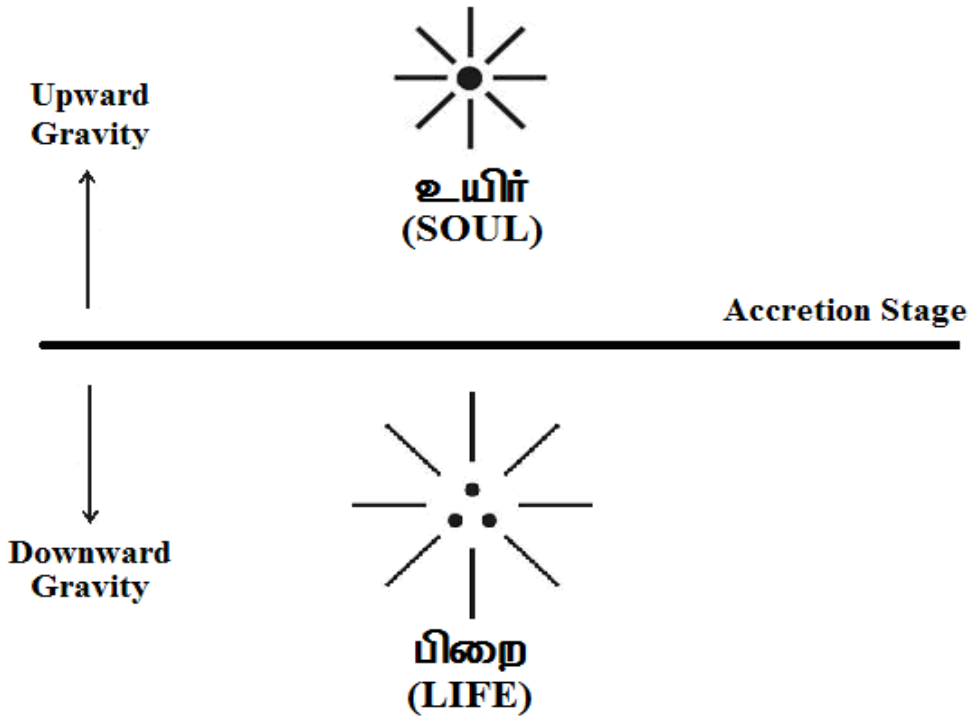

It is further hypothesized that the etymology of word "**HOLY**" might be derived from proto Indo Europe root word "**OLI**" as described below.

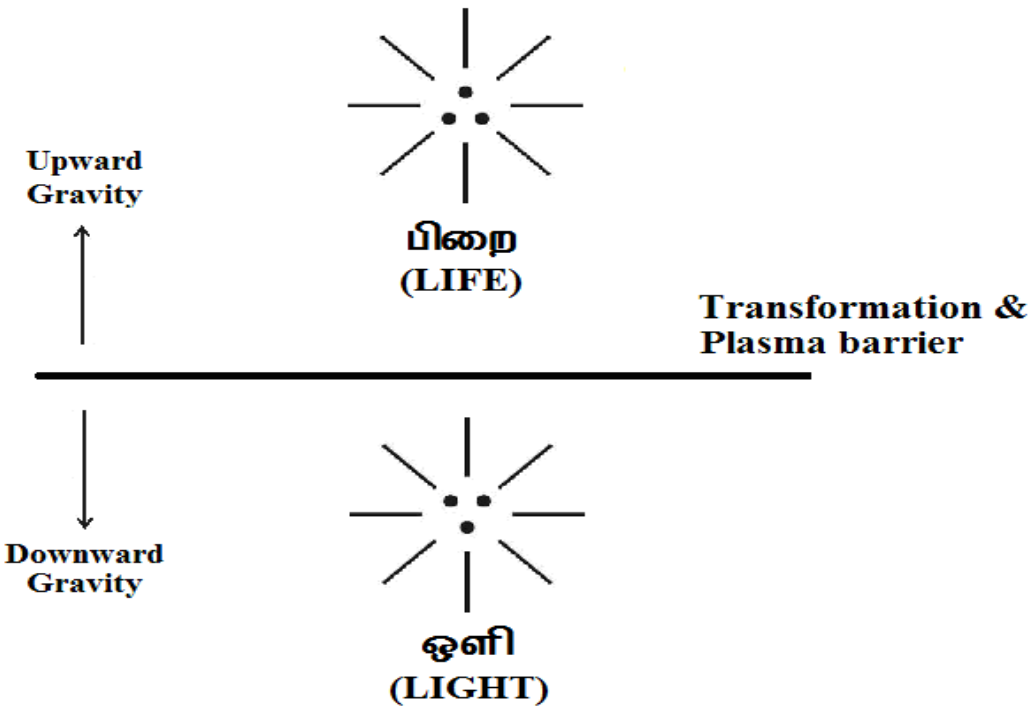

> *"**WHITE**" is like "**SOUL**"*
> *"**BLACK**" is like "**LIFE**"*
> *"**HOLY**" is like "**LIGHT**"*
>
> ***- M.Arulmani***
> ***Tamil based Indian***

f) Kachcha Theevu is source of Black Money?...

It is hypothesized that Kachcha Theevu (virgin island) shall be considered as origin of first land mass on the earth planet descended from **white planet** during the course of expanding Universe. In proto Indo-Europe language root the Kachcha Theevu shall also be called as "**KANDI**". Further Kachcha Theevu shall be considered as the natural source of **DARK ASSETS** such as coal, coke, crude oil etc., which shall be considered as the source of "**BLACK MONEY**".

g) Case study on "JAI HIND"?...

Case study shows that the phrase "**JAI HIND**" is considered closely associated with slogan during freedom fight for India which means "**HAIL MOTHER LAND**".

It is hypothesized that "**White money**" (Kandi), **Black money** (Kundi) shall be considered having distinguished "**GENDER VALUE**" as described below.

i) ***KANDI*** *shall mean* ***MALE PLANET*** *(White planet)*
ii) ***KUNDI*** *shall mean* ***FEMALE PLANET*** *(Earth planet)*
a) ***KANDI MONEY*** *shall mean* ***Father of mars***
b) ***KUNDI MONEY*** *shall mean* ***Mother of Earth***
c) ***JAI HIND*** *shall mean* ***Mother of India***

- Author

h) Case study on "VANDE MATARAM"?...

Case study shows that Vande mataram is concerned with National songs of India which mean "**Mother I salute to thee**"

In secular India the philosophy of Vande mafaram was not accepted by other religions as it refer Idol worship of nation as mother. Hence in 1950 after Independence India "**National Anthem**" wrote by Rabindranath Tagore was accepted in place of "**National song**" of India.

It is hypothesized that Earth planet shall be considered as Female gender and the philosophy of land of India might be considered as "**MOTHER**". Further the "**J-RADIATION**" (Zero hour radiation) of universe shall be considered as "**Mother of radiations**". In proto Indo Europe language root "**J-RADIATION**" shall be called as "**JAYAM THEE**"

ஜெயம் தீ
(MOTHER INDIA)

It is further hypothesized that the philosophy of "**Vande mataram**" might be derived from the **Three-in-one culture** of Ancient India.

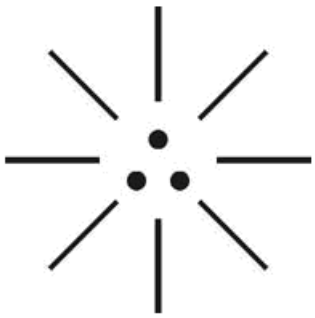

(Salute to Mother)

i) Right dot is "**NANDRI**" (like mind)
ii) Left dot is "**VANAKKAM**" (like Body)
iii) Centre dot is "**VAZHA**" (like Heart)

II. CONCLUSION:

It is focused that global level expert not yet confined where is the source of **White money, Black money**?... It is hypothesized that "**SUPERNATURE**" (GOD) shall be considered as the "**Source of money**" having infinite level of Dark matter, Dark Energy kept in the "**BLACK BOX CASH CHEST**" of "**DARK LAW**".

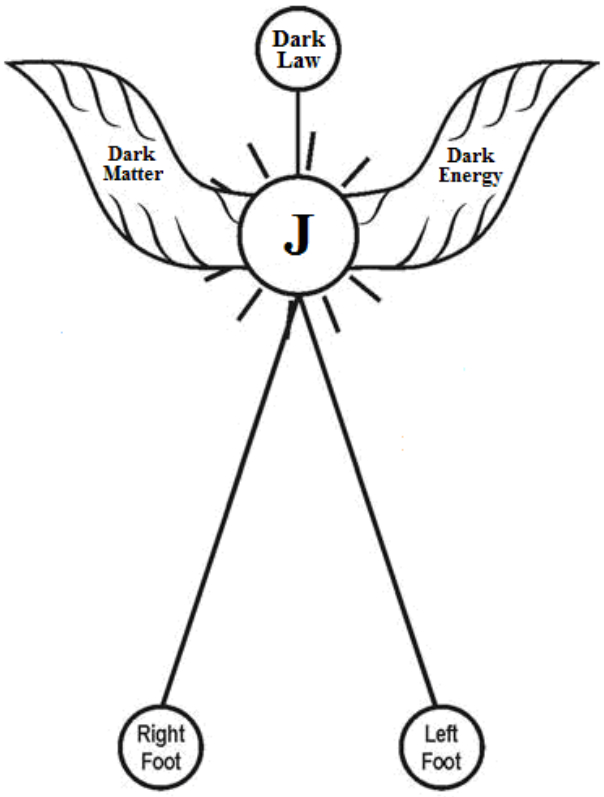

கரி மணி

(SUPERNATURE)

Previous Publication: The philosophy of origin of first life and human, the philosophy of model Cosmo Universe, the philosophy of fundamental neutrino particles have already been published in various international journals mentioned below. Hence this article shall be considered as **extended version** of the previous articles already published by the same author.

[1] Cosmo Super Star – IJSRP, April issue, 2013

[2] Super Scientist of Climate control – IJSER, May issue, 2013

[3] AKKIE MARS CODE – IJSER, June issue, 2013

[4] KARITHIRI (Dark flame) The Centromere of Cosmo Universe – IJIRD, May issue, 2013

[5] MA-AYYAN of MARS – IJIRD, June issue, 2013

[6] MARS TRIBE – IJSER, June issue, 2013

[7] MARS MATHEMATICS – IJERD, June issue, 2013

[8] MARS (EZHEM) The mother of All Planets – IJSER, June issue, 2013

[9] The Mystery of Crop Circle – IJOART, May issue, 2013

[10] Origin of First Language – IJIRD, June issue, 2013

[11] MARS TRISOMY HUMAN – IJOART, June issue, 2013

[12] MARS ANGEL – IJSTR, June issue, 2013

[13] Three principles of Akkie Management (AJIBM, August issue, 2013)

[14] Prehistoric Triphthong Alphabet (IJIRD, July issue, 2013)

[15] Prehistoric Akkie Music (IJST, July issue, 2013)

[16] Barack Obama is Tamil Based Indian? (IJSER, August issue, 2013)

[17] Philosophy of MARS Radiation (IJSER, August 2013)

[18] Etymology of word **"J"** (IJSER, September 2013)

[19] NOAH is Dravidian? (IJOART, August 2013)

[20] Philosophy of Dark Cell (Soul)? (IJSER, September 2013)

[21] Darwin Sir is Wrong?! (IJSER, October issue, 2013)

[22] Prehistoric Pyramids are RF Antenna?!... (IJSER, October issue, 2013)

[23] HUMAN IS A ROAM FREE CELL PHONE?!... (IJIRD, September issue, 2013)

[24] NEUTRINOS EXIST IN EARTH ATMOSPHERE?!... (IJERD, October issue, 2013)

[25] EARLY UNIVERSE WAS HIGHLY FROZEN?!... (IJOART, October issue, 2013)

[26] UNIVERSE IS LIKE SPACE SHIP?!... (AJER, October issue, 2013)

[27] ANCIENT EGYPT IS DRAVIDA NAD?!... (IJSER, November issue, 2013)

[28] ROSETTA STONE IS PREHISTORIC "THAMEE STONE" ?!... (IJSER, November issue, 2013)

[29] The Supernatural "CNO" HUMAN?... (IJOART, December issue, 2013)

[30] 3G HUMAN ANCESTOR?... (AJER, December issue, 2013)

[31] 3G Evolution?... (IJIRD, December issue, 2013)

[32] God Created Human?... (IJERD, December issue, 2013)

[33] Prehistoric "J" – Element?... (IJSER, January issue, 2014)

[34] 3G Mobile phone Induces Cancer?... (IJERD, December issue, 2013)

[35] "J" Shall Mean "JOULE"?... (IRJES, December issue, 2013)

[36] "J"- HOUSE IS A HEAVEN?... (IJIRD, January issue, 2014)

[37] The Supersonic JET FLIGHT-2014?... (IJSER, January issue, 2014)

[38] "J"-RADIATION IS MOTHER OF HYDROGEN?... (AJER, January issue, 2014)

[39] PEACE BEGINS WITH "J"?... (IJERD, January issue, 2014)

[40] THE VIRGIN LIGHT?... (IJCRAR, January issue 2014)

[41] THE VEILED MOTHER?... (IJERD, January issue 2014)

[42] GOD HAS NO LUNGS?... (IJERD, February issue 2014)

[43] Matters are made of Light or Atom?!... (IJERD, February issue 2014)
[44] THE NUCLEAR "MUKKULAM"?... (IJSER, February issue 2014)
[45] WHITE REVOLUTION 2014-15?... (IJERD, February issue 2014)
[46] STAR TWINKLES!?... (IJERD, March issue 2014)
[47] "E-LANKA" THE TAMIL CONTINENT?... (IJERD, March issue 2014)
[48] HELLO NAMESTE?... (IJSER, March issue 2014)
[49] MOTHERHOOD MEANS DELIVERING CHILD?... (AJER, March issue 2014)
[50] E–ACHI, IAS?... (AJER, March issue 2014)
[51] THE ALTERNATIVE MEDICINE?... (AJER, April issue 2014)
[52] GANJA IS ILLEGAL PLANT?... (IJERD, April issue 2014)
[53] THE ENDOS?... (IJERD, April issue 2014)
[54] THE "TRI-TRONIC" UNIVERSE?... (AJER, May issue 2014)
[55] Varied Plasma Level have impact on "GENETIC VALUE"?... (AJER, May issue 2014)
[56] JALLIKATTU IS DRAVIDIAN VETERAN SPORT?... (AJER, May issue 2014)
[57] Human Equivalent of Cosmo?... (IJSER, May issue 2014)
[58] THAI-e ETHIA!... (AJER, May issue 2014)
[59] THE PHILOSOPHY OF "DALIT"?... (AJER, June issue 2014)
[60] THE IMPACT OF HIGHER QUALIFICATION?... (AJER, June issue 2014)
[61] THE CRYSTAL UNIVERSE?... (AJER July 2014 issue)
[62] THE GLOBAL POLITICS?... (AJER July 2014 issue)
[63] THE KACHCHA THEEVU?... (AJER July 2014 issue)
[64] THE RADIANT MANAGER?... (AJER July 2014 issue)
[65] THE UNIVERSAL LAMP?... (IJOART July 2014 issue)
[66] THE MUSIC RAIN?... (IJERD July 2014 issue)
[67] THIRI KURAL?... (AJER August 2014 issue)
[68] THE SIXTH SENSE OF HUMAN?... (AJER August 2014 issue)
[69] THEE… DARK BOMB?... (IJSER August 2014 issue)
[70] RAKSHA BANDHAN CULTURE?... (IJERD August 2014 issue)
[71] THE WHITE BLOOD ANCESTOR?... (AJER August 2014 issue)
[72] THE PHILOSOPHY OF "ZERO HOUR"?... (IJERD August 2014 issue)
[73] RAMAR PALAM?... (AJER September 2014 issue)
[74] THE UNIVERSAL TERRORIST?... (AJER September 2014 issue)
[75] THE "J-CLOCK"!... (AJER September 2014 issue)
[76] "STUDENTS" AND "POLITICS"?... (IJERD October 2014 issue)
[77] THE PREGNANT MAN?... (AJER September 2014 issue)
[78] PERIAR IS ATHEIST?... (IJSER September 2014 issue)
[79] A JOURNEY TO "WHITE PLANET"?... (AJER October 2014 issue)
[80] Coming Soon!... (AJER October 2014 issue)
[81] THE PREJUDICED JUSTICE?... (IJERD October 2014 issue)
[82] BRITISH INDIA?... (IJSER October 2014 issue)
[83] THE PHILOSOPHY OF "HUMAN RIGHTS"?... (IJERD October 2014 issue)
[84] THE FOSTER CHILD?... (AJER October 2014 issue)
[85] WHAT DOES MEAN "CRIMINAL"?... (IJERD October 2014 issue)
[86] 1000 YEARS RULE?... (AJER November 2014 issue)
[87] AM I CORRUPT?... (IJSER November 2014 issue)

REFERENCE

[1] Intensive Internet "e-book" study through, Google search and wikipedia
[2] M.Arulmani, "3G Akkanna Man", Annai Publications, Cholapuram, 2011
[3] M. Arulmani; V.R. Hemalatha, "Tamil the Law of Universe", Annai Publications, Cholapuram, 2012
[4] Harold Koontz, Heinz Weihriah, "Essentials of management", Tata McGraw-Hill publications, 2005
[5] M. Arulmani; V.R. Hemalatha, "First Music and First Music Alphabet", Annai Publications, Cholapuram, 2012
[6] King James Version, "Holy Bible"
[7] S.A. Perumal, "Human Evolution History"
[8] "English Dictionary", Oxford Publications
[9] Sho. Devaneyapavanar, "Tamil first mother language", Chennai, 2009
[10] Tamilannal, "Tholkoppiar", Chennai, 2007
[11] "Tamil to English Dictionary", Suravin Publication, 2009
[12] "Text Material for E5 to E6 upgradaton", BSNL Publication, 2012
[13] A. Nakkiran, "Dravidian mother", Chennai, 2007
[14] Dr. M. Karunanidhi, "Thirukkural Translation", 2010
[15] "Manorama Tell me why periodicals", M.M. Publication Ltd., Kottayam, 2009
[16] V.R. Hemalatha, "A Global level peace tourism to Veilankanni", Annai Publications, Cholapuram, 2007
[17] Prof. Ganapathi Pillai, "Sri Lankan Tamil History", 2004
[18] Dr. K.K. Pillai, "South Indian History", 2006
[19] M. Varadharajan, "Language History", Chennai, 2009
[20] Fr. Y.S. Yagoo, "Western Sun", 2008
[21] Gopal Chettiar, "Adi Dravidian Origin History", 2004
[22] M. Arulmani; V.R. Hemalatha, "Ezhem Nadu My Dream" - (2 Parts), Annai Publications, Cholapuram, 2010
[23] M. Arulmani; V.R. Hemalatha, "The Super Scientist of Climate Control", Annai Publications, Cholapuram, 2013, pp 1-3

American Journal of Engineering Research (AJER)
e-ISSN : 2320-0847 p-ISSN : 2320-0936
Volume-03, Issue-11, pp-150-166
www.ajer.org

Research Paper Open Access

Study the Effectiveof Seismic load on Behavior of Shear Wall in Frame Structure

Dr.Hadi Hosseini[1], Mahdi Hosseini[2], Ahmad Hosseini[3]

[1,]*Aerospace Engineering , working in International Earthquake Research Center of America (IERCA)*
[2,]*Master of Technology in Structural Engineering, Dept. of Civil Engineering, Jawaharlal Nehru Technological University Hyderabad (JNTUH), Hyderabad, Telengana , India*
[3,]*Graduate Student in Mechanical Engineering, Dept. of Mechanical Engineering,Kakatiya University Warangal, Telengana, India*

ABSTRACT : *Structural walls, or shear walls, are elements used to resist lateral loads, such as those generated by wind and earthquakes. Structural walls are considerably deeper than typical beams or columns. This attribute gives structural walls considerable in-plane stiffness which makes structural walls a natural choice for resisting lateral loads. In addition to considerable strength, structural walls can dissipate a great deal of energy if detailed properly. Walls are an invaluable structural element when protecting buildings from seismic events. Buildings often rely on structural walls as the main lateral force resisting system. Shear walls are required to perform in multiple ways. Shear walls can then be designed to limit building damage to the specified degree. The load-deformation response of the structural walls must be accurately predicted and related to structural damage in order to achieve these performance goals under loading events of various magnitudes. The applied load is generally transferred to the wall by a diaphragm or collector or drag member. The performance of the framed buildings depends on the structural system adopted for the structure The term structural system or structural frame in structural engineering refers to load-resisting sub-system of a structure. The structural system transfers loads through interconnected structural components or members. These structural systems need to be chosen based on its height and loads and need to be carried out, etc. The selection of appropriate structural systems for building must satisfy both strength and stiffness requirements. The structural system must be adequate to resist lateral and gravity loads that cause horizontal shear deformation and overturning deformation. The efficiency of a structural system is measured in terms of their ability to resist lateral load, which increases with the height of the frame. A building can be considered as tall when the effect of lateral loads is reflected in the design. Lateral deflections of framed buildings should be limited to prevent damage to both structural and nonstructural elements. In the present study, the structural performance of the framed building with shear wall will be analysis.*

KEY WORDS: *Structural walls,Shear walls,frame structure,Seismic Load,frame system*

I. INTRODUCTION

Seismic Load : Earthquake forces experienced by a building result from ground motions (accelerations) which are also fluctuating or dynamic in nature, in fact they reverse direction some what chaotically. The magnitude of an earthquake force depends on the magnitude of an earthquake, distance from the earthquake source(epicenter), local ground conditions that may amplify ground shaking (or dampen it), the weight(or mass) of the structure, and the type of structural system and its ability to with stand abusive cyclic loading. In theory and practice, the lateral force that a building experiences from an earthquake increases in direct proportion with the acceleration of ground motion at the building site and the mass of the building (i.e., a doubling in ground motion acceleration or building mass will double the load).This theory rests on the simplicity and validity of Newton's law of physics: F = m x a, where 'F' represents force, 'm' represents mass or weight, and 'a' represents acceleration. For example, as a car accelerates forward, a force is imparted to the driver through the seat to push him forward with the car(this force is equivalent to the weight of the driver multiplied by the acceleration or rate of change in speed of the car). As the brake is applied, the car is decelerated and a force is imparted to the driver by the seat-belt to push him back toward the seat. Similarly, as the ground accelerates back and forth during an earthquake

it imparts back-and-forth(cyclic) forces to a building through its foundation which is forced to move with the ground. One can imagine a very light structure such as fabric tent that will be undamaged in almost any earthquake but it will not survive high wind. The reason is the low mass (weight) of the tent. Therefore, residential buildings generally perform reasonably well in earthquakes but are more vulnerable in high-wind load prone areas. Regardless, the proper amount of bracing is required in both cases.

Why Are Buildings With Shear Walls Preferred In Seismic Zones?

Reinforced concrete (RC) buildings often have vertical plate-like RC walls called Shear Walls in addition to slabs, beams and columns. These walls generally start at foundation level and are continuous throughout the building height. Their thickness can be as low as 150mm, or as high as 400mm in high rise buildings. Shear walls are usually provided along both length and width of buildings. Shear walls are like vertically-oriented wide beams that carry earthquake loads downwards to the foundation.

"We cannot afford to build concrete buildings meant to resist severe earthquakes without shear walls." Mark Fintel, a noted consulting engineer in USA Shear walls in high seismic regions requires special detailing. However, in past earthquakes, even buildings with sufficient amount of walls that were not specially detailed for seismic performance (but had enough well-distributed reinforcement) were saved from collapse. Shear wall buildings are a popular choice in many earthquake prone countries, like Chile, New Zealand and USA. Shear walls are easy to construct, because reinforcement detailing of walls is relatively straight-forward and therefore easily implemented at site. Shear walls are efficient; both in terms of construction cost properly designed and detailed buildings with Shear walls have shown very good performance in past earthquakes. The overwhelming success of buildings with shear walls in resisting strong earthquakes is summarized in the quote: And effectiveness in minimizing earthquake damage in structural and non- Structural elements (like glass windows and building contents).

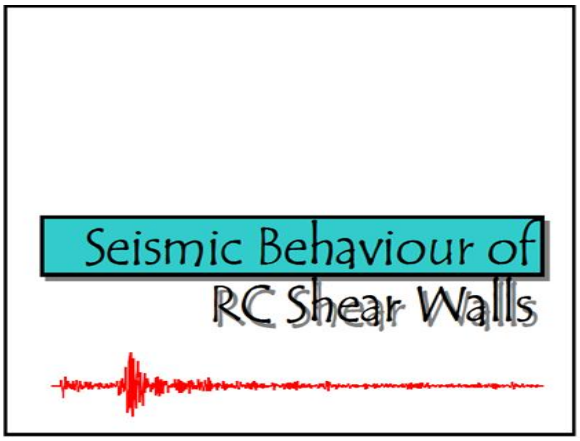

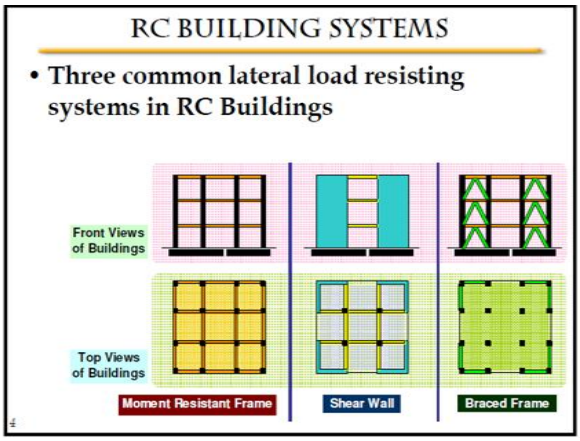

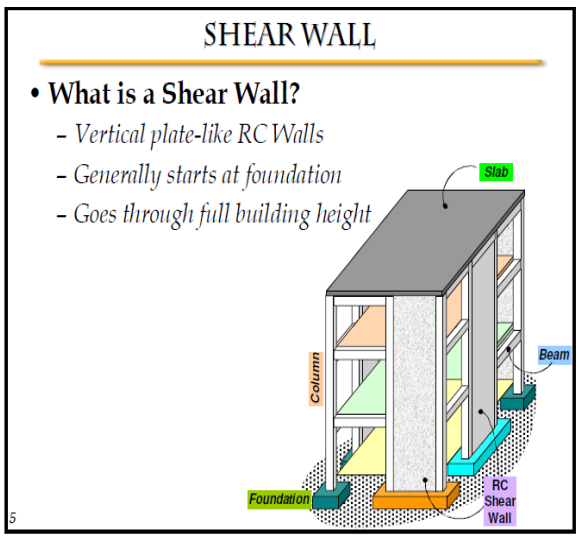

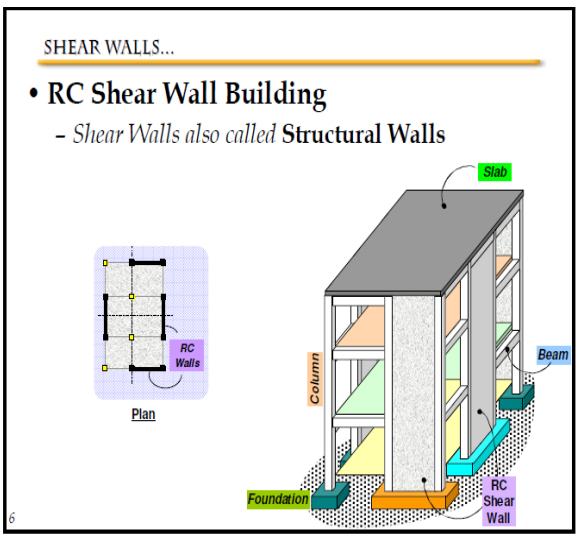

SHEAR WALLS...

- **Principal attributes**
  - *Large Strength*
  - *High Stiffness*
  - *Ductility*
    - **Shear wall can be detailed to have large ductility**

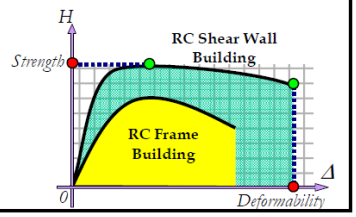

7

SHEAR WALLS...

- **Role of Shear Walls**
  - *Smooth transfer of seismic forces*
  - *Vertically oriented wide beams*

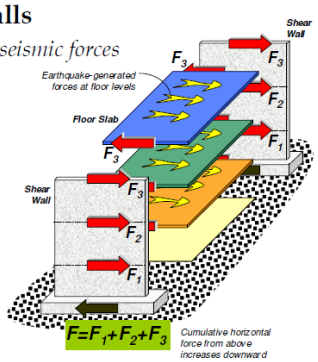

8

SHEAR WALLS...

- **Advantages of Shear Walls...**
  - *Lesser lateral displacement than frames*
  - *Lesser Damage to structural and non-structural elements*

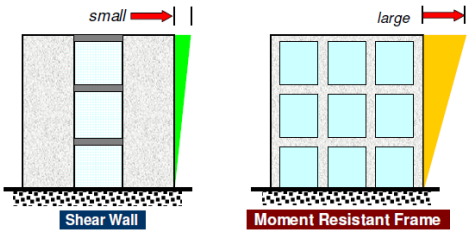

11

SHEAR WALLS...

- **Current Use of Shear Walls**
  - *Popular choice in many earthquake prone countries*
    - **Chile, Canada, USA and New Zealand**
  - *In general, used in medium and high rise buildings*
    - **10 storeys and higher**

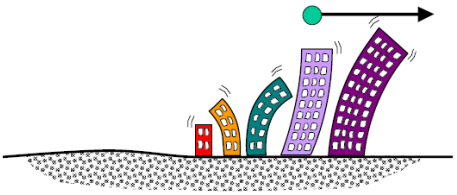

12

ARCHITECTURAL ASPECTS

- **Walls must be preferably in both directions**
  - *in plan*

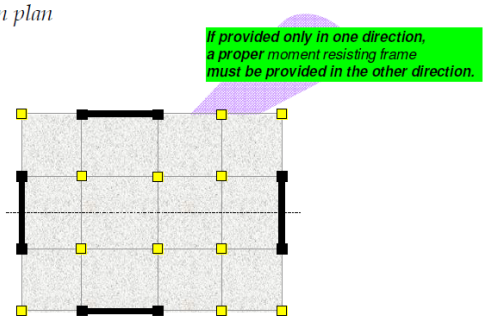

13

ARCHITECTURAL ASPECTS...

- **If provided only in one direction, a proper moment resisting frame must be provided in the other direction.**

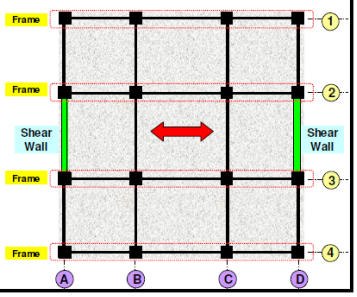

14

ARCHITECTURAL ASPECTS...

- **Shear wall can extend over the full width of building, or even over partial width**

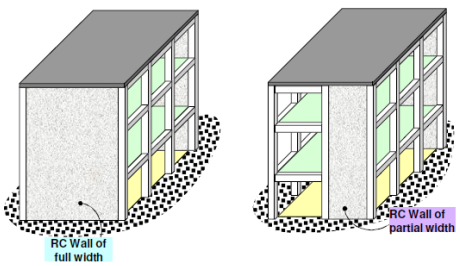

15

ARCHITECTURAL ASPECTS...

- **Walls should be throughout the height**
  - *Cannot be interrupted in lower levels*

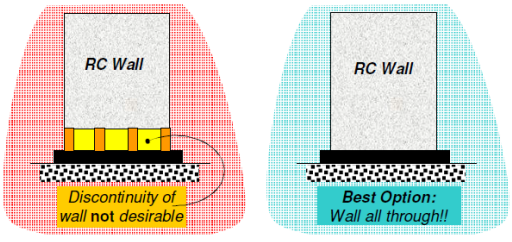

16

ARCHITECTURAL ASPECTS...

- **Walls should be throughout the height**
  - *Cannot be interrupted in* upper *levels*

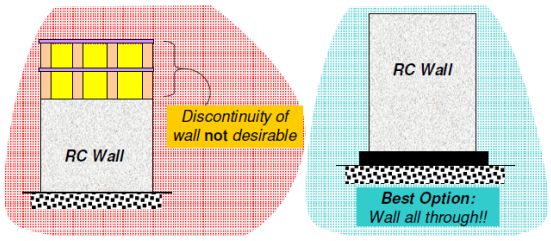

17

ARCHITECTURAL ASPECTS...

- **Walls should be along perimeter of building**
  - *Improves resistance to twist*

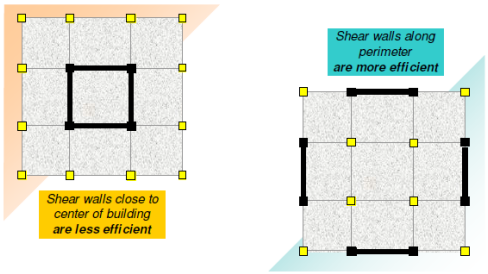

18

ARCHITECTURAL ASPECTS...

- **Walls must be symmetrically placed in plan**

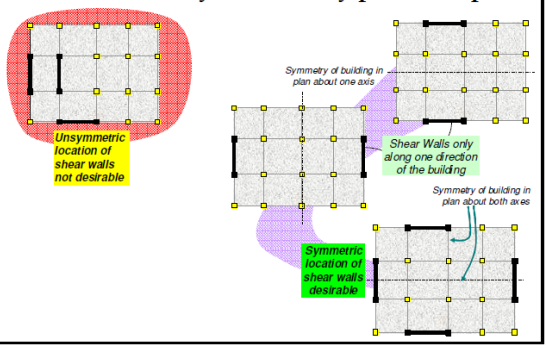

19

ARCHITECTURAL ASPECTS...

- **Shear wall building should not be narrow**
  - *Earthquakes cause significant overturning effects*
  - *Special care is required in design of their foundations*

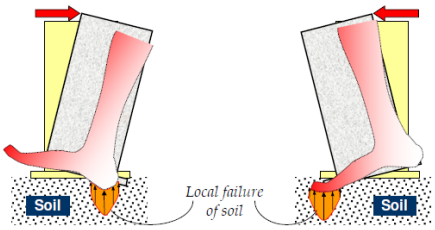

20

SEISMIC BEHAVIOUR...

- **Undesirable Mode of Failure**

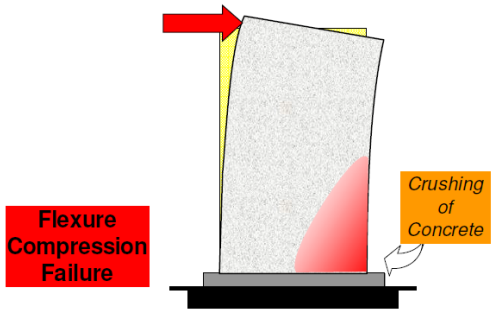

23

SEISMIC BEHAVIOUR...

- **Desirable Mode of Failure**

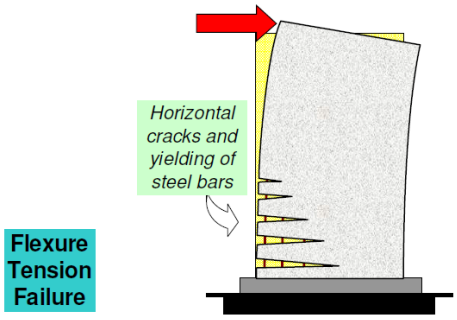

24

SEISMIC BEHAVIOUR...

- **Shear demand is more in lower storeys**

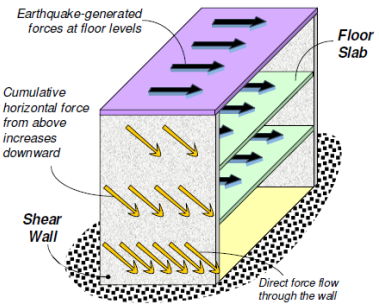

25

SEISMIC BEHAVIOUR...

- **Shear demand is more in lower storeys...**

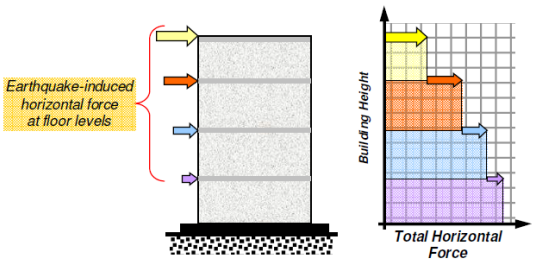

26

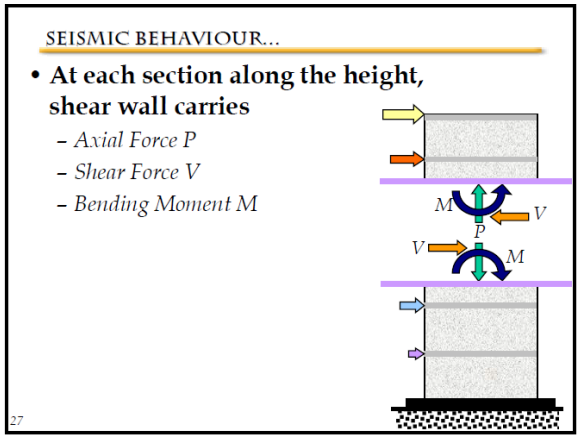

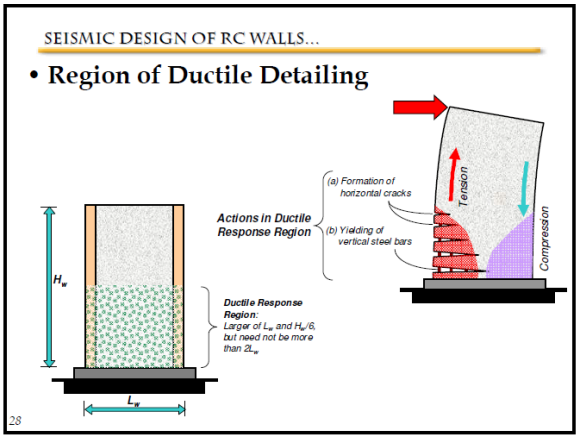

II. METHODOLOGY

Earthquake motion causes vibration of the structure leading to inertia forces. Thus a structure must be able to safely transmit the horizontal and the vertical inertia forces generated in the super structure through the foundation to the ground. Hence, for most of the ordinary structures, earthquake-resistant design requires ensuring that the structure has adequate lateral load carrying capacity. Seismic codes will guide a designer to safely design the structure for its intended purpose.

Quite a few methods are available for the earthquake analysis of buildings; two of them are presented here:
[1] Equivalent Static Lateral Force Method (pseudo static method).
[2] Dynamic analysis.
I. Response spectrum method.
II. Time history method.

Equivalent lateral Force (Seismic Coefficient) Method : This method of finding lateral forces is also known as the static method or the equivalent static method or the seismic coefficient method. The static method is the simplest one and it requires less computational effort and is based on formulae given in the code of practice.
In all the methods of analyzing a multi storey buildings recommended in the code, the structure is treated as discrete system having concentrated masses at floor levels which include the weight of columns and walls in any storey should be equally distributed to the floors above and below the storey. In addition, the appropriate amount of imposed load at this floor is also lumped with it. It is also assumed that the structure flexible and will deflect with respect to the position of foundation the lumped mass system reduces to the solution of a system of second order differential equations. These equations are formed by distribution, of mass and stiffness in a structure, together with its damping characteristics of the ground motion.

Dynamic Analysis : Dynamic analysis shall be performed to obtain the design seismic force, and its distribution in different levels along the height of the building, and in the various lateral load resisting element, for the following buildings:

Regular buildings: Those greater than 40m in height in zones IV and V, those greater than 90m in height in zone II and III.

Irregular buildings: All framed buildings higher than 12m in zones IV and V, and those greater than 40m in height in zones II and III.
The analysis of model for dynamic analysis of buildings with unusual configuration should be such that it adequately models the types of irregularities present in the building configuration. Buildings with plan irregularities, as defined in Table 4 of IS code: 1893-2002 cannot be modeled for dynamic analysis.
Dynamic analysis may be performed either by the TIME HISTORY METHOD or by the RESPONSE SPECTRUM METHOD

Time History Method : The usage of this method shall be on an appropriate ground motion and shall be performed using accepted principles of dynamics. In this method, the mathematical model of the building is subjected to accelerations from earthquake records that represent the expected earthquake at the base of the structure.

Response Spectrum Method : The word spectrum in engineering conveys the idea that the response of buildings having a broad range of periods is summarized in a single graph. This method shall be performed using the design spectrum specified in code or by a site-specific design spectrum for a structure prepared at a project site. The values of damping for building may be taken as 2 and 5 percent of the critical, for the purposes of dynamic of steel and reinforce concrete buildings, respectively. For most buildings, inelastic response can be expected to occur during a major earthquake, implying that an inelastic analysis is more proper for design. However, in spite of the availability of nonlinear inelastic programs, they are not used in typical design practice because:

[1] Their proper use requires knowledge of their inner workings and theories. design criteria, and
[2] Result produced are difficult to interpret and apply to traditional design criteria , and
[3] The necessary computations are expensive.
[4] Therefore, analysis in practice typically use linear elastic procedures based on the response spectrum method. The response spectrum analysis is the preferred method because it is easier to use.

III. NUMERICAL ANALYSES

STRUCTURE
G+19 earthquake resistant structure with shear walls

Problems In The Building Due To Earthquake : Main problems that would be arising due to earthquake in the structure are story drift and deflection of the building due to its large height and also torsion and others, so if the structure is proved to be safe in all the above mentioned problems than the structure would be safe in all cases in respect earthquake.

Geometrical Properties
[1] .No.of stories of the Building model=20
[2] Column size=500 mm x 500 mm
[3] Beam size= 700 mm x 500 mm
[4] Slab thickness=200mm

Loads
[1] Live Load=3KN/m2
[2] Wall Load=12.4KN/m
[3] Floor Finishing =1KN/m2
[4] Wind load

Wind coefficients
[1] Wind Speed=50m/s
[2] Terrain Category =2
[3] Structure Class=B
[4] Risk Coefficient(k1)=1
Topography(k3)=1

Seismic loading
[1] Seismic zone factor(Z)=0.36
[2] Soil Type= Medium(II)
[3] Response Reduction factor(R) =5%
[4] Story Range=Base to 20
[5] Important factor(I)=1

IV. MATERIAL PROPERTIES

Table I The materials used in structure and their general properties are

Material Text	Unit weight KN/m3	Elastic Modulus KN/m2	Shear Modulus KN/m2	Poisson Ratio Unit less	Thermal expansion coefficient 1/C
Concrete	23.563	24855578.28	10356490.95	0.2	0.0000099
Rebar steel	76.973	199947978.8	76903068.77	0.3	0.0000117
Bar steel	76.9730	199947978.8	769030068.77	0.3	0.0000117

Load Combinations : Load combination is the foremost important criteria for designing any structure and more important is the distribution of those loads on to various components of the structure like beams, columns, slabs and in our case shears walls and concrete core wall too. There are many kinds of loads existing depending on the location of the where the structure is to be constructed for example in a place where wind is frequent there we have to consider the wind loads and places where rains are heavy rain loads are included and same way all the other loads such as snow loads, earthquake load and etc. are included however DEAD LOADS, LIVE LOADS AND IMPOSEDLOADS are always included. Dead loads are all common depending on the structural components and specific gravity of the structure, to get the self weight of the structural component volume or area of the component is multiplied by the specific gravity of the component. Live loads depend on the purpose we are constructing the building. Imposed loads depend on the seismic loads, dead loads and according to are 1893 part 1 percentage of those values is finally considered.

The following Load Combinations have been considered for the design

1.	1.5(DL+ LL)	DL – Dead Load
2.	1.5(DL ± EQXTP)	LL – Live Load
3.	1.5(DL ± EQYTP)	EQTP–Earthquake load
4.	1.5(DL ± EQXTN)	With torsion positive
5.	1.5(DL ± EQYTN)	EQTN–Earthquake load
6.	1.2(DL + LL ± EQXTP)	With torsion negative
7.	1.2(DL + LL ± EQYTP)	WL- Wind load
8.	1.2(DL + LL ± EQXTN)	
9.	1.2(DL + LL ± EQYTN)	
10.	1.5(DL ± WLX)	
11.	1.5(DL ± WLY)	
12.	1.2(DL + LL ± WLX)	
13.	1.2(DL + LL ± WLY)	

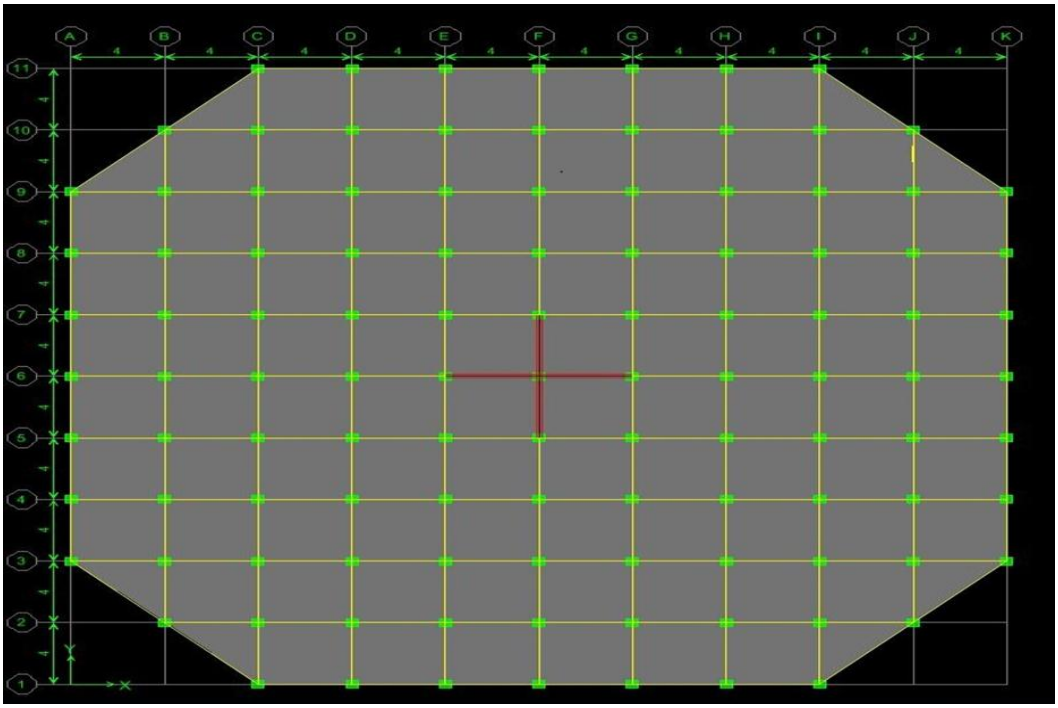

Figure 1: Basic Plan of The Building

Table II: Axial force, Shear Force, Torsion and Moment for columnC1

Story	Column	Load	Loc	AXIAL FORCE	SHEAR FORCE	TORSION	MOMENT
STORY1	C1	1.2DLLLEQY	2.5	-5981.12	2.99	0.699	-20.004
STORY2	C1	1.2DLLLEQY	2.5	-5679.2	-10.81	0.888	-31.458
STORY3	C1	1.2DLLLEQY	2.5	-5385.39	-15.63	0.899	-40.218
STORY4	C1	1.2DLLLEQY	2.5	-5097.36	-20.13	0.898	-45.37
STORY5	C1	1.2DLLLEQY	2.5	-4812.42	-23.46	0.894	-48.001
STORY6	C1	1.2DLLLEQY	2.5	-4528.9	-25.99	0.887	-48.977
STORY7	C1	1.2DLLLEQY	2.5	-4245.72	-27.88	0.876	-48.786
STORY8	C1	1.2DLLLEQY	2.5	-3962.1	-29.24	0.861	-47.741
STORY9	C1	1.2DLLLEQY	2.5	-3677.43	-30.17	0.841	-46.02
STORY10	C1	1.2DLLLEQY	2.5	-3391.19	-30.76	0.816	-43.719
STORY11	C1	1.2DLLLEQY	2.5	-3102.89	-31.04	0.784	-40.883
STORY12	C1	1.2DLLLEQY	2.5	-2812	-31.08	0.746	-37.525
STORY13	C1	1.2DLLLEQY	2.5	-2517.98	-30.93	0.7	-33.647
STORY14	C1	1.2DLLLEQY	2.5	-2220.24	-30.63	0.646	-29.246
STORY15	C1	1.2DLLLEQY	2.5	-1918.14	-30.24	0.584	-24.333
STORY16	C1	1.2DLLLEQY	2.5	-1611.02	-29.82	0.512	-18.94
STORY17	C1	1.2DLLLEQY	2.5	-1298.25	-29.44	0.431	-13.185
STORY18	C1	1.2DLLLEQY	2.5	-979.21	-29.34	0.339	-6.978
STORY19	C1	1.2DLLLEQY	2.5	-653.62	-28.53	0.236	-2.515
STORY20	C1	1.2DLLLEQY	2.5	-320.5	-36.26	0.125	11.945

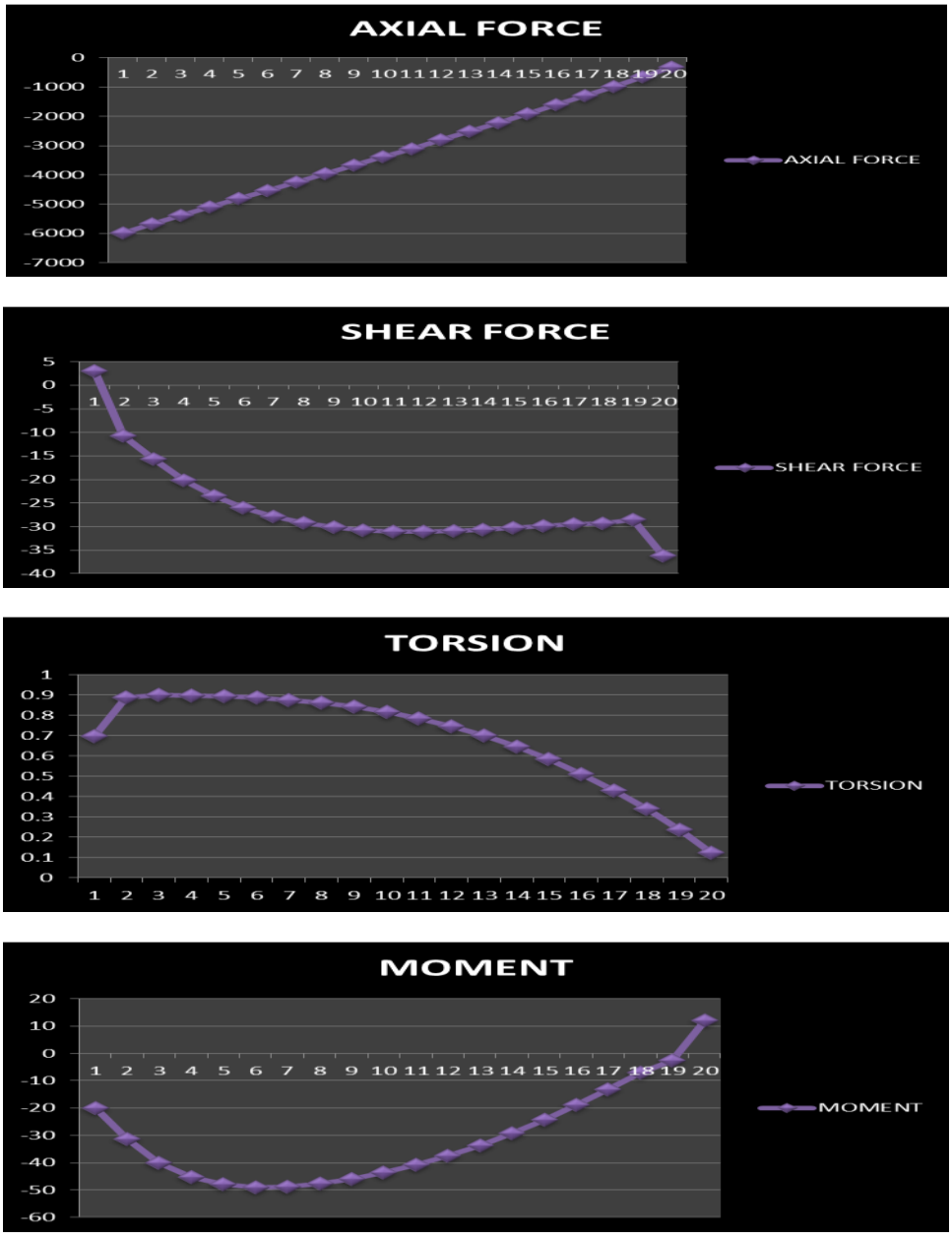

Figure 2: Axial force, Shear Force, Torsion and Moment for columnC1

Table III: Axial force, Shear Force, Torsion and Moment for columnC2

Story	Column	Load	Loc	AXIAL FORCE	SHEAR FORCE	TORSION	MOMENT
STORY1	C2	1.2DLLLEQY	2.5	-6603.93	7.94	0.699	-36.262
STORY2	C2	1.2DLLLEQY	2.5	-6226.23	1.01	0.888	-54.111
STORY3	C2	1.2DLLLEQY	2.5	-5863.39	-6.1	0.899	-65.904
STORY4	C2	1.2DLLLEQY	2.5	-5510.34	-12.14	0.898	-73.576
STORY5	C2	1.2DLLLEQY	2.5	-5165.54	-17.46	0.894	-78.05
STORY6	C2	1.2DLLLEQY	2.5	-4827.32	-22.1	0.887	-80.374
STORY7	C2	1.2DLLLEQY	2.5	-4494.32	-26.15	0.876	-81.122
STORY8	C2	1.2DLLLEQY	2.5	-4165.4	-29.66	0.861	-80.672
STORY9	C2	1.2DLLLEQY	2.5	-3839.61	-32.72	0.841	-79.246
STORY10	C2	1.2DLLLEQY	2.5	-3516.17	-35.38	0.816	-76.972
STORY11	C2	1.2DLLLEQY	2.5	-3194.43	-37.71	0.784	-73.916
STORY12	C2	1.2DLLLEQY	2.5	-2873.88	-39.76	0.746	-70.11
STORY13	C2	1.2DLLLEQY	2.5	-2554.1	-41.58	0.7	-65.572
STORY14	C2	1.2DLLLEQY	2.5	-2234.76	-43.24	0.646	-60.317
STORY15	C2	1.2DLLLEQY	2.5	-1915.64	-44.78	0.584	-54.377
STORY16	C2	1.2DLLLEQY	2.5	-1596.61	-46.25	0.512	-47.82
STORY17	C2	1.2DLLLEQY	2.5	-1277.66	-47.7	0.431	-40.764
STORY18	C2	1.2DLLLEQY	2.5	-958.94	-49.18	0.339	-33.472
STORY19	C2	1.2DLLLEQY	2.5	-640.18	-50.37	0.236	-26.108
STORY20	C2	1.2DLLLEQY	2.5	-325.91	-58.95	0.125	-22.275

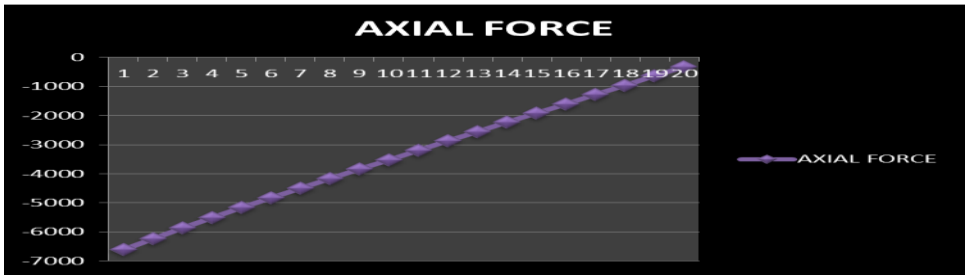

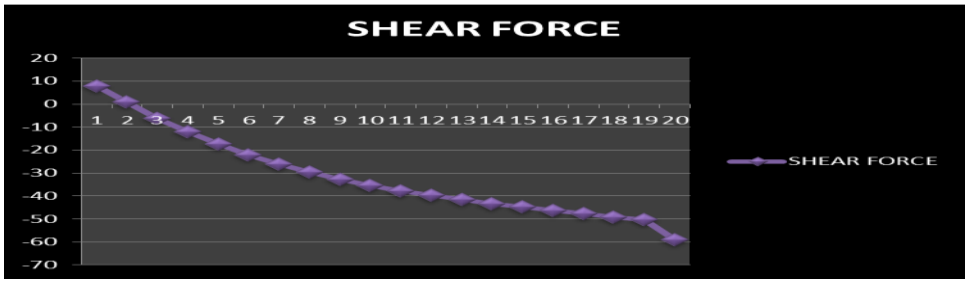

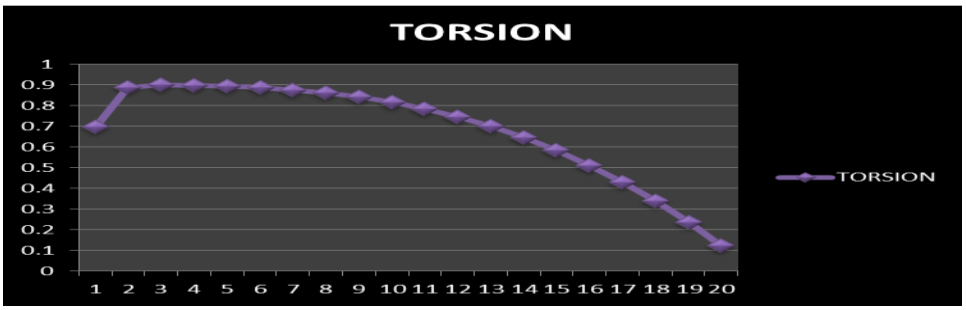

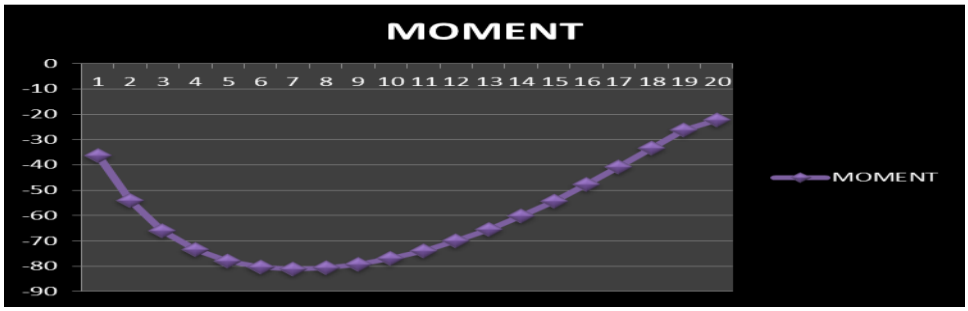

Figure 3: Axial force,Shear Force, Torsion and Moment for columnC2

Table IV: Axial force, Shear Force, Torsion and Moment for columnC4

Story	Column	Load	Loc	AXIAL FORCE	SHEAR FORCE	TORSION	MOMENT
STORY1	C4	1.2DLLLEQY	2.5	-6840.36	1.14	0.699	-38.844
STORY2	C4	1.2DLLLEQY	2.5	-6459.07	-4.4	0.888	-60.572
STORY3	C4	1.2DLLLEQY	2.5	-6087.55	-9.9	0.899	-75.858
STORY4	C4	1.2DLLLEQY	2.5	-5723.32	-14.58	0.898	-86.567
STORY5	C4	1.2DLLLEQY	2.5	-5365.25	-18.7	0.894	-93.676
STORY6	C4	1.2DLLLEQY	2.5	-5012.27	-22.29	0.887	-98.253
STORY7	C4	1.2DLLLEQY	2.5	-4663.56	-25.44	0.876	-100.899
STORY8	C4	1.2DLLLEQY	2.5	-4318.45	-28.18	0.861	-102.02
STORY9	C4	1.2DLLLEQY	2.5	-3976.41	-30.57	0.841	-101.862
STORY10	C4	1.2DLLLEQY	2.5	-3636.98	-32.67	0.816	-100.58
STORY11	C4	1.2DLLLEQY	2.5	-3299.78	-34.5	0.784	-98.267
STORY12	C4	1.2DLLLEQY	2.5	-2964.53	-36.12	0.746	-94.983
STORY13	C4	1.2DLLLEQY	2.5	-2964.53	-36.12	0.746	-94.983
STORY14	C4	1.2DLLLEQY	2.5	-2298.8	-38.85	0.646	-85.679
STORY15	C4	1.2DLLLEQY	2.5	-1967.91	-40.01	0.584	-79.77
STORY16	C4	1.2DLLLEQY	2.5	-1638.13	-41.08	0.512	-73.147
STORY17	C4	1.2DLLLEQY	2.5	-1309.29	-42.08	0.431	-65.97
STORY18	C4	1.2DLLLEQY	2.5	-981.35	-43.02	0.339	-58.545
STORY19	C4	1.2DLLLEQY	2.5	-653.82	-43.61	0.236	-50.801
STORY20	C4	1.2DLLLEQY	2.5	-329.82	-50.76	0.125	-51.899

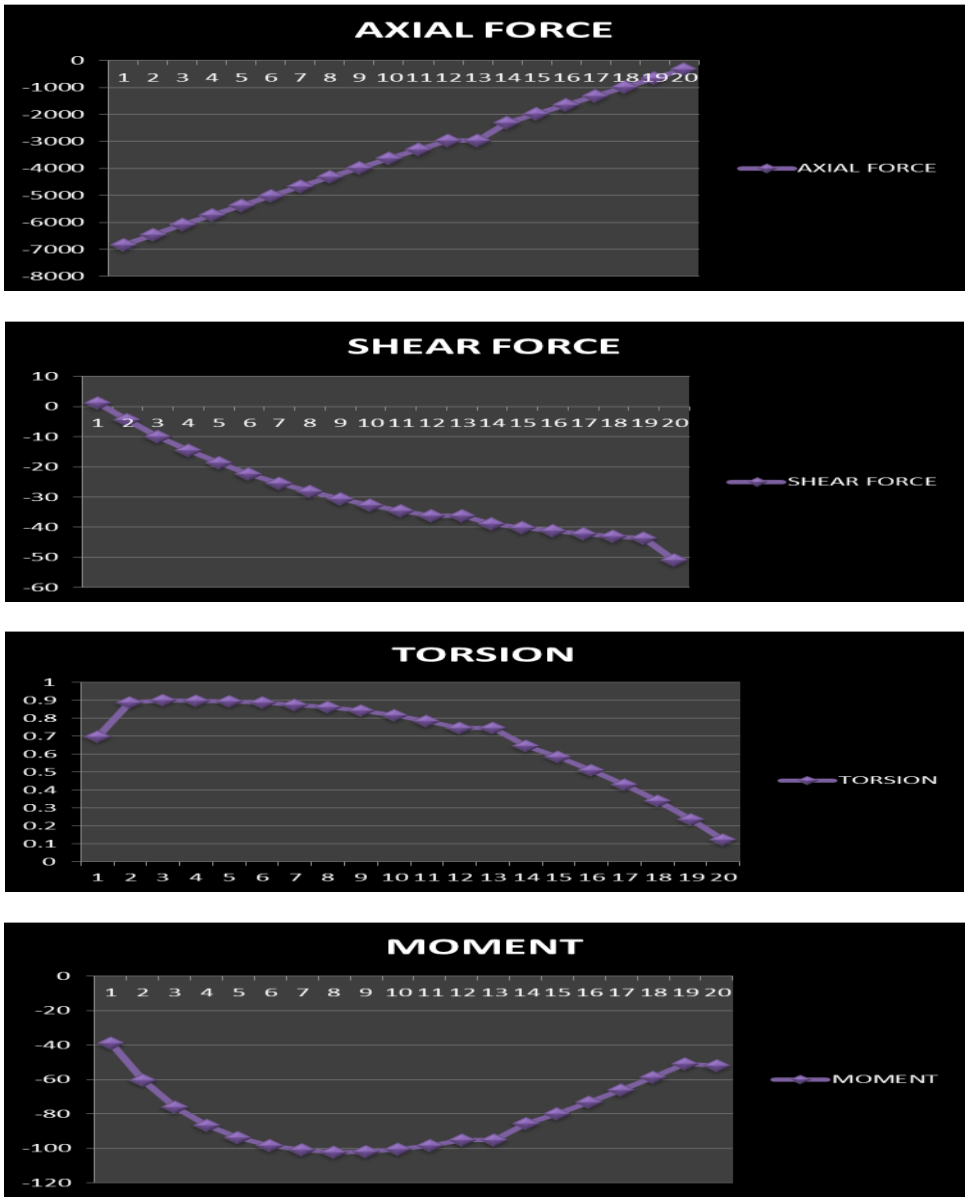

Figure 4:Axial force, Shear Force, Torsion and Moment for columnC4

Table V: Axial force, Shear Force, Torsion and Moment for columnC6

Story	Column	Load	Loc	AXIAL FORCE	SHEAR FORCE	TORSION	MOMENT
STORY1	C6	1.2DLLLEQY	2.5	-6936.63	-6.34	0.699	-38.329
STORY2	C6	1.2DLLLEQY	2.5	-6555.77	-11.89	0.888	-59.426
STORY3	C6	1.2DLLLEQY	2.5	-6183.69	-17.1	0.899	-74.085
STORY4	C6	1.2DLLLEQY	2.5	-5818.14	-21.54	0.898	-84.178
STORY5	C6	1.2DLLLEQY	2.5	-5458.03	-25.42	0.894	-90.682
STORY6	C6	1.2DLLLEQY	2.5	-5102.37	-28.79	0.887	-94.67
STORY7	C6	1.2DLLLEQY	2.5	-4750.38	-31.7	0.876	-96.745
STORY8	C6	1.2DLLLEQY	2.5	-4401.43	-34.2	0.861	-97.318
STORY9	C6	1.2DLLLEQY	2.5	-4055.02	-36.34	0.841	-96.638
STORY10	C6	1.2DLLLEQY	2.5	-3710.71	-38.15	0.816	-94.864
STORY11	C6	1.2DLLLEQY	2.5	-3368.17	-39.67	0.784	-92.093
STORY12	C6	1.2DLLLEQY	2.5	-3027.13	-40.94	0.746	-88.387
STORY13	C6	1.2DLLLEQY	2.5	-2687.35	-41.97	0.7	-83.795
STORY14	C6	1.2DLLLEQY	2.5	-2348.65	-42.8	0.646	-78.365
STORY15	C6	1.2DLLLEQY	2.5	-2010.88	-43.44	0.584	-72.164
STORY16	C6	1.2DLLLEQY	2.5	-1673.91	-43.91	0.512	-65.296
STORY17	C6	1.2DLLLEQY	2.5	-1337.63	-44.23	0.431	-57.929
STORY18	C6	1.2DLLLEQY	2.5	-1002.01	-44.39	0.339	-50.339
STORY19	C6	1.2DLLLEQY	2.5	-666.63	-44.11	0.236	-42.732
STORY20	C6	1.2DLLLEQY	2.5	-334.27	-49.99	0.125	-41.405

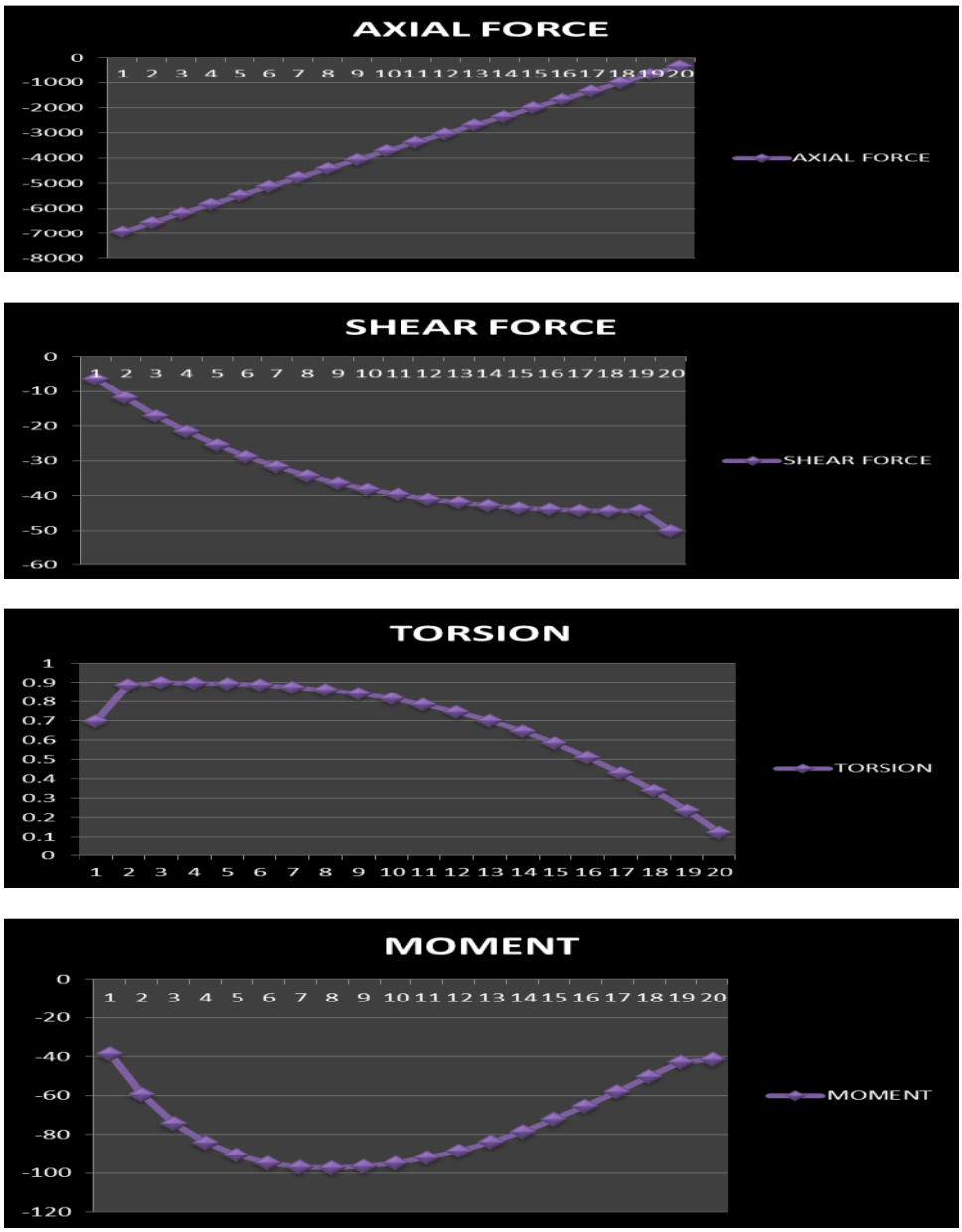

Figure 5: Axial force, Shear Force, Torsion and Moment for columnC6

Table VI: Axial force, Shear Force, Torsion and Moment for columnC1

Story	Column	Load	Loc	AXIAL FORCE	SHEAR FORCE	TORSION	MOMENT
STORY1	C1	1.2DLLLEQX	2.5	-5981.13	36.35	-0.701	5.976
STORY2	C1	1.2DLLLEQX	2.5	-5679.21	36.16	-0.894	12.12
STORY3	C1	1.2DLLLEQX	2.5	-5385.4	44.31	-0.905	17.009
STORY4	C1	1.2DLLLEQX	2.5	-5097.37	48.38	-0.904	21.094
STORY5	C1	1.2DLLLEQX	2.5	-4812.42	50.23	-0.9	24.17
STORY6	C1	1.2DLLLEQX	2.5	-4528.91	50.59	-0.893	26.484
STORY7	C1	1.2DLLLEQX	2.5	-4245.73	49.9	-0.882	28.185
STORY8	C1	1.2DLLLEQX	2.5	-3962.1	48.43	-0.867	29.387
STORY9	C1	1.2DLLLEQX	2.5	-3677.43	46.33	-0.847	30.179
STORY10	C1	1.2DLLLEQX	2.5	-3391.19	43.69	-0.822	30.628
STORY11	C1	1.2DLLLEQX	2.5	-3102.89	40.54	-0.791	30.792
STORY12	C1	1.2DLLLEQX	2.5	-2812	36.89	-0.752	30.72
STORY13	C1	1.2DLLLEQX	2.5	-2517.98	32.73	-0.707	30.461
STORY14	C1	1.2DLLLEQX	2.5	-2220.24	28.08	-0.653	30.064
STORY15	C1	1.2DLLLEQX	2.5	-1918.14	22.94	-0.591	29.584
STORY16	C1	1.2DLLLEQX	2.5	-1611.03	17.37	-0.519	29.095
STORY17	C1	1.2DLLLEQX	2.5	-1298.25	11.49	-0.438	28.65
STORY18	C1	1.2DLLLEQX	2.5	-979.21	5.35	-0.346	28.612
STORY19	C1	1.2DLLLEQX	2.5	-653.62	0.4	-0.243	27.185
STORY20	C1	1.2DLLLEQX	2.5	-320.5	-10.39	-0.132	39.994

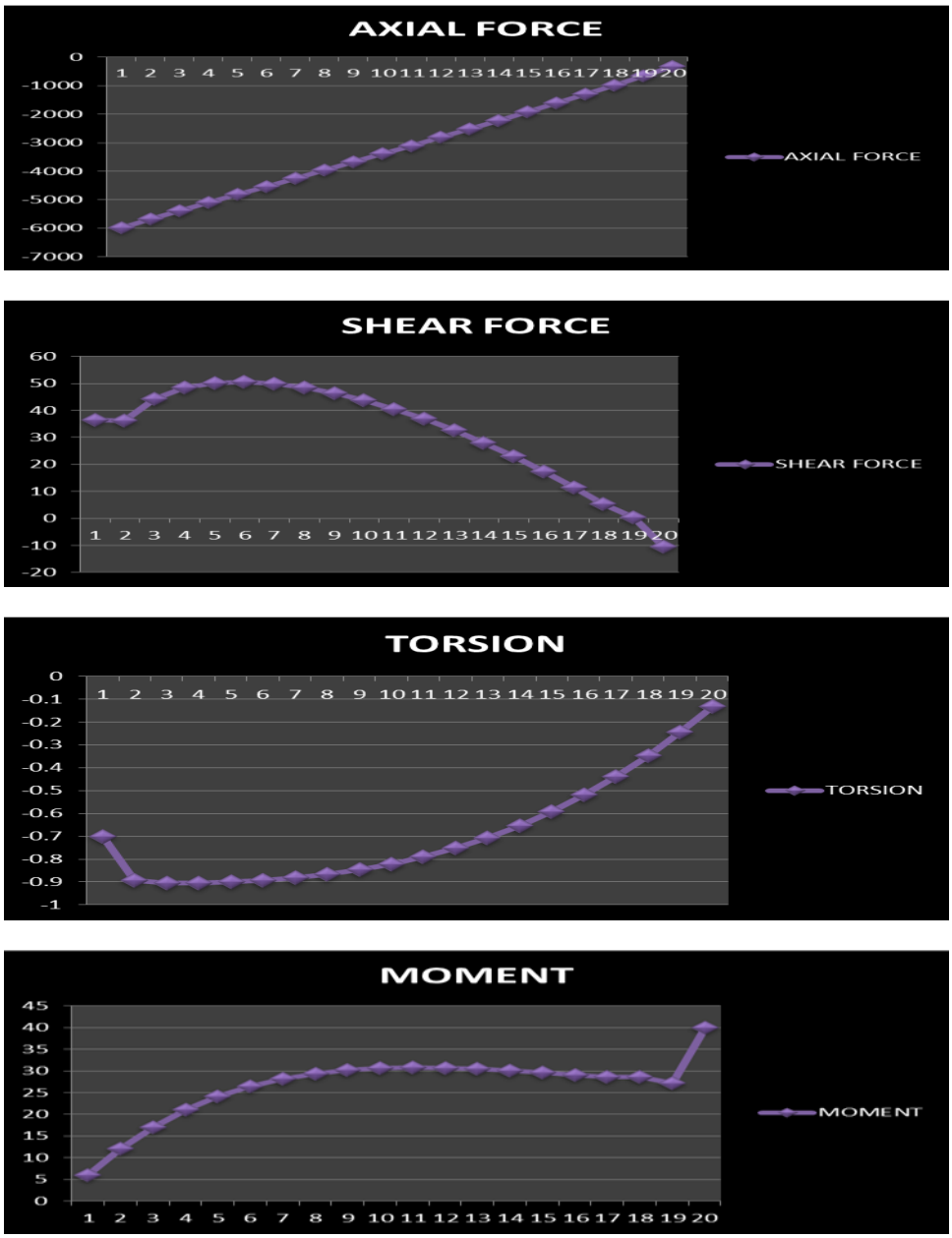

Figure 6:Axial force, Shear Force, Torsion and Moment for columnC1

TableVII:Axial force, Shear Force, Torsion and Moment for columnC2

Story	Column	Load	Loc	AXIAL FORCE	SHEAR FORCE	TORSION	MOMENT
STORY1	C2	1.2DLLLEQX	2.5	-6476.29	48.2	-0.701	-10.762
STORY2	C2	1.2DLLLEQX	2.5	-6096.56	53.97	-0.894	-10.749
STORY3	C2	1.2DLLLEQX	2.5	-5734.07	58.9	-0.905	-8.508
STORY4	C2	1.2DLLLEQX	2.5	-5383.03	60.68	-0.904	-6.505
STORY5	C2	1.2DLLLEQX	2.5	-5041.85	59.93	-0.9	-4.794
STORY6	C2	1.2DLLLEQX	2.5	-4708.64	57.69	-0.893	-3.356
STORY7	C2	1.2DLLLEQX	2.5	-4381.79	54.43	-0.882	-2.15
STORY8	C2	1.2DLLLEQX	2.5	-4059.91	50.47	-0.867	-1.136
STORY9	C2	1.2DLLLEQX	2.5	-3741.81	45.96	-0.847	-0.277
STORY10	C2	1.2DLLLEQX	2.5	-3426.48	40.98	-0.822	0.468
STORY11	C2	1.2DLLLEQX	2.5	-3113.12	35.54	-0.791	1.135
STORY12	C2	1.2DLLLEQX	2.5	-2801.04	29.64	-0.752	1.762
STORY13	C2	1.2DLLLEQX	2.5	-2489.71	23.25	-0.707	2.387
STORY14	C2	1.2DLLLEQX	2.5	-2178.74	16.35	-0.653	3.049
STORY15	C2	1.2DLLLEQX	2.5	-1867.87	8.96	-0.591	3.79
STORY16	C2	1.2DLLLEQX	2.5	-1556.96	1.12	-0.519	4.653
STORY17	C2	1.2DLLLEQX	2.5	-1246.04	-7.07	-0.438	5.686
STORY18	C2	1.2DLLLEQX	2.5	-935.34	-15.36	-0.346	6.918
STORY19	C2	1.2DLLLEQX	2.5	-624.64	-22.99	-0.243	8.398
STORY20	C2	1.2DLLLEQX	2.5	-318.84	-35.86	-0.132	12.237

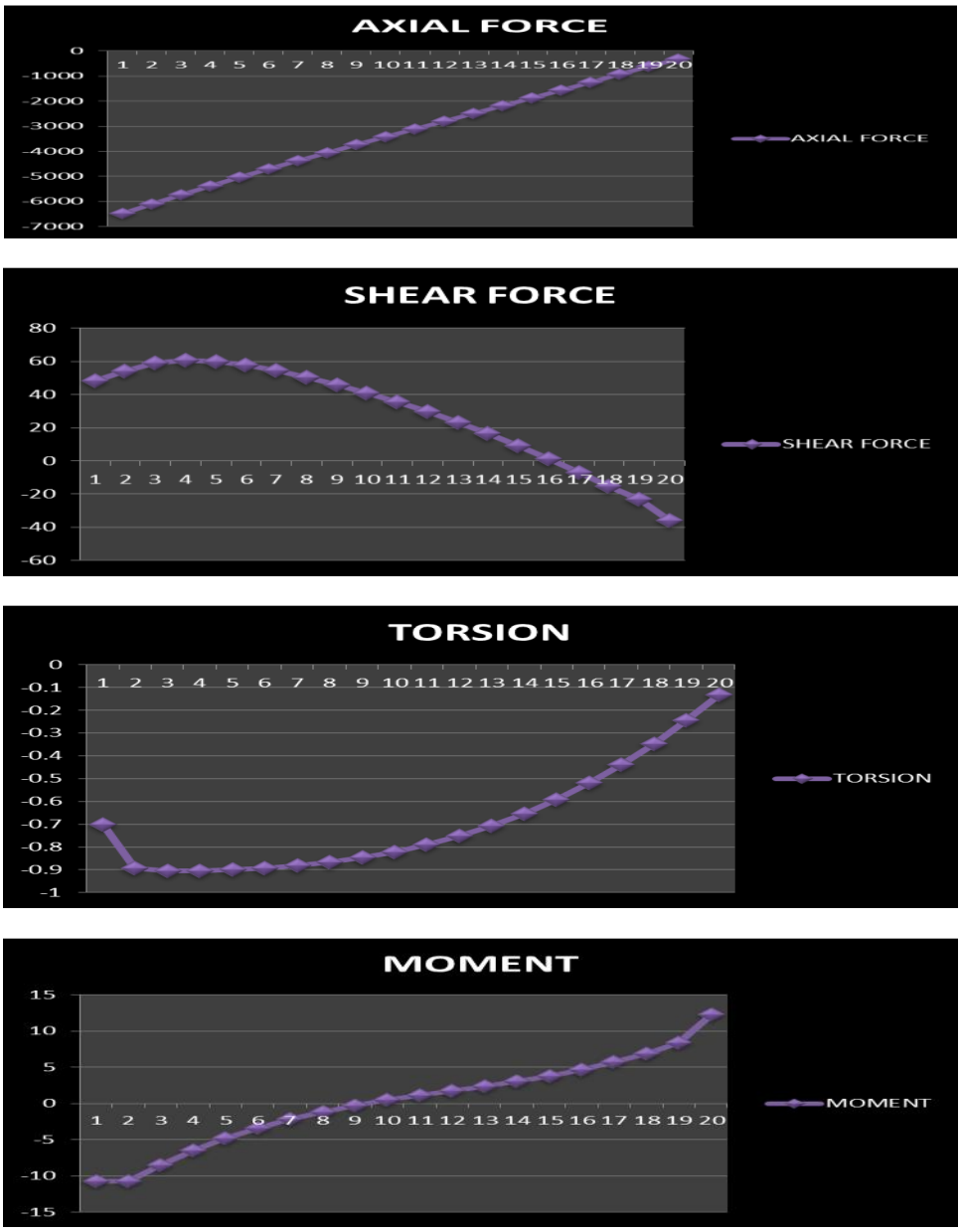

Figure 7: Axial force, Shear Force, Torsion and Moment for columnC2

TableVIII:Axial force, Shear Force, Torsion and Moment for columnC4

Story	Column	Load	Loc	AXIAL FORCE	SHEAR FORCE	TORSION	MOMENT
STORY1	C4	1.2DLLLEQX	2.5	-6562.56	56.71	-0.701	-12.67
STORY2	C4	1.2DLLLEQX	2.5	-6176.39	64.1	-0.894	-15.803
STORY3	C4	1.2DLLLEQX	2.5	-5804.63	69.85	-0.905	-16.353
STORY4	C4	1.2DLLLEQX	2.5	-5443.44	72.38	-0.904	-16.732
STORY5	C4	1.2DLLLEQX	2.5	-5091.64	72.2	-0.9	-17.052
STORY6	C4	1.2DLLLEQX	2.5	-4747.82	70.41	-0.893	-17.31
STORY7	C4	1.2DLLLEQX	2.5	-4410.74	67.5	-0.882	-17.492
STORY8	C4	1.2DLLLEQX	2.5	-4079.29	63.77	-0.867	-17.586
STORY9	C4	1.2DLLLEQX	2.5	-3752.52	59.38	-0.847	-17.58
STORY10	C4	1.2DLLLEQX	2.5	-3429.61	54.4	-0.822	-17.461
STORY11	C4	1.2DLLLEQX	2.5	-3109.85	48.84	-0.791	-17.218
STORY12	C4	1.2DLLLEQX	2.5	-2792.66	42.69	-0.752	-16.837
STORY13	C4	1.2DLLLEQX	2.5	-2477.58	35.93	-0.707	-16.309
STORY14	C4	1.2DLLLEQX	2.5	-2164.21	28.53	-0.653	-15.622
STORY15	C4	1.2DLLLEQX	2.5	-1852.3	20.5	-0.591	-14.763
STORY16	C4	1.2DLLLEQX	2.5	-1541.66	11.88	-0.519	-13.723
STORY17	C4	1.2DLLLEQX	2.5	-1232.19	2.78	-0.438	-12.488
STORY18	C4	1.2DLLLEQX	2.5	-923.95	-6.53	-0.346	-11.066
STORY19	C4	1.2DLLLEQX	2.5	-616.5	-15.33	-0.243	-9.26
STORY20	C4	1.2DLLLEQX	2.5	-313.9	-29.36	-0.132	-8.944

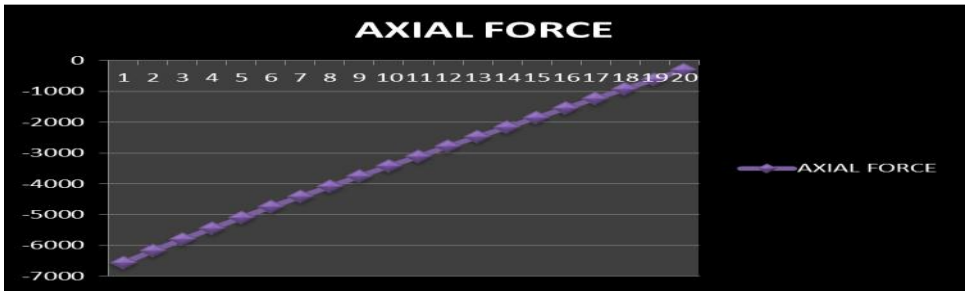

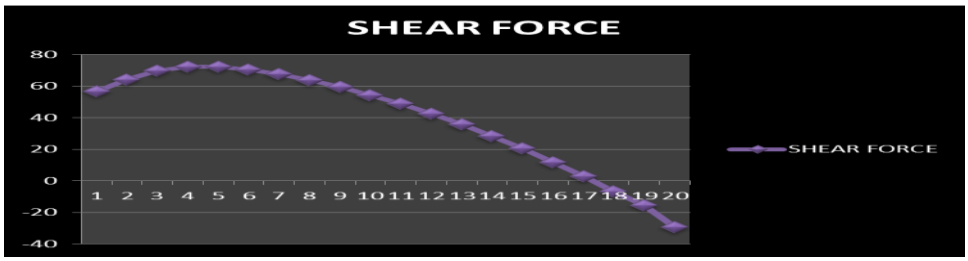

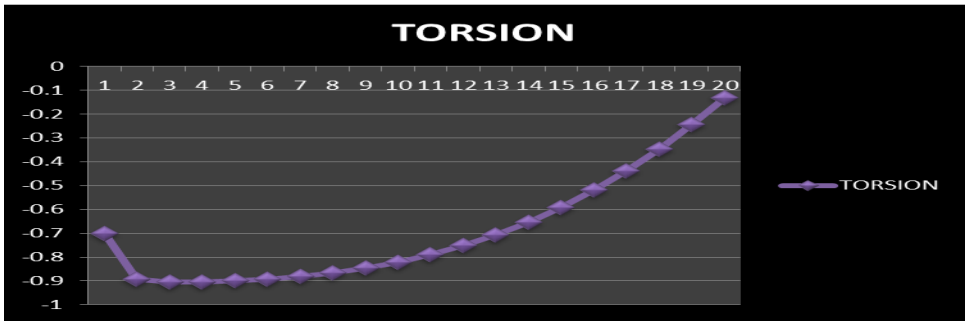

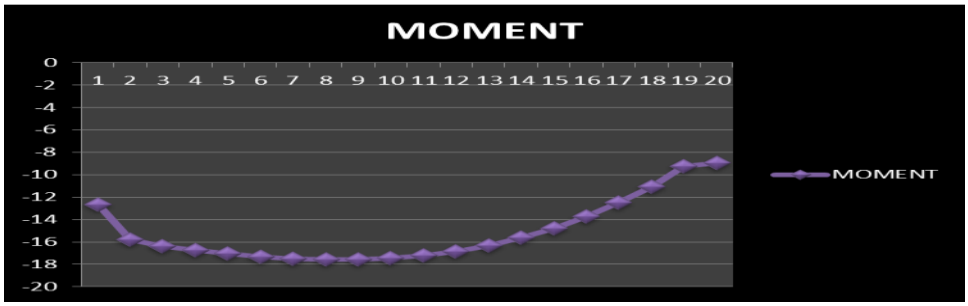

Figure 8: Axial force, Shear Force, Torsion and Moment for columnC4

Table IX:Axial force Shear Force, Torsion and Moment for columnC6

Story	Column	Load	Loc	AXIAL FORCE	SHEAR FORCE	TORSION	MOMENT
STORY1	C6	1.2DLLLEQX	2.5	-6554.88	64.22	-0.701	-12.18
STORY2	C6	1.2DLLLEQX	2.5	-6167.73	71.66	-0.894	-14.702
STORY3	C6	1.2DLLLEQX	2.5	-5795.59	77.13	-0.905	-14.645
STORY4	C6	1.2DLLLEQX	2.5	-5434.36	79.43	-0.904	-14.425
STORY5	C6	1.2DLLLEQX	2.5	-5082.8	79.04	-0.9	-14.159
STORY6	C6	1.2DLLLEQX	2.5	-4739.39	77.04	-0.893	-13.845
STORY7	C6	1.2DLLLEQX	2.5	-4402.86	73.91	-0.882	-13.475
STORY8	C6	1.2DLLLEQX	2.5	-4072.03	69.94	-0.867	-13.039
STORY9	C6	1.2DLLLEQX	2.5	-3745.93	65.3	-0.847	-12.53
STORY10	C6	1.2DLLLEQX	2.5	-3423.7	60.04	-0.822	-11.937
STORY11	C6	1.2DLLLEQX	2.5	-3104.61	54.18	-0.791	-11.253
STORY12	C6	1.2DLLLEQX	2.5	-2788.06	47.68	-0.752	-10.469
STORY13	C6	1.2DLLLEQX	2.5	-2473.57	40.51	-0.707	-9.577
STORY14	C6	1.2DLLLEQX	2.5	-2160.75	32.64	-0.653	-8.566
STORY15	C6	1.2DLLLEQX	2.5	-1849.34	24.08	-0.591	-7.429
STORY16	C6	1.2DLLLEQX	2.5	-1539.16	14.86	-0.519	-6.156
STORY17	C6	1.2DLLLEQX	2.5	-1230.12	5.08	-0.438	-4.74
STORY18	C6	1.2DLLLEQX	2.5	-922.3	-5.02	-0.346	-3.156
STORY19	C6	1.2DLLLEQX	2.5	-615.31	-14.68	-0.243	-1.525
STORY20	C6	1.2DLLLEQX	2.5	-313.27	-29.88	-0.132	1.428

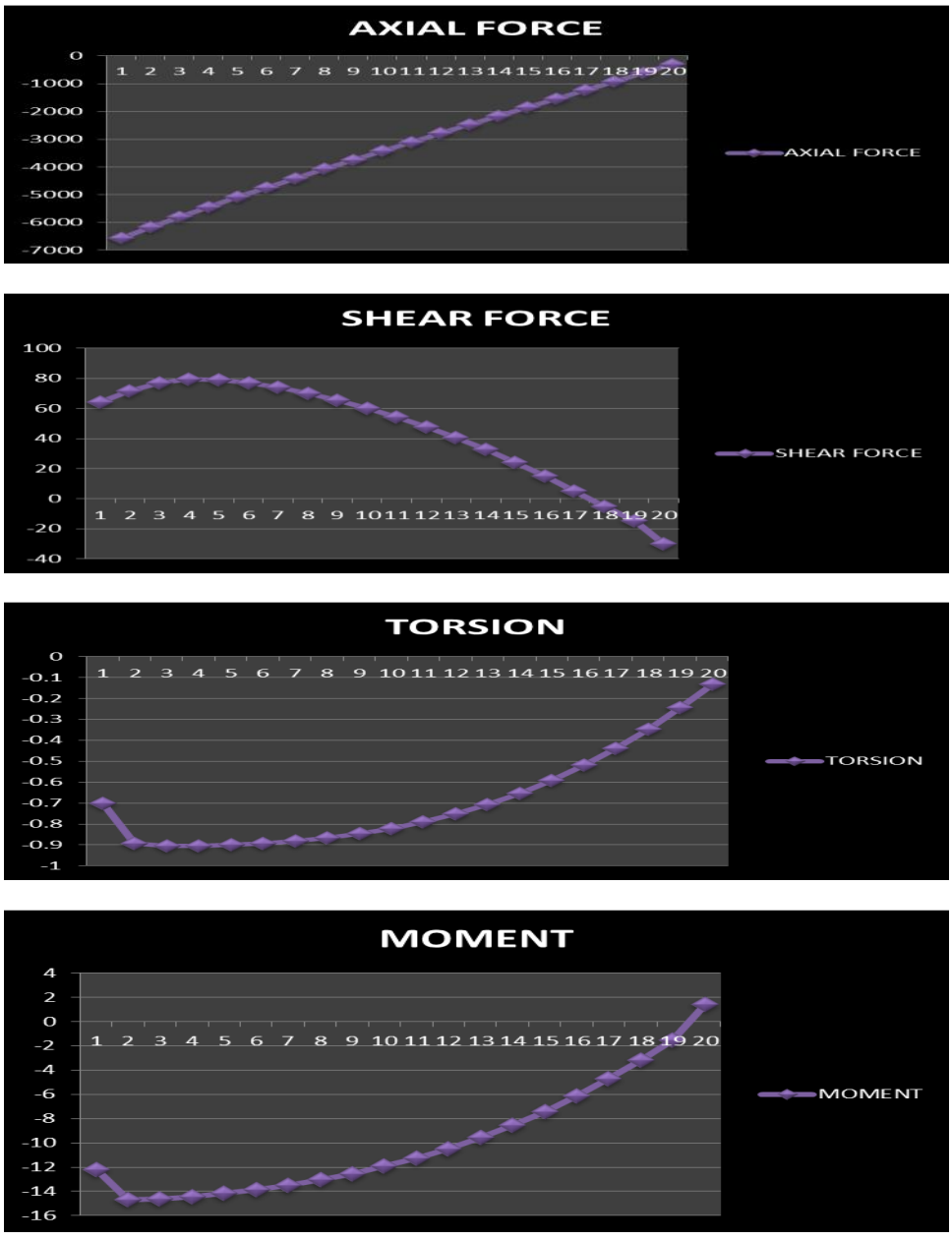

Figure 9: Axial force, Shear Force, Torsion and Moment for columnC6

V. DISCUSSION ON RESULTS

The structural prototype is prepared and lots of data is been collected from the prototype. All the aspects such as safety of structure in shear, moment and in story drift have been collected. So now to check whether to know whether the structure is safe with established shear walls and all construction of core wall in the center we need to compare the graphical values of structure with the shear wall and a simple rigid frame structure.The tallness of a structure is relative and cannot be defined in absolute terms either in relation to height or the number of stories. The council of Tall Buildings and Urban Habitat considers building having 9 or more stories as high-rise structures. But, from a structural engineer's point of view the tall structure or multi-storied building can be defined as one that, by virtue of its height, is affected by lateral forces due to wind or earthquake or both to an extent. Lateral loads can develop high stresses, produce sway movement or cause vibration. Therefore, it is very important for the structure to have sufficient strength against vertical loads together with adequate stiffness to resist lateral forces. So lateral forces due to wind or seismic loading must be considered for tall building design along with gravity forces vertical loads. Tall and slender buildings are strongly wind sensitive and wind forces are applied to the exposed surfaces of the building, whereas seismic forces are inertial (body forces), which result from the distortion of the ground and the inertial resistance of the building. These forces cause horizontal deflection is the predicted movement of a structure under lateral loads . Lateral deflection and drift have three effects on a structure; the movement can affect the structural elements (such as beams and columns); the movements can affect non-structural elements (such as the windows and cladding); and the movements can affect adjacent structures. Without proper consideration during the design process, large deflections and drifts can have adverse effects on structural elements, nonstructural elements, and adjacent structures. When the initial sizes of the frame members have been selected, an approximate check on the horizontal drift of the structures can be made. In this study analysis is done with changing structural parameters to observe the effect on the lateral deflection of the tall building due to earthquake loading. There are three major types of structures were identified in this study, such as rigid frame, coupled shear wall and wall frame structures.

VI. CONCLUSION

[1] Based on the analysis and discussion ,shear wall are very much suitable for resisting earthquake induced lateral forces in multistoried structural systems when compared to multistoried structural systems whit out shear walls. They can be made to behave in a ductile manner by adopting proper detailing techniques.

[2] Shear walls must provide the necessary lateral strength to resist horizontal earthquake forces.
[3] When shear walls are strong enough, they will transfer these horizontal forces to the next element in the load path below them, such as other shear walls, floors, foundation walls, slabs or footings.
[4] Shear walls also provide lateral stiffness to prevent the roof or floor above from excessive side-sway.
[5] When shear walls are stiff enough, they will prevent floor and roof framing members from moving off their supports.
[6] Also, buildings that are sufficiently stiff will usually suffer less nonstructural damage
[7] It is evident from the observing result that the shear wall are making value of torsion very low.
[8] It is evident from the observing result that for combination loads 1.2 DLLLEQX&1.2DLLLEQY ,maximum value of moment at story one and minimum value of shear force also at story one . The Moment is maximum when the shear force is minimum or changes sign.
[9] The vertical reinforcement that is uniformly distributed in the shear wall shall not be less than the horizontal reinforcement .This provision is particularly for squat walls (i.e. Height-to-width ratio is about 1.0).However ,for walls whit height-to-width ratio less than 1.0, a major part of the shear force is resisted by the vertical reinforcement. Hence ,adequate vertical reinforcement should be provided for such walls.

REFRENCES

[1] IS-456-2000-Code of Practice for Plane and Reinforced Concrete .
[2] IS 1893(Part 1)-2002:Eriteria for Earthquake Resistant Design of Structure .
[3] IS:875(Part1)-1987- Code of Practice for Design Load(other than earthquake) for Buildings andStructure –Dead loads
[4] IS:875(Part2)-1987- Code of Practice for Design Load(other than earthquake) for Buildings andStructure –Imposed Load
[5] IS:875(Part2)-1987- Code of Practice for Design Load(other than earthquake) for Buildings andStructure –Wind Load
[6] Mark fintel-Hand Book of Concrete Engineering. Second Edition .CBS Publishers &Distributors-New Delhi,2004
[7] Anil k.Chopra-Dynamics of Structure :Theory and Application to Earthquake Engineering, SecondEdition ,Pearson Education (Singapore) Pvt.Ltd 2005
[8] Mariopaz-Structure Dynamics : Theory and Computations,(Second Edition) , .CBS Publishers&Distributors-New Delhi,2004
[9] Indian Society of Earthquake Technology –Proceedings of the Sixth World Conference EarthquakeEngineering,Vol.1,Published by Sarita Prakashan,Merut,1977.
[10] A.r.chandrasekharan and D.s.prakashrao –a Seismic Design of Multi –Storied RCC Buildings (published in the proceeding ot the 12th symposium on earthquake engineering held iit-roorkee in dec 2002)
[11] Medhekar,m.s,andJain,s,k, Seismic Behavior ,Design and Detailing of RC Shear Wall,part 1:behavior and strength –an icj compilation .
[12]. Kaustubhdasgupta ,C.v.r.murty and Shaileshk.agrawal,Seismic Shear Design of RC Structural Walls

897-971.
[13] Crandell, J., and S. Herrenbruck. 2006.Residential wall bracing principles and design options. Journal of Building Safety. August2006
[14] Mahdi hosseini , Ahmed najim Abdullah alaskari, Prof.N.V.RamanaRao, International Journal of Civil Engineering and Technology (IJCIET), ISSN 0976 –6316(Online), Volume 5, Issue 8, August (2014)
[15] Mahdi hosseini,dr,hadihosseini,ahmadhosseini,American journals of engineering and research ,october 2014

AUTHOR'S PROFILE:

I. Dr.Hadi hosseini , Aerospace Engineering , working in International Earthquake Research Center of America (IERCA)

II. Mahdi hosseini , Master of Technology in Structural Engineering, Dept. of Civil Engineering, Jawaharlal Nehru Technological University Hyderabad (JNTUH), Hyderabad, Telengana , India
Research interest: Structural Engineering ,Structural Dynamics ,Structural Optimization, structural design, Reinforced Concrete Structures, Finite element analysis ,Earthquake Engineering

III.Ahmad hosseini, Graduate Student in Mechanical Engineering, Dept. of Mechanical Engineering,Kakatiya University ,Warangal, Telengana, India
Research interest: solar panels, energy

American Journal of Engineering Research (AJER)
e-ISSN : 2320-0847 p-ISSN : 2320-0936
Volume-03, Issue-11, pp-167-197
www.ajer.org

Research Paper Open Access

Conceptual Design of Solar-micro Hydro Power Plant to Increase Conversion Efficiency for Supporting Remote Tribal Community of Bangladesh

[1.]Anmona Shabnam Pranti , [2.]A M Shahed Iqubal , [3.]A. Z. A. Saifullah

[1] *Faculty, Department of Electrical and Electronics Engineering, IUBAT—International University of Business Agriculture and Technology, Dhaka, Bangladesh*

[2] *Faculty, Department of Mechanical Engineering, IUBAT—International University of Business Agriculture and Technology, Dhaka, Bangladesh*

[3*] *Professor & Chair, Department of Mechanical Engineering, IUBAT—International University of Business Agriculture and Technology, Dhaka, Bangladesh*

ABSTRACT: *Bangladesh is endowed with people along with limited primary energy sources and low electrification rate. Most of the hilly areas are out of the coverage of national grid where tribal people, a significant part of the country, are dwelling. The economic development of the whole country depends upon their advancement which is related to the electrification rate. Available micro hydro potential in hilly region could be a solution for this crisis if modified design is used. This paper deals with a new design of water power potential conversion efficiency increment of a micro hydro power plant to 95% from about 50% by using solar power for heating the water. In this proposed hybrid design, a parabolic reflector is considered to be used after comparative solar intensity analysis on different micro hydro power sites in Bangladesh to increase the velocity as well as the flow rate through penstock by heating the water to increase power production and efficiency. The main purpose of this concept is to supply electricity to more people, especially, remote tribal community by available renewable energy sources for economic development.*

KEYWORDS: *Bangladesh, Tribal Community, Energy Crisis, Renewable Energy, Solar Hybrid Micro Hydro Power Plant*

I. INTRODUCTION

The national security of a country depends on energy reserve and economic growth is determined by the amount of use of electricity which increases the GDP rate. In this era of modernization and globalization, everyday electricity is needed to run necessary and luxurious commodities like refrigerator, air-conditioner, television, and computer for social, educational and technological growth as well as to be connected to the outer world through internet. Energy security has become a burning question for Bangladesh, a South Asian developing country with limited energy resources compared to recent population and industrialization growth. The average electrification rate is very low. Most of the people using electricity live in urban areas and facing massive load shading. The energy policy must facilitate energy access to all Bangladesh citizens with necessary improvements [1]. The government has to encourage the Rural Electrification Board (REB) and its network of rural cooperatives (Palli Biddyut Samitee – PBS) to create small-scale generating capacity whose power would be distributed on a priority basis independently of the national grid to customers in the local participating PBS [1, 2]. To fight with the current situation electricity generation from renewable sources is inevitable to support remote areas. Thus another recommendation for the REB is to explore the potential of getting financing for renewable energy projects from firms investing carbon emission offsets [2]. Small scale hydroelectric power plant has eliminated electricity scarcity problem in developing countries like Nepal, Sri Lanka and Brazil. However, Bangladesh has some suitable sites for micro range hydro electricity production but the proven potential is not significant to support vast community. On the other hand huge amount solar energy can be tracked because of suitable geographical location. The main objective of this study is to focus on the possible increase of electricity production from the available limited hydro potential by a fusion of hydro and solar potential for social and economic development of the deprived tribal community of Bangladesh.

II. GEOGRAPHIC AND SOCIOECONOMIC ARCHITECTURE OF REMOTE TRIBAL AREAS OF BANGLADESH

Bangladesh is on the tropic of cancer with warm weather [3]. It has been blessed by vast population of about 160 million [106] with a growth rate of 1.19% [107] in a limited land of 147,570 km^2 [3]. More than half (80%) of the people reside in a limited modern facility rural areas[94, 4, 5] and a significant part of minority and tribal community lives in hilly regions, an inevitable part for determining national economic prosperity which depends on daily electricity use[4]. In Bangladesh, per capita electricity consumption is 136 kwh/year which is one among the countries having lowest energy consumption in the world [6]. Different tribal people live in Mymensingh, Sylhet, Rajshahi , Bandorban, Khagrachori, Rangamati and Chittagong district [7] like 50,000 Manipuri, Khasia and Tripura in Moulvi Bazar [8], 2, 88,077 ethnic minorities (Chakma, Marma, Tanchangya, Tripura, Pankua, Lushai & Khiang) in Rangamati [9], 524,961 mostly Chakma and Tripura in Mong Circle Khagrachori [10, 11] and 12 ethnic groups 125,000 Chakma, 66,000 Marma, 37,000 Tippera, 16,000 Mru, 8,000 Tanchangya, 2,000 Chaks, 2,000 Kumis, 2,000 Kuki/Lushais, 2,000 Khyang, 2,000 Pankho, 2,000 Bangoji and 2,000 Mrung in Chitrtagong[12]. Most of the tribal people, 778,425 among 897828, live in rural areas with limited facilities and electricity supply [7].Table 1 show the respective literacy rate of that district where mostly the tribal people live. From Table 1, it is clear that the literacy rate of each district is below that of the national and capital (Dhaka) 57.91% [19] and 96.9% [18] respectively. The difference of urban and rural literacy rate is 14.02% (65.83% and 51.81% respectively) [20]. Education is the most important key of economic development and electrification is one of the preconditions of educational enhancement in remote areas.

93% power of Bangladesh is produced by Coal, oil and gas [21], where the reserve are 3.3 Billion tons [23], 5,724 bbl/day [24] and 20 TCF [22] respectively and is used in industry like cement, fertilizer or for running vehicles [25]. Only 7% is hydro power in the electrical power mix [99] to support electrification to 52% people [26], 6066MW electricity is necessary, and current generation capacity, 4162 MW [21], is not enough for all people getting supply of electricity. Primary energy purchase from abroad for conventional power generation in near future after finishing the reserve will not be economical while we are already importing 90% of our oil [31, 28]. So it is quite unrealistic to think about new electrification unless introducing renewable power production.

III. METHODOLOGY AND ESTIMATION

3.1. Different power production procedures respective to Bangladesh: Total installed capacity (according to BPDB) is 6693 MW of which 250 MW coal based, 1127 MW oil and 5086 MW gas based and 230 MW Hydro power plant [29]. Though conventional power generation will stop before 2020 for gas reserve deduction, the prime source of thermal power [31], renewable power production is not convenient yet where technologically improved renewable energy plant is important for sustainability [31]. Bangladesh is very close to the equatorial line (24 North). Solar energy falls almost perpendicularly and day lengths difference of winter and summer is less. Therefore, it is a suitable place for tracking solar energy [30]. However, roof top solar cell is not admirable because of the low conversion efficiency, 30% theoretically and 10-15% practically [32]. Diesel engine plant has low installation cost but its operational (fuel) cost is high [33]. In Bangladesh wind power production is not possible because of low wind profile [31], approximately 6.5m/s [32]. Nuclear power needs high technological support [32]. Hilly region micro hydro site in Bangladesh can be the best option for decentralized power supply as low cost scheme, which has been shown in Peru through experiment [33, 31]. But it is not considered because of low available potential and efficiency.

3.2. Fusion of solar and hydro power for electrifying rural off grid Bangladesh: Electricity is produced by using stored potential and kinetic energy in micro hydro power plant [34] and the Greeks learned the procedure first [34]. Hydro power is the dominating factor in the national energy mix in many developing countries. Now-a-days small hydro power is used for removing power deficiency problem in Nepal, India, China, Peru and a country like USA [34]. This plant, capacity =<100 KW [28, 34, 95, 35], uses run off river system suitable for hilly areas where small rivers run with high current [34, 28]. The total installation capacity of small range hydro power in our neighbor country India is 12,841.81 MW [37], in Nepal is 14.6 MW [38] and in Sri Lanka is 181 MW [39]. However the total estimated small scale hydro power potential by BPDB and BWDB in Bangladesh is only 1.129 MW [31] which is the lowest in South Asian countries. The amount of power production from a micro hydro power plant depends on the stream power [95]. Though 1 m/s current velocity has an energy density of 500 W/m^2, very little amount of this can be converted into electricity [40, 41]. Generally the efficiency of this type of power plant is considered as much as 55% [109]. The conversion efficiency depends upon various factors among which velocity of the falling water is the most important. Hydro power production process is the oldest process of harnessing energy which can be

improved by the development of technology and its contribution can be significant to supply electricity to people of remote off grid area. Full utilization of water power through micro hydro power plant by using improved technologies can be a smart solution to provide electrical power to the remote hilly region. The geographical location of our county is suitable for tracking solar energy. We can utilize the huge amount of incident sun power to increase the conversion efficiency of a micro hydro power plant situated in our country. A hybrid system can be made with the water potential available in the hilly region of our country along with solar power to support more people who are still in dark. As we cannot increase the total available potential of our country, so it is the only way to construct more efficient micro hydro power plant than the existing one so that the impact of low available potential can be relaxed by generating more power by the same stream available in our country.

3.3. Main Concept for the hybrid plant: Financial, technical, organizational and social intermediation is needed to design a successful plant among which technical intermediation is our prime concern. A study on Nepali power plant has pointed out that 30% of installed power plant remain ineffective due to poor hydrology estimation and inefficient design of channel (penstock) through which water is conveyed to the turbine [33, 34].

The power production from water entirely depends upon the flow rate (Q) of the water and the head of the water (H) and is proportional to the flow rate for constant head and constant conversion efficiency of the turbine [42, 34]. The theoretical power depends upon flow rate and head of water which is the vertical distance between the water entering points from intank to water leaving point of penstock to the turbine which depends upon the characteristics of the pipeline [34, 42, 43, 68].

Theoretical power (P) = Flow rate (Q in m^3/s) × Head (H in m) × Gravity (g in m/s^2)

$$P= (9.81\times Q\times H)\ KW$$

At the time of energy conversion, some energy is lost due to work done [28]. The flow rate is the product of the cross sectional area (A) of penstock and the velocity of the fluid (V) [34, 44].

$$Q=A\times V$$

So, water velocity is an important factor in order to increase the electrical power production.

Viscosity is a property of a liquid which controls the flow rate by the cohesion between liquid particles [114]. For constant diameter of penstock, the flow rate of water through the pipe depends on the velocity as well as the viscosity of the water [96]. In case of liquids, viscosity and temperature and viscosity and velocity have inverse relationship [45, 46, 54].

Temperature $\propto$ 1/resistance to flow

Considering laminar flow through penstock, the Hagen-Poiseuille law of viscous flow can be expressed as below [114].

$$P_1-P_2= (32\times\mu\times V\times L)/D^2$$

where,

L= penstock length

D= penstock internal diameter

V= Velocity of water in pipe

μ= water Dynamic viscosity

P_1-P_2= pressure loss through the pipe.

The pressure drop will decrease rather than increase with the decrement of the viscosity of the water which is more advantageous for enhancing the power production as net head H= available head - pressure drop. As pressure has no effect on viscosity [46], so dynamic viscosity and velocity has an inverse relationship when pressure drop is considered constant for a specific pipe. With the increment of temperature, the viscosity of water will decrease as well as the velocity and flow rate will increase which will causes more power production from the same available potential.

A parabolic concave mirror has the capability to converge all incident parallel rays to the focal point (F) and very high temperature can be achieved which may cause fire [110]. This high temperature can be utilized in micro hydro power plant to increase the flow rate of the flowing water. Because of geographical location every year we have at least 300 sunny days [101].

POTENTIAL OF MICRO HYDRO POWER IN BANGLADESH: Around 232 rivers flow through Bangladesh [31]. It is quite easy to find out suitable run off river micro hydro power plant site in our country. Moreover, 12% hilly area of Bangladesh [97] has stream flow which can be used for electricity production for supplying to the leg behind tribal community. The first micro hydro power plant installed in Bamerchara, Chittagong (10 MW) [31] was

a demo power plant to test the feasibility of micro hydro power in Bangladesh to provide electricity to 140 families in the village and to a Buddhist Temple [98]. One 20 KW micro hydro power plant has been installed at Barkal, Rangamati [98] and two are possible to install at Madhobkundo (10-20 KW) in Moulovi Bazar and Sailipropat (5-10 KW) in Bandarban respectively [31]. Some experts pointed out in 1981 according to IECO Master Plan that 11, 56,320 KWh of energy could be generated in Chittagong-Bandarban area, 63,06,041 KWh in Mymensingh-Sherpur area and18,70752 KWh in the greater Dinajpur-Rangpur area annually. Their identified sites are Foy's Lake at Pahartali, Choto Kumira in Chittagong, Sealock in Bandarban, Nikhari Chara and Madhabchar at Baralekhamin Moulavibazar, Ranga Poni Gung at Jaintiapur in Sylhet, Bhugai Kangsha and Marisi in Sherpur, Punarbhaba and Talma in Thakurgaon and Pathraj in Dinajpur [48]. Through another survey of Bangladesh Water Development Board (BWDB) and Bangladesh Power Development Board (BPDB) in 1981, the potential of micro hydro power was identified in 12 places of our country, 1.1 GWh in Chittagong-Bandarban area, 6.3 GWh in Sylhet-Moulovi Bazar area, 8.6 MWh in Mymensingh-Sherpur area and 1.8 GWh in Dinajpur-Rangpur area [49]. Another study has been done by LGED-Local Government Engineering Department of Bangladesh on three hilly districts [31].Table 2 shows the site from the result of BPDB and BWDB joint survey in 1981[98] and the potential site of LGED survey [31].There are some other micro hydro sites in Chittagong. One is Choto Kumira Canal (power potential 19.19 KW) and another is Mahamaya Chora, (power potential 4.95 KW) [4]. Moreover, micro hydro power can be generated at Sangu and Matamuhuri River identified by BPDB [98].Table 3 shows some potential micro hydro power sites, their flow rate, available head and possible electricity production on which the calculation has been done.

INCIDENT SOLAR ENERGY ON DIFFERENT MICRO HYDRO POWER SITES OF BANGLADESH

The amount of solar electromagnetic flux incident on earth surface per unit area perpendicular to the rays is solar constant [50]. The geographical location of Bangladesh (23.50 North latitude), nearest to equatorial line, has made it a suitable place for tracking huge amount of solar energy falling almost perpendicularly throughout the year as the difference between winter and summer season's day length is smaller than most other countries of the world. Bangladesh has also appropriate climatic condition as we get almost 300 sunny days in a year [101]. The average incident solar power in our neighbor country India is about 4.5 KWh/m^2 which is equivalent to 5 trillion KWh/yr [100]. The estimated value of solar constant in early January is about 1.412 KW/m² and in early July is 1.321 KW/m² after absorbing 6.9% by the atmosphere [50]. Average value of solar constant is about 137 MW/cm^2 [51]. Only a small part of this power can be concentrated by a reflector which has the capability to damage our eyes [52]. The intensity of the reflected rays is the highest at the focal point of a curved mirror. It is possible to achieve up to 3,500 °C temperature by concentrating solar energy with special and expensive instrument. And, 700°C can be achieved by low cost ordinary equipment which is being used in India [53]. Solar constant on the earth entirely depends up on the latitude of the specific place. Incident solar energy per square centimeter is calculated by the equation [51]

E = (MW/cm^2) x (Area in cm^2) x (Time in sec) MJ

The total amount of energy incident on the solar collector is 5.9 x 10^6 MJ/cm^2 in 12 hr duration [51]. The sun does not remain constant directly overhead on any particular place throughout the year and the declination can be calculated by the formula [54]

Declination $\Theta = 23.5° \sin((T / 365.25) * 360°)$

where,

T= number of days counted from the vernal equinox (March 21), Θ=0º at equator [51, 55].

The declination varies from 23.5° north latitude on June 21 to 23.5° south latitude on December 21 [54].

The declination on 1st April of the year $\Theta = 23.5 \text{ Sin } \{360(10/365.25)\} = 4.023º$

Table 4 indicates the solar declination on the 1st day of each month of the year in Bangladesh after the calculation. The latitude of a particular place is also a determinant of solar declination and intensity of a particular place. Rangamati is a southeastern Hill District at 23^0 44´ north latitudes [9] and other two districts Khagrachori and Bandarbon of Chittagong hill track are at 23.166667 North [56, 57] and 22 North [58] latitude respectively where most of the micro- hydro power sites are situated. Some other micro- hydro power plant potential is also in Sylhet, Chittagong and Moulvi Bazar district which are at 24° 53' North [59], 22° 20' North [60], 24.35º north [8] latitude respectively.

The solar constant for a particular day for a particular place can be calculated by [51, 61]

σ_D = (137mW/cm^2) cos (L(site latitude) - Θ)

The solar constant of Bandarban on 1st May is σ_D = (137MW/cm^2) cos(22 -14.924)º=135.957613 MW/cm^2.

Though actual day Length (sunset to sunrise) differs from day to day. In Bangladesh we get sun energy almost eight hours a day throughout the year with a little variation [102]. Actual day length is calculated by the equation [51]

$T_D = (24/\pi)\ Cos^{-1}\{(-\tan \Theta)\ (\tan L)\}$ hour

where

Θ= solar declination

L= observer's latitude

Time from sunset to sun rise at Khagrachori on 1st May

$T_D = (24/\pi)\ \cos^{-1}\{(-\tan 14.924)(\tan 23.167)\} = 12.54893$ hours

The amount of energy collected by collector/unit area is dependent on time duration between sunrise and sunset [62]

$E = \sigma_D\ (3{,}600\ T_D\ /\pi)$ MJ

The amount of energy per unit area at Rangamati on 1st April

$E = \{128.983875\ (3{,}600 \times 12.04385\ /\pi)\}$ MJ

$= 1781040$ MJ $= 1.7\times10^6$ KJ

The calculated value of solar intensity, day hours and energy captured on earth surface of different districts of micro- hydro power site in Bangladesh and Kramer Junction, California for the first day of each month of the year is given in Table 5.

Figure 1 shows comparative solar intensity curve of different districts of micro- hydro power site in Bangladesh and Kramer Junction, California. From figure 1, it is clear that the variation of solar intensity on different sites of micro-hydro power plant in Bangladesh is almost constant throughout the year and in every month it is higher than that of Kramer Junction, California, USA, latitude 34.992 North [63], where a 33 MW Solar Thermal Power Plant is situated and sun energy is used to raise the temperature of liquid flowing through a pipe in order to produce electricity [64]. We should best use of this huge amount of energy, the gift of nature, for electricity production to lessen the current scarcity in Bangladesh.

IV. CONCEPTUAL DESIGN OF PROPOSED POWER PLANT

Large or small amount of electricity can be produced by utilizing the potential energy of water by creating dam or using run off river water. Figure 2 shows classification hydroelectric power plants [42]. According to other conception, large scale hydro power is considered up to 100 MW, small scale is up to 5 MW and micro hydro power is up to 100 KW [65, 66]. The ranges of hydro power plant higher than 30 MW is large, small hydro is 30 MW-2 MW, mini hydro is 2 MW-100 KW, micro hydro is 100 KW-10 KW and Pico hydro is less than 10 KW [67]. According to another information 10 KW-200 KW capacity plant is also called micro hydro power plant [33]. No dam is necessary in micro hydro power scheme (run off river) [68, 69]. Some civil works are needed - like wire and channel for diverting water in to in tank, penstock for conveying water to the turbine, tail race to divert used water from turbine, power house for housing turbine coupled with generator, small control and transmission system, inverters for electrical power control and a battery for storing power for using at pick hours [42, 34, 43]. Figure 3 and 4 shows the conventional micro hydro power plant design and the conventional micro hydro power plant with penstock view respectively. Figure 5 shows penstock and reflector design in proposed system. As found in Table 3, most of the micro hydro power site in Bangladesh have net available head of not more than 10 m.The smooth internal surface pipe is to be used as penstock because when friction loss is only 1/3 (gross head),we can get maximum power output. Maximum 10-15% loss is acceptable for better design [27, 114].

As penstock has to bear weight and pressure of water, for low pressure PVC pipe(range upto160-350 psi) and for higher pressure Galvanized steel, welded steel pipe**,** high density polyethylene pipe are used after considering power loss and economic tradeoff [27, 43**,** 70]. A metal tube (steel) is considered to be used in this system as an inner case because conductivity is higher, and the tube should pass through the focal line of the reflector. The outer periphery of the penstock tube should be built with general glossy glass to reduce the heat loss [71]. Special solar-selective coating will prevent oxidation and heat radiation loss [72, 71]. The average length of penstock has been considered as 50 m which is the practical length of one micro hydro power plant in our country and 300 mm diameter has been considered which is generally used in 4-11 m head micro hydro power plant [27]. For high head plant Pelton wheel, for low head plat Francis turbine, for medium head plant multi-jet Pelton turbine, for small scale low head plant cross flow impulse turbine and for micro hydro power plant cross flow Pelton turbine is used [43, 73, 42]. However, cross flow turbine and synchronous generator is suitable for off grid micro hydro power plant sites in Bangladesh

[49, 31]. Though According to the Fermat's principle, sun rays always travel minimum path, up to 80%, not all rays, can be concentrated to the focal point by large curve mirror (spherical and cylindrical) because of spherical aberration [75, 103, 72, 52] and only 200°C temperature can be earned by burning glasses [72]. A parabolic reflector, used in Newtonian telescopes and to collect energy from distant source, has the capacity to concentrate all parallel sun light closer to the reflector and to achieve high temperature by concentrating as incident and reflection angle of inner surface is same [74, 52, 75, 72]. One axis tracking system of parabolic reflector consisting of curved mirrors, 182.88 m^2 area and 50 m in length has been considered in our design.

V. CALCULATION OF EFFICIENCY INCREMENT

100% theoretical power which depends upon head and volume of water flow cannot be harnessed. Minimum 5 m head and 1 litre/second flow rate are needed to produce electrical power [76]. The low head low speed micro hydro power plant turbines and generators are less efficient and according to different information turbine efficiency is 80% [42] or 95% [43], generator efficiency is 95%[43], turbine generator sets efficiency is 40-80% [77] and transmission efficiency is 98% [43]. The overall efficiency remains almost 55%. For system beyond 10 KW efficiency is 60-70% [28], for mini hydro efficiency is 75-85% [65] and for micro hydro efficiency is 60-80% or 65-75% [65]. The general efficiency of a micro hydro power plant considered according to different information is 79% [43] or 55% [109] or 53% [34] or 50% [42, 77, 28, 65, 49, 78]. Based on all information, overall efficiency of 50% is taken for calculating output power in Bangladesh:

Potential available $P=9.81\times Q(m^3/s)\times H(m)$ KW

Electrical power can be generated $P_e=0.5\times 9.81\times Q(m^3/s)\times H(m)$ KW [78]

Table 6 shows flow rate, available head, potential available and electrical power output in different micro hydro power site in Bangladesh selected for calculation.

Kramer Junction, California, USA, Solar thermal power plant (33 MW) is at 35.019804756678 º North Latitude [64] where average solar intensity is 97.32827505 MW/cm^2[calculated] and uses 836.1236 m^2 (20×450 $feet^2$)[79] parabolic trough reflector to achieve 700° F temperature by synthetic oil flowing through the receiver tube [79].

The respective temperature could be produced by 836.1236 m^2 solar parabolic reflector of that kind for a specific place is

$T_1=\{(\sigma_D\times 700)/97.32827505\}^oF$

$=\{(5/9)[\{(\sigma_D\times 700)/ 97.32827505\}-32]\}^oC$ [80]

In this design the area of reflector is considered=182.88 m^2.

Temperature could be raised $T_2= \{T_1*(182.88/836.12736)\}^oC$ in Synthetic Oil heat exchanger in a particular place.

Temperature rise in water can be calculated by the formula [11]

$S_o / S_w = (m_w\times\Delta T_w)/(m_o\times\Delta T_o)$--------(1)

Mass of oil and water are m_o and m_w respectively. Temperature difference in oil is ΔT_o and water is ΔT_w.

Specific heat of liquid water is S_w= 4.1796 kJ/kg ºC [83] and that of Synthetic Oil is S_o=2.341 kJ/kg ºC[84].

And, $m_w=(d_w /d_o)\times m_o=1.125\times m_o$ kg [85],

Where, density of water is d_w = 997.0479 kg/m3 [86] and density of synthetic oil is d_o = 886.2 kg/m3 at 0ºC [87].So,

Temperature rise in water= $\Delta T_w = 0.4978\times\Delta To$---------- (2),

Table7 shows dynamic viscosity for different temperature obtained by the solar concentrator for micro hydro power plant.

According to Hagen-Poiseuille law [114],

$P_1-P_2 = 32\times\mu \times V \times L / D$

Where

P_1-P_2 = Pressure drop

μ = Dynamic viscosity

V = Water velocity

L = Pipe length and

D = Pipe diameter

$V=\{(P_1- P_2)\times 0.3\times 10^6\}/(32\times\mu\times 50)$

As steel pipe, welded new, unpickled, with roughness factor of 0.03mm has been chosen for the design, constant pressure loss is considered for the calculation. Cross sectional area of the pipe is $A = \pi r^2$ = 0.070685834 m^2, where D = 300mm [44] and flow rate through penstock

Q =A×V [44]

=0.070685834×V m^3/s

Available water potential is P_1=9.81×Q (Litre/second)/1000)×H(meter) KW

and possible electrical power production is P_2= 0.5×9.81×Q (Litre/second)/1000)×H(meter) KW.

Table 8 shows all the calculated comparative data of velocity, flow rate, power production and conversion efficiency in proposed system and conventional current system. At 25ºC Dynamic viscosity 891×10^-6 μ Ns/m^2 is considered [111]. The respective current velocity of water is calculated in ft/s by software "Pressure Drop Online-Calculator for Mobile and PDA" downloaded from internet and converted in m/s. [88]
X= power output in proposed system and Y=efficiency of water energy conversion.

VI. DISCUSSION

Advantages and social impact of this hybrid power plant in Bangladesh need to be paid attention very carefully. Current available energy service is not sufficient for supporting the need for the poor, found in a study of UN, was the Millennium Development Goals of 'The UN-Energy Paper'[105] and it has become a great challenge for the government and general people of Bangladesh to supply electricity to all people within 2021. Because, reliable and affordable energy supply to the poor population is the precondition of sustainable development. Almost 1.6 billion people of the world is out of electricity [105]. Although lack of electricity supply slows down local economic development, youth opportunities and enhances social crimes and problems, the electrification rate of the rural areas of many developing countries are not more than 10% [112]. The scenario is quite worst in Bangladesh. Overall 52% [26], in Urban Areas 80% [89] and in rural areas only 25%[90] people are connected with national grid but are continuously facing massive load shading.

Generally the demand of an off grid village is very low (5 KW-50 KW) [113], less than the loss in transformer [91]. It is quite uneconomic to construct new transmission line in hilly tribal areas for too small load which needs 0.875 USD for 1KWh energy transmission [91]. Moreover, significant amount of power is lost on the way as transmission loss. Besides, distribution loss of Bangladesh is 26% [26].People are now looking for modern, decentralized and environment friendly renewable energy scheme like Micro hydro power plant [28] which is economical [31], non-polluting, does not emit CO_2 and destroy ecology like large hydro plant [92, 104, 28]. Power production remains almost constant unlike solar cell and wind power [31]. 20% world energy will come from renewable sources by 2020 [36]. European Union is producing 13% electricity from Hydro electric power plant to reduce 67 million tons CO2 emission/year [92] according the target, of a seminar at Kyoto, of reducing green house effect by 8% in Europe and 5% in other industrial countries [92]. Though the installation cost of micro hydro power plant is very high, in Sri Lanka and Nepal it is 2762.5(21.2% civil cost) and 1587.5(43.8% civil cost) USD/KW respectively and in general 3085 USD/KW [33], compared with other plant of same capacity like diesel plant [28]. It is useful for developing countries because of low maintenance or running cost [33, 34, 31] as least investment [91] and no fuel purchasing is needed and power production cost is almost USD 0.018/KWh compared with 0.6/KWh grid power [91]. However economic success depends upon the objective as the scheme is usually used to supply electricity to rural, remote and off grid community. Effect of high installation cost can be neutralized by meeting the demand of more people (tribal community) by setting more efficient proposed design for long term by using only extra parabolic reflector and free fuel (sunlight and water).The efficiency of micro hydro power plant in our country is considered as 50%. But by using this hybrid power plant 95% available hydro potential can be converted to electricity As our main concern is to supply electricity to more people by our existing resource, a trade-off between efficiency and investment cost should considered.

Micro hydro power plants are being used for poverty reduction and economic and social development in rural areas of Nepal by achieving 80% secondary school success [92], Sri Lanka, Pakistan, Peru, Zimbabwe [33], and China where there are more than 85000 small scale micro hydro power plants [42]. In China, one village per capita income and electrification rate changes from 19 to 115 USD and 60% to 99% respectively because of a micro hydro power plant [91]. Academic performances of rural children, who need to compete with technologically advance urban children at tertiary level to maintain development harmony, depend upon the use of electricity as they cannot access services like internet, cable TV and mobile phones which are used to communicate them with the outer world. Without electricity, it is not possible to run evening adult education centre in rural hilly areas for agricultural villagers to change their life style and socio-economic condition which has been done in a village of Nepal to raise the literacy rate from 30% by introducing a micro hydro power plant [92]. CO2 emission can be reduced and village children time spent in collecting fire wood for cooking can be saved for studying by the use electricity [92]. Not only the advanced livelihood but also small enterprise is necessary to develop socio economic condition of a remote community and a micro hydro power plant can be a smart solution. Though Bangladesh has limited potential of micro hydro power, it is possible to accelerate economic growth in remote areas by the best use of it to obtain economic sustainability.

VII. CONCLUSION

Energy plays a vital role in human development and electricity is the most usable form of energy. A great portion of household's expenditure is on energy and per day 1 to 4 hours of a woman, in collection fire woods, is spent for energy [93]. So for reducing dependency on CO_2 creating fossil fuel, increasing electrification rate in remote hilly regions, a significant part of our country and achieving energy security for the county, alternative sources of renewable energy is necessary. We cannot think our national prosperity without social and economic growth of the unprivileged poor community of the remote hilly areas. In 30 years, micro hydro power plant has not got importance and financial assistance from the government [33], though natural water fall of hilly areas could be an added advantage [31] and in some circumstances it can be beneficial for rural people with improved design. To implement a successful plant although the cost is strongly site specific, the cost can be minimized by local advanced design. It is needed to consider many tasks. The tasks include not only the arrangement of sufficient finance but also the intermediation of current technology. But the potential is not significant. On the other hand, the solar power alone cannot be the solution for supplying electricity to these people as the efficiency is very low. That is why it could be the best way to built a hybrid power plant by using solar and micro hydro power potential in rural off grid hilly areas in order to obtain a sustainable development for the country. Micro hydro power plant conversion efficiency can be increased by 90% by using this solar hybrid technology.

Actually the main objective of a micro hydro power plant is to generate electricity for the remote hilly area people who are leg behind from the modern world and to improve their socio economic condition. So the main concern of a micro hydro power plant should be to generate more electricity from the available stream by improving the design to enlighten the leg behind community of our society to increase the economic growth of our country which mostly depends upon the electrification rate of our country. Although a micro hydro power plant can play a vital role to improve the economic condition of developing countries, no definite strategies has been taken to identify the role of this kind of power plant in energy sector development for rural growth [33]. AS ADB provides subsidies for rural electrification program like micro hydro power plant system up to 100 KW [33], the government of Bangladesh can get help, if they will take the strategy of this kind of power plant for electrifying tribal community. Certainly it is not possible to cover all poor rural un-electrified area of our country by micro hydro power plant, but its impact can be significant in reducing the difference between the level of livelihood of on grid people and off grid tribal people who are a significant part of our country.

REFERENCES

[1] Dr. M. Alimullah Miyan, John Richards, Ph.D., Energy Policy for Bangladesh, CPR Commentary No. 3, Summer 2004, pp. 10, 11.

[2] B.D. Rahmatullah, Nancy Norris, John Richads, a New Mandate for the Rural Electrification Boards (Area – Based Planning Initiatives to Relieve Power Shortages), CPR Commentary No. 6, summer 2006. pp. 9-11.

[3] "Geography of Bangladesh", Wikipedia, the free encyclopedia, modified on 5th October 2012, Available at: http://en.wikipedia.org/wiki/Geography_of_Bangladesh, Access on 18th November 2012.

[4] Khizir Mahmud, Md. Abu Taher Tanbir & Md. Ashraful Islam, "Feasible Micro Hydro Potentiality Exploration in Hill Tracts of Bangladesh", Global Journal of Researches in Engineering, Electrical and Electronics Engineering, Volume 12 Issue 9, Version 1.0, 2012, available at: https://globaljournals.org/GJRE_Volume12/3-Feasible-Micro-Hydro-Potentiality-Exploration.pdf

[5] Kenji Momota, Power Distribution and Efficiency Enhancement Project, field survey report, IC Net Limited, January 2009. Available at: http://www2.jica.go.jp/en/evaluation/pdf/2008_BD-P49_4.pdf, accesses on 31st march 2013

[6] "Electricity Sector in Bangladesh", Wikipedia, the free encyclopedia, modified on 15 January 2013, available at: http://en.wikipedia.org/wiki/Electricity_sector_in_Bangladesh, accessed on 2 February 2013

[7] "Bangladesh Ethnicity and Linguistic Diversity", ita, , available at: http://www.photius.com/countries/bangladesh/society/bangladesh_society_ethnicity_and_lingui~225.html, Accessed on 25 July 2013

[8] "Maulvi Bazar District", wikipedea, the free encyclopedia, modified on 10 September 2012, available at: http://en.wikipedia.org/wiki/Maulvi_Bazar_District, accessed on February 25 2013.

[9] "Overview of Rangamati", Rangamati Hill District Council, official website, 2011, available at: http://www.rhdcbd.org/about_rangamati.php, accessed on July 12 2012.

[10] "Khagrachari District", wikipedea, the free encyclopedia, modified on 10 September 2012, available at: http://en.wikipedia.org/wiki/Khagrachari_District, Accessed on February 25 2013

[11] "About Khagrachori", bdt, Bangladesh Tourism Direction, 2010, available at: http://www.btd.com.bd/tourist-destination/khagrachori.html, Accessed on 25 July 2012

[12] BertocciPeter J., "Chittagong Hill Tribes of Bangladesh", Culture & Survival, Resource Development and Ethnic Conflict, published on 17 February, 2010, available at: http://www.culturalsurvival.org/publications/cultural-survival-quarterly/bangladesh/chittagong-hill-tribes-bangladesh, Accessed on 25 July, 2013

[13] "Rangamati Hill District", Wikipedia, the free encyclopedia, modified on 25 October 2012, Available at: http://en.wikipedia.org/wiki/Rangamati_Hill_District, 25 April, 2013

[14] "Bandarban District", Wikipedia, the free encyclopedia, modified on 3 November 2012, available at: http://en.wikipedia.org/wiki/Bandarban_District, Accessad on 12 July, 2013

[15] "Sylhet District", Wikipedia, the free encyclopedia, modified on 11 October 2012, available at: http://en.wikipedia.org/wiki/Sylhet_District, accessed on 12 July 2013.

[16] "Chittagong District" Wikipedia, the free encyclopedia, modified on 12 August 2012, available at: http://en.wikipedia.org/wiki/Chittagong_District, accessed on 27 February 2013.

[17] "Mymensingh District", Wikipedia, the free encyclopedia, modified on 8 January 2013, available at http://en.wikipedia.org/wiki/Mymensingh_District, accessed on 27 February 2013.

[18] "Dhaka District", Wikipedia, the free encyclopedia, modified on 7 October 2012, available at http://en.wikipedia.org/wiki/Dhaka_District, Accessed on 27 February 2013.

[19] Government of Bangladesh, PRELIMINARY REPORT ON HOUSEHOLD INCOME & EXPENDITURE SURVEY-2010, BANGLADESH BUREAU OF STATISTICS, Statistics Division, Ministry of Planning, June 2011, available at: http://www.bbs.gov.bd/webtestapplication/userfiles/image/HIES/HIES-PR.pdf

[20] Government of Bangladesh, Report on the Bangladesh Literacy Survey, 2010, Industry and Labor Wing, Bangladesh Bureau of Statistics, Statistics Division Ministry of Planning , June 2011 , Available at: http://www.bbs.gov.bd/WebTestApplication/userfiles/Image/Survey%20reports/Bangladesh%20Literacy%20Surver%202010f.pdf

[21] Literature Values For Water Specific Heat Capacity, THERMAL APPLICATIONS NOTE, Thermal Analysis & Rheology, TA Instruments, Available at: http://www.tainstruments.co.jp/application/pdf/Thermal_Library/Applications_Notes/TN015.PDF, Accessed on 05 July 2013

[22] The Government of Peoples Republic of Bangladesh, Energy and Mineral Resource Division (EMRD), Ministry of Power, Energy and Mineral Resources, Official website, modified in 2009, available at: http://www.emrd.gov.bd/43221.html, accessed on 13 February 2013.

[23] Country comparison> Oil- Production, indexmundi, Source: CIA World Factbook, 01 January, 2012, available at: http://www.indexmundi.com/g/r.aspx?t=0&v=88&l=en, Accessed on February 15, 2013

[24] "Natural Gas in Bangladesh", Wikipedia, the free encyclopedia, modified on 17 December 2012, available at: http://en.wikipedia.org/wiki/Natural_gas_in_Bangladesh, Accessed on 25 July 2013

[25] "Bangladesh Energy Sector: Crisis Compounding," published 13 October, 2010, available at: http://www.energybangla.com/index.php?mod=article&cat=SomethingtoSay&article=2803Sweeden--

[26] Engr. Abdur Rouf, Engr. KM Nayeem Khan, Eng. Shazibul Hoque, Bangladesh Power Sector Data, Power Cell, June 2006, available at: http://www.e-powerexpo.net/BD/Bangladesh%20Power%20Data.pdf, Accessed on 13 June, 2013.

[27] Green Energy Solutions for a Sustainable Future, Micro Hydro Power-Small hydro power, small hydro turbine, micro hydro turbine, micro hydro power, 2012, available at: http://www.sunecochina.com/Micro-Hydro-Power-Generator.html, accessed on 15 February, 2013

[28] A Buyer's Guide, Micro Hydro Power System, Natural Resources Canada, the Government of Canada, 2004, Available at: http://www.builditsolar.com/Projects/Hydro/CanadaMicroHydroGuide.pdf, Accessed on 25 July, 2013

[29] Bangladesh Power Development Board, Government official website, 2011, Available at: http://www.bpdb.gov.bd/bpdb/index.php?option=com_content&view=article&id=150&Itemid=16, Accessed on 05 June 2013

[30] Jahidul Islam Razan, Riasat Siam Islam, Rezaul Hasan, Samiul Hasan, and Fokhrul Islam, "A Comprehensive Study of Micro-Hydropower Plant and its Potential in Bangladesh", International Scholarly Research Network, ISRN Renewable Energy, Volume 2012, available at: http://www.hindawi.com/isrn/re/2012/635396/

[31] Bangladesh latitude Longitude map, Maps of World, Media Kit, 2013, Available at: http://www.mapsofworld.com/lat_long/bangladesh-lat-long.html Accessed on 1 August 2013

[32] Dr Masud Hasan Chowdhury, Green Future for Bangladesh through Solar Power Generation, The NEWAGE, Online Edition, 22 October, 2011, Available at: http://newagebd.com/newspaper1/archive_details.php?date=2011-10-22&nid=37769, accessed on 25 May, 2013

[33] Smail Khennas and Andrew Barnett, BEST PRACTICES FOR SUSTAINABLE DEVELOPMENT OF MICRO HYDRO POWER IN DEVELOPING COUNTRIES FINAL SYNTHESIS REPORT, The Department for International Development, UK and The World Bank, March, 2000, available at: http://www.afghaneic.org/renewable/2%20bestpractsynthe.pdf

[34] Small Hydropower Systems, ENERGY EFFICIENCY AND RENEWABLE ENERGY, the National Renewable Energy Laboratory (NREL), the U.S. Department of Energy (DOE), Department of Energy, United States of America, July 2011, Available at: http://www.nrel.gov/docs/fy01osti/29065.pdf

[35] "Micro Hydro", Wikipedia, the free encyclopedia, modified on 05 December 2013, available at: http://en.wikipedia.org/wiki/Micro_hydro#Head_and_flow_characteristics, accessed on 8 December 2013

[36] Renewable energy, Technology Roadmap, 20% by 2020, European Renewable Energy Council, available at: http://www.erec.org/fileadmin/erec_docs/Documents/Publications/Renewable_Energy_Technology_Roadmap.pdf

[37] Praveen Saxena, Small Hydro Development In India, International Conference on Small Hydropower -Hydro Sri Lanka, 22-24 October, 2007, available at: http://www.ahec.org.in/links/International%20conference%20on%20SHP%20Kandy%20Srilanka%20All%20Details%5CPapers%5CPolicy,%20Investor%20&%20Operational%20Aspects-C%5CC27.pdf

[38] Micro-hydro Yearbook of Nepal: 2003 published, news@microhydropower.net, CADEC Micro-hydro e-news No 17, available at: http://www.microhydropower.net/news/viewnews.php?ID=27, accessed on 22 July 2013.

[39] Harshini Perera and Sanjeevi Jayasuriya, The Daily News, Online, Srilanka's National News Paper, Published on 22 June 2010, available at: http://www.dailynews.lk/2010/06/22/bus02.asp, accessed on 10 January 2013

[40] Ion BOSTAN, Valeriu DULGHERU, Viorel BOSTAN, Anatol SOCHIREANU, Oleg CIOBANU, Radu CIOBANU , "HIDRAULICA", Magazine of Hydraulics, Pneumatics, Tribology, Ecology, Sensorics, Mechatronic, Volume 03, issue 04, 2012, available at: http://www.fluidas.ro/hidraulica/2012/3_4/15_21.pdf

[41] BASHAR A. SINOKROT, JOHN S. GULLIVER, "In-stream flow impact on river water temperatures", JOURNAL OF HYDRAULIC RESEARCH, VOL. 38, NO. 5, 30 April, 200, available at: http://www.iahr.org/publications/assets/jhr38-5/Bashar_Gulliver.pdf

[42] How to Plan a micro hydro power plant, Hydropedea, modified on 17 November 2010, available at: http://en.howtopedia.org/wiki/How_to_Plan_a_Micro_Hydro-power_Plant#Short_Description, accessed on 25 November 2013

[43] Micro Hydro Electric Power Plant overview and Power Calculation, TRIPOD, available at: http://members.tripod.com/hydrodocs_1/calculations.html, accessed on 25 June 2013

[44] Asher Azenkot, Irrigation Systems Design, Ministry of Agriculture Extension Service, Field Service, 18 April, 2004, available at: http://dc338.4shared.com/doc/Iw10Aj5u/preview.html, accessed on 22 February 2013.

[45] Jarviscochrane, "How Flow Rate = Low short Temperature in HX?", published on 6 February, 2011, available at: http://www.home-

barista.com/espresso-machines/high-flow-rate-low-shot-temperature-in-hx-t16600.html, accessed on 22 July 2013
[46] Gray, "What is the relationship between viscosity, flow rate, and temperature!", Available at: http://answers.yahoo.com/question/index?qid=20110321184749AAhc9bx, accessed on 22 March 2013
[47] "In 100 years of Nepalese Hydroelectricity, People still Suffer Scarcity, Increasing Load-shedding remains at least for five more years," published May 25, 2010, available at: http://english.ohmynews.com/ArticleView/article_sangview.asp?menu=c10400&no=386090&rel_no=1, accessed on 20 July 2013
[48] Md. Asadullah Khan, Small hydropower generating units can ease power crisis, The Daily Star, an English daily of Bangladesh, Published on 01 August 2009, available at: http://www.thedailystar.net/newDesign/news-details.php?nid=99488, accessed on 10 July 2013
[49] A.K.M. Sadrul Islam, M. Q. Islam, M. Z. Hossain, M. I. Khan and S. A. Uddin, "Appropriate Low Head Micro Hydro Systems for Bangladesh", Second International Conference on Electrical and Computer Engineering, ICECE 2002, 26-28 December 2002, Dhaka, Bangladesh, available at: http://www.buet.ac.bd/icece/publ2002/paper_055.pdf,
[50] Solar Constant, Wikipedia, the free encyclopedia, modified on 4 September 2012, available at: http://en.wikipedia.org/wiki/Solar_constant, accessed on 5 June 2013
[51] Calculating the Energy from Sunlight over a 12-Hour Period, Math & Science Resources, LTP, NASA official, available at: http://www.grc.nasa.gov/WWW/k-12/Numbers/Math/Mathematical_Thinking/sun12.htm, accessed on 22July 2013
[52] Mirrors and Images, PHYSCLIPS, A multilevel Multimedia Resources, Science UNSW, available at: http://www.animations.physics.unsw.edu.au/jw/light/mirrors-and-images.htm, accessed on 23 June 2013
[53] Solar Furnace, Wikipedia, the free encyclopedia, modified on 25 September 2013, available at: http://en.wikipedia.org/wiki/Solar_furnace, accessed on 22 October 2013.
[54] Richard Perez and Sam Coleman, "PV Module Angles", Home Power, August/September 1993, available at: http://labman.phys.utk.edu/phys221/modules/m9/viscosity.htm, accessed on 25 January 2013
[55] March Equinox: March 20, timeanddate.com, available at: http://www.timeanddate.com/calendar/march-equinox.html, accessed on 05 September 2013
[56] Khagrachori District, Satelite Views.net, available at: http://www.satelliteviews.net/cgi-bin/w.cgi?c=bg&UF=217465&UN=271597&DG=ADM2, accessed on 25 August 2013.
[57] Khagrachori District, get a map.net, available at: available at: http://www.getamap.net/maps/bangladesh/bg80/_khagracharidistrict/, accessed on 23 July 2013
[58] Bandarban District, get a map.net, available at: available at http://www.getamap.net/maps/bangladesh/chittagong/_bandarban_district/, accessed on 23 July 2013
[59] Current Local Time in Sylhet, timeanddate.net, available at: http://www.timeanddate.com/worldclock/city.html?n=936, accessed on 23 July 2013
[60] Current Local Time in Chittagong, timeanddate.net, available at: http://www.timeanddate.com/worldclock/city.html?n=469, accessed on 23 July 2013
[61] Ashok Kumar, N.S.Thakur, Rahul Makade, Maneesh Kumar Shivhare, International Journal of Engineering Science and Technology (IJEST) , Vol. 3 No. 4 Apr 2011 , available at: http://www.ijest.info/docs/IJEST11-03-04-254.pdf
[62] Factoring in the Actual Length of Day for Solar Energy Calculations, Math & Science Resources, LTP, NASA official, available at: http://www.grc.nasa.gov/WWW/k-12/Numbers/Math/Mathematical_Thinking/sun12b.htm, accessed on 22 July 2013
[63] Profile for Kramer Junction, California, CA, PODUNK, the power of Place, available at: http://www.epodunk.com/cgi-bin/genInfo.php?locIndex=10358, accessed on 22 May 2013.
[64] Identifiers for solar thermal, Global Energy Observatory, available at: http://globalenergyobservatory.org/geoid/5320, accessed on 22 May, 2013
[65] Mini & Micro Hydro Power Generation, EBARA Hatakeyama Hatakeyama Memorial Fund, Tokyo, Japan, available at: http://nrec.mn/data/uploads/Nom%20setguul%20xicheel/Water/MHP%28Mongolia%20%5C%2707%29F.pdf, accessed on 25 May 2013
[66] Mini & Micro Hydro Power, Renewable Cogen Asia, 2010, available at: http://www.rcogenasia.com/renewable-electricity/mini-micro-hydro-power/, accessed on 22 March 2013
[67] Ogeya Mbeo, Research Scientist – Energy Technologies Kenya Industrial Research and Development Institute (KIRDI), ROLE OF RENEWABLE ENERGY - (HYDROPOWER THE CASE OF KENYA), EFFECTIVE NATURAL RESOURCE MANAGEMENT FOR INCLUSIVE AND SUSTAINABLE GROWTH, available at: http://www.odi.org.uk/sites/odi.org.uk/files/odi-assets/events-documents/4751.pdf, accessed on 25 November 2013
[68] Emil Bedi, CANCEE and HAKAN Falk, "Energy Saving Now", Small Hydro Power Plants, energysavingnow.com, 2010, available at: http://energy.saving.nu/hydroenergy/small.shtml, accessed on 22 March 2013
[69] Micro hydro power, Practical Action, UK, available at: http://practicalaction.org/micro-hydro-power, accessed on 22 June 2013
[70] The Micro Hydro Plant, Implementing my Paradise, Homo Ludens, available at: http://ludens.cl/paradise/turbine/turbine.html, accessed on 22 February 2013
[71] Jian Li, Zhifeng Wanga, Dongqiang Lei, Jianbin Li, Hydrogen permeation model of parabolic trough receiver tube, Solar Energy, 7 February 2012, available at: http://www.chsel.com/ois/uploadfile/com_content/133594818593275600.pdf
[72] Solar thermal power plants Technology Fundamentals, published in Renewable Energy World 06/2003, pp. 109-113, available at: http://www.volker-quaschning.de/articles/fundamentals2/index.php, accessed on 17 May 2013
[73] Sivasakthy Selvakumaran (SID), Low Cost Structures in Micro-Hydroelectric Power Generation, Fourth-year undergraduate project in Group D, 2009/2010, available at: http://www.ewb-uk.org/filestore/FINAL%20REPORT_Sakthy%20Selvakumaran.pdf
[74] Parabolic Reflector, Wikipedia, the free encyclopedia, modified on 23 January 2014, available at: http://en.wikipedia.org/wiki/Parabolic_reflector, accessed on 28 January 2014
[75] Finding the Focal Point, Saved By the Sun || student handout, NOVA, WGBH Educational Foundation, 2007, available at: http://www.pbs.org/wgbh/nova/education/activities/pdf/3406_solar_03.pdf, accessed on 22 June 2013
[76] Joe Cole, Hydroelectric Power - Water power - micro hydro systems, Electro vent, available at: http://www.green-trust.org/hydro.htm, accessed on 22 May 2013
[77] Hydroelectric Information, nooutage.com, modified on Dec 5, 2011, available at: http://www.nooutage.com/hydroele.htm#Rebates%20&%20Incentives, accessed on 22 March 2013
[78] Mukhtiar Singh, Ambrish Chandra, Modeling and Control of Isolated Micro-Hydro Power Plant with Battery Storage System, IEEE

Annual Conference, available at: http://bhagirathi.iitr.ac.in/dspace/bitstream/123456789/1048/1/RES008.pdf
[79] Concentrating Solar Power, SEIA, Solar Energy Industries Association, available at: http://www.seia.org/policy/solar-technology/concentrating-solar-power, accessed on 23 February 2013
[80] Convert Fahrenheit & Celsius, available at: http://www.manuelsweb.com/temp.htm, accessed on 26 May 2013
[81] Prof. N. De Leon, Specific Heat and Heat Capacity, C101 Class Notes, available at: http://www.iun.edu/~cpanhd/C101webnotes/matter-and-energy/specificheat.html, accessed on 22 June 2013
[82] Specific Heat, HyperPhysics, Thermodynamics, Available at: http://hyperphysics.phy-astr.gsu.edu/hbase/thermo/spht.html, accessed on 26 July 2013
[83] Annual report, 2009, Bangladesh power development board, available at: www.bpdb.gov
[84] SYNTHETIC TRANSFORMER OIL For Cooler Transformers, Royal Purple, Beyond Synthetic, available at: http://www.ro-quip.com/Technical_Docs/Royal%20Purple/Heat%20Transfer%20oils/Transformer%20Oil_psro.pdf, accessed on 20 June 2013.
[85] Density Equation and Formulas Calculator, Science - Physics, Mathematical Physics, 2012, available at: http://www.ajdesigner.com/phpdensity/density_equation_volume.php, accessed on 22 February, 2013.
[86] Anne Marie Helmenstine, Ph.D., What Is the Density of Water?, about.com Chemistry, available at: http://chemistry.about.com/od/waterchemistry/f/What-Is-The-Density-Of-Water.htm, accessed on 22 February 2013
[87] Ionic Liquids as Thermal Energy Storage Media for Solar Thermal Electric Power Systems, THE UNIVERSITY OF ALABAMA, Class Lecture, available at: http://www.nrel.gov/csp/troughnet/pdfs/rreddy_ionicfluids.pdf
[88] Pressure Drop Online-Calculator, Pressure Drop Online-Calculator for Mobile and PDA, available at: http://www.druckverlust.de/Online-Rechner/dp.php, accessed on 25 May 2013
[89] Ram M. Shrestha, S. Kumar, Sudhir Sharma and Monaliza J. Todoc, Institutional Reforms and Electricity Access: Lessons from Bangladesh and Thailand, Energy Field of Study, School of Environment, Resources and Development, Asian Institute of Technology, available at: http://www.afrepren.org/project/gnesd/esdsi/ait.pdf
[90] Bangladesh Energy Situation, Energypedia, modified on 05 December 2013, available at: https://energypedia.info/index.php/Bangladesh_Country_Situation, accessed in 07 December 2013
[91] Charlie Dou, Charlie Dou, case study report, Self-supported development of micro-hydro power by village community, UN, UNDP, 2011, available at: http://www.growinginclusivemarkets.org/media/cases/China_Microhydro_2011.pdf
[92] Anup Gurung, Ian Bryceson, Jin Ho Joo, Sang-Eun Oh, Socio-economic impacts of a micro-hydropower plant on rural livelihoods, Scientific Research and Essays Vol. 6(19), pp. 3964-3972, 8 September, 2011, available at: http://www.academicjournals.org/sre/pdf/pdf2011/8Sep/Gurung%20et%20al.pdf
[93] Soma Dutta, Energy as a key variable in eradicating extreme poverty and hunger: A gender and energy perspective on empirical evidence on MDG #1, Discussion Paper, DFID/ENERGIA project on Gender as a Key Variable in Energy Interventions, December 2005 , available at: http://r4d.dfid.gov.uk/PDF/Outputs/Energy/R8346_mdg_goal1.pdf
[94] Khalid Md. Bahauddin, Tariq Md SalahUdin, Impact of Utilization of Solar PV Technology among Marginalized Poor People in Rural Area of Bangladesh, Proc. of International Conference on Environmental Aspects of Bangladesh (ICEAB10), Japan, Sept. 2010, available at: http://benjapan.org/iceab10/24.pdf
[95] Small Hydro, Wikipedia, the free encyclopedia , modified on 16 January, 2014, available at: http://en.wikipedia.org/wiki/Small_hydro, accessed on 22 January, 2014
[96] Keith Gibbs, The flow of liquid through a tube, School Physics, 2013, available at: http://www.schoolphysics.co.uk/age16-19/Properties%20of%20matter/Viscosity/text/Flow_of_liquid_through_a_tube/index.html, accessed on 15 June 2013
[97] Bangladesh, Chittagong, UNJobs, a Swiss Association, available at: http://unjobs.org/duty_stations/bangladesh/chittagong/bandarban, accessed on 22 November 2013
[98] M.A. Wazed, Shamsuddin Ahmed, A Feasibility Study of Micor-Hydroelectric Power Generation at Sapchari Waterfall, Khagrachari, Bangladesh, Science Alert, Journal of Applied Sciences, 9: pp. 372-376, available at: http://scialert.net/fulltext/?doi=jas.2009.372.376
[99] "South Asia Regional Overview," last modified October, 2004, available at: http://www.eia.doe.gov/emeu/cabs/nepal.html, accessed on 15 October 2010.
[100] Dr Masud Hasan Chowdhury, Green future for Bangladesh through solar power generation, the Bangladesh Economics News, published on 26 October 2011, available at: http://bangladesheconomy.wordpress.com/2011/10/26/6071/, accessed on 25 August, 2013
[101] CDKN Asia, Explosion of solar power in Bangladesh, Climate and Development Knowledge Network, 6 July 2011, available at: http://cdkn.org/2011/07/explosion-of-solar-power-in-bangladesh/, accessed 25 October, 2013,
[102] SHAKIR-ul haque Khan, TOWFIQ-ur-Rahman, SHAHADAT Hossain, A BRIEF STUDY OF THE PROSPECT OF SOLAR ENERGY IN GENERATION OF ELECTRICITY IN BANGLADESH, Cyber Journals: Multidisciplinary Journals in Science and Technology, Journal of Selected Areas in Renewable and Sustainable Energy (JRSE), June Edition, 2012, available at: http://www.cyberjournals.com/Papers/Jun2012/02.pdf
[103] Curved Mirror, modified on 30 December 2013, available at: http://en.wikipedia.org/wiki/Curved_mirror, accessed on 05 January 2014
[104] Micro Hydro, GVEP International, Global Village Energy Partnership: Accelerating Access to Energy, available at: http://www.gvepinternational.org/en/business/micro-hydro, accessed on 25 February 2013
[105] The Energy Challenge for Achieving the Millennium Development Goals, UN-Energy, Knowledge network, published in December 2004, available at: http://www.un-energy.org/publications/50-the-energy-challenge-for-achieving-the-millennium-development-goals
[106] Population of Bangladesh, Bangladesh Information, the mirror of Bangladesh, Published on 16 January, 2013, available at: http://bangladesh-information24.blogspot.com/2013/01/population-of-bangladesh.html, accessed on 05 July 2013.
[107] Population Growth (Annual %) in Bangladesh, Densiti, Hints and Tips, available at: http://www.tradingeconomics.com/bangladesh/population-growth-annual-percent-wb-data.html, accessed on 26 July 2013
[108] Maulvi Bazar District, Banglapedea, National Encyclopedia of Bangladesh, available at: http://www.bpedia.org/M_0188.php, Accessed on 28 September 2013
[109] Benjamin Root, Microhydro Myths & Misconceptions, Home power, January 2012, available at: http://www.homepower.com/articles/microhydro-power/design-installation/microhydro-myths-misconceptions, accessed on 22 February 2013
[110] ISAAC ASIMOV, UNDERSTANDING PHYSICS 2, LIGHT, MAGNETISM AND ELECTRICITY, available at: http://www.arvindguptatoys.com/arvindgupta/phys2.pdf

[111] Dynamic viscosity of liquid water from 0 ℃ to 100 ℃, www.vaxasoftware.com, available at: http://www.vaxasoftware.com/doc_eduen/qui/viscoh2o.pdf
[112] Deepak Bajracharya, Rural Energy Planning in China and Other Developing Countries of Asia, Pp 32, available at: http://books.google.com.bd/books?id=_qXci2YWxq4C&pg=PA32&lpg=PA32&dq=the+electrification+rate+of+the+rural+areas+of+many+developing+countries+are+not+more+than+1
[113] Off-Grid Electrification using Micro hydro power schemes- Sri Lankan Experience (A survey and Study on existing off-grid electrification schemes), available at: http://www.pucsl.gov.lk/tamil/wp-content/uploads/2013/03/Off-Grid-5.3-su-cov-page.pdf
[114] R.S. Khurmi, A Textbook of Hydraulics, Fluid Mechanics and Hydraulics Machines, S. Chand & Company Ltd, Ramnagar, New Delhi, Edition 2010, pp 9,242,341.

Figures and Tables

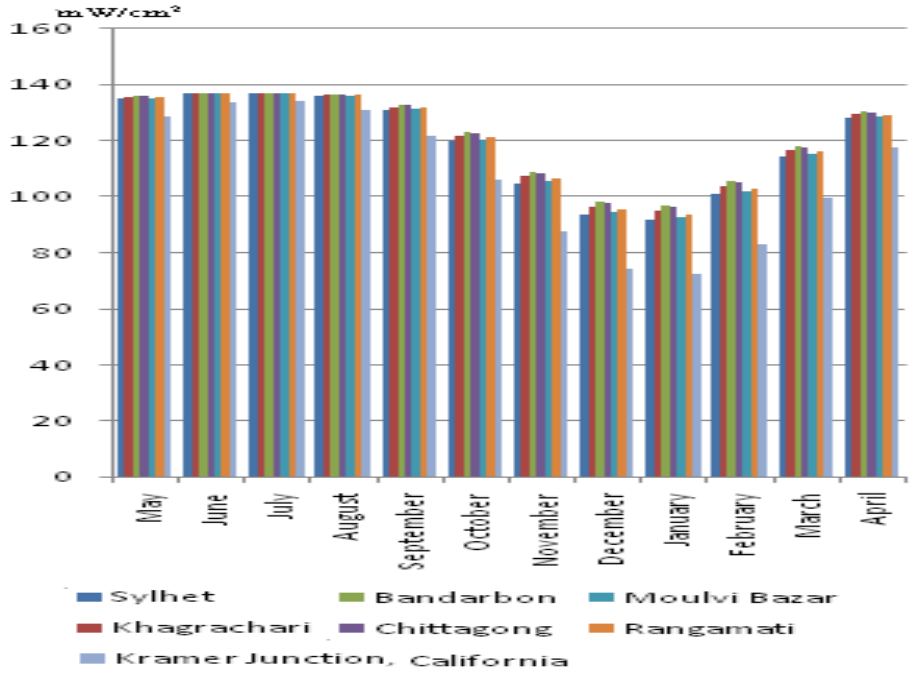

Figure 1: Solar intensity curve of different districts of micro- hydro power sites in Bangladesh and Kramer Junction, California.

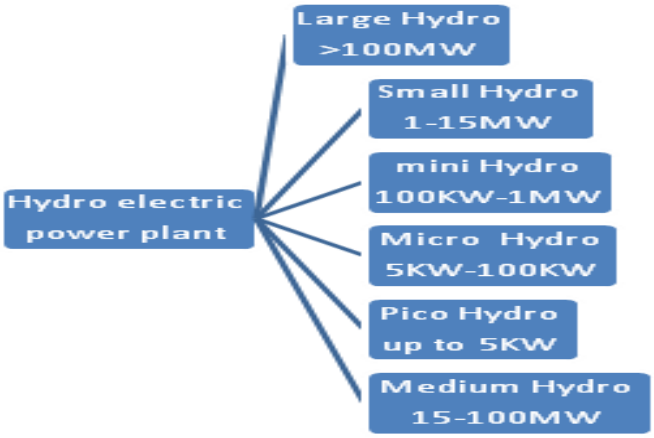

Figure 2: Classification of hydroelectric power plant

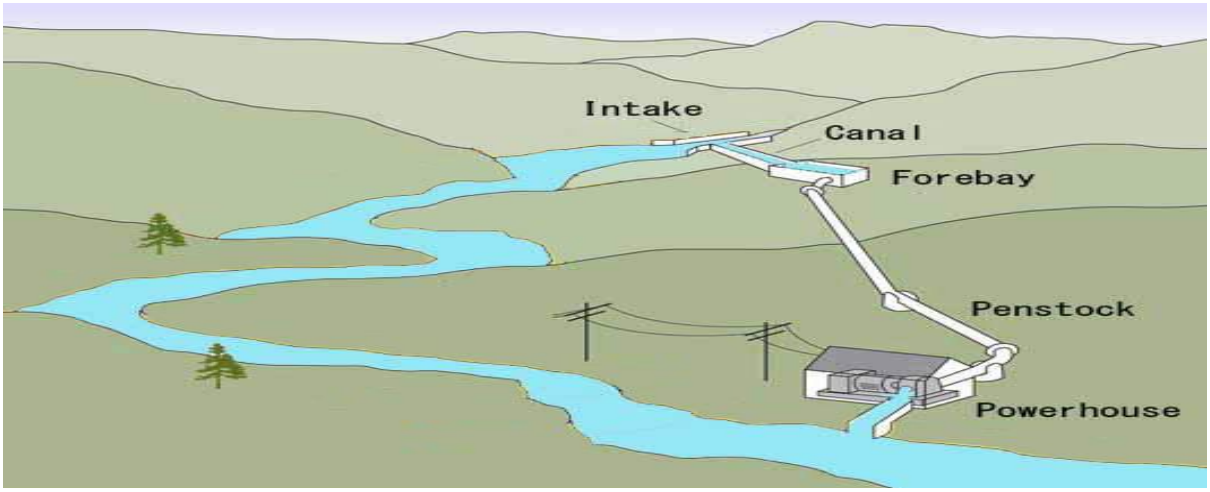

Figure 3: Conventional micro hydro power plant

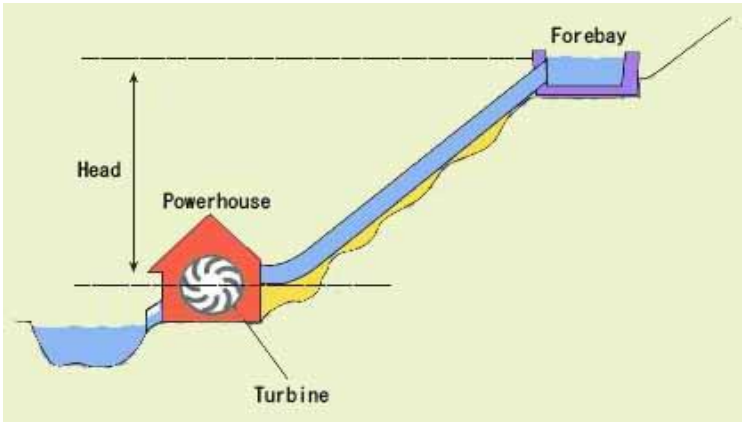

Figure 4: Conventional micro hydro power plant with penstock view

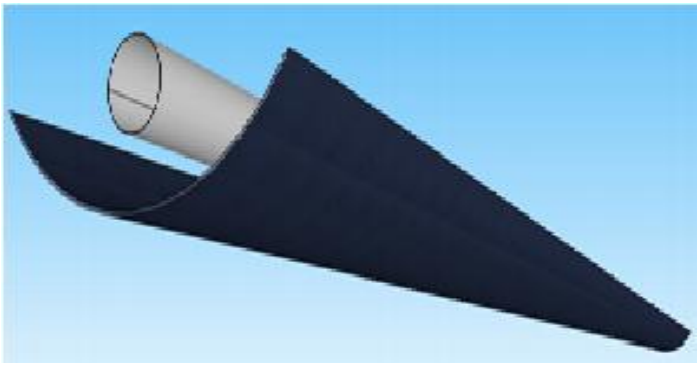

Figure 5: Penstock and reflector view in proposed design

Table 1: Literacy rate of different tribal districts of Bangladesh

District	Rangamati	Bandorban	Khagracori	Sylhet	Chittagong	Mymensingh	Moulvi Bazar	Dhaka	National
Literacy Rate	36.5% [13]	43% [14]	26.3% [10]	46% [15]	43.2% [16]	25.42% [17]	30.8% [108]	96.9% [18]	57.91% [19]

Table 2: Micro-hydro site pointed out in BPDB and BWDP joint survey and LGED survey

Site Name	***Sectional Area***	***Power Potential (kW)***
Nunchari Tholi Khal	11	5
Choto kumira	128.2	15
Hinguli chara	-	12
Lungi chara	545	10
Budia chara	660	10
Madhub chara	83.7	78
Bhugai kongsa	704	65.5
marisi	692.3	32.5
Sealock Khal	25	30
Taracha Khal	35	20
Rowangchari Khal	30	10
Hnara Khal	20	10
Hanara Khsl	25	30
Monjaipara	15	10
Bamar chara	-	10

Table 3: List of micro hydro power site with their flow rate, available head and possible electricity production

Site Name	*District*	*Flow Rate (liter/second)*	*Head (meter)*	*Power Potential Available (KW)*
Sailopropat	Bandarban	100	6	2.94
Madhabkundu	Moulovibazar	150	10	7.36
Faizlake	Chittagong	42.5	12	2.50
Sealck	Bandarban	1132	4	22.21
Madhunaghat bridge	Chittagong	7870	3.28	126.61
Sapchari waterfall	Khagrachori	38	10	1.86
Nikhari chara	Sylhet	480	6.8	16.01
Madhab chara	Sylhet	996	9.9	48.37
Lungichara	Chittagong	425	3	6.25
Budia chara	Chittagong	170	7.6	6.34
Chota karina chara	Chittagong	311	6	9.15
Bamar chara	Chittagong	150	10	7.36
Mahamaya Chara	chittagong	552	.9144	2.48
Ruanchori canal	Bandarban	771	5	18.91

Table 4: Solar declination on the 1st day of each month of the year in Bangladesh

Day (1st day of each month)	*Declination Θ in degree*
May	14.924
June	22.079
July	23.17
August	17.97
September	7.78
October	-4.172
November	-15.35
December	-22.13
January	-23.075
February	-17.612
March	-8.4
April	4.023

Table 5: Solar intensity, day hours and energy falls on earth surface of different districts of micro- hydro power site in Bangladesh and Kramer Junction, California for the first day of each month of the year.

District	*Latitude*	σ_D	*Day*	*Td* *hours*	*E* *MJ*
Sylhet	24.88	134.9389777	May	12.54893	1941408
Sylhet	24.88	136.8364899	June	13.26801	2081519
Sylhet	24.88	136.9390512	July	13.41243	2105754
Sylhet	24.88	136.0058887	August	12.81075	1997585
Sylhet	24.88	130.9497365	September	12.14863	1823915
Sylhet	24.88	119.7796679	October	12.04671	1654339
Sylhet	24.88	104.6252304	November	12.58197	1509239
Sylhet	24.88	93.4579613	December	13.27452	1422355
Sylhet	24.88	91.79398732	January	13.39943	1410177
Sylhet	24.88	101.0547034	February	12.77681	1480307
Sylhet	24.88	114.5539886	March	12.1726	1598697
Sylhet	24.88	128.0316551	April	12.04385	1767892
Khagrachari	23.167	135.5860729	May	12.54893	1950718
Khagrachari	23.167	136.9753254	June	13.26801	2083631
Khagrachari	23.167	136.9999998	July	13.41243	2106691
Khagrachari	23.167	136.437383	August	12.81075	2003923
Khagrachari	23.167	132.0942694	September	12.14863	1839857
Khagrachari	23.167	121.7129784	October	12.04671	1681041
Khagrachari	23.167	107.221078	November	12.58197	1546685
Khagrachari	23.167	96.40919203	December	13.27452	1467271
Khagrachari	23.167	94.79158367	January	13.39943	1456227
Khagrachari	23.167	103.7734052	February	12.77681	1520132
Khagrachari	23.167	116.7479435	March	12.1726	1629316
Khagrachari	23.167	129.4311451	April	12.04385	1787216
Bandarbon	22	135.957613	May	12.54893	1956063
Bandarbon	22	136.9998699	June	13.26801	2084004
Bandarbon	22	136.9714661	July	13.41243	2106252
Bandarbon	22	136.6615955	August	12.81075	2007216
Bandarbon	22	132.806507	September	12.14863	1849777

Bandarbon	22	122.9679309	October	12.04671	1698374
Bandarbon	22	108.9348381	November	12.58197	1571406
Bandarbon	22	98.37060899	December	13.27452	1497122
Bandarbon	22	96.78541744	January	13.39943	1486857
Bandarbon	22	105.5726307	February	12.77681	1546488
Bandarbon	22	118.183016	March	12.1726	1649343
Bandarbon	22	130.3184507	April	12.04385	1799469
Chittagong	22.33	135.8582576	May	12.54893	1954634
Chittagong	22.33	136.9986867	June	13.26801	2083986
Chittagong	22.33	136.9852919	July	13.41243	2106465
Chittagong	22.33	136.6039332	August	12.81075	2006369
Chittagong	22.33	132.6106719	September	12.14863	1847049
Chittagong	22.33	122.6182056	October	12.04671	1693544
Chittagong	22.33	108.4547748	November	12.58197	1564481
Chittagong	22.33	97.82006577	December	13.27452	1488743
Chittagong	22.33	96.2256403	January	13.39943	1478257
Chittagong	22.33	105.068257	February	12.77681	1539100
Chittagong	22.33	117.7821527	March	12.1726	1643749
Chittagong	22.33	130.0730028	April	12.04385	1796079
Moulvi Bazar	24.35	135.1520893	May	12.54893	1944474
Moulvi Bazar	24.35	136.8925065	June	13.26801	2082371
Moulvi Bazar	24.35	136.9709762	July	13.41243	2106245
Moulvi Bazar	24.35	136.1523865	August	12.81075	1999737
Moulvi Bazar	24.35	131.3163948	September	12.14863	1829022
Moulvi Bazar	24.35	120.3893401	October	12.04671	1662760
Moulvi Bazar	24.35	105.4384725	November	12.58197	1520970
Moulvi Bazar	24.35	94.38010782	December	13.27452	1436390
Moulvi Bazar	24.35	92.73032247	January	13.39943	1424561
Moulvi Bazar	24.35	101.9056209	February	12.77681	1492771
Moulvi Bazar	24.35	115.2438161	March	12.1726	1608324
Moulvi Bazar	24.35	128.476929	April	12.04385	1774040
Rangamati	23.73	135.3867264	May	12.54893	12.54893
Rangamati	23.73	136.9431842	June	13.26801	13.26801

Rangamati	23.73	136.993463	July	13.41243	13.41243
Rangamati	23.73	136.3089899	August	12.81075	12.81075
Rangamati	23.73	131.7310678	September	12.14863	12.14863
Rangamati	23.73	121.0894774	October	12.04671	12.04671
Rangamati	23.73	106.3783688	November	12.58197	12.58197
Rangamati	23.73	95.44860079	December	13.27452	13.27452
Rangamati	23.73	93.81559236	January	13.39943	13.39943
Rangamati	23.73	102.8899733	February	12.77681	12.77681
Rangamati	23.73	116.0382777	March	12.1726	12.1726
Rangamati	23.73	128.983875	April	12.04385	12.04385
Kramer Junction, California [151]	35.0198	128.6677273	May	12.54893	1851181.684
Kramer Junction, California [151]	35.0198	133.5239797	June	13.26801	2031130.198
Kramer Junction, California [151]	35.0198	134.0833774	July	13.41243	2061841.366
Kramer Junction, California [151]	35.0198	130.9849423	August	12.81075	1923839.992
Kramer Junction, California [151]	35.0198	121.8216185	September	12.14863	1696775.539
Kramer Junction, California [151]	35.0198	106.2097935	October	12.04671	1466918.637
Kramer Junction, California [151]	35.0198	87.42972191	November	12.58197	1261190.671
Kramer Junction, California [151]	35.0198	74.37307159	December	13.27452	1131898.678
Kramer Junction, California [151]	35.0198	72.4663709	January	13.39943	1113257.82
Kramer Junction, California [151]	35.0198	83.20075906	February	12.77681	1218772.024
Kramer Junction, California [151]	35.0198	99.5443561	March	12.1726	1389225.277
Kramer Junction, California [151]	35.0198	117.4552008	April	12.04385	1621849.724

Table 6: Flow rate, available head, potential available and Electrical power output in different micro hydro power site in Bangladesh.

Site	*District*	*Q (litter/second)*	*H (meter)*	*Potential Available in Water P (KW)*	*Electrical Power Output P_e (KW)*
Sailopropat	Bandarban	100	6	5.8	2.943
Madhabkundu	Moulovibazar	150	10	15	7.3575
Faizlake	Chittagong	42.5	12	5	2.50155
Sealck	Bandarban	1132	4	44.42	22.20984
Madhunaghat bridge	Chittagong	7870	3.28	253.23	126.61
Sapchari waterfall	Khagrachori	38	10	3.7278	1.8639
Nikhari chara	Sylhet	480	6.8	32.01984	16.00992
Madhab chara	Sylhet	996	9.9	95.753448	48.365262
Lungichara	Chittagong	425	3	12.50775	6.253875
Budia chara	Chittagong	170	7.6	12.67452	6.33726
Chota karina chara	Chittagong	311	6	18.30546	9.15273
Bamar chara	Chittagong	150	10	14.715	7.3575
Mahamaya Chara	Chittagong	552	.9144	4.952	2.475792864
Ruanchori canal	Bandarban	771	5	37.81755	18.908775

Table 7: Dynamic viscosity of water for different temperature obtained by the solar concentrator for micro hydro power plant

District	*Temperature rise in synthetic oil for 182.4 m^2 reflector in ºC*	*Temperature rise in water in ºC*	*1st day of the month*	*Dynamic viscosity $\times 10^{-6}$ N-s/m^2*
Sylhet	114.039806	56.56374377	May	504
Sylhet	115.6981127	57.38626391	June	504
Sylhet	115.7877449	57.43072149	July	504
Sylhet	114.9722193	57.02622079	August	504
Sylhet	110.5534593	54.83451579	September	504
Sylhet	100.7915194	49.99259362	October	547
Sylhet	87.54749085	43.42355546	November	595
Sylhet	77.78799762	38.58284682	December	652
Sylhet	76.33378865	37.86155917	January	652

Sylhet	84.42707407	41.87582874	February	652
Sylhet	96.22460324	47.72740321	March	547
Sylhet	108.003239	53.56960656	April	504
Khagrachari	114.6053267	56.84424204	May	504
Khagrachari	115.8194463	57.44644537	June	504
Khagrachari	115.8410102	57.45714104	July	504
Khagrachari	115.3493184	57.21326192	August	504
Khagrachari	111.5537093	55.33063981	September	504
Khagrachari	102.4811116	50.83063134	October	547
Khagrachari	89.81609901	44.54878511	November	595
Khagrachari	80.36718831	39.8621254	December	652
Khagrachari	78.95349998	39.16093599	January	652
Khagrachari	86.80304904	43.05431232	February	595
Khagrachari	98.14198227	48.67842321	March	547
Khagrachari	109.2263056	54.17624757	April	504
Bandarbon	114.9300294	57.00529458	May	504
Bandarbon	115.8408966	57.45708473	June	504
Bandarbon	115.8160735	57.44477244	July	504
Bandarbon	115.545266	57.31045196	August	504
Bandarbon	112.1761603	55.63937549	September	504
Bandarbon	103.5778614	51.37461926	October	547
Bandarbon	91.31381789	45.29165368	November	595
Bandarbon	82.08134379	40.71234652	December	652
Bandarbon	80.69598573	40.02520892	January	652
Bandarbon	88.37545939	43.83422786	February	595
Bandarbon	99.39614571	49.30048827	March	547
Bandarbon	110.001755	54.56087049	April	504
Chittagong	114.8431991	56.96222673	May	504
Chittagong	115.8398626	57.45657186	June	504
Chittagong	115.8281564	57.45076558	July	504
Chittagong	115.4948728	57.28545688	August	504

Chittagong	112.0050127	55.55448628	September	504
Chittagong	103.2722234	51.22302281	October	547
Chittagong	90.89427269	45.08355925	November	595
Chittagong	81.60020352	40.47370094	December	652
Chittagong	80.2067756	39.7825607	January	652
Chittagong	87.93466836	43.61559551	February	595
Chittagong	99.04581628	49.12672488	March	547
Chittagong	109.7872489	54.45447547	April	504
Moulvi Bazar	114.2260522	56.65612189	May	504
Moulvi Bazar	115.7470677	57.41054559	June	504
Moulvi Bazar	115.8156454	57.44456012	July	504
Moulvi Bazar	115.1002492	57.08972362	August	504
Moulvi Bazar	110.8738956	54.99345224	September	504
Moulvi Bazar	101.3243347	50.25687001	October	547
Moulvi Bazar	88.25821347	43.77607388	November	595
Moulvi Bazar	78.59389588	38.98257236	December	652
Moulvi Bazar	77.15208689	38.2674351	January	652
Moulvi Bazar	85.17072261	42.24467841	February	652
Moulvi Bazar	96.82746926	48.02642475	March	547
Moulvi Bazar	108.3923805	53.76262074	April	504
Rangamati	114.4311103	56.75783073	May	504
Rangamati	115.7913569	57.43251302	June	504
Rangamati	115.8352974	57.45430752	July	504
Rangamati	115.2371108	57.15760696	August	504
Rangamati	111.2362938	55.17320173	September	504
Rangamati	101.9362108	50.56036056	October	547
Rangamati	89.07962397	44.18349349	November	595
Rangamati	79.52769176	39.44573511	December	652
Rangamati	78.10054475	38.73787019	January	652
Rangamati	86.03098495	42.67136854	February	595
Rangamati	97.52177891	48.37080234	March	547

Rangamati	108.8354195	53.98236807	April	504

Table 8: velocity, flow rate, output and efficiency of power conversion in conventional design for selected micro hydro power site in Bangladesh

Micro hydro power site	*Velocity at 25^0C ft/s*	*Velocity in m/s*	*Pressure drop P_1-P_2 N/m2*	*Previous output power in KW*	*Water energy can be harnessed in previous system*
Sailopropat	4.64	1.41427	6.705535	2.943	50.74137931
Madhabkundu	6.96	2.12141	10.0583	7.3575	49.05
Faiz Lake	1.97	0.60046	2.846962	2.50155	50.031
Sealock	52.54	16.0142	75.92862	22.20984	49.9996398
Madhunaghat bridge	365.28	111.337	527.8875	126.61	49.99802551
Sapchari water fall	1.76	0.53645	2.543479	1.8639	50
Nikharichara	22.28	6.79094	32.19813	16.00992	50
Madhab Chara	46.23	14.0909	66.80967	48.365262	50.51020408
Lungi Chara	19.73	6.0137	28.51298	6.253875	50
Budia Chara	7.89	2.40487	11.4023	6.33726	50
Chota Karina Chara	14.43	4.39826	20.85364	9.15273	50
Bamar Chara	6.96	2.12141	10.0583	7.3575	50
Mahamaya Chara	25.62	7.80898	37.02496	2.475792864	49.99581712
Ruangchori Chanal	35.79	10.9088	51.72222	18.908775	50

Table 9 : velocity, flow rate, output and efficiency of power conversion in proposed design for selected micro hydro power site in Bangladesh

Site	*Month*	*Dynamic Viscosity $\times 10^{-6}$ N-m/s^2*	*Velocity increase m/s*	*Flow rate m^3/s*	*Q litter/s*	*Current power output KW*	*Water energy can be harnessed in current system*
Sailopropat	May	467	2.692265113	0.190305005	190.3050049	5.600676294	96.56338438

Sailopropat	June	467	2.692265113	0.190305005	190.3050049	5.600676294	96.56338438
Sailopropat	July	467	2.692265113	0.190305005	190.3050049	5.600676294	96.56338438
Sailopropat	August	467	2.692265113	0.190305005	190.3050049	5.600676294	96.56338438
Sailopropat	September	504	2.494618667	0.176334201	176.334201	5.189515534	89.47440577
Sailopropat	October	547	2.298515188	0.162472463	162.472463	4.781564587	82.44076875
Sailopropat	November	595	2.113088753	0.149365441	149.3654408	4.395824923	75.79008488
Sailopropat	December	652	1.928355534	0.136307419	136.3074192	4.011527346	69.16426458
Sailopropat	January	652	1.928355534	0.136307419	136.3074192	4.011527346	69.16426458
Sailopropat	February	595	2.113088753	0.149365441	149.3654408	4.395824923	75.79008488
Sailopropat	March	547	2.298515188	0.162472463	162.472463	4.781564587	82.44076875
Sailopropat	April	504	2.494618667	0.176334201	176.334201	5.189515534	89.47440577
Madhabkundu	May	504	3.741927999	0.264501301	264.5013013	12.97378883	86.49192554
Madhabkundu	June	467	4.038397669	0.285457507	285.4575072	14.00169073	93.34460486
Madhabkundu	July	467	4.038397669	0.285457507	285.4575072	14.00169073	93.34460486
Madhabkundu	August	467	4.038397669	0.285457507	285.4575072	14.00169073	93.34460486
Madhabkundu	September	504	3.741927999	0.264501301	264.5013013	12.97378883	86.49192554
Madhabkundu	October	547	3.447772781	0.243708694	243.7086945	11.95391146	79.69274309
Madhabkundu	November	595	3.169633128	0.224048161	224.0481611	10.9895623	73.26374869
Madhabkundu	December	652	2.892533299	0.204461129	204.4611286	10.02881836	66.85878907

Madhabkundu	January	652	2.892533299	0.204461129	204.4611286	10.02881836	66.85878907
Madhabkundu	February	652	2.892533299	0.204461129	204.4611286	10.02881836	66.85878907
Madhabkundu	March	547	3.447772781	0.243708694	243.7086945	11.95391146	79.69274309
Madhabkundu	April	504	3.741927999	0.264501301	264.5013013	12.97378883	86.49192554
Faiz Lake	May	467	1.143052214	0.080797599	80.79759906	4.755746681	95.11493362
Faiz Lake	June	467	1.143052214	0.080797599	80.79759906	4.755746681	95.11493362
Faiz Lake	July	467	1.143052214	0.080797599	80.79759906	4.755746681	95.11493362
Faiz Lake	August	467	1.143052214	0.080797599	80.79759906	4.755746681	95.11493362
Faiz Lake	September	504	1.059137667	0.074866029	74.86602929	4.406614484	88.13228968
Faiz Lake	October	547	0.975878216	0.068980766	68.98076556	4.060207861	81.20415722
Faiz Lake	November	595	0.897151906	0.063415931	63.41593069	3.732661681	74.65323361
Faiz Lake	December	652	0.818719914	0.0578719	57.87189994	3.406340031	68.12680061
Faiz Lake	January	652	0.818719914	0.0578719	57.87189994	3.406340031	68.12680061
Faiz Lake	February	595	0.897151906	0.063415931	63.41593069	3.732661681	74.65323361
Faiz Lake	March	547	0.975878216	0.068980766	68.98076556	4.060207861	81.20415722
Faiz Lake	April	504	1.059137667	0.074866029	74.86602929	4.406614484	88.13228968
Sealock	May	467	30.48526058	2.154876068	2154.876068	42.27866846	95.17935269
Sealock	June	467	30.48526058	2.154876068	2154.876068	42.27866846	95.17935269
Sealock	July	467	30.48526058	2.154876068	2154.876068	42.27866846	95.17935269

Sealock	August	467	30.48526058	2.154876068	2154.876068	42.27866846	95.17935269
Sealock	September	504	28.24725533	1.996680802	1996.680802	39.17487733	88.19197957
Sealock	October	547	26.02672155	1.839720519	1839.720519	36.09531659	81.25915485
Sealock	November	595	23.92708687	1.691306091	1691.306091	33.1834255	74.70379446
Sealock	December	652	21.83530167	1.543446509	1543.446509	30.28242051	68.17294127
Sealock	January	652	21.83530167	1.543446509	1543.446509	30.28242051	68.17294127
Sealock	February	595	23.92708687	1.691306091	1691.306091	33.1834255	74.70379446
Sealock	March	547	26.02672155	1.839720519	1839.720519	36.09531659	81.25915485
Sealock	April	504	28.24725533	1.996680802	1996.680802	39.17487733	88.19197957
Madhunaghat bridge	May	467	211.9462502	14.98159746	14981.59746	241.0299325	95.18221874
Madhunaghat bridge	June	467	211.9462502	14.98159746	14981.59746	241.0299325	95.18221874
Madhunaghat bridge	July	467	211.9462502	14.98159746	14981.59746	241.0299325	95.18221874
Madhunaghat bridge	August	467	211.9462502	14.98159746	14981.59746	241.0299325	95.18221874
Madhunaghat bridge	September	504	196.386704	13.88175796	13881.75796	223.3352748	88.19463522
Madhunaghat bridge	October	547	180.9486267	12.79050459	12790.50459	205.7787541	81.26160174
Madhunaghat bridge	November	595	166.3510905	11.75866557	11758.66557	189.1781151	74.70604395
Madhunaghat bridge	December	652	151.808127	10.73068407	10730.68407	172.6395375	68.1749941
Madhunaghat bridge	January	652	151.808127	10.73068407	10730.68407	172.6395375	68.1749941
Madhunaghat bridge	February	595	166.3510905	11.75866557	11758.66557	189.1781151	74.70604395

Madhunaghat bridge	March	547	180.9486267	12.79050459	12790.50459	205.7787541	81.26160174
Madhunaghat bridge	April	504	196.386704	13.88175796	13881.75796	223.3352748	88.19463522
Sapchari water fall	May	467	1.021204009	0.072184657	72.18465703	3.540657427	94.97981188
Sapchari water fall	June	467	1.021204009	0.072184657	72.18465703	3.540657427	94.97981188
Sapchari water fall	July	467	1.021204009	0.072184657	72.18465703	3.540657427	94.97981188
Sapchari water fall	August	467	1.021204009	0.072184657	72.18465703	3.540657427	94.97981188
Sapchari water fall	September	504	0.946234667	0.066885387	66.88538657	3.280728211	88.0070876
Sapchari water fall	October	547	0.871850589	0.061627486	61.62748598	3.022828187	81.08879735
Sapchari water fall	November	595	0.801516424	0.056655857	56.65585686	2.778969779	74.54718008
Sapchari water fall	December	652	0.731445202	0.051702814	51.70281416	2.536023035	68.03001863
Sapchari water fall	January	652	0.731445202	0.051702814	51.70281416	2.536023035	68.03001863
Sapchari water fall	February	595	0.801516424	0.056655857	56.65585686	2.778969779	74.54718008
Sapchari water fall	March	547	0.871850589	0.061627486	61.62748598	3.022828187	81.08879735
Sapchari water fall	April	504	0.946234667	0.066885387	66.88538657	3.280728211	88.0070876
Nikharichara	May	467	12.92751438	0.913792136	913.7921355	30.47862289	95.18668078
Nikharichara	June	467	12.92751438	0.913792136	913.7921355	30.47862289	95.18668078
Nikharichara	July	467	12.92751438	0.913792136	913.7921355	30.47862289	95.18668078
Nikharichara	August	467	12.92751438	0.913792136	913.7921355	30.47862289	95.18668078
Nikharichara	September	504	11.97847067	0.846708189	846.7081891	28.24110494	88.19876969

Nikharichara	October	547	11.03683586	0.780147948	780.1479475	26.02105464	81.2654112
Nikharichara	November	595	10.14646927	0.717211643	717.2116425	23.92187712	74.70954609
Nikharichara	December	652	9.259431312	0.654510625	654.5106247	21.83054738	68.17819007
Nikharichara	January	652	9.259431312	0.654510625	654.5106247	21.83054738	68.17819007
Nikharichara	February	652	9.259431312	0.654510625	654.5106247	21.83054738	68.17819007
Nikharichara	March	595	10.14646927	0.717211643	717.2116425	23.92187712	74.70954609
Nikharichara	April	504	11.97847067	0.846708189	846.7081891	28.24110494	88.19876969
Madhab Chara	May	467	26.82401211	1.896077667	1896.077667	92.07258348	96.1558935
Madhab Chara	June	467	26.82401211	1.896077667	1896.077667	92.07258348	96.1558935
Madhab Chara	July	467	26.82401211	1.896077667	1896.077667	92.07258348	96.1558935
Madhab Chara	August	467	26.82401211	1.896077667	1896.077667	92.07258348	96.1558935
Madhab Chara	September	504	24.854789	1.756881489	1756.881489	85.31328668	89.09682989
Madhab Chara	October	547	22.90093904	1.618771976	1618.771976	78.60675775	82.09287434
Madhab Chara	November	595	21.05346833	1.488181967	1488.181967	72.26537225	75.47025591
Madhab Chara	December	652	19.21290438	1.35808017	1358.08017	65.947694	68.87239611
Madhab Chara	January	652	19.21290438	1.35808017	1358.08017	65.947694	68.87239611
Madhab Chara	February	652	19.21290438	1.35808017	1358.08017	65.947694	68.87239611
Madhab Chara	March	595	21.05346833	1.488181967	1488.181967	72.26537225	75.47025591
Madhab Chara	April	504	24.854789	1.756881489	1756.881489	85.31328668	89.09682989

Lungi Chara	May	467	11.44792903	0.809206411	809.2064108	11.90747234	95.20075422
Lungi Chara	June	467	11.44792903	0.809206411	809.2064108	11.90747234	95.20075422
Lungi Chara	July	467	11.44792903	0.809206411	809.2064108	11.90747234	95.20075422
Lungi Chara	August	467	11.44792903	0.809206411	809.2064108	11.90747234	95.20075422
Lungi Chara	September	504	10.60750567	0.749800385	749.8003847	11.03331266	88.21180996
Lungi Chara	October	547	9.773643246	0.690858124	690.8581241	10.1659773	81.27742636
Lungi Chara	November	595	8.98518127	0.635125032	635.1250317	9.345864842	74.72059197
Lungi Chara	December	652	8.199666956	0.579600297	579.6002973	8.528818375	68.18827028
Lungi Chara	January	652	8.199666956	0.579600297	579.6002973	8.528818375	68.18827028
Lungi Chara	February	595	8.98518127	0.635125032	635.1250317	9.345864842	74.72059197
Lungi Chara	March	547	9.773643246	0.690858124	690.8581241	10.1659773	81.27742636
Lungi Chara	April	504	10.60750567	0.749800385	749.8003847	11.03331266	88.21180996
Budia Chara	May	467	4.578011154	0.323600536	323.6005365	12.0631808	95.17662837
Budia Chara	June	467	4.578011154	0.323600536	323.6005365	12.0631808	95.17662837
Budia Chara	July	467	4.578011154	0.323600536	323.6005365	12.0631808	95.17662837
Budia Chara	August	467	4.578011154	0.323600536	323.6005365	12.0631808	95.17662837
Budia Chara	September	504	4.241927001	0.299844148	299.8441479	11.17759014	88.18945526
Budia Chara	October	547	3.908466561	0.276273219	276.2732185	10.29891304	81.25682897
Budia Chara	November	595	3.593161695	0.253985631	253.9856311	9.468076357	74.70165622

Budia Chara	December	652	3.279035596	0.231781366	231.7813658	8.640345756	68.17098995
Budia Chara	January	652	3.279035596	0.231781366	231.7813658	8.640345756	68.17098995
Budia Chara	February	595	3.593161695	0.253985631	253.9856311	9.468076357	74.70165622
Budia Chara	March	547	3.908466561	0.276273219	276.2732185	10.29891304	81.25682897
Budia Chara	April	504	4.241927001	0.299844148	299.8441479	11.17759014	88.18945526
Chota Karina Chara	May	467	8.37271241	0.59183216	591.8321596	17.41762046	95.14986488
Chota Karina Chara	June	467	8.37271241	0.59183216	591.8321596	17.41762046	95.14986488
Chota Karina Chara	July	467	8.37271241	0.59183216	591.8321596	17.41762046	95.14986488
Chota Karina Chara	August	467	8.37271241	0.59183216	591.8321596	17.41762046	95.14986488
Chota Karina Chara	September	504	7.758048999	0.548384164	548.3841637	16.13894594	88.16465655
Chota Karina Chara	October	547	7.148184087	0.505275354	505.2753538	14.87025366	81.23397971
Chota Karina Chara	November	595	6.571523858	0.464513645	464.5136446	13.67063656	74.68065025
Chota Karina Chara	December	652	5.997019472	0.423904323	423.9043229	12.47550422	68.1518204
Chota Karina Chara	January	652	5.997019472	0.423904323	423.9043229	12.47550422	68.1518204
Chota Karina Chara	February	595	6.571523858	0.464513645	464.5136446	13.67063656	74.68065025
Chota Karina Chara	March	547	7.148184087	0.505275354	505.2753538	14.87025366	81.23397971
Chota Karina Chara	April	504	7.758048999	0.548384164	548.3841637	16.13894594	88.16465655
Bamar Chara	May	467	4.038397669	0.285457507	285.4575072	14.00169073	95.15250241
Bamar Chara	June	467	4.038397669	0.285457507	285.4575072	14.00169073	95.15250241

Bamar Chara	July	467	4.038397669	0.285457507	285.4575072	14.00169073	95.15250241
Bamar Chara	August	467	4.038397669	0.285457507	285.4575072	14.00169073	95.15250241
Bamar Chara	September	504	3.741927999	0.264501301	264.5013013	12.97378883	88.16710045
Bamar Chara	October	547	3.447772781	0.243708694	243.7086945	11.95391146	81.23623149
Bamar Chara	November	595	3.169633128	0.224048161	224.0481611	10.9895623	74.68272038
Bamar Chara	December	652	2.892533299	0.204461129	204.4611286	10.02881836	68.15370955
Bamar Chara	January	652	2.892533299	0.204461129	204.4611286	10.02881836	68.15370955
Bamar Chara	February	595	3.169633128	0.224048161	224.0481611	10.9895623	74.68272038
Bamar Chara	March	547	3.447772781	0.243708694	243.7086945	11.95391146	81.23623149
Bamar Chara	April	504	3.741927999	0.264501301	264.5013013	12.97378883	88.16710045
Mahamaya Chara	May	467	14.86548108	1.050778928	1050.778928	4.712882195	95.17128826
Mahamaya Chara	June	467	14.86548108	1.050778928	1050.778928	4.712882195	95.17128826
Mahamaya Chara	July	467	14.86548108	1.050778928	1050.778928	4.712882195	95.17128826
Mahamaya Chara	August	467	14.86548108	1.050778928	1050.778928	4.712882195	95.17128826
Mahamaya Chara	September	504	13.774166	0.973638411	973.6384114	4.366896795	88.18450718
Mahamaya Chara	October	547	12.6913705	0.897100109	897.1001085	4.023612404	81.25226987
Mahamaya Chara	November	595	11.66752885	0.824729007	824.7290073	3.699018462	74.6974649
Mahamaya Chara	December	652	10.64751482	0.752628465	752.6284653	3.375638014	68.16716506
Mahamaya Chara	January	652	10.64751482	0.752628465	752.6284653	3.375638014	68.16716506

Mahamaya Chara	February	595	11.66752885	0.824729007	824.7290073	3.699018462	74.6974649
Mahamaya Chara	March	547	12.6913705	0.897100109	897.1001085	4.023612404	81.25226987
Mahamaya Chara	April	504	13.774166	0.973638411	973.6384114	4.366896795	88.18450718
Ruangchori Chanal	May	467	20.76641561	1.467891406	1467.891406	36.00003674	95.19399523
Ruangchori Chanal	June	467	20.76641561	1.467891406	1467.891406	36.00003674	95.19399523
Ruangchori Chanal	July	467	20.76641561	1.467891406	1467.891406	36.00003674	95.19399523
Ruangchori Chanal	August	467	20.76641561	1.467891406	1467.891406	36.00003674	95.19399523
Ruangchori Chanal	September	504	19.241897	1.360129537	1360.129537	33.3571769	88.20554717
Ruangchori Chanal	October	547	17.72927987	1.253208934	1253.208934	30.7349491	81.27165589
Ruangchori Chanal	November	595	16.29901864	1.152109726	1152.109726	28.25549102	74.71528701
Ruangchori Chanal	December	652	14.87410443	1.051388477	1051.388477	25.78530239	68.1834291
Ruangchori Chanal	January	652	14.87410443	1.051388477	1051.388477	25.78530239	68.1834291
Ruangchori Chanal	February	595	16.29901864	1.152109726	1152.109726	28.25549102	74.71528701
Ruangchori Chanal	March	547	17.72927987	1.253208934	1253.208934	30.7349491	81.27165589
Ruangchori Chanal	April	504	19.241897	1.360129537	1360.129537	33.3571769	88.20554717

American Journal of Engineering Research (AJER)
e-ISSN : 2320-0847 p-ISSN : 2320-0936
Volume-03, Issue-11, pp-198-203
www.ajer.org

Research Paper Open Access

Comparative Evaluation for Experimental and Analytical Mode for Tensile Behavior of High Strength Fibre Reinforced Concrete

Dr. Abhijit P. Wadekar[1], Prof. Rahul D. Pandit[2]
1(Principal of People's Education Society's, P. E. S. College of Engineering, Aurangabad, Maharashtra, India.
2(Faculty of CSMSS's, Chh. Shahoo College of Engineering, Kanchanwadi, Aurangabd, Maharashtra, India.

ABSTRACT: *The use of High Strength Concrete (HSC) is incérasse rapidly. From the study of expérimental investigation, It has been observe that HSC is relatively brittle material. Fibres are added to improve its ductility. Experimental study is carried out to assess comparative study in between two types of fibres for mechanical properties of high strength fibre reinforced concrete (HSFRC) of grade M80. In addition to normal materials, silica fume, fly Ash and two types of fibres viz. polypropylene fibre and sound crimped steel fiber, are used. The content of silica fume and fly ash is 5% and 10% respectively by weight of cement. Water to cementitious material ratio was 0.25. Mixes are produced by varying types of fibres and for each type of fibre its volume fraction is varied from 0.5% to 4.0 % with an increment of 0.5% by weight of cementitious materials. 27 specimens each of cylinders (100×200mm) are tested to study the effect type and volume fraction of fibres on split tensile strength and of HSFRC. The results indicated the comparative evaluation for experimental and analytical mode for tensile behavior of HSFRC.*

KEYWORDS : *Polypropylene Fibres, sound crimped steel fiber, Waving steel fibre, High Strength Fibre Reinforced Concrete, Split Tensile Strength.*

1. INTRODUCTION

Concrete is a man made rocks which commonly used as construction material. It traditionally consists of cement, fine aggregate, coarse aggregate and water. However modern concrete is produced by adding mineral and chemical admixtures also. IS 456-2000 suggested the use of fly ash, silica fume, ground granulated blast furnace slag (ggbfs), metakaoline, rice husk ash (RHA) in the production of concrete. Concrete has been categorized as ordinary, standard and high strength based on characteristic compressive strength at the age of 28 days. High strength concrete is being produced due to growing demand for taller and larger structures. As per IS 456, High strength concrete is a concrete with strength between 60 to 80 MPa. Such a concrete demands the use of supplementary cementitious materials (SCM) and super plasticizer in order to reduce cement consumption, increase strength, decrease permeability, and improve durability. It is noticed that high strength concrete is a relatively brittle material possessing lower tensile strength. Internal micro cracks are inherently present in the concrete and its poor tensile strength is due to the propagation of such micro cracks, eventually leading to brittle fracture of the concrete. It has been recognized that the addition of small, closely spaced and uniformly dispersed fibres in the concrete would act as crack arresters and would substantially improve its flexural strength. The toughness of HSFRC depends upon the percentage content of silica fume, fly ash, type of fibre, its volume fraction and aspect ratio. Such a concrete is in demand wherein resistance to cracking is a performance requirement of the structure e.g. liquid storage tanks.

Literature Review: Various researchers have carried out **e**xperimental investigation to study the mechanical behaviour of high strength fibre reinforced concrete. The markable investigation carried out on mechanical properties of high strength fibre reinforced concrete (HSFRC) by P.S.Song and S. Hwang that the brittleness with low tensile strength and strain capacities of high strength concrete (HSC) can be reduce by the addition of steel fibres [1]. It is reported that the use of steel fibres in concrete decrease the workability of concrete but increase split tensile strength,flexural strength, modulus of elasticity and poisons ratio [3,4]. P.Balaguru and Mahendra Patel studied the flexural toughness of steel fibre reinforced concrete by using deformed and hooked end fibres. The results indicated that hooked end fibres provided better results than deformed fibre [5]. The experimental investigation is carried out to study the influence of fibre content on the compressive strength,

modulus of rupture, toughness and splitting tensile strength [6,7,12]. S.P.Singh and S.K.Kaushik carried out an experimental program to study fatigue strength of steel fibre reinforced concrete (SFRC), in which they obtained the fatigue-lives of SFRC at various stress level and stress ratio. There results indicated that the statistical distribution of equivalent fatigue-life of SFRC is in agreement with the two-parameter Weibull distribution. The coefficient of the fatigue equation were determined corresponding to different survival probabilities so as to predict the flexural fatigue strength of SFRC for the desired level of survival probability [9]. The use of mineral admixtures such as silica fume and fly ash in high strength concrete gives the smaller paste porosity as compared to controlled concrete which increases the compressive strength, split tensile strength and flexural strength [10, 11, 13, 14, 17]. The production of good concrete can be done using automation and controlled environment but it not possible to alter its inherent brittle nature and the lack of any tensile strength. The addition of polypropylene fibres in plane concrete, it has increased the ductility and energy absorption capacity of concrete [18]. In the present investigation comparative evaluation for experimental and analytical mode for tensile behavior of HSFRC is studied by incorporating various types of fibres.

Need for Investigation : The ductility is the most important parameters in the design of RCC structures. However, it is observed that ductility of concrete reduces with increase in cement content in concrete as per the increase in grade.

Objectives and Scope : The investigation is focused to comparative study of experimental and analytical effect of various types of fibres on split tensile strength of HSFRC. The water to cementitious material ratio considered for the study of HSFRC of M80 grade was 0.25. The content of silica fume and fly ash in every mix was 5% and 10% by the weight of cementitious material. Three types of fibres considered for the study include, Polypropylene Fibres (PF), Sound Crimped Steel Fibres (SCSF) and Waving Steel Fibre (WSF). Dosage of fibre was varied from 0.5% to 4% at an interval of 0.5% by weight of cementitious material. Type of cement, fine aggregate, coarse aggregate, type of superplasticiser and its dosage are kept constant in every mix. The comparative investigation is done by using Dr. Y. M. Ghugalas formula, i.e.

$$f_{cys} = \left[1.011 + V_f \left(\frac{E_m}{E_f} \right) \right] \log_e f_{cu}$$

II. EXPERIMENTAL PROGRAM

There are 8 mixes cast using single type of fibre. Thus there are in all 24 mixes cast using three types of fibres.

The details of the experimental programme are given in Table 2.1

Table 2.1: Schedule of Experimental Program

Sr. No.	Mix designation of M80 grade HSFRC	Fibre content (%)	No. of specimen (cubes, cylinders and prisms each) using types of Fibres		
			PF	SCSF	WSF
1	M0	0.0	3		
2	M1	0.5	3	3	3
3	M2	1.0	3	3	3
4	M3	1.5	3	3	3
5	M4	2.0	3	3	3
6	M5	2.5	3	3	3
7	M6	3.0	3	3	3
8	M7	3.5	3	3	3
9	M8	4.0	3	3	3

Materials : Ordinary Portland Cement of 53 Grade conforming to IS: 12269-1987 was used in the investigation. The properties of cement are presented in Table 2.2 .

Table 2.2: Physical Properties of Ordinary Portland Cement (OPC)

Sr. No.	Description of Test	Results
01	Fineness of cement (residue on IS sieve No. 9)	6%
02	Specific gravity	3.15
03	Setting time of cement a) Initial setting time b) Final setting time	 118 minute 322 minute
04	Soundness test of cement (with Le-Chatelier's mould)	1mm
06	Compressive strength of cement (a) 3 days (b) 7 days (c) 28 days	 41.03 N/mm^2 55.44 N/mm^2 77.82 N/mm^2

Crushed stone metal with a maximum size of 12.5 mm from a local conforming to the requirements of IS: 383-1970 was used. Locally available river sand passing through 4.75 mm IS sieve conforming to grading zone-II of IS: 383-1970 was used.The properties of aggregates are presented in Table 2.3

Table 2.3: Physical Properties of Fine and Coarse Aggregate

Sr. No	Property	Results	
		Fine Aggregate	Course aggregate
1.	Particle Shape, Size	Rounded, 4.75 mm down	Angular, 10mm down
2.	Fineness Modulus	2.38	6.87
3.	Silt content	2%	
4.	Specific Gravity	2.624	2.684
5.	Bulking of sand	4.16%	0.4%
6.	Bulk density	1586.26 kg/m^3	1565 kg/m^3
7.	Surface moisture	Nil	Nil

Sulphonated melamine based super plasticizer supplied by Roff. Chemicals India Pvt. Ltd. Mumbai is used as water reducing and self retarding admixture in the experimental work. The properties comply with the requirements of IS 9103-1999 (Amended 2003) as well as ASTM C 494-type F.

The fly ash are used which available from Nashik. The specific gravity of fly ash was 2.3. The properties of fly ash are presented in Table 2.4

2.4: Physical Properties of Fly Ash

Sr. No.	Description of Test	Results
01	Specific Gravity	2.3
02	Colour	Grayish white
03	Bulk Weight	Approx. 0.9 metric ton per cubic meter
04	Specific density	Approx. 2.3 metric ton per cubic meter
05	Average Particle size	0.14mm
06	Particle shape	Spherical

The properties of various types of fibres considered for the study are presented in Table 2.4

Table 2.4: Properties of Fibres used

Sr. No.	Property	Properties of two types of fibres		
		PF	SCSF	WSF
2.	Length (mm)	40	30	40
3.	Width (mm)	1.20	-	0.25
4.	Diameter (mm)	0.50	0.45	
6.	Aspect Ratio	-	66.66	160
7.	Colour	White	White	White
8.	Specific Gravity	0.9	7.85	------
9.	Density kg/m^3	1.36	1.36	1.36
10.	Tensile strength MPa	400-800	400-1000	1000

11.	Melting point	253 $^{\circ}C$	253^{0}C	253 $^{\circ}C$
10	Young's modulus kN/mm^2	11.3	25.19	25.19
13.	Water absorption	0.04%	0.04%	0.04%
14.	Minimum elongation	8%	8%	8%
15.	Resistance to alkali in high strength concrete	Excellent	Excellent	Excellent
16.	% Elongation	8	8	8
17.	Effective Diameter mm	0.874	0.456	0.456

2.2: **Production of HSFRC Concrete :** The high strength concrete of M80 grade was designed as per DOE method. Table 2.5 shows the weights of various constituents of HSFRC.

Table 2.5: Mix Proportion

Sr. No	Material	Weight of material in Mass kg/m^3
1	Ordinary Portland Cement (85 % of CM)	472.6
2	Silica fume (5 % of CM)	27.8
3	Fly Ash (10 % of CM)	55.6
4	Fine Aggregate	702
5	Coarse Aggregate	1042
6	Water	150
7	Superplasticizer	18 ml per kg of Cement
8	Water Binder Ratio	0.25

II. RESULT AND DISCUSSION

Effect of fibres content (%) on Split Tensile Strength of High Strength Concrete : The comparative evaluation for experimental and analytical mode and effects of Silica fume, fly ash and three types of fibres on split tensile strength of a high strength fibres reinforced concrete has been shown in figure 3.1, 3.2 and 3.3. The fibre volume fraction is indicated on X-axis and split tensile strength is on Y-axis. A continuous increase in strength is observed up to a limit. The 3 % of fibres content has given maximum increase in split tensile strength as compared to that of normal concrete. Polypropylene fibre was higher than that of concrete with Sound crimped steel fibres at the same volume fractions of fibres up to the limit maximum split tensile strength of 7.21N/mm^2.

The Comparative Results of Experimental and Analytical Method of Split Tensile Strength of Normal and High Strength Concrete for Polypropylene Fibres, 80 MPa

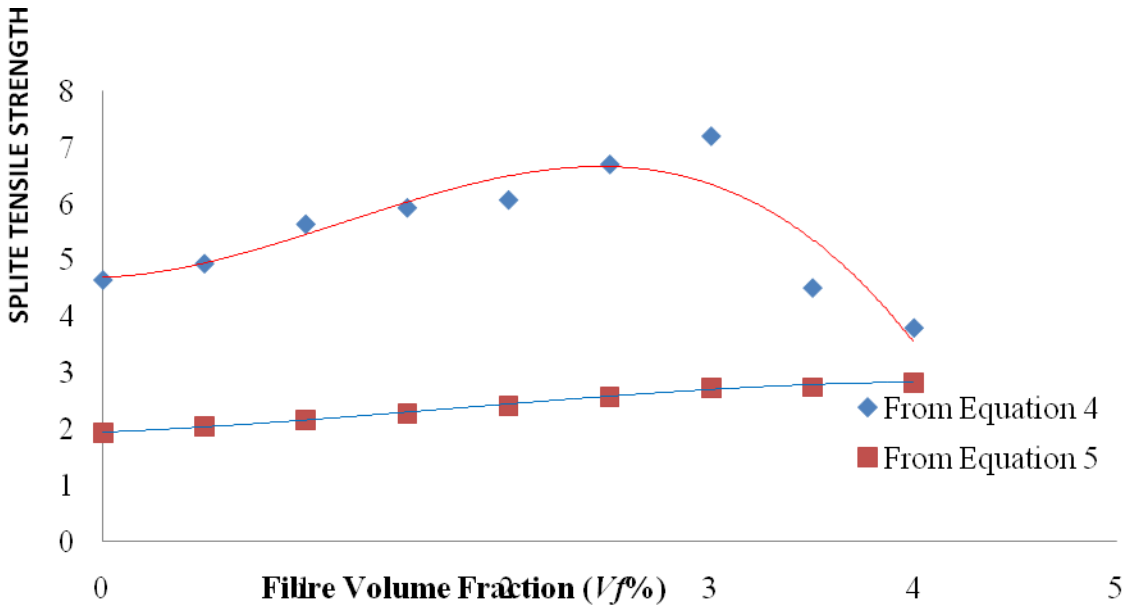

Fig. 3.1 Variation at Split Tensile Strength at the Age of 28 Days With respect to Percentage Fibre Volume Fraction

The Comparative Results of Experimental and Analytical Method of Split tensile Strength of Normal and High Strength Concrete for Sound Crimped Steel Fibres, 80 MPa

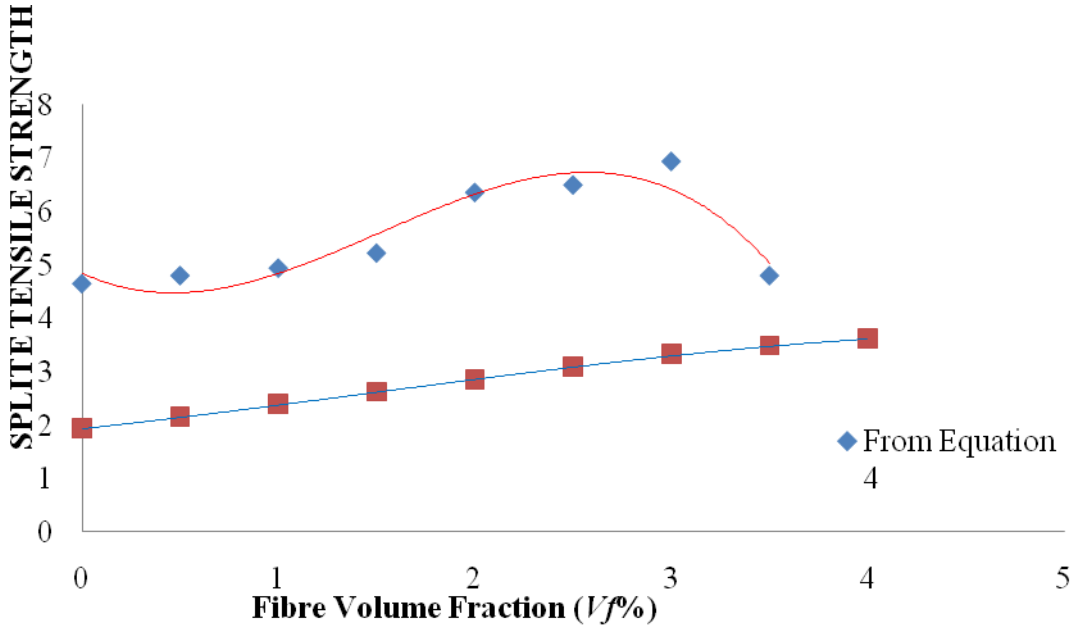

Fig. 3.2 Variation at Split Tensile Strength at the Age of 28 Days With respect to Percentage Fibre Volume Fraction

2.1. The Comparative Results of Experimental and Analytical Method of Split tensile Strength of Normal and High Strength Concrete for Flat Steel Fibres, 80 MPa

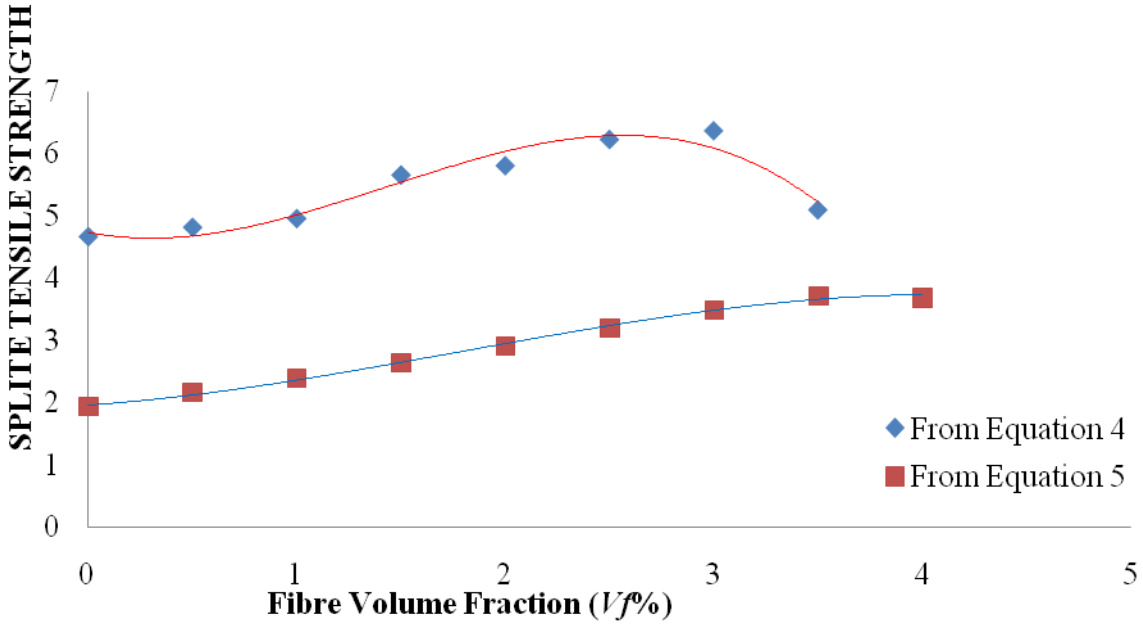

Fig. 3.3 Variation at Split Tensile Strength at the Age of 28 Days With respect to Percentage Fibre Volume Fraction

III. CONCLUSION

From the results discussed in the previous section, following conclusions are drawn.

[1] HSC without fibres is relatively brittle and fails suddenly when compared with HSFRC with different types of fibres.
[2] The split tensile strength of HSC improves with addition of fibres. The maximum strength was occurred at 3% of volume fraction of each fibres. The obtained strength for two types of fibres viz. polypropylene fibre and sound crimped steel fiber is as follws i.e 7.21 and. From the results the higher compressive strength is obtained 7.21 Mpa for polypropylene fibre fibre.
[3] The results obtained in the study are plotted in graphs for each types of test. The study of graph has been concluded that the maximum variations are obtained in experimental evaluation as compared to analytical method of split tensile strengths graph.

.

REFERENCES

[1] P.S.Song., S. Hwang., "Mechanical properties of high strength steel fibre-reinforced concrete", Construction and Building MATERIALS, 18 (2004) 669-673
[2] S.P.Singh and S.K.Kaushik, "Flexural Fatigue Analysis of steel fibre reinforced concrete",ACI Material Journal, Vol.98,No.4,July-August2001,pp.306-312.
[3] Fuat Koksal and Fatih Altun, "Combine effect of Silica fume and steel fibre on the mechanical properties of high strength concrete", Construction and building materials, 23(2007), pp.441-454.
[4] Job Thomas and Ananth Ramaswamy, " Mechanical Properties of Steel Fibres Reinforced Concrete", Journal of Materials in Civil Engineering, May2007, Vol. 19,No.5, pp.385-392.
[5] P.Balaguru, Ramesh Narahari and Mahendra Patel "Flexural Toughness of Steel Fiber Reinforced Concrete", ACI Materials Journal,Nov-Dec.1992, Vol.89, No.6, pp.-541-546.
[6] Faisal F.Wafa and Samir A. Ashour, "Mechanical Properties of high strength fibre-reinforced concrete", ACI Materials Journal,Nov-Dec.1992, Vol.89, No.5, pp.-449-455.
[7] Paviz Soroushian and Ziad Bayasi, "Fiber-Type Effect on the Performance of Steel Fiber Reinforced Concrete", ACI Materials Journal, March-April.1991, Vol.88, No.2, pp.-.291-134.
[8] K.H.Tan, P.Paramasivam and K.C.Tan, "Instaneous and Long-Term Deflectgion of Steel Fiber Reinforced Concrete Beam", ACI Structural Journal, July-August.1994, Vol.91, No.4, pp.-.384-393.
[9] S.P.Singh and S.K.Kaushik, "Fatigue Strength of Steel Fibre Reinforced Concrete in Flexural", Cement and Concrete Composites, 2 September 2002, Vol.25, pp.-.779-786.
[10] C.S.Poon, S.C.Kou and L.Lam, "Compressive Strength, Chloride Diffusivity and Pore Structure of High Performance Metakaolin and Silica Fume Concrete", Construction and Building Materials, August 2005, Vol. 20, pp.-.858-865.
[11] S.Bhaskar, Ravindra Gettu, B.H.Bharatkumar and M.Neelamegam, "Strength, Bond and Durability Related Properties of Concretes with Mineral Admixtures", The Indian Concrete Journal, February 2012, pp.-.09-15.
[12] Avinash S. Pant and Suresh R. Parekar, "Steel Fibres Reinforced Concrete Beam Without Reinforcement Under Combined Bending, Shear and Torsion", The Indian Concrete Journal, April 2012, pp.-.39-43.
[13] Vivek Bindiganavile, Farnaz Batool and Narayana Suresh, " Effect of Fly Ash on thermal properties of cement based foams avaluated by transient plane heat source", The Indian Concrete Journal, November 2012, pp.-.7-13.
[14] Subhash Mitra, Pramod K. Gupta and Suresh C. Sharma, " Time-dependant strength gain in mass concrete using mineral admixtures", The Indian Concrete Journal, November 2012, pp.-.15-22.
[15] IS: 516-1959, Edition 1.2 (1991-07), "Indian Standard for Methods of test for strength of concrete.
[16] Sadr Momtazi A, Ranjbar M. M., Balalaei F, Nemati R, "The effect of Iran's Silica fume in enhancing the concrete compressive strength", Cement and Concrete Research,May 2011, pp.-1-7.
[17] Jian-Tong Ding and Zonglin Li, " Effect of Metakaolin and Silica Fume on Properties of Cocrete", ACI Material Journal, July-August 2002, Vol. 99, PP.-. 393-398.
[18] Rahul Jain, rishi Gupta, makrand G. Khare and Ashish A. Dharmadhikari, " Use of Polypropylene fibre reinforced concrete as a construction material for rigid pavements", The Indian Concrete Journal, March 2011, pp.-.45-53.
[19] IS: 456-2000, "Indian Standard for code of practice for plain and reinforced concrete".
[20] IS: 383-1970. "Specification for course and Fine Aggregates from natural sources for concrete." Bureau of Indian standards, New Delhi.

American Journal of Engineering Research (AJER)
e-ISSN : 2320-0847 p-ISSN : 2320-0936
Volume-03, Issue-11, pp-204-212
www.ajer.org

Research Paper Open Access

Overview of Very Small Aperture Terminal for Television Transmission

[1]Alumona T. L., [2]Ugbem C. A., [3]Ohaneme C.O.
[1]*Department of Electronic & Computer Engineering, NAU Awka*
[2]*Silverbird Television, UHF-30 Awka, Nigeria*
[3]*Department of Electronic & Computer Engineering, NAU Awka*

ABSTRACT : *This paper provides an overview of very small aperture terminal (VSAT) network systems for television transmission. In this context, "broadband" means that the application requires a data transfer rate greater than 100 kbps and should allow broadcast, multi and unicast, and interactive bi-directional services to fixed locations. The systems examined include digital broadcasting (e.g., DVB) with IP encapsulation, and bi-directional VSAT star networks. Detailed comparisons of various transmission parameters and standards are provided to help evaluate currently available satellite and ground equipment capabilities.*
In recent times, file transfer application requires support of file broadcast or IP multicast. Typical applications include audio and video broadcast. A VSAT network is inherently broadcast in nature. Thus VSAT networks naturally and efficiently support these new broadcast applications.

KEYWORDS*: VSAT, DVB, TDMA, FDMA, IRD, QPSK.*

I. INTRODUCTION

The acronym VSAT which stands for Very Small Aperture Terminal is the earth station antenna used at the VSAT earth stations. In VSAT the earth station antenna size is typically less than 2.4m in diameter and the trend is towards even smaller dishes not more than 1.8 m in diameter. According to European Telecommunication standard Institute, VSAT is referred as satellite transmit – receive system that has an aperture size smaller than 2.8m. VSATs provide cost effective solutions for the growing telecommunication needs throughout the world. The architecture of the networks is of two types. One is star topology and the other is mesh topology.The star topology is the traditional VSAT network topology, here the communication link are between the hub and the remote terminal. This topology is well suited for data broadcasting or data collection. The access techniques used in a star network can be both frequency domain multiple access (FDMA) and time domain multiple access (TDMA).

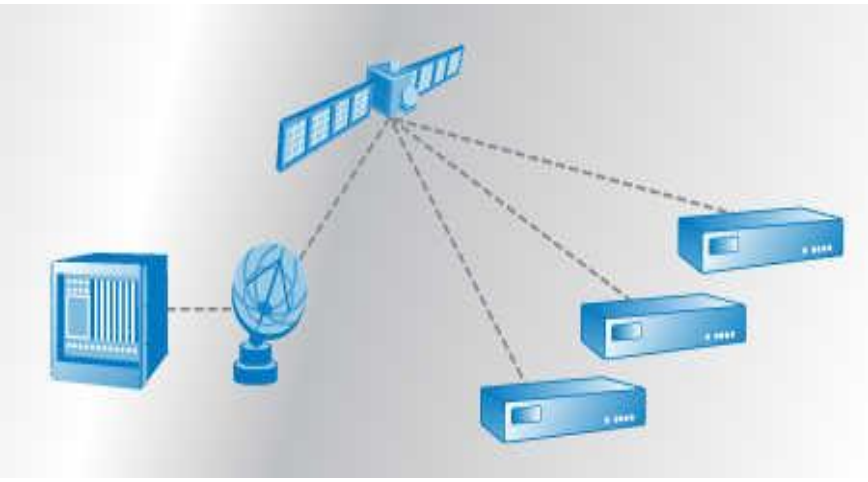

Figure 1.0: A typical VSAT star topology

In mesh topology there is a direct communication between the remote VSAT terminals. This minimizes the time delay which is concerned with speech services. The access method used in a mesh network is FDMA. The links from the hub to the VSAT are called outbound links. The links from the VSAT to the hub are called inbound links. Both inbound and outbound links consist of two parts, uplink and downlink as shown below[1].

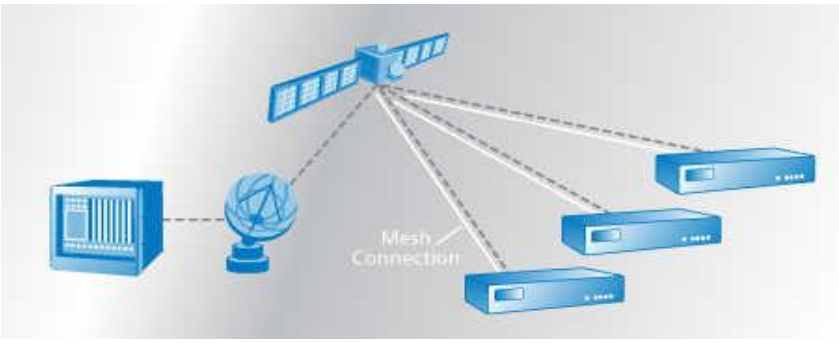

Figure 1.1: A typical VSAT mesh topology

Since the invention of television in the 1920s [2], various analogue television standards have been developed which include Phase Alternating Line (PAL), SéquentielCouleur à MémoireSysteme(SECAM) and National Television Systems Committee (NTSC). These standards are basically spectrum sharing techniques which have their inherent flaws prominent among which are cross-colour, cross luminance and "relatively poor chrominance definition" [3]. The move towards digital transmission of video signals has not been a sudden switch; auxiliary digital services employed to improve image quality have been developed all along. In the 1970s, Vertical Insertion Test signals (VITs) were employed while Video Programmes System (VPS), Multiple Subsampling Encoding system (MUSE), Multiplexed Analogue Components (MAC), D2MAC and High Definition-MAC (HD-MAC) were developed in the 1980s [4]. These efforts in the digital direction had the advantages of less susceptibility to degradation in quality, unique visual effect and ease of television interoperability [5]. Digital video broadcasting (DVB) holds much promise especially in areas of spectrum utilization, high definition content delivery, mobile television integration, high user television interactivity and internet incorporation. The Digital Video Broadcasting (DVB) Project; an organization made of over 260 countries [6], was set up originally to develop technologies for digital video broadcasting via the three traditional broadcasting distribution media; Cable network, satellite systems and terrestrial networks leading to three earlier standards viz DVB-C, DVB-S and DVB-T respectively and its standards have enjoyed wider deployment around the world [7].

II. PROPOSED METHOD

The Internet itself is the last and probably most important interface in the context of data communications. Organizations in the private and public sector have either converted their data communications over to the Internet Protocol, or are in the process of doing so. The interface that is growing to dominate the data world is the simple RJ-45 modular jack associated with the Ethernet standards, 10baseT and 100baseT. Higher rates than 100Mbps demand Gigabit Ethernet or the optical speeds of the Synchronous Digital Hierarchy (e.g., OC-3, OC-48). Such speeds are presently beyond a practical HSA service from currently operating C and Ku band GEO satellites [8]. This could be the domain of the coming generation of broadband satellites employing Ka band spot beams and on-board processing as shown in figure 2.0 below.

Figure 2.0: Ka Band Antenna

A. Broadcast, Multicast and Unicast : Terrestrial networks, including the Internet, are effective for point-to-point transfer of digital media and content. Multicast service over the Internet must employ several point-to-point links to emulate a broadcast system, and therefore has difficulty assuring timely delivery of content to all receivers. A broadcasting station from a local television tower or GEO satellite affords timely delivery of content with a consistent bandwidth. Guaranteeing delivery is usually less of a problem because receivers are designed to directly play the content (a local recording device can allow later playback, if desired).Included in the DVB standard is a data transfer capability called Internet Protocol Encapsulation (IPE). This allows a single broadcast carrier to transfer both television programming and Internet content on the same transport stream. At the subscriber end, the carrier is detected by an integrated receiver decoder (IRD) that extracts the data and delivers it to a local PC or LAN as shown in figure 2.1 below.

Figure 2.1: Scopus IRD 2900 Professional Receiver Decoder [23]

This vehicle allows satellite broadcasters to introduce broadband data into their multiplexed transmissions. The data that rides the MPEG stream may be encrypted along with the digital video and audio, or can be processed with its own unique encryption system. To this may be added a terrestrial return channel for bi-directional service to the desktop or other computational device. Many applications can be supported in this asymmetrical manner since the greater demand is for megabit per second transfer over the satellite in the outbound direction. One must not neglect the potential of this mode for reaching locations that cannot transmit directly over the satellite [9].

B. Digital Video Broadcasting – Return Channel Satellite (DVB-RCS) Network : A DVB-RCS VSAT network is a satellite-based communications system that provide interconnection between users who are exchanging real time (and non-real time) applications based on several data types (e.g. text, voice, images, video etc.). There are two transmission paths, the Forward Channel from a centralized Hub location to the remote location and a Return Channel from the remote location to the central Hub. The DVB-RCS VSAT system underwent final standardization by the European Telecommunications Standards Institute (ETSI) in 2000. The standard calls for a forward link based on a DVB/MPEG-2 data format and a return link using Multi-Frequency – Time Division Multiple Access (MF-TDMA) scheme, allowing a two-way exchange of data. The DVB/MPEG-2 format carries from 1 Mbps up to 45 Mbit/s in the forward link and the MF-TDMA scheme allows from 64 kbps up to 4 Mbps per carrier.

A recent revision of the DVB-RCS standard added support for the new DVB-S2 transmission standard, including adaptive coding and modulation features. The network consists of a central earth station Hub station, the communication satellite and VSAT at the remote sites. Forward traffic to the users at the remote stations (VSATs) is multiplexed into a conventional DVB/MPEG-2 broadcast stream at the Hub and broadcast via the satellite to the VSATs. This broadcast stream is transmitted using QPSK modulation and concatenated convolutional and Reed-Solomon coding (providing a maximum forward data rate of approximately 45 Mbit/s in a 36 MHz transponder) in each transponder used. The return link uses the highly efficient and fast MF-TDMA satellite access scheme together with turbo-coding in order to provide seamless internetworking with other networks. Industry standards are used for carrying data from the VSATs to the Hub Station, in particular Internet Protocol (IP) and Asynchronous Transfer Mode (ATM), or MPEG.

C. Hardware-Implementation : To implement this kind of communication, a user will require a device called a "SIT", ("Satellite Interactive Terminal", "astromodem" or Satellite modem). A suitable satellite-dish is also required. Some systems are supplied as a pre-built combination. The user receives multimedia stream transmissions via the downlink-signals from the satellite. The user sends requests for service signals via the "SIT" and the uplink channel to the satellite. Upon receipt of the command from the user the satellite sends the user request data to the service provider.

D. This takes about 0.5 seconds to connect each way with the satellite. (1 second total for satellite up and downlinks, and another second to the service provider and back, a total of 2 seconds Round-trip delay time).
The protocol used for the SIT portion of the journey is Multiple Frequency Time Division Multiple Access (MF-TDMA). Using this protocol, the user receives data in packets (bursts) that may not be a continuous stream, but when stored and rearranged will generate a virtual 2-dimensional data array. A scheduler is used to maintain these bursts and eliminate duplicates. This protocol is implemented in such a way that different users will receive varying amounts of packet bursts, this helps to regulate the data stream from the satellite-link according to user demands. The forward path (hub to remotes) of the system is based on the relevant ETSI/DVB standards that are shared with the current direct-to-home (DTH) delivery of broadcast television and radio. Thus, both data and video services can be paired (or multiplexed) together to take advantage of existing infrastructure and space segment capacity.

The VSAT employs a scheduled MF-TDMA scheme to access the network and participate in bi-directional communications. MF-TDMA allows a group of VSATs to communicate with a Hub using a set of carrier frequencies, each of which is divided into time-slots. The Hub allocates to each active VSAT a series of bursts; each defined by a frequency, bandwidth, start time and duration. This collection of carrier frequencies and time-slots is referred to as a frame. Each time/frequency slot contains exactly one packet (the packet content being either portions of IP packets or concatenated ATM cells). Frequency-agile VSATs access a pattern of time/frequency slots within these frames. Having established knowledge of the MF-TDMA structure via forward link tables, the VSAT accesses the network using a slotted ALOHA burst. Thereafter, traffic capacity is allocated dynamically, allowing the VSAT to operate in a contention-less mode. A VSAT can only transmit once the VSAT has forward channel reception. Moreover the VSAT must have synchronized itself to the forward link, logged in and have been allocated capacity (in terms of MF-TDMA slots).

Bandwidth and Power Efficiency : Since bits/Hz drive data transmission costs over satellite, and today's satellite bandwidth costs can represent over 20% of direct costs for service to end users, it is in this area that service providers and satellite operators often first focus their evaluation of a DVB-RCS system versus that of other access systems. Most DVB-RCS solution provides for highly-efficient bits/Hz on the forward channel – utilizing 45 Mbps in a 36 MHz transponder as well as taking advantage of every iota of satellite power available rather than wasting it as can happen in a system that is non-capable of saturating a satellite transponder.

Network Scale Efficiency : DVB-RCS is fundamentally designed to be scalable to large populations of terminals. MF-TDMA offers a significant efficiency advantage over other access schemes through the "pooling effect" inherent in statistical multiplexing of large terminal populations in not just one, but two dimensions (frequency and time) simultaneously.

Channel Coding : Channel coding effectively sacrifices bandwidth efficiency for improved reliability of transmission. DVB-RCS uses Turbo coding, which offers excellent bandwidth efficiency for given bit-error ratio (and therefore power efficiency).

Modulation Scheme : Most return channel uses QPSK, which is commonly acknowledged as the optimal trade-off between power and bandwidth efficiency in modulation for multiple access IP over satellite applications. An open standard modulation scheme using QPSK which permits use of linear radios that allows the remote VSAT user to use any qualified L-Band BlockUp converter (BUC) manufactured on the market. [10]

III. RESEARCH METHOD

Standards for digital video broadcasting can be viewed or studied from the standpoint of the distribution media or by looking at the technical specifications for each stage of the broadcast process.

A. The Satellite Standard : Designing a system of moving pictures with accompanying audio which employs satellite communication will require considering the drawbacks of this distribution medium. Satellite channels suffer from signal degradation due to the course travelled by the transmitted signal to arrive at the receiver(s) and this in turn decreases carrier-to-noise ratio. This explains the choice of Quadrature Phase Shift Keying (QPSK) as a modulation technique for the DVB-S standard which was developed in 1994.The DVB-S system based on the Moving Picture Experts Group-2(MPEG-2) for source coding is able to provide multi-programming services through Time Division Multiplexing (TDM) [11]. Error correction is achieved by combining convolutional forward error correction (FEC) for inner coding and Reed-Solomon (RS) codes for outer coding to ensure a balance between power efficiency and spectrum utilization.

DVB-S2 essentially builds upon DVB-S and DVB-DSNG (DVB-Digital Satellite News Gathering) adding to them advancement in coding schemes and flexibility to satisfy users' demand for capacity and interactivity [12]. It employs Adaptive Coding and Modulation (ACM) which allows transmission parameters variation instead of the constant coding and modulation(CCM) used in DVB-S. The DVB-S2 standard specifies8PSK, 16APSK and 32APSK modulation schemes in addition to the QPSK in the earlier standards. A combination of Bose-Chaudhuri-Hocquenghem(BCH) for outer coding, Low Density Parity Check(LDPC) for inner coding and bit interleaving provides robust forward error coding suitable for the noise prone satellite channel. Furthermore a backward compatibility feature of DVB-S2 allows for the accommodation of already existing DVB-S equipment while its non-backward compatibility mode ensures full utilization of the digital "dividend" provided by its deployment [13 – 15]. A summary of the differences between DVB-S and DVB-S2 parameters is shown in Table 3.0.

TABLE 3.0
COMPARISON OF DVB-S AND DVB-S2 FEATURES [14]

	DVB-S	DVB-S2
Modulation	QPSK	QPSK, 8PSK, 16ASK, 32ASK
Coding Scheme	Viterbi and Reed Solomon	LDPC AND BCH
Coding Rates	½, 2/3, ¾, 5/6, 7/8	¼, 1/3, 2/5, ½, 3/5, 2/3, ¾, 4/5, 5/6, 8/9, 9/10
Adaptive Coding	No(CCM only)	VCM and ACM* (*Requires return channel)
Roll-Off	0.35	0.20, 0.25, 0.35
Spectral Efficiency	1.0 – 1.75 bits/Hz	0.5 – 4.5 bits/Hz

B. The Cable Standard : Similar to the satellite standard, presently there are two generations of the cable standard. Developed in 1994, the DVB-C (DVB-over cable standard) is built upon the Quadrature Amplitude Modulation (QAM) accommodating 16 to 256-QAM constellations with a roll-off factor of 0.15. The cable medium is relatively less noisy since it is shielded and so error protection is based upon a shortened Reed-Solomon (RS) Code while convolutional interleaving ensures protection of the error protected packets against burst errors [16]. With improvement in coding techniques, the specifications for digital broadcasting over cable was expanded to allow for higher order modulation in DVB-C2, adaptable input formats which added to the MPEG transports stream of DVB-C. There is a parallel between the format for error protection in DVB-C2 and DVB-S2; both use FEC encoding which employs BCH outer coding, LDPC inner coding and bit interleaving which allows for cable retransmission of received satellite signals. The higher order QAM mappings are implemented up to the level of 4096QAM [17]. Furthermore in DVB-C2, the single carrier modulation method is replaced by the multi-carrier Orthogonal Frequency Division Multiplexing (OFDM). The performance of DVB-C2 shows low impact of narrow band interference and negligible impact of burst errors and impulsive noise under simulated conditions [18].

C. The Terrestrial Standard : Terrestrial broadcasting has been the mainstay of local broadcasting especially in the analogue mode. It suffers from less attenuation when compared to satellite broadcasting but its channel is not as secure as the cable channel. It is arguable that terrestrial broadcasting in the analogue mode holds attraction in areas where affording set top boxes and (or) satellite dishes is beyond the financial capacity of locals. Figure 3.1 below is a typical mast housing Silverbird Terrestrial TV antenna transmitting on channel 30 UHF Awka, Nigeria.

Figure 3.0: A 450ft Mast housingSTV UHF-30 Antenna [22]

In the DVB-T system, the RS code is implemented on the MPEG-2 transport stream for outer coding coupled with a punctured Viterbi Convolutional code for inner coding. This combination serves to provide error protection while OFDM transmission provides good multipath performance for the QPSK, 16-QAM, and 64QAM modulated data carriers [19]. Digital Video Broadcasting over terrestrial systems- second generation (DVB-T2) deployed in 2009, nine years after the first generation standard extends the performance of the earlier standard by adding LPDC, BCH and interleaving(bit, cell, time and frequency interleaving) FEC for error protection; constellation rotation; Multiple Physical Layer Pipes; extended interleaving and optional Multiple Input, single Output (MISO) transmission mode. It also adds a higher modulation level of 256-QAM, uses the active constellation and tone detection techniques to reduce the Peak to Average Power Ratio (PAPR) [20]. Comparisons of some features of both generations are shown in Table 3.1.DVB-T2 is not the only standard for Digital Terrestrial Television Broadcasting; in the United States, the Advanced Television Systems Committee (ATSC) has standards which bear its name; in Japan there is the Integrated Services Digital Broadcasting-Terrestrial (ISDB-T) standard and in China the Digital Terrestrial Multimedia Broadcast (DTMB) standard is deployed. Similar among these standards is their progress into the second generation. The progress of the development of the digital television standards has helped free up spectrum for incorporation of internet services on the broadcasting channel creating avenue for interactive services, reception of satellite and cable services on mobile devices leading to specifications for handheld terminals, internet protocol based broadcasting(Internet Protocol Television) and possible convergence of the broadcasting standards. These feats have employed cutting edge technologies for example in DVB-S2 and DVB-C2, the Shannon's limit has been nearly reached raising doubts over a next generation's standard.

	DVB-T	**DVB-T2**
Coding Scheme	Convolutional Coding + Reed Solomon	LDPC and BCH
Coding Rates	½, 2/3, ¾, 5/6, 7/8	¼, 1/3, 2/5, ½, 3/5, 2/3, ¾, 4/5, 5/6, 8/9, 9/10
Modes	QPSK, 16QAM, 64QAM	QPSK, 16QAM, 64QAM, 256QAM
Guard Interval	¼, 1/8, 1/16, 1/32	¼, 19/128, 1/8, 19/256, 1/16, 1/32, 1/128
Fast Fourier Transform(FFT) Size	2k, 8k	1k,2k, 4k, 8k, 32k
Bandwidth	6, 7, 8 MHz	1.7, 5, 6, 7, 8, 10 MHz
Maximum Data Rate(at 20dB C/N)	3.17Mbit/s	45.5Mb/s
Required C/N ratio(at 24Mbit/s)	16.7 dB	10.8 dB

TABLE 3.1 : COMPARISON OF FEATURES OF DVB-T AND DVB-T2 [21]

IV. RESULTS AND DISCUSSIONS

DVB systems distribute data using a variety of approaches, including by satellite (DVB-S, DVB-S2 and DVB-SH; also DVB-SMATV for distribution via SMATV); cable (DVB-C); terrestrial television (DVB-T, DVB-T2) and digital terrestrial television for handhelds (DVB-H,DVB-SH); and via microwave using DTT (DVB-MT), the MMDS (DVB-MC), and/or MVDS standards (DVB-MS). These standards define the physical layer and data link layer of the distribution system. Devices interact with the physical layer via a synchronous parallel interface (SPI), synchronous serial interface (SSI), or asynchronous serial interface (ASI). All data is transmitted in MPEG-2 transport streams with some additional constraints (DVB-MPEG). A standard for temporally-compressed distribution to mobile devices (DVB-H) was published in November 2004.These distribution systems differ mainly in the modulation schemes used and error correcting codes used, due to the different technical constraints. DVB-S (SHF) uses QPSK, 8PSK or 16-QAM. DVB-S2 uses QPSK, 8PSK, 16APSK or 32APSK, at the broadcaster's decision. QPSK and 8PSK are the only versions regularly used. DVB-C (VHF/UHF) uses QAM: 16-QAM, 32-QAM, 64-QAM, 128-QAM or 256-QAM. Lastly, DVB-T (VHF/UHF) uses 16-QAM or 64-QAM (or QPSK) in combination with COFDM and can support hierarchical modulation.

The DVB-T2 specification was approved by the DVB Steering Board in June 2008 and sent to ETSI for adoption as a formal standard. ETSI is expected to publish the standard in July 2009. The DVB-T2 standard will give more-robust TV reception and increase the possible bit-rate by over 30% for single transmitters (as in the UK) and is expected to increase the max bit-rate by over 50% in large single-frequency networks.

A. **Content :** Besides audio and video transmission, DVB also defines data connections (DVB-DATA - EN 301 192) with return channels (DVB-RC) for several media (DECT, GSM, PSTN/ISDN, satellite etc.) and protocols (DVB-IPTV: Internet Protocol; DVB-NPI: network protocol independent).Older technologies such as teletext (DVB-TXT) and vertical blanking interval data (DVB-VBI) are also supported by the standards to ease conversion. However, for many applications more advanced alternatives like DVB-SUB for sub-titling are available.

B. **Return channel :** DVB has standardized a number of return channels that work together with DVB (-S/T/C) to create bi-directional communication. RCS is short for Return Channel Satellite, and specifies return channels in C, Ku and Ka frequency bands with return bandwidth of up to 2 Mbit/s. DVB-RCT is short for Return Channel Terrestrial, specified by ETSI EN 301958.

C. **Technology :** Satellites used for television signals are generally in either naturally highly elliptical (with inclination of +/-63.4 degrees and orbital period of about 12 hours, also known as Molniya orbit) or geostationary orbit 37,000 km (22,300 miles) above the earth's equator as shown in figure 4.1 below. Satellite television, like other communications relayed by satellite, starts with a transmitting antenna located at an uplink facility. Uplink satellite dishes are very large, as much as 9 to 12 meters (30 to 40 feet) in diameter. The increased diameter results in more accurate aiming and increased signal strength at the satellite. The uplink dish is pointed toward a specific satellite and the uplinked signals are transmitted within a specific frequency range, so as to be received by one of the transponders tuned to that frequency range aboard that satellite. The transponder 'retransmits' the signals back to Earth but at a different frequency band (a process known as translation, used to avoid interference with the uplink signal), typically in the band (4–8 GHz) or Ku-band (12–18 GHz) or both. The leg of the signal path from the satellite to the receiving Earth station is called the downlink.

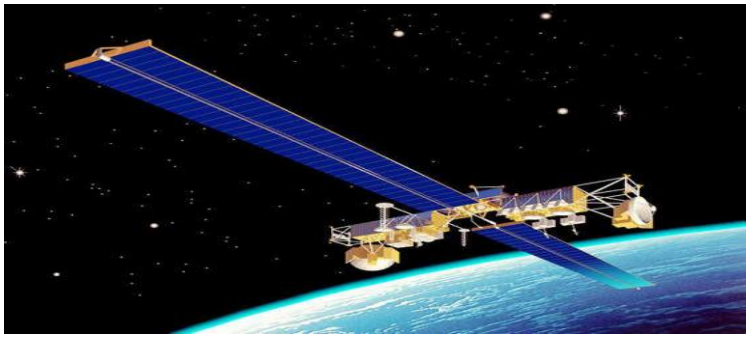

Figure 4.0: Television Satellite in space [23]

A typical satellite has up to 32 transponders for Ku-band and up to 24 for a C-band only satellite, or more for hybrid satellites. Typical transponders each have a bandwidth between 27 MHz and 50 MHz Each geo-stationary C-band satellite needs to be spaced 2 degrees from the next satellite (to avoid interference). For Ku the spacing can be 1 degree. This means that there is an upper limit of 360/2 = 180 geostationary C-band satellites and 360/1 = 360 geostationary Ku-band satellites. C-band transmission is susceptible to terrestrial interference while Ku-band transmission is affected by rain (as water is an excellent absorber of microwaves at this particular frequency). The downlinked satellite signal, quite weak after traveling the great distance (see inverse-square law), is collected by a parabolic receiving dish, which reflects the weak signal to the dish's focal point. Mounted on brackets at the dish's focal point is a device called a feedhorn. This feedhorn is essentially the flared front-end of a section of waveguide that gathers the signals at or near the focal point and 'conducts' them to a probe or pickup connected to a low-noise block downconverter or LNB. The LNB amplifies the relatively weak signals, filters the block of frequencies in which the satellite TV signals are transmitted, and converts the block of frequencies to a lower frequency range in the L-band range. The evolution of LNBs was one of necessity and invention.

The original C-Band satellite TV systems used a Low Noise Amplifier connected to the feedhorn at the focal point of the dish as shown in figure 4.1 below.

Figure 4.1: 1.2M C-Band Satellite Antenna for Outdoor STV Broadcast [22]

The amplified signal was then fed via 50 Ohm impedance coaxial cable to an indoor receiver or in other designs fed to a downconverter (a mixer and a voltage tuned oscillator with some filter circuitry) for downconversion to an intermediate frequency. The channel selection was controlled, typically by a voltage tuned oscillator with the tuning voltage being fed via a separate cable to the headend. But this simple design evolved. Designs for microstrip based converters for Amateur Radio frequencies were adapted for the 4 GHz C-Band. Central to these designs was concept of block downconversion of a range of frequencies to a lower, and technologically more easily handled block of frequencies (intermediate frequency).The advantages of using an LNB are that cheaper cable could be used to connect the indoor receiver with the satellite TV dish and LNB, and that the technology for handling the signal at L-Band and UHF was far cheaper than that for handling the signal at C-Band frequencies. The shift to cheaper technology from the 50 Ohm impedance cable and N-Connectors of the early C-Band systems to the cheaper 75 Ohm technology and F-Connectors allowed the early satellite TV receivers to use, what were in reality, modified UHF TV tuners which selected the satellite television channel for down conversion to another lower intermediate frequency centered on 70 MHz where it was demodulated. This shift allowed the satellite television DTH industry to change from being a largely hobbyist one where receivers were built in low numbers and complete systems were expensive (costing thousands of Dollars) to a far more commercial one of mass production. Direct broadcast satellite dishes are fitted with an LNBF, which integrates the feedhorn with the LNB.

The satellite receiver demodulates and converts the signals to the desired form (outputs for television, audio, data, etc.). Sometimes, the receiver includes the capability to unscramble or decrypt; the receiver is then called an integrated receiver/decoder or IRD. The cable connecting the receiver to the LNBF or LNB must be of the low loss type RG-6, quad shield RG-6 or RG-11, etc. It cannot be standard RG-59 [23].

V. CONCLUSION

Progress in digital video broadcasting standards shows the benefits of digital broadcasting. This offers opportunities for developing countries like Nigeria to explore cooperative efforts to overcome their challenges. Television stations with many remote out-stations can create a private high-speed satellite intranet, which links the main office reliably with all remote VSATs as is the cast of Silverbird Television (STV). These networks, comparable to the corporate or institutional networks of large multinational companies or international institutions, today need high speed, reliable and cost-effective communications. This is especially true when the locations are dispersed over remote regions and barely connectable via a terrestrial network infrastructure as is the case of Silverbird Television whose headquarter is located in Lagos with about six (6) out-stations spread across Nigeria.

REFERENCES

[1] T. Pratt, C . Bostian , J.Allnutt, *"Satellite Communication"* John Wiley and Sons, 2nd Edition.
[2] R. William, *Television: Technology and Cultural Form.* London: Fontana, 1974, pp. 18
[3] E. Trundle, *Newnes Guide to Television and Video*, 3rd ed. Oxford: Newnes, 2001, pp. 49-50
[4] P. Dambacher, *"History of the development of digital Transmission techniques in broadcasting" in Digital Terrestrial Television Broadcasting: Designs, Systems and Operation*, P. Dambacher, Ed. Berlin: Springer, 1998, pp. 1-2
[5] H. Benoit, *Digital Television: MPEG-1, MPEG-2 and Principles of the DVB System*, 2nded. Focal press, 2002, pp. 15

[6] U. Reimers. *"Digital television- a first summary" in DVB The family of International Standards for Digital Video Broadcasting*, 2nd ed. U. Reimers, Ed. Berlin: Springer, pp. 6

[7] T. Kratvochvil, (2008). *"From analogue to digital television-the common way how to digitize European broadcasting."Presented at History of Telecommunications Conference*, 2008. IEEE. [Online]. Available:IEEEXplore, DOI:10.1109/HISTELCON.2008.4668734. [Accessed: 26 Feb. 2013].

[8] Kadish, Jules E. and Thomas W.R. East, *Satellite Communications Fundamentals*, Artech House, Boston, MA, 2001.

[9] Elbert, Bruce R., *Introduction to Satellite Communication* – second edition, Artech House, Boston, MA, 1999

[10] Advantech Wireless Solutions. Available: www.advantechwireless.com/datasheet/govt-enterprise-vsat-solutions.

[11] M. Cominetti, V. Mignone, A. Morello, M. Visintin, (1995). *The European system for digital multi-programme television by satellite, IEEE Transactions on Broadcasting*, [Online]. vol.41 (2), pp. 49-62. Available: IEEEXplore, DOI: 10.1109/11.392832 .[Accessed: 8 Mar. 2013]

[12] B. Bennet, C. Holt, M. Skowrunski, E. Summers, B. Hamilton (2005). *"DVB-S2 benefits for military broadcast systems." Presented at IEEE Military Communications Conference*, 2005. MILCOM 2005. [Online]. Available: IEEEXplore, DOI: 10.1109/MILCOM.2005.1605678. [Accessed: 8 Mar. 2013]

[13] Ibid. 11

[14] B. Labsky and T. Kratochvil(2010). *"DVB-S/S2 satellite television broadcasting measurement and comparison." Presented at 2010 20th International Conference*Radioelektronika (RADIOELEKTRONIKA). [Online]. Available:IEEEXplore, DOI: 10.1109/RADIOELEK.2010.5478588. [Accessed: 8 Mar. 2013]

[15] DVB Project, (2012, July). *Digital Video Broadcasting (DVB); Second Generation Framing Structure, Channel Coding and Modulation Systems for Broadcasting, Interactive Services, News Gathering and other Broadband Satellite Applications*[Online]. Available: http://www.dvb.org/technology/standards/A83_DVB-S2.pdf. [Accessed: 8 Mar. 2013]

[16] *Digital Video Broadcasting (DVB); Framing Structure, Channel Coding and Modulation for Cable Systems.* EN 300 429 V1.2.1, 1998. Edition (1998-04)

[17] *Digital Video Broadcasting (DVB); Frame Structure Channel Coding and Modulation for a Second Generation Digital Transmission System for Cable Systems*, ETSI EN 302 769V1.2.1, 2011. Edition (2011-04)

[18] P. Hasse, D. Jaeger and J. Robert, (2010). *"DVB-C2 – a standard for improved robustness in cable networks." Presented at IEEE 14th International SymposiumonConsumer Electronics (ISCE)*, 2010 [Online]. Available: IEEEXplore, DOI: 10.1109/ISCE.2010.5523733. [Accessed: 10 Mar. 2013]

[19] *Digital Video Broadcasting (DVB); Framing Structure, Channel Coding and Modulation for Digital Terrestrial Television*, ETSI EN 300 744 V1.6.1, 2009. Edition (2009-01).

[20] *Digital Video Broadcasting (DVB); Framing Structure, Channel Coding and Modulation for a Second Generation Digital Terrestrial Television Broadcasting System*, ETSI EN 302 755 V1.3.1. Edition (2012-04)

[21] DVB Project, (2013, Feb). *DVB-C2:2nd Generation Terrestrial The World's Most Advanced Terrestrial TV System.*[Online].Available:http://www.dvb.org/technology/fact_sheets/DVB-T2_Factsheet.pdf[Accessed: 12 Mar 2013]

[22] Silverbird TV, UHF-30 Awka, Nigeria.

[23] *TV Broadcast Solutions, TV Technologies*, DVB. Available: http://www.broadcast-integration.com/115145/Products

American Journal of Engineering Research (AJER)
e-ISSN : 2320-0847 p-ISSN : 2320-0936
Volume-3, Issue-11, pp-213-221
www.ajer.org

Research Paper Open Access

Estimation of Capacity at Un-Signalized Intersections under Mixed Traffic Flow Conditions

[1,]Ramesh Surisetty, [2,]S. Siva Gowri Prasad
[1](Corresponding Author and Post graduate student)
[2*](Assistant Professor)
Department of Civil Engineering, GMR Institute of Technology, Rajam, AP, India

ABSTRACT : *The methodology for the analysis of unsignalized intersections has been established where identical traffic conditions are depending upon the present traffic scenario. There are several attempts made to develop different approaches for the analysis of unsignalized intersections under Mixed, Major and Minor traffic conditions. Conflict technique is a recent development, which is based on practically simplified concept, considering interaction and impact between flows at intersection and using different mathematical models by calibrating their accuracy. In present study, capacity of unsignalized intersection was calculated from Conflict technique. Surveys were conducted in Visakhapatnam, to measure different traffic parameters Volume, Flow and Capacity to this method. Movement capacities were evaluated by using HCM (2000) for comparison with approach wise capacities obtained from conflict technique from different directions on the study area.*

KEYWORDS: *Capacity, Conflict technique, Surveys, Tanner Model, Traffic Parameters, Unsignalized Intersection*

I. INTRODUCTION

The rapid development in India has brought an increase to the cost of living of the citizen. It influenced the travel pattern of the community from their origin to any destination. The development also affects the transportation system as shown by the annual increase in the No. of vehicles on Roads. In India carry different types of vehicles like high speed automobiles, low speed cycles, cycle rickshaws and animal drawn carts. This will lead to complex interaction between the vehicles and study of such traffic behavior needs special attention. This will result in increased interactions between vehicles; then they tend to move in clusters rather than one after the other.

Traffic consists on Indian roads of bi-directional freedom traffic such as two or three wheeled vehicles and uni-directional vehicles such as four wheelers. While the above tend to overtake or turning or crossing or turn right even if a small gap is available. Hence, to determine the intersection capacity traffic engineer requires a clear understanding of gaps being accepted or rejected by various modes of traffic. Besides, in these mixed traffic conditions, users do not usually follow lane discipline and can occupy any lateral position on the road. To prevent traffic accidents, conflicting traffic streams are separated either in space or in time.

There are several types of capacity analysis models for unsignalized T-intersections. Capacity at unsignalized intersection is measured with two methods. First approach consists of Gap Acceptance Procedure (GAP). Second approach consists of Empirical Regression method. GAP method mostly used in United states and European Countries which is based on Critical-Gap acceptance and Follow-up times of vehicles from the minor road. By the Collection of field data and Estimation of Capacity of Minor movements and measures of traffic performance at approaches to Urban major/minor priority junctions. Third approach is the conflict technique with pragmatically simplified concept where the interaction and impact between flows/streams from each approaches of intersection was based on the mathematical formulation.

II. OBJECTIVE AND SCOPE OF PRESENT STUDY

[1] To study the different traffic parameters for conflict technique by using HCM method.
[2] To identify the traffic conflicts in a Major & Minor Streams in a particular intersection or junction.
[3] To know the priorities an intersection/junction by using Mathematical Model.

III. AREA OF STUDY

The major traffic conflicts occur in T-Intersections is identified by Visakhapatnam are:
[1] Urvasi Junction
[2] Kancharpalem Junction
[3] Gnanapuram Junction

IV. DATA COLLECTION AND ANALYSIS

The study of traffic behaviour is useful for traffic engineers to design intersections, for developing traffic control warrants, traffic signal timings, to design the vehicle storage lanes. Data is needed for analysis and understanding of the traffic conditions. The data can be collected by manual method.

This method employs a field team to record traffic volume on the prescribed record sheets. By this method it is possible to obtain data which cannot be collected by mechanical counters, such as vehicle classification, turning movements and counts where the loading conditions or No. of occupants are required. By selecting typical short count periods, the traffic volume study is made by manual counting. Manual counts are typically used for periods of less than a day. Normal intervals for a manual count are 5, 10, or 15 minutes. Then by statistical analysis the peak hourly traffic volumes as well as the average daily traffic volumes are calculated. This method is very commonly adopted due to specific advantages over other methods.

The main objective of this study is to find the capacity of unsignalized intersection using conflict technique and to compare the results with the HCM (2000) procedure, which is based on the gap acceptance procedure. For this the following field observations are necessary.

[1] Travelled distance for each movement on each approach.
[2] Times of arrival and departure at reference lines for each vehicle from each stream.
[3] Approach speed of the vehicles.
[4] Volume at unsignalized intersection movement-wise.

Manual Counts are typically used where,

- Small data samples are required
- Automatic equipment is not available, or the effort and expense of using automated equipment are not justified
- The count period is less than a day

Manual counts are typically used to gather data about the following:

- Turning movements
- Direction of move
- Pedestrian actions

The number of people need to collect data depends on the length of the count period, type of data being collected, number of lanes or cross walks being observed, and traffic volume.

Volume Count Study : To determine the number, movement and classification of roadway vehicles at a given location. The number of observers needed to count the vehicles depends upon the number of lanes in the highway on which the count is to be taken and the type of information desired. The indications in table can be used as rough guides. It is perhaps more desirable to record traffic in each of travel separately and past separate observer for each direction enumerators should be literate persons with preferably middle or matriculation level for the purpose.

Gap Acceptance Study : Pedestrians preparing to cross the roadway must access the gaps in conflicting traffic determine whether sufficient length is available for crossing & decide to cross the road. Following experiments presents a method for collecting field data to identify the minimum usable gap. As if any traffic engineering analysis recognition & definition of the difference between the standard values of the observed values & the observed values increase the accuracy.

Gap Acceptance Capacity Model : This method is based on critical gap acceptance and follow up times of vehicles from the minor road**.** The theory of gap-acceptance is the major concept for unsignalized intersection analysis. The modified Tanner's formula was found to be the most suitable model.Tanner proposed a theoretical model to relate the various parameters connected with the delay problem in dealing with an Intersection of a Major and Minor road and for finding capacity at unsignalized intersections and the expression is as follows:

$$C_p = \frac{q_M(1-\lambda t_p)e^{-\lambda(t_c-t_p)}}{1-e^{-\lambda t_f}}$$

Where,
$\lambda = q_M/3600$ (veh/s)
t_p=minimum headway in the major traffic stream
t_c= critical gap
q_M= number of major stream headway
t_f = follow-up gap respectively

Tables & Figures : Table (1) and Figure (3) shows the maximum number of vehicles in the peak hours is 200 in the direction from Minor Street to Right side in the morning hours and away from complex in the major street in the evening hours.Table (2) and Figure (5) shows the maximum number of vehicles in the peak hours is 212 in the direction from Minor Street to Left side which is obtained in the evening hours.
Table (3) and Figure (7) shows the maximum number of vehicles in the peak hours is 211 in the direction from Minor Street to Right side which is obtained in the evening hours.

V. CONCLUSIONS & RECOMMENDATIONS

[1] The data like Volume, Flow, and Capacity of each type of vehicle can be obtained from the field study where as for gap acceptance models.
[2] Based on the traffic flow measurements, the maximum flow of a stream, the total capacity of an intersection can be calculated.
[3] By Comparing all the 3 T-intersections
[1] The study area of Kancharpalem Junction has shown the Mixed traffic conditions.
[2] The maximum number of vehicles in the peak hours is 212 in the direction from Minor Street to left side which is obtained in the evening hours.
[3] The study area of Gnanapuram Junction has shown the Major Stream.
[4] The maximum number of vehicles in the peak hours is 211 in the direction from Minor Street to right side which is obtained in the evening hours.
[5] The study area of Urvasi Junction has shown the Minor Stream.
[6] The maximum number of vehicles in the peak hours is 200 in the direction from Minor Street to right side in the morning hours and away from complex in the Major street in the evening hours.

[1] The signal should be provide at Kancharpalem and Gnanapuram Junctions.
[2] Critical gap, follow-up time (tc, tf) are Calculated by 3 Junctions within the limit of HCM (2000).
[3] The conflict approach is suitable to calculate the capacity of unsignalized intersections under mixed traffic flow, especially for India as an alternative instead of using the Highway Capacity Manual (2000).

VI. SCPOE FOR FURTHER STUDY

The present work can be extended as indicated below

[1] Pedestrians are not considered in this study, further study can be focused on pedestrian movements along with vehicle movements.
[2] It was recommended to extend the study for more than two hours and the speed can be counted in order to achieve a better prediction.

The equation used for T-junctions and the same can also be used for four-legged intersections which gives more accuracy in data analysis.

REFERENCES

[1] A. ALDIAN, MICHAEL A.P .TAYLOR *"Selecting Priority Junction Traffic models to determine U-turn Capacity at median opening". Proceedings of the Eastern Asia Society for Transportation Studies.Vol.3. No.2, October, (2001).*

[2] HWANG ZUNHWAN, KIM JUMSAN and RHEE SUNGMO *" Development of a New Highway Capacity Estimation Method" Proceedings of the Eastern Asia Society for Transportation Studies, Vol. 5, pp. 984-995, (2005).*

[3] IAN C. ESPADA, TAKASHI NAKATSUJI and YORDPHOL TANABORIBOON *"A Discharge Capacity Formula for Priority T-Intersection and its Application to Macroscopic Simulation of Urban Networks". J Infrastructure Plan and Man JSCE, No.695/IV-54,177-186, January (2002).*

[4] JANUSZ CHODUR *"Capacity Models and Parameters for Unsignalized Urban Intersections in Poland" Journal of Transportation Engineering ASCE/December (2005).*

[5] JANUSZ CHODUR *"Capacity of Unsignalized Urban Junctions" Transportation Research Circular E-C018: 4th International Symposium on Highway Capacity (1998).*

[6] JIAN-AN TAN AND FRANCO TUFO *"A Capacity Analysis Procedure for Unsignalized Intersections in Switzerland" Third International Symposium without Traffic Signals (1997).*

[7] JOEWONO PRASETIJO *"Development of a new method of Capacity Analysis at Unsignalized Intersections under mixed Traffic flow (Preliminary Design for Indonesia)" Proceedings of the Eastern Asia Society for Transportation Studies, Vol. 5, pp. 967-983, (2005).*

[8] MICHAEL KYTE and GEORGE LIST *"A Capacity Model for All-Way Stop-Controlled intersections based on stream interactions" Transportation Research Part A 33 (1999) 313-335.*

[9] MOSHE A. POLLATSCHEK, ABISHAI POLUS and MOSHE LIVNEH *"A Decision Model for Gap-Acceptance and Capacity at intersections" Transportation Research Part B 36 (2002) 649-663.*

[10] NING WU *"Capacity of Shared-Short Lanes at Unsignalized Intersections" Transportation Research Part A 33 255-274 (1999).*

[11] NING WU *"Determination of Capacity at All-Way Stop-Controlled (AWSC) Intersections" (Published in Transportation Research Record 1710, TRB National Research Board, Washington, D.C., USA (2000).*

[12] RAHIM AKCELIK *"A Review of Gap-Acceptance Capacity Models" 29th Conference of Australian Institutes of Transport Research (CAITR 2007), University of South Australia, Adelaide, Australia, December (2007).*

[13] S.SIVA GOWRI PRASAD, RAMESH SURISETTY and SURESH KUMAR CH. *"A Study on Gap Acceptance of Unsignalized intersection under mixed traffic conditions" IJRET Volume.3 Issue: 08, August-2014.*

[14] TIAN ET. AL "Implementing the Maximum Likelihood Methodology to measure a driver's critical gap", Transportation Research, Part A, No.33 pp 187-197 (1999).

[15] UNSIGNALIZED INTERSECTIONS CHAPTER-17 *"Highway Capacity Manual (2000)".*

[16] WAN IBRAHIM, W.H and SANIK M.E *"Estimating Critical Gap Acceptance for unsignalized T-intersection under Mixed Traffic Flow Condition", Proceedings of the Eastern Asia Society for Transportation Studies, Vol.6, (2007).*

[17] WERNER BRILON, NING WU and KERSTIN LEMKE *"Capacity at unsignalized two-stage priority intersections", Transportation Research Part A 33, pp: 275-289 (1996).*

[18] WERNER BRILON, ROD J. TROUT BECK and RALPH KOENIG *"Useful Estimation Procedures for Critical Gaps" 3rd International Symposium on Intersections without Traffic Signals, Portland Oregon, PP. 71-87, July (1997).*

[19] WERNER BRILON and NING *WU "Two Stage Gap-Acceptance Some Clarifications" (Published in Transportation Research Record 1852, TRB National Research Council, Washington, D.C, USA (2003).*

[20] WERNER BRILON and NING WU *"Unsignalized Intersections – A Third method for Analysis" Proceedings of the 15th International Symposium on Transportation and Traffic Theory Australia, pp. 157-178 (2002).*

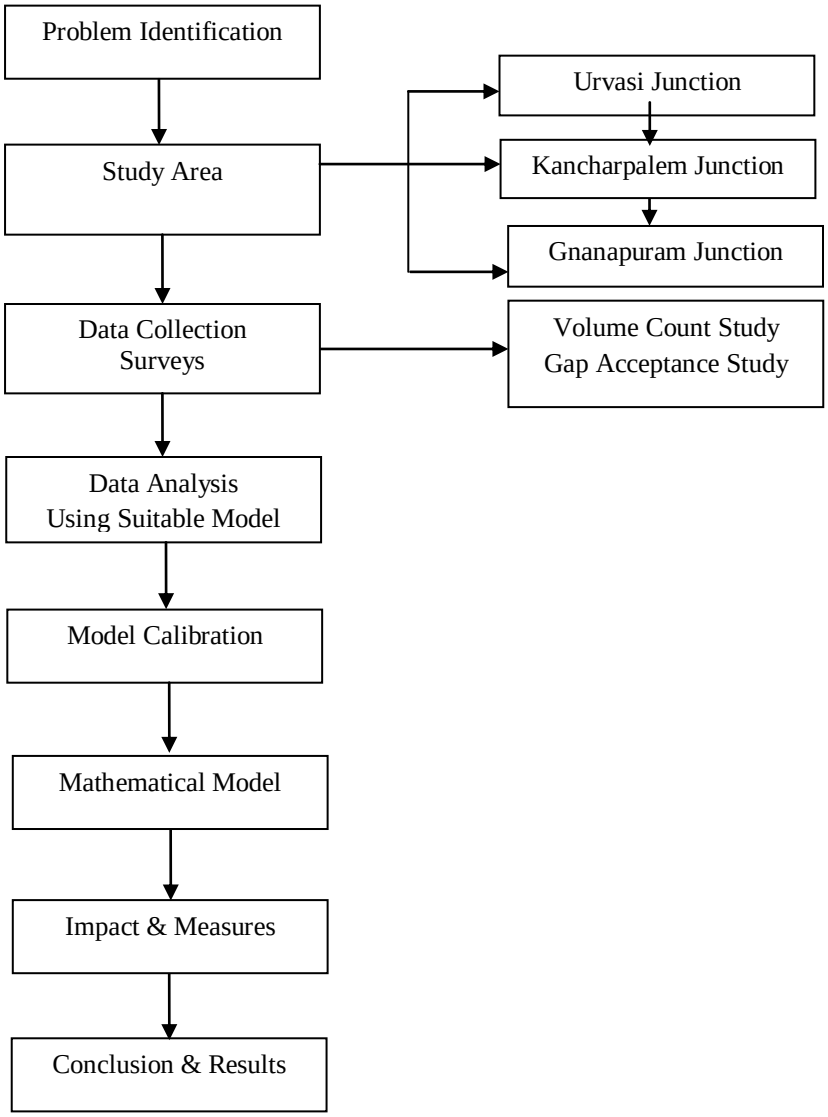

Figure-1 Methodology

(a) (b)

Figure-(a) & (b) Author collecting the traffic data in the study area

Hourly Variations of Traffic in the Study Areas

Table: 1 Comparison of the Peak Hour Traffic Variations at URVASI JUNCTION

Name of the Junction	Conflict	Maximum No. of Vehicles		Maximum values of capacity	
		Morning	Evening	Morning	Evening
Urvasi	Towards Complex	190	189	22.8	58.07
	Left side	182	191	30.6	53.07
	from Complex	187	200	20.49	48.29
	Right side	200	189	20.79	51.8

Figure-2 Site View of Urvasi Junction

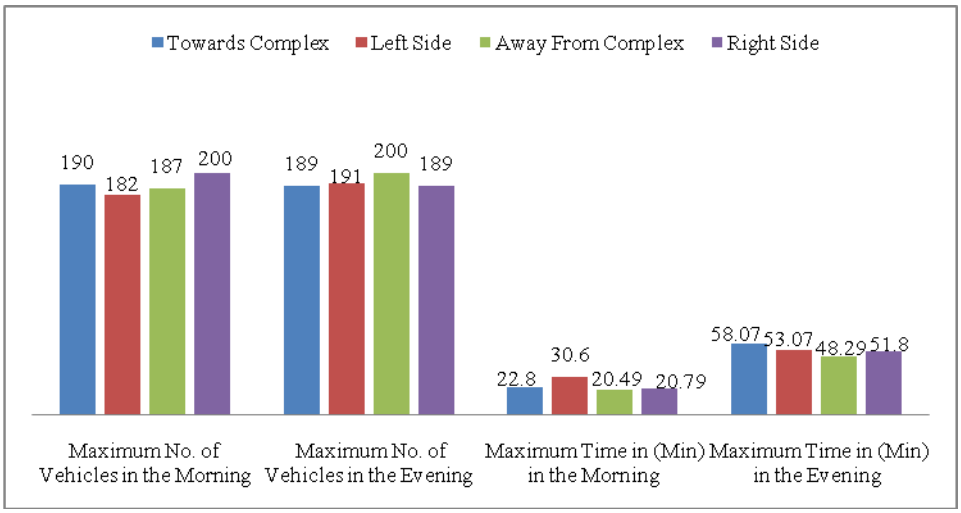

Figure-3

Table: 2 Comparison of the Peak Hour Traffic Variations at KANCHARPALEM Junction

Name of the Junction	Conflict	Maximum No. of Vehicles		Maximum values of capacity	
		Morning	Evening	Morning	Evening
Kancharpalem	Towards Convent	205	196	58.18	33.63
	Left side	197	212	32	31.57
	Away from Convent	191	209	52.98	44.62
	Right side	199	207	58.07	37.23

Figure-4 Site View of Kancharpalem Junction

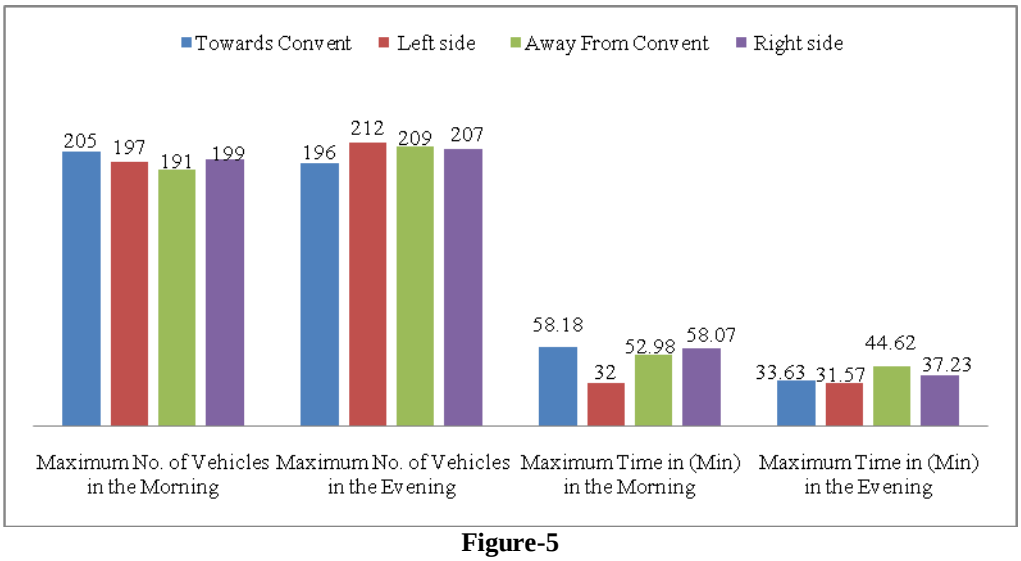

Figure-5

Table: 3 Comparison of the Peak Hour Traffic Variations at GNANAPURAM Junction

Name of the Junction	Conflict	Maximum No. of Vehicles		Maximum values of capacity	
		Morning	Evening	Morning	Evening
Gnanapuram	Towards Dondaparthy	206	196	45.67	57.8
	Left side	206	204	54.03	58.75
	Away from Complex	206	211	29.88	48.1
	Right side	203	198	48.64	60.14

Figure-6 Site View of Gnanapuram Junction

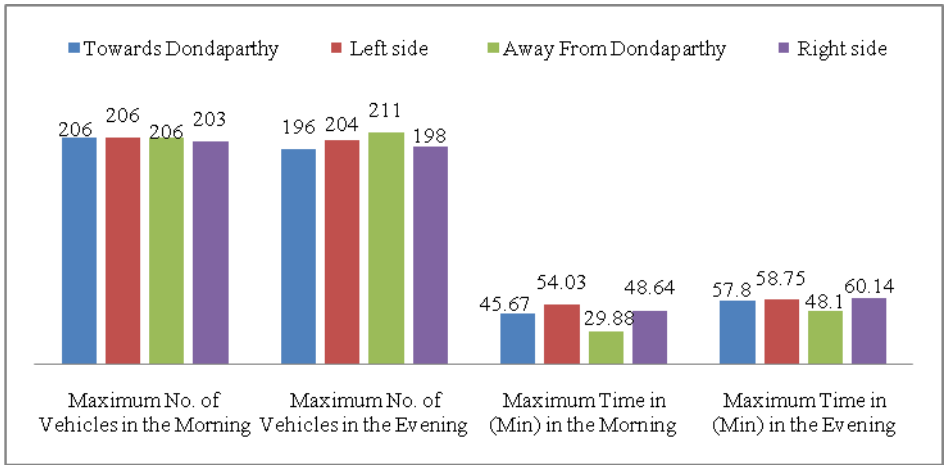

Figure-7

AUTHOR'S BIOGRAPHY:

Ramesh Surisetty, presently pursuing M-Tech Transportation engineering in Department of Civil Engineering, GMR Institute of Technology, Rajam, AP, India. He has a total 2 years of experience in Infrastructure projects.

Mr. S. Siva Gowri Prasad is currently associated as Assistant Professor in Department of Civil Engineering at GMR Institute of Technology, Rajam, A.P, India. He has a total 10 years of experience in Industrial projects and academics.

American Journal of Engineering Research (AJER)
e-ISSN : 2320-0847 p-ISSN : 2320-0936
Volume-03, Issue-11, pp-222-232
www.ajer.org

ResearchPaper Open Access

Multivariable LMI Approach for Robust Control of Tractor Trailer System with State Delay and Parametric Uncertainty

[1,]Shyma Muhammed , [2,]ADolly Mary, [3,]Abraham T Mathew
(Department of Electrical Engineering, National Institute of Technology Calicut India)

ABSTRACT: *The design of controllers for systems which are subject to uncertain time delays is a challenging problem for control engineers. This is due to the potential for closed-loop instability contributed by the uncertainty in the processphase.This paper gives a robust method to control a Wheeled Mobile Robot trailer system with time delay. This articulated vehicle being a complicated non holonomic system, the number of control inputs is less compared to the number of generalized coordinates. A robust H-infinity output feedback controller is synthesized using LMI algorithms for the nominal plant considering the model uncertainties in unstructured form and also the output disturbances. Analysis of the system without the output disturbance, with a first order output disturbance and with a second order output disturbance have been carried out. The simulation results indicate that the WMR trailer system is stable with the proposed LMI H_∞ controller.Also this paper describes a linearized model of WMR trailer system which is highly nonlinear in the presence of output disturbances, uncertainties and time delays.*

KEYWORDS: *LMI,robust control, time delay, tractor trailer, uncertainty.*

I. INTRODUCTION

The Tractor-Trailer system, especially the articulated form that uses several trailers, forms a unique class of control systems because of the variety of control issues existing in the motion of this type of articulated vehicles. In such systems, the complexity in tracing a pre-defined path for the forward and backward movementincreases as the number of trailers increases. These vehicles are assumed to be moving on plane surfaces without any guide ways or rail lines. Thus the controlled motions have to be achieved by the operation of the wheels both for traction as well as steering. Articulated vehicles made of wheeled mobile robots have advantages in terms of their suitability for experimentation. These types of vehicle have nonlinearity in the control loops and there are many constraints. The two wheeled mobile robot can be connected as tractor trailer system so that the effect of steering control for trailer units as a subsidiary control can be studied. It is seen that when the vehicle is having freedom to move without connecting power or data wires linked to it from the terrestrial control station, then we have two constraints: one requirement is to conserve battery and extend the life, and secondly, to communicate from the control station with the WMR drive circuit on board the WMR. This data link could be wireless and packet switched scheme can be employed to make use of the technology of sensor networks. This networking of sensors and controllers may cause time delays in the system model. Hence such a scenario is investigated here.

Control of these articulated systems is ahighly nonlinear problem. Nonlinear control strategies for a WMR based on feedback linearization were proposed in [1-2] where the emphasis was for solving the trajectory tracking and the posture stabilization, by employing the kinematics of the system. Tracking control schemes, where adaptive tracking controllers for kinematic model and adaptive back stepping controllers for dynamic models were designed for nonholonomic mobile robots with unknown parameters [3]. Adaptive control using back stepping designed for tracking reference trajectory and point stabilization were proposed in [4-5] where the asymptotic convergence of tracking error to zero is said to be achieved. A robust tracking control design for wheeled vehicle systems with trailer, based on adaptive fuzzy elimination technique was proposed in [6]. Here, anH-infinity minimax control equipped with adaptive fuzzy elimination scheme is used to achieve a robust tracking performance, despite the parameter uncertainties and external disturbance.

The static control method used requires tuning with constant control law updating when subjected to disturbances. In [7] a robust H-infinity output feedback controller is designed using mu synthesis for a tractor

trailer system subjected to model uncertainties in unstructured form and output disturbances. An LMI based H_∞ design is proposed in [8] for both the steering control and the fault detection. But in all the above cases the effect of time delay was not taken in to account. In the conventional mathematical description of a physical process, one generally assumes that the behavior of the considered process depends on the current process. However, there exist situations where such an assumption is not satisfied and the use of a 'current state' model in analysis would cause a poor performance or even destabilization. These systems are called time delay systems.The performance and stability of a control system can be directly affected by a time-delay located either in its input, output, or both. In the case of a mobile robot, an input time-delaymay become critical in different situations, such as when vision is used as the localization technique and a high frame per second rate is demanded, or when centralized control of multiple agents is desired, or even if very accurate regulation or tracking performance is required [9]. The time delay affects the system due to the fact that the controller and the robot are linked via a delay inducing communication channel, by which the performance and stability of the system are possibly compromised. The time delay can be imposed in transmission of the data between the system components. It is known that the existence of time delay in a system is the main source of instability and poor performance. In previous researches, scattering theory and passivity based control are used to guarantee the stability in case time delay exists [10-11].This paper gives a robust method to control a wheeled mobile robot trailer system with time delay. A robust H-infinity output feedback controller is synthesized using LMI algorithms for the system when subjected to model uncertainties in unstructured form and output disturbances. Analysis of the system without considering the output disturbance and also with a first order and second order output disturbance have been performed for different values of time delays. The simulation results indicate that the WMR trailer system is stable with the proposed LMI H_∞ controller. Also this paper describes a linearized model of WMR trailer system which is highly nonlinear in the presence of output disturbances, uncertainties and time delays.

The remaining part of the paper is organized as follows: In Section 2, system description and problem formulation are discussed. The mathematical modeling of the WMR trailer system with time delay is discussed in Section 3.Section 4deals with the control Design. Section 5deals with theH_∞ control scheme for WMR trailer system.The simulation results are presented in Section 6.Finally, Section 7 concludes the paper followed by the references used.

II. SYSTEM DESCRIPTION AND PROBLEM FORMULATION

Consider a wheeled mobile robot trailer system with time delay described by the state equation

$$\dot{x}(t) = A_1 x(t) + A_d x(t-\tau) + B_1 w(t) + B_2 u(t)$$
$$z(t) = Cx(t) \qquad (1)$$

where$\boldsymbol{x(t)} \in \boldsymbol{R^n}$is the state, $\boldsymbol{u(t)} \in \boldsymbol{R^m}$ is the control input,$\boldsymbol{w(t)} \in \boldsymbol{R^l}$ is the external disturbance, which belongs to $\boldsymbol{L_2[0,\infty]}$ and $\boldsymbol{z(t)} \in \boldsymbol{R^p}$ is the controlled system output.$\boldsymbol{A_1}$,$\boldsymbol{A_d}$,$\boldsymbol{B_1}$,$\boldsymbol{B_2}$and $\boldsymbol{C}$are known constant matrices with appropriate dimensions, $\boldsymbol{\tau > 0}$ is the time delay. One important assumption for completing the description of dynamic system of (1) is that all of the system states are measurable.

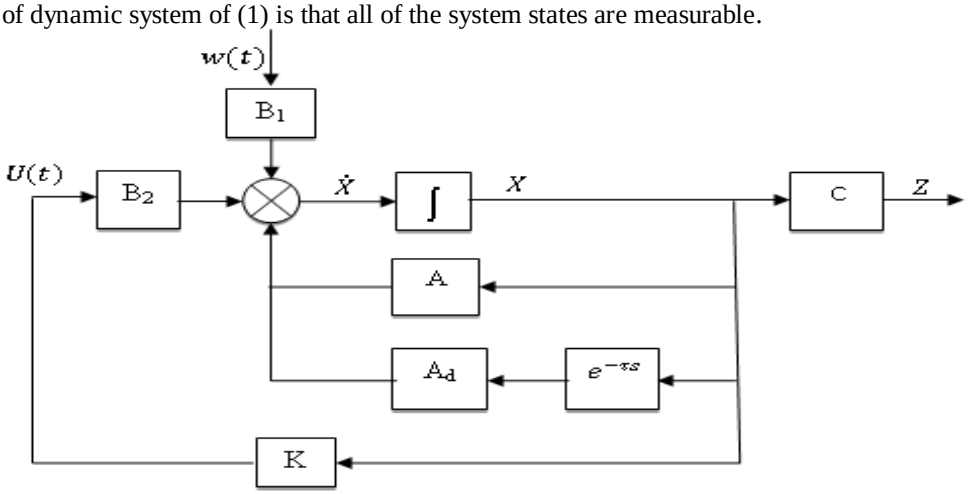

Figure:1. Control scheme for a WMR Trailer time delay system represented by Eqn (1)

The output feedback structure for the proposed Hinfinity control scheme is shown in Fig.2. The system consists of a linear time invariant augmented system *P* which belongs to the class P of uncertain system.*P* comprises the nominal model and weighting functions corresponding to model uncertainties and disturbances. The inputs w and u represents the exogenous and control inputs whereas zandy represent the controlled and measured outputs.

The relation between output and input can be represented as

$$\begin{bmatrix} z \\ y \end{bmatrix} = \begin{bmatrix} P_{11} & P_{12} \\ P_{21} & P_{22} \end{bmatrix} \begin{bmatrix} w \\ u \end{bmatrix} \quad (2)$$

Considering the invariance of the plant P and the separability of the variables for the linear setting, the system has been partitioned into the state space for as given in Eq.(3)

$$\begin{aligned} \dot{x} &= A_1 x + B_1 w + B_2 u + A_d \, \mathrm{x}(\mathrm{t} - \tau) \\ z &= C_1 x + D_{11} w + D_{12} u \\ y &= C_2 x + D_{21} w + D_{22} u \end{aligned} \quad (3)$$

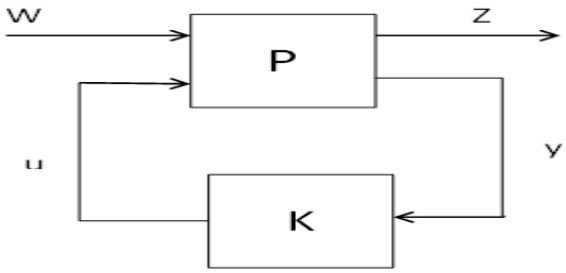

Figure:2. H-infinity feedback control

Assume that (A_1,B_1) is stabilizable; (A,C_1) is detectabl;(A,B_2) is controllable;and (A,C_2) is observable. With a feedback $u=K(s)\,y$, the closed loop transfer function from disturbance w to controlled output z is as in (4)

$$F_l(P,K) = P_{11} + P_{12}K(I - P_{22}K)^{-1}P_{21} \quad (4)$$

With the above cited assumptions, we can obtain a proper real rational controller for the closed loop system so that the system remains internally stable. The control problem is: with a feedback $u=K(s)\,y$, find an admissible internally stabilizing control K which would be attenuating disturbances such that the norm of the stable closed loop system from the disturbances to the controlled outputs is less than γ which is equal to 1 for optimal and slightly greater than 1 for suboptimal control [7]. The control objective is stated in the mathematical form in Eq.(5)

$$\|F_l(P,K)\|_\infty = sup_{\omega \epsilon R} / F_l(P,K)(j\omega) / < \gamma \quad (5)$$

III. MATHEMATICAL MODEL OF THE WHEELED MOBILE ROBOT TRAILER SYSTEM WITH TIME DELAY

The schematic diagram shown in Fig.3 represents the kinematics of the WMR trailer system having time delay. As shown in the figure, there is the front mobile differential drive robot made of rigid body and non-deforming wheels which acts as the tractor. It is assumed that the vehicle moves on a plane without slipping. The robotic tractor has a platform with two driving wheels mounted on the same axis with independent actuators and one free castor wheel for balancing purposes. The mobile robot is steered by changing the relative angular velocities of the driving wheels. The trailer is neither powered nor controlled in its motion.

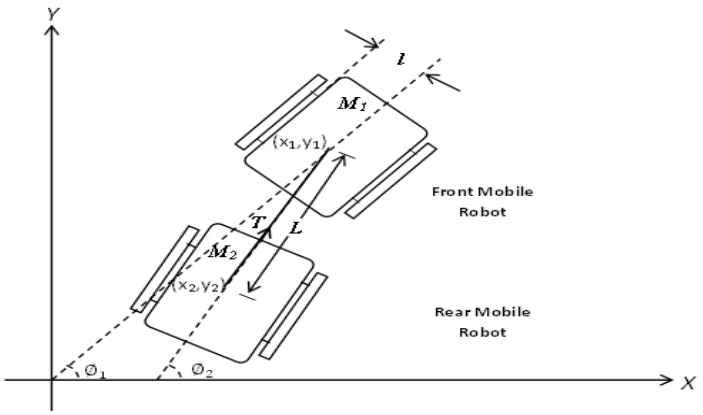

Figure:3. Wheeled mobile robot with trailer

Let the wheeled vehicle with two independent driving wheels be rigid, moving on the plane as shown in Fig. 3, where X-Y indicates the absolute (fixed) coordinates on the plane. The following assumptions are made for dealing with the wheeled vehicle.

Assumptions

1) The running wheeled vehicle satisfies both the pure rolling and non-slipping conditions.
2) The link bar of the wheeled vehicle crosses the centers of gravity of the front and rear wheeled vehicles, i.e.,$d_L = 0$

Under the above assumptions, the model of such wheeled vehicle can be composed of the following equations [12-13].

1) The dynamic equation of the front mobile robot

$$I_v\ddot{\emptyset}_1 - Td_L = D_r l - D_l l \tag{6}$$
$$M_1\dot{v}_1 - T\cos(\emptyset_2 - \emptyset_1) = D_r + D_l$$

2) The dynamic equation of the driving systems for right and left wheels of the front mobile robot

$$I_w\ddot{\theta}_r + c\dot{\theta}_r = ku_r - rD_r \tag{7}$$
$$I_w\ddot{\theta}_l + c\dot{\theta}_l = ku_l - rD_l \tag{8}$$

3) Pure rolling constraints

$$r\dot{\theta}_r = v_1 + l\dot{\emptyset}_1 \tag{9}$$
$$r\dot{\theta}_l = v_1 - l\dot{\emptyset}_1 \tag{10}$$

4) Nonslipping constraints

$$\dot{x}_1\sin\emptyset_1 - \dot{y}_1\cos\emptyset_1 = 0 \tag{11}$$
$$\dot{x}_2\sin\emptyset_2 - \dot{y}_2\cos\emptyset_2 = 0 \tag{12}$$

Or

$$\dot{x}_1 = v_1\cos\emptyset_1 \tag{13}$$
$$\dot{y}_1 = v_1\sin\emptyset_1 \tag{14}$$
$$\dot{x}_2 = v_2\cos\emptyset_2 \tag{15}$$
$$\dot{y}_2 = v_2\sin\emptyset_2 \tag{16}$$

5) Relationships between front and rear wheeled vehicles

$$T = M_2\dot{v}_2 \tag{17}$$
$$v_2 = v_1\cos(\emptyset_2 - \emptyset_1) \tag{18}$$
$$\dot{\emptyset}_2 = -\frac{1}{L}v_1\sin(\emptyset_2 - \emptyset_1) \tag{19}$$

Substituting Eqn(9) &Eqn (10) and its derivatives in Eqn(7)&Eqn(8) we get

$$\frac{I_w}{r}(\dot{v}_1 + l\ddot{\emptyset}_1) + \frac{c}{r}(v_1 + l\dot{\emptyset}_1) = ku_r - rD_r \tag{20}$$
$$\frac{I_w}{r}(\dot{v}_1 + l\ddot{\emptyset}_1) + \frac{c}{r}(v_1 - l\dot{\emptyset}_1) = ku_l - rD_l \tag{21}$$

From Eqn(20) &Eqn(21) we have

$$D_r = \frac{k}{r}u_r - \frac{I_w}{r^2}(\dot{v}_1 + l\ddot{\emptyset}_1) - \frac{c}{r^2}(v_1 + l\dot{\emptyset}_1) \tag{22}$$
$$D_l = \frac{k}{r}u_l - \frac{I_w}{r^2}(\dot{v}_1 - l\ddot{\emptyset}_1) - \frac{c}{r^2}(v_1 - l\dot{\emptyset}_1) \tag{23}$$

Because of the second assumption$d_L = 0$ Eqn(6) becomes

$$I_v\ddot{\emptyset}_1 = D_r l - D_l l \tag{24}$$

Substituting Eqn(22)&Eqn(23) in Eqn(24) we will get

$$(I_v + \frac{2l^2}{r^2}I_w)\ddot{\emptyset}_1 = -\frac{2l^2c\dot{\emptyset}_1}{r^2} + \frac{lk}{r}(u_r - u_l) \tag{25}$$

Again from Eqn(6) we have

$$M_1\dot{v}_1 = T\cos(\emptyset_2 - \emptyset_1) + D_r + D_l \tag{26}$$

With

$$T = M_2\cos(\emptyset_2 - \emptyset_1)\dot{v}_1 + \frac{1}{L}M_2v_1\sin^2(\emptyset_2 - \emptyset_1)v_1 + M_2v_1\sin(\emptyset_2 - \emptyset_1)\dot{\emptyset}_1 \tag{27}$$

SubstitutingEqns (22),(23) & (27) in Eqn(26) ,we have

$$\left[M_1+\frac{2I_w}{r^2}-M_2cos^2(\emptyset_2-\emptyset_1)\right]\dot{v}_1 = \frac{k}{r}(u_r+u_l)-\frac{2c}{r^2}v_1 + \frac{1}{L}M_2\sin^2(\emptyset_2-\emptyset_1)\cos(\emptyset_2-\emptyset_1)v_1+M_2v_1\sin(\emptyset_2-\emptyset_1)\cos(\emptyset_2-\emptyset_1)\dot{\emptyset}_1 \quad (28)$$

From Eqns(13),(15),(19),(25)&(28), the state equations of the above system can be written as

$$\dot{x}_1 = x_5\cos x_3$$
$$\dot{x}_2 = x_5\sin x_3$$
$$\dot{x}_3 = x_6$$
$$\dot{x}_4 = -\frac{x_5}{L}\sin(x_4-x_3)$$
$$\dot{x}_5 = \frac{k}{rP}((u_r+u_l)-\frac{2cx_5}{r^2P}+\frac{M_2}{LP}\sin^2(x_4-x_3)\cos(x_4-x_3)x_5 + \frac{M_2}{P}\sin(x_4-x_3)\cos(x_4-x_3)x_5x_6$$
$$\dot{x}_6 = \frac{lk}{r\vartheta}(u_r-u_l)-\frac{2l^2c}{r^2\vartheta}x_6$$

Where $P = M_1+\frac{2I_w}{r^2}-M_2cos^2(\emptyset_2-\emptyset_1)and\vartheta = (I_v+\frac{2l^2}{r^2}I_w)$.

The nominal parameters of this wheeled vehicle system [14] are shown in Table 1.

Table 1: The nominal parameters of the WMR Trailer system

Parameter	Nominal value
$I_v(kgm^2)$	10
$I_w(kgm^2)$	0.005
$M_1(kg)$	200
$M_2(kg)$	100
$l(m)$	0.3
c(kgm^2/s)	0.05
$r(m)$	0.1
$L(m)$	1.2
K	5

Time delay in WMR system appears in two situations1) In local controller, position signal from robot to sensor and the execute signal from actor to robot cause time delay; 2)In remote network controller, the signal transmission cause time delay. Also the transmission of control error signals from the control center to the robot can cause the delay. So in order to accommodate the time delay of the system, a matrix A_d is also introduced in the system.

Substituting the nominal values of the parameters in the nominal model linearized at a constant velocity of 1m/s yields G_{nom} for the system.Thus the state space representation of the nominal system with time delay can be represented as

$$\dot{x}_n = A_nx_n+B_nu+A_dx(t-\tau)$$
$$y = C_nx$$

Where$A_n = \begin{bmatrix} 0 & 0 & -0.3536 & 0 & 0.7071 & 0 \\ 0 & 0 & 0.3536 & 0 & 0.7071 & 0 \\ 0 & 0 & 0 & 0 & 0 & 1 \\ 0 & 0 & 0.3915 & -0.3915 & 0.285 & 0 \\ 0 & 0 & 0.16 & -0.16 & -0.0075 & -0.1426 \\ 0 & 0 & 0 & 0 & 0 & -0.0892 \end{bmatrix}$ $B_n = \begin{bmatrix} 0 & 0 \\ 0 & 0 \\ 0 & 0 \\ 0 & 0 \\ 0.4437 & 0.4437 \\ 1.4866 & -1.4866 \end{bmatrix}$

$C_n = \begin{bmatrix} 1 & 0 & 0 & 0 & 0 & 0 \\ 0 & 1 & 0 & 0 & 0 & 0 \end{bmatrix}$ $A_d = \begin{bmatrix} 0.3 & 0 & 0 & 0 & 0 & 0 \\ 0.1 & 0.2 & 0 & 0 & 0 & 0 \\ 0.1 & 0 & 0.2 & 0 & 0 & 0 \\ 0.1 & 0 & 0 & 0.2 & 0 & 0 \\ 0 & 0 & 0 & 0 & 0 & 0 \\ 0 & 0 & 0 & 0 & 0 & 0 \end{bmatrix}$

IV. CONTROL DESIGN

In order to synthesize a robust H-infinity output feedback controller using LMI algorithms for the nominal plant when subjected to model uncertainties in unstructured form and output disturbances, the corresponding linear matrix inequalities have to be formulated first. The LMI solvers in MATLAB® are used for solving the inequalities.

Theorem: The system (1) is asymptotically stable and the norm of system transfer function from the disturbance w to the output y, $\|T_{wy}\| <= \gamma, \gamma > 0$, for $\tau > 0$ if there exist real symmetric matrices $P > 0, Q > 0$ satisfying the Arithmetic Riccatti Equations

$$PA + A^T P + Q + PA_d Q^{-1} {A_d}^{-1} P + C^T C + \gamma^{-2} P B_1 {B_1}^T P < 0$$

The above inequality can be expressed as an LMI.

A Lyapunov function candidate for the system represented by Eqn(1) is given by

$$V(x,t) = x(t)^T P x(t) + \int_{t-\tau}^{t} x(\sigma)^T Q x(\sigma) d\sigma \qquad (29)$$

where $P, Q \in R^{nxn}$ are positive definite symmetric matrices [15]. If $P > 0, Q > 0$ satisfies $\dot{V}(x,t) < 0$ for every x satisfying Eqn(1), then the system (1) is stable, i.e., $x(t) \to 0$ as $t \to \infty$

Let $u(t) = Kx(t)$, then the resulting closed loop system is

$$\dot{x} = (A_1 + B_2 K)x(t) + A_d x(t-\tau) + B_1 w(t) \qquad (30)$$

The time derivative of $V(x,t)$ along the trajectory of the system represented by Eqn(30) is given by $L(x,t) = \dot{V}(x,t)$

$$= x(t)^T P[(A_1 + B_2 K)x(t) + A_d x(t-\tau) + B_1 w(t)] + [(A_1 + B_2 K)x(t) + A_d x(t-\tau) + B_1 w(t)]^T P x(t) + x(t)^T Q x(t) - x(t-\tau)^T Q x(t-\tau)$$

Introduce the following performance measure

$$J = \int_0^\infty [z^T(t) z(t) - \gamma^2 w^T(t) w(t)] dt$$

This can be rewritten as $J \le [\int_0^\infty (z^T(t) z(t) - \gamma^2 w^T(t) w(t) + L(x,t)] dt \qquad (31)$

Substituting $z(t)$ and $L(x,t)$ in the Eqn(31), it can be written as

$$J \le \int_0^\infty \{[cx(t)]^T [cx(t)] - \gamma^2 w^T(t) w(t) + x(t)^T P[(A_1 + B_2 K)x(t) + A_d x(t-\tau) + B_1 w(t)] + [(A_1 + B_2 K)x(t) + A_d x(t-\tau) + B_1 w(t)]^T P x(t) + x(t)^T Q x(t) - x(t-\tau)^T Q x(t-\tau)\} dt$$

From this performance measure inequality we get the linear matrix inequality for the system represented by Eqn (1) as

$$\begin{bmatrix} (A_1 X + B_2 Y)^T + A_1 X + B_2 Y + Q & B_1 & (C_1 X)^T & A_d X \\ B_1^T & -\gamma I & 0 & 0 \\ C_1 X & 0 & -\gamma I & 0 \\ X A_d^T & 0 & 0 & -Q \end{bmatrix} < 0 \qquad (32)$$

X>0

Where $X(=X^T), Q$ and Y are the matrices and γ is the H_∞ performance attenuation bound. A_1, A_d, B_1, B_2 and C_1 are known constant matrices with appropriate dimension. Using LMI tool box in MATLAB® we can get suitable matrices X and Y by the MATLAB code X=dec2mat(lmis,xfeas,x) and Y=dec2mat(lmis,xfeas,y). Then a state feedback robust H_∞ controller $u = YX^{-1}x(t)$ can be obtained to guarantee the stability of the system [16].

V. H-INFINITY CONTROL SCHEME

Because of the uncertainty in the system model, the model parameters may not be exact and are subjected to variations. These uncertainties due to the factors like modeling errors, parameter uncertainties and nonlinearities of the system should also be taken in to account while designing a robust controller, so that we get satisfactory control over a wider range of the operating variables. Based on the nominal model and the set of perturbed models in the neighborhood of the nominal model, a formulation of uncertainty is obtained and is represented as the uncertainty weight matrix. The perturbed model is represented in multiplicative input uncertainty form with the mathematical equation,

$$G_p = G_{nom}(I + W_m \Delta_m), \|\Delta_m\|_\alpha \le 1$$

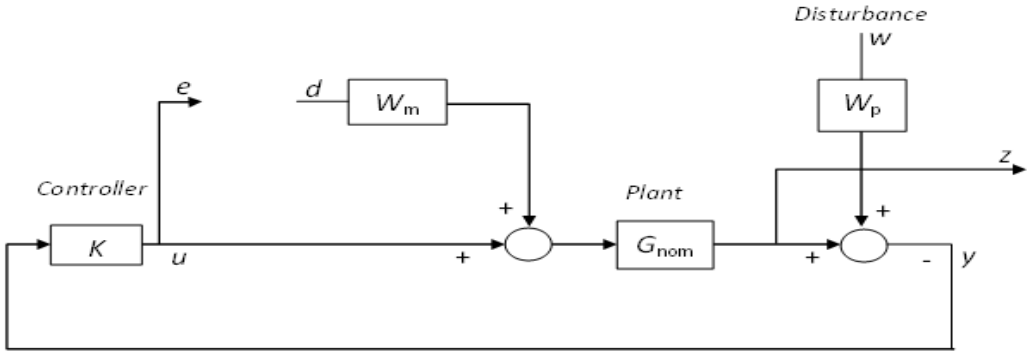

Figure:4. Augmented structure of Wheeled mobile robot with trailer

A suitable value of W_m can be selected in such a way that its magnitude covers all model perturbations. This model uncertainty weighting W_m can be represented as $W_m = C_m(sI - A_m)^{-1}B_m$.Again consider an output disturbance weighting W_p acting on the system which can be represented as$W_p = C_p(sI - A_P)^{-1}B_p$.

The augmented structure of the perturbed plant with Δ_m open is shown in Fig.4. Then the augmented state space representation of the perturbed system is in the form

$$\dot{x} = Ax + B_1 w + B_2 u + A_d x(t-\tau)$$
$$y = C_2 x$$
$$z = C_1 x$$

Where

$$A = \begin{bmatrix} A_n & B_n C_m & 0 \\ 0 & A_m & 0 \\ 0 & 0 & A_P \end{bmatrix} \quad B_1 = \begin{bmatrix} B_n D_m & 0 \\ B_m & 0 \\ 0 & B_p \end{bmatrix}$$

$$B_2 = \begin{bmatrix} B_n \\ 0 \\ 0 \end{bmatrix} \qquad C_1 = \begin{bmatrix} 0 & 0 & 0 \\ c_z & 0 & 0 \end{bmatrix} \qquad C_2 = [-C_n \quad 0 \quad -C_p]$$

VI. SIMULATION RESULTS AND DISCUSSION

In order to establish the effect of time delay in the WMR trailer system, three cases are considered. In the first case there is no output disturbance to the system. In this case the output disturbance weighting W_p becomes zero, and then only the model uncertainty weighting W_m is acting on the system. In the second case a first order output disturbance weighting W_p is acting on the system along with the model uncertainty weighting.

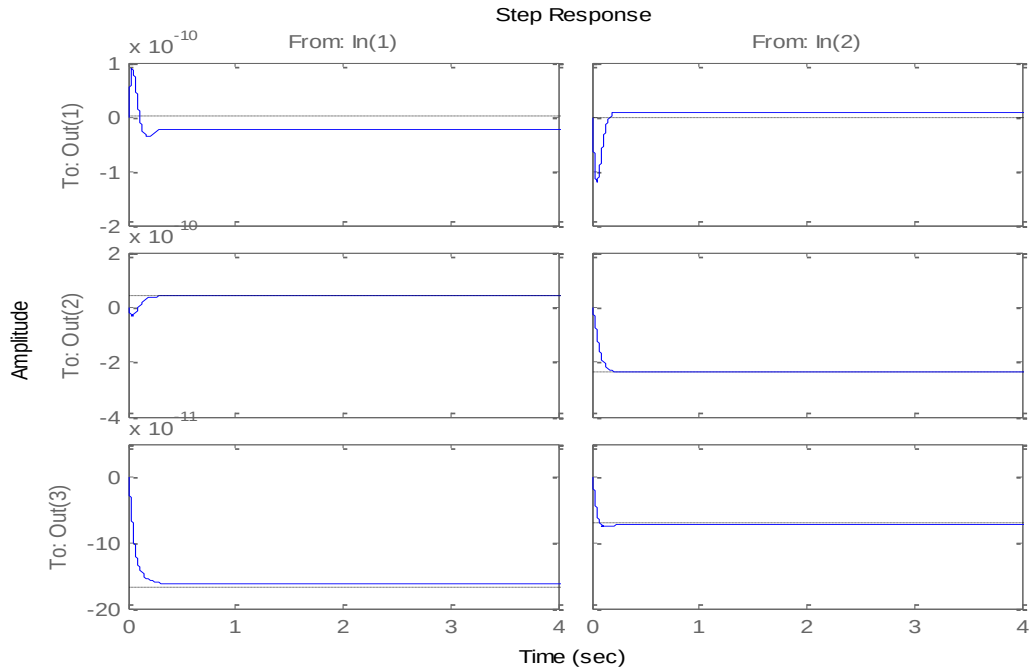

In the third case the output disturbance weighting W_p acting on the system is of second order. For all the above three cases an H-infinity controller is synthesized in MATLAB®with the help of LMI solvers. The closedloop

responses of the system for different values of timedelay are plotted. Fig.5 & Fig.6 shows the closed loop responses of the given WMR trailer system having the time delay 0.1 sec& 0.5 sec respectively. From this

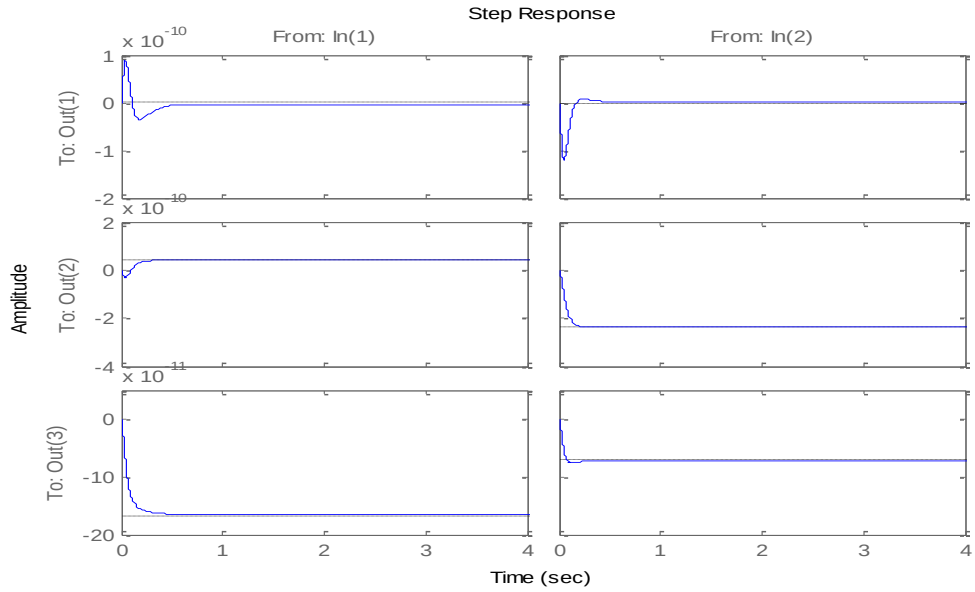

figure it can be seen that the given WMR system is stabilized by the proposed LMI H_∞control.

Figure:5. Closed loop response of the given WMR trailer system with time delay 0.1 sec.

Figure:6. Closed loop response of the given WMR trailer system with time delay 0.5 sec.

Table 2 gives the Performance specification of the above WMR trailer system having different values of time delay .The optimum value of disturbance attenuation bound is obtained as 0.00025.

Table 2 Performance specification of the WMR Trailer system having different values of time delay

Time delay (sec)	Settling time(sec)	Steady state error
0	0.715	0
0.1	0.73	0
0.5	0.527	0
1	0.828	0
2	0.828	0
3	0.828	0
4	0.828	0
5	0.828	0

From the Table 2 it can be seen that, as the value of time delay increases from 0 sec to 0.1 sec, the settling time also increases from 0.715 sec to 0.73 sec. When the time delay becomes 0.5 sec, the settling time decreases to 0.527 sec. As the delay reaches 1sec, the settling time increases to 0.828 sec and then remains constant for different values of delays.

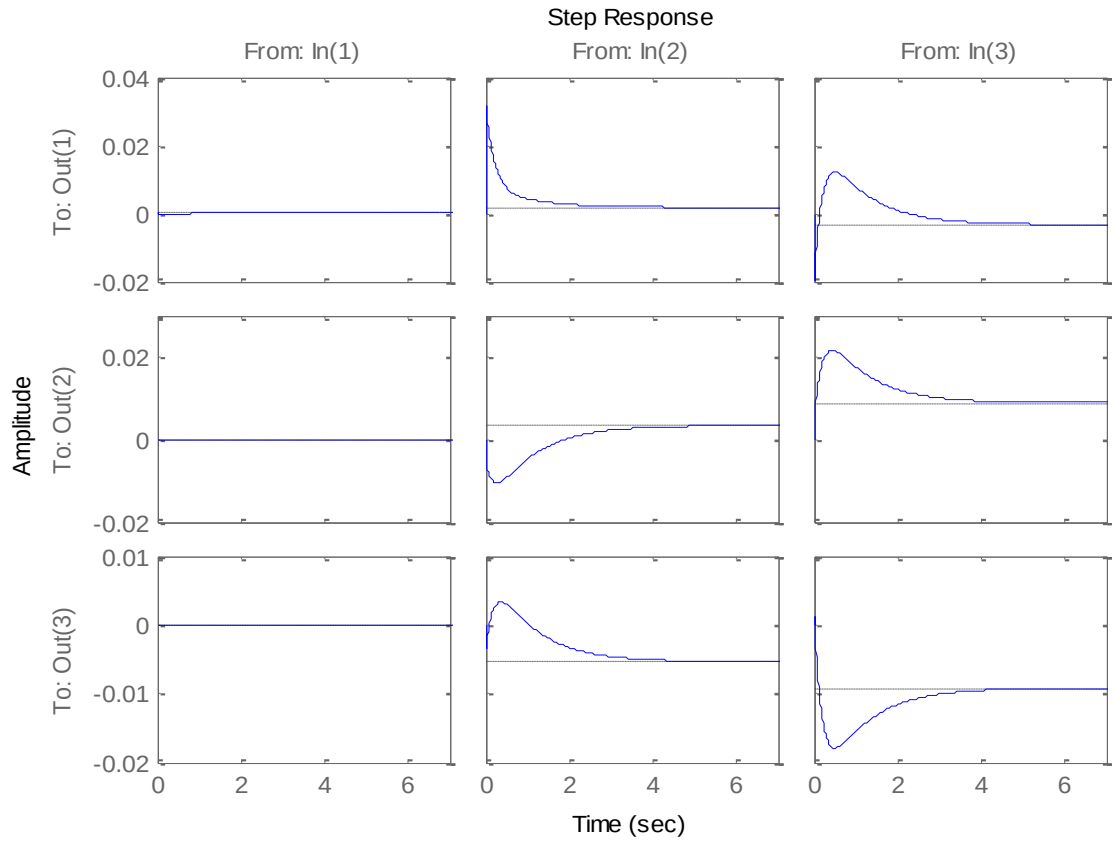

Figure:7. Closed loop response of the given WMR trailer system with $W_p = \frac{.0019s+.6}{s+1}$having no delay

Fig.7 shows the closed loop responses of the given WMR trailer system with$W_p = \frac{.0019s+.6}{s+1}$having no delay. As in the previous case here also it can be seen that the given WMR trailer system is stabilized by the proposed LMI H_∞controller. Table 3 gives the Performance specification of the above WMR trailer systemwith $W_p = \frac{.0019s+.6}{s+1}$ having different values of time delay. The optimum value of disturbance attenuation bound is obtained as 0.2027.

Table: 3 Performance specification of the WMR Trailer system with $W_p = \frac{.0019s+.6}{s+1}$having different values of time delay.

Time delay(sec)	Settling time(sec)	Steady state error
0	4.59	0.00178&-0.0033 0.00337&0.00885 -0.00537&-.00919
0.1	4.59	0.00178&-0.0033 0.00337&0.00885 -0.00537&-.00919
0.5	4.71	0.00178&-0.0033 0.00337&0.00885 -0.00537&-.00919
1	4.99	0.00178&-0.0033 0.00337&0.00885 -0.00537&-.00919
2	5.85	0.00178&-0.0033 0.00337&0.00885 -0.00537&-.00919
3	6.23	0.00178&-0.0033 0.00337&0.00885 -0.00537&-.00919
4	6.29	0.00178&-0.0033 0.00337&0.00885 -0.00537&-.00919
5	6.3	0.00178&-0.0033 0.00337&0.00885 -0.00537&-.00919

From the Table 3 it can be seenthat,the settling time increases as the time delay increases.But the steady state error remains constant for every values of delays

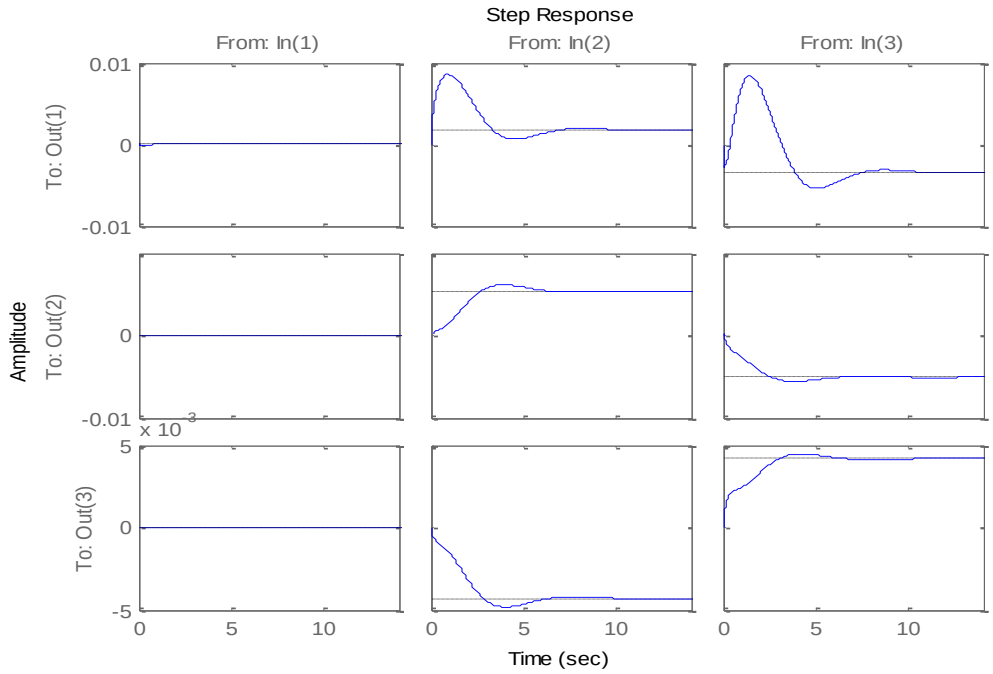

Figure:8. Closed loop response of the given WMR trailer system with $W_p = \frac{.0019s+.6}{s^2+s+1}$ having the delay 0.1 sec.

Fig.8 shows the closed loop responses of the given WMR trailer system with$W_p = \frac{.0019s+.6}{s^2+s+1}$having the delay 0.1 sec. As in the previous case here also it can be seen that the given WMR trailer system is stabilized by the proposed LMI H_∞controller. Table 4 gives the Performance specification of the above WMR trailer systemwith $W_p = \frac{.0019s+.6}{s^2+s+1}$having different values of time delay . The optimum disturbance attenuation bound obtained is 0.1594.

Table 4 Performance specification of the WMR Trailer system with $W_p = \frac{.0019s+.6}{s^2+s+1}$having different values of time delay

Time delay(sec)	Settling time(sec)	Steady state error
0	9.52	0.00179&-0.00343 0.00542&-0.00505 -0.00429&0.00418
0.1	9.53	0.00179&-0.00343 0.00542&-0.00505 -0.00429&0.00418
0.5	9.61	0.00179&-0.00343 0.00542&-0.00505 -0.00429&0.00418
1	9.75	0.00179&-0.00343 0.00542&-0.00505 -0.00429&0.00418
2	9.9	0.00179&-0.00343 0.00542&-0.00505 -0.00429&0.00418
3	10.9	0.00179&-0.00343 0.00542&-0.00505 -0.00429&0.00418
4	11.9	0.00179&-0.00343 0.00542&-0.00505 -0.00429&0.00418
5	13.1	0.00179&-0.00343 0.00542&-0.00505 -0.00429&0.00418

As in the previous case,here also it can be seen that as the time delay increases the settling time also increases, but the steady state error remains constant.It can be seen that even though the robust control of time delay systems are more complicated than that of the system without time delay, the proposed LMI H_∞controller is successful in controlling the WMR trailer system with both delay and uncertain disturbances.

VII. CONCLUSIONS

Robust control of WMR trailer system in the presence of disturbance as well as delay using LMI techniques was discussed here.Also this paper gives a linearized model of the WMR trailer system in the presence of disturbances, uncertainties and delays.A robust H-infinity output feedback controller is synthesized using LMI algorithms for the nominal plant when subjected to model uncertainties in unstructured form and output disturbances.The LMI solvers inMATLAB®were madeuse of for solving the inequalities.Analysis of the system without the output disturbance, with a first order output disturbance and with a second order output disturbance have been performed for different values of delays. The simulation results indicate that the WMR trailer system is stable with the proposed LMI H_∞ controller.

REFERENCES.

[1] GiuseppaOriolo,Alessandra De Luca and MarilenaVendittelli, "WMR Control Via Dynamic Feedback Linearization: Design, Implementation, and Experimental Validation ", *IEEE Transactions on Control Systems Technology*, vol. 10, no. 6, Nov. 2002

[2] Mohammad Eghtesad, Dan S. Necsulescu, "Experimental study of the dynamic based feedback linearization of an autonomous wheeled ground vehicle*", Robotics and Autonomous systems,* vol.47 pp. 47-63, 2004.

[3] TakanoriFukao, Hiroshi Nakagawa and Norihiko Adachi, "Adaptive Tracking Control of a Nonholonomic Mobile Robot", *IEEE Transactions on Robotics and Automation*, vol. 16, no.5,Oct. 2000.

[4] FarzadPourboghrat, Mattias P. Karlsson," Adaptive control of dynamic mobile robots with nonholonomic constraints", *Computers and Electrical Engineering*, vol. 28, pp.241-253, 2002.

[5] Jinbo WU, Guohua XU, "Robust adaptive control for a nonholonomic mobile robot with unknown parameters", *J. Control Theory Appl.* , vol. no. 2,pp. 212-218,2009.

[6] Bor-Sen Chen, Charng-Shi Wu, Huey-JianUang, "A minimax tracking design for wheeled vehicles with trailer based on adaptive fuzzy elimination scheme", IEEE Transactions on Control Systems Technology, Vol. 8, Issue 3, pp. 418-434, 2000.

[7] A Dolly Mary, Abraham T Mathew, Jeevamma Jacob "A Robust H-infinity Control Approach of Uncertain Tractor Trailer System"IETE Journal of Research Vol.59 ,Issue 1 ,pp 38-47,2013

[8] S.Mammar,V.BadalBaghdassarian,D.Koenig "Robust Control and Fault Detection Synthesis with Application to Tractor-Semitrailer Automatic Steering" Proceedings of the 2000 IEEE International Conference on Control Applications Anchorage, Alaska, USA September 25-27, 2000

[9] Alejandro Alvarez-Aguirre "Predictor Based Control Strategy for WheeledMobile Robots Subject to Transport Delay" Eindhoven University of Technology Eindhoven, The Netherlands,2002

[10] Y. Kawai and M. Fujita, "A Design Scheme of Bilateral Teleoperationof Constrained System with Time Delay," IEEJ Transactions onElectronics Information and Systems, vol. 29, no. 9, pp. 1655–1661,2009.

[11] T. Namerikawa, "Bilateral Control with Constant Feedback Gains forTeleoperation with Time Varying Delay," Proceedings of the Joint 48thIEEE Conference on Decision and Control and 28th Chinese ControlConference, pp. 7527–7532, 2009.

[12] Pappas G.J,Kyriakopoulos K.J "Modeling and feedback control of nonholonomic mobile vehicles," *Proc. 31st Conf. Decision Contr.*, Tucson, AZ, 1992, pp. 2680–2685.

[13] K.Watanable, J. Tang, M. Nakamura, S. Koga, and T. Fukuda, "A fuzzy-Gaussian neural network and its application to mobile robot control," *IEEE Trans. Contr. Syst. Technol.*, vol. 4, pp. 193–199, 1996.

[14] Wenping Jiang2008.; Robust H Infinity Controller Design for Wheeled Mobile Robot with Time-delay.*International Conference on Intelligent Computation Technology and Automation*

[15] Boyd S, Ghaoui L, Feron E, and Balakrishnan V (1995) Linear Matrix Inequalities in System and Control Theory Society for Industrial and Applied Mathematics Philadelphia

[16] Gahinet P, Nemirovski A, Lamb A.J and Chilali M, *LMIControlToolbox: for use with MATLAB.* The Mathworks, Inc.Natick, MA. 1995.

American Journal of Engineering Research (AJER)
e-ISSN : 2320-0847 p-ISSN : 2320-0936
Volume-03, Issue-11, pp-233-239
www.ajer.org

ResearchPaper Open Access

Characterization and Optimization of Biodiesel Production from Crude Mahua Oil by Two Stage Transesterification

* Hariram.V[1] and Vagesh Shangar.R[2]
[1,2](Department of Automobile Engineering, Hindustan Institute of Technology & Science, Hindustan University, Chennai, Tamil Nadu, India)
* Corresponding author : connect2hariram@gmail.com

ABSTRACT : *Biodiesel production from Mahua seed was experimentally investigated in the present study. Expeller method was employed to extract mahua oil from its seed and was subjected to two stage transesterification due to the presence of more than 18% of free fatty acid content. In the primary stage, the FFA content was reduced to less than 2% by acid esterification using concentrated H_2SO_4 and methanol and followed by base catalyzed transesterification to convert the vegetable oil into biodiesel. The properties like density, viscosity, Calorific value, flash and fire point were analyzed and compared with other prominent biodiesel. GC/MS and FT-IR analysis were also studied to identify and confirm the presence of fatty acid methyl esters. The yield of mahua oil biodiesel was compared with reaction time and molar ratio at various temperatures and 65^oC was found to optimum for the production of biodiesel.*

KEYWORDS : *Transesterification, biodiesel, molar ratio, free fatty acid, viscosity*

I. INTRODUCTION

Petroleum diesel fuels have been found to have a very important role in the world economy. Nowadays vegetable oils show potential replacement for petro diesel due to the absence of sulphur content and friendly storage. The viscosity of Trans-esterified vegetable oil blends was found to be very close with petroleum diesel with enhanced lubricating properties. The biodegradability, non-toxicity and renewability make the vegetable oil biodiesel more suitable to be used with diesel in Internal Combustion engines. The usage of vegetable oil also helps in higher international exchanges and also contributes to carbon di-oxide sequestration and thereby helps in green house effect [1, 2]. Vegetable oil on comparison with conventional fossil fuel emits lesser quantity of unburned hydrocarbons, Particulates and Oxides of nitrogen and carbon.

The Production of biodiesel with high fatty acid contents was carried out by two step pretreatment process in which Sulphuric acid was used as a primary catalyst. In the second step methanol and Potassium hydroxide were used to produce Mahua oil biodiesel at 60°C. The comparisons of molar ratio to methanol, amount of catalyst and reaction temperature were investigated to produce palm oil biodiesel at 95°C for nine hours. It was found that the addition of Butanol enhanced the biodiesel production up to 90% with higher cetane number [4] .The rubber seed oil was found to be a promising alternative to petroleum diesel. The FFA content of rubber seed oil was found to be very much higher which was reduced to less than 2% in two step acid alkaline catalyzed transesterification process which ultimately produced fatty acid methyl esters and glycerol at the end of the reaction. The calorific value of rubber seed oil was found to be 14% less than petroleum diesel with similar other physio-chemical properties with diesel [14]. The two stage acid esterification and base esterification was carried out to produce biodiesel from Jatropa curcas L oil. Since the FFA content was more than 16%,the biodiesel yield was only less than 50% with lesser stability.$H_2SO_4$was treated as a catalyst at 60°C for 1 hour which reduced the FFA content to less than 2% and a highly stable Jatropha biodiesel was obtained at an yield of 96% [18]. The Mahua seed is found enormously in India especially in tribal and forest regions. The kernels of Mahua seed were estimated to produce nearly 35 to 45 % of oil depending upon the growth and geographical factors which is highly viscous at room temperature.

To reduce the viscosity, various methods can be employed namely heating, thermal cracking, pyrolysis, dilution and Transesterification [16]. Generally Mahua oil biodiesel was obtained by employing two stage transesterification with Acid/base catalyst, biocatalyst and supercritical Methanolysis process. The two stage trans-esterification process comprises of primarily Acid esterification to reduce the Free Fatty Acid contents and base catalyzed esterification to convert the vegetable oil into Fatty Acid Methyl ester [15-17]. In the present study, mahua seed was used to extract mahua oil by expeller process. A two step trans-esterification process was employed comprising of acid catalyzed esterification and base catalyzed esterification to convert mahua oil with higher FFA content into its corresponding biodiesel. During the transesterification reaction, Sodium hydroxide and methanol were mixed to form sodium methoxide for the production of Mahua Oil Methyl Esters. The fatty acid methyl esters were subjected to Gas chromatography/Mass Spectrometry analysis and Fourier Transform Infrared technique to identify the various FAMEs present in it. The physio chemical properties of mahua oil biodiesel was also analyzed and found within ASTM standards. An optimization study was also conducted by varying parameters like Molar ratio, reaction time, Reaction temperature and quantity of Methanol and Sodium hydroxide.

Nomenclature and Abbreviations	
GC/MS	Gas chromatography/ Mass spectrometry
FT-IR	Fourier Transform Infrared Spectroscopy
FFA	Free Fatty acid
FAME	Fatty Acid Methyl Ester
ASTM	American Society of Testing Materials
NIST	National Institute of Standards and Testing
v\v	Volume to volume ratio
w/w	Weight to weight ratio
KOH	Potassium hydroxide
NaOH	Sodium hydroxide
CO	Carbon monoxide
OH	Hydroxide
MJ	Mega joule
H_2SO_4	Sulphuric acid

II. MATERIALS AND METHODS

The Mahua seeds were collected from Thanjavur district of Tamil Nadu and maintained with less than 6% of moisture. Expeller process was used to extract mahua oil at the quantity of 350 ml per kg of mahua seed. It was found that the free fatty acid content was about 18% by titration method. The properties of raw Mahua oil and Mahua biodiesel were determined and can be seen in Table 1 and 2 and the pictorial view of raw Mahua oil extracted and Mahua biodiesel can be seen in Fig (2). A two stage esterification process was employed with Acid esterification followed by base catalyzed esterification. The pretreatment and Transesterification experiments were conducted in laboratory conditions which consisted of 1000 cc inverted neck flask with air tight conditions. The reaction environment was maintained between room temperature and 65°C with 5% Concentrated Sulphuric acid and 0.36 v/v methanol to oil ratio. The reactant mixture was continuously stirred at 450 rpm for about 90 minutes with an interval of 15 minutes. The acid value was continuously monitored at these intervals by titration method till the optimum value was achieved. The pretreatment process was followed by base catalyzed reaction in which a molar ratio of 1:6 (oil to methanol molar ratio) was employed.0.8% (w/w of Sodium hydroxide to oil) was used as a catalyst to treat and neutralize the fatty acids [3,13].

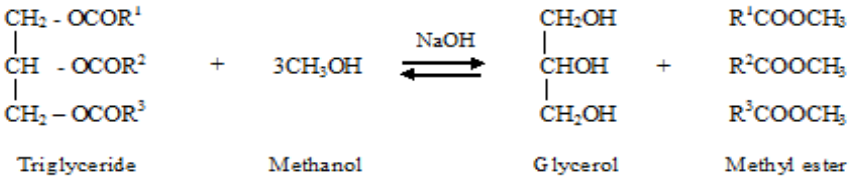

Fig 1. Transesterification reaction of Mahua oil biodiesel

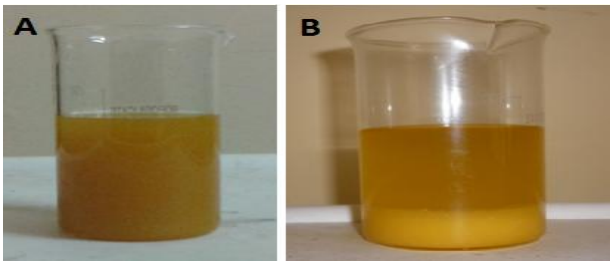

Fig 2. Comparison of Raw Mahua oil (A) with trans-esterified Mahua oil biodiesel (B)

Table 1
Comparison of Physio-Chemical Properties of Raw Mahua oil with diesel and vegetable oil

Properties	ASTM D6751	Straight Diesel [a]	Mahua Oil	Jatropha Oil [b]	Rubber seed oil [c]
Density at 15°C (Kg/m³)	860-900	839	955	912	910
Kinematic viscosity at 40°c(mm^2/s)	1.9-6.0	3.18	24.58	8.72	66.2
Calorific value (MJ/Kg)	……..	44.8	36	40	37.5
Flash point (°c)	Min 130	68	232	125	198
Carbon residue (%)	……..	0.1	3.7	…..	….
Ash content(%)	<0.02	0.01	0.9	…..	….
Acid value, mg KOH	<0.8	0.35	38	10.47	34
Cetane number	……..	51	……	57	……

[a]Sinha et al(2008),[b]Deng.X et al(2010),[c]Ramadhas et al(2005)

The reaction was carried out in a 1000cc inverted glass funnel as a separator which separates fatty acid methyl esters and glycerol as given in Scheme 1.The Transesterified Mahua biodiesel along with glycerol settlement is shown in the Fig 2. Gas chromatography and Mass spectrometry analysis was performed on the fatty acid methyl esters using JEOL GC MATE II and the FAME's were identified as given in the Table 3 and Fig 3. The Fourier Transform Infra red analysis was also performed on the sample to confirm the presence of fatty acid methyl esters as given in Fig 4. The physio chemical properties like density, viscosity, flash point, fire point, calorific value, carbon residue, ash content, acid value, cetane number were determined and found to be within ASTM standards as shown in Table 2 [6,7].

Table 2
Comparison of Physio Chemical Properties of Mahua Oil Methyl Ester with other biodiesel

Properties	ASTM D6751 Biodiesel	Straight diesel [a]	Mahua Biodiesel	Jatropha biodiesel [b]	Rubber seed oil Biodiesel [c]
Density at 15°C (Kg/m³)	860-900	839	872	880	874
Kinematic viscosity at 40°c(mm^2/s)	1.9-6.0	3.18	3.9	4.328	5.81
Calorific value (MJ/Kg)	…….	44.8	39	40	36.5
Flash point (°c)	min 130	68	205	140	130
Fire point (°c)	min 145	103	218	155	145
Carbon residue(%)	…….	0.1	0.2	0.25	0.24
Ash content(%)	<0.02	0.01	0.02	0.02	0.02
Acid value, mg KOH	<0.8	0.35	0.5	0.32	0.118
Cetane number	…….	51	52	57	54

[a]Sinha et al(2008),[b]Raheman et al(2005),[c]Ramadhas et al(2005).

Characterization of Biodiesel : Gas chromatography /Mass spectrometry analysis and Fourier Transform Infrared analysis were employed to study the Trans esterification reaction. JEOL GC MATE II data system equipped with a double focusing and high resolution impact helium gas was used as a carrier. The time range was 60 to 600 ionizations. The scan range of FTIR spectrometry was found to be MIR 450 to 4000 cm^{-1} and the resolution was 1.0cm^{-1}.The biodiesel samples were injected at a particular time intervals and its corresponding peaks for the presence of monoglycerides, triglyceride, glycerol and other methyl esters were compared with NIST library as given in Table 3 [17]. In the FT IR analysis as shown in Fig.4, a strong signal was identified in between wave numbers 1500 cm^{-1} to 2000 cm^{-1} which confirmed the presence of fatty acid methyl esters. A group of carboxylic acid compounds was found between 2855 cm^{-1} and 2926cm^{-1}.Aliphatic chloro and fluoro compounds were found between 723 cm^{-1} and 1117 cm^{-1}.The presence of alcohols with OH and CO stretch were also seen [8].

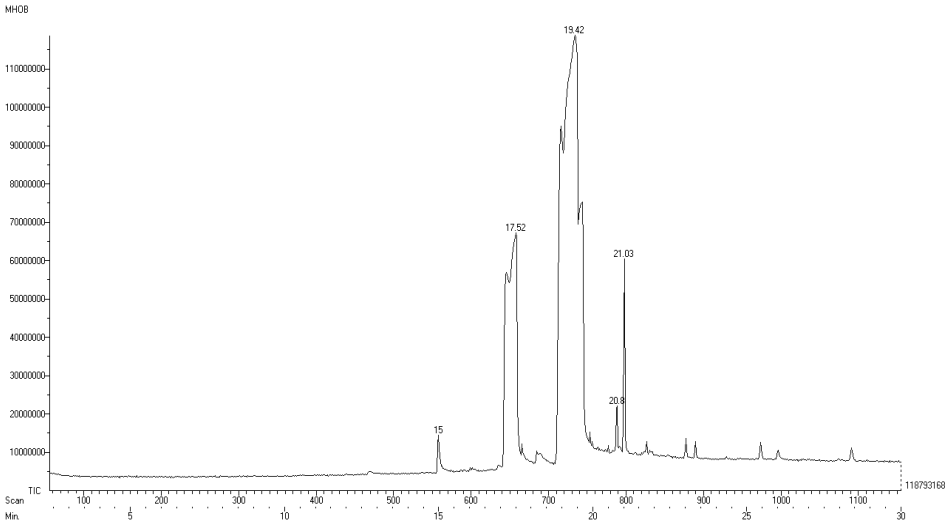

Fig 3. GC/MS Mass Spectrum of Mahua Biodiesel

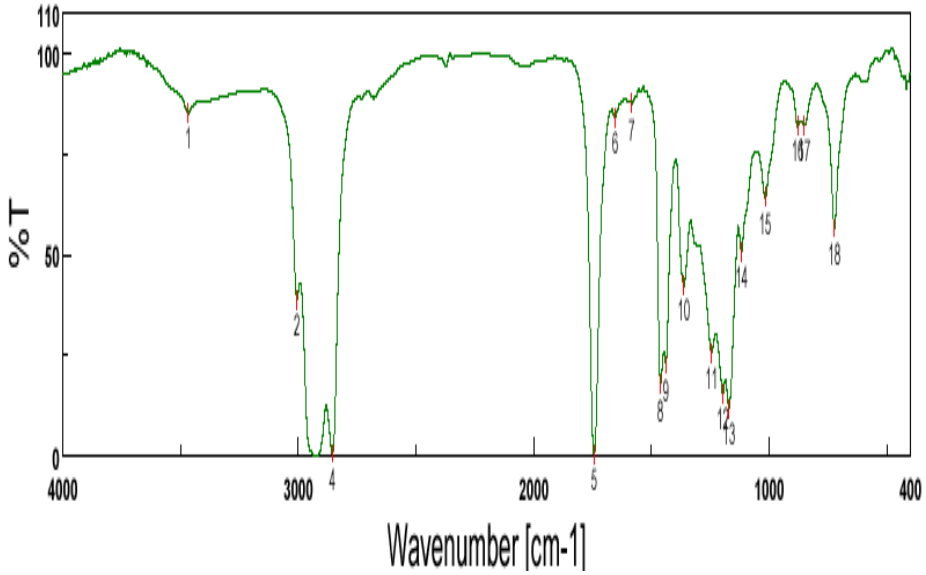

Fig 4. Fourier Transform Infrared spectrum of Mahua Biodiesel

Table 3
Composition of Fatty Acid methyl ester in Mahua biodiesel

Peak No	Retention time(min)	Description of the ester	Name of the Acid	Chemical formulae	Scan	Ions
1	15.00	Tridecanoic acid 12 methyl methyl ester	Pentadecanoic acid	$C_{15}H_{30}O_2$	558	1716
2	17.57	Pentadecanoic acid 14 methyl methyl ester	Margaric Acid	$C_{17}H_{34}O_2$	660	3262
3	19.72	10 Octadecanoic acid Methyl ester	Nonadecylic acid	$C_{19}H_{36}O_2$	746	3223
4	20.80	Methyl 9,12 epithio 9,11 octadecanoate	Palmitic acid	$C_{16}H_{32}O_2S$	789	2237
5	21.50	Mono(2,2,6,6-tetramethyl-4-piperidinyl) ester	Decanedioic acid	$C_{19}H_{24}NO_4$	799	2535

III. RESULTS AND DISCUSSION

Acid Catalyzed esterification : The Fig 5 shows the variation of FFA with reaction time at various reaction Temperatures. The Acid value of Mahua oil was initially found to be 18% (36mgKOH/g) which makes the Mahua oil unsuitable for engine operation. The raw Mahua oil was treated with 3.5% (v/v) of Concentrated H_2SO_4 and 0.35(v/v) of Methanol to oil ratio. The pretreatment reaction was carried out at room temperature, 50°C and 60°C with the above said composition of Methanol and Concentrated H_2SO_4. At room temperature the conversion efficiency was only 50% and with increase in reaction temperature, the FFA content was brought down to less than 2% as shown in the Fig 5 which may be due to formation of moisture at elevated temperatures. The Methanol to oil at 0.35(v/v) at 65°C for 90 minutes reaction was found to be optimum to reduce the free fatty acid content [5].

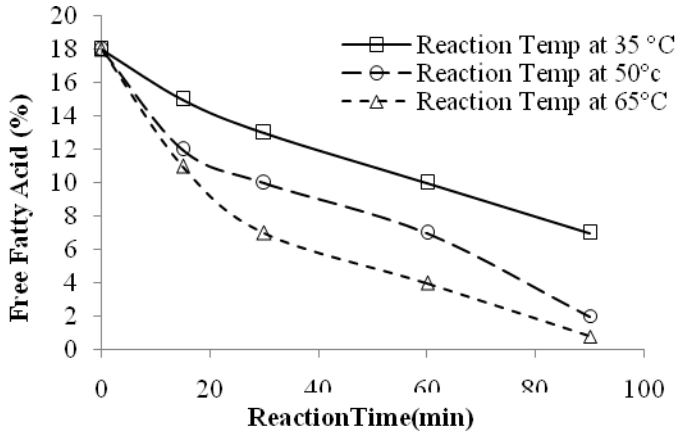

Fig 5. Effect of Reaction time on FFA reduction

Base Catalyzed Transesterification: The base catalyzed transesterification reaction was carried out at various molar ratios of 3:1,6:1 and 9:1.The reaction temperatures were maintained at 35°C,50°C and 65°C and methanol was mixed in the proportions of 0.29 (v/v) with 0.8% of Sodium hydroxide to form Sodium meth-oxide and the entire mixture was mixed with acid esterified oil. The mixture was stirred at 450 rpm using a magnetic stirrer for 2 hours to neutralize the triglycerides into fatty acid methyl esters and glycerol was obtained as by product. At 35°C the yield of biodiesel was found to be 77% for 90 minutes at molar ratio 1: 6 as shown in Fig 6 whereas at 50°C and 65°c the yield of biodiesel was found to be 82% and 89% respectively.

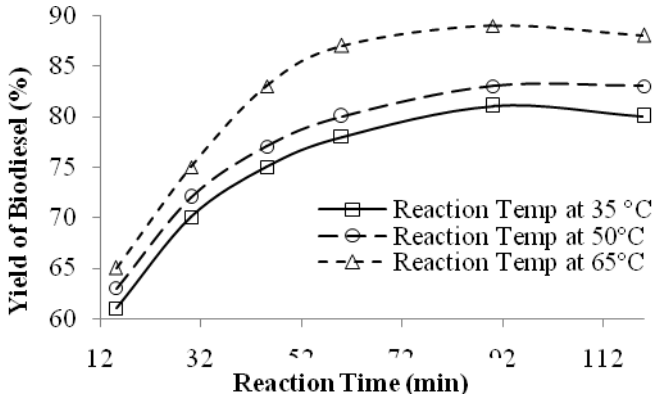

Fig 6. Effect of Reaction time on Biodiesel yield

The optimum yield of biodiesel was noticed at 65°C reaction temperature for a continuous stirring of 90 to 100 minutes as shown in Fig 6 . At higher reaction temperature (more than 65°C), the transesterification reaction was found to deteriorate which may be due to methanol evaporation [10,12] .

3.3 Effect of Methanol to oil molar ratio on Biodiesel yield

The Fig 7 shows the variation in the yield of biodiesel with molar ratios at 35°C,50°C and 65°C reaction temperatures respectively. It can be seen that at 35°C reaction temperature the conversion efficiency of oil to biodiesel was found to be 77% at molar ratio 3:1.The conversion efficiency showed a slight increase up to 82% at the molar ratio 6:1 and with further increase in molar ratio, the biodiesel yield was found to decrease gradual manner.

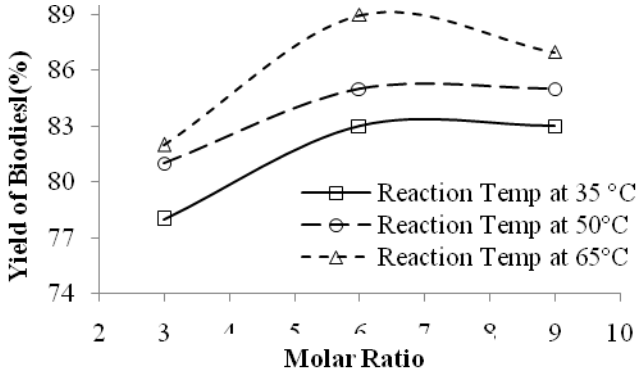

Fig 7. Effect of Methanol to oil molar ratio on Biodiesel yield

On increase in the reaction temperature to 50°C and 65°C the yield of biodiesel showed a noticeable increase up to 84% and 89% respectively at 6:1 molar ratio as shown in the Fig 7.Further increase in methanol showed no significant yield of biodiesel. The excess methanol added during the process has been removed by fractional distillation continued by washing [11].

IV. CONCLUSION

The expeller method was found to be suitable for extracting Mahua oil at 350 ml per kg of Mahua seed. Using titration technique, the free fatty acid content of mahua oil was found to be 18% which was reduced to less than 2% by acid esterification in which 5% of concentrated Sulphuric acid and methanol were added. The base catalyzed transesterification with sodium hydroxide and methanol at molar ratio of 1:6 was found to be very effective which yielded 89 % of biodiesel. The biodiesel production was optimized with reaction temperature, reaction time and molar ratio in which the reaction temperature of 65°C yield more than 85% of

mahua oil biodiesel than 35^{o}C and 50^{o}C of reaction temperature. The Mahua oil biodiesel was characterized using Gas chromatography Mass spectrometry and Fourier transform Infrared techniques in which Pentadecanoic acid, Margaric Acid, Nonadecylic acid, Palmitic acid and Decanedioic acids were found in prominent quantities.

V. ACKNOWLEDGEMENT

The author would like to thank Sophisticated Analytical Instrumentation Facility (SAIF) and Department of Chemistry in Indian Institute of Technology Madras and ITA lab, Chennai for their support in analyzing the fuel properties.

REFERENCES

[1] Agarwal AK. Vegetable oil versus Diesel fuel: development and use of biodiesel in a compression ignition engine. *TIDE* 1998;8(3):191-204.
[2] Bryan R. Moser. Biodiesel production, properties, and feed stocks. Springer In Vitro Cell.Dev.*Biol-Plant* 2009: 45:229–266
[3] Demirbas A. Biodiesel fuels from vegetable oils via catalytic and non-catalytic supercritical alcohol transesterification and other methods: *Energy Conversion and Management* 2003;44:2093–109.
[4] Edward Crabbe, Cirilo Nolasco-Hipolito, Genta Kobayashi, Kenji Sonomoto, Ayaaki Ishizaki. Biodiesel production from crude palm oil and evaluation of butanol extraction and fuel properties. *Process Biochemistry* 2001: 37 : 65–71.
[5] Ghadge SV, Raheman H. Procees optimization for biodiesel production from mahua oil using response surface methodology.*Biores Technol* 2005.
[6] Hariram V and Mohan Kumar G. Identification and characterization of FAME's in Algal oil methyl ester using FT IR,NMR, and GC/MS. *International Journal of Emerging trends in Engineering and Development* 2012: Issue 2 Vol 5 :653-662.
[7] Jefferson S de Oliveiraa, Polyanna M Leitea, Lincoln B de Souzaa, Vinı´cius M Melloa, Eid C Silvab, Joel C Rubima, Simoni M.P, Meneghettib, Paulo A.Z Suareza. Characteristics and composition of Jatropha gossypiifolia and Jatropha curcas L. oils and application for biodiesel production. *Biomass and Bioenergy* 2009 :33: 449 – 453.
[8] Ji-Yeon Park & Deog-Keun Kim & Zhong-Ming Wang, Pengmei Lu & Soon-Chul Park & Jin-Suk Lee Production and Characterization of Biodiesel from Tung Oil, *Appl Biochem Biotechnol* 2008: 148:109–117.
[9] McLafferty. Mass Spectrometric Analysis, molecular arrangement, *Anal.Chem* 1959:31:82-87.
[10] Ma F, Hanna MA. Biodiesel production: a review. *Bioresource Technology* 1999:70:1-15.
[11] Meher LC, Naik SN, Das LM. Methanolysis of Pongamia pinnata (karanja) oil for production of biodiesel. *Journal of Scientific & Industrial Research* 2004:63 : 913-918.
[12] Patni Neha, Bhomia Chintan, Dasgupta Pallavi and Tripathi Neha. Use of Sunflower and Cottonseed Oil to prepare Biodiesel by catalyst assisted Transesterification. *Research Journal of Chemical Sciences* 2013:Vol. 3(3), 42-47.
[13] Padhi SK, Singh RK. Optimization of esterification and transesterification of Mahua (Madhuca Indica) oil for production of biodiesel. *J.Chem.Pharm.Res*. 2010,2(5):599-608.
[14] Ramadhas AS, Jayaraj S, Muraleedharan C. Biodiesel production from high FFA rubber seed oil. *Fuel* : 2005:84: 335-340.
[15] Rajesh Kumar K, Channarayappa, Prasanna KT, Balakrishna Gowda .Evaluation of Aphanamixis polystachya(Wall.) R. Parker as a potential source of biodiesel. *J Biochem Tech* 2012: 3(5): S128-S133.
[16] Shashikant Vilas Ghadge, Hifjur Raheman. Biodiesel production from mahua (Madhuca indica) oil having high free fatty acids. *Biomass and Bioenergy* 28 2005:601 –605.
[17] Shailendra Sinha, Avinash Kumar Agarwal, Sanjeev Garg. Biodiesel development from rice bran oil: Transesterification process optimization and fuel characterization. *Energy Conservation and Management* 2008:49 : 1248-1257.
[18] Xin Deng, Zhen Fang, yun-hu Liu.Ultrasonic transesterification of Jatropha curcas L.oil to biodiesel by a two-step process. *Energy Conservation and Management* 2010 : 51 : 2802-2807.

American Journal of Engineering Research (AJER)
e-ISSN : 2320-0847 p-ISSN : 2320-0936
Volume-03, Issue-11, pp-240-244
www.ajer.org

ResearchPaper Open Access

Characterization of Garko and Kura Rice Husks

O.A Oyelaran[1], Y.Y. Tudunwada[2],
Department of Research and Development,
Hydraulic Equipment Development Institute, Kano-Nigeria
Department of Business technology Development,
Hydraulic Equipment Development Institute, Kano-Nigeria

ABSTRACT: *A characterization studies have been carried out on Garko and Kura rice husk samples from Kano state of Nigeria. The results of Garko and kura rice husk are Moisture content of 5. 90 and 5.30%; Ash content of 17.10 and 15.70; Silica 95.10 and 93.08; alumina 2.56 and 1.91%; Calcium Oxide 0.45 and 0.31. Other results are Garko has 12.86% Carbohydrate, 15.40 crude fibre, 73.91 fat extract and 0.45 protein. Other results of Kura husk are 9.90% Carbohydrate, 13.50 crude fibre, 71.17 fat extract and 0.52 protein. The coking results reveals that there were increasing weight loss as the temperature is increased. In some cases at higher and at longer period of time some constancy were observed, implying optimal ash content. From the studies carried out both rice husks samples have good properties for both agricultural and industrial applications. However, comparative basis, Garko rice husk possesses better agricultural and metallurgical properties than Kura rice husk.*

KEYWORDS : *Rice husk, Silica, metallurgical, Agricultural,*

I. INTRODUCTION

Rice (Oryza sativa) is a cereal plant belonging to the grass family. They are monocotyledonous like wheat, barely, maize etc. Rice is widely grown in many parts of Nigeria in states like Kano, Ebonyin, Plateau etc. The constituents of rice include bran, grain, endosperm and husk. Rice husks are a fibrous, non-digestible commodity, accounting for about 20% of the dried paddy on stalk [1]. Rice husk removal during rice processing, generates disposal problem due to less commercial interest. Also, handling and transportation of rice husk is challenging due to its low density. Rice husk is a great environment threat causing damage to land and surrounding area where it is dumped. Rice husks posses both organic and inorganic components. The organic components includes crude protein, carbonhydrates, lipid, lignin, vitamins and organic acids [2]. The inorganic constituents having ash as the major component which is between 13.2 to 29.0% of the weight of rice husk [3]. Rice husk is unusually high in ash compared to other biomass fuels The silica content is between 87 – 97% [4]. The other components of ash are K_2O, CaO, Fe_2O_3, P_2O_5, SO_3, Na_2O, MgO and Cl [5]. Majority of the husk are disposed usually by burning in the open field creating problem of pollution to human and entire environment. Suitability of rice husk to be used for different applications depends upon the physical and chemical properties of the husk such as ash content, silica content etc. Direct use of rice husk as fuel has been seen in power plants. Apart from its use as fuel, Rice husk finds its use as sources of raw material for synthesis and development of new phases and compounds.

Various factors which influence ash properties are incinerating conditions (temperature and duration), rate of heating, burning technique, crop variety and fertilizer used. The main aim of this work, is to characterized the two rice husk for possible industrial applications. Despite so many well established uses of rice husk, only little portion of rice husk produced is utilized in a meaningful way developing nations, the remaining part is allowed to burn in open air or dumped as a solid waste. The large number of industrial applications which rice husk can be put to use necessitated the desire to study Garko and Kura rice husk with a view of identifying the best way they can be put to use.

II. MATERIALS AND METHODS

2.1 Materials : The materials used for this project were rice husk from Garko and Kura in Kano state of Nigeria. The husks were collected in large quantities from the rice mills located in both towns. They were than taken to Kano were the test was carried out.

2.2 Experimentation

2.2.2 Leaching : 5%g of each of the sample was measured into a washed and oven dried 250 ml conical flask. 5 mole NaOH and NH_4OH (33% purity) were added separately into the conical flasks containing the samples. The conical flasks were left to stand for 2 hours before filtration is carried out.

2.2.1Coking : 10g of the sample were measured into stainless cups and charge into the furnace. They were then burnt at temperatures of 200^0C, 300^0C, 400^0C, 500^0C, 600^0C and 700^0C for time intervals of 1, 2, 3, 4, and 5 hours. After every hour at the selected temperature a cup was withdrawn and the weight lost measured.

III. RESULTS AND DISCUSSIONS

The results of the chemical analysis are shown on **Tables** 1 and 2; the result of leaching is shown on Table 3, while the result of the coking experiment is presented in figure 1 to 6. From the result obtained (Table 1) Garko husk had higher values of silica, Alumina and ash. As a source of Silica and Silicon compounds, rice husk a promising raw material source for a number of silicon compounds such as silicon carbide, silicon nitride, silicon tetrachloride, zeolite, silica, and pure silicon [6, 7]. Rice husk ash has been widely used in various industrial applications such as processing of steel, refractory industry etc. Suitability of rice husk ash mainly depends on the chemical composition of ash, predominantly silica content in it. Rice husk ash is found to be superior to other supplementary materials like slag, silica fume and fly ash [8]. Rice husk ash has been used as silica source for cordierite production. Replacement of kaolinite with rice husk silica in the mixture composition, yields higher cordierites with a lower crystallize temperature and decrease in activation energy of crystallization [9].Silica aerogels prepared from RHA finds application in super thermal insulators, catalyst supports and dielectric materials (Goncalves, 2007). Based on the above usage of silica in the various industries mentioned Garko husk is superior to Kura husk for industrial applications. Agriculturally also, Garko husk shows superiority in terms of the fat, carbonhydrate and crude fibre, hence will posses more nutritional value than Kura husk as seen on Table 2.

From the results of leaching it is deduced that the solvents had considerable influence on the rice husk samples. It means that each of the solvent leached out a certain percentage of the inorganic constituents alongside the organic matter that were previously leached out during the digestion process. Calcium oxide, silica and magnesia were considerable reduced by the action of all the solvents with H_2SO_4 and NaOH showed more evere reduction in the values of the three oxides than HNO_3, NH_4OH and HCl. Surprisingly, the value of FeO in all the media increased more than its original value in the chemical analyses results. These increases might have resulted from some chemical reactions between the media and the constituents may have led to the formation of FeO instead of its removal from the complex, thereby increasing its value in the residue. The result is corroborated by the colour changes noticed when the solvents were added to the husks

Table 1: Results of Chemical Analysis of Garko and Kura Rice Husks

Constituents	Garko Rice Husk	Kura Rice Husk
Moisture Content %	5.90	5.30
Ash Content %	17.10	15.70
Silica (SiO_2) %	95.10	93.08
Calcium Oxide (CaO) %	0.45	0.31
Ferric Oxide (FeO) %	0.18	0.19
Magnesia (MgO) %	0.41	0.46
Alumina (Al_2O_3) %	2.56	1.91

Table 2: Results of essential food content of Garko and Kura Rice Husks

Constituents	Garko Rice Husk	Kura Rice Husk
Carbonhydrate	12.86	5.90
Crude fibre	15.40	13.50
Fats extract	73.91	71.17
Protein	0.45	0.63

Table 3: Result of leaching experiment on Garko and Kura Rice Husks

Rice Husk Sample	Leaching Chemical	CaO	FeO	MgO	SiO_2
Garko	HCl	033	0.24	0.19	91.21
	HNO_3	0.35	0.25	0.19	91.58
	H_2SO_4	0.27	0.23	0.15	90.80
	NaOH	0.35	0.25	0.17	91.05
	NH_4OH	0.76	0.26	0.16	93.60
Kura	HCl	0.39	0.25	0.18	91.60
	HNO_3	0.42	0.26	0.20	91.60
	H_2SO_4	0.35	0.26	0.16	91.10
	NaOH	0.34	0.26	0.17	91.20
	NH_4OH	0.45	0.27	0.18	93.50

than HNO_3, NH_4OH and HCl. Surprisingly, the value of FeO in all the media increased more than its original value in the chemical analyses results. These increases might have resulted from some chemical reactions between the media and the constituents may have led to the formation of FeO instead of its removal from the complex, thereby increasing its value in the residue. The result is corroborated by the colour changes noticed when the solvents were added to the husks From Figure 1 to 6, clearly shows that weight loss increased with both coking time and coking temperatures. This is true since the higher the temperature, the higher the rate of volatilization of organic matter and the longer the holding time, the higher the rate of volatilization.

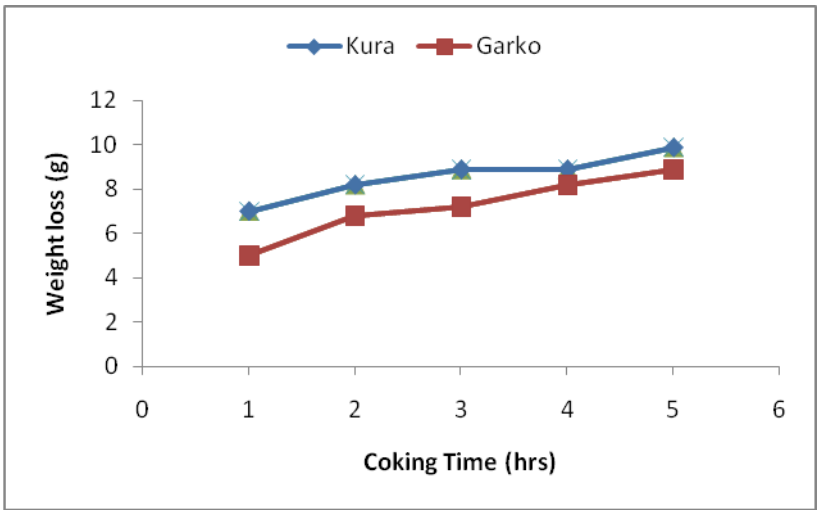

Figure 1: weight losses against coking time at 200^0C

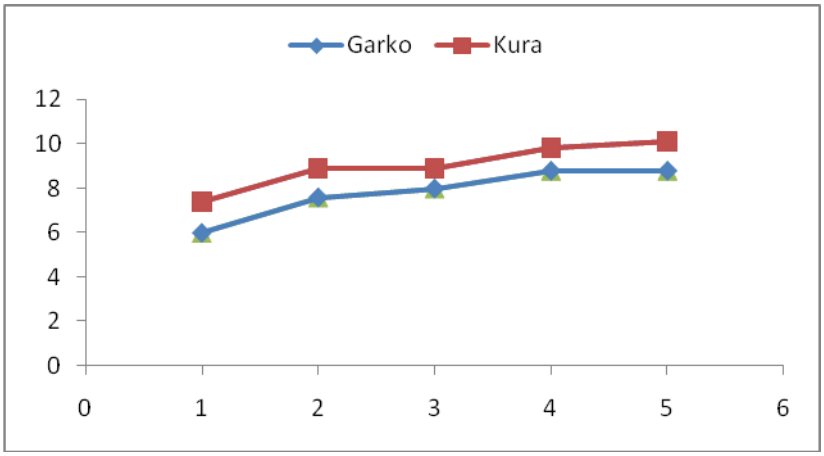

Figure 2: weight losses against coking time at 300^0C

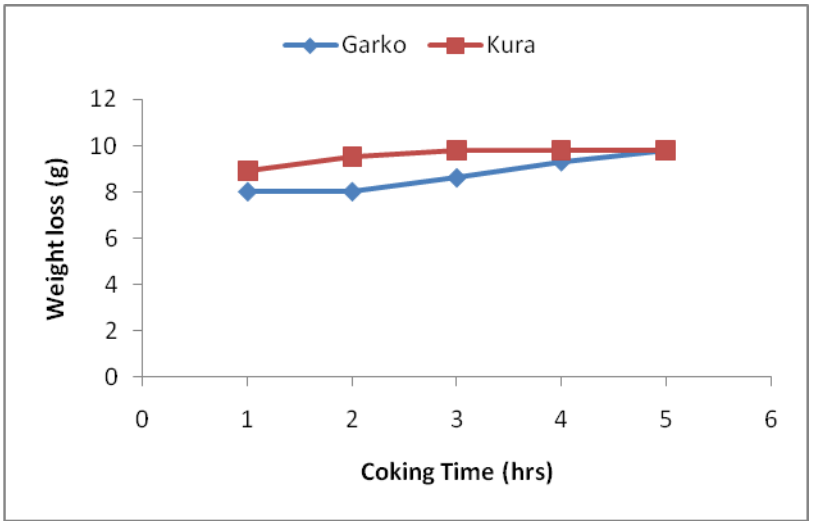

Figure 3: Weight losses against coking time at 400^0C

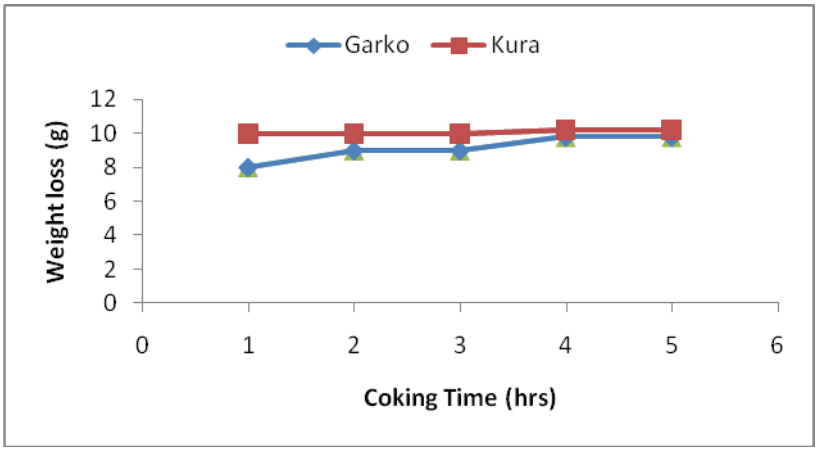

Figure 4: Weight losses against coking time at 500^0C

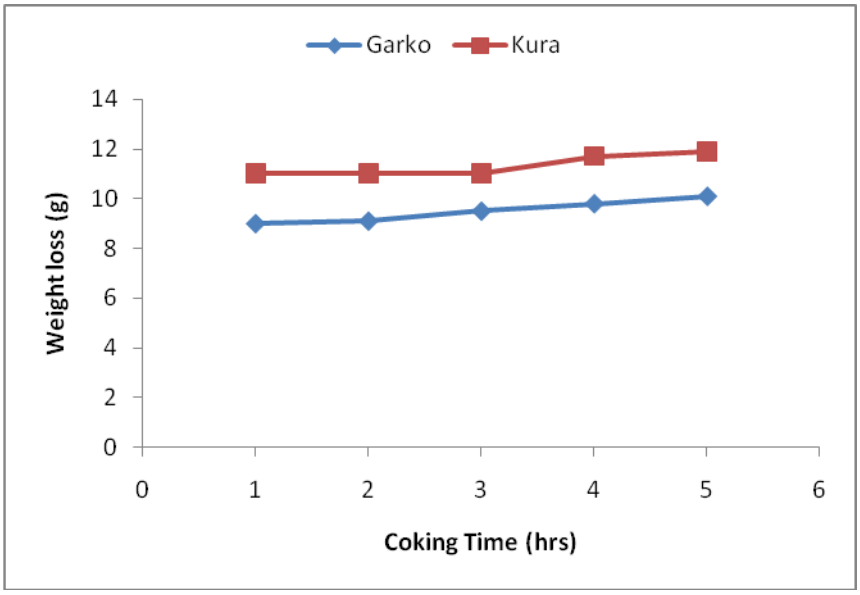

Figure 5: Weight losses against coking time at 600^0C

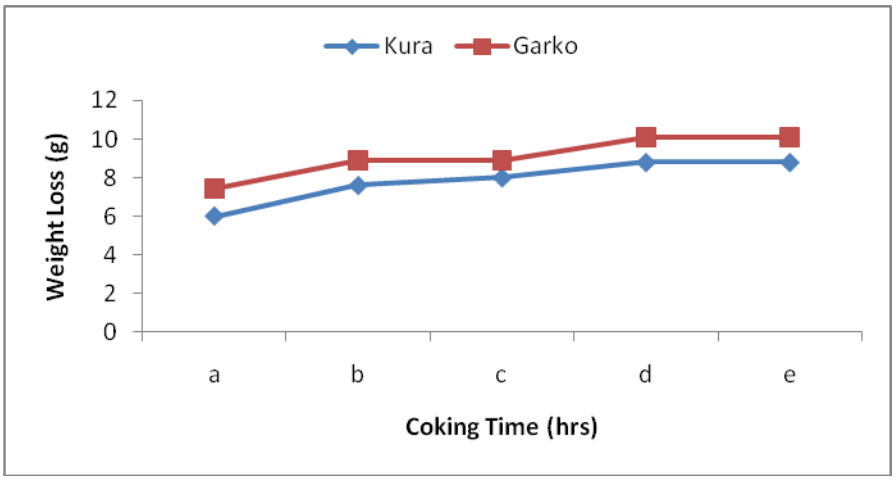

Figure 6: Weight losses against coking time at 700^0C

IV. CONCLUSION

Rice husk has been used directly or in the form of ash as a value added material for manufacturing and synthesizing new materials and as a low cost substitute material for modifying the properties of existing products. Presence of silica is an additional advantage in comparison to other byproduct materials which makes rice husk an important material for a wide range of manufacturing and application processes. From the study carried out Garko and Kura rice husk possesses the requirement for both agricultural and industrial applications. However comparing the two husk, Garko rice husk is best used in the metallurgical and materials industries because of its higher content of silica, alumina and ash. Agriculturally also Garko is better utilized than Kura husk because of higher content of fat extract, crude fibre and carbonhydrates value.

REFERENCES

[1] T. H. Lious, and F. W. Chang, The Nitridation Kinetics of Pyrolyzed rice Husk, *Ind. Eng.Chem.Res., 35(10)* 1996, 3375 – 3383..
[2] M.T. Tsay, and F.W. Chang, Characterization of Rice Husk Ash – Supported Nickel Catalysts Prepared by ion Exchange. *Appl. Catal. A. 203(1)* , 2000, 15 – 22.
[3] D.J. Minson, The Effect of Pelleting and Wafering on the Feeding Value of Roughage. *British Grassland Soc. Rev.J. 18*, 1963, 39 – 44.
[4] M. Rozainee, S.P. Ngo, A.A. Salema, Effect of fluidising velocity on the combustion of rice husk in a bench-scale fluidised bed combustor for the production of amorphous rice husk ash, *Bioresource Technology 99*, 2008 703–713
[5] F.B. Morrison, *Feeds and feeding: A hand book for Student and Stockman*, (22nd Edition, Morrison Publishing Co., Ithaca, N.Y. 1959)
[6] K.A. Matori, and M.M Haslinawati Producing Amorphous White Silica from Rice Husk. *MASAUM Journal of Basic and Applied Sciences, 1(3)*, 2009, 512
[7] G. T Adylov., Sh. A Faiziev., M. S. Paizullakhanov, Silicon Carbide Materials Obtained from Rice Husk, *Technical Physics Letters, Vol. 29, No. 3*, 2003, pp. 221–223
[8] Sun Luyi , Silicon-Based Materials from Rice Husks and Their Applications. *Ind. Eng. Chem. Res., 40*, 2001, 5861-5877
[9] El Fadaly , Recycling of Ceramic Industry Wastes in Floor Tiles Recipes. *Journal of American Science*, 2010.
[10] M.R.F. Goncalves, Thermal insulators made with rice husk ashes: Production and correlation between properties and microstructure. *Construction and Building Materials 21* (2007) 2059–2065

American Journal of Engineering Research (AJER)
e-ISSN : 2320-0847 p-ISSN : 2320-0936
Volume-03, Issue-11, pp-245-250
www.ajer.org

Research Paper Open Access

Investigation of the Thermal Insulation Properties of Selected Ceiling Materials used in Makurdi Metropolis (Benue State-Nigeria)

Gesa, F. Newton[1], Atser A. Roy[2]& Aondoakaa, I. Solomon[3]
[1,2,3](Department of Physics, College of Science/ University of Agriculture, Nigeria).

ABSTRACT: *In this research, the thermal insulation properties of three selected materials namely: Plaster of Paris (P.o.P), Plywood and Isorel (Masonite) used as ceiling boards in Makurdi, Benue state-Nigeria have been investigated. The selection of these insulation materials is based upon their predominant usage as padding materials in the tropical Makurdi metropolis. To achieve this, the steady-state method using Lee-Charton's apparatus was adopted to analyze the thermal conductivities of the chosen materials. The results obtained show that, P.o.P exhibits the best insulation property followed by Plywood then Isorel ceiling board with thermal conductivities of 0.1185w/mk, 0.1768w/mk and 0.4498w/mk respectively. Their corresponding thermal resistivities are 8.4388mk/w, 5.6561mk/w and 2.2232mk/w. From the results, P.o.P is recommended for its best insulation property. The research therefore provides a guide to intending builders and civil Engineers for selecting of housing insulation materials in Makurdi metropolis as well as other humid zones of tropical Africa.*

KEYWORDS: *Thermal Insulation, P.o.P, Plywood, Isorel (Masonite), Lee-Charlton's method, Makurdi.*

Preamble: Makurdi metropolis is situated in the tropics of Nigeria on 7.74°N, 8.51°E and has an elevation 104m above the sea level. The city which is located on the banks of River Benue, a major tributary of the River Niger, has a land area of about 3,993.3 Km^2 [1] with a population of about 292,645 inhabitants [2]. As a result of her location, the city has an adversely high average annual temperatures of up to 35^oC within the year. This has left the inhabitants of the city with choices of various ceiling boards in search of a naturally aesthetic cool shelter. Between luxury and comfort, the elite class have been caught in the web of preference to some insulating materials such as, plywood, Isorel (Masonite) and plaster of Paris popularly known as P.o.P among other types. This work therefore investigates the thermal insulating behavior of these materials commonly used as ceiling pads in housing construction in Makurdi metropolis, Benue State.

I. INTRODUCTION

Thermal insulators have been used in heat storage systems to prevent temperature gradient thereby minimizing heat losses to the surroundings [3]. In housing construction, insulators are used to prevent heat exchange across the boundaries of shelters. These insulating materials are usually made in various types, varieties and forms like loose fill, rigid boards, pipes and foam. Proper selection of insulating material is based on the thermal property which includes the thermal conductivity, specific heat capacity and thermal diffusivity [4]. The thermal insulation is provided by embedding insulation materials at least on the roof areas and the vertical walls of the system [5]. Poor thermal insulation in heat reservoirs and shelter systems leads to high heat losses or heat gains as the case may be [6].Plywood, Isorel (Masonite) and Plaster of Paris (P.o.P) ceiling boards are currently used as thermal insulation materials for the ceiling purpose in Benue State, Nigeria mainly due to availability in the market or their stunning appearance and not on their low thermal conductivity. However, some of these thermal insulators are not suitable ceiling materials to be used in Makurdi. This work therefore sets to determine among other things, the insulation material(s) that provides better solution as ceiling materials in terms of thermal conductivity or resistivity thereby provides a guide for civil Engineers and builders.

II. THERMAL CONDUCTIVITY

The thermal conductivity (k) of a material is a measure of the effectiveness of the material in conducting heat [8]. Good heat insulators should have low thermal conductivities in order to reduce the total coefficient of heat transmission. The thermal conductivity of a material therefore represents the quantity of heat that passes through a meter thickness per square per second with one degree difference in temperature between the faces. In a steady state, that is, where the temperature at any point in the material is constant with time; thermal conductivity is the parameter which controls heat transfer by conduction [4]. The rate of heat flow, H is given by Fourier's law:

$$H = -kA\frac{\partial\theta}{\partial x} \quad (1)$$

where k is the thermal conductivity, A is the area of the test piece normal to the heat flow and $\frac{\partial\theta}{\partial x}$ is the temperature gradient.

Thermal conductivity is regarded as the most important characteristic of a thermal insulation since it affects directly the resistance to transmission of heat that a material offers. The lower the thermal conductivity value, the lower the overall heat transfer. The thermal conductivity of insulating materials has been found to vary with density, moisture content, temperature, direction of heat flow with respect to grain for fibrous materials, the presence of defects in the material and porosity [8].

Measurement of Thermal Conductivity of Insulators: The methods of measurement of thermal conductivity can be divided into steady state methods and non-steady state methods. Steady state methods are widely used as they are mathematically simpler. For materials of low thermal conductivity, steady state methods can be very time consuming and involve expensive apparatus. Non-steady state methods have experimental advantages once the much more difficult mathematical treatment has been worked out. In non-steady state methods, heat transfer have the potential of directly determining thermal diffusivity, however they are not as accurate as steady state methods when applied to dry materials [9]. A steady state method is therefore preferred in analyzing the thermal conductivity of dry materials. The Lee-Charlton's method as a steady state method is therefore employed in this research.

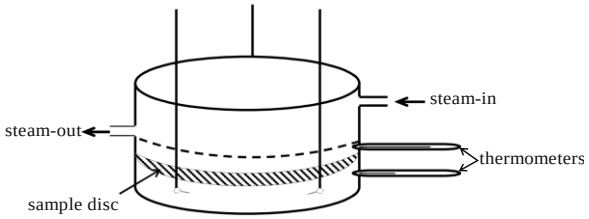

Figure 1. Lee-Charlton's Disc for Measurement of Thermal Conductivity

By measuring how fast the brass cools at the steady state temperature T_1, the rate of heat loss can be determined. If the disc cools down at a rate, $\frac{dT}{dt}$ then the rate of heat loss is given by

$$H = mc\frac{dT}{dt} \quad (2)$$

where, m is mass of the brass disc, C is specific heat capacity of brass.

At steady state, heat conducted through the bad conductor (sample disc) per second will be equal to heat radiated per second from the exposed portion of the metallic disc.

$$kA\left[\frac{T_2-T_1}{x}\right] = mc\frac{dT}{dt} \quad (3)$$

Therefore, k is defined as, $k = \frac{Mc\frac{dT}{dt}}{A\frac{(T_2-T_1)}{x}}$ (4)

where k is the coefficient of thermal conductivity of the sample, A is area of the sample in contact with the metallic disc, x is thickness of the sample, T_2 -T_1 is temperature difference across the sample thickness, m is

mass of the metallic disc, C is heat capacity of the metallic disc and $\frac{dT}{dt}$ is rate of cooling of the metallic disc at T_1.

Thermal diffusivity, δ and resistivity, r are calculated using equation (5) and (6)

$$\delta = \frac{k}{cp} \quad (5)$$

$$r = \frac{1}{k} \quad (6)$$

where δ is thermal diffusivity, k is thermal conductivity, r is thermal resistivity, cp is volumetric heat capacity expressed as: cp = Specific heat capacity x density (*i.e* $cp = C \times \rho$) (7)

III. MATERIAL AND METHODS

Materials : Circular discs of the three predominantly used insulating materials in Makurdi: Plaster of Paris (P.o.P), Plywood and Isorel (Masonite), vernier caliper, micrometer screw gauge, mass balance, retort stands, heat source, steam boiler, water, Mercury in glass thermometers, stop watch and Lee-Charlton's apparatus.

Table 1. Material Specification

Materials	Thickness (m)	Mass (Kg)	Specific heat capacity (J/kgk)	Diameter (m)	Mean surface Area (m^2)
Plywood	0.003	0.0168	2500	0.11	0.0095
P.o.P	0.003	0.0250	1090	0.11	0.0095
Isorel(Masonite)	0.003	0.0256	2100	0.11	0.0095

Method: Sample Plywood and Cardboard were obtained from building material shops at modern market Makurdi, Benue State while P.o.P board was obtained from the building site along International Market Road Makurdi. The samples were shaped to have equal cross-sectional areas. Using mass balance, micrometer screw gauge and vernier caliper, the mass (kg), height (m) and diameter (m) respectively of the samples were obtained and related parameters calculated and presented in table 1. The setup was then arranged as shown in appendix A3.The steam boiler was filled with water to nearly half and heated to produce steam that causes the rise in temperature of the brass disc and sample specimen until steady temperatures T_1 and T_2 were obtained after a certain time interval.The specimen was then removed and the brass disc heated directly by the steam chamber till its temperature was slightly above T_1. The steam chamber was then removed and sample specimen placed on the brass disc. The initial temperature was noted and cooling temperature drop recorded continually in intervals of one minute till there was no observable change in temperature. The result was tabulated as shown in table 2. From the temp.-time plot (fig. 2), cooling rates were determined from the slopes then thermal properties computed.

IV. TESTS AND ANALYSIS OF RESULTS

Table 2. Cooling Rate of the Selected Insulation Materials

Ambient Temperature = 31°C

Time	Temperature Variation (°C)		
x 60 (s)	P.o.P	Plywood	Isorel
0	88	94	94
1	83	90	91
2	80	87	88
3	77	84	86
4	75	82	84
5	73	79	82
6	71	77	80
7	69	76	78
8	68	74	77
9	66	73	75
10	65	71	74

Using equation (4), $k = (Mc\ dT/dt)/[A\ (T_2 - T_1)/X]$and fig. 1, the thermal conductivity of each of the selected material was calculated and presented in table table 3.0.

Table 3. Thermal Properties of the Selected Ceiling Boards

Sample	Density (kg/m^3)	Thermal Conductivity (k) (w/mk)	Thermal Diffusivity(δ) (m^2/s)$\times 10^{-7}$	Thermal Resistivity (r) (mk/w)
Isorel	898.25	0.4498	2.3845	2.2232
P.o.P	876.55	0.1185	1.2403	8.4388
Plywood	589.47	0.1768	1.1997	5.6561

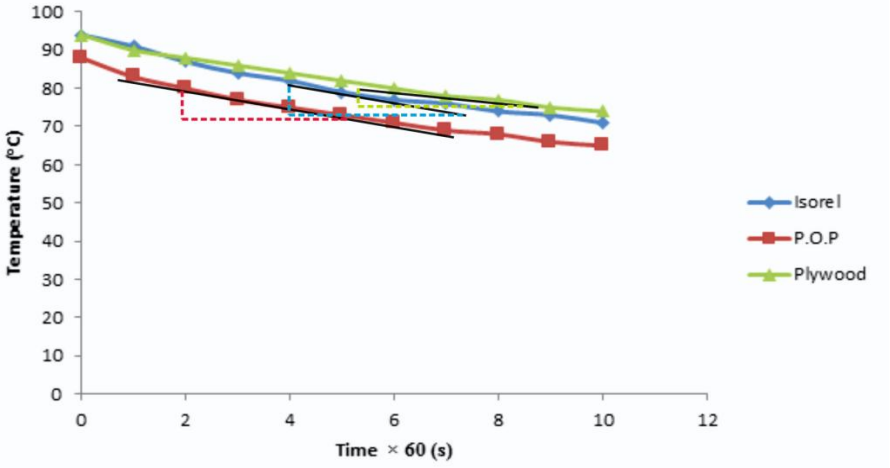

Figure 1. The Cooling Curve for the Three Selected Materials

V. DISCUSSION OF RESULTS

Table 1 is the material specification of the selected materials showing the thickness, area, mass and specific heat capacity of the chosen samples. Since thermal conductivity is a function of thickness and area, the specimens were carefully prepared with equal thicknesses and cross-sectional areas. Table 2 and Fig. 1 show the cooling rates of the selected materials at ambient temperature of 31°C. The results show that within the prevailing tests, P.o.P exhibits the best cooling rate followed by plywood then isorel (Masonite). The cooling curves of the three sampled materials taken at every one minute show that both materials have a similar cooling pattern. Table 3 presents the calculated thermal parameters such as thermal conductivity, k; thermal diffusivity, δ and thermal resistivity, r for the three selected materials. The results show that, all the materials are good insulating materials since their thermal conductivities fall within the conductivities of construction and heat-insulating materials given by [10], as 0.023 - 2.9$Wm^{-1}\ k^{-1}$.

Isorel popularly called Masonite Ceiling has a thermal conductivity of 0.4498$Wm^{-1}\ k^{-1}$, Thermal diffusivity of 2.3845 $\times$ 10^{-7} m^2/s and thermal resistivity of 2.2232mk/W. P.o.P has a thermal conductivity of 0.1185$Wm^{-1}\ k^{-1}$, Thermal diffusivity of 1.2403 $\times$ 10^{-7} m^2/s and thermal resistivity of 8.4388mk/W while Plywood has a thermal conductivity of 0.1768$Wm^{-1}\ k^{-1}$, Thermal diffusivity of 1.1997 $\times$ 10^{-7} m^2/s with thermal resistivity of 5.6561mk/W. theoretically, a substance with a large thermal conductivity value is a good conductor of heat; one with a small thermal conductivity value is a poor heat conductor, that is a good insulator. In order words a good insulation material will have high resistivity-value for thickness other than 1m.Thermal diffusivity measures the ability of a material to transmit a thermal disturbance. It indicates how quickly a material's temperature will change. Thermal diffusivity therefore increases with the ability of a body to conduct heat and decreases with the amount of heat needed to change the temperature of a body. It is of little interest in many thermal insulation systems since in these, approximately steady state conditions normally exist.

VI. CONCLUSION

From the results in Table 3, we have observed that among the materials studied, P.o.P provides the best thermal insulation since it has the lowest thermal conductivity (highest thermal resistivity) followed by Plywood then Isorel (Masonite) ceiling board. From the result of the research, the best insulation material to be used in the tropical city like Makurdi is P.o.P. However, from the economic point of view, it is commendable to choose an insulating material with a lower thermal conductivity and more affordability to average number of inhabitants when considering housing construction in a densely populated city like Makurdi. Hence Plywood is recommended for the lower or middle class who cannot cope with the exorbitant cost of P.o.P since it is less expensive and offers better insulation property than Isorel (Masonite).

REFERENCES

[1] Ityavyar J.A, Inah E.I and Akosim, C- Assessment of Captive Management of Nile Crocodile, *Crocodylus niloticus*, in Three Towns of Benue State, Nigeria in *Journal of Research in Forestry, Wildlife And Environment*. Volume 3 No. 2 September, 2011.

[2] GeoNames geographical database, 18th, January 2012.

[3] Turner W.C and Malloy J. F, "Thermal Insulation Handbook'', Published by McGray-Hill Book Company New York 1988.

[4] Ayugi G, "Thermal properties of selected Materials for Thermal Insulation available in Uganda" B.Sc thesis Dept. of Physics Makerere University. 2009

[5] Novo A. V, Bayon J.R, Castro-Fresno D and Rodriguez-Hernandez J. ' Review of Seasonal heat Storage in Large Basin: Water Tanks and Gravel Water Pits. Applied Energy, 87: 390, 397. 2010

[6] Bauer D, Marx R, Nulbicker-Lux J, Ochs F, Heidemann W and Muller- Steinhagen H, "German Central Solar Heating Plants with Seasonal heat Storage, Solar Energy 84:612, 623. 2010

[7] Mohammad Al-Homoud S, "Performance characteristics and Practical application of Common Building Thermal Insulation Materials. Building and Environment, 40: 353, 366. 2005

[8] Rajput. Engineering thermodynamics, New Delhi: Lax Mi Publications, 2005.

[9] Mohesemin N, M, "Thermal Properties of food and Agricultural Materials. Gordon and Breach Science Publishers, New York. 1980.

[10] Mahhrer Y, "Journal of Soil Science, 134 (6), 381-387, 1982

[11] The World Gazetteer". Archived from the original on 2013-02-09

ACKNOWLEDGMENT: **Department of Physics, Federal University of Agriculture, Makurdi- Benue State.**

APPENDIX

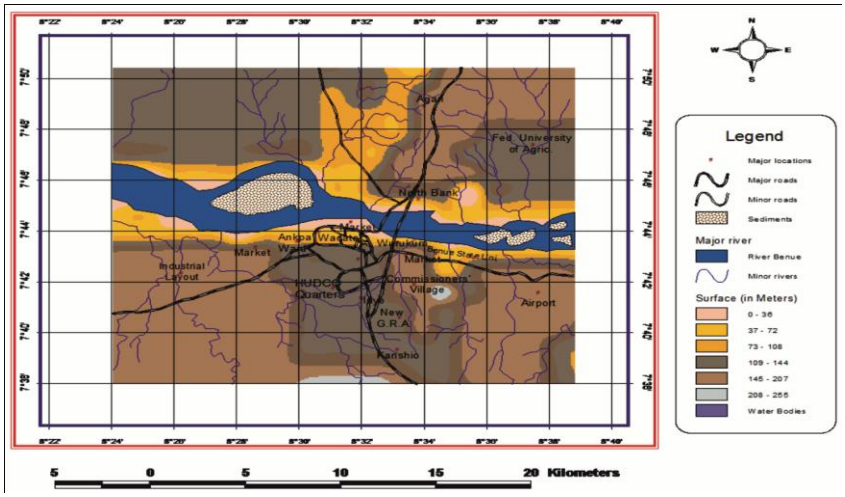

A1: Map of Benue State Showing the Study Area

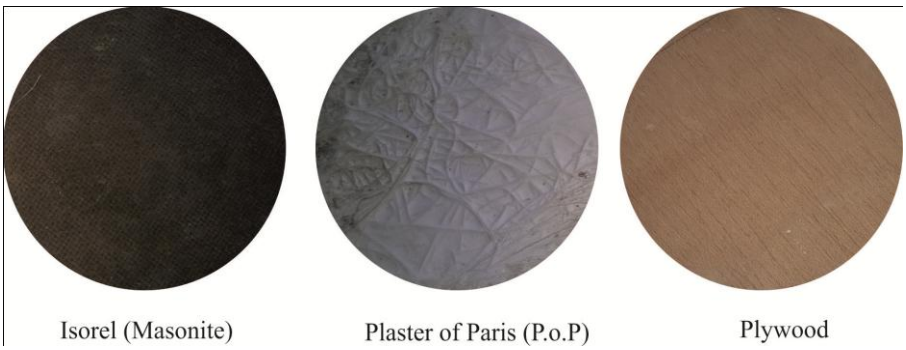

A2: Test Specimens Showing the Selected Insulating Materials

A3: Experimental Set-up of Lee-Charton's Method in Determination of Thermal Conductivity

American Journal of Engineering Research (AJER)
e-ISSN : 2320-0847 p-ISSN : 2320-0936
Volume-03, Issue-11, pp-251-259
www.ajer.org

Research Paper Open Access

Simulation Study for Production of Hydrocarbons from Waste

[1,]Ameen Sayal , [2,]Vikas K. Sangal , [3,]Parminder Singh
[1,2,3,]*Department of Chemical Engineering, Thapar University, Patiala 147004, Punjab, India*

ABSTRACT : This paper presents a simplified process simulation model on conversion of waste plastic to hydrocarbons using Aspen Hysys. A simulation model has been developed based on a degradation scheme, considering product fractions to be gas, naphtha, middle distillate (diesel) and bottom product and their hydrocarbon composition paraffin, olefin, napthenes and aromatic. Material and energy flows, sized unit operations blocks can be used to conduct economic assessment of each process and optimize each of them for profit maximization. A detailed sensitivity analysis investigating the effects of various process parameters, including variation across the stages, bed capacity and heat duty has been presented. Diesel product and Naptha obtained from waste plastic has final boiling to be 372 ^{0}C and 204 ^{0}C respectively, which is in accordance with euro standards. The simulation model developed can also be used as a guide for understanding the process and the economics.

KEYWORDS: *Waste plastic, Aspen Hysys, Hydrocarbons, paraffin, olefin, Simulation*

I. INTRODUCTION

Plastics light weight, durability and energy efficiency makes them a vital part of our everyday activities [1]. Therefore they have a profound contribution towards the advancement in the recent technologies and new scientific achievements. Plastics have wide applications owing to their functional superiority and cost effectiveness over the traditional packaging materials. Due to this, the world's annual plastic consumption increased dramatically from around 2 million tonnes in the 1950s to about 245 million tonnes in 2006 with a 10% increase yearly [2]. The increased use of different types of plastics has also increased its waste release into the environment. Recycling waste plastics into reusable plastic products is a conventional strategy followed to address this problem for years. However this technique has not given remarkable results. Another possible treatment of the waste plastics is incineration, it is an intensive process which can also be rejected due to its further contribution to the pollution in the form of gases and soot particles and even no useful product is obtained. Similarly various other methods such as mechanical, biological and other chemical recycling approaches are operational, but still appeared inadequate or not in position to conform with current environmental regulations [2-3].

Tertiary recycling (also known as feedstock recycling) is the processing of waste into fuels or basic chemicals. Pyrolysis is one such technique where the polymers are thermally and catalytically converted into useful products that can be used as fuel oil like industrial diesel, gaseous fuel, carbon black etc [4]. Although literature and process data from pyrolysis applications report a high oil/wax product yield, there are concerns that its energy requirement, and subsequent carbon footprint, make this process undesirable. Catalytic conversion followed by pyrolysis which is a chemical recycling technique that involves the conversion of polymers to recover useful liquid products may be the suitable method. Catalytic conversion occurs at considerably low temperature and forms hydrocarbons. In such degradation process, the most valuable fuel is obviously liquid fuel, like gasoline, diesel. A maximum liquid yield of about 86.6 wt.% was produced during the catalytic degradation of HDPE using silica/alumina (SA) catalyst in a powdered particle fluidized bed reactor [5]. Kumar et al., [6] gave a very good review on tertiary recycling of high-density polyethylene to fuel.A number of solid bases and solid acids have been used as catalysts for the catalytic degradation of different types of waste plastic polymers [2]. Zeolites based catalysts are able to convert the waste plastic at lower temperature effectively as compared to the basic catalysts such as $BaCO_3$, bimetallic catalyst and FCC catalyst [7].

Fernandes et al., [8] studied the degradation of high-density polyethylene (HDPE) alone and in presence of an acidic catalyst (silicoaluminophosphate, SAPO-37) using only TGA technique. Lin et al., [9] worked on the pyrolysis of HDPE over various catalysts using a laboratory fluidised-bed reactor. They found that catalysed degradation resulted in much larger amounts of gaseous hydrocarbons. Neves et al., [10] studied the catalytic degradation of HDPE using a mesoporous aluminosilicate (AlTUD-1) catalyst but the study was limited to only TGA analysis. Lin et al., [11] presented a combined kinetic and mechanistic modelling of the catalytic degradation of polymers. Csukas et al. [12] studied the thermal pyrolysis of plastic wastes in tubular reactor with direct computer mapping based simulation methodology, combined with genetic algorithm.

As discussed by Sahu et al., [13], Catalytic Conversion of PP, PE PS simulation model did not discuss the variation of parameters with number of trays in distillation column, heat duty and other optimization parameters. Most of the detailed polymer degradation models in the literature are valid to the given pyrolysis system and evaluate only the formation of light molecular weight product fractions. Therefore more robust model is needed to model the pyrolysis process of real plastic waste. Most of the researchers optimized the plant based on gasification process or thermal degradation [14]. To the author's knowledge, there are no reports in the literature on the study of simulation and optimization of distillation column, heat duty and bed capacity for the production of hydrocarbons from waste. Even no work was done using Aspen Hysys simulator. Based on the review of the literature, the objectives of this study are set as (i) the simulation of plastics degradation process using commercial simulation software Aspen Hysys (ii) to successfully test and demonstrate the applicability of Aspen Hysys to simulate the catalytic conversion process for one of the most abundantly used plastic, polyethylene (PE), (iii) to analyze the performance of a plastics degradation process and optimization of process parameters.

II. CATALYTIC PROCESS

Figure 1 illustrates the process flow sheet of the simplified catalytic pyrolysis model of PE. HDPE in resin form, allowed it to pass through hopper, then it was passing through moving heating chamber where the temperature varies from 50^0C to 350^0C. The molten plastic is then carried to the pyrolyser reactor where thermal cracking of the plastic occurs where the temperature varies from 350^0C to 550^0C and metal oxide was used to provide the homogeneous heating. These vapours produced in pyrolyser are sent to catalytic reactor for reforming and promotion of secondary reactions using zeolite based catalyst. The temperature of catalytic bed was kept at 340^0C approximately. The products from catalytic reactor were send to distillation column, where we got the LPG, naptha and diesel product.

III. PLANT SIMULATION AND OPTIMIZATION

3.1. Simulation : In the present work, fractionation of hydrocarbon mixture (C_1-C_{20}) obtained after pyrolysis and catalytic conversion of the waste plastic is considered. The reboiler duty and the heat required to preheat the feed are considered as the total energy requirement for the fractionating column. The Peng Robinson was used as fluid package. This package was appropriate for hydrocarbons which are non polar. Figure 2 shows the schematic representation of the simulation flow sheet.

The parameters required to be specified for the operation of the fractionating column under varying operating conditions are listed in Table 1. D86 data is added to oil manager defining the cuts at different boiling points shown in Table 2. D86 data was obtained from ASTM distillation to define cuts in variation of temperature. From the simulation model, results were obtained for the different simulated products (Diesel, LPG, Naptha) which were then compared with literature data. Table 3 shows the simulated D86 data of cracked residue. From Table 3 it was clear that the final boiling point of the cracked residue is 372^0C. According to the Euro III and Indian Standards diesel have the final boiling point of 370^0C. It means that the product obtained was of diesel range, since other properties like density (832 kg/m^3), cetane index (46), viscosity at temperature 40^0C (2.9 Centistokes), obtained after simulating these results also matches so these findings confirmed that the product obtained was diesel. So the side stream originating at tray number 15, from which we were getting diesel was appropriate corresponding to a tower constituting 20 trays. Similarly the final boiling point of Naptha was obtained to be 204^0C which is according to Euro and Indian Standards shown in Table 4. Also properties like motor octane number (82), Reid vapour Pressure (60 kPa), obtained after simulating these results also matched, which confirmed that the product obtained was Naptha. So the side stream originating at tray number 8, from which we were getting Naptha was appropriate corresponding to a tower constituting 20 trays. In this the tray numbered as top to bottom i.e. top tray is numbered as 1 and bottom as 20. Variation of temperature, mole fraction, density, and molar flow rate of hydrocarbon were obtained after the simulation of fractionator showing the variation with respect to stages. Figure 3 shows the variation of pressure with number of stages.

From figure 3, it was clear that the pressure at top is less and at bottom is more and pressure drop across the column is 30kPa. The profile obtained was appropriate since pressure at bottom is always more than at top because at bottom reboiler and at top condensor is there. Even the profile obtained was linear which shows that pressure increases linearly as we move down the stage, giving the appropriate variation.The variation of liquid, vapour molar flow rate of hydrocarbons is shown with variation of trays in Figure 4. Net molar flow of vapour hydrocarbon was maximum at tray 1, since vapour were maximum at top, then it decreases drastically from stage 2 (feed tray) up to stage 3, the stage below feed stage and reaches to zero, then increases non linearly with increase in stages upto 8^{th} tray (naptha outlet side stream) corresponding pressure to be 1.2 kgmole/hr then again decreases and again increases and reached upto 1.5 kgmole/hr on stage 15 (diesel outlet side stream). This type of profile was obtained due to the positioning of side streams and feed stream. Similarly liquid molar flow increases to 1.8 kgmole/hr till 8^{th} stage (naptha outlet side stream) and then drastic decrease from stage 8^{th} to 9^{th}. Then again the flow rate increases till 15^{th} (diesel outlet side stream) and then decreases.

Figure 5 shows the variation of temperature with tray position in column. The temperature was minimum at tray 1 and maximum at tray 20 similar to that of pressure but temperature increases non linearly with number of trays. Temperature plays vital role in the positioning of side stream for particular product requirement that is diesel or naptha. The profile obtained was appropriate since pressure at bottom is always more than at top because at bottom reboiler is there and at top condensor. So corresponding to pressure temperature varies directly with a positive order not linearly. Sudden changes in the slope of curve is due to the positioning of side streams that is 8^{th} and 15^{th} corresponding naptha outlet side stream and diesel outlet side stream respectively.

Among the lighter hydrocarbons, it was obtained that propane was maximum at top, then butane and then ethane and lastly the methane. These lighter hydrocarbon were found till stage 5 after that higher fractions were found. These lighter hydrocarbons are in vapour phase. This type of profile was shown in figure 6. Mole fraction of propane is much more as compared to other lighter hydrocarbons so this was an optimised model since it was producing LPG (main constituent's propane and butane) also. Mole fraction plays a vital role in showing up the variations of molecular weight and K value in Figure 7 and 8 respectively. Propane being maximum in mole fraction among lighter hydrocarbons and K value of propane being increasing as precedence of tray (in Figure 8) result in increasing trend of molecular weight across the precedence of tray (in Figure 7).
Density of light(vapour phase) would be maximum at top, since low temperature at top. Density was maximum at stage 2, since feed was entering at stage 2. Density of lighter hydrocarbon decreases non linearly till stage 20 as temperature increases and sudden changes in the slope of curve is due to the presence of side streams that is 8^{th} and 15^{th} corresponding naptha outlet side stream and diesel outlet side stream respectively. Molecular weight varies some how differently for light(vapour phase). It suddenly increases till stage 2 due to presence of feed stream and then decreases till 5^{th} tray and then again increases till last tray non linearly. Figure 7 shows the variation. Due to increase in K value of propane from tray 1 to 20, which is having the maximum molar fraction among the lighter components the molecular weight increases. Since K value is directly proportional to intrinsic viscosity and molecular weight.

Figure 8 shows the profile of K values with tray position of lighter hydrocarbons(Methane, Ethane, Propane, Butane). Methane being the lightest having maximum K value at top and rest three hydrocarbons have less Kvalues. K value of methane and ethane decreases whereas that of propane and butane increases and converges to certain range (12-22), easily visualised from the curve. K value is empirically parameter closely related to intrinsic viscosity based on molecular mass of polymeric material. As the K value of methane decreases with stage the intrinsic viscosity decreases and corresponding molecular weight decreases, some different pattern adopted by ethane, in this K value increases and then decreases, but as we proceed from 1^{st} to last tray the K value of ethane was fallen down so molecular weight decreases as per relation of K value with viscosity and molecular weight. But some different pattern adopted by propane and butane, in this the K value increases from 1^{st} tray to last tray and the variation is due to that molecular weight increases of heavier hydrocarbons. Even from figure 6, mole fraction of propane is more so more amount is present and this will be key to check molecular weight and due to this reason the molecular weight shown in Figure 7 increases due to major composition of propane present in proceeding trays.

After simulating the whole plant, work was done on optimization of the process, the above results the variation of all parameters with respect to tray position were on optimized model i.e. at 100^0c and 20 trays. The plant was simulated at higher and lower temperature but the product obtained was not according to Euro and Indian Standards shown in Table 5 . When the plant was simulated at lower temperature the the heat duty raised to 1.23*e^5 KJ/hr whereas the optimum condition i.e. 100^0c, the product obtained was according to standards

and even the heat duty was 7.834*e^4 KJ/hr. Number of trays were also optimized shown in the Table 6 and the optimum no. of trays were obtained to be 20. The Capacity of Fractionator corresponding to the optimum no. of tray was 77172 litres. Simulating the plant helped to calculate the accurate sizes of the equipments and to optimize the heat duty and other parameters.

IV. CONCLUSION

In the present work, an easy simulation and optimization procedure for waste plastic to hydrocarbons was proposed. A commercial process simulator Aspen Hysys is used for simulation. In this work a simulation model of distillation column was developed. A sensitivity study investigating the effects of various process parameters has been presented. The optimum temperature where the diesel and naptha product was similar to that of Euro standards was found to be 100^0C. The simulation model developed for the conversion of waste plastic to hydrocarbons can also be used as a guide for understanding the process. Diesel and Naptha obtained from waste plastic are in accordance with euro standards.

V. ACKNOWLEDGEMENTS

The Authors acknowledge the Indian Institute of Petroleum and would like to thank Dr Ajay Kumar (Indian Institute of Petroleum) for their kind help in making layout and design of the simulation model.

References

[1] A Singhabhandhu, T Tezuka: The waste-to-energy framework for integrated multi- waste utilization: Waste cooking oil, waste lubricating oil, and waste plastics. Energy.2010, 35, 2544-2551.

[2] A.K. Panda, R.K. Singh, D.K. Mishra, Thermolysis of waste plastics to liquid fuel: a suitable method for plastic waste management and manufacture of value added products a world prospective, Renewable Sustainable Energy.2010, 14, 233–248

[3] Shent HT, Pugh RJ, Forssberg E: A review of plastics waste recycling and the flotation of plastics. Resources Conservation and Recycling. 1999, 25, 85-109.

[4] C. Breen, P.M. Last, S. Taylor, P. Komadel, Synergic chemical analysis — the coupling of TG with FTIR, MS and GC–MS 2. Catalytic transformation of the gases evolved during the thermal decomposition of HDPE using acid-activated clays, Thermochim. Acta 2000, 363, 93–104

[5] G. Luo, T. Suto, S. Yasu, K. Kato, Catalytic degradation of high density polyethylene and polypropylene into liquid fuel in a powder-particle fluidised bed, Polym. Degrad. Stab. 2000, 70, 97–102.

[6] Sachin Kumar, Achyut K. Panda, R.K. Singh, A review on tertiary recycling of high- density polyethylene to fuel, Resources, Conservation and Recycling. 2011, 55, 893–910.

[7] B. Saha, A. K. Chowdhury, and A. K. Ghoshal. "Catalyzed Decomposition of Propylene and Hybrid Generic Algorithm for Kinetics Analysis". Applied Catalysis B: Environmental. 2008, 83, 265-276.

[8] G.J.T. Fernandes, V.J. Fernandes Jr., A.S. Araujo, Catalytic degradation of polyethylene over SAPO-37 molecular sieve, Catal. 2002, 75, 233–238.

[9] Y.H. Lin. "Production of valuable hydrocarbons by catalytic degradation of a mixture of post-consumer plastic waste in a fluidized-bed reactor". Polymer Degradation and Stability. 2009, 94, 1924-1931.

[10] I.C. Neves, G. Botelho, A.V. Machado, P. Rebelo, S. Ramoa, M.F.R. Pereira, A. Ramanathan, P. Pescarmona, Feedstock recycling of polyethylene over AlTUD-1 mesoporous catalyst, Polym. Degrad. Stab. 2007, 92, 1513–1519.

[11] Y.-H. Lin, W.-H. Hwu, M.-D. Ger, T.-F. Yeh, J. Dwyer, A combined kinetic and

[12] mechanistic modelling of the catalytic degradation of polymers, Journal of Molecular Catalysis A: Chemical. 2001, 171, 143–151.

[13] B. Csukás, M. Varga, N. Miskolczi,, S. Balogh, A. Angyal, L. Bartha, Simplified dynamic simulation model of plastic waste pyrolysis in laboratory and pilot scale tubular reactor, Fuel Processing Technology. 2013, 106, 86-200.

[14] J.N. Sahu, K.K. Mahalik, Ho Kim Nam, Tan Yee Ling,Teoh Swee Woon, Muhammad Shahimi bin Abdul Rahman, Y.K. Mohanty,N.S. Jayakumar, feasibility study for catalytic cracking of waste plastic to produce oil and simulation using aspen plus.

[15] 2013, 1346-1356.

[16] Pravin Kannan, Ahmed Ali Shoaibi and C. Srinivasakannan, optimisation of waste plastic gasification process using Aspen plus. 2012, 279-296.

Table 1: Specifications of Fractionator

Conditions/Specifications	Values
Overall hydrocarbon mixture flow rate	208 kg/hr
Number of stages/trays	20
Feed stages	2
Hydrocarbon mixture Liquid flow rate	55.34 kg/hr
Hydrocarbon mixture Vapour flow rate	152.9 kg/hr
Temperature of inlet Hydrocarbon mixture	100 ^{0}C
Pressure of inlet Hydrocarbon mixture	500 kPa
Composition of product conditions Diesel Naptha LPG Bottom Product	 70% 8% 7% 15%
Tray efficiency	0.5
Pressure drop across column	30kPa
Reboiler heat duty KJ/hr	7.83* e^4
Preheater duty KJ/hr	1.77* e^5

Table 2: D86 Data

Volume %	Temperature ^{0}C
5	151
10	165
20	171
30	184
40	199
50	220
60	239
70	254
80	239
90	242
100	243

Table 3: Diesel Product Cut Point at different Temperature Ranges

Cut Point	TBP ^{0}C	ASTM D86 ^{0}C	D86 Crack Reduced ^{0}C
0	109.14	149.69	149.69
1	120.49	156.96	156.96
2	130.41	163.42	163.42
3.5	142.29	171.31	171.31
5	150.59	176.92	176.92
7.5	161.38	184.34	184.34
10	170.29	190.57	190.57
20	199.42	211.62	211.62
30	221.51	228.29	228.29
40	248.27	249.53	249.53
50	273.62	270.09	266.26
60	293.14	285.73	280.64
70	317.33	305.64	298.43
80	337.23	323.20	313.50
90	361.91	345.05	331.29
100	445.88	403.55	372.56

Table 4: Naptha Product Cut Point at different Temperature Ranges

Cut Point	TBP ^{0}C	ASTM D86 ^{0}C	D86 Crack Reduced ^{0}C
0	-75.99	-30.61	-30.61

1	-56.88	-20.37	-20.37
2	-46.87	-14.75	-14.75
3.5	-41.52	-11.06	-11.06
5	-9.63	14.18	14.18
7.5	-5.38	17.89	17.89
10	-1.98	20.89	20.89
20	54.34	72.15	72.15
30	78.37	91.99	91.99
40	94.66	103.07	103.07
50	109.00	112.67	112.67
60	123.56	123.00	123.00
70	138.48	134.15	134.15
80	153.91	146.62	146.62
90	172.93	162.81	162.81
100	219.59	204.13	204.13

Table 5: Optimization of Temperature

Temperature	Reboiler Heat duty KJ/hr	Diesel Final boiling point cut	Naptha final boiling point cut
112^0C	$6.78*e^4$	379.8 ^{0}C	216 ^{0}C
100^0C	$7.83*e^4$	372.6 ^{0}C	204.1 ^{0}C
60^0C	$1.04*e^5$	366.4 ^{0}C	179.3 ^{0}C
31^0C	$1.23*e^5$	362.1 ^{0}C	170.6 ^{0}C

Table 6: Optimization of number of stages

Number of Stages	Reboiler Heat duty KJ/hr	Diesel Final boiling point cut	Naptha final boiling point cut
20	$7.83*e^4$	372.6 ^{0}C	204.1 ^{0}C
17	$7.54*e^4$	378.6 ^{0}C	207.1 ^{0}C
09	$7.12*e^5$	382.4 ^{0}C	212.3 ^{0}C
07	$6.78*e^5$	384.1 ^{0}C	217.6 ^{0}C

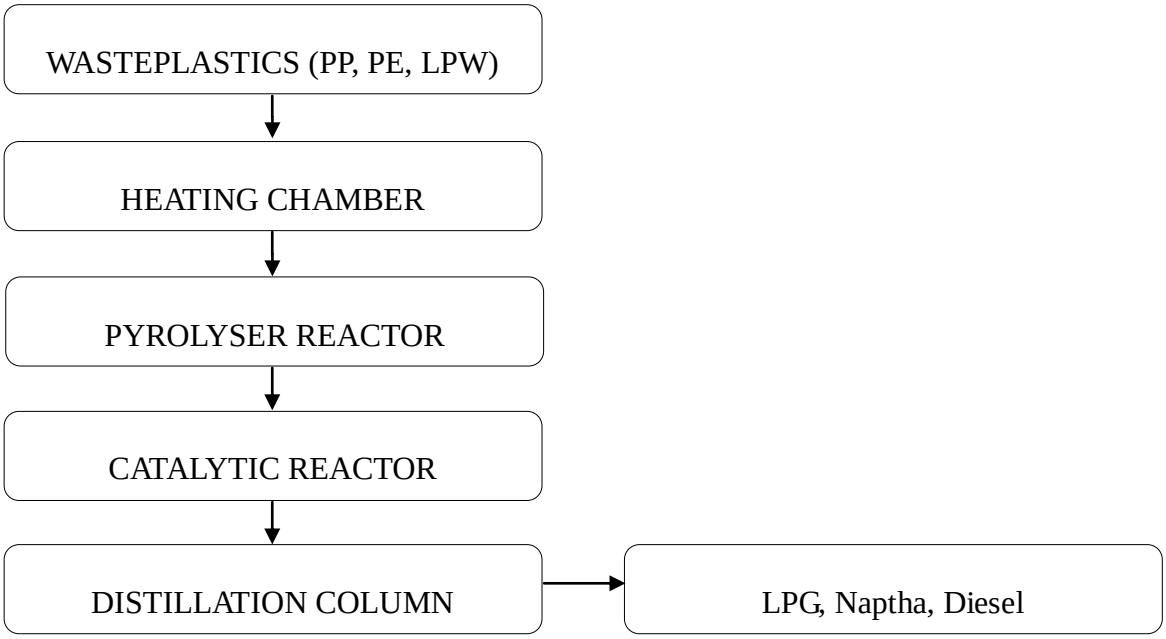

Figure 1: Process Flow Diagram

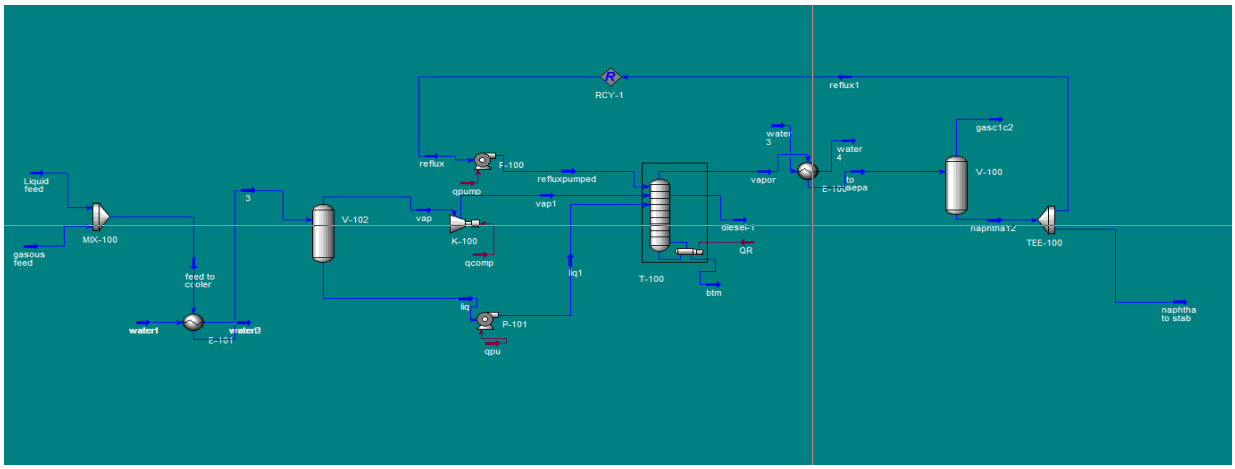

Figure 2: Simulation Flow Sheet

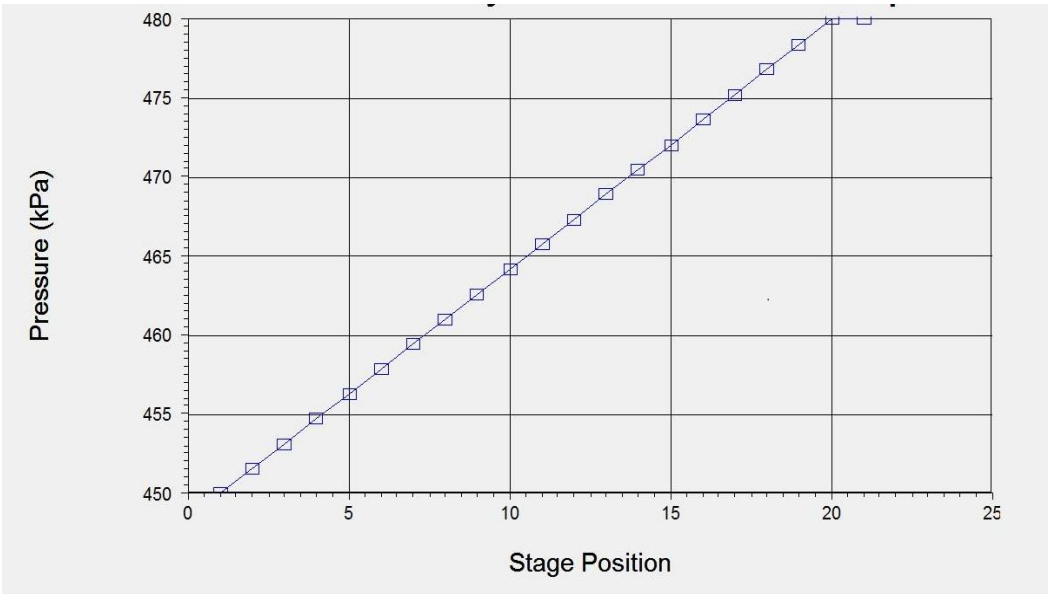

Figure 3: Pressure v/s no. of trays

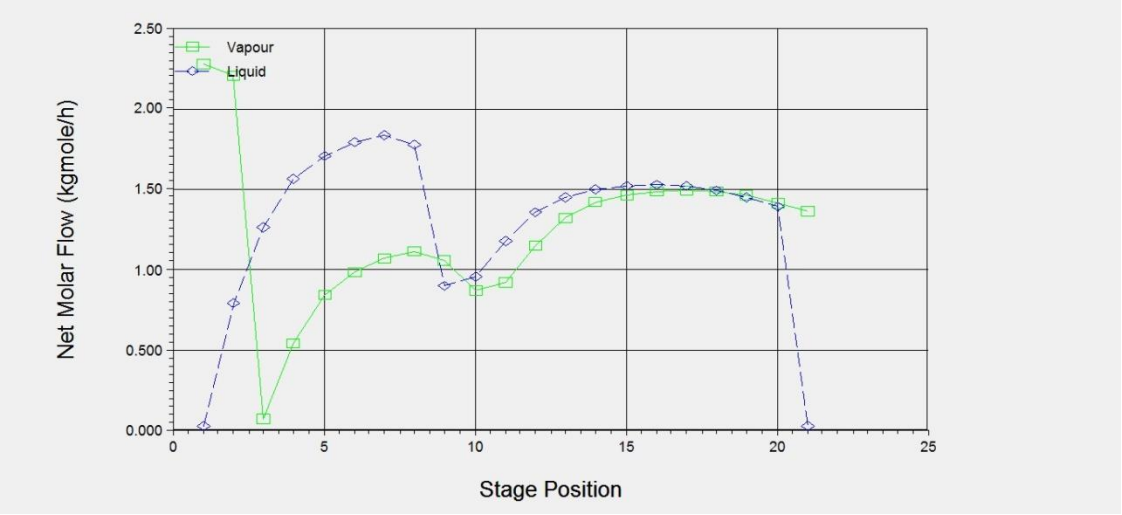

Figure 4: Molar flow v/s no. of trays

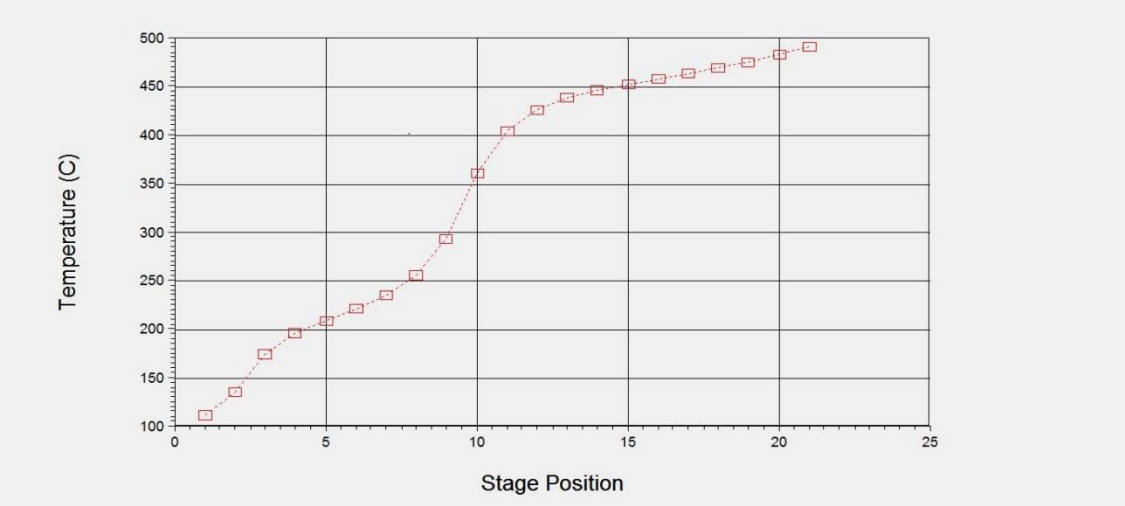

Figure 5: Temperature v/s no. of trays

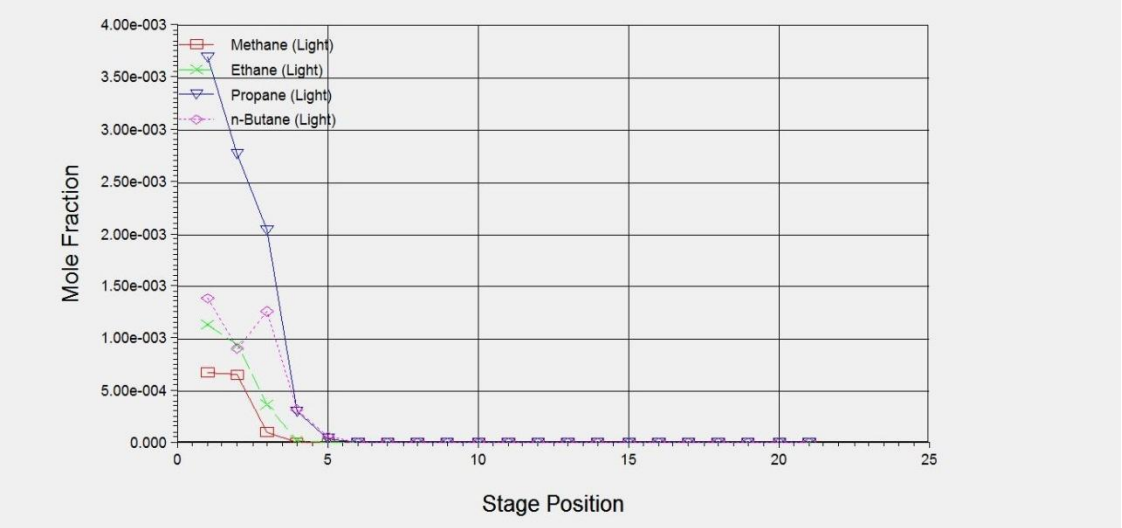

Figure 6: Composition v/s no. of trays

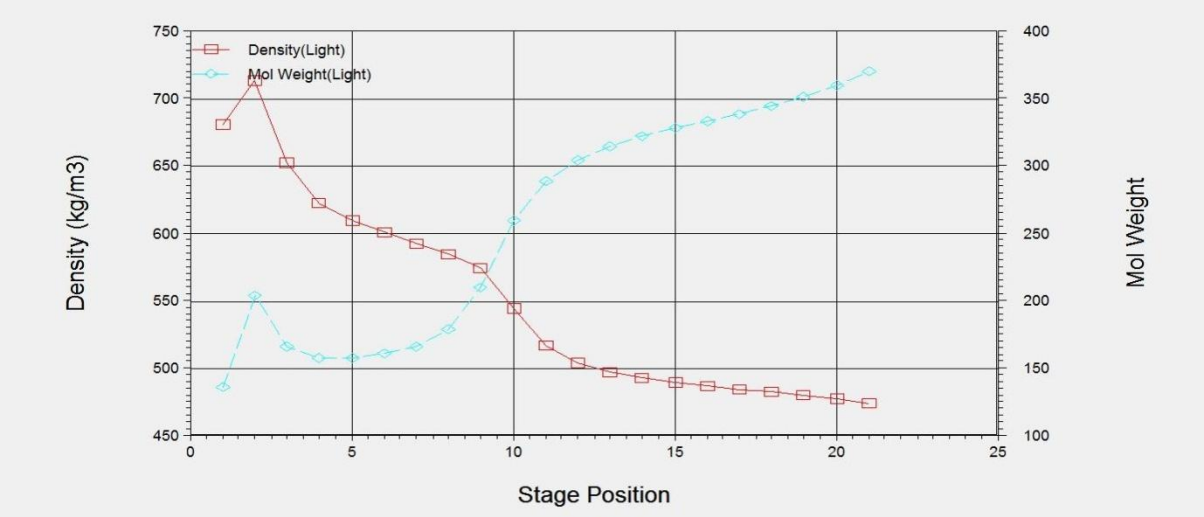

Figure 7: Column Properties v/s no. of trays

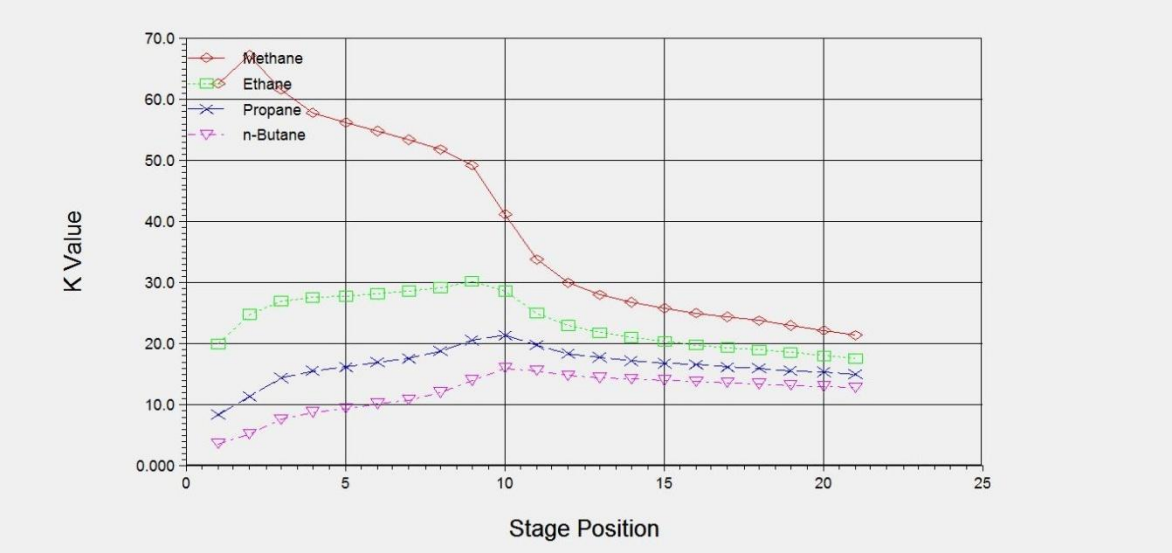

Figure 8: K Values v/s no. of trays

American Journal of Engineering Research (AJER)
e-ISSN : 2320-0847 p-ISSN : 2320-0936
Volume-03, Issue-11, pp-260-266
www.ajer.org

Research Paper Open Access

Assessment and ranking of traffic management Method for passenger safety in Zabol

[1,]Gholam Ali Khammar, [2,]Mohammad Podine
Assistant professor in Department of Geography and Urban Planning, University of Zabol, Zabol, Iran
MSc student in Department of Geography and Urban Planning, University of Zabol, Zabol, Iran

ABSTRACT : *The risk of accidents on the roads and the cost-benefit ratio of immunization impact, there is a direct connection. The Urban priority for immunization is important. To set priorities road safety with risk of accident, it is necessary to use quantitative methods for determination of dangerous conditions. Risk index ranking of streets or intersections are used in safety studies. In this regard, the present study aimed to assess and set priorities risk pathways index is in Zabol. Analytical method based on a library of documents and researches the type of field studies and surveys are used. For data analysis, the AHP model will be used. According to an analysis made of the 8 indicators for the safety of pedestrian traffic management: index (A) Improved control intersections (traffic islands - control priority - creating ways to turn right - creating fields - Installation Symptoms) weighing 0.258 intersection improvements In the ranked first, and the index (B) one-way streets in eighth place with a weight of 0.079 Placed in the eighth ranking.*

KEY WORDS: *priorities Passages, risk indicators, Traffic, Zabol*

I. INTRODUCTION

With the arrival of the industrial revolution in the eighteenth century, the city's population focus, activities and technological developments were intense. A waive of new industries and advanced manufacturing industries, including the cities began to rise. Quick and easy access to the vehicle and posterity of the results, such as traffic, pollution and accidents along. Vehicle accidents on urban roads is one of the major challenges of urbanization. This year many financial and physical damage afflicted on the citizens. Among the factors that cause an increase in traffic accidents each year are as follows. Urban population growth, the increasing number of vehicles, lack of enough investment in urban infrastructure, engineering and scientific principles to the design of other passages (Ghaforyan & Hakakzadah, 2010, 2).

To extend the life and increase car traffic in cities and roads in the past half century, unfortunately, the number and severity of traffic accidents is increasing rapidly. The economic and social benefits arising from to develop communication and speed of movement of goods and passengers had to be sought. Financial losses of life and property caused by accidents imposes a load on society. Therefore in the advanced industrialized countries and a broad range of research in universities and research centers on the causes and to occur traffic accidents and ways to avoid them or is in progress. Rate and calculate the waste and the costs to society are also included in this research. These countries through the application of these findings are much success in lessening the number and severity of crashes have achieved gains. Traffic engineering, to meet the needs of new and immerging problems of displacement, mobility and transport there is, is the product of social conditions. This means that new fields based on social conditions and community needs that arise and then changes. If the invention opens, it usually takes a longtime to understand it's implications for their users, but never realize they have it all. As technology is changing to meet the needs of the needs of the community, it's needs and new technologies are created. Engineers, who are constantly trying to meet these needs. (Hossayni, 2007, 25).

Based on studies of traffic accidents in Iran in comparison with developed nations and even in developing countries, much more. Loss of personnel was the worst results of accidents that high social and economic costs of irreparable affects on the community. The death toll in traffic accidents resulting in pedestrian accidents is very high. So, according to available statistics on accidents in urban traffic pedestrians 31.5% of

deaths within the city, as well about 43 percent of total deaths in crashes (urban and suburban) form (Hossayni, 2007, 25). Because little research has been done in the field of accidents pedestrians than other factors, such as neglected diseases society of accidents can be named.Obviously, with the current trend soon we will be witnessing a national bad luck. Because accidents are pedestrians, a multifactorial affect, remove the causes of accidents and pedestrians harness unpleasant subject, a comprehensive partnership between the organizations to demand ISPs. In this study, we tried to set priorities the passage of the comprehensive factors should be used to secure them.

II. BACKGROUND RESEARCH

Studies in the twenty-first century America has predicted more attention to issues of safety and security of transport, new technology and sustainable design directed and teal, 2002, 12) Daniel). In other studies, traffic safety management is the most important factor in traffic safety control are discussed. Traffic safety and management measures described in (Hu and Zhu, 2005, 2067). In the studies, to cultural issues have been discussed in the traffic safety and safety culture issues into three passages and the environment, and human error issues and problems associated with the automotive division (Adrian, 2006).Badgley and Jacobs to study traffic safety situation in developing countries are discussed. The result of their research is to remark a hierarchy of geometric design and safety in this country is one of the main problems (Baguley and Jacobs, 2001).
Stijn and Wets the study decided converting intersections to reduce accidents in the field. However, this study has proposed to review this matter, crash rates before and after to convert pedestrians and cyclists to explore the intersection (Stijn, Wets, 2006). In studies in Turkey because of the horizontal elements, most of geometric design. Vertical geometric design elements have been identified (Xiaoming etal, 2007).

Research Goals

- Identification of safety problems associated with traffic and for citizens
- Crash costs in cities
- Creating quiet to the streets to promote the welfare, safety and comfort

III. MATERIALS AND METHODS

The issues of decision variables related to problems in the real world, more and qualitative variables are interactive. These variables must be converted to numbers, mathematical decision models are applied to the decision making several models exist in between the multiple attribute decision making model (MADM) is noted. Technique (AHP) by Prof. Thomas L. Saaty In the late seventies. Passion is presented. This model is one of the best multi-criteria decision making models and it is great. This method is the most comprehensive system designed for multiple criteria decision making, because this technique to formulate the problem and provides a hierarchy of qualitative and quantitative indicators, as well as to consider the issue. Accordingly, this paper introduces the study area, indicators were selected by the study were analyzed in three stages.Finally, a scheme of priorities the-current criteria for the use of the AHP model has been done. The population of this study consisted of managers and planners. Random sampling and systematic sampling using Cochran formula to collect data from questionnaires, use of library resources and Internet sites. All data gathered originally collected and subsequently processed by Excel software Expert Choice Software is a specialized application for AHP model has been analyzed.

Theoretical Foundations

Urban Spaces : Difference and diversity in cities puts people together who have different patterns of life and makes the city an attractive place. But another aspect of this variation is unknown, the way humans that happens in a public place at a different time units (eg, streets, restaurants, etc.) Are not strangers to each other. Increases the anonymity of urban conditions. This could lead to increased human suffering, particularly for women and those who are more physically vulnerable.Urban spaces, social life and social fields to display different views of the city major identity, collective expression of urban areas, where the spirit of collective cooperation to strengthen compliance with the last goal of human civilized societies are social (Hanifiasal , 2009, 19).

Security : Security is one of important topics in the humanities, like many other concepts (society, culture, values, etc.) and the complexity innate and essential credit is being dumb. So Buzan, the leading theorists in this regard stated, every take on to understand the concept of security, without inconsistencies and lack of enough knowledge of these ideas is simplified (Tajik, 2000, 37).Canadian Defense Academy (1989), maintain security acceptable way of life for all people by the needs and lawful hopes of the citizens well-being. This includes, insisting the military, internal subversion and destruction of political values, economic and social, which are essential for quality of life (Buzan, 1999, 31).

Place of Security Studies in Geography and Urban Planning : Urban security in various fields of city planning concept that has been studied. By reviewing the literature, it is hard to separate the different academic disciplines in this category to be defined. This is mainly "because of the adoption of interdisciplinary perspectives and interdisciplinary study of man is freed from accepting any abstraction boundaries (Rahimi, 2011, 28).On the issue of urban insecurity as a subset of studies on the psychological aspects of quality of life in a form that describes the environmental quality of life of citizens. Lavinthal remarks came in second and third domain is the geographic studies. But as an urban geographer specializing in Security Studies, Rachel Paine wrote. Most new and interesting things about the fear out of the field of geographic space has been carried out. He also believes that most things in this case with emphasis on the physical environment is gone. While the concept of security and fear within the spatial and social exclusion can best be described (Pain, 2000, 366).

IV. AREA OF STUDY

Sistan region with an area of 15,197 sq km in the geographic range between 30°C and 5 minutes to 31 degrees 28 minutes latitude and 60 degrees 15 minutes to 61 degrees 50 minutes longitude in southeastern Iran and the northern part of the province and Balochistan by about one eighth of the total area allocated to the province. Average annual rainfall in the region 6/59 mm, mean annual temperature of 22°C and the average annual relative humidity is 38 Drsdmy.According to the classification criteria land Domarten 9/1 is classified as Frakhshk areas. One of the hallmarks of the region, which winds 120 days in the mountains between Afghanistan and plain air pressure, occurs. The wind almost from early June starting at about 4 months of the year continues in Zabol plain and almost Dravst September (late August) is terminated.

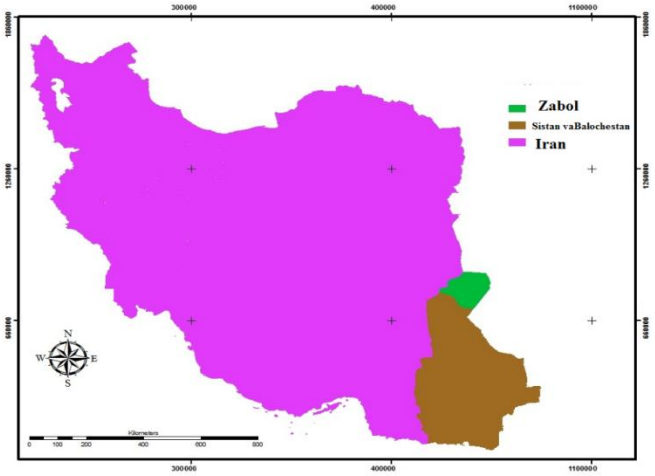

Figure (1): position in the region, Sistan-Baluchistan province, Source: research findings

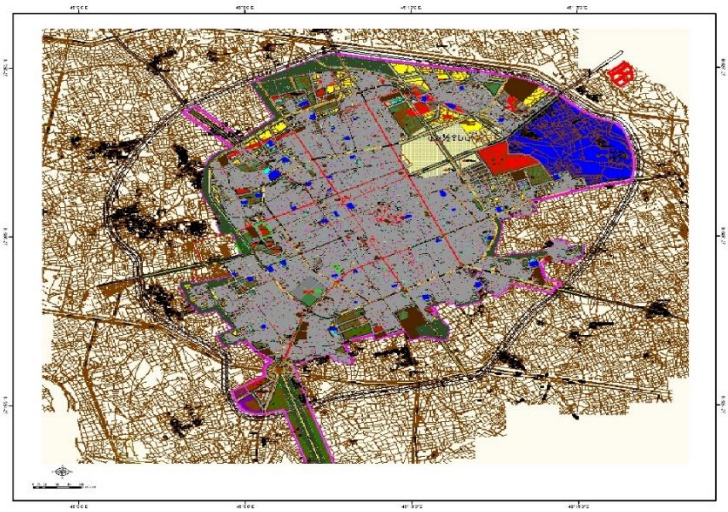

Figure (2): Map of Zabol, Source: research findings

V. DISCUSSION AND CONCLUSIONS

Traffic management measures for the safety of pedestrians

- control, parks, street and parking design optimization
- one-way streets
- the traffic calming measures
- color streets (line drawing, colored asphalt(
- Improved control intersections (traffic islands - control priority - creating ways to turn right - creating fields - Installation Symptoms)
- maintain the security of pedestrian crossing (passage - creating a protective fence)
- Crossing Constraints
- Measures to build sidewalks

First, the problems of converting a hierarchical structure that includes a three-level hierarchy of objectives, criteria, and be choices are

Table (1): Indicators for traffic management techniques for pedestrian safety

A	control, parks, street and parking design optimization
B	one-way streets
C	the traffic calming measures
D	color streets (line drawing, colored asphalt)
E	Improved control intersections (traffic islands - control priority - creating ways to turn right - creating fields - Installation Symptoms)
F	maintain the security of pedestrian crossing (passage - creating a protective fence)
G	Crossing Constraints
H	Measures to build sidewalks

Source: research findings

Comparison matrix to determine the binary parameters (A =ahj) question are results and their importance and expertise of specialists in this field is used.

Table (2): Matrix A couple of indicators

H	G	F	E	D	C	B	A	Indicators
1.4	1.3	1.7	1.8	1.2	7	1	2	A
3	4	1.3	1.5	4	2	5	1	B
5	7	1.3	3	1.2	1	1.7	1.2	C
6	8	1.2	2	1	2	2	1.4	D
2	6	1.3	1	1.2	1.3	8	5	E
5	8	1	3	2	3	7	3	F
1.3	1	1.8	1.6	1.8	1.7	3	1.4	G
1	3	1.5	1.2	1.6	1.5	4	1.3	H
24.07	38.03	10.09	15.01	13.08	19.05	31.7	16.03	∑

Source: research findings

Matrix pair (two for binary) index is obtained as follows:

It is to fill this matrix; scale of 1 to 9 is used to determine the relative importance of each element relative to other elements.

Table (3): 9 Saaty scale quantitative comparison of binary options

Intensity of importance	1	3	5	7	9	2-4-6-8
Definitaion	Equal importance	Weak importance of one over another	Essential of strong importnace	Demonstrated importance	Absoloute importance	Intermediate values

Source: research findings

After forming the matrix of paired comparisons and values should be the norm. For this purpose, the value of each column of the matrix corresponding to the sum will be divided.

Table (4): Paired comparison matrix normalized relative indicators and weights

H	G	F	E	D	C	B	A	Indicators
0.056	0.033	0.155	0.119	0.086	0.358	0.031	0.122	A
0.121	0.104	0.119	0.099	0.298	0.102	0.157	0.061	B
0.202	0.182	0.119	0.198	0.086	0.051	0.053	0.073	C
0.242	0.208	0.110	0.132	0.072	0.102	0.063	0.085	D
0.080	0.156	0.119	0.066	0.086	0.066	0.252	0.306	E
0.202	0.208	0.091	0.198	0.144	0.153	0.220	0.184	F
0.052	0.026	0.165	0.105	0.130	0.087	0.094	0.085	G
0.040	0.078	0.137	0.079	0.115	0.076	0.126	0.079	H

Source: research findings

The logical consistency of judgments : now the same steps for all choices of (a, b, c,) we do. This step must be calculated to determine whether the inconsistency rate between paired comparisons we are compatible or not. Here are just a couple of inconsistency rate for comparisons of account we choices of similar operations to be performed on every indicator. Inconsistency rate can be obtained from the following relationship be:

$$I..R. = \frac{I..I.}{I..I..R.}$$

Inconsistency rate (IR): the table below is extracted:

N	1	2	3	4	5	6	7	8	9	10
$I..I..R$	0	0	0/58	0/9	1/12	1/24	1/32	1/41	1/45	1/45

So the inconsistency rate calculations in the present study, 0.060 is .Since IR = 0.060 smaller than 0/1 , then the paired comparisons , there is a remarkable consistency All calculations of the eigenvector (eigenvector) is carried out .In the questionnaire, and explain briefly introduce the measure compiled and presented in Table values for comparison of paired preference, paired- comparison was requested to be completed. The sample questionnaire, and program managers are urban planners. After collection, analysis and verification questionnaire, the following results were obtained:

A (L: 0.161) B (L: 0.079) C (L: 0.206) D (L: 0.092) E(L: 0. 258) F (L: 0.207) G (L: 0. 103) H H(L: 0.122)

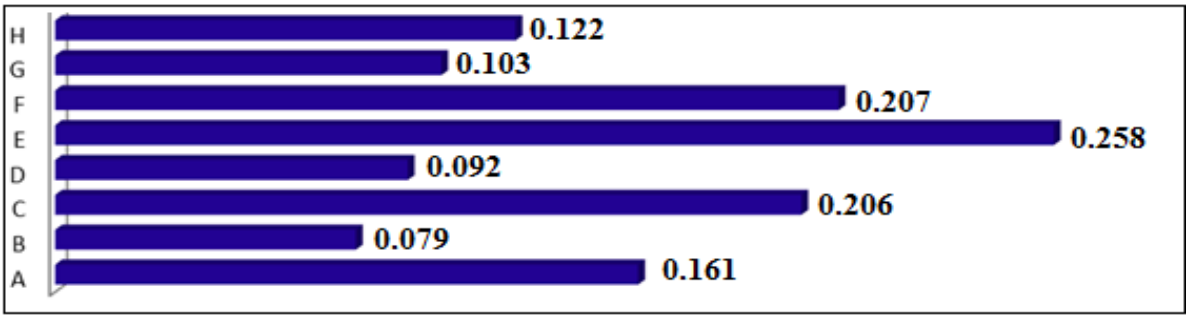

Inconsistency = 0.060
With 0 missing judgment
Figure (3): Results of hierarchical analysis using expert choice software, Source: research findings

Table (5): Prioritize and weight standard methods of traffic management parameters for pedestrian safety

Weight	Criterion	Indicators
0.161	control, parks, street and parking design optimization	A
0.079	one-way streets	B
0.206	the traffic calming measures	C
0.092	color streets (line drawing, colored asphalt)	D
0.258	Improved control intersections (traffic islands - control priority - creating ways to turn right - creating fields - Installation Symptoms)	E
0.207	maintain the security of pedestrian crossing (passage - creating a protective fence)	F
0.103	Crossing Constraints	G
0.122	Measures to build sidewalks	H

Source: research findings

According to an analysis made of the 8 indicators for the safety of pedestrian traffic management:
index (E) Improved control intersections (traffic islands - control priority - creating ways to turn right - creating fields - Installation Symptoms) weighing 0.258 intersection improvements In the ranked first,
The Second rank, the index (F) maintain the security of pedestrian crossing (passage - creating a protective fence) with a standard weight of 0.207.
The Third rank, the index (C) the traffic calming measures, weighing 0.206,
The Fourth rank, the index (A) control, parks, street and parking design optimization of weighing 0.161,
The Fifth rank, the index (H) Measures to build sidewalks weighing 0.122 metric.
The sixth rank, the index (G) Crossing Constraints the weight 0.103.
The seventh rank, the index (D) color streets (line drawing, colored asphalt) with a standard weight of 0.092.
Finally, the eighth rank, the index (B) one-way streets in eighth place with a weight of 0.079 criterion.

VI. CONCLUSIONS

Given the above, promote safety should be a priority agenda guardians of safety of urban street network, so traffic accidents are usually killed and wounded civilians, may be lessened. One of the most important reasons of urban road safety promotion, pay attention to all the little issues at planning and urban design. Meanwhile, the city streets should be the main factor of movement and on the other hand, all factors must be considered to prevent the accident. A citizen in an urban street network should be able to benefit from intelligent transport systems, knowledge based, at least time to reach its destination safely and comfortably. Necessary for a safe trip, the design and definition of safe access routes to the city and the street network without stopping chemists using different modes of transport is. This is no integrated street network and travel exchange points is not possible.According to an analysis made of the 8 indicators for the safety of pedestrian traffic management: index (A) Improved control intersections (traffic islands - control priority - creating ways to turn right - creating fields - Installation Symptoms) weighing 0.258 intersection improvements In the ranked first, and the index (B) one-way streets in eighth place with a weight of 0.079 Placed in the eighth ranking.
At the end of the speech in favor of the Messenger of Islam as saying "the city in which the server is not secure, not cities", it is hoped to be able to complete to develop an urban street network, reducing travel time and promote the culture of passage among people, the most advanced and integrated transport network traffic to provide citizens with the use of different modes of transport and infrastructure communication, traffic systems available, safe, smooth, comfortable and clean home We promote safety and street network and global transport system and urban traffic assist.

VII. SUGGESTIONS

- Different routes of public transport to access the city center and main hub with access from one system to another in minimum time.
- Proper design of space stations. In order to properly cover the districts of Zabol public transport system in terms of demand.
- Design and defining the access routes to all networks Zabol road.
- Increase the comfort and safety of passengers getting on and off and on during the trip and pay special attention to the elderly and disabled.
- Safety inspection infrastructure in urban street network.
- Laws and rules and uphold them.
- Rapid implementation and low cost of transport and traffic.
- Improve the efficiency of existing facilities, considering the needs of different users of the street.

REFERENCE:

[1] Adrian, roy, (2006), Traffic Safety Issues of the Future: A Long Range Research Agenda, Federal Highway Administration National Highway Traffic Safety Administration.
[2] Baguley and G D Jacobs, (2001), TRAFFIC SAFETY ISSUES FOR THE NEXT MILLENNIUM, Transport Research Laboratory.
[3] Buzan,B, (1999), People, States and Fear, Publication Research Institute of Strategic Studies.
[4] Daniel b. fambro, john c. collings, john c. collings, john c. collings, john m. mason, jr, (2002), Geometric Design: Past, Present, and Future, Texas A&M University report.
[5] Ghaforyan, M. Hakakzadah M., (2010), because of traffic accidents on the roads within the city of Kerman province in 88, Conference on Traffic Safety, p 2.
[6] Hanifiasal.Y, (2009). Safety assessment of the role of women in to plan urban spaces Uremia with the PUA. Master's thesis, Supervisor: Akbar Kiani, Zabol University, Department of Geography: pp 100 1.
[7] Hossayni, P, (2007), studies of pedestrians in Khorramabad, MS Thesis, Police since University, 25.
[8] Hu Qionghong, Zhou Zhiyun, (2005), Study on the urban road traffic safety management, Proceedings of the Eastern Asia Society for Transportation, Studies, Vol. 5, pp. 2062 – 2074.
[9] Pain, Rachel, (2000), Place, Social relation and the fear of crime:review,Progress in human Geography ,Vlo 24, pp 365-387.

[10] Rahimi jagh jaghi, H, (2011), analyzes the concept of security from the prospective of social groups in the city center (Case Study: 9 in twelve districts of Tehran), Master's thesis, Tarbiat Modares University.
[11] Stijn Daniels, Geert Wets, (2006), Traffic safety effects of roundabouts: a review with emphasis on bicyclist's safety, Hasselt University, Transportation Research Institute (IMOB), Wetenschapspark 5, 3590 Diepenbeek, Belgium.
[12] Tajik, M. R, (1999); safe in dialogue Khatami, Tehran: Ney Publication.
[13] Xiaoming Zhong, Yuanyuan Wang, Liande Zhong, Xinzheng Zhu, JiaJia, Ming Zhao, Jianming Ma, Xiaoming Liu, (2007), Study on the Relationship of Intersection Design and Safety of Urban Unsignalized Intersection in China, 3rd Urban Street Symposium of the Transportation Research Board.

American Journal of Engineering Research (AJER)
e-ISSN : 2320-0847 p-ISSN : 2320-0936
Volume-03, Issue-11, pp-267-276
www.ajer.org

Research Paper Open Access

Michael Is Chief Angel?...
(A New Theory On "Nephilim")

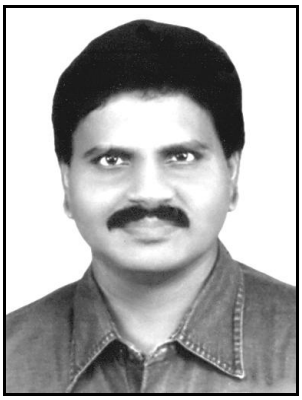

M.Arulmani,
B.E.
(Engineer)

V.R.Hema Latha,
M.A., M.Sc., M.Phil.
(Biologist)

ABSTRACT: ***"Michael" is chief of all Angels?... No… No… No…*** *The "**HOLY ADAM**" shall be considered as **Chief of all Angels**. Michael shall mean "**FALLEN ANGEL**".*

*This scientific research attempts to clarify certain fundamental questions about **Holy Angel, Archangel, Angel of Lord, Fallen Angel** based on global level religion, Christian Faith and how "**Angel**" differs from "**Human**".*

*This research focus that the Biblically stated "**ADAM**" shall be considered as "**HOLY ADAM**" belong to "**ANGEL FAMILY**" Human race lived in **WHITE PLANET** (White Mars) before eating "**forbidden fruit**", and descended to **EARTH PLANET** as "**Fallen Angels**" after eating forbidden fruit.*

*This research further focus that the Angel populations lived in **white planet** in the early Universe shall be considered as '**SUPER HUMAN RACE**' also called as '**NEPHILIM**'. The Nephilim shall be considered as the **Natural Human** originated due to impact of '**J-RADIATION**' (Zero hour radiation) and considered lived under **Endothermic and Microgravity environment**.*

JOULE
(Zero Hour Radiation)

It is further focused that **Nephilim Race** (Angel family) shall be considered as the human populations where '**Male**' is responsible for '**Pregnancy**' and regenerate population through "**EGG**" due to impact of "**J-**

RADIATION" composed of fundamental particles without involvement of any '**sexual act**' between **male angel, female angel** of Nephilim race. Female angel shall be considered as a **guardian angel** for assisting male angel for **safe delivery**.

> *"**HOLY ADAM** shall be considered as **Father of all Angels**; "**HOLY EVE**" shall be considered as **mother of all angels**. "**MICHAEL**" shall be considered as one of the Angels of Nephilim race descended to earth planet. The fallen angels on the Earth planet shall be considered belong to **Woman Race** responsible for **Female pregnancy** through sexual act subsequently. All angels like Gabriel, Raphael, Metatron, Uriel, Sariel, Raguel, Remiel, Jophiel, Chamuel etc shall be considered as pertain to Nephilim race of **white planet**."*
>
> ***…M. Arulmani, Tamil Based Indian***

KEY WORDS:
a) Philosophy of '**Supernature**'?...
b) Philosophy of '**Creator**'?...
c) Philosophy of '**Archangel**'?...
d) Philosophy of '**Angel of Lord**'?...
e) Etymology of word '**Michael**'?...
f) Son of man differs from '**Son of God**'?...

I. INTRODUCTION:

Case study shows that in ancient Greek, Hebrew mythology there are so many theories about the philosophy of '**Nephilim**'. Nephilim is considered as **heavenly beings** who came to '**Earth**' and had sexual intercourse with woman and regenerate earthly populations. In Hebrew Nephilim means '**Giant**' and perceived as "**fallen Angel**".

In Christian theology the philosophy of Angel is considered as follows:

[1] Angels are spirit beings (Heb 1:14)
[2] Angels are Higher creatures than Human (Psalm 8:5)
[3] Angels need not consume Eucharist
[4] Angels need not be redeemed by Jesus.
[5] Angels do not have married life.

This scientific research focus that Angels shall be considered as **natural populations** evolved of **J-RADIATION** (Zero Hour Radiation) just like birth of **Mushroom** due to impact "**Lightning**". The Angels shall be considered as **Superior human race** and ancestors to **Earthly human race**.

II. HYPOTHESIS AND NARRATIONS

Angels are born of "Soul"?...

It is hypothesized that Angels shall be considered as born of "**J-Radiation**" consists of fundamental particles **photon, electron, proton** having zero mass or negligible man exists under zero gravity (or) upward gravity. The J-Radiation shall also be called as "**Soul**". **If so… What is the source of soul?...**

It is hypothesized that "**SPIRIT**" shall be considered as the source of '**SOUL**' as described below. The spirit shall also be called as "**Supernature**" and the soul shall be called as '**Nature**'.

(i)

(SUPER NATURE)

(ii)

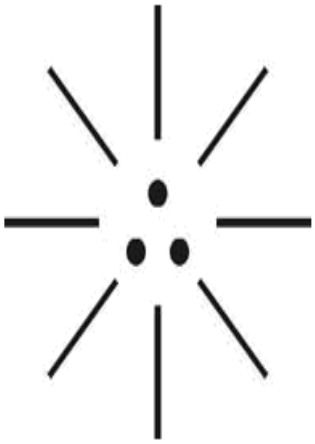

(NATURE)

(iii)

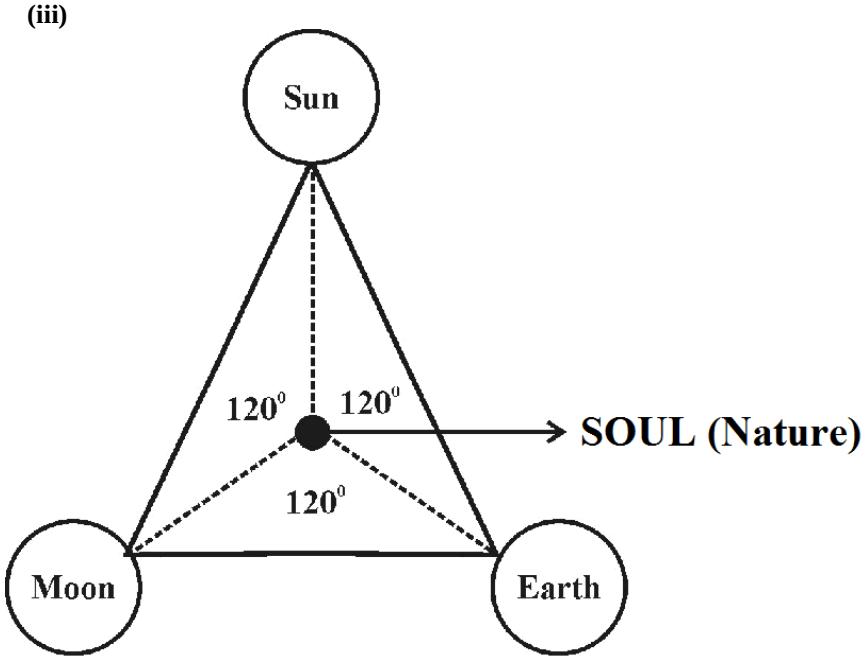

SPIRIT
(Super Nature)

a) Philosophy of 'Creator"?...

It is hypothesized that the '**supernature**' shall be considered as '**creator**' also called as '**Archangel**'.

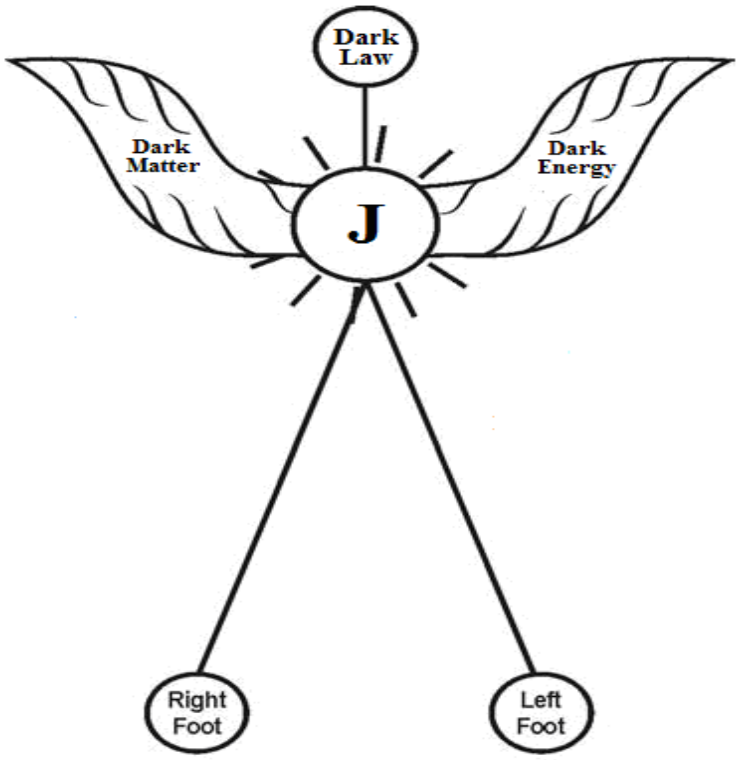

ARCHANGEL
(Creator)

b) Philosophy of Angel of Lord?...

Based on Biblical faith, '**JESUS CHRIST**' shall be hypothetically considered as the '**Angel of Lord**' or '**Archangel**' also called as '**Son of God**'. Further it is emphasized that son of God shall be considered as having distinguished meaning from '**Son of man**' as described below.

(i)

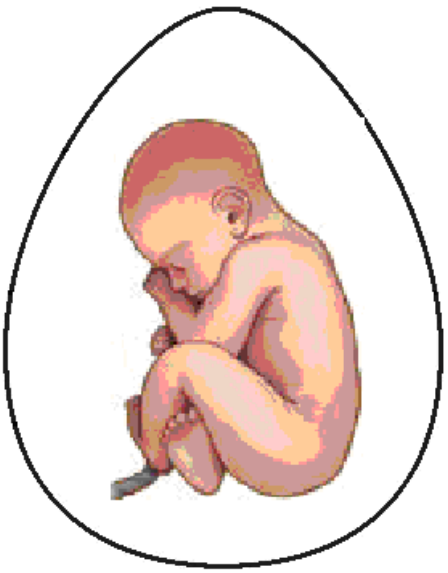

ARCHANGEL
(Son of God)

(ii)

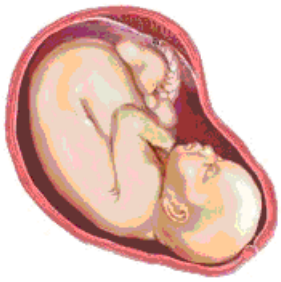

FALLEN ANGEL
(Michael)

(iii)

EVANGELIC ANGEL
(Son of Man)

c) Philosophy of immortal Soul?...

Soul is immortal?... Yes… Yes… Yes… It is hypothesized that soul shall be considered as zero hour energy which enables formation of billions of natural matters (virgin matter) in the early Universe. The natural matters shall be considered as **distinguished angels.** Alternatively "**SOUL**" shall be considered as "**ANGEL**".

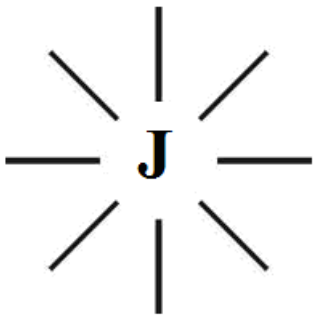

ANGEL
(Immortal Soul)

After death of a person the departed soul of every one right from Adam, Eve, Noah, Abraham, Isaac, Jacob, Moses, Daniel etc shall be considered as transformed as **ANGELS** with **material body**. The transformed souls shall be considered as **LIVING ANGELS** exist in upper atmosphere just like viewed sitting inside the

FLIGHT called as **ANGEL FLIGHT** till **FINAL JUDGEMENT.** The **demon, evil spirit** shall be considered as temporary impact on fellow human during transformation and ultimately becoming **angel**.

MODEL ANGEL FLIGHT
(Living Angels)

"Soul neither be created nor destroyed but it can be transformed from soul to angel or angel to soul"

…Author

d) Philosophy of Soul of Mother Mary?...

It is hypothesized that **MOTHER MARY** shall be considered as integral part of heavenly father and Son of God and cannot be separated. Mother Mary shall be considered as **LIVING ANGEL** exist in the **ANGEL FLIGHT** until final judgment.

[1] **JESUS CHRIST** is like **PILOT**
[2] **MOTHER MARY** is like **AIRHOSTESS**
[3] **HEAVENLY FATHER** is like **BLACK BOX**
[4] **PETER** is like **COPILOT** (Assisting Jesus Christ)

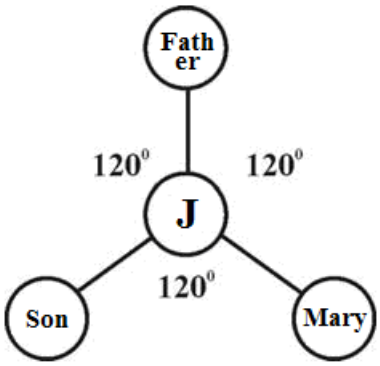

(ARCHANGEL)

e) Philosophy of 1000 Years Rule?...

It is hypothesized that birth of Jesus Christ shall be considered as **FIRST ADVENT** and **RESURRECTION** of Jesus Christ shall be considered as **SECOND ADVENT**. It is speculated that 1000 Years rule already started the day when Jesus Christ Resurrected. Second resurrection shall be considered as the day when Mother Mary has been resurrected after resurrection of Jesus Christ. It is focused that presently the earthly population shall be considered under third extension of **gracious period** of 1000 years and it may go up to 3000AD for end of Universe and for **NEW LIFE** (Matt 24:31, 25:31,41).

f) Etymology of word Michael?...

Case study shows that Michael in Hebrew language means **WHO IS LIKE GOD?...** It is hypothesized that the '**HOLY ADAM**" before consuming **Forbidden fruit** shall be called as **HOLY ANGEL** who shall be considered as the **Chief of all Angels**. The etymology of word **Michael, Mega** might be derived from philosophy of proto Indo Europe root word **'MIKAI', 'MIKKAR'**. Mikkar shall mean "**Superior**" (Giant). Michael shall be considered as the **FALLEN ANGEL** or **DARK ADAM.**

(i)

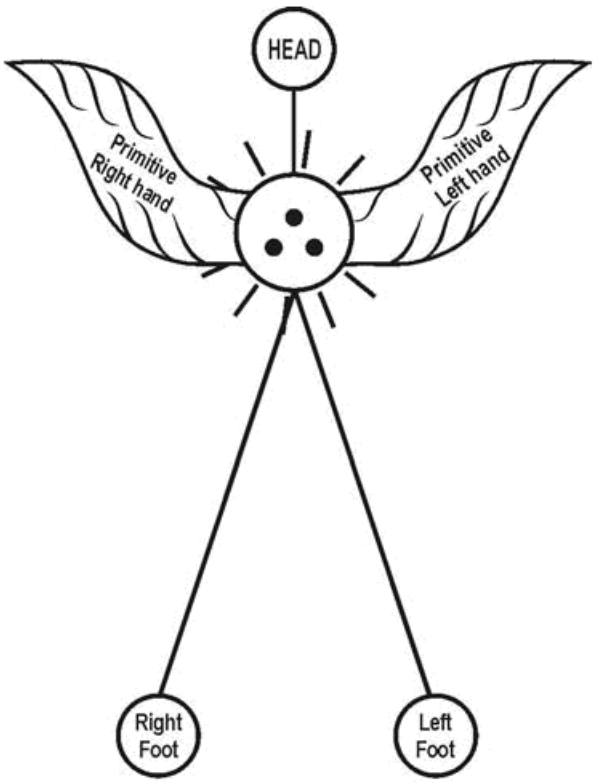

மிக்கார்
(HOLY ADAM)

(ii)

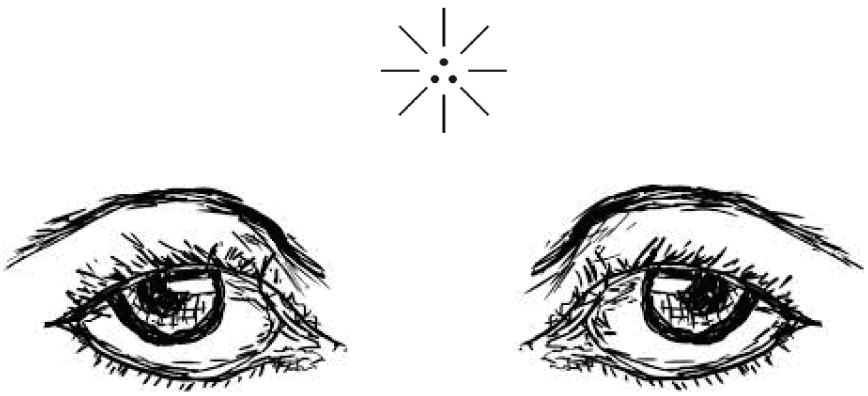

மீகா
(HOLY EVE)

g) Case study on "Nephilim"

[1] The Nephilim were offspring of "**Sons of God**" and "**Daughters of men**" before the Deluge
i. (Genesis 6:4)

[2] ii) Nephilim are **Heavenly beings** who came to Earth.
[3] -New American Bible Commentry.

[4] iii) Nephilim are "**anecdote of Superhuman race**"
- Jerusalem Bible

II. CONCLUSION:

Nephilim shall be considered as natural human population belong to angel family lived in white planet. In Nephilim population, male is responsible for pregnancy and regeneration. In earthly population, female is responsible for pregnancy and regeneration. Angel shall alternatively mean soul.

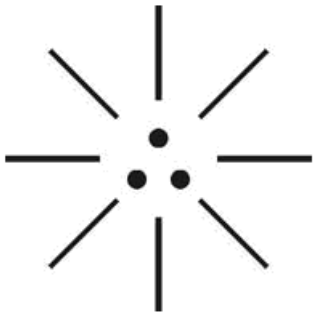

ANGEL
(Soul Logo)

III. PREVIOUS PUBLICATION:

The philosophy of origin of first life and human, the philosophy of model Cosmo Universe, the philosophy of fundamental neutrino particles have already been published in various international journals mentioned below. Hence this article shall be considered as **extended version** of the previous articles already published by the same author.

[1] Cosmo Super Star – IJSRP, April issue, 2013
[2] Super Scientist of Climate control – IJSER, May issue, 2013
[3] AKKIE MARS CODE – IJSER, June issue, 2013
[4] KARITHIRI (Dark flame) The Centromere of Cosmo Universe – IJIRD, May issue, 2013
[5] MA-AYYAN of MARS – IJIRD, June issue, 2013
[6] MARS TRIBE – IJSER, June issue, 2013
[7] MARS MATHEMATICS – IJERD, June issue, 2013
[8] MARS (EZHEM) The mother of All Planets – IJSER, June issue, 2013
[9] The Mystery of Crop Circle – IJOART, May issue, 2013
[10] Origin of First Language – IJIRD, June issue, 2013
[11] MARS TRISOMY HUMAN – IJOART, June issue, 2013
[12] MARS ANGEL – IJSTR, June issue, 2013
[13] Three principles of Akkie Management (AJIBM, August issue, 2013)
[14] Prehistoric Triphthong Alphabet (IJIRD, July issue, 2013)
[15] Prehistoric Akkie Music (IJST, July issue, 2013)
[16] Barack Obama is Tamil Based Indian? (IJSER, August issue, 2013)
[17] Philosophy of MARS Radiation (IJSER, August 2013)
[18] Etymology of word **"J"** (IJSER, September 2013)
[19] NOAH is Dravidian? (IJOART, August 2013)
[20] Philosophy of Dark Cell (Soul)? (IJSER, September 2013)
[21] Darwin Sir is Wrong?! (IJSER, October issue, 2013)
[22] Prehistoric Pyramids are RF Antenna?!... (IJSER, October issue, 2013)
[23] HUMAN IS A ROAM FREE CELL PHONE?!... (IJIRD, September issue, 2013)
[24] NEUTRINOS EXIST IN EARTH ATMOSPHERE?!... (IJERD, October issue, 2013)

[25] EARLY UNIVERSE WAS HIGHLY FROZEN?!... (IJOART, October issue, 2013)
[26] UNIVERSE IS LIKE SPACE SHIP?!... (AJER, October issue, 2013)
[27] ANCIENT EGYPT IS DRAVIDA NAD?!... (IJSER, November issue, 2013)
[28] ROSETTA STONE IS PREHISTORIC "THAMEE STONE" ?!... (IJSER, November issue, 2013)
[29] The Supernatural "CNO" HUMAN?... (IJOART, December issue, 2013)
[30] 3G HUMAN ANCESTOR?... (AJER, December issue, 2013)
[31] 3G Evolution?... (IJIRD, December issue, 2013)
[32] God Created Human?... (IJERD, December issue, 2013)
[33] Prehistoric "J" – Element?... (IJSER, January issue, 2014)
[34] 3G Mobile phone Induces Cancer?... (IJERD, December issue, 2013)
[35] "J" Shall Mean "JOULE"?... (IRJES, December issue, 2013)
[36] "J"- HOUSE IS A HEAVEN?... (IJIRD, January issue, 2014)
[37] The Supersonic JET FLIGHT-2014?... (IJSER, January issue, 2014)
[38] "J"-RADIATION IS MOTHER OF HYDROGEN?... (AJER, January issue, 2014)
[39] PEACE BEGINS WITH "J"?... (IJERD, January issue, 2014)
[40] THE VIRGIN LIGHT?... (IJCRAR, January issue 2014)
[41] THE VEILED MOTHER?... (IJERD, January issue 2014)
[42] GOD HAS NO LUNGS?... (IJERD, February issue 2014)
[43] Matters are made of Light or Atom?!... (IJERD, February issue 2014)
[44] THE NUCLEAR "MUKKULAM"?... (IJSER, February issue 2014)
[45] WHITE REVOLUTION 2014-15?... (IJERD, February issue 2014)
[46] STAR TWINKLES!?... (IJERD, March issue 2014)
[47] "E-LANKA" THE TAMIL CONTINENT?... (IJERD, March issue 2014)
[48] HELLO NAMESTE?... (IJSER, March issue 2014)
[49] MOTHERHOOD MEANS DELIVERING CHILD?... (AJER, March issue 2014)
[50] E–ACHI, IAS?... (AJER, March issue 2014)
[51] THE ALTERNATIVE MEDICINE?... (AJER, April issue 2014)
[52] GANJA IS ILLEGAL PLANT?... (IJERD, April issue 2014)
[53] THE ENDOS?... (IJERD, April issue 2014)
[54] THE "TRI-TRONIC" UNIVERSE?... (AJER, May issue 2014)
[55] Varied Plasma Level have impact on "GENETIC VALUE"?... (AJER, May issue 2014)
[56] JALLIKATTU IS DRAVIDIAN VETERAN SPORT?... (AJER, May issue 2014)
[57] Human Equivalent of Cosmo?... (IJSER, May issue 2014)
[58] THAI-e ETHIA!... (AJER, May issue 2014)
[59] THE PHILOSOPHY OF "DALIT"?... (AJER, June issue 2014)
[60] THE IMPACT OF HIGHER QUALIFICATION?... (AJER, June issue 2014)
[61] THE CRYSTAL UNIVERSE?... (AJER July 2014 issue)
[62] THE GLOBAL POLITICS?... (AJER July 2014 issue)
[63] THE KACHCHA THEEVU?... (AJER July 2014 issue)
[64] THE RADIANT MANAGER?... (AJER July 2014 issue)
[65] THE UNIVERSAL LAMP?... (IJOART July 2014 issue)
[66] THE MUSIC RAIN?... (IJERD July 2014 issue)
[67] THIRI KURAL?... (AJER August 2014 issue)
[68] THE SIXTH SENSE OF HUMAN?... (AJER August 2014 issue)
[69] THEE… DARK BOMB?... (IJSER August 2014 issue)
[70] RAKSHA BANDHAN CULTURE?... (IJERD August 2014 issue)
[71] THE WHITE BLOOD ANCESTOR?... (AJER August 2014 issue)
[72] THE PHILOSOPHY OF "ZERO HOUR"?... (IJERD August 2014 issue)
[73] RAMAR PALAM?... (AJER September 2014 issue)
[74] THE UNIVERSAL TERRORIST?... (AJER September 2014 issue)
[75] THE "J-CLOCK"!... (AJER September 2014 issue)
[76] "STUDENTS" AND "POLITICS"?... (IJERD October 2014 issue)
[77] THE PREGNANT MAN?... (AJER September 2014 issue)
[78] PERIAR IS ATHEIST?... (IJSER September 2014 issue)
[79] A JOURNEY TO "WHITE PLANET"?... (AJER October 2014 issue)
[80] Coming Soon!... (AJER October 2014 issue)
[81] THE PREJUDICED JUSTICE?... (IJERD October 2014 issue)
[82] BRITISH INDIA?... (IJSER October 2014 issue)
[83] THE PHILOSOPHY OF "HUMAN RIGHTS"?... (IJERD October 2014 issue)
[84] THE FOSTER CHILD?... (AJER October 2014 issue)

[85] WHAT DOES MEAN "CRIMINAL"?... (IJSER October 2014 issue)
[86] 1000 YEARS RULE?... (AJER November 2014 issue)
[87] AM I CORRUPT?... (IJSER November 2014 issue)
[88] BLACK MONEY?... (AJER November 2014 issue)
[89] DEAD PARENTS ARE LIVING ANGELS?... (IJERD November 2014 issue)

REFERENCE

[1] Intensive Internet "e-book" study through, Google search and wikipedia
[2] M.Arulmani, "3G Akkanna Man", Annai Publications, Cholapuram, 2011
[3] M. Arulmani; V.R. Hemalatha, "Tamil the Law of Universe", Annai Publications, Cholapuram, 2012
[4] Harold Koontz, Heinz Weihriah, "Essentials of management", Tata McGraw-Hill publications, 2005
[5] M. Arulmani; V.R. Hemalatha, "First Music and First Music Alphabet", Annai Publications, Cholapuram, 2012
[6] King James Version, "Holy Bible"
[7] S.A. Perumal, "Human Evolution History"
[8] "English Dictionary", Oxford Publications
[9] Sho. Devaneyapavanar, "Tamil first mother language", Chennai, 2009
[10] Tamilannal, "Tholkoppiar", Chennai, 2007
[11] "Tamil to English Dictionary", Suravin Publication, 2009
[12] "Text Material for E5 to E6 upgradaton", BSNL Publication, 2012
[13] A. Nakkiran, "Dravidian mother", Chennai, 2007
[14] Dr. M. Karunanidhi, "Thirukkural Translation", 2010
[15] "Manorama Tell me why periodicals", M.M. Publication Ltd., Kottayam, 2009
[16] V.R. Hemalatha, "A Global level peace tourism to Veilankanni", Annai Publications, Cholapuram, 2007
[17] Prof. Ganapathi Pillai, "Sri Lankan Tamil History", 2004
[18] Dr. K.K. Pillai, "South Indian History", 2006
[19] M. Varadharajan, "Language History", Chennai, 2009
[20] Fr. Y.S. Yagoo, "Western Sun", 2008
[21] Gopal Chettiar, "Adi Dravidian Origin History", 2004
[22] M. Arulmani; V.R. Hemalatha, "Ezhem Nadu My Dream" - (2 Parts), Annai Publications, Cholapuram, 2010
[23] M. Arulmani; V.R. Hemalatha, "The Super Scientist of Climate Control", Annai Publications, Cholapuram, 2013, pp 1-3

American Journal of Engineering Research (AJER)
e-ISSN : 2320-0847 p-ISSN : 2320-0936
Volume-03, Issue-11, pp-277-280
www.ajer.org

Research Paper Open Access

State of art an Overview on the Tensile Strength and Flexural Strength of Concrete in different Curing Methods

J. Allen Paul Edson[1], M. Kamesh Amudhan[2]
[1](Department of Civil Engineering, SRR Engineering College, India)
[2](Department of Civil Engineering, SRR Engineering College, India)

ABSTRACT : *The concrete is made of different ingredients such as cement, fine aggregate, and coarse aggregate but it is a homogeneous material when it is in a harden concrete. The strength of concrete decides the life span of any concrete structure. The factors which affect the strength of concrete are the type of material used, size of aggregate, water cement ratio, improper compaction and improper curing. Curing is one of the major factors in the failure of concrete. Curing is defined as the process of promoting the hydration of cement. The grade used in the manufacture of concrete may be M20, M30 grade. This paper deals with the overview on the tensile strength and flexural strength of concrete when the concrete is exposed to various curing methods such as Water curing (Ponding and Immersion), Air Curing (Dry air curing), and plastic film curing at 3 days, 7 days, 28 days and 56 days. It is studied that the tensile and flexural strength of concrete during immersion method is high when compared with Air curing and plastic film curing. It is found that the water curing is the most effective method of curing with the maximum of 10% increase in tensile strength and 15% increase in flexural strength of concrete when compared with other curing methods. On comparison with self compacting concrete (SCC) and Normal cement concrete (NCC) under different curing methods the tensile strength and flexural strength of SCC is high than NCC.*

KEYWORDS : *Air Curing, Flexural Strength, Immersion Curing, Plastic Film Curing, Tensile strength.*

I. INTRODUCTION

The concrete is the soul material for the civil engineers. Many engineers and researches were involved in research to increase the strength of concrete. There are different factors which involve in the affecting the strength of concrete (i) Type of material (ii) size if aggregate (iii) water cement ratio (iv) Mix proportion (v) Improper compaction (vi) Improper curing. Nowadays the failure of structure is because the concrete cannot attain its strength due to the following above mentioned factors. Improper curing is one reason for the maximum number of failure structures. This paper deals with the state of art on the tensile strength and flexural strength of concrete in different curing methods at 3days, 7days, and 28days. Curing is the process of promoting hydration in the cement. Curing is done to prevent the loss of moisture content from the concrete, ineffective curing results in the evaporation of moisture content from the concrete which results in the shrinkage cracks and temperature cracks.

II. MATERIAL INVESTIGATION

Ajay Goel et.al, Suggested ordinary Portland cement of 43 grade conforming to IS 383:1970. The specific gravity of cement is 3.15. Fine aggregate of river sand with the fineness modulus 2.163 conforming to zone III of IS 383-1970. Coarse aggregate of crushed stone aggregate of size 10mm and 20mm is used. The specific gravity of coarse aggregate is 2.40. It is generally suggested to use M20 grade of concrete with cement of 43 grade or 53 grade, fine aggregate of size 4.75mm passing through sieve with coarse particles present with the fineness modulus of 2.65 and coarse aggregate of size 10mm and 20mm but not more than 20mm should be used.J.R. al-feel and N.S. al-saffar used limestone powder passing sieve no.200 and it is used at 8% of cement weight. The cement content of the mix used is 460 kg/m^3.

III. EXPERIMENTAL PROGRAMME

Split tensile strength is an indirect method to determine the tensile strength of concrete. The M20 grade concrete is prepared and placed in the mould (cylinder) of size 150mm x 300mm. A layer of oil or grease is applied on the walls of the mould. The concrete is placed in three layers and compacted using a tamping rod of 25 blows. Now allow the concrete in the mould to set for 24 hours, then remove the mould and place the

specimen for curing at 3days, 7days, 28days and 56days. Similarly prepare mould for different curing methods. After stipulated days test the specimens for split tensile test by applying the compressive line load along the opposite generators of the cylinder and determine the tensile strength of concrete in different curing methods at 3days, 7days, 28days and 56days. To determine the flexural strength of concrete prepare the concrete and place it in the mould of size 100mm x 100mm x 500mm and repeat the same procedure. The load is applied at the third point of the span of 400mm.

3.1 Curing methods

3.1.1 Ponding method : Ponding is one of the ideal methods for curing the slab element which ensures the slab do not lose its moisture content. The temperature of water used in Ponding should be constant. Freezing and thawing of water temperature results in thermal cracks in concrete.

3.1.2 Immersion method : In this method the concrete specimen is made to get immersed in the water, it is mostly used in the laboratory to immerse the concrete (Cube, cylinder, Prism) test specimens. The Ponding and immersion method can be done only in the horizontal surfaces.

3.1.3 Membrane Curing method: A membrane (Sealers) compound like wax, polythene sheets, chlorinated rubber etc. These materials should be laid on the surface of the concrete. The main purpose of membrane is to resist the moisture content enter into the concrete and to maintain the moisture content within the concrete. It is only possible to apply the membrane only on the horizontal surfaces not on the vertical surfaces.

3.1.4 Sprinkling Curing method: This method of curing can be done anywhere but the other methods are more effective than this method. Sprinkling method is especially for column because it is a vertical member.

3.1.5 Air Curing: The concrete will be laid on the open dry yard in order to allow the concrete to cure in its room temperature. This method is not effective when compared with water curing and membrane curing.

IV. RESULTS AND DISCUSSIONS

Ajay Goel et.al, made a study on the "A comparative study on the effect of curing on the strength of concrete" with air curing, plastic film and water curing at 3daqys, 7days, 28days, 56days and found that the average split tensile strength of concrete at 3 days in plastic film is 1.72 N/mm^2 where the split tensile strength of concrete at 3 days in water curing is 2.51 N/ mm^2 and in air curing is 1.63 N/ mm^2. It is studied that the split tensile strength of concrete at 3 days in water curing increases by 31.47%. At 7 days the split tensile strength of concrete in water curing increases by 22.79%. At 28 days, the split tensile strength of concrete in water curing increases by 30.26%. At 56 days, the split tensile strength of concrete in water curing increases by 27% as shown in table I.

Table I. shows the split tensile strength of concrete in different curing methods and the percentage difference in strength.

S.No	Days of Curing	Split Tensile Strength N/mm^2			% Difference
		Water Curing	Air Curing	Plastic Film Curing	
1	3 days	2.51	1.63	1.72	31.47
2	7 days	2.94	2.13	2.27	22.79
3	28 days	3.9	2.47	2.72	30.26
4	56 days	4.0	2.52	2.92	27

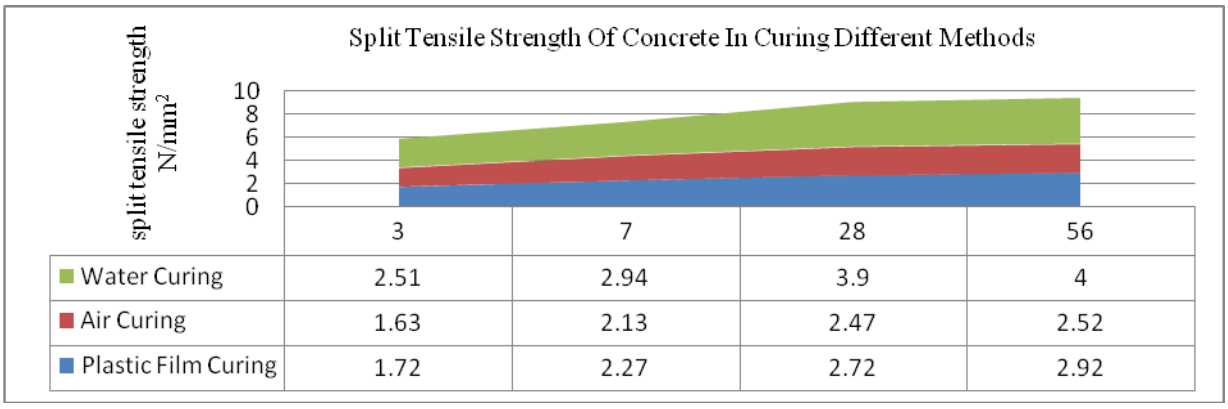

Figure 1. Shows the Split tensile strength of concrete in different curing methods.

"A comparative study on the effect of curing on the strength of concrete" by Ajay Goel et.al, with air curing, plastic film and water curing at 3daqys, 7days, 28days, 56days and found that the average flexural strength of concrete at 3 days in plastic film is 3.75 N/mm^2 where the flexural strength of concrete at 3 days in water curing is 4.12 N/ mm^2 and in air curing is 3.08 N/ mm^2. It is studied that the split tensile strength of concrete at 3 days in water curing increases by 31.47%. At 7 days the flexural strength of concrete in water curing increases by 15.33%. At 28 days, the flexural strength of concrete in water curing increases by 5.59%. At 56 days, the flexural strength of concrete in water curing increases by 5.56% as shown in table II.

Table II. Shows the flexural strength of concrete in different curing methods and the percentage difference in strength.

S.No	Days of Curing	Flexural Strength N/mm^2			% Difference
		Air Curing	Plastic Film Curing	Water Curing	
1	3 days	3.08	3.75	4.12	8.98
2	7 days	4.54	3.92	4.63	15.33
3	28 days	5.76	6.08	6.44	5.59
4	56 days	5.84	6.12	6.48	5.56

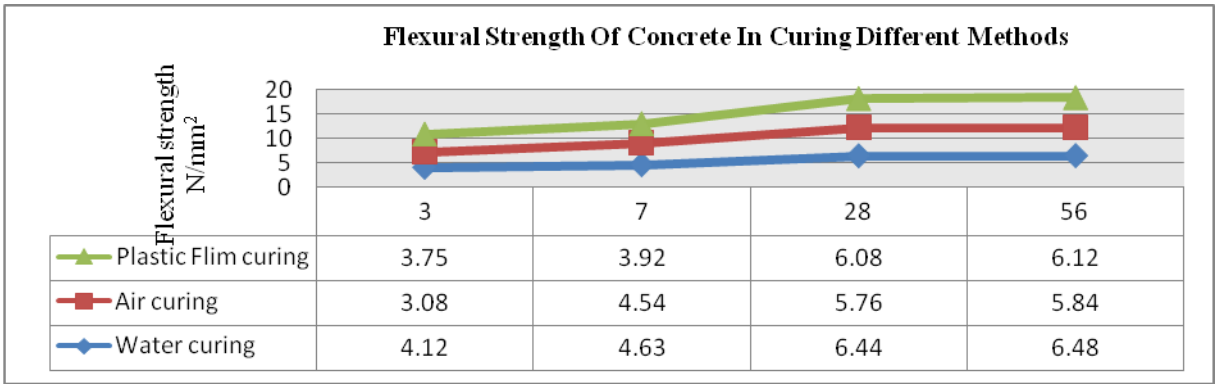

Figure 3. Shows the flexural strength of concrete in different curing methods.

J.R.Al-Feel et.al, made a study on the " Properties of self compacting concrete at different curing conditions and their comparison with properties of Normal concrete" he made a comparative study on the split tensile strength of self compacting concrete(SCC) and normal cement concrete(NCC) under different curing conditions at 7 days,14 days and 28 days. It is found that the split tensile strength of self compacting concrete is high when compared with split tensile strength of normal cement concrete at water curing method and air curing method. The values of the tensile strength of SCC and NCC are shown in table III.

Table III. Shows the split tensile strength of SCC and NCC at water curing and Air curing.

S.No	Days of Curing	Split tensile Strength N/mm^2			
		water curing		Air curing	
		SCC	NCC	SCC	NCC
1	7 days	4.45	3	3.8	2.75
2	14 days	5.1	3.65	4.45	3.35
3	28 days	5.3	3.8	4.5	3.45

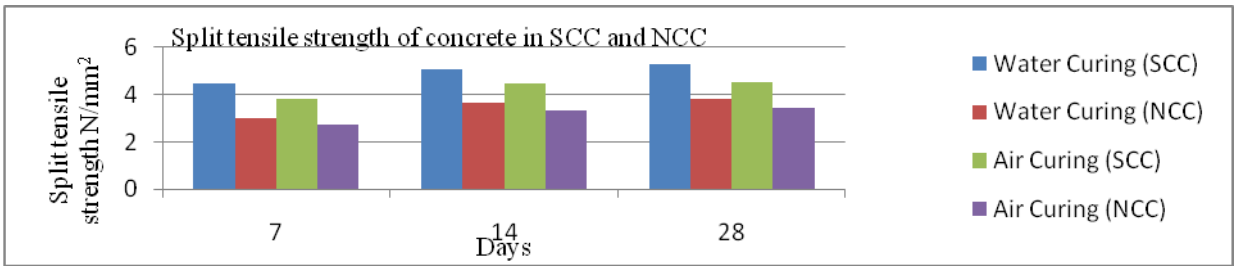

Figure 3.Shows the split tensile strength of SCC & NCC concrete in different curing methods.

J.R. Al-Feel et.al also made a study on the flexural strength of the concrete for SCC and NCC under different curing condition at 28 days. The values of the flexural strength of SCC and NCC are shown in table IV

Table IV. Shows the flexural strength of SCC and NCC at water curing and Air curing.

S.No	Days of Curing	Flexural Strength N/mm^2			
		water curing		Air curing	
		SCC	NCC	SCC	NCC
1	28 days	4.41	3.00	3.91	2.50

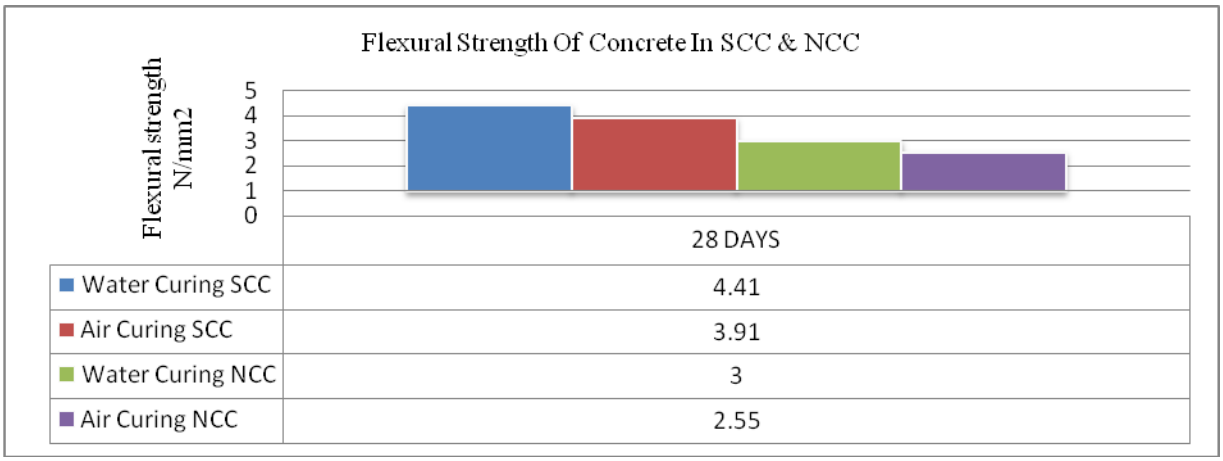

Figure 4. Shows the flexural strength of SCC & NCC concrete in different curing methods.

V. CONCLUSION

Water curing method is the most effective method for curing the concrete, since both the tensile strength and flexural strength of the concrete get increased in this curing method. This method proves effective because there is an improve in pore structure and the degree of hydration of cement reaction will not lose any moisture content from the concrete. It is found that the water curing is the most effective method of curing with the maximum of 10% increase in tensile strength and 15% increase in flexural strength of concrete when compared with other curing methods. It can be observed that the average split tensile strength at 3 days in case of air curing and plastic curing is minimum. Whereas it is maximum under water curing. The flexural strength of the concrete increase in water curing method and it is minimum in the air curing and plastic film curing. But the increase of flexural and tensile strength of concrete is not high when compared to increase of compressive strength in the concrete under different curing methods. Curing method seems to be detrimental to the development of compressive strength then to its flexural and split tensile strength.

REFERENCES

[1] O. James, P.N.Ndoke and S.S.Kolo, Department Of Civil Engineering, Federal University of Technology, Minna. "Effect of Different Curing Methods on the Compressive Strength of Concrete".

[2] J. R. Al-Feel N. S. Al-Saffar, Civil Engineering Department, Mosul University, "Properties of Self Compacting Concrete at Different Curing Condition and their Comparison with properties of Normal Concrete.

[3] Ajay Goel, Jyoti Narwal, Vivek Verma, Devender Sharma, Bhupinder Singh, A Comparative Study on the Effect of Curing on The Strength of Concrete. International Journal of Engineering and Advanced Technology (IJEAT) ISSN: 2249 – 8958, Volume-2, Issue-6, August 2013.

[4] Nirav R Kholia, Prof. Binita A Vyas, Prof. T. G. Tank, Effect on concrete by different curing method and efficiency of curing compounds – A Review.

[5] Md. Safuddin, S.N. Raman and M.F.M. Zain, 2007, "Effect of Different Curing Methods on the Properties of Microsilica Concrete", Australian Journal of Basic and Applied Sciences, 1(2): 87-95, ISSN 1991-8178.

[6] Akeem Ayinde, Raheem, Aliu Adebayo Soyingbe, Amaka John Emenike, "Effect of Curing Methods on Density and Compressive Strength of Concrete". International Journal of Applied Science and Technology Vol. 3 No. 4; April 2013.

American Journal of Engineering Research (AJER)
e-ISSN : 2320-0847 p-ISSN : 2320-0936
Volume-03, Issue-11, pp-281-289
www.ajer.org

Research Paper Open Access

Analysis of Parallel Topology for Active Power Factor Correction Using Single and Dual Mode Boost Converters

Md. Mosfiqur Rahaman[1], Md. Tanvir Ahad[1], Akib Yusuf[1],Md. Rifat Rahamatullah[1], Safayat-Al-Imam[2]

[1](*Research Scholar, Department of Electrical & Electronic Engineering, Ahsanullah University of Science & Technology, Bangladesh)*

[2](*Assistant Professor, Department of Electrical & Electronic Engineering, Ahsanullah University of Science & Technology, Bangladesh)*

ABSTRACT: *The ratio between real or average power and apparent power known as power factor has a high impact on power system industries. Efficient usage of the real power is very indicative in developing a power system. With the profusely development of technology in power semiconductor devices, the rate of using power electronic systems has expanded to new and wide application range that include residential, commercial, aerospace and other systems. In the nonlinear system, loads are the main source of harmonics. So that nonlinear behavior puts a question mark on their high efficiency. The current drawn by power electronic interfaces from the line is distorted resulting in a high total Harmonic Distortion and low p.f. this creates adverse effects on the power system include increased magnitudes of neutral currents in three phase systems, overheating in transformers and induction motors. This paper aims to develop a circuit for PFC by using active filtering approach by implementing two (single & dual) boost converters arranged in parallel, for improving circuit quality and switching loss. This work actually involves simulation of basic power electronic circuit and it starts with simple circuit with a gradual increase in complexity by inclusion of new components and their subsequent effect on current and voltage wave forms. We focused to improve the condition of input current waveforms for making it sinusoidal by tuning the circuits.*

KEYWORDS: *Boost converter, Power factor, Dual Boost converter, Harmonics, Active PFC, Passive PFC, Average current mode control.*

I. INTRODUCTION

Converters are very essential elements in power electronics industries. AC to DC converter has a diode bridge rectifier with a high value of capacitor for filtering purpose. This capacitor cut downs the cost of the converter and makes it robust. However due to the presence of harmonic ac line current, the power factor is poor [1]. The most common power quality disturbance is instantaneous power interruption. Various power factor correction (PFC) techniques are employed to overcome these power quality problems out of which the boost converter topology has been extensively used in various ac/dc and dc/dc applications. In fact, the frontend oftoday's ac/dc power supplies with power-factor correction (PFC) is almost exclusively implemented with boost topology [2][3]. The basic boost topology does not provide a high boost factor. This has needed many proposed topologies as cascaded boot tapped inductor boost etc. This paper introduces another variation dual Boost PFC convertor addition in parallel with rectifier circuit to provide a higher boost factor and also provides proper controlling. This paper involves with PSPICE simulation of different types of electronic conventional rectifier circuit and voltage waveforms. It starts with simple rectifier circuit and different MOSFETs and switches to improve by implementing advanced techniques such as active PFC, where we mainly focusing on the objective of improving the input current waveform. All the simulation work is carried out/done in PSICE simulation manager.

II. POWER FACTOR WITH DIFFERENT LOADS

Power factor is defined as the cosine of the angle between voltage and current in an ac circuit. If the circuit is inductive, the current lags behind the voltage and power factor is referred to as lagging. However, in a capacitive circuit, current leads the voltage and the power factor is said to be leading.

Linear System: It is AC electrical loads where the voltage and current waveforms are sinusoidal. The current at any time is proportional to voltage. Power factor is determined only by the phase difference between voltage and current.

Non Linear System: Applies to those ac loads where the current is not proportional to voltage. The nature of the nonlinear current is to generate harmonics in the current waveform. This distortion of the current waveform leads to distortion of voltage waveform. Under this condition, the voltage waveform is no longer proportional to current. For sinusoidal voltage and non-sinusoidal current P.F can be expressed.

$$PF = \frac{V_{RMS} I_{1RMS}}{V_{RMS} I_{RMS}} \cos\theta \text{ or } PF = \frac{I_{1RMS}}{I_{RMS}} \cos\theta \text{ or } PF = K_p \cos\theta \text{ ; Here, } K_p = \frac{I_{1RMS}}{I_{RMS}},\ K_p \approx [0-1]$$

cosθ is the displacement factor of the voltage and current. *Kp* is the purity factor or the distortion factor. Another important parameter that measures the percentage of distortion is known as the current total harmonic distortion (THDi) which is defined as follows:

III. EFFECTS OF HARMONICS ON POWER QUALITY

The contaminative harmonics can decline power quality and affect system performance in several ways [4]. As presence of harmonics declaims the transmission efficiency and also creates thermal problems, both conductor and iron loss are increased. In 3-0 system, neutral conductor becomes unprotected due to odd harmonics. Triggering are misconducted as the peak harmonics create currents which interrupts the protection system of an automatic relay. Huge current flows through the ground conductor of system with four wire 3-0 when odd number of n- current is present in harmonics. Finally, harmonics could cause other problems such as electromagnetic interference to interrupt communication, degrading reliability of electrical equipment, increasing product defective ratio, insulation failure, audible noise etc [5]-[8].

IV. RECTIFIERS

A rectifying circuit is one which links an ac supply to dc load, that is, it converts an alternating voltage supply to a direct voltage. The direct voltage so obtained is nor normally level, as from a battery, but contains an alternating ripple component superimposed on the mean (dc) level.

Uncontrolled Rectifiers: The simplest uncontrolled rectifier use can be found in single-phase circuits. There are two types of uncontrolled rectification. They are (1) half-wave rectification and (2) full-wave rectification. Half-wave and full-wave rectification techniques have been used in single-phase as well as in three-phase circuits. As mentioned earlier, uncontrolled rectifiers make use of diodes. Diodes are two-terminal semiconductor devices that allow flow of current in only one direction. The two terminals of a diode are known as the anode and the cathode.

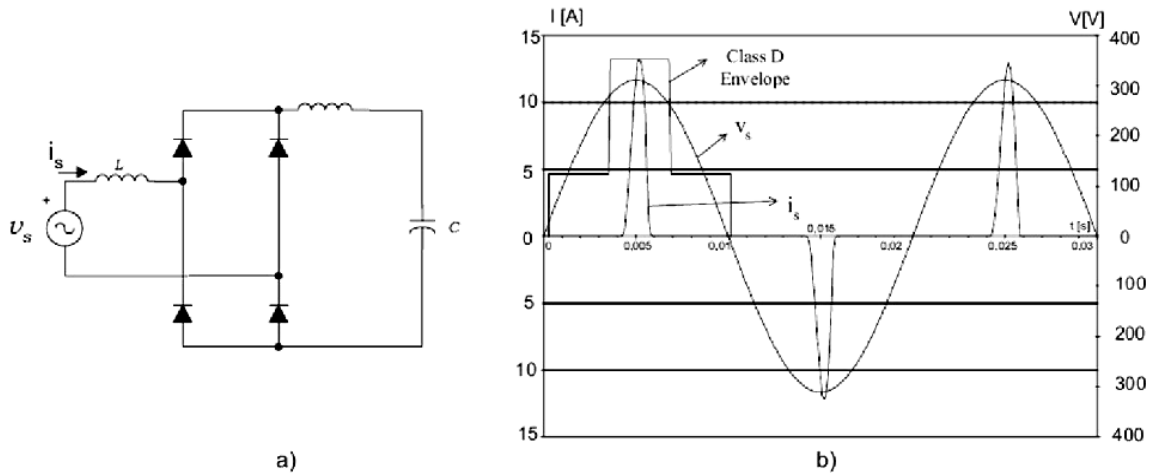

Figure 1: Single phase rectifier (a) circuit (b) waveforms of input voltage and current [9].

Controlled Rectifiers: Controlled rectifier circuits make use of devices known as "thyristors." A thyristor is a four-layer (*pnpn*), three-junction device that conducts current only in one direction similar to a diode. The last (third) junction is utilized as the control junction and consequently the rectification process can be initiated at will provided the device is favorably biased and the load is of favorable magnitude.

The presence of harmonics in the waveform of the network voltage can be attributed to various causes such as rectifiers, variable speed drives, thyristors, saturated transformer, arc furnaces etc[9]-[14].Problems like interferences in telecommunications systems and equipment, distortion of the electricity supply voltage, erratic operation of control and protection relays, failures in transformers and motors due to overheating caused by core losses are caused by harmonies in system. Amplification of both voltage and current at the same time will occur if the resonant frequency is close or equal to one of the harmonic frequencies present in the distribution system. The power feeder (overhead line or underground cable) have an inductive impedance. By putting a capacitor in parallel with the load (for Power factor correction) it is possible for the combined system to have a resonance condition. As the power factor of a three phase system decreases, the current rises. The heat dissipation in the system rises proportionately by a factor equivalent to the square of the current rise. Power factor correction is necessary for overcome above mention problem.

TYPES OF POWER FACTOR CORRECTION

Passive PFC : The simplest form of PFC is passive (Passive PFC). A passive PFC uses a filter at the AC input to correct poor power factor. The passive PFC circuitry uses only passive components: an inductor and some capacitors (Figure. 1).

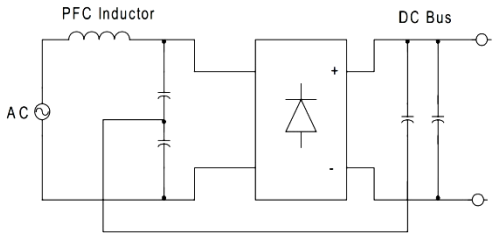

Figure 2: A passive PFC circuit requires only a few components to increase efficiency, but they are large due to operating at the line power frequency [5], [9].

Although pleasantly simple and robust, a passive PFC rarely achieves low Total Harmonic Distortion (THD). Also, because the circuit operates at the low line power frequency of 50Hz or 60Hz, the passive elements are normally bulky and heavy.

Active PFC : Active PFC offers better THD and is significantly smaller and lighter than a passive PFC circuit. To reduce the size and cost of passive filter elements, an active PFC operates at a higher switching frequency than the 50Hz/60Hz line frequency.

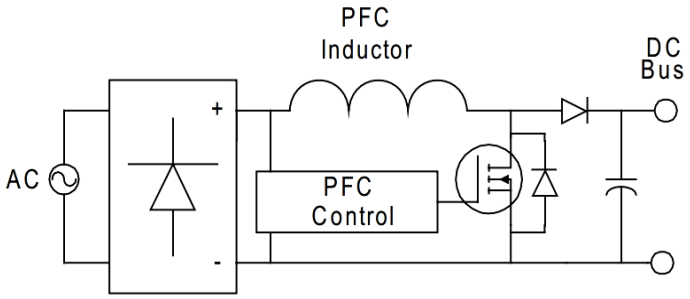

Figure 3: An active PFC circuit produces low THD and uses relatively small passive component [5].

BASIC PRINCIPLE OF BOOST CONVERTER: Stepping up the power stage without isolating topology, the boost converter works perfectly. In practical field of power designing, required output should be always higher that input voltage. This topology is fulfilled perfectly with boost power stage. The basic working principle of boost converter is to generate non-pulsating input current to output diode as diode conducts only during a portion of the switching cycle. The output capacitor supplies the entire load current for the rest of the switching cycle. Figure 4 shows a simplified schematic of the boost power stage. Inductor L and capacitor C make up the effective output filter.

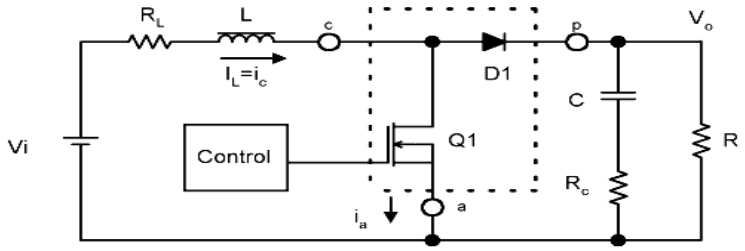

Figure 4: Boost Power Stage Schematic diagram

Boost power stage can work out both in modes considering continuity of current in the inductor. This current inductor mode current flows either continuously in the inductor during the entire switching cycle in steady-state operation or inductor current is zero for a portion of the switching cycle. A periodicity is maintained as it approaches towards peak value from zero and returns back to it during each switching cycle. It is desirable for a power stage to stay in only one mode over its expected operating conditions because the power stage frequency response changes significantly between the two modes of operation.

V. BASIC PRINCIPLE OF DUAL BOOST CONVERTER

Conventionally, boost converters are used as active Power factor correctors. However, a recent novel approach for PFC is to use dual boost converter i.e. two boost converters connected in parallel. Circuit diagrams for both types of PFCs are as given below:

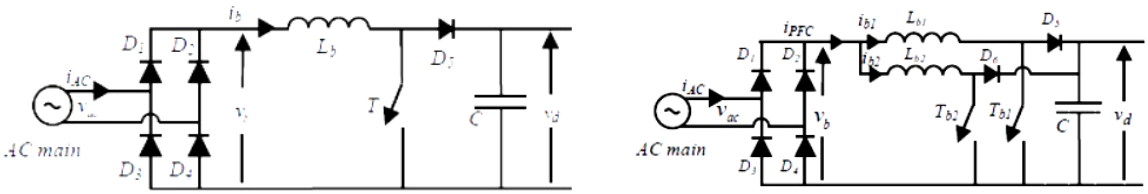

Figure 5: (a) Classical PFC circuit (b) Dual Boost PFC circuit [9]

Here, we use a parallel scheme, where choke L_{b1} and switch T_{b1} are for main PFC while L_{b2} and T_{b2} are for active filtering. The filtering circuit serves two purposes i.e. improves the quality of line current and reduces the PFC total switching loss. The reduction in switching losses occurs due to different values of switching frequency and current amplitude for the two switches. The parallel connection involves phase shifting of two or more boost converters connected in parallel and operating at the same switching frequency.

VI. CONTROL PRINCIPLE OF DC-DC CONVERTERS

Control strategy for an electrical system is intended to develop a set of actions that can detect the time evolution of electrical quantities and to impose them to follow a desired time evolution. In general, a control algorithm can be split into three functional sub-blocks:

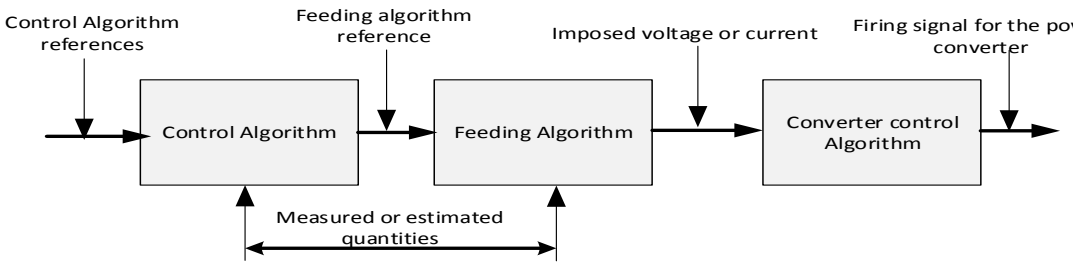

Figure 7: Basic description and splitting of the Control algorithm [6]

Control Algorithm operates to generate reference values to the feeding algorithm on the basis of reference values imposed to the controller. On the other hand, feeding algorithm gives the voltage or current values to impose at the considered system in order to follow the time evolution of the reference values coming

from the control algorithm. And finally, converter control algorithm provides the right sequence of firing pulses for management of the power modules based on the information derived from control and feeding algorithm.
A dc-dc converter provides a regulated dc output voltage under varying load and input voltage conditions. The converter component values are also changing with time, temperature and pressure. Hence, the control of the output voltage should be performed in a closed-loop manner using principles of negative feedback.

VII. SIMULATION AND RESULT

This paper deals with the current control common closed loop mode approach for PWM dc-dc converters, Signals in current form have a natural advantage over voltage signals. Voltage being an accumulation of electron flux, is slow in time as far as control mechanism is concerned. This led to the development of a new area in switch mode power supply design, i.e. the current mode control. Here, the averaged or peak current of magnetic origin is employed in the feedback loop of the switch mode power converters. It has given new avenues of analysis and at same time introduced complexities in terms of multiple loops[9].

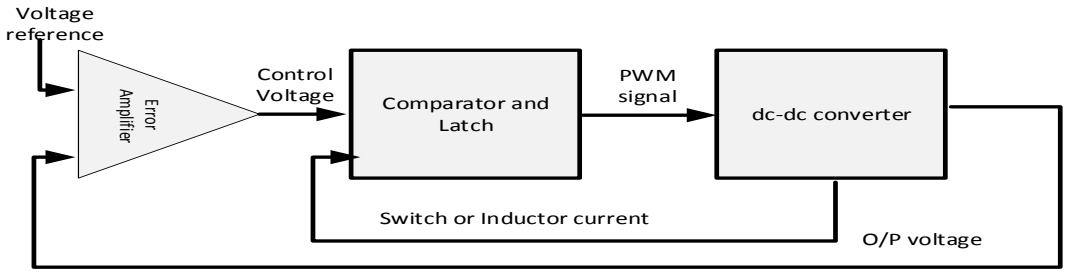

Figure 8: A current control mode

A schematic diagram of current mode control is shown in Fig 8. It comprises of an additional inner control loop. The inductor current signal, converted to its voltage analog fed back by this loop is compared to the control voltage. The dynamic behavior of the converter is significantly altered by this modification of replacing the saw tooth waveform by the converter current signal. The key difference between voltage and current mode control is the way the reference map is generated. In the case of voltage mode control, the ramp is external from the viewpoint of the power plant, whereas for current mode control, it is internal.

The main approach of the paper to adopt a circuitry approach of a PFC circuit with parallel boost converter with feedback loop. Furthermore, the circuit is simulated through PSPICE and parameters are observed.

Circuitry and simulation diagrams of a PFC circuit without any feedback: The classical boost regulated PFC circuit is implemented here .IRF 540 power MOSFET used as switch .No feedback part is attached with. That is why full control over circuit is absent here.

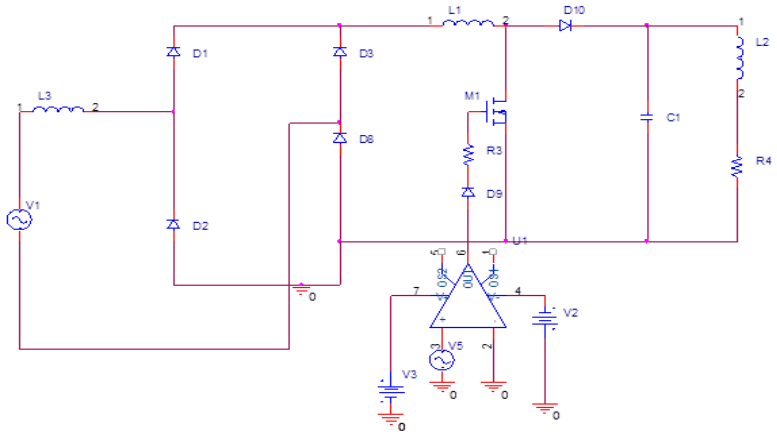

Figure 9: PFC circuit without feedback

Here in fig (9) we found the PFC circuit without feedback. The difference in this circuit is the absence of variable pulse width generation supply in feedback loop. Here the RMS wave contributes to calculate the power factor.

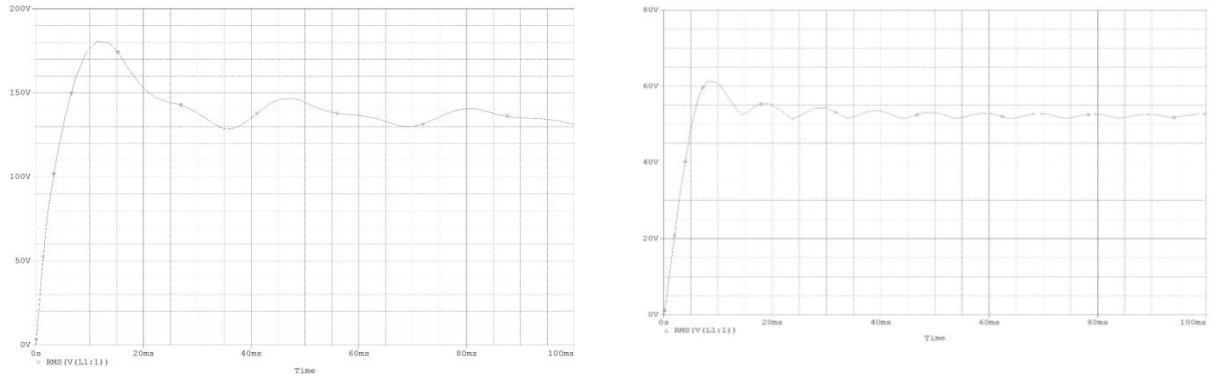

Figure 10: RMS wave of input and output voltage

Here in fig (20) we found the ultimate input & output voltage of the RMS wave. RMS wave contributes to calculate the power factor.

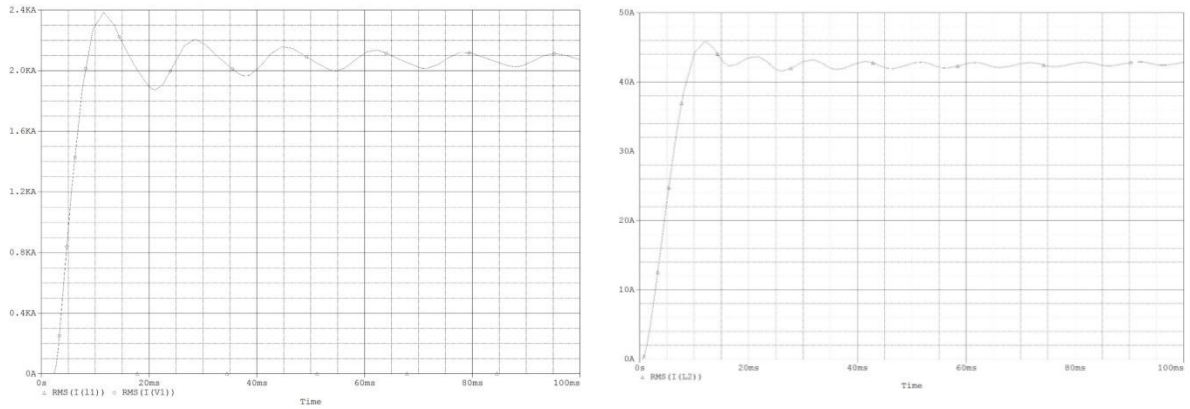

Figure 11: RMS wave of input and output current

Here in fig (11) we found the ultimate input and output current of the RMS wave. RMS wave contributes to calculate the power factor.

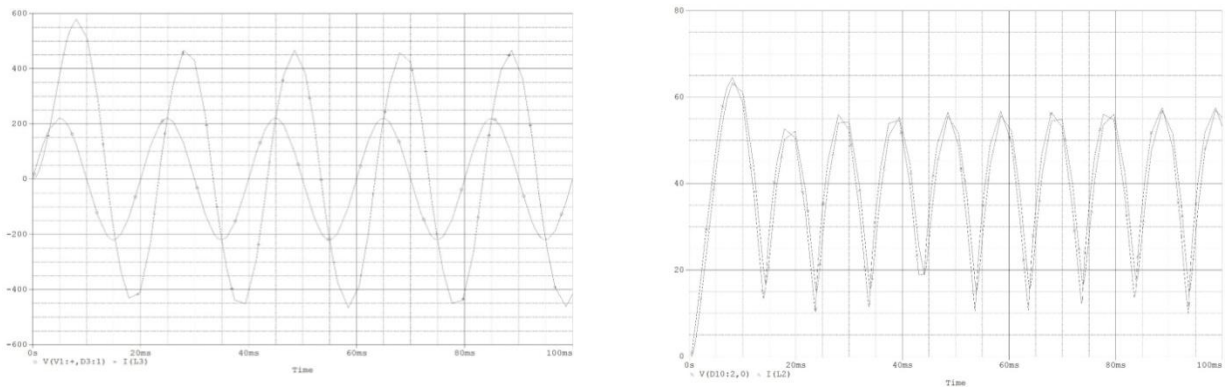

Figure 12: Input and output curves PFC circuit using boost converter without feedback.

Here, in fig (12) we found the ultimate input & output curves of the PFC circuit using boost converter without feedback as inductive load is connected current lags. Because of comparative better power factor, harmonics reduces. This least situation is also improved within next PFC design.

Circuitry and simulation diagram of a PFC circuit having Parallel Boost Converter with Feedback

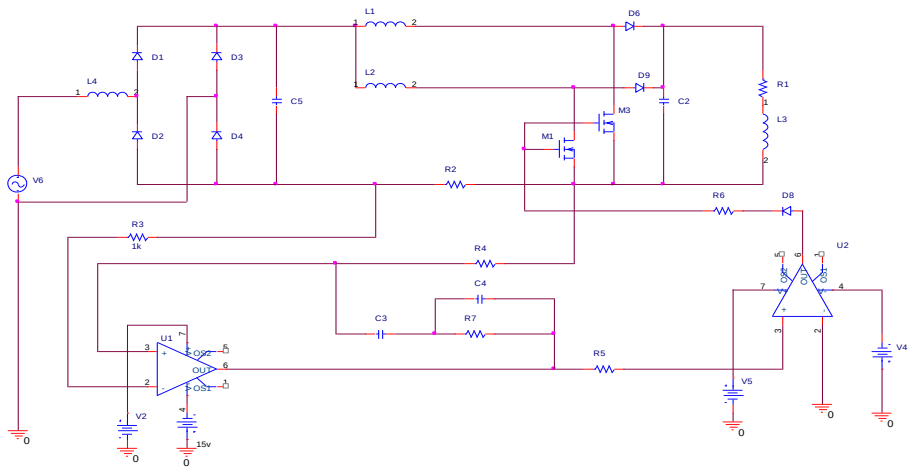

Figure 13:PFC circuit with parallel boost converter feedback

Here fig (13) shows our final effort-boost controlled PFC circuitry with feedback system. The key which makes the difference, is the usage of two different type of power MOSFET, P-type and N-type. Which specify the specified boost regulator loop at separate time. The PWM creates a square wave by comparing the saw-tooth with the sinusoidal wave which came from CEA. The output of CEA varies with the variation of load. A gate drive IC should have to be implemented which was given at ACM control mode design but is absent here. Cause the accurate gate drive IC model IR2771C was not available in out library and the IR26771 model is obsolete. We used a resistance and diode instead. Sometimes in practical, the MOSFET supplies back some of the current that which is harmful for the system. To avoid this, a diode is used as reverse for that backing current. MOSFET needs 1-2 A current flow to its gate to work as a switch.

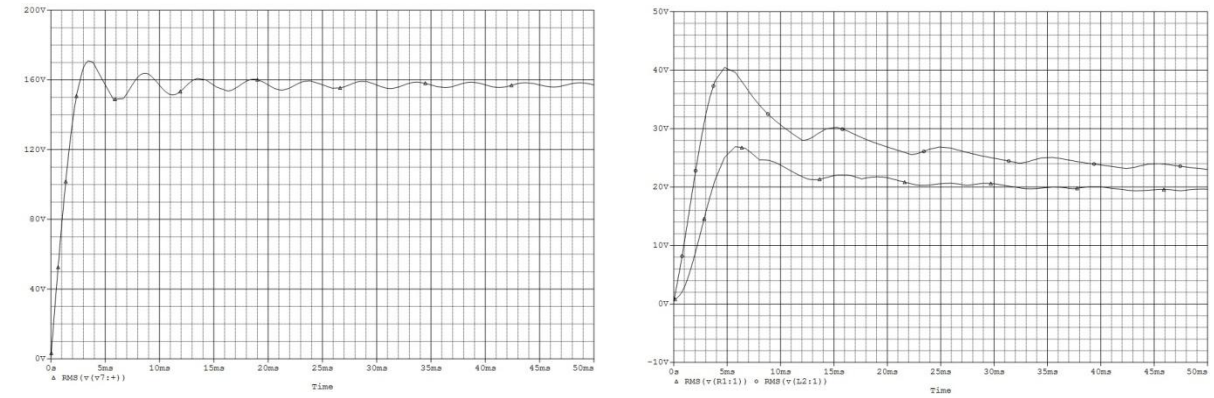

Figure 14: RMS wave of Input and Output Voltage.

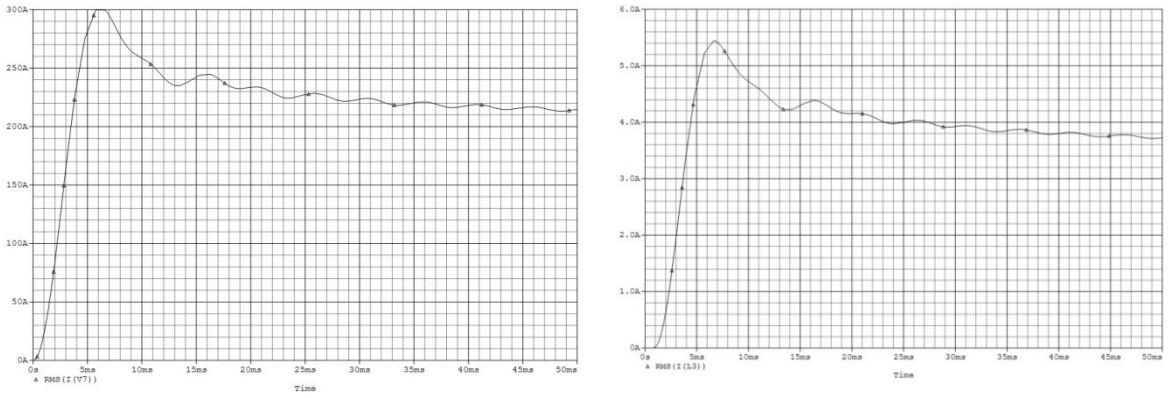

Figure15: RMS wave of input and output current

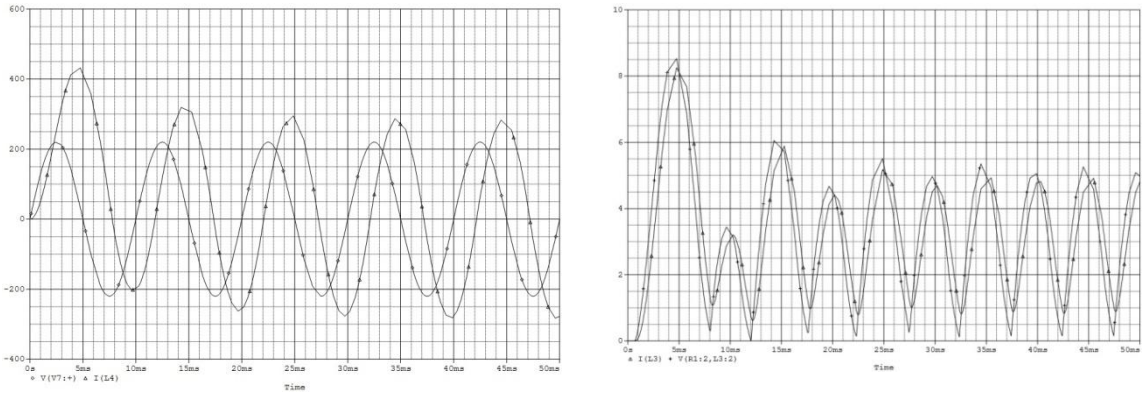

Figure 16: Input Voltage and current wave shape as a function of time

Here fig (16) shows Input V-I wave shape and Output V-I wave shape. Here we have found our longed curve which represents a very successful power factor as practical. On the previous circuit, the power factor could be recommended as better and this could be the best.

VIII. COMPARISON BETWEEN THE OUTPUT WAVE SHAPES OF LAST TWO CIRCUITRY-

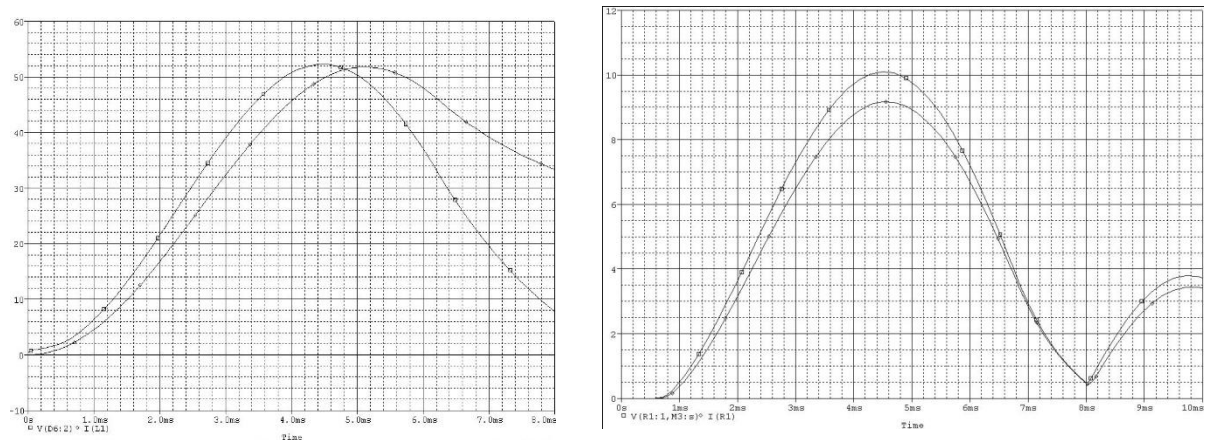

Figure 17: PFC circuit using boost converter (a) without feedback (b) with feedback

This figure shows that with feedback and using parallel boost converter which the PFC circuit works. Here ,in the 1st figure ,we see that without using feedback circuit the V-I curve starts at approximately in millisecond ,which represents that p.f is not that improved .But if we add a feedback circuit thisphenomenon is been improved.

Table I.: Analysis of different PFC circuits[9]

SI.No	Circuit	Power Factor
1	Conventional Rectifier (without boost converter)	0.9706[9]
2	Boost Converter without feedback	0.989[9]
3	Boost Converter with feedback	0.99

IX. CONCLUSION

The power factor corrections with boost converters are simulated by PSPICE simulator link. In this paper conventional converter, we used the parallel topology of boost converter to correct the power factor and brought it near unity by elimination of harmonics effects step by steps, when first one improves and second one filtering the power factor. Here we use one n-type and one p-type MOSFET instead of using two a kind and a smaller fractional value of PF range capacitor across the R-L load, this paper will be most innovative and important handbook to improve the power factor for non-linear loads.

REFERENCES

[1] Hussain S. Athab, IEEE Member, P. K. Shadhu Khan, senior IEEE Member, A Cost Effective Method of Reducing Total Harmonic Distortion (THD) in Single-Phase Boost Rectifier 1-4244-0645-5/07/$20.00©2007 IEEE.

[2] Tiago Kommers Jappe & Samir Ahmad Mussa, Federal University of Santa Catarina, INEP-Power Electronics Institute lorian´opolis, SC, Brazil, Current control techniques applied in PFC boost converter at instantaneous power interruption - 978-1-4244-4649-0/09/$25.00 ©2009 IEEE.

[3] Shikha Singh G.Bhuvaneswari Bhim Singh, Department of Electrical Engineering, Indian Institute of Technology, Delhi Hauz Khas, New Delhi-110016 INDIA. Multiple Output SMPS with Improved Input Power Quality - 978-1-4244-6653-5/10/$26.00 ©2010 IEEE.

[4] Yungtaek Jang, Senior Member, IEEE, Milan M. Jovanovic´, Fellow, IEEE, Kung-Hui Fang, and Yu-Ming Chang, High-Power-Factor Soft-Switched Boost Converter IEEE TRANSACTIONS ON POWER ELECTRONICS, VOL. 21, NO. 1, JANUARY 2006 - 0885-8993/$20.00 © 2006 IEEE.

[5] Dash, R (2011),"Power factor correction using parallel boost converter", (Doctoral dissertation)

[6] Rashid M., Power Electronics Handbook.

[7] Purton K.D and Lisner R.P, Average Mode Control in Power Electronic converters-analog versus digital, Department Of Electrical and computer system engineering, Monash University,Australia

[8] "Power System Harmonics". Rockwell Automation. Allen-Bradley.**(Harmonics)**

[9] P.Vijaya Parasuna, J.V.G.Rama Rao, Ch.M.Lakshm," Improvement in Power Factor & THD Using Dual Boost Converter",International Journal of Engineering Research and Application(IJERA),Vol 2 ,Issue4 , July-August,2012, pp. 2368-2376

[10] "Making -5V 14-bit Quiet (page 54)" by Kevin Hoskins 1997 **(DC to DC converter)**

[11] "DC-DC CONVERTERS: A PRIMER". 090112 jaycar.com.au Page 4 **(Voltage and Current control method)**

[12] "DC-DC Converter Basics". 090112 powerdesigners.com (DC to DC converter)

[13] Authoritative Dictionary of Standards Terms (7th ed.), IEEE, ISBN 0-7381-2601-2, Std. 100. **(Power factor correction)**

[14] Sankaran, C. (1999), "Motors", Effects of Harmonics on Power Systems, Electro-Test, "The interaction between the positive and negative sequence magnetic fields and currents produces torsional oscillations of the motor shaft. These oscillations result in shaft vibrations." **(Harmonics and power factor correction)**

[15] A New Active Power Factor Correction Controller using Boost Converte--Sridevi J. Department of Electrical and Electronics Engineering, Gokaraju Rangaraju Institute of Engineering and Technology,Bachupally , Kukatpally, Hyderabad, A.P, INDIA, Available online at: www.isca.in.

American Journal of Engineering Research (AJER)
e-ISSN : 2320-0847 p-ISSN : 2320-0936
Volume-03, Issue-11, pp-290-298
www.ajer.org

Research Paper Open Access

Study of Biodiesel Emissions and Carbon Mitigation in Gas Turbine Combustor

Mohamed Alalim Altaher[1], Gordon E. Andrews[2] and Hu Li[2]
[1]*Petroleum and Chemical Engineering Department Sebha University, PO Box 18758, Sebha, Libya*
[2]*Energy Research Institute, School of Chemical and Process Engineering , The University of Leeds, Leeds, LS2 9JK, UK*

ABSTRACT: *The energy security and reduction of carbon emissions have accelerated the R&D of the alternative fuels in the transport, heating and power generation sectors in last decade. The heating and power generation sectors are two of the major contributors to carbon dioxide emissions, which are due to the combustion of petroleum fuels. A gas turbine combustor test rig was used to study the combustion and emission characteristics of waste cooking oil methyl ester (WME) biodiesel. A 140mm diameter atmospheric pressure premixed combustion test rig was used at 600K inlet air temperature and Mach number 0.017. The tests were conducted using pure WME and blend with kerosene. The central fuel injection was used for liquid fuels and wall injection was used for NG (Natural Gas). The exhaust samples for smoke and gaseous emissions (NOx, UHC, CO and CO_2) have been analysed on dry basis and corrected to 15% O_2 over range of different fuel rate. The results showed that the biodiesel had lower CO, UHC emissions and higher NOx emissions than the kerosene. The blend B20 had lowest NOx emissions comparing with pure biodiesel (B100) and B50. The optimum conditions for WME with lowest emissions were identified. The carbon dioxide emissions per 100 megawatts of heat generated for each fuel were calculated. The relative carbon emissions and mitigations by biodiesel were compared. The results can be used to estimate pollutant emissions and carbon reductions by biodiesel in power generation industry and other sectors where gas turbine engines are used.*

KEYWORDS: *Biodiesel, Gas turbine, Gaseous Emissions, carbon mitigation.*

I. INTRODUCTION

During the last decade, global warming from the increase in greenhouse gases has become a major scientific and political issue. The level of these gases is increasing in the atmosphere as a result of human activity such as fossil fuel combustion(oil, coal and natural gas) and land use (largely deforestation)[1]. Fossil fuel is a primary source for the energy supply and Figure.1 shows that the petroleum and natural gas comprised of ~60% of energy supply worldwide in 2005[2].

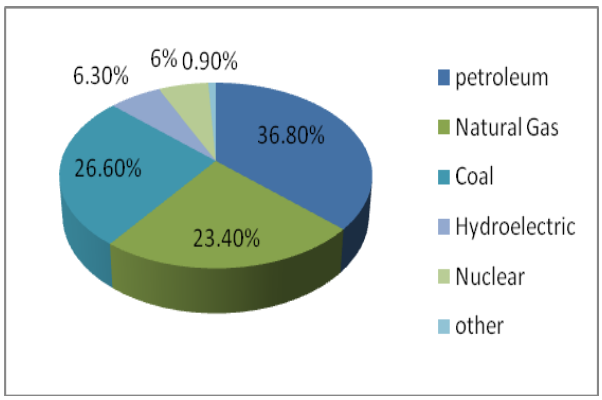

Fig.1 : Fractions of sources for Energy production in 2005[2].

The main greenhouse gases (GHGs) that are produced by human activities and have direct contributions to global warming potentials are carbon dioxide (CO_2), methane (CH_4), nitrous oxide (N_2O) and some special chemicals (halogenated compounds) and their proportional contributions are shown in Figure.2. [3]. CO_2 is a dominant GHG and its level in the atmosphere has been increased by some 25% during the past 200 years and continuing to increase at 0.4% per year[4].The results showed that the average earth surface temperature will increase by some 2° to 6°C and sea level will rise of between 50 and 200 centimetres in this century[5, 6]. Figure.3 shows the three major contributors of carbon dioxide emissions by sectors: power plants, factories and home heating systems and transport[3]. Each sector contributes one third of carbon dioxide emissions.

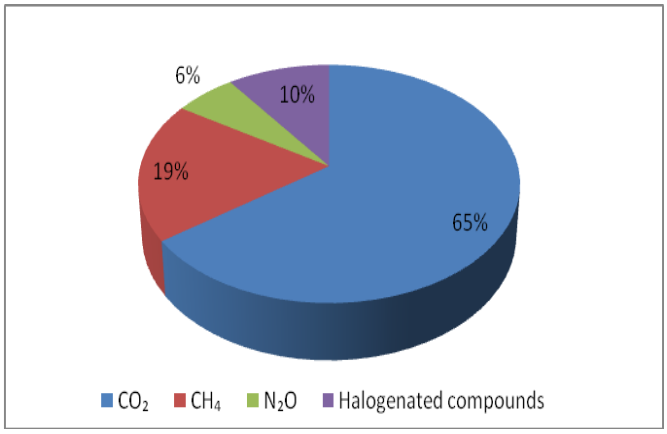

Fig.2: Proportional contributions of greenhouse gases to climate change[1]

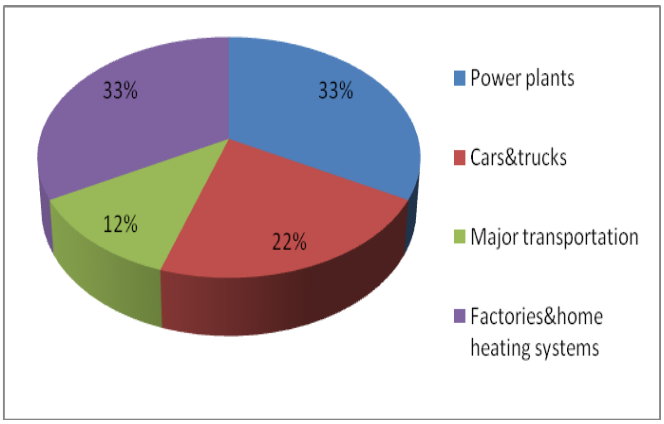

Fig.3: Contributions of each sector to CO_2 emissions[3]

The concerns of environmental impacts and energy security have led the R&D of alternative energy sources such as biofuels, solar and wind energy. Biofuels have attracted huge attention in different countries due to their renewability and environmental benefits. Biofuels include bio-alcohols, biodiesel, biomass and other biomass derived fuels. Biodiesel is one of the most popular biofuels being used in the transport sector. Many studies have shown that the characteristics of biodiesel is very close to diesel fuel and can be used in diesel engine with little or no modification[7]. Moreover, the combustion of biodiesels shown a reduction in smoke opacity, particulate matter (PM), hydrocarbons and carbon monoxide emissions in the exhaust gas compared with diesel fuel[8]. Thus, the results showed significant reduction of smoke and gases emissions with biodiesel blends and the optimum ratios for biodiesel/diesel were 20/80 and 30/70[8]. One of the main drawbacks of biodiesel is the cost and sustainability. The use of waste cooking oils is one way to reduce the cost of biodiesel and utilise the waste [8].There are substantial researches on the applications of biodiesel on diesel engines but the studies on the applications of biodiesel on gas turbine engines are limited. This paper will assess and compare the environmental impact of waste cooking oil methyl ester (WME) and kerosene using a radial swirler industrial low NOx gas turbine combustor under atmospheric pressure and 600K preheated air.

A. Biodiesel sources : In the last century petroleum fuel have been playing an important role in transportation, industrial growth with agricultural and energy sector [9, 10]. Depletion of fossil fuels and increasing concerns of environmental impacts have led scientists to identify alternative fuel sources [10, 11]. Biofuels such as biodiesel have attracted more and more attentions recently and become alternative fuels to liquid fossil fuels due to its renewability and its environmental benefits [9, 11, 12]. Biodiesel is one of the best available sources and promising alternative fuels to liquid fossil fuel [9, 10]. Biodiesel can be made from alcohol and vegetable oils or animal fats which are both agriculturally derived products[8]. Biodiesel is biodegradable and nontoxic and defined as the monoalkyl esters of long chain fatty acids derived from renewable feed stocks like vegetable oils or animal fats[13, 14]. Although there are over 350species of oil producing plants, only a few can potentially be used for biodiesel productions such as rapeseed, sunflower, soybean and oil palm[10]. Figure.4 gives the fractions of commonly used oil crops worldwide in terms of annual oil yield[15]

Rapeseed oil represents the largest contribution of world biodiesel production with 84%, whereas palm and soybean are the lowest[15]. However, the rapeseed oil is not the one having highest oil yield and instead the oil palm gives the highest harvest and oil yield per unit of land. The molecule of vegetable oil is composed of three fatty acid chains attached to a molecule of glycerine and known as triglycerides[16]. Many researchers have concluded that vegetable oils have a great potential to be alternative fuels for diesel engines[15]. However, using raw vegetable oils for diesel engines can cause numerous engine problems. The high viscosity and low volatility of oils compared with diesel lead to engine cold start problems, engine deposits, injector coking and piston ring sticking[7]. These problems can be solved by two ways: heating the vegetable oils to reduce the viscosity and lower the emissions or through transesterification of vegetable oils to form an ester (biodiesel) to reduce the viscosity [10, 17].

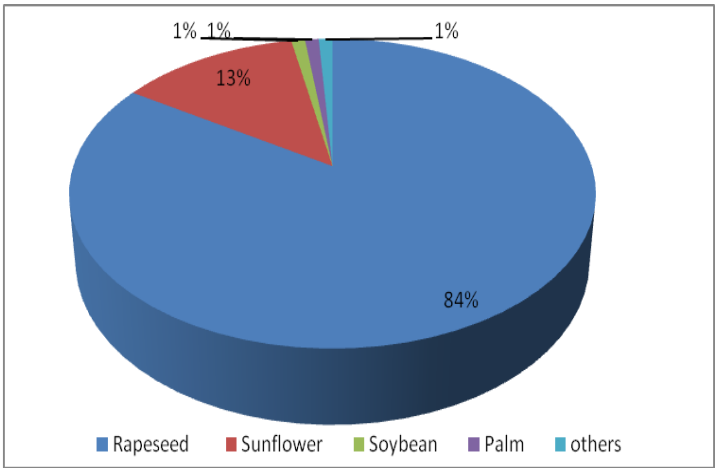

Fig. 4: Oil crops yield for biodiesel[15].

B. Biodiesel production process : Transesterification is defined as chemical reaction of vegetable oils or animal fats with alcohol in the presence of catalyst to form fatty acid methyl esters (FAME) and include glycerol by-product.[17-19]. Methanol, ethanol, propanol, butanol and amyl alcohol are alcohols used in transesterification process. Methanol is a most commonly used alcohol in this process due to its cost and its physical and chemical properties that can make the reaction with triglycerides quicker[14]. It was found that a 3:1 molar ratio of alcohol to triglycerides is needed to complete the transesterification process. Nevertheless, to improve the reaction rate, catalyst (alkalis, acids) or enzymes are usually used[14, 19].Moreover, alkali catalyst has been most often used commercially due to their fast reaction rate than its acid catalyst counterpart [20]. The typical alkali catalysts used in transesterification process are sodium hydroxide, potassium hydroxide or alkali methoxides[11]. However, acid –catalyzed transesterification has less usage because it has relatively slow reaction rate and its insensitivity to free fatty acids in feedstock oil than its alkali catalyst counterpart[19]. Sulphuric acid, sulfonic acids and hydrochloric acid are used as acid catalysts; sulphuric acid is the most commonly used in the reaction as acid catalyst[14, 19]. Nevertheless, acid –catalyzed transesterification can be used if there is more water and free fatty acid (more than 1) in the triglycerides [14].

C. Characteristics of biodiesel : Biodiesel is sulphur-free, non-toxic, biodegradable, oxygenated compounds and renewable fuels and has high cetane numbers. The major advantage of biodiesel is the reduction of CO2 emissions. Many researchers have shown that the properties of biodiesel are similar to diesel fuel. Therefore, biodiesel can be used in diesel engine with little or no modification of the engines[16]. It shows that the density,

cetane number, pour point and flash point of biodiesel are higher whereas the heating value is about 10% lower compared to diesel. The kinematic viscosity of both fuels is similar. Moreover, biodiesel prolongs the engine life and has better lubricating qualities than fossil fuels. However, there are some drawbacks of biodiesel such as reduced energy density which increases mass fuel consumption and the higher cost of production than diesel [16]. The use of waste cooking oils and animal fats for biodiesel production provides not only a resource for biodiesel but also saving the environment as it avoids these oils and fats pouring into sewer systems which is harmful for the environment and human health [17, 18].

II. MATERIAL AND METHODS

A. Rig Description : Premixed Gas turbine combustor test rig was used to study the combustion and emission characteristics of biodiesel fuel. The apparatus used for the combustion experiments consisted of a combustion chamber, an air supply line, venturi air flow meter, 250mm diameter air plenum chamber, a fuel supply line and an exhaust gas analyse system. The combustion experiments were carried out at atmospheric pressure. To ensure high gas temperature of compressed air in the system air was heated to the required inlet temperature (600K) by a 150KW electrical heater. The primary zone combustion chamber was 6.4mm thick stainless steel, cylindrical shape with an inner diameter of 140mm and length of 330mm. Thus, a premixing fuel injector with holes on centres of equal area, 2m long and 76mm diameter mixing tube was sued to inject biodiesel and kerosene in this study. The flame stabilizer was positioned in between the flame tube and the mixing tube.

The combustor was positioned in parallel in the test room and supplied by air from two independent approach pipes which connected to the air supply pipe downstream of the electrical heaters. The inlet temperature (of 600K)was measured 100mm upstream of the Swirler using chrome-alumel type K thermocouple and investigated at M=0.017. This Mach number typically represents ~40% of the total combustor airflow entering the lean primary zone through the radial swirler. The ignition was carried out by electrical discharge from the spark igniters.

B. Emission Measurement : Mean exhaust gas samples were obtained using an 'X' configuration stainless steel water cooled probe with 40 holes at centres of equal area. The sample gases were passed into a 190°C heated sample line and on through a 190°C heated filter and pump to a 190°C heated gas analysis system. The gas analyses results were processed to provide air fuel ratio, combustion efficiency and mean adiabatic flame temperature. The NOx emissions were measured hot on wet gas basis using a chemiluminescence NOx analyser (signal Instruments, UK) with vacuum ozone reaction chamber. It had a minimum scale of 1-4ppm with a 0.05ppm resolution. Whereas, the unburnt hydrocarbons was measured using a heated FID. However, the CO and CO_2 were measured on a dry gas basis using NDIR with luft cell detectors (ADC). The gas analysis results were processed to provide an air to fuel ratio and mean adiabatic flame temperature and all emissions will be corrected to 15% O_2 over a range of different fuel rate.

C. Fuel preparation and injection : Kerosene was stored in a 200 litre barrel whereas WME and blends were stored in a 40 litre tank. They were pumped from the barrel or tank and delivered to injection fuel points after passing through rotameters for measuring fuel flow. Two rotameters were used with different measurement ranges. These two rotameters were calibrated for kerosene, WME and blends respectively as the density for these liquid fuels are different and thus the mass flow is different for the same indicated readings

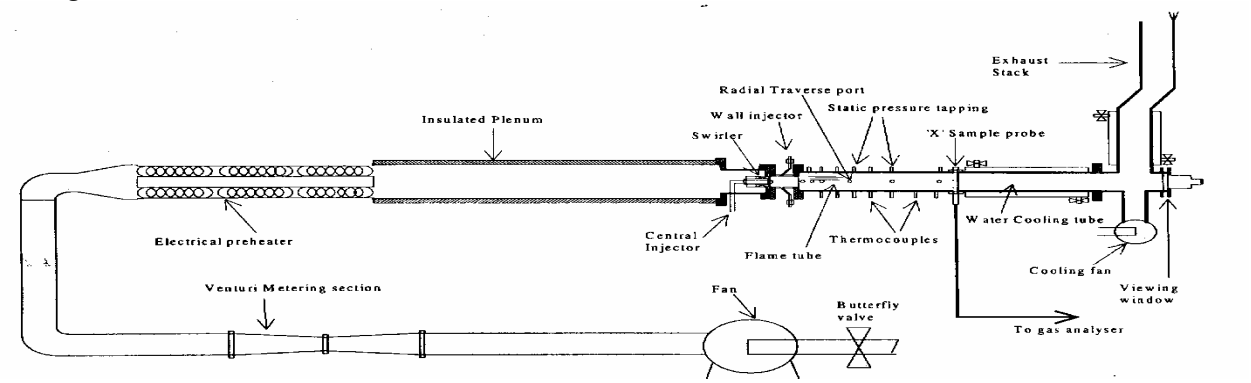

Fig.5: combustion Rig

Liquid fuels (B100, B50, B20 and Kerosene) were injected and premixed with incoming air in a premixed fuel injector with holes on centres of equal area. The air fuel ratio (equivalence ratio) is increased in small steps by increasing fuel flow rate whereas keeping air flow rate constant. The gas sample for smoke and gaseous emissions (NOx, NO UHC, CO and CO_2) have been analysed on dry basis and corrected to 15% O_2 over the rang of different fuel rate.

III. RESULTS AND DISCUSSIONS

A. UHC, CO & NOx Emissions : All emissions results are corrected to 15%oxygen and plotted as a function of the equivalence ratio for 600K inlet temperature and Mach number of 0.017. The influence of equivalence ratio and fuel type on gaseous emissions of, UHC, CO and NOx are shown from Figure 6 to Figure 8. Comparison between pure biodiesel (B100), Kerosene and blends (B20, B50) fuels regarding UHC is given in Figure6. In this study, UHC, CO and NOx emissions are evaluated in ppm in the exhaust gas. The UHC emissions for all fuels were reduced as the primary zone was operated richer. Generally, pure biodiesel and blend fuels (B20&B50) had slightly lower UHC emissions than kerosene in all operating conditions. However, kerosene fuel had a higher UHC than biodiesel and biodiesel blend fuels in lean conditions (Φ< 0.6). Moreover, the results showed that B20 had a big impact on UHC emissions in all conditions. The reduction of biodiesel UHC emissions is due the fact that biodiesel has long carbon chains and the absence of aromatic content make cetane number higher than fossil fuels which prompt the combustion[7, 8]. Generally, the emissions of UHC for all types of fuels are low which indicated that the atomization of liquid fuels was good.

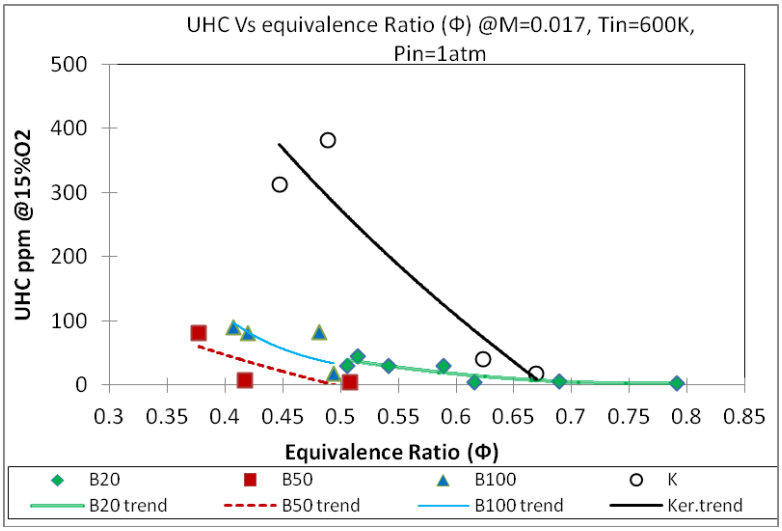

Fig.6. UHC emissions as a function of equivalence ratio for pure biodiesel, kerosene and blend.

Comparison among B20, B50, B100 and Kerosene fuels with regard CO at Mach number 0.017 and air inlet temperature 600K is given in Figure7. The CO emissions for all fuels were reduced markedly as the primary zone was operating leaner. The range of CO emissions were almost (330-630ppm) in all type of fuels operating leaner than Φ=0.53. However, the CO emissions for kerosene fuel was about 2.5 times those for B20 and about 5times those for B100 and B20 of the mixture richer than 0.55.whereas the lowest CO emissions around 450ppm was recorded with B100 for equivalence ratio Φ=0.48. The behaviour of CO & UHC emissions of biodiesel and blend fuels in gas turbine engine is in an agreements with previous studies in diesel engines[8].Thus, characteristics of CO emissions for pure biodiesel, B50 and kerosene are similar at Φ=0.48.The CO results indicated that complete combustion was achieved with biodiesel and biodiesel blend fuels which has higher oxygen content than kerosene.

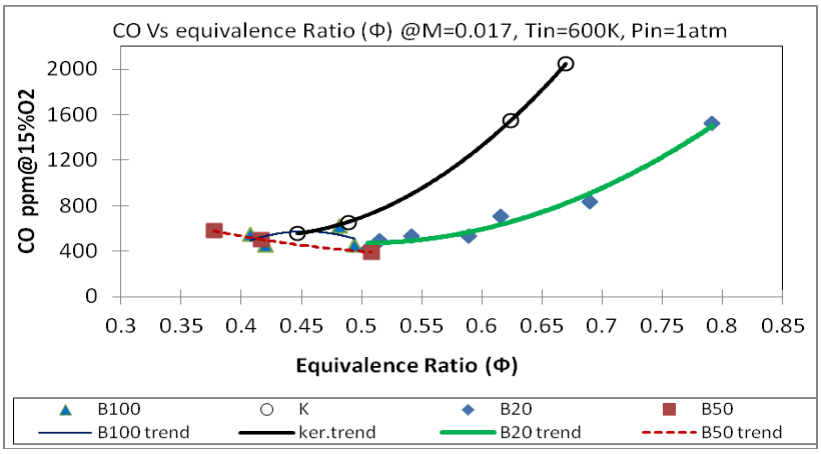

Fig.7. CO emissions as a function of equivalence ratio for pure biodiesel, kerosene and blend.

The NOx emissions as function of equivalence ratio for biodiesel, kerosene and two blends (B20 and B50) at Much number 0.017 with an air inlet temperature of 600K were presented in Figure8.It is seen that Nox emissions level decreases with increasing equivalence ratio for all type of fuels. B50 and B100 fuels had higher NOx emissions than kerosene and B20 when the equivalence ratio was 0.4 to 0.5. However, NOx emissions of B100 and B50 fuels were about 27% higher than that of B20 and their characteristics behaviour were completely identical. However, NOx emissions increased as the concentration of biodiesel increased. This is mainly related to the oxygen content in the biodiesel and has a shorter delay time which is cause a peak pressure and temperature to enhance Nox formation. Thus, NO emissions were measured for all types of fuels and have the same trends of NOx emissions.

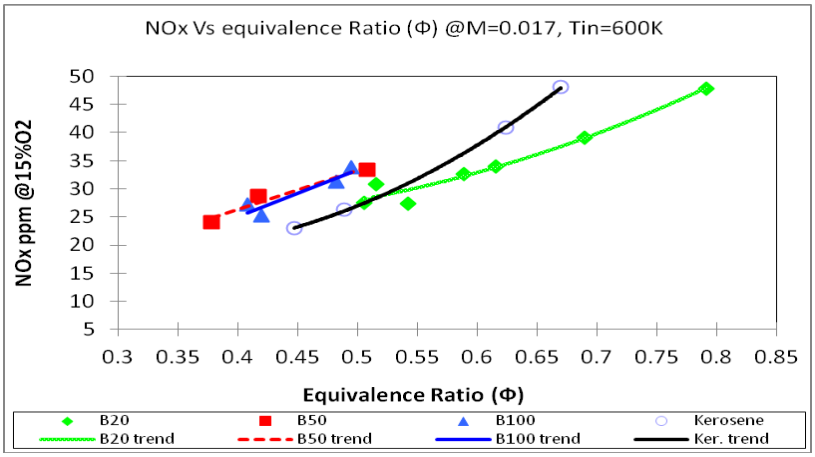

Fig.8. NOx emissions as a function of equivalence ratio for pure biodiesel, kerosene and blend.

B. CO_2 emissions : CO_2 emissions are a direct reflection of the fuel consumption and related to fuel compositions. As the air flow is constant in the tests the CO_2 emissions increase as the equivalence ratio increases. However, the variation of CO_2 emissions was not significant between kerosene, WME and blends and CO_2 emissions were around 4.6%. The CO_2 emissions from co-firing with NG showed notable decrease due to low carbon content in NG and have a value of 4%.

C. CO_2 reductions by biodiesel comparing with fossil fuel : As described earlier, biodiesel has a lower CO, UHC emissions and renewable. It can be used in diesel engines with little or no modifications. The biggest benefit of biodiesel is theoretically carbon neutral, which means that the CO_2 emitted in the combustion of biodiesel is absorbed by plants during their growth. The net effect is therefore theoretically zero carbon emissions. However, the real net effect is not zero carbon emissions. This is due to that the production of biodiesel consumes energies and thus emits CO_2. Figure.9 shows the CO_2 reduction as a function of biodiesel fraction in blends. The maximum CO_2 reduction by biodiesel is ~80% with B100, indicating a loss of ~20% due to biodiesel's production.

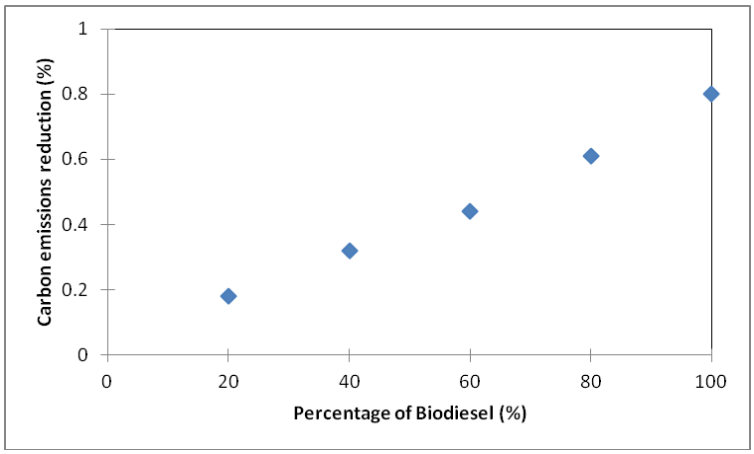

Fig.9: Effect of biodiesel blend level on CO_2 emissions[21]

The emission of CO_2 when combusting Natural gas, Kerosene and pure biodiesel are approximately (0.23, 0.26 and 0.11 kg/kWh) respectively[22]. However, based on these figures the CO_2 emissions were calculated per 100 MJ of heat energy generated for each fuel scenario and presented in Figure.10.

The emission index (EI) of Kg CO_2 per Kg fuel was calculated by multiply the calorific value of each fuel (CV) by CO_2 emission factor (EF). The EI for kerosene and NG is the CO_2 produced in a complete combustion. The EI for the WME is the CO_2 produced during its production not the CO_2 by a complete combustion. The table 2 lists the calorific value (CV), emission factor (EF) and EI of each fuel.

Table.1: Calorific value and EI for each fuel[22].

Fuel	Calorific value (CV) MJ/kg	CO_2 emissions factor(EF)* kgCO2/MJ	Emission index (EI) kgCO2/kg fuel EI=CV*EF
Kerosene	44	0.93	41
Natural gas	50.1	0.82	41
Biodiesel(B100)	39.8	0.39	15.5
B50	41.9	0.66	27.6
B20	43.2	0.82	35.5

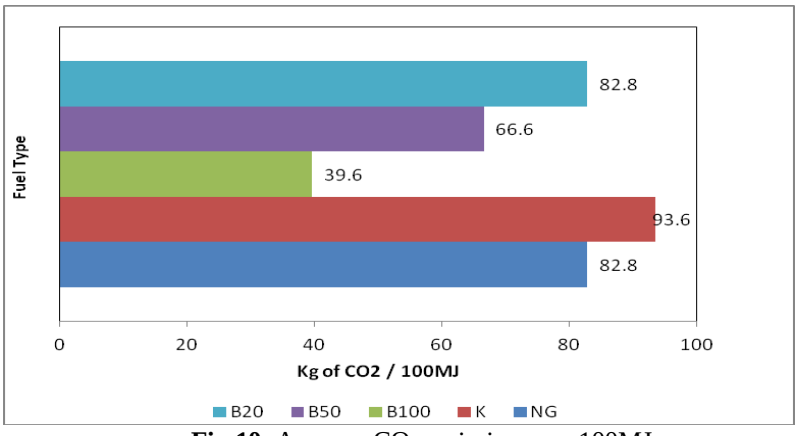

Fig.10: Average CO_2 emissions per 100MJ

Figure.10 shows the comparison among NG, Kerosene, B100, B50 and B20 fuels with regard CO_2 emitted to produce 100MJ of heat energy. It can be seen that kerosene fuel had the highest CO_2 emissions compared with pure biodiesel and its blends as well as natural gas. However, pure biodiesel had the lowest CO_2 emissions with 39.6Kg. These emissions were produced during production of biodiesel not in combustion process. Moreover, B50 produced less CO_2 emissions than B20 as the percentage of reduction increased as the concentration of biodiesel increased as shown in Figure.8.

Figure.11 shows the CO_2 emissions as a function of fuel type based on kerosene fuel to produce 100MJ of heat energy. i.e. all the CO2 emissions were normalised to kerosene CO2 emissions. The NG produced lower CO2 emissions due to its higher H/C ratio. The CO_2 emissions were reduced up to ~60% for B100, 30% for B50 and 20% for B20 compared to kerosene. Also, in this study, the mass of carbon emitted to produce 100MJ of heat energy was calculated for different type of fuel and compared and presented in Figure.12. This enables a direct comparison of carbon emissions and mitigations by biodiesel compared with fossil fuels. These results can be used to estimate pollutant emissions and carbon reductions by biodiesel in power generation industry and other sectors where gas turbine engines are used.

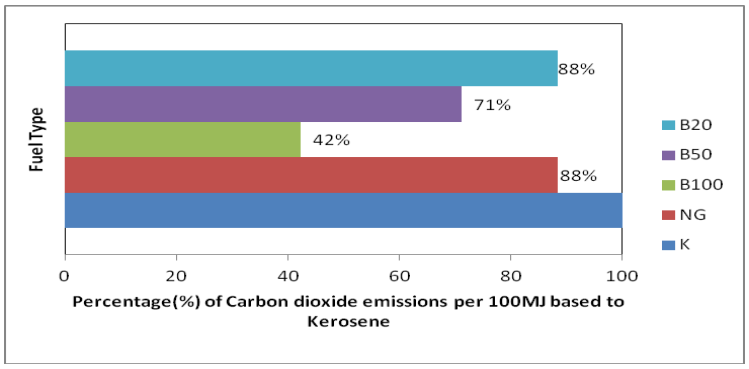

Fig.11. The Percentage (%) of Carbon dioxide emissions per 100MJ based to Kerosene

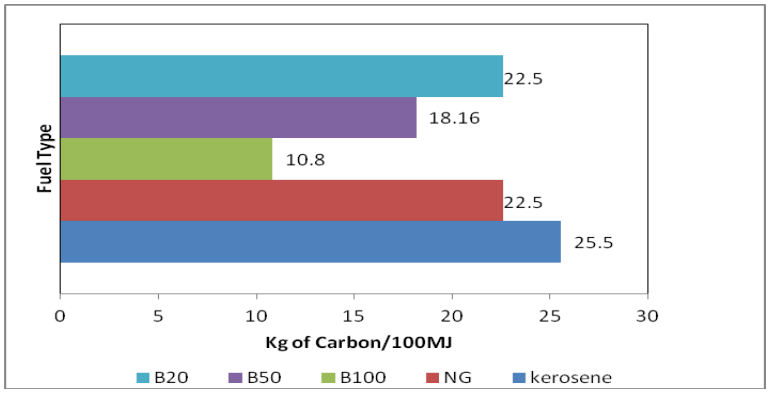

Fig.12. The average Carbon emissions per 100MJ.

III. CONCLUSIONS

In this study, combustion experiments on waste cooking oil derived methyl ester biodiesel (WME) on a radial swirler industrial low NOx gas turbine combustor under atmospheric pressure and 600K were conducted. The principle findings are as follows:

[1] Blends and pure fuels had much lower UHC emissions than kerosene until Φ=0.65 where all fuels produced the same level of emissions.
[2] Blends and pure biodiesel fuels produced lower CO emissions than kerosene fuel.
[3] Pure biodiesel and its blends had higher Nox emissions than kerosene fuel.
[4] Nox emissions of B100 and B50 fuels were higher than that of B20 and their characteristics behaviour were completely identical.
[5] Nox emissions increased as the concentration of biodiesel increased.
[6] The optimum conditions for WME with lowest CO, UHC and NOx emissions were around Φ=0.55.
[7] CO_2 emissions for kerosene, pure biodiesel and blends are similar and at around 4.6%. The co-firing with NG reduced CO2 emissions to 4%.
[8] The replacement of fossil fuels with biodiesel can reduce carbon emissions significantly due to biodiesel's carbon neutral (or nearly neutral) characteristics.
[9] CO_2 emissions per 100MJ of heat energy generated were reduced up to 30% for B50 and 20% for B20 and NG
[10] There was massive reduction in CO_2 emission with pure biodiesel up to 60% compared to kerosene fuel.
[11] From the above finding, WME is considered to be a promising alternative fuel for gas turbines

IV. NOMENCLATURE

CO: Carbon monoxide

NOx: oxides of nitrogen

HC: Unburned hydrocarbon

NG: Natural gas

WME: Waste cooking oil Methyl Ester

FID: Flame Ionization Detector

NDIR: Non-Dispersive Infrared

REFERENCES

[1]. Programme, I.G.G.R.D., Greenhouse Gases, IEA Greenhouse Gas R&D Programme.
[2]. Administration, E.I., Renewable Energy Trends in Consumption and Electricity, 2005, USA Government: USA.
[3]. Hopwood, N. and J. Cohen, Greenhouse Gases and Society. 2009.
[4]. Reserch, C.M.., Greenhouse Gases. 2008, the online enviromental community. p. 3.
[5]. Titus, J.G., "Greenhouse Effect, Sea Level Rise, and Land Use". 1990, Land use policy. p. 138-53.
[6]. Schneider, S.H., The Greenhouse Effect: Science and Policy Science, 1989. 243,p. 771 - 781
[7]. Canakci, M., Performance and emissions characteristics of biodiesel from soybean oil. 2005, Faculty of Technical Education, Kocaeli University. p. 915-922.
[8]. Lue, Y.-F., Y.-Y. Yeh, and C.-H. Wu, The Emission Characteristics of a Small D.I.Diesel Engine using Biodiesel Blended Fuel. Environmental Science and Health, 2001. A36(5): p. 845-859.
[9]. Hashimoto, N., et al., Fundamental combustion characteristics of palm methyl ester (PME) as alternative fuel for gas turbines. Fuel, 2008. 87(15-16): p. 3373-3378.
[10]. Basha, S.A., K.R. Gopal, and S. Jebaraj, A review on biodiesel production, combustion, emissions and performance. Renewable and Sustainable Energy Reviews. 13(6-7): p. 1628-1634.
[11]. Phan, A.N. and T.M. Phan, Biodiesel production from waste cooking oils. Fuel, 2008. 87(17-18): p. 3490-3496.
[12]. Jha, S.K., S. Fernando, and S.D.F. To, Flame temperature analysis of biodiesel blends and components. Fuel, 2008. 87(10-11): p. 1982-1988.
[13]. Bhale, P.V., N.V. Deshpande, and S.B. Thombre, Improving the low temperature properties of biodiesel fuel. Renewable Energy, 2009. 34(3): p. 794-800.
[14]. Ma, F. and M. A.Hanna, Biodiesel production: a review. Bioresource Technology, 1999. 70: p. 1-15.
[15]. Mckibben, G.P.B., Biodiesel Growing a New Energy Economy. frst edition ed. 2005: Chelsea Green. 281.
[16]. Bozbas, K., Biodiesel as an alternative motor fuel: Production and policies in the European Union. Renewable and Sustainable Energy Reviews, 2008. 12(2): p. 542-552.
[17]. de Souza, G.R., et al., Evaluation of the performance of biodiesel from waste vegetable oil in a flame tube furnace. Applied Thermal Engineering, 2009. 29(11-12): p. 2562-2566.
[18]. Lapuerta, M., J. Rodríguez-Fernández, and J.R. Agudelo, Diesel particulate emissions from used cooking oil biodiesel. Bioresource Technology, 2008. 99(4): p. 731-740.
[19]. Zhang, Y., et al., Biodiesel production from waste cooking oil: 2. Economic assessment and sensitivity analysis. Bioresource Technology, 2003. 90(3): p. 229-240.
[20]. Dorado, M.P., et al., An approach to the economics of two vegetable oil-based biofuels in Spain. Renewable Energy, 2006. 31(8): p. 1231-1237.
[21]. Coronado, C.R., J.A. de Carvalho Jr, and J.L. Silveira, Biodiesel CO2 emissions: A comparison with the main fuels in the Brazilian market. Fuel Processing Technology, 2009. 90(2): p. 204-211.
[22]. Agency, I.E., CO2 emissions from fuel combustion. 2009.